OAK RIDGE NATIONAL LABORATORY
OPERATED BY UNION CARBIDE CORPORATION • FOR THE DEPARTMENT OF ENERGY

OAK RIDGE NATIONAL LABORATORY
CENTRAL RESEARCH LIBRARY
CIRCULATION SECTION
4500N ROOM 175
LIBRARY LOAN COPY
DO NOT TRANSFER TO ANOTHER PERSON
If you wish someone else to see this report, send in name with report and the library will arrange a loan.

ORNL/RSIC-42

A REVIEW OF THE THEORY AND APPLICATION OF SENSITIVITY AND UNCERTAINTY ANALYSIS

PROCEEDINGS OF A SEMINAR-WORKSHOP, OAK RIDGE, TENNESSEE

AUGUST 22–24, 1978

RADIATION SHIELDING INFORMATION CENTER

Printed in the United States of America. Available from
National Technical Information Service
U.S. Department of Commerce
5285 Port Royal Road, Springfield, Virginia 22161
Price: Printed Copy $13.00; Microfiche $3.00

This report was prepared as an account of work sponsored by an agency of the United States Government. Neither the United States Government nor any agency thereof, nor any of their employees, contractors, subcontractors, or their employees, makes any warranty, express or implied, nor assumes any legal liability or responsibility for any third party's use or the results of such use of any information, apparatus, product or process disclosed in this report, nor represents that its use by such third party would not infringe privately owned rights.

ORNL/RSIC-42

Contract No. W-7405-eng 26

Radiation Shielding Information Center
Engineering Physics Division

A REVIEW OF THE THEORY AND APPLICATION OF SENSITIVITY AND UNCERTAINTY ANALYSIS PROCEEDINGS OF A SEMINAR-WORKSHOP, OAK RIDGE, TENNESSEE

August 22–24, 1978

Edited and Compiled by:
C. R. Weisbin, R. W. Roussin, H. R. Hendrickson, and E. W. Bryant

Date Published: February 1979

OAK RIDGE NATIONAL LABORATORY
Oak Ridge, Tennessee 37830

operated by

UNION CARBIDE CORPORATION

for the

DEPARTMENT OF ENERGY

TABLE OF CONTENTS

Page

Abstract viii

Foreword ix

Acknowledgments ix

Summary, C. R. Weisbin, Oak Ridge National Laboratory 1

Session I: Sensitivity and Uncertainty Analysis for Fast and Thermal Reactors, C. R. Weisbin, Oak Ridge National Laboratory, Chairman

1. "The Use of Cross-Section Sensitivities in the Analysis of Fast Reactor Integral Parameters," P. J. Collins and M. J. Lineberry (Argonne National Laboratory, Idaho). 13

2. "Advances in Fast Reactor Sensitivity and Uncertainty Analysis," J. H. Marable and C. R. Weisbin (Oak Ridge National Laboratory). 25

3. "Controlled Cross-Section Adjustment by Integral Data," U. Salmi, J. J. Wagschal, A. Ya'ari, and Y. Yeivin (Racah Institute of Physics, The Hebrew University, Israel). 49

4. "Sensitivity Analysis Applied to the Calculation of Detector-Response Kernels," W. H. Scott, Jr. (Science Applications, Inc., La Jolla), and P. J. McDaniel, J. H. Renken, and S. A. Wright (Sandia Laboratories, New Mexico). 61

5. "Sensitivity of Water Reactor Fuel Cycle Parameters and Costs to Nuclear Data," M. Becker, D. R. Harris, B. Quan, and J. M. Ryskamp (Rensselaer Polytechnic Institute). 75

6. "Nonlinear Model Fitting of Thermal Neutron Data and its Application in Resonance Parameter Uncertainty Analysis," J. K. Thompson (Battelle Pacific Northwest Laboratories). 89

7. "Fission Product Decay Power and Uncertainties After Realistic Reactor Operating Histories," T. J. Trapp (Battelle Pacific Northwest Laboratory), and B. I. Spinrad (Oregon State University). 105

Session II: Sensitivity and Uncertainty Analysis for Dosimetry and Fusion Reactor Applications, E. Greenspan, Nuclear Research Center—Negev, Israel, Chairman

1. "Testing of ENDF/B Cross-Section Data in the Californium-252 Neutron Benchmark Field," W. Mannhart (Physikalisch-Technische Bundesanstalt, Braunschweig, FRG). 119

2. "Use of HEDL Codes in the Sensitivity and Uncertainty Analysis of the Pressure Vessel Embrittlement Damage Function Problem," G. L. Guthrie, F. Schmittroth, R. L. Simons, and E. P. Lippincott (Hanford Engineering Development Laboratory), and C. Oster (Battelle Pacific Northwest Laboratories). 135

3. "Varied Applications of a New Maximum-Likelihood Code with Complete Covariance Capability," F. Schmittroth (Hanford Engineering Development Laboratory). 145

4. "Sensitivity and Uncertainty Analysis Applied to the NBS-ISNF," B. L. Broadhead (University of Tennessee), and J. H. Marable (Oak Ridge National Laboratory). 161

5. "Sensitivity Analysis Applied to an Integral Test of Niobium Cross Sections," D. T. Ingersoll (Oak Ridge National Laboratory), and B. W. Wehring (University of Illinois). 179

6. "The Application of Uncertainty Analysis in Conceptual Fusion Reactor Design," T. Wu and C. W. Maynard (University of Wisconsin). 191

7. "Uncertainty Analysis for Secondary Energy Distributions," S. A. W. Gerstl (Los Alamos Scientific Laboratory). 219

Session III: Advances and Future Extensions for Sensitivity and Uncertainty Analysis, F. Perey, Oak Ridge National Laboratory, Chairman

1. "High Order Effects in Cross-Section Sensitivity Analysis," E. Greenspan, Y. Karni, and D. Gilai (Nuclear Research Center–Negev and Ben Gurion University of the Negev, Israel). 231

2. "Sensitivity Theory for Reactor Thermal-Hydraulics Problems," E. M. Oblow (Oak Ridge National Laboratory). 251

3. "A New Approach to the Adjustment of Group Cross-Sections Fitting Integral Experiments," Y. Chao (Carnegie-Mellon University). 281

4. "Sensitivity Theory for Depletion Analysis," M. L. Williams, J. R. White, J. H. Marable, and E. M. Oblow (Oak Ridge National Laboratory). 299

5. "Expectations for ENDF/B-V Covariance Files: Coverage, Strength and Limitations," F. G. Perey (Oak Ridge National Laboratory). 311

Additional Papers Related to the Seminar (Not Presented Orally).

1. "Fuel-Motion Unfolding Based on Point Detector Responses," P. J. McDaniel and S. A. Wright (Sandia Laboratories, New Mexico). 319

2. "Sensitivity of LWR Fuel Cycle Costs to Uncertainties in Detailed Thermal Cross Sections," J. M. Ryskamp, M. Becker, and D. R. Harris (Rensselaer Polytechnic Institute). 329

3. "The Linearity Assumption in Adjustment Procedures," Y. Yeivin (Racah Institute of Physics, The Hebrew University, Israel). 343

4. "First and Higher Order Perturbation Techniques and Their Application in System Analysis and Data Adjustments," A. Gandini (CNEN-CSN, Casaccia, Rome, Italy). 351

5. "The Use of Error Files in Uncertainty Analysis and Data Adjustment," M. M. Chesnutt (Imperial College, London), and A. K. McCracken (AEE Winfrith, England). 363

6. "Influence of Cross-Section Structure on Unfolded Neutron Spectra," C. Ertek, M. F. Vlasov, B. Cross, and P. M. Smith (International Atomic Energy Agency, Vienna, Austria). 375

ABSTRACT

This review consists of manuscripts of 25 papers submitted to the Radiation Shielding Information Center Seminar-Workshop on "Theory and Application of Sensitivity and Uncertainty Analysis" held at Oak Ridge, Tennessee, August 22-24, 1978. The papers are grouped in three sessions which were conducted at the Seminar. Additional papers which were submitted, but not given orally, are also included in this report. The sessions were titled, "Sensitivity and Uncertainty Analysis for Fast and Thermal Reactors," "Sensitivity and Uncertainty Analysis for Dosimetry and Fusion Reactor Applications," and "Advances and Future Extensions for Sensitivity and Uncertainty Analysis."

A summary of the papers presented and the discussions and comments which were made is also included to provide an indication of the state-of-the-art of sensitivity and uncertainty analysis.

FOREWORD AND ACKNOWLEDGMENTS

This review deals with the second of two seminar-workshops held by the Radiation Shielding Information Center in 1978. The seminar-workshop allows the dissemination in a few days of an extensive amount of technical information in particular areas. The seminar portion involves formal presentations and discussions among representatives of installations developing or using similar technology. The workshop concentrates on a specific package of computing technology related to the theme of the meeting. The proceedings of the first, held in March 1978, have been published as ORNL/RSIC-41, "A Review of Multigroup Nuclear Cross-Section Processing, Proceedings of a Seminar-Workshop," compiled by D. K. Trubey and H. R. Hendrickson.

The August 1978 seminar-workshop concentrated on the theory and application of sensitivity and uncertainty analysis. The workshop featured ORNL's FORSS Sensitivity and Uncertainty Analysis Code System which is now packaged in the RSIC collection as PSR-129/FORSS.

One of the goals of this meeting was to try to provide more of a state-of-the-art review of the field than is normally provided by publishing the formal papers. For that reason attempts were made to provide ample time for questions and discussions among participants. To try to capture the sense of where the field now stands, a summary of the seminar presentations and discussions has been prepared by C. R. Weisbin and published as part of this document.

The papers published in this report were submitted to the Seminar portion of the meeting. We are grateful to the authors of the papers for submitting their manuscripts in camera-ready form. The three sessions of the Seminar were chaired by C. R. Weisbin, E. Greenspan, and F. G. Perey. Their guidance provided stimulating discussions.

The Workshop on the FORSS Sensitivity and Uncertainty Analysis Code System was managed in great part by J. L. Lucius of the UCND-CSD staff. His many weeks of effort were largely responsible for the success of the Workshop. Presentations at the Workshop were made by J. D. Smith (University of Tennessee), J. Drischler, J. Marable, E. Oblow, F. Perey, R. W. Roussin, and C. R. Weisbin (ORNL-EPD), and W. E. Ford, III and R. Q. Wright (UCND-CSD).

We thank Barbara Beem, Jan Gentry, Nancy Mauney, Brenda Neeley, and Cathy Oldham for typing materials for the Workshop.

All the members of the RSIC staff helped to make the seminar-workshop run smoothly. We are grateful to Mildred Landay who was responsible for registration. We also thank Marie Anthony, Ann Gustin, and Betty McGill for help in preparing the final documents used at the workshop.

R. W. Roussin
Radiation Shielding Information Center
Oak Ridge National Laboratory

SUMMARY
RSIC SEMINAR/WORKSHOP
"THEORY AND APPLICATION OF SENSITIVITY AND UNCERTAINTY ANALYSIS"
Royal Scotsman Inn, Oak Ridge, Tennessee
August 22-24, 1978

C. R. Weisbin

The enclosed summary represents my view of the conference and is intended to provide a "snapshot" of the substance, issues, and state-of-the-art which evolves from such a meeting. No attempt was made to achieve consensus by the participants regarding any of my observations or conclusions.

The meeting was made intentionally broad in scope, covering theory and application of both sensitivity and uncertainty analyses for fast and thermal reactors, dosimetry and fusion applications and generalizations and extensions to new fields. Seventy-six scientists participated representing mostly all of the major U.S. work in this field as well as work in the U.K., Italy, France, West Germany and Israel. The round table meeting format and equal allotment of paper presentation time (15 minutes) and question time (15 minutes) led to lively and stimulating discussions.

In Sections I-III below, I have attempted to very briefly comment on the papers presented in the three formal sessions (organizations are listed explicitly in the program--see Appendix II). Section IV summarizes some of the discussions which were stimulated on a variety of topics and some of my observations and conclusions. Finally, Section V presents briefly a commentary on the workshop part of the meeting.

I. Highlights of Session I: Sensitivity and Uncertainty Analysis for Fast and Thermal Reactors

The paper of Collins and Lineberry discussed the ANL experience with cross section adjustment procedures for the analysis of various discrepancies obtained in the prediction of a range of critical experiments as well as differences in predictions of power distributions and control rod worths between homogeneous and heterogeneous LMFBR designs. One unique feature of this paper is the availability of quantified *covariance matrices for measured integral parameters* including k_{eff} and reaction rate ratios. This type of information is absolutely essential for credible adjustments! In the future, the authors expect to include reactivity worth and spectrum measurements. The following paper, by Marable and Weisbin, summarized the ORNL status and future directions for reactor sensitivity analysis. The paper elaborated on recently developed procedures for the *inclusion of methods uncertainties* (as well as nuclear data and integral experiment uncertainties) into the adjustment procedure. Significant future work is required in the evaluation of the biases and uncertainties associated with particular analysis approaches. A limited start in this direction is being made by the Data Testing Subcommittee of CSEWG. Y. Yeivin presented the next paper which warned against the pitfalls of "blind" application of adjustment codes. The approach taken by the Yeivin group emphasized

rejection of dubious integral data found by *successive adjustments* using different groupings of the available integral data. These three interesting papers were followed by a coffee break.

P. McDaniel presented the next paper, a novel development and application of sensitivity analysis to *unfold signals* generated by small fission detectors *to determine fuel motion* in a melting reactor-fuel-pin test assembly. Forward and adjoint three-dimensional angular flux densities calculated with the MORSE Monte Carlo code were coupled to generate the response kernels required for unfolding. J. M. Ryskamp presented the next paper, a quantification of the *sensitivity of fuel cycle cost to uncertainties in detailed thermal cross sections*. The sensitivities for GE (BWR-6) and B&W (PWR) reactors are highest near the peak of the hardened Maxwellian flux. Although simplified models are employed, significant conclusions have evolved from studies of this type emphasizing the *importance of considering the entire fuel cycle* (when performing sensitivity analysis) due to buildup and depletion of various nuclides, throwaway or recycle of fissionable material, and time dependent spectral changes. Jack Thompson next presented a non-linear least squares fitting of experimental thermal neutron data. This work provided an interesting example of an evaluation procedure which *yields directly best estimates of the nuclear data parameters and their associated uncertainties*. An example of the application of this procedure to ^{240}Pu data was given. The last paper of the morning was presented by T. J. Trapp on the subject of fission product decay power and uncertainties. His paper demonstrated the *propagation of uncertainties in fission product yields and decay energies to uncertainties in decay power* from 0-10,000 seconds. The analysis included appropriate constraints (e.g., summation of yields) and treated fission product capture as a correction term.

II. Highlights of Session II: Sensitivity and Uncertainty Analysis for Dosimetry and Fusion Reactor Applications

The Tuesday afternoon session began with the paper of Mannhart regarding the testing of ENDF/B data in the ^{252}Cf neutron benchmark field. Activation measurements for ^{197}Au(n,γ), ^{115}In(n,n'), etc. are available and this simplest of all fields presents a unique opportunity to verify the data files. However, as common to many papers in this meeting, *lack of detailed covariance files* makes it difficult to draw supported conclusions. This paper also discussed *analytic approximations for the calculation of the sensitivity* of group averaged cross sections to changes in *microscopic data, energy shifts, and fission spectrum shape*. The next paper by Guthrie, et al, dealt with the application of sensitivity methodology to the LWR pressure vessel damage function unfolding problem. There is an ongoing effort to *correlate neutron exposure data* measured at a surveillance position *with the rate of embrittlement* of the metal at the 1/4 thickness position in the pressure vessel wall. A companion paper by Schmittroth described new HEDL methodology being employed to treat this same problem. Schmittroth's adjustment code FERRET is *based upon a general log-normal formulation* to ensure positivity and to cope with asymmetric limits. Schmittroth has also applied this tool to fission product cross section

evaluations for ENDF/B-5 and for the evaluation of fission product after-heat. The next paper, presented by Broadhead, described a benchmark analysis of ISNF reaction rate measurements including *calculated flux covariances* as well as activation and cross section uncertainties. Use of detailed calculations (171 groups) and proposed ENDF/B-5 ^{235}U fission spectra led to a consistent adjustment. A coffee break followed with lively discussion pertaining to this entire field of dosimetry.

D. Ingersoll led off the fusion session describing a sensitivity analysis of an integral test (measurement of leakage spectra) of Nb cross sections. Specific *re-evaluation requests* were made for the inelastic cross sections above 1 MeV and all data above 10 MeV deduced from comparison of calculation with measurement. This was followed by the Wisconsin paper presented by Wu which briefly reviewed the theories of sensitivity and uncertainty analysis and then applied them to a new conceptual tokamak fusion reactor design NUWMAK. An interesting approach was taken in this paper to determine the *cost/benefit of performing different experiments* based upon the total reduction in response uncertainty as determined by the a posteriori variance from the adjustment procedures. The final paper of this session was given by Gerstl on the important subject of *building the methodology to analyze uncertainties due to secondary energy and angular distributions*, data not typically included in many data uncertainty analyses. Sensitivities to changes in the mean spectrum energy (or mean scattering angle) and characterization of the associated uncertainties were developed in this work which *require a minimum of additional computation and permits rough estimates of spectral shape uncertainty* to be considered quantitatively.

Following this paper was a two hour discussion session, which along with the "concluding panel" will be briefly described in Section IV. The day was finally concluded with a much appreciated buffet.

III. Highlights of Session III: Advances and Future Extensions for Sensitivity and Uncertainty Analysis

E. Greenspan presented the lead-off paper in this session which described investigations into *higher order effects in sensitivity theory*. The first example is the common practice of adjusting only infinitely dilute cross sections assuming that associated changes in f-factors are of second order. The paper demonstrated that such *fine structure effects can have a significant impact on group constants*, which becomes more important with decreasing energy. This should potentially be of interest for analysis of Doppler effect in fast reactors and all adjustment approaches for thermal reactors. The second part of this paper described the theory and application of *second order sensitivity analysis* with example being the *non-linear effect of changes in the 297 keV* sodium minima. The paper concludes that second order analysis provides satisfactory accuracy for cross section uncertainty analysis for problems of this type. E. M. Oblow presented the

next paper which dealt with the *formulation of a sensitivity theory for coupled, non-linear equations* such as those which arise in the area of thermal hydraulics. This methodology is potentially important, not only for safety problems, but for the expansion of the entire "sensitivity field" to more general problems and applications. It currently appears feasible to use existing codes, with appropriate modification of source terms and preservation of important intermediate quantities, to compute the required adjoint functions. Yung-An Chao then presented his new approach to the adjustment of group cross sections fitting integral measurements. This approach attempts *to determine mathematically whether negligence errors in the input data sets should be suspected,* and indeed how bad they are. The data is then adjusted in such a manner as to account for suspected negligence errors (decision theory is not used in the adjustment step). The problem then turns to the physicist to find and correct those sources of error after which the input data can be statistically combined. The view offered that "adjustment makes sense only if the data sets are not statistically consistent", a position that was heatedly debated, was in my view an attempt by Chao to make clear that one can always combine statistically consistent data (this process is *not* called adjustment by Chao) but one has to adjust, fix, etc. data sets that are determined to be inconsistent (this "fixing" process is what he calls adjustment). Viewed in this light, the subject appears to me to be much less controversial. The mathematical procedures adopted by Chao are used to discover that a discrepancy really exists; *it still remains with the physicist to fix it! The major issue at present is what to do while waiting*! Another coffee break followed.

M. L. Williams presented the next paper discussing a general perturbation theory for two of the common approximations used in burnup analysis. It was shown that *three adjoint equations* (for the flux shape, the flux normalization, and the nuclide density) *are required to fully develop a perturbation theory which accounts for the coupled variations in the neutron and nuclide fields.* The last paper, presented by F. G. Perey, dealt with the basic definitions and determination of the input quantities we all require in uncertainty analyses. Based on experience, he suggests that the general term "errors" be avoided and the terms "estimated data covariances", "known mistakes" and "unknown mistakes" be used appropriately to avoid confusion in meaning. *According to Perey, covariance information is only valid if no mistakes, known or suspected, have been made in obtaining them.* Finally, logical inferences which can be made on the basis of limited, incomplete or inconsistent information is closely related to decision theory, an area that should receive more attention in the future.

Due to lack of time, to insufficient travel funds, etc., there were several papers which were not formally presented in the meeting but which appear in these proceedings. These include a paper by Chestnutt and McCracken on "The Use of Error Files in Uncertainty Analysis and Data Adjustment" wherein upper limit estimates of calculated quantities are shown to be significantly reduced by the use of ENDF/B data covariance files and recently published few group covariance matrices. Other papers include "The Linearity Assumption in Adjustment Procedures" by Yeivin (a reminder that systems are often non-linear and that this assumption should always be checked), "Influence of Cross Section Structure on Unfolded Neutron Spectra" by Ertek, et

al. and "First and Higher Order Perturbation Techniques and Their Application in Systems Analysis and Data Adjustments" by Gandini.

Two are also included whose content was covered during the presentation at the seminar of closely related papers. These are "Fuel-Motion Unfolding Based on Point Detector Responses" by McDaniel and Wright and "Sensitivity of LWR Fuel Cycle Costs to Uncertainties in Detailed Thermal Cross Section" by Ryskamp et al.

IV. Highlights of the Discussion Session and "Concluding Panel" Session

In preparation for this conference, I prepared a list of questions which along with the papers would serve to stimulate discussion. These questions are listed in Appendix I. It is appropriate to remind the reader at this point that it is always difficult to summarize free-wheeling discussion. Hence, the view presented below is intended only to characterize a subjective interpretation of what actually took place.

Clearly the most discussion centered on the topic of cross section adjustment, its usefulness and role, now and in the future. This question really envelops those relating to the credibility of covariance files, the quantification of methods uncertainties, the level at which adjustment is to take place (point or multigroup) and the need to include higher order effects. The data base required for credible adjustments is now actively being formulated and tested. Probably the least advanced component is the quantification of methods bias and uncertainties; such quantification requires considerable work. "First round" data for integral experiment uncertainties has been reported for many types of systems. ENDF/B-5 is expected to contain a great deal of nuclear data covariance information but since this also will be the first time that a significant body of such data is accumulated, it is natural to expect "known mistakes", "unknown mistakes", and a non-uniform quality of nuclear data covariance evaluations. It should be clear that the adjustment process is intended as an aid to differential and integral evaluators and analysts, not as a substitute for them. The timing is such that the evaluation and data testing processes for the next version of ENDF/B could be significantly improved using data and methodology of this type.

A great variety of methods improvements and expansion of the scope of perturbation theory was presented but much of the effort is still apparently in the demonstration stage and hasn't really affected most designers or evaluators yet. Sensitivity coefficients describing fuel cycle cost, pressure vessel damage, fuel motion detector development, and thermal data evaluation, etc., hold great promise for near term exploitation by the application community but such use is likely to be made in the near future only if an active effort is made to disseminate this technology to the scientific community and to follow up questions which will inevitably develop. Long standing discrepancies such as overprediction of $^{28}c/^{48}f$ and central worths need to be attacked using this new technology. Promising new areas for continued development and testing include uncertainty analysis of secondary distributions, depletion sensitivity, cost/benefit analysis of future experiment requirements, quantification of methods bias and uncertainties, expansion to non-linear coupled systems of equations, and investigation of spectral fine structure effects.

Several other issues were substantive enough to produce considerable discussion. "Modelling uncertainties" reflecting our current inability to represent known measured data within restrictive computerized formats (e.g., detailed angular distributions, resonance structure in the unresolved range, etc.) must be accounted for and ultimately eliminated. We are not yet able (at least in the U.S.) to select group structures in an automated sense using sensitivity theory. Also, since fuel cycle cost (or other "dollar" related parameters) are often time dependent, and sensitive to the state of the economy, more physical parameters such as ore requirements might be used as the figure-of-merit in future experiment planning.

V. Highlights of the Workshop on the FORSS Sensitivity Analysis Code System

After some four years of development, the first version of the driver-controlled FORSS sensitivity and uncertainty analysis code system was packaged, distributed through RSIC, and presented to the user community with oral presentations, documentation, sample problems and questions and answers. The system is available on the IBM system and is being converted to the CDC system on the Berkeley machine. The presentations are described in the Program (Appendix II) and included overview and detailed discussions on each module. Important capabilities exist to generate sensitivity coefficients, project response changes based upon data changes, perform data uncertainty analysis and cross section adjustment. In addition to program utilization, existing libraries of cross sections, covariance matrices, and sensitivity coefficients were summarized.

Appendix I

Stimulating Questions for the Sensitivity Seminar/Workshop

C. R. Weisbin

1. How credible are (and will be) uncertainty files; what is the precision with which currently developed covariance files are defined? Will it be possible to predict uncertainties with enough confidence to reduce design margins?

2. Can methods uncertainties ever really be quantified for a specific problem, for classes of problems, etc.?

3. Is second order theory, with its associated computational complexity, necessary and worthwhile?

4. What is the difference between the conventional designer approach C/E plus bias, and the adjustment approach to uncertainty analysis?

5. Should adjustment proceed if at all, on the point (ENDF/B) level rather than the multigroup level? Are adjustments already implicitly performed?

6. Is it necessary to approach cross section uncertainty analysis using sophisticated tools (e.g. multidimensional, generalized adjoints, etc.) or are simpler computational models (e.g. slowing down theory etc. one dimension etc.) good enough?

7. Can sensitivity theory be employed to meaningfully select multigroup structures in an automated sense?

8. What constraints (e.g. criticality) need to be employed in the determination of sensitivity coefficients for built, and to-be-built reactor systems? Are there similar constraints required in the sensitivity analysis of shield designs?

9. Should cost really be the objective function in integral experiment planning, given its time dependent nature?

10. What is contamination and how does one know when he's got it; can one trust computed generalized adjoints whose magnitudes are very small (e.g. 10^{-7})?

Appendix II

RSIC SEMINAR-WORKSHOP

THEORY AND APPLICATION OF SENSITIVITY AND UNCERTAINTY ANALYSIS

ROYAL SCOTSMAN INN, OAK RIDGE, TENNESSEE

August 22—24, 1978

PROGRAM

OPENING—8:15 a.m.

SESSION I: Sensitivity and Uncertainty Analysis for Fast and Thermal Reactors

Tuesday Morning, August 22, 1978

Chairman, E. Greenspan, Nuclear Research Center, Negev, Israel

8:30 a.m.
The Use of Cross-Section Sensitivities in the Analysis of Fast Reactor Integral Parameters, P. J. Collins and M. J. Lineberry (Argonne National Laboratory, Idaho).

9:00 a.m.
Advances in Fast Reactor Sensitivity and Uncertainty Analysis, J. H. Marable and C. R. Weisbin (Oak Ridge National Laboratory).

9:30 a.m.
Controlled Cross-Section Adjustment by Integral Data, U. Salmi, J. J. Wagschal, A. Yaari, and Y. Yeivin (Hebrew University, Israel).

10:00 a.m. ***Break***

10:15 a.m.
Sensitivity Analysis Applied to the Calculation of Detector Response Kernels, W. H. Scott, Jr. (Science Applications, Inc.), P. J. McDaniel, J. R. Renken, and S. A. Wright (Sandia Laboratories).

10:45 a.m.
Sensitivity of Water Reactor Fuel Cycle Parameters and Costs to Nuclear Data, M. Becker, D. R. Harris, B. Quan, and J. M. Ryskamp (Rensselaer Polytechnic Institute).

11:15 a.m.
Nonlinear Model Fitting of Thermal Neutron Data and its Application in Resonance Parameter Uncertainty Analysis, J. K. Thompson (Battelle Pacific Northwest Laboratories).

11:45 a.m.
Fission Product Decay Power and Uncertainties After Realistic Reactor Operating Histories, T. J. Trapp and B. J. Spinrad (Oregon State University).

12:15 p.m. ***Lunch Break***

SESSION II: Sensitivity and Uncertainty Analysis for Dosimetry and Fusion Reactor Applications

Tuesday Afternoon

Chairman, F. Perey, Oak Ridge National Laboratory

1:15 p.m.
Testing of ENDF/B Cross-Section Data in the Californium-252 Neutron Benchmark Field, Wolf Mannhart (Physikalish-Tech., Braunschweig, Germany).

1:45 p.m.
Use of HEDL Codes in the Sensitivity and Uncertainty Analysis of the Pressure Vessel Embrittlement Damage Function Problem, G. L. Guthrie, F. Schmittroth, R. L. Simons, E. P. Lippincott (Battelle Northwest Laboratory), and C. Oster (Westinghouse Hanford).

2:15 p.m.
Varied Applications of a New Maximum-Likelihood Code with Complete Covariance Capability, Frank Schmittroth (Westinghouse Hanford).

2:45 p.m.
Sensitivity and Uncertainty Analysis Applied to the NBS-ISNF, B. Broadhead and J. H. Marable (Oak Ridge National Laboratory).

3:15 p.m. ***Break***

3:30 p.m.
Sensitivity Analysis Applied to an Integral Test of Niobium Cross Sections, Dan Ingersoll (Oak Ridge National Laboratory) and B. Wehring (University of Illinois, Urbana).

4:00 p.m.
The Application of Uncertainty Analysis in Conceptual Fusion Reactor Design, C. W. Maynard (University of Wisconsin).

4:30 p.m.
Sensitivity and Uncertainty Analysis for Secondary Energy Distributions, S. A. W. Gerstl (Los Alamos Scientific Laboratory).

5:00 p.m.
DISCUSSION SESSION: Discussion of Sessions I and II: Limitations and Future Directions

7:00 p.m.
RECEPTION and BANQUET:

SESSION III: Advances and Future Extensions for Sensitivity and Uncertainty Analysis

Wednesday Morning, August 23, 1978

Chairman, C. Weisbin, Oak Ridge National Laboratory

8:30 a.m.
High Order Effects in Cross Section Analysis Sensitivity, Ehud Greenspan, Y. Karni, and D. Gilai (Nuclear Research Center, Negev).

9:00 a.m.
Sensitivity Theory for Reactor Thermal-Hydraulics Problems, E. M. Oblow (Oak Ridge National Laboratory).

9:30 a.m.
A New Approach to the Adjustment of Group Cross-Sections Fitting Integral Experiments. (Y. Chao (Carnegie-Mellon University).

10:00 a.m. ***Break***

10:15 a.m.
Sensitivity Theory for Depletion Analysis, M. L. Williams, J. R. White, J. H. Marable, and E. M. Oblow (Oak Ridge National Laboratory).

10:45 a.m.
Expectations for ENDF/B-V Uncertainty Files: Coverage, Strengths, and Limitations, F. G. Perey and R. W. Peelle (Oak Ridge National Laboratory).

11:15 a.m.
SESSION IV: Concluding Panel

1:00 p.m. ***Lunch Break***

WORKSHOP on FORSS

Wednesday Afternoon

2:00 p.m.
FORSS: An Overview of FORSS Sensitivity and Uncertainty Methodology, C. R. Weisbin.

2:30 p.m.
Overview of the FORSS System: An Introduction of the Modules and Their Interaction, J. L. Lucius.

3:00 p.m. ***Break***

3:15 p.m.
FORSS Cross-Section Requirements and Preparation: MINX-SPHINX; AMPX; AXMIX, W. E. Ford, III.

4:00 p.m.
Error Files, Covariance Matrices, the COVERX File, J. D. Smith and F. G. Perey.

4:30 p.m.
FORSS-ANISN, E. M. Oblow.

5:00 p.m. ***Adjournment***

WORKSHOP on FORSS

Thursday Morning, August 24, 1978

8:30 a.m.
JULIET: Calculation of Generalized Sources, Responses, Normalization Parameters, and Sensitivity Coefficients, J. L. Lucius.

9:00 a.m.
The SENPRO File and the SENPRO Service Module, J. L. Lucius.

9:25 a.m.
SENTINEL: Analysis of the Effect of Cross-Section Changes, R. Q. Wright.

9:45 a.m.
COVERT and CAVALIER: Uncertainties Due Exclusively to Nuclear Data Uncertainties, J. H. Marable.

10:05 a.m. ***Break***

10:20 a.m.
SENPRO and COVERX Files Available from RSIC, R. W. Roussin.

10:40 a.m.
Improved FIDO, J. H. Marable.

10:55 a.m.
UNCOVER: Uncertainties With Integral Experiments Taken Into Account, J. H. Marable.

11:25 a.m.
COVERS: Data Preparation for UNCOVER, J. L. Lucius.

11:40 a.m.
NTCRKR: The Inverse Problem, J. H. Marable.

12:00 ***Lunch Break***

1:30 p.m.
Discussion of the Use of FORSS and Demonstration With Sample Problems, **All.**

5:00 p.m. ***Adjournment***

THE USE OF CROSS SECTION SENSITIVITIES IN THE ANALYSIS OF FAST REACTOR INTEGRAL PARAMETERS

P.J. Collins and M.J. Lineberry
Argonne National Laboratory
Idaho Falls, Idaho U.S.A.

ABSTRACT

A cross section adjustment system has been developed at Argonne National Laboratory to study the various discrepancies obtained in the prediction of a range of reactor parameters. Cross section sensitivities are calculated with a generalized perturbation theory code. Discrepancies with experiment are minimized by a least squares adjustment of multigroup cross sections. Correlation data between cross sections and between integral measurements is included where available. The sensitivity information permits the correlation of C/E results for a variety of parameters and assemblies having different material compositions and spectra. The integral data at present includes k_{eff} and reaction rate ratios for four ZPR "benchmark" assemblies and seven zero-leakage test zones built in the UK. Reactivity worths for several materials and the use of spectrum measurements are being studied. In addition, sensitivity analysis has been employed for the study of differences in prediction of power distributions and control rod worths between homogeneous and heterogeneous LMFBR designs.

1. INTRODUCTION

The use of cross section sensitivities at ANL-West in the analysis of fast reactor integral experiments at present falls into two main areas. The first involves the results from relatively simple benchmark critical experiments and studies discrepancies in calculated eigenvalues and central core measurements of reaction rate ratios, reactivity worths and spectra. The second area concerns the analysis of assemblies more typical of power reactor designs such as cores with two enrichment zones and heterogeneous designs. The two sets of analyses are, of course, closely related through the common cross-section base in the calculations. However, while the benchmark cores are easily calculated using simple models and corrections for analytical approximations are (hopefully) well known and easily applied, the analysis of the more prototypical cores requires, in many cases, more care in evaluating methods corrections. Work in the latter area is at an early stage.

The benchmark studies use a least squares method of adjusting multigroup cross sections to minimize the residual discrepancies between calculation and experiment for a range of integral parameters. This work has several aims: by relating a wide range of integral parameters through their sensitivities to the cross section base we are able to study for example, (i) the relation between discrepancies for different integral parameters in a given assembly, (ii) the relation between a given parameter measured in different assemblies with different composition and spectra, and (iii) the possible identification of unreliable experimental results. Finally, as an aid in cross section data testing, it is useful to find if reasonable adjustments to the cross sections can account for the discrepancies in calculation.

The sensitivities for power reactor parameters have been studied only recently. Several of the calculated properties of the heterogeneous LMFBR cores built on ZPPR proved more sensitive to nuclear data then did their homogeneous core counterparts. However, these cores also proved to be more sensitive to the analytical approximations and a considerable number of corrections were applied before even preliminary conclusions regarding data sensitivities could be drawn. The present studies have mostly been confined to one-group sensitivities but it is possible that some of the "spatial parameters" may be usefully included in the multigroup data adjustment code.

2. THE LEAST SQUARES ADJUSTMENT CODE

The multigroup data adjustment code follows closely the method described by Mitani and Kuroi[1] except for the addition of correlations between integral parameters. The quantity minimized is

$$Q = \begin{bmatrix} V_1^T & V_2^T \end{bmatrix} \begin{bmatrix} \rho_1^{-1} & 0 \\ 0 & \rho_2^{-1} \end{bmatrix} \begin{bmatrix} V_1 \\ V_2 \end{bmatrix} \tag{1}$$

where V_1 is the vector of weighted residual discrepancies between calculated and experimental values of the integral parameters, V_2 is the vector of weighted residual discrepancies between adjusted and original values of the multigroup cross sections, ρ_1 is the correlation matrix of integral measurements uncertainties, and ρ_2 is the multigroup cross section correlation matrix. The adjusted values of the integral parameters are given by

$$C_i' = C_i + \sum_{j=i}^{n} a_{ij} \left(\sigma_j' - \sigma_j\right) \tag{2}$$

where C_i, a_{ij}, σ_j', and σ_j are the initial calculated value of the integral parameter, the sensitivity coefficient and the adjusted and multigroup cross sections, respectively.

The code is written for a general group structure and includes a group collapse option, by summation of sensitivities over subgroups. The sensitivities are calculated using the generalized perturbation option of VARI-ID, a one-dimensional diffusion code based on the variational method of Stacey[2]. The code is currently being extended to two and three spatial dimensions.

Correlations between cross sections have been obtained through ORNL processing of ENDF/B covariance files. Presently the multigroup covariance library derived by Weisbin for the ZPR-6/7 spectrum is used, and includes correlations for ^{235}U, ^{238}U, ^{239}Pu, ^{240}Pu, and ^{241}Pu cross sections[3].

3. INTEGRAL DATA AND UNCERTAINTIES

The integral data being used (Table 1) comes from four benchmark assemblies, ZPR-3/48, ZPR-6/6A, ZPR-6/7, and ZPR-9/31 and seven zero-leakage test zones of the ZEBRA-8 series[4]. The integral parameters are k or k_∞, reaction rate ratios and central reactivity worths. Typical uncertainties in the data are 2 to 3% for reaction rate ratios (5% in the earlier measurements in ZPR-3/48), 0.3% for the ZEBRA k_∞ values and a few percent for small sample worths. Experimental uncertainties in critical masses are negligible but uncertainties of a few

TABLE 1. Integral Parameters Used in the Adjustment Code

Assemblies	Parameters	Number
1. ZPR "Benchmarks"		
ZPR-3/48 (Pu)	k_{eff}	4
ZPR-6/6A (U)	Reaction rate ratios	10
ZPR-6/7 (Pu)	Central reactivity worths[a]	19
ZPR-9/31 (Pu)	Spectrum ratios[a]	5
2. Zebra 8 Zero-Leakage Zones		
Zebra 8A (Pu)	k_∞	7
8B "	Reaction rate ratios	20
8C "		
8D "	Relative reactivity worths[a]	30
8E "		
8F "	Spectrum ratios[a]	20
8H (U)		

[a]These data are available but only some items are presently included.

tenths of a percent are estimated for approximations in the calculated effects of heterogeneity, streaming, etc. Sensitivity coefficients for the benchmark assemblies were generated by Bohn(5) and McKnight(6).

The correlation matrix being used for reaction rates in the benchmark assemblies is shown in Table 2. These data are currently being refined but it is believed that the correlations shown are realistic and will change only in detail. Correlation data for ZEBRA 8 have been reported by the experimenters and include correlated errors of 1 to 1.5% between reaction rate ratios and a small correlation of tenths of a percent between k_∞ and the reaction rates due to the zero-leakage technique. Sensitivity data for the neutron spectrum in ZPR-9/31 have been generated for proton-recoil data. While the uncertainties in the experimental group fluxes are of the order of 5 to 10%, uncertainties in flux ratios for adjacent groups can be reasonably small so that the derivation of these correlations is vital in order to make effective use of the data(7).

TABLE 2. Correlation Matrix for ZPR Reaction Rate Ratios[a]

ZPR-3/48										
$^{28}c/^{25}f$	1	0.53	0.32	0.00	0.28	0.00	0.01	0.00	0.00	0.00
$^{28}f/^{25}f$		1	0.00	0.19	0.00	0.18	0.00	0.00	0.00	0.00
ZPR-6/6A										
$^{28}c/^{25}f$			1	0.29	0.31	0.00	-0.38	0.08	0.00	-0.18
$^{28}f/^{25}f$				1	0.00	0.48	-0.25	0.00	0.42	-0.30
ZPR-6/7										
$^{28}c/^{49}f$					1	0.24	0.40	0.17	0.11	0.13
$^{28}f/^{49}f$						1	0.33	0.04	0.71	0.23
$^{25}f/^{49}f$							1	0.04	0.22	0.55
ZPR-9/31										
$^{28}c/^{49}f$								1	0.22	0.26
$^{28}f/^{49}f$									1	0.44
$^{25}f/^{49}f$										1

[a]Column labelling is the same as for rows.

Calculations for the integral assemblies were made within the Argonne Reactor Computation (ARC) system. Cross section processing and cell heterogeneity treatment was generally done with the MC^2-II and SDX codes using an intermediate library in 150 to 200 groups which was collapsed to 28 groups for the final reactor calculations. It is very important to ensure that the calculations of integral parameters be as elaborate as necessary to minimize errors due to modelling. This is illustrated in Table 3 for two difficult cases, ZEBRA 8A and 8C. Both of these test zones are very heterogeneous; 8A had a relatively soft spectrum and 8C contained steel as the only diluent. The initial calculations with the SDX code gave relatively low values of k_∞ in 8C and

TABLE 3. Comparison of VIM and SDX Calculations

Parameter	Calculation	ENDF/B-IV C/E	Adjusted C/E
Zebra 8A k_∞	MC^2/SDX	0.998	1.003
	VIM	0.969	0.990
Zebra 8A $^{28}c/^{49}f$	MC^2/SDX	0.997	0.961
	VIM	1.041	0.998
Zebra 8C k_∞	MC^2/SDX	0.957	0.995
	VIM	0.968	0.996
Zebra 8C $^{28}c/^{49}f$	MC^2/SDX	1.029	0.992
	VIM	1.031	0.995
Adjustments to steel capture	MC^2/SDX		-1% to -40%
	VIM		-1% to -20%

of $^{28}c/^{49}f$ ($^{238}U(n,\gamma)/^{239}Pu(n,f)$) in 8A. Because of the heterogeneity, further calculations were made with the VIM Monte Carlo code which gave significant increases in these parameters. The adjustment code was able to fit the k_∞ for 8C since no other parameter in the system was very sensitive to steel data. However large reductions in steel capture of up to 40% were required with the SDX calculations and these were approximately halved when the VIM calculations were used. The code was unable to give a good fit to the $^{28}c/^{49}f$ ratio in 8A when the SDX calculations were used because of the constraints imposed by many other parameters with a high sensitivity to ^{238}U capture. The MC^2/SDX path has been extensively tested against VIM for the ZPR-6/7 unit cell and very good agreement was obtained[8]. Recent developments include the RABANL option for improved resonance shielding capability and an improved treatment of steel resonance data. These have not yet been used for the ZEBRA 8A and 8C cases.

4. RESULTS FROM THE DATA ADJUSTMENT STUDIES

A detailed comparison of the integral parameters calculated with ENDF/B-IV data and the parameters after data adjustment was given in Reference 9. Since those calculations were made, the carbide benchmark assembly, ZPR-9/31 has been added to the system. A summary of the results for k and reaction rates is given in Table 4. In this summary the results from the ZEBRA 8 zones have been averaged and compared with those from the ZPR assemblies. For the adjustments only k and reaction rates were included. The principal adjustments to the multigroup data are also given in Reference 9.

The adjustments result in increases in k values of 1 to 2%. The $^{28}c/^{49}f$ ratios decrease by 3 to 5% but the values for ZPPR cores remain higher than those for ZEBRA. Thus there is an indication of a

TABLE 4. Integral Parameters Before and After Data Adjustment

Parameter	Assembly	ENDF/B-IV C/E	Adjusted C/E
k_{eff} or k_∞	Mean Zebra 8	0.979 ± 0.010[a]	0.997 ± 0.007[a]
	ZPR-3/48	0.991	1.002
	ZPR-6/6A	0.987	1.000
	ZPR-6/7	0.984	1.000
	ZPR-9/31	0.988	1.000
$^{28}c/^{49}f$	Mean Zebra 8	1.030 ± 0.010	0.995 ± 0.004
	ZPR-3/48	0.926	0.899
	ZPR-6/7	1.084	1.037
	ZPR-9/31	1.066	1.000
$^{28}f/^{49}f$	Mean Zebra 8	0.979 ± 0.020	0.985 ± 0.018
	ZPR-3/48	0.990	1.021
	ZPR-6/7	0.968	0.996
	ZPR-9/31	0.960	0.991
$^{25}f/^{49}f$	Mean Zebra 8	0.992 ± 0.021	0.994 ± 0.022
	ZPR-6/7	1.033	1.032
	ZPR-9/31	0.958	0.959
$^{28}c/^{25}f$	Zebra 8H	1.038	1.008
	ZPR-6/6A	1.028	0.989
$^{28}f/^{25}f$	Zebra 8H	1.022	1.015
	ZPR-6/6A	0.962	0.993

[a]RMS deviation from the mean.

systematic difference in the two measurement techniques. Values of C/E for this ratio are generally in the range 1.06 to 1.10 for a large number of measurements in ZPPR(10). The low value for ZPR-3/48 is an exception but the experimental uncertainty is about 5%. The ^{238}U capture cross sections are reduced by 3 to 7% by the adjustment(9) and well within the estimated standard deviations. As noted earlier large reductions in steel capture of up to 20% are required to fit the k_∞ for ZEBRA 8C but this is the only parameter included which has a high sensitivity to steel data. Values of the $^{25}f/^{49}f$ ratio are only marginally improved by the adjustment but these were originally within one to two standard deviations of experiment. The recent measurement for ZPR-9/31 gives the lowest C/E value for this ratio.

Central reactivity worths were not included in the data adjustment calculations described above. These are potentially valuable in data studies because large C/E discrepancies are generally obtained. Table 5 shows the effect of adding central worths to the set of parameters used in Table 4. Because of the uncertainty of about 5% in the β_{eff} values and reactivity scale, the effects of using worths relative to the ^{239}Pu worth as well as absolute worths are included separately. Although the ^{10}B worth was included the boron data itself was not

adjusted. With relative worths in the fitting, values for ^{10}B and sodium are readily fit to the value of 1.16 for ^{239}Pu in ZPR-6/7, with only small changes in the fit for the other parameters. With the absolute worths included, the C/E for ^{239}Pu obtained is 1.08 while those for ^{10}B and sodium are close to unity. The mean C/E for the ^{238}U capture ratio is decreased by 1% in this case. The value of 1.08 is consistent with results from adjusted data sets which have β_{eff} values some 5-7% higher than ENDF/B[11] and which yield C/E values close to unity for central worths. It is also consistent with comparisons of calculated and experimental β_{eff} values in ZPR cores which have C/E in the range 0.90 to 0.95 but with about 5% uncertainty in the measurement. The principal data changes required to fit the central worth results were for ^{239}Pu capture; changes of up to 30% were made and these were large compared with the estimated uncertainties of 10 to 20%. Changes of up to 10% were produced for ^{240}Pu capture and of 1 to 5% in steel and ^{238}U capture but these were small compared with the uncertainties. Changes of up to 10% occured for scattering data in steel, sodium, and oxygen in order to fit the sodium worth, but the other parameters in the fit have only small sensitivity to these data.

TABLE 5. Studies of Central Worth C/E's

		Worths in Fit		
Parameter	ENDF/B-IV	None	Relative Worths	Absolute Worths
ZPR-6/7 Worth(^{239}Pu)	1.19	1.16	1.16	1.08
ZPR-6/7 Worth (^{10}B)	1.12	1.09	1.16	1.03
ZPR-6/7 Worth(Na)	1.43	1.34	1.17	1.02
ZPR-6/7 k_{eff}	0.984	1.000	1.000	0.999
Mean Zebra-8 k_∞	0.979	0.997	0.998	0.997
Mean Zebra-8 $^{28}c/^{49}f$	1.030	0.995	1.001	0.985

5. SENSITIVITY STUDIES FOR POWER REACTOR MOCK-UP CORES

One of the principal results of the recent studies of a heterogeneous core in ZPPR was to show significant errors in calculated radial power distributions. Reaction rates at outer core positions were calculated several percent higher than near the core center. Correspondingly, radial biases in C/E values were found for other spatially dependent parameters. This behavior was not found in previous studies of two-zone homogeneous cores of similar size.

ZPPR-7A was a benchmark in the heterogeneous core series which contained a central blanket zone and three internal blanket rings but no central rod positions. Errors in calculated ^{235}U fission distributions are illustrated in Table 6. The C/E ratio in the outer core region was 4.6% higher than near the center. The relative (statistical)

TABLE 6. Errors in the Radial $^{235}U(n,f)$ Distributions in ZPPR-7A

	First Core Ring	Outer Core Ring	Difference
Reference C/E with xy transport S_4-P_1[a]	1.004	1.050	+4.6%
Correction factors:			
Streaming	1.008	0.997	-1.1%
$(S_8-P_1)/(S_4-P_1)$	1.002	0.997	-0.5%
$(S_8-P_3)/(S_8-P_1)$	0.999	1.002	+0.3%
Mesh size (S_8-P_3)	1.000	1.000	0.0
Buckling Approximation	1.002	0.999	-0.3%
Space-dependent group collapse	1.003	0.999	-0.4%
Total Correction	1.014	0.994	-2.0%
Corrected C/E	1.018	1.044	+2.6%

[a]Scattering was treated with a P_0 expansion, corrected for transport effects.

accuracy of the experiments was about 0.7%. Similar results were found for other non-threshold reactions. More detail of the results is given in Reference 10. A detailed investigation of approximations in the calculation method was made. Corrections were derived for streaming effects, higher order angular quadrature, anisotropic scattering, mesh size, zone and group dependent buckling approximations and spatially-dependent group collapse. The relative corrections totaled 2% and reduced the original discrepancy to 2.6%.

In order to understand the residual discrepancy a number of data sensitivity studies were made. In these the multigroup data was changed by the same percentage over all energies using a cylindrical model of the reactor. The same variations were made for a model of a conventional core, ZPPR-2. As shown in Table 7 a significantly greater sensitivity was found in the heterogeneous core for several cross sections, principally ^{238}U capture and inelastic scattering and transport cross sections. A five percent reduction in ^{238}U capture, consistent with the benchmark studies (Section 4), gave an improvement of 1% in the power shape of 7A relative to ZPPR-2. These same data alterations were found to give similar changes in k_{eff} for both cores, consistent with the critical mass predictions.

A similar sensitivity was found for control rod predictions in the heterogeneous core. In ZPPR-7B, the reference calculations gave a C/E for outer ring control rod worths 11% higher than for the inner ring. Relatively large methods corrections were found which reduced this discrepancy to 5%. As for the power distributions, it was found that this difference was halved by a reduction in ^{238}U capture of 5%[10].

TABLE 7. Effect of Cross Section Alterations on Power Density Shape

Cross Section	Alteration, %	Effect on Power Density Tilt[a], %	
		ZPPR-7A	ZPPR-2
$^{238}U(n,\gamma)$	-5	+1.6	+0.5
$^{238}U(n,f)$	+5	+0.2	+0.1
$^{238}U(n,n')$	-10	+0.8	∿0
$^{239}Pu(n,\gamma)$	+10	-0.1	-0.2
$^{239}Pu(n,f)$	+1	∿0	∿0
$Fe(n,\gamma)$	-10	+0.1	+0.1
Σ_{tr}	-5	+2.2	+0.4
Σ_{tr} (core only)	-5	+0.9	--

[a]Ratio of C/E near the core center to that near the core edge.

Data sensitivity studies for power distributions and control rod worths are being extended for ZPPR-2, ZPPR-9 (a 700 MWe size assembly), and a 1300 MWe core similar to that used in recent international comparisons[11]. It is important to determine how far the comparisons of calculation and experiment in ZPPR-9 will go in predicting the accuracy of calculations in the larger core. Some results for the inner core power shape, with cross section sensitivities in one group, are shown in Table 8. For this parameter, the sensitivities increase significantly on going to the large core size. Sensitivities for ZPPR-9 are about 60 to 70% of those for the 1300 MWe core for the most important cross section items. Using the one group cross section changes, shown in reference 11, together with these sensitivities, we can account for a large part of the power shape differences between ENDF/B-IV and the adjusted data sets.

6. SUMMARY

The data adjustment method is valuable for studying the significance of calculational discrepancies for a wide range of integral parameters. The present results for several benchmark parameters show good consistency between eigenvalue and $^{28}c/^{49}f$ comparisons. A possible bias between UK and US measurements of this ratio is indicated and a few measurements of other reaction rate ratios fall somewhat outside the expected range with the currently evaluated errors. Further study of the central reactivity worth results and inclusion of more independently measured parameters is desirable. Preliminary studies of sensitivities for spatial parameters in power reactor type cores have been useful in showing that calculational discrepancies observed are consistent with uncertainties in the multigroup data. The extension of this work into the data adjustment code may be possible, but special care is required in making corrections in the calculation model.

TABLE 8. Sensitivities for the Inner Core Power Shape

Cross-Section		Sensitivity for Center/Edge Ratio of $^{239}Pu(n,f)$ in the Inner Core		
		ZPPR-2	ZPPR-9	1300 MWe Core
^{238}U	c	-0.084	-0.254	-0.365
	f	+0.010	+0.032	+0.036
	ν	+0.014	+0.054	+0.061
	(n,n´)	-0.001	-0.047	-0.065
^{239}Pu	c	-0.015	-0.021	-0.022
	f	+0.001	+0.001	+0.020
	ν	-0.009	-0.050	-0.050
^{240}Pu	c	-0.002	-0.002	-0.004
	f	-0.003	-0.009	-0.024
^{241}	c	--	--	-0.001
	f	+0.001	+0.003	+0.026
^{242}Pu	c	--	--	-0.001
	f	--	--	-0.003
Fe	c	-0.006	-0.011	-0.020
Cr	c	-0.003	-0.005	-0.010
Ni	c	-0.001	-0.002	-0.007
Radial diffusion coefficient		+0.135	+0.414	+0.721

ACKNOWLEDGMENTS

The data adjustment code was brought to its present state of sophistication by the work of Gary Grasseschi and Kord Smith. The reaction rate covariance data were derived by David Olsen and we are grateful for many helpful discussions with Stu Carpenter. Calculations of the power reactor sensitivity data were made by Trudy Rempel.

REFERENCES

1. H. Mitani and H. Kuroi, "Adjustment of Group Cross Sections by Means of Integral Data", J. Nuclear Science and Technology, 9, p. 383, (1972).

2. W.M. Stacey, Jr., "Variational Estimates of Reactivity Worths and Reaction Rate Ratios in Critical Nuclear Reactors", Nuc. Sci. Eng., 48, p. 444 (1972).

3. J.H. Marable and C.R. Weisbin, "Uncertainties in the Breeding Ratio of a Large LMFBR", Proc. Advances in Reactor Physics, Gatlinburg, CONF-780401, p. 231 (1978).

4. P.J. Collins and M.J. Lineberry, "Calculations for the ZEBRA-8 Series of Zero-Leakage Test Zones Using ENDF/B Version IV Data", Trans. Am. Nuc. Soc., 24, p. 481 (1973).

5. E.M. Bohn, "The Central Worth Discrepancy in Three Fast Reactor Benchmark Critical Assemblies", ANL-75-14, (1975).

6. R.D. McKnight, "Sensitivity Analyses for the Advanced Fuels Program Carbide Benchmark Critical Assembly", Proc. Advances in Reactor Physics, Gatlinburg, CONF-780401, p. 67 (1978).

7. C.G. Campbell and J.L. Rowlands, "The Relationship of Microscopic and Integral Data", Nuclear Data for Reactors, Vol. II, Proc. Helsinki Conf. IAEA, Vienna, p. 391 (1970).

8. D.C. Wade, Internal ANL Reports.

9. P.J. Collins, et al., "Consistency of Fast Reactor Integral Measurements Using Cross Section Adjustment", Trans. Am. Nuc. Soc., 27, p. 884 (1977).

10. P.J. Collins, et al., "A Comparison Between Physics Parameters in Conventional and Heterogeneous LMFBRs Using Results from ZPPR", Proc. Advances in Reactor Physics, Gatlinburg, CONF-780401, p. 207 (1978).

11. L.G. LeSage, et al., "Assessment of Evaluated Nuclear Data Files via Benchmark Calculations - A Preliminary Report on the NEACRP/IAEA International Comparison Calculation of a Large LMFBR", Proc. Advances in Reactor Physics, Gatlinburg, CONF-780401, p. 1, (1978).

ADVANCES IN FAST REACTOR SENSITIVITY AND UNCERTAINTY ANALYSIS*

J. H. Marable and C. R. Weisbin
Oak Ridge National Laboratory
Oak Ridge, Tennessee 37830

ABSTRACT

A review of present methods and existing computer codes at ORNL as well as elsewhere indicates an enormous capability not only to calculate sensitivity coefficients but also to apply them to a variety of purposes. Extensive files of sensitivity coefficients have been created and gathered for fast benchmark experiments and for two-dimensional models of fast power reactors of several designs, including k-reset effects when appropriate. These sensitivity files have been combined with covariance files which quantify the uncertainty in the differential nuclear data to predict the uncertainty in calculated performance parameters. Recent applications of these files have been made to adjust a large amount of both integral and differential data by incorporating benchmark experiment values and their covariances. By means of adjustments of this type, it is hoped that the differential data base as well as the integral data base can be improved.

However, there are still many limitations to our present capabilities. One of these limitations has been our inability to include in a complete and systematic way the effect of methods uncertainties on the determination of adjusted data, which depends in general not only on experimental measurements, but also on estimates of covariances associated with the measurements and the methods. Also, the uncertainty in adjusted data contains contributions from uncertainties in covariance estimates which contributions we have heretofore neglected. A new and comprehensive approach to include effects of methods uncertainties is presented here, and all sources which contribute to the uncertainty of the adjusted data are considered. This new approach is demonstrated using rough estimates for the methods uncertainties as applied to a simplified representation of the ZPR-6/7 fast benchmark. The results indicate that it may be essential to include methods uncertainties if integral experiments are to be used for the creation of adjusted nuclear data libraries. A careful evaluation of methods bias and uncertainties must still be performed.

1.0. INTRODUCTION AND BACKGROUND

The primary goal of sensitivity and uncertainty analysis is to answer reactor physics questions of importance to design.[1] Such analysis is

*Research sponsored by the Division of Reactor Research and Technology, U. S. Department of Energy, under contract W-7405-eng-26 with the Union Carbide Corporation.

especially applicable to (1) measuring the significance of individual contributions to calculated performance parameters, (2) pinpointing sources of significant uncertainty in performance parameters, (3) quantifying the impact of uncertainties in data bases and of changes in data bases, (4) reducing the sources of uncertainty by (a) giving guidance to planning integral and differential experiments, (b) giving guidance to methods development and (c) giving guidance to evaluators for adjusting data bases and methods so as to be most consistent with all the available information, and (5) providing tools for the optimization of design performance parameters of economic importance.

The present ability of the ORNL FORSS sensitivity and uncertainty analysis system to accomplish the foregoing is indicated by the present status information in Table 1. These accomplishments over the past several years are substantial achievements, not only with respect to the quantity and quality of the work but also with regard to the impact of this work. For example, sensitivity and uncertainty analysis has played an important role in evaluating the effect of going from ENDF/B-IV to a proposed preliminary version of ENDF/B-V.[2]

Table 1. Present Status of ORNL Sensitivity and Uncertainty Analysis.

- One-dimensional driver-controlled version of FORSS[3] (released through RSIC) calculates sensitivities[4] of k_{eff}, reaction-rate ratios, and worths.
- Calculate sensitivities of two-dimensional models using DOT-IV[5] and VENTURE.[6]
- Calculate sensitivities of design reactors with k reset to unity using enrichment.[7]
- Compare sensitivities quantitatively by magnitude and by energy-dependent shape over and above that imposed by group structure.[8]
- Calculate effect on performance parameters due to a change in data base (e.g., ENDF/B-IV proposed ENDF/B-V).[2]
- Calculate uncertainties in performance parameters due to uncertainties in nuclear data.[1]
- Adjust large arrays of integral and differential data to make them consistent with prescribed calculational methods.[9]
- Determine the least expensive differential-data measurement program which will meet prescribed uncertainties of calculated performance parameters.[1]
- Calculate sensitivities of elementary time-dependent systems.[10]

An elementary example of the type of information available from a sensitivity analysis is presented in Table 2. These data are from a study[8] in which the sensitivities of three LMFBRs at equilibrium cycle were compared; a plutonium-fueled breeder, a 20% denatured ^{233}U-Th breeder, and a ^{233}U fueled breeder. Table 2 gives energy-integrated relative sensitivities of k to the fission cross sections of various nuclides. From this table we see, for example, that a relative error (or change) in the ^{241}Pu fission cross section is 50% more significant to the multiplication factor of the conventional plutonium-fueled LMFBR than an equal relative error (or change) in the ^{238}U fission cross section. On the other hand, we may note that a relative error (or change) in the ^{239}Pu fission cross section is as significant to the multiplication factor of the 20% denatured-fueled LMFBR as an equal relative error (or change) in the ^{238}U fission cross section is to the multiplication factor of the conventional fast breeder design.

Table 2. Total Sensitivities of k to Fission for the three LMFBR Designs Indicate Similarities for the Principal Fuel Nuclides.

	k(Pu)[a]	k(20%)[b]	k(U-233)[c]
Th-232		.007	.015
U-233		.507	.583
U-235	.009	.002	
U-238	.083	.046	
Pu-239	.453	.084	
Pu-240	.038	.001	
Pu-241	.120	.000	
Pu-242	.008	.000	

[a]A conventional Pu-fueled LMFBR.

[b]A 20% denatured LMFBR.

[c]A ^{233}U-Th LMFBR; data from R. D. McKnight and R. B. Turski of ANL.[11]

An example of the results of applying uncertainty analysis to the multiplication factor and the breeding ratio (fertile capture to fissile absorption ratio at mid-equilibrium cycle) of a conventional 1200 MWe LMFBR[7,9] is shown in Table 3. In this table the nuclear-data-induced uncertainties associated with calculations of these performance parameters are compared with the uncertainties which would result from using a nuclear data set adjusted to fit the six benchmark integral experiments shown. The effect of maintaining k equal to unity (k-reset) by enrichment is also shown. These results in Table 3 show that adjustment of differential nuclear data so as to be consistent with integral experiments can help bring uncertainties of calculated performance parameters within acceptable limits.

Table 3. Standard Deviations of Performance Parameters in Percent.

Assembly	k	B.R.	$\frac{^{28}c}{^{49}f}$	$\frac{^{28}f}{^{49}f}$	$\frac{^{28}f}{^{25}f}$	$\frac{^{49}f}{^{25}f}$
ZPR-6/7	2.27		7.20	3.41		
(adjusted)[a]	0.40		1.54	1.34		
ZPR-3/56B	1.72				3.99	3.77
(adjusted)[a]	0.36				1.49	1.43
LCCEWG model[b]	2.09	6.37(2.74)[c]				
(adjusted)[a]	0.39	1.63(1.41)[c]				

[a]The adjusted standard deviations are based on a 1/2% error in experimental values of k and a 2% error in reaction rate ratios for the ZPR-6/7 and ZPR-3/56B benchmarks.

[b]This LMFBR model is described in Ref. 12.

[c]Quantities in parentheses are k-reset.

In spite of these accomplishments, however, there still remains much to be done in order to achieve the goals set forth. There are still many limitations to present capabilities, and many needed data are incomplete or missing. Some of the important limitations are summarized in Table 4.

Table 4. Present Limitations.

- Sensitivities are for group-averaged self-shielded cross sections, not with respect to ENDF/B data directly.
- Covariance files are incomplete, especially regarding integral experiments, resonance parameters, and secondary distributions.
- Uncertainty of calculational methods has not been included in a complete and systematic way.
- Integral experiments have not been included in the inverse problem and cost functions for data measurements have not been entirely realistic.
- Depletion and fuel management have not been treated in a time-dependent fashion for sensitivity analysis.
- Sensitivity analysis has not been applied to design problems, such as core design optimization, in the framework of a complete overall cost-benefit program.

One of the important limitations mentioned in Table 4 is our present inability to include methods uncertainties in a practical and realistic way. This limitation is made manifest through (1) lack of methods uncertainty data and (2) lack of a technique of using such data in our present uncertainty analyses.

The remainder of this paper addresses this latter problem, namely: How can one include methods uncertainty data (assuming this is available) in uncertainty analyses? In particular, we ask what roles methods uncertainties play with regard to the total uncertainties in calculated performance parameters and also with regard to the adjustment of data? Finally, we demonstrate this new technique of including methods uncertainties by using simplified data for ZPR-6/7.

2.0. A GEOMETRIC APPROACH

It is convenient as well as enlightening to consider the process of data adjustment from a geometrical viewpoint. For this purpose we form a multidimensional space of certain selected relevant physical observables, which are the integral measurements and the evaluated differential measurements (cross sections, etc.). For our present purposes, we do not include design specifications as variables in this space. Figure 1 is a plot of two dimensions of such a space. The horizontal axis represents a nuclear datum which results from an evaluation of differential measurements and the vertical axis corresponds to an integral measurement.

In this space the point x_{exp} represents the results of all the experimental measurements, integral as well as differential. Its coordinates are the best values (using weighted means and other evaluation techniques) of the experiments.

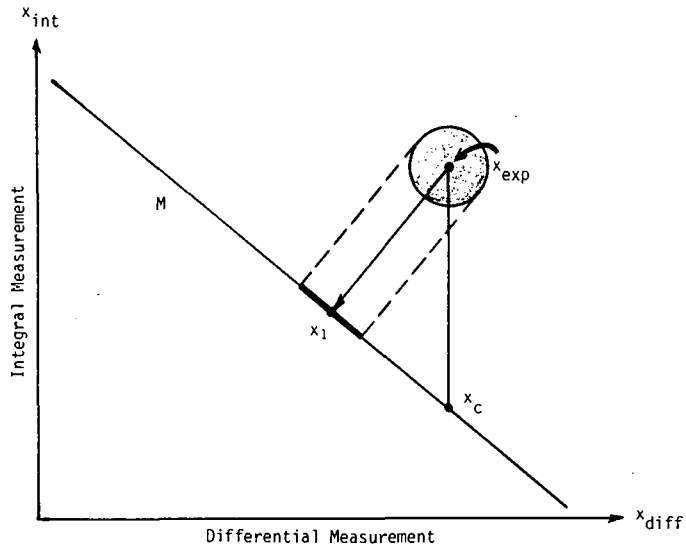

Figure 1. The experimental point x_{exp} is usually compared against the calculational point x_c, but x_1 is the "closest" point consistent with the method M.

2.1. A Natural Metric

Uncertainties are associated with this experimental point x_{exp}. In its most general form these uncertainties are represented by a distribution. It will suit our present purposes to represent the uncertainties by a covariance matrix B. This covariance B is a symmetric matrix and has an inverse. The symmetry property is not an assumption, but is inherent in the definition of covariance (superscript T indicates the transpose)

$$B = \langle \delta x_{exp} \; \delta x_{exp}^{T} \rangle \quad . \tag{1}$$

The geometric significance of the covariance matrix can be seen by plotting the quadratic surface

$$(x - x_{exp})^T B^{-1} (x - x_{exp}) = 1 \quad . \tag{2}$$

This surface forms an ellipsoid about the experimental point x_{exp} as shown in Fig. 1. The directions of the principal axes of the ellipsoid correspond to uncorrelated linear combinations of measurements, and the half-lengths of the principal axes of the ellipsoid are simply the standard deviations for these uncorrelated combinations. These principal axes form a complete orthogonal basis for the space, and the unit of distance along each principal axis can be chosen to be one standard deviation. Thus the matrix B^{-1} forms a natural metric with which distance is measured in terms of standard deviations.

2.2. The Calculational Method

We assume that we have a calculational method by which we can calculate each of the integral quantities from the basic differential nuclear data. Thus we have for each of N_o integral experiments

$$(x_c)_i = f_i(x_d), \qquad i = 1, N_o \quad , \tag{3}$$

where $(x_c)_i$ is the calculated value of the i'th integral experiment, N_o is the number of integral experiments, and the functions f_i represent the calculational method. These functions depend on design data associated with the individual integral experiments as well as the differential experiment variables x_d.

For each i Eq. (3) represents a hypersurface. The intersection of the N_o hypersurfaces forms a hyperspace M which we call the calculational manifold because it geometrically represents the calculational method as applied to the totality of integral experiments. We assume here that this generally curved hyperspace M is linear in the vicinity of the experimental point x_{exp}, as shown by the straight line in the two dimensions of Fig. 1.

2.3. Two Conventional Approaches to Adjustment

As one would expect, it turns out that the experimental point x_{exp} almost never lies in the calculational manifold M. In fact, the calculational manifold M frequently does not even overlap the 1-σ ellipsoid around x_{exp}. A Procrustean response to this situation is made according to whether one is an experimenter or an analyst. It is as if there were two Procrustean beds, the first on which heads are lined up at one end and feet chopped off at the other end, and the second in which feet are lined up and then heads are chopped off at the other end. In either case one achieves his goal: the resulting bodies match the beds. Some observers like to point out that there is a difference between chopping off heads and chopping off feet — still others are more squeamish and try to avoid the whole bloody business. But we will not be squeamish here, and, hopefully, we will not be guilty of the alternative Procrustean response of stretching the body of data beyond the natural limits imposed by associated covariances.

Let us conjecture the viewpoint of an integral experimenter. He assumes the integral components of x_{exp} to be truth. His view of the method is focussed on the single point x_c (Fig. 1), which is determined by the measured differential experiment values and by the values of the integral quantities as calculated from the differential data. This point is especially convenient since only the integral experiment components differ from the experimental point. He therefore moves this point x_c to a point x_c' determined so as to obtain as good agreement as possible with the integral experiment values and at the same time maintain a few constraints. These constraints are that biases or relative biases associated with corresponding similar integral experiments (e.g., k_{eff} in two different assemblies) should be equal, or at least nearly equal. In this light

the experimenter considers his experiments as measurements of the bias (or C/E) and also assigns uncertainties to these biases using standard methods.[13,14] By these techniques he is frequently able to arrive at an adjusted calculated point x_c' whose 1-σ uncertainty overlaps part of the 1-σ of the integral experiment.

The analyst finds it difficult to assign physical meaning to a bias factor which satisfies no known equation of the theory. On the other hand, he is guided by Boltzmann's principal that nothing is more practical than a good theory and by the belief that his calculational method represents "truth." He therefore projects onto M the experimental point x_{exp}, i.e., he finds that point x_1 on the manifold M which is closest to the experimental point x_{exp} using the metric B^{-1}, and then he assigns an uncertainty indicated by the projection of the quadratic B onto the hyperspace M, as shown in Fig. 1.

2.4. Adjusting the Data to the Method

Let us look more closely into the process described in the foregoing paragraph. For this it is convenient to introduce the concept of a projection operator. Let $P_\perp$ denote the operator which projects an arbitrary vector onto the perpendicular to the manifold M and $P_{||}$ projects parallel to the manifold M.

Then we have the following properties

$$P_\perp + P_{||} = 1 \tag{4}$$

$$P_\perp P_{||} = P_{||} P_\perp = 0 \tag{5}$$

$$P^T B^{-1} = B^{-1} P \quad . \tag{6}$$

Equations (4) and (5) are general properties concerning the completeness and orthogonality of the complementary projection operators $P_\perp$ and $P_{||}$, Eq. (6) relates an arbitrary projection operator P and its transpose P^T to the metric B^{-1}. We must yet relate our projection operator to the calculational manifold M. Because this manifold M is linear, it can be represented by a matrix $\mathscr{S}$ such that

$$\mathscr{S}\, x = s_0 \quad , \tag{7a}$$

where s_0 is a vector of suitable biases or displacements along the directions corresponding to the integral experiments and x is any point lying in the calculational manifold. An alternative to Eq. (7a) is

$$\mathscr{S}\,(x-x_0) = 0 \tag{7b}$$

for any two points x and x_0 which lie in the hyperspace M.

The elements of $\mathscr{S}$ are essentially sensitivity coefficients. More explicitly, $\mathscr{S}$ may be expressed by

$$\mathscr{S} = [-I, S] \tag{8}$$

where -I is the negative unit matrix with order equal to the number of integral experiments and S is a matrix whose row vectors give the sensitivities of the calculated integral experiments with respect to the differential data. We are using here absolute and not relative sensitivities.

We also have the condition

$$\mathscr{S} P_{||} = 0 \tag{9}$$

since $P_{||}$ projects onto the hyperspace M.

From the requirements of Eqs. (4), (5), (6), and (9) it follows (as shown in Appendix A) by algebraic processes that

$$P_{\perp} = B\mathscr{S}^{T} G^{-1} \mathscr{S} \tag{10}$$

where

$$G = \mathscr{S} B \mathscr{S}^{T} \quad . \tag{11}$$

It follows that the point x_1 is determined by the following equation

$$x_1 = x_{exp} + P_{\perp} (x_o - x_{exp}) \tag{12}$$

where x_0 is any point lying on the calculational manifold M. Usually it is convenient to choose the point x_0 as the calculated point x_c. Equation (12) is the basis for many adjustment schemes.

2.5. The Uncertainty Associated with the Adjusted Data

The uncertainty in the adjusted point x_1 is usually given by the covariance B_1 found by projecting the experimental covariance B onto the calculational manifold M. Geometrically this is represented by the orthogonal projection of the 1-σ ellipsoid, as shown in Fig. 1. Algebraically this adjusted covariance B_1 is given by

$$\begin{aligned} B_1 &= P_{||} B P_{||}^{T} \\ &= B - P_{\perp} B \end{aligned} \tag{13}$$

where the final expression with reduced matrix multiplication results from applying Eqs. (4) through (6).

Although Eq. (13) is the expression usually given for the uncertainty in the adjusted point x_1, in order to arrive at the total uncertainty in x_1 one should include all contributions. All contributions are found by

considering the following expressions, valid to first order, and which comes from Eq. (12), as shown in Appendix B,

$$\begin{aligned} \delta x_1 = {} & P_{||}\, \delta x_{exp} \\ & + P_{\perp}\, \delta x_o \\ & + P_{||}\, \delta B\, B^{-1}\, P_{\perp}\, (x_o - x_{exp}) \\ & + B\, \Delta\, (x_o - x_{exp}) \quad , \end{aligned} \tag{14}$$

where

$$\Delta = P_{||}^{T}\, \delta \mathscr{S}^{T}\, G^{-1}\, \mathscr{S} + \mathscr{S}^{T}\, G^{-1}\, \delta \mathscr{S}\, P_{||} \quad . \tag{15}$$

The geometric interpretation of Eq. (14) is exactly as one would expect. If one keeps the calculational method (represented geometrically by the manifold M and algebraically by $\mathscr{S}$ and x_o) fixed, then any change such as δx_{exp} or δB can only result in a change δx_1 which lies in the manifold M. On the other hand, a change in x_o (i.e., in the bias) results in a change δx_1 perpendicular to the manifold M. And a change $\delta\mathscr{S}$ in the sensitivities, which determine the slopes of M, causes a change δx_1 which has components perpendicular and parallel to M. However, if the calculational point x_o (assumed to remain fixed while $\mathscr{S}$ varies) is chosen to be x_1, then a change $\delta\mathscr{S}$ results in a δx_1 lying entirely in M.

From this first order expression we find the corresponding covariance

$$\begin{aligned} \langle \delta x_1\, \delta x_1^{T} \rangle = {} & P_{||} \langle \delta x_{exp}\, \delta x_{exp}^{T} \rangle P_{||}^{T} \\ & + P_{\perp} \langle \delta x_o\, \delta x_o^{T} \rangle P_{\perp}^{T} \\ & + P_{||} \langle \delta B\, B^{-1}\, P_{\perp} (x_o - x_{exp})(x_o - x_{exp})^{T}\, P_{\perp}^{T}\, B^{-1}\, \delta B \rangle P_{||}^{T} \\ & + B \langle \Delta (x_o - x_{exp})(x_o - x_{exp})^{T}\, \Delta^{T} \rangle B \\ & + [P_{||} \langle \delta x_{exp}\, \delta x_o^{T} \rangle P_{\perp}^{T}] + \text{transpose} \\ & + [P_{||} \langle \delta B\, B^{-1}\, P_{\perp} (x_o - x_{exp})\, \delta x_{exp}^{T} \rangle P_{||}^{T}] + \text{transpose} \\ & + [P_{||} \langle \delta B\, B^{-1}\, P_{\perp} (x_o - x_{exp})\, \delta x_o^{T} \rangle P_{\perp}^{T}] + \text{transpose} \\ & + [B \langle \Delta (x_o - x_{exp})\, \delta x_{exp}^{T} \rangle P_{||}^{T}] + \text{transpose} \\ & + [B \langle \Delta (x_o - x_{exp})\, \delta x_o^{T} \rangle P_{\perp}^{T}] + \text{transpose} \\ & + [B \langle \Delta (x_o - x_{exp})(x_o - x_{exp})^{T}\, P_{\perp}^{T}\, B^{-1}\, \delta B \rangle P_{||}^{T}] + \text{transpose.} \end{aligned} \tag{16}$$

We note that the usual expression given for the covariance of x_1 [Eq. (13)] is actually only the first term of the sixteen terms on the right of Eq. (16) and thus has many missing contributions. In the

following we shall consider only the first four terms. The remaining six pairs of terms we expect on first guess to be small. They will be examined more closely in a later study.

Assume the method is fixed. They Eq. (12) gives the expression for the so-called "best" point x_1, and the uncertainty in x_1 is given by the covariance of Eq. (16). Since the method is fixed, there should be no contribution from uncertainties in $\mathscr{S}$ and x_0, but there are still the contributions from δB, due to the imprecision with which covariance matrices are currently estimated.

If the relative uncertainties in B are perfectly correlated so that $\delta B = B\ \delta\mu$ where $\delta\mu$ is a scalar, then it is easy to see geometrically as well as algebraically that there is zero contribution from the uncertainty in B. However, if the uncertainties are not perfectly correlated, then there will be a contribution. For example, assume that we can partition B into

$$B = \begin{pmatrix} B_1 & 0 \\ 0 & B_2 \end{pmatrix} \tag{17}$$

where B_1 is the integral experiment covariance and B_2 is the differential experiment covariance, and further assume that

$$\delta B = \begin{pmatrix} B_1\delta\mu_1 & 0 \\ 0 & B_2\delta\mu_2 \end{pmatrix} \tag{18}$$

so that the uncertainties in the integral experiment covariances are strongly correlated and the uncertainties in the differential experiments are strongly correlated. Then we can write

$$\delta B = B\left(\frac{\delta\mu_1 + \delta\mu_2}{2}\right) + \begin{pmatrix} B_1 & 0 \\ 0 & -B_2 \end{pmatrix}\left(\frac{\delta\mu_1 - \delta\mu_2}{2}\right) \quad . \tag{19}$$

The assumption of Eq. (18) might represent a situation in which the covariances of the integral measurements were calculated by one evaluator using his methods and the covariances of the differential measurements were calculated by another evaluator using different methods. Such uncorrelated uncertainties in the integral and differential covariances give rise to an uncertainty in the direction of projecting onto M as shown in Fig. 2.

The third term of Eq. (16) may be expressed

$$\langle(\delta\mu_1-\delta\mu_2)^2\rangle \begin{pmatrix} B_1G^{-1}SB_2S^TG^{-1} \\ B_2S^TG^{-1}B_1G^{-1} \end{pmatrix} (x_c-x_{exp})_I (x_c-x_{exp})_I^T (G^{-1}SB_2S^TG^{-1}B_1 \qquad G^{-1}B_1G^{-1}SB_2) \tag{20}$$

The subscript I refers to the truncated vectors containing only integral components.

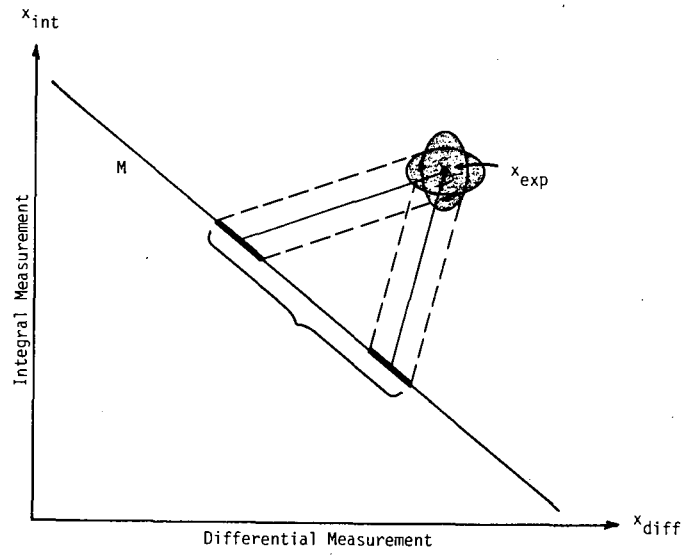

Figure 2. Dispersion in the covariance of the experimental measurements gives rise to a dispersion in the projection of the experimental point onto the method manifold M.

The first factor $\langle(\delta\mu_1-\delta\mu_2)^2\rangle$ vanishes if $\delta\mu_1 = \delta\mu_2 = \delta\mu$ as discussed previously. If $\delta\mu_1$ and $\delta\mu_2$ are uncorrelated, i.e., if the uncertainty of the integral experiment covariance is uncorrelated with the uncertainty in the differential experiment covariance, then

$$\langle\delta\mu_1 \ \delta\mu_2\rangle = 0 \tag{21}$$

and

$$\langle(\delta\mu_1 - \delta\mu_2)^2\rangle = \langle\delta\mu_1{}^2\rangle + \langle\delta\mu_2{}^2\rangle \quad . \tag{22}$$

Now it has been estimated that the uncertainties in the differential and integral experiment covariances used for the adjustment in Ref. 9 are of the order of 50%.[12] Accordingly, each term on the right of Eq. (22) would be 0.25, with a corresponding value of 0.5 for the sum.

We may express our final results for the third term of Eq. (16) by

$$(\langle\delta\mu_1{}^2\rangle + \langle\delta\mu_2{}^2\rangle)\begin{pmatrix} G-B_1 \\ B_2S^T \end{pmatrix} \ \mathcal{X} \ (G-B_1 \ SB_2) \tag{23}$$

where

$$\mathcal{X} = A\,A^T \tag{24}$$

and

$$A = G^{-1}\,B_1\,G^{-1}\,(x_c-x_{exp})_I \quad . \tag{25}$$

These results are valid under the assumptions given in Eqs. (18) and (21), namely that the uncertainties of the integral experiment covariances are correlated with correlation coefficient of unity and that the uncertainties of the differential experiment covariances are similarly correlated, but that the integral and differential measurements are uncorrelated. Note that there is no attempt here to prove the validity of the above assumptions, only to evaluate the consequences of such assumptions in the absence of more concrete information.

2.6. Adjustment of Both Data and Method

It should be noted that Eq. (16) gives the uncertainty in x_1 which is defined by Eq. (12). We have not yet considered the question of whether this x_1 really defines the "best" point consistent with all the data. It can be considered to be the best point only if the calculational method as given by M represents absolute truth. This, however, is generally not the case.

The calculational method will in general have uncertainties associated with it, as shown by the shaded portion surrounding M in Fig. 3. These uncertainties can be represented by uncertainties in the parameters which define the calculational manifold M. Under our previous assumptions this is a linear manifold and is represented by sensitivities $\mathscr{S}$ and by a bias δ [Eq. (7a)], or by a representative point x_0.

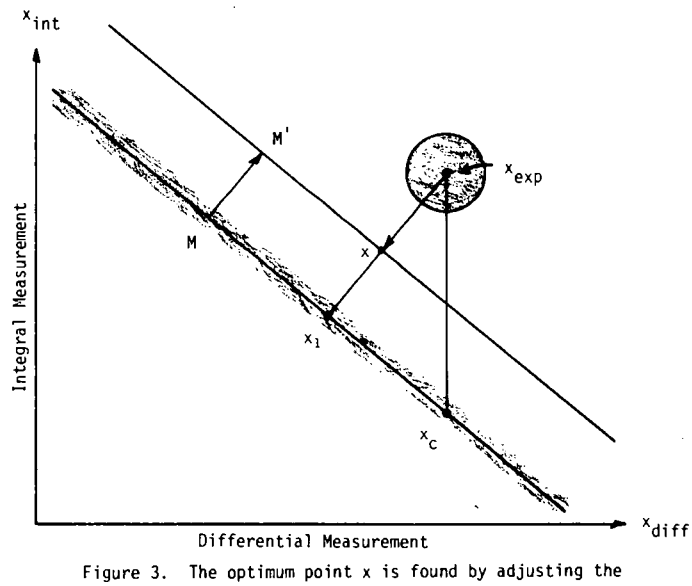

Figure 3. The optimum point x is found by adjusting the method from M to M' and the data point from x_{exp} to x.

When we look for the "best" point x consistent with all the data, we should be free to vary our method parameters as well as our integral and differential values. Thus we should like to find a method M' with parameters x, $\mathscr{S}$, and δ which minimizes the "distance"

$$\begin{pmatrix} x - x_{exp} \\ \underline{\mathscr{S}} - \underline{\mathscr{S}}_o \\ \mathscr{s} - \mathscr{s}_o \end{pmatrix}^T \begin{pmatrix} B_{ext}^{-1} \end{pmatrix} \begin{pmatrix} x - x_{exp} \\ \underline{\mathscr{S}} - \underline{\mathscr{S}}_o \\ \mathscr{s} - \mathscr{s}_o \end{pmatrix} \tag{26}$$

where B_{ext} is an extended covariance matrix including the methods uncertainties in $\mathscr{S}$ and $\mathscr{s}$ as well as the data uncertainties in x. The column vector $\underline{\mathscr{S}}$ consists of the elements of the rectangular matrix $\mathscr{S}$. A similar relation holds between $\underline{\mathscr{S}}_o$ and $\mathscr{S}_o$. This minimization is subject to the constraint

$$\mathscr{S}\, x = \mathscr{s} \quad . \tag{27}$$

We can in like manner relate the initial method parameters $\mathscr{S}_o$ and $\mathscr{s}_o$ to either the calculational point x_c or the initial projected point x_1

$$\mathscr{S}_o\, x_c = \mathscr{s}_o \tag{28}$$

$$\mathscr{S}_o\, x_1 = \mathscr{s}_o \quad . \tag{29}$$

The above problem of minimization subject to a quadratic restraint is a nonlinear optimization problem. In the following we will simplify the problem in order to readily find solutions to be able to illustrate and assess the impact of these results.

We first assume that there are no correlations between experimental and methods uncertainties or between methods sensitivities and methods biases as represented by $\mathscr{S}$ and $\mathscr{s}$. Our extended covariance then has the partitioned form

$$B_{ext} = \begin{pmatrix} B_{exp} & 0 & 0 \\ 0 & B_{sens} & 0 \\ 0 & 0 & B_{bias} \end{pmatrix} . \tag{30}$$

Note that B_{exp} is the integral and differential experiment covariance matrix denoted in previous sections simply by B.

Combining Eqs. (26) through (30) we find that we wish to minimize the following

$$\begin{aligned} &(x-x_{exp})^T B_{exp}^{-1} (x-x_{exp}) + (x-x_1)^T \mathscr{S}_o^T B_{bias}^{-1} \mathscr{S}_o (x-x_1) \\ &+ (\underline{\mathscr{S}} - \underline{\mathscr{S}}_o)^T B_{sens}^{-1} (\underline{\mathscr{S}} - \underline{\mathscr{S}}_o) + x^T (\mathscr{S} - \mathscr{S}_o)^T B_{bias}^{-1} (\mathscr{S} - \mathscr{S}_o)\, x \\ &+ 2\, x^T (\mathscr{S} - \mathscr{S}_o)^T B_{bias}^{-1} \mathscr{S}_o (x-x_1) \quad . \end{aligned} \tag{31}$$

For our illustration we further assume that the sensitivities are so well determined that the last three terms can be neglected. In other words we are assuming

$$\mathscr{S} = \mathscr{S}_o \quad . \tag{32}$$

It follows that the first two terms of Expression (31) are to be minimized by suitable choice of x. In Appendix C it is shown that the solution is given by

$$x = x_{exp} + Q(x_o - x_{exp}) \tag{33}$$

where Q (not generally a projection operator) is given by

$$Q = B_{exp} \mathscr{S}_o^T G^{-1} [1 - (1-\lambda)(1 + B_i B_{bias}^{-1})^{-1}] \mathscr{S}_o \quad . \tag{34}$$

B_i is a matrix defined in Appendix C and λ is a scalar defined by

$$\lambda = \frac{\chi_{ib}^2}{\chi_{exp}^2 + \chi_{ib}^2} \tag{35}$$

where

$$\chi_{exp}^2 = (x_c - x_{exp})_I^T G^{-1} (x_c - x_{exp})_I \tag{36}$$

and

$$\chi_{ib}^2 = (x_c - x_{exp})_I^T [B_{bias} + B_i]^{-1} (x_c - x_{exp})_I \quad . \tag{37}$$

The resulting value for the minimum of the first two terms of Expression (31) is

$$\chi^2 = \lambda \chi_{exp}^2 = \frac{\chi_{ib}^2 \chi_{exp}^2}{\chi_{ib}^2 + \chi_{exp}^2} \quad . \tag{38}$$

Dividing this χ^2 by the number of integral experiments N_o gives the chi-square per degree of freedom, which is often used to evaluate the goodness of fit.

The uncertainty associated with the adjusted point x may be calculated in the same manner as the uncertainty in x_1 was calculated above in Section 2.5. Thus the equivalent of Eq. (16) would be calculated by first calculating the equivalent of Eq. (14). However, the complexities of the formulae are too great to allow their inclusion here, and they will be given in another paper.

3.0. ADJUSTMENT APPLIED TO ZPR-6/7

An example of the application of the above-developed adjustment technique is supplied by a simplified picture of the ZPR-6/7 fast reactor benchmark. In particular, we have chosen two performance parameters, the multiplication factor k and the ^{238}U-capture to ^{239}Pu-fission ratio $^{28}c/^{49}f$. Three pertinent effective one-group nuclear data parameters have been chosen, the fission cross section of ^{239}Pu, the capture cross section of ^{238}U and the effective yield per fission $\bar{\nu}$. The data chosen are based on Reference 1, with C/E's of .99 and 1.08 for k and $^{28}c/^{49}f$, respectively. Estimated uncorrelated experimental standard deviations are given in column 3 of Table 5. Based on Reference 4, sensitivity coefficients for k were chosen to be 0.6, -0.25, and 1.0 for σ_f^{49}, σ_c^{28}, and $\bar{\nu}$, respectively. Corresponding sensitivity coefficients chosen for $^{28}c/^{49}f$ were -1.0, 0.9, and 0.0 respectively. Folding these sensitivities with the standard deviations of column 3 led to the calculated standard deviations shown in column 4.

Table 5. A Simplified Picture of k_{eff} and $^{28}c/^{49}f$ in ZPR-6/7 Appears Consistent.

Variable	E/C-1 (%)	Exp. St.[a] Dev.(%)	Cal. St. Dev. from Data(%)	Assumed[b] Methods St. Dev(%)
k	1.01	0.2	2.4	1.0
$^{28}c/^{49}f$	-7.41	2.0	6.5	1.0
σ_f^{49}	0	3.0	-	-
σ_c^{28}	0	6.0	-	-
$\bar{\nu}$	0	0.3	-	-

[a]These are assumed to be uncorrelated.

[b]These are assumed to be correlated with a correlation coefficient of -0.5.

If one observes the standard deviations of the experiment and the standard deviations of the calculations, then the experiment-calculation difference appears to be marginally consistent. Because of the importance of these performance parameters and because these comparisons are sometimes viewed as being discrepant in view of their magnitudes, it is instructive to consider the effect of adjustments with and without the inclusion of methods uncertainties. Three adjustments are shown in Table 6. The first adjustment results from the biases which a designer might apply to the calculated results in order to reach agreement with the measured integral experiments. The second adjustment assumes the method is fixed and corresponds to the point x_1 in Fig. 3. The third adjustment shown in Table 6 corresponds to the point x in Fig. 3 and results from assuming an uncertainty in the method. This methods uncertainty is characterized by estimated standard deviations of 1% in both k and the ratio $^{28}c/^{49}f$ as shown in Table 5, and by an estimated correlation coefficient of -0.5. The chi-square per degree of freedom was 1.37 for adjustment without methods uncertainties and became 1.10 for adjustment with methods uncertainties included.

Table 6. Effects of Methods Uncertainties in this Application to ZPR-6/7 Can be Significant for Adjustment of Differential Data.

Variable	Adjustments to Calculated Values in Percent[a]		
	Design Bias Only	Adjustment Without Methods Uncertainties[b]	Adjustment With Methods Uncertainties
k	1.01(0.20)	1.05(0.20)(0.20)	1.04
$^{28}c/^{49}f$	-7.4 (2.0)	-5.36(1.5) (1.7)	-5.85
σ_f^{49}	0 (3.0)	-1.06(1.5) (1.6)	-0.12
c^{28}	0 (6.0)	-7.14(3.1) (3.5)	-6.57
$\bar{\nu}$	0 (0.3)	-0.09(0.3) (0.3)	-0.06

[a]Values in parentheses are standard deviations of the adjusted values.

[b]Second set of standard deviations include a 50% relative standard deviation in the covariance matrix.

The results as shown in Table 6 are interpreted as follows. Considered independently, both integral experiment discrepancies tend to decrease σ_c and to increase σ_f. However, the ratio of the c/f discrepancy to the k discrepancy is 8 whereas the ratio of sensitivities is 4 and 2 for σ_c^{28} and σ_f^{49}, respectively. Hence correcting c/f greatly overcorrects k. A change in the yield $\bar{\nu}$ within its estimated uncertainties is not able to take care of this. Thus the adjustment without inclusion of methods uncertainties decreases c/f by decreasing σ_c^{28} and then compensates for k by also decreasing σ_f^{49}. When methods uncertainties are included, the overcorrected k is alleviated by the methods uncertainties, and the requirement that σ_f^{49} compensate for it is greatly reduced, although the adjustment on σ_f^{49} is still very slightly negative. Thus, inclusion of methods uncertainties, even with a marginally consistent set of data, can lead to adjustments significantly different from those obtained neglecting methods uncertainties.

4.0. CONCLUSIONS

The present capability of the ORNL FORSS sensitivity and uncertainty analysis has been reviewed in light of its primary goal of answering reactor physics questions of importance to design. This capability includes the creation and handling of large data files including multidimensional sensitivities as well as covariance matrices. Problem solving includes the inverse problem and data adjustment of large arrays, and effects of k-reset by enrichment can be taken into account.

However, there are still many limitations. The treatment of time-dependent responses and systems is limited, covariance files need to be expanded, and our uncertainty analyses including adjustment procedures need to include the effects of methods uncertainties. In general, our framework and that of the designer must be brought into closer interaction.

In this paper we have eliminated one of our present limitations by addressing the problem of including quantified methods uncertainties in

our adjustment procedure. It is hoped that the inclusion of methods uncertainties will lend more credibility to the results of the adjustment procedures. This adjustment procedure is based on a minimization principle, the expression to be minimized being given by Eq. (26). The resulting formula for the adjustment which includes the effects of methods uncertainties is given by Eq. (33) as derived in Appendix C. We have also indicated how to calculate uncertainties associated with adjusted data, and we have, in particular, given explicit formulae [Eq. (16)] for such uncertainties when adjustments do not include the effects of methods uncertainties. Equation (16) contains many terms which previously were neglected.

These new techniques have been applied to a simplified representation of the fast reactor benchmark ZPR-6/7 using rough estimates for methods uncertainties. The inclusion of methods uncertainties in the adjustment procedure leads to moderate corrections to adjustment changes of calculated integral values. However, the inclusion of methods uncertainties leads to a reduction in the adjustment change of σ_f^{49}, a differential parameter, by a factor of ten (from a decrease of 1.1% without methods uncertainties to a decrease of 0.1% with). This indicates that the inclusion of methods uncertainties may be essential for the general application of integral experiments to the determination of nuclear data. We have yet to perform a careful evaluation of methods uncertainties and of methods biases.

ACKNOWLEDGEMENTS

The authors wish to thank G. de Saussure and R. W. Peelle for their concern with the need for addressing methods uncertainties, F. G. Perey for stimulating discussions, F. C. Maienschein and P. B. Hemmig for their interest and support, J. D. Drischler for technical assistance, and Jan Gentry for typing and preparing the manuscript in its final form.

REFERENCES

1. C. R. Weisbin, E. M. Oblow, J. H. Marable, R. W. Peelle, and J. L. Lucius, "Application of Sensitivity and Uncertainty Methodology to Fast Reactor Integral Experiment Analysis," Nucl. Sci. Eng. 66, 307 (1978).

2. C. R. Weisbin, J. H. Marable, J. Hardy, Jr., and R. D. McKnight, "Projections of ENDF/B Version V Performance for Fast and Thermal Reactors Using Sensitivity Coefficients," Proceedings of American Nuclear Society Topical Meeting, "Advances in Reactor Physics," Gatlinburg, Tennessee, edited by E. G. Silver (April 10-12, 1978).

3. J. L. Lucius, C. R. Weisbin, J. H. Marable, J. D. Drischler, R. Q. Wright, and J. E. White, "A User's Manual for the FORSS Sensitivity and Uncertainty Analysis Code System," Oak Ridge National Laboratory Report ORNL-5316 (to be published).

4. J. H. Marable, J. L. Lucius, and C. R. Weisbin, "Compilation of Sensitivity Profiles for Several CSEWG Fast Reactor Benchmarks," ORNL-5262 (ENDF-234) (March 1977).

5. R. L. Childs, J. H. Marable, and C. R. Weisbin, "Two-Dimensional Reactor Sensitivity Analysis Using Discrete-Ordinates Transport Theory," Trans. Am. Nucl. Soc. 27, 909 (1977).

6. D. R. Vondy and T. B. Fowler, "The Code PERTUBAT for Processing Neutron Diffusion Theory Neutronics Results for Perturbation Analyses," Oak Ridge National Laboratory Report ORNL-5376 (March 1978).

7. J. H. Marable and C. R. Weisbin, "Performance Parameter Uncertainties for a Large LMFBR," Trans. Am. Nucl. Soc. 26, 542 (1977).

8. J. H. Marable and C. R. Weisbin, "Sensitivity Analyses of Fast Reactor Systems Including Thorium and Uranium," Trans. Am. Nucl. Soc. 28, 718 (1978).

9. J. H. Marable and C. R. Weisbin, "Uncertainties in the Breeding Ratio of a Large LMFBR," Proceedings of American Nuclear Society Topical Meeting, "Advances in Reactor Physics," Gatlinburg, Tennessee, edited by E. G. Silver (April 10-12, 1978).

10. M. L. Williams and C. R. Weisbin, "Sensitivity and Uncertainty Analysis for Functionals of the Time-Dependent Nuclide Density Field," ORNL-5393 (ENDF-263) (April 1978).

11. R. D. McKnight and R. B. Turski, "Nuclear Data Sensitivity Coefficients for a ^{233}U-^{232}Th Fueled LMFBR," Argonne National Laboratory Report ZPR-TM-298 (November 1977).

12. E. Kujawski and H. S. Bailey, "Benchmark Analysis of Liquid Metal Fast Breeder Reactor Nuclear Design Methods," Nucl. Sci. Eng. 64, 90 (September 1977).

13. R. A. Doncals, J. A. Lake, and N. C. Paik, "Use of Integral Data in the Development of Design Methods for Fast Reactors," Proceedings of American Nuclear Society Topical Meeting, "Advances in Reactor Physics," Gatlinburg, Tennessee, edited by E. G. Silver (April 10-12, 1978).

14. P. A. Ombrellaro, R. A. Bennett, J. W. Daughtry, R. D. Dobbin, R. A. Harris, J. V. Nelson, R. E. Peterson, and R. B. Rathrock," Biases for Current FFTF Calculational Methods," *ibid.*

15. R. W. Peelle, private communication, August 1978.

APPENDIX A

We want to find the form of the projection operator $P_\perp$ which projects perpendicular to the calculational manifold M. We assume the conditions expressed by Eqs. (4), (5), (6), and (9). First we eliminate $P_{||}$ from these equations to find the following conditions

$$P_\perp P_\perp = P_\perp \tag{A1}$$

$$P_\perp B = B P_\perp^T \tag{A2}$$

and

$$\mathscr{S} P_\perp = \mathscr{S} \quad , \tag{A3}$$

where

$$\mathscr{S} x = 0 \tag{A4}$$

if and only if the vector x lies in the calculational manifold M.

Define the square matrix

$$G = \mathscr{S} B \mathscr{S}^T \quad . \tag{A5}$$

Since B is symmetric and positive definite, and the rows of $\mathscr{S}$ are linearly independent, the matrix G is symmetric and positive definite and hence has an inverse.

From (A3) and (A5)

$$\begin{aligned} \mathscr{S} P_\perp &= \mathscr{S} \\ &= G\, G^{-1} \mathscr{S} \\ &= \mathscr{S} B\, \mathscr{S}^T G^{-1} \mathscr{S} \quad . \end{aligned} \tag{A6}$$

This last result may be written

$$\mathscr{S}(P_\perp - B\, \mathscr{S}^T G^{-1} \mathscr{S}) = 0 \quad . \tag{A7}$$

Hence because of (A4) the operator $P_\perp - B\, \mathscr{S}^T G^{-1} \mathscr{S}$ brings any vector into the calculational manifold. But from (A1), (A2), and (A3)

$$P_\perp - B\, \mathscr{S}^T G^{-1} \mathscr{S} = P_\perp (P_\perp - B\, \mathscr{S}^T G^{-1} \mathscr{S}) \tag{A8}$$

and hence the operator $P_\perp - B\, \mathscr{S}^T G^{-1} \mathscr{S}$ brings every vector into the subspace orthogonal to the calculational manifold. But only the null vector lies in both the calculational manifold and the subspace orthogonal to it. Hence

$$(P_{\perp} - B\,\mathscr{S}^{T}\,G^{-1}\,\mathscr{S})\,x = 0 \tag{A9}$$

for each and every x and therefore

$$P_{\perp} - B\,\mathscr{S}^{T}\,G^{-1}\,\mathscr{S} = 0 \tag{A10}$$

or

$$P_{\perp} = B\,\mathscr{S}^{T}\,G^{-1}\mathscr{S} \quad . \tag{A11}$$

APPENDIX B

We calculate the increment dx_1 by considering all the increments in the quantities determing x_1 as given in Eq. (12). Thus, by making the appropriate substitutions into the terms of Eq. (12) we have

$$\begin{aligned} x_1 + \delta x_1 &= x_{exp} + \delta x_{exp} \\ &+ (B+\delta B)(\mathscr{S}+\delta\mathscr{S})^{T}(G+\delta G)^{-1}(\mathscr{S}+\delta\mathscr{S})(x_o+\delta x_o-x_{exp}-\delta x_{exp}) \ . \end{aligned} \tag{B1}$$

We observe that to first order the following is valid

$$\begin{aligned} (G + \delta G)^{-1} &= G^{-1} - G^{-1}\,\delta\,G\,G^{-1} \\ &= G^{-1} - G^{-1}(\delta\mathscr{S}B\mathscr{S}^{T} + \mathscr{S}B\delta\mathscr{S}^{T} + \mathscr{S}\delta B\mathscr{S}^{T})G^{-1} \quad . \end{aligned} \tag{B2}$$

After subtracting off the zero order terms in Eq. (B1) — these are the same as in Eq. (12) — the remaining first order terms give

$$\begin{aligned} \delta x_1 = {} & (1 - B\mathscr{S}^{T}G^{-1}\mathscr{S})\delta x_{exp} \\ & + B\mathscr{S}^{T}G^{-1}\,\mathscr{S}\,\delta x_o \\ & + (1 - B\mathscr{S}^{T}G^{T}\mathscr{S})\delta B\mathscr{S}^{T}G^{-1}\,\mathscr{S}(x_o - x_{exp}) \\ & + (B - B\mathscr{S}^{T}G^{-1}\mathscr{S}B)\delta\mathscr{S}^{T}G^{-1}\mathscr{S}(x_o - x_{exp}) \\ & + B\mathscr{S}^{T}G^{-1}\delta\mathscr{S}(1 - B\mathscr{S}^{T}G^{-1}\mathscr{S})(x_o - x_{exp}) \quad . \end{aligned} \tag{B3}$$

The application of Eqs. (4) and (10) along with the well known formula for taking the transpose of a product then allows Eq. (B3) to be written

$$\begin{aligned} \delta\,x_1 = {} & P_{||}\,\delta\,x_{exp} \\ & + P_{\perp}\,\delta\,x_o \\ & + P_{||}\,\delta\,B\,B^{-1}\,P_{\perp}(x_o - x_{exp}) \\ & + B[P_{||}{}^{T}\,\delta\,\mathscr{S}^{T}\,G^{-1}\,\mathscr{S} + \mathscr{S}^{T}\,G^{-1}\delta\,\mathscr{S}\,P_{||}](x_o - x_{exp}). \end{aligned} \tag{B4}$$

APPENDIX C

We want to minimize the expression

$$(x-x_{exp})^T B_{exp}^{-1}(x-x_{exp}) + (x-x_1)^T \mathscr{S}_o^T B_{bias}^{-1} \mathscr{S}_o(x-x_1) \quad . \tag{C1}$$

We first break the displacement $x-x_{exp}$ into two perpendicular components so that

$$x = x_{exp} + \Delta_{||} + \Delta_{\perp} \tag{C2}$$

where $\Delta_{||}$ lies in the calculational manifold M_o, i.e.,

$$\mathscr{S}_o \Delta_{||} = 0 \quad . \tag{C3}$$

The requirement that $\Delta_{\perp}$ be perpendicular to $\Delta_{||}$ is expressed by

$$\Delta_{||}^T B_{exp}^{-1} \Delta_{\perp} = 0 \quad . \tag{C4}$$

We further break $\Delta_{\perp}$ into two perpendicular components

$$\Delta_{\perp} = \lambda(x_1-x_{exp}) + \xi \tag{C5}$$

where λ is a scalar to be determined and ξ is a vector perpendicular to the displacement x_1-x_{exp} as well as to the calculational manifold, i.e.,

$$\xi^T B_{exp}^{-1}(x_1-x_{exp}) = 0 \quad . \tag{C6}$$

In terms of these components the Expression (C1) to be minimized becomes the following

$$\begin{aligned} &\Delta_{||}^T B_{exp}^{-1} \Delta_{||} + \lambda^2\chi_{exp}^2 + (1-\lambda)^2 \chi_{bias}^2 \\ &+ \xi^T B_{exp}^{-1} \xi + \xi \mathscr{S}_o^T B_{bias}^{-1} \mathscr{S}_o \xi \\ &+ 2(1-\lambda) (x_{exp}-x_1)^T \mathscr{S}_o^T B_{bias}^{-1} \mathscr{S}_o \xi \end{aligned} \tag{C7}$$

where χ_{exp}^2 and χ_{bias}^2 are defined

$$\begin{aligned}\chi^2_{exp} &= (x_1-x_{exp})^T B^{-1}_{exp}(x_1-x_{exp}) \\ &= (x_o-x_{exp})^T \mathscr{S}_o^T G^{-1} \mathscr{S}_o(x_o-x_{exp}) \\ &= (x_c-x_{exp})_I^T G^{-1}(x_c-x_{exp})_I \quad . \end{aligned} \tag{C8}$$

$$\begin{aligned}\chi^2_{bias} &= (x_1-x_{exp})^T \mathscr{S}_o^T B^{-1}_{bias} \mathscr{S}_o(x_1-x_{exp}) \\ &= (x_o-x_{exp})^T \mathscr{S}_o^T B^{-1}_{bias} \mathscr{S}_o(x_o-x_{exp}) \\ &= (x_c-x_{exp})_I^T B^{-1}_{bias}(x_c-x_{exp}) \quad . \end{aligned} \tag{C9}$$

In order to find the component vectors $\Delta_{||}$ and ξ and the scalar λ which minimize Expression (C7) it is convenient to use the projection operators such that

$$\Delta_{||} = P_{||}\, y \tag{C10}$$

$$\xi = P_\xi\, z \quad . \tag{C11}$$

Here $P_{||}$ projects onto the calculational manifold M_o and P_ξ projects perpendicular to M_o and to the displacement x_1-x_{exp}. $P_{||}$ is simply $1-P_\perp$ where $P_\perp$ is defined by Eq. (10). We will see how to construct P_ξ.

The vectors y and z introduced above have complete freedom to range throughout the entire space. Hence we can take derivatives with respect to their components without restrictions or constraints. Taking derivatives of (C7) with respect to components of y gives

$$\Delta_{||} = 0 \quad . \tag{C12}$$

This result is fairly obvious by inspection since B^{-1}_{exp} is a positive quadratic form. Taking derivatives of Expression (C7) with respect to components of z gives

$$B^{-1}_{exp}\,\xi + P_\xi^T \mathscr{S}_o^T B^{-1}_{bias} \mathscr{S}_o\,\xi + (1-\lambda)P_\xi^T \mathscr{S}_o^T B^{-1}_{bias} \mathscr{S}_o(x_{exp}-x_1) = 0 \quad . \tag{C13}$$

We can readily solve for $\mathscr{S}_o\xi$ by pre-multiplying each term of Eq. (C13) by $\mathscr{S}_o B_{exp}$. The result is

$$\mathscr{S}_0\xi = (1-\lambda)\,(1+H)^{-1}\,H\,\mathscr{S}_0(x_1-x_{exp}) \tag{C14}$$

where the operator H is defined by

$$H = \mathscr{S}_0\,B_{exp}P_\xi^{\,T}\,\mathscr{S}_0^{\,T}\,B_{bias}^{-1} \quad . \tag{C15}$$

Substituting the result (C12) back into the second term of Eq. (C11) gives

$$\xi = (1-\lambda)\,B_{exp}\,P_\xi^{\,T}\,\mathscr{S}_0^{\,T}\,B_{bias}^{-1}(1+H)^{-1}\,\mathscr{S}_0(x_1-x_{exp}) \quad . \tag{C16}$$

In order to actually carry through these operations an explicit expression for the projection operator P_ξ is required. In order to find P_ξ we first construct a matrix T with N_0 (the number of integral experiments) columns and N_0-1 rows and of rank N_0-1 such that

$$T\,\mathscr{S}_0(x_1-x_{exp}) = 0 \quad . \tag{C17}$$

Actually, we know that in Eq. (C17) x_1 can be replaced by x_c or any other point x_0 which lies in the calculational manifold M_0. We know also that such a matrix T can always be constructed and in many different ways; i.e., it is not unique. The particular choice of T is here irrelevant. With $\mathscr{S}$ defined by Eq. (8), a convenient choice for T is the following

$$(T)_{ij} = \begin{cases} (x_c)_{i+1} & j=i \\ -(x_c)_i & j=i+1 \\ 0 & \text{otherwise} \quad \text{for } i=1,\ N_0-1;\ j=1,\ N_0. \end{cases} \tag{C18}$$

The operator $T\mathscr{S}_0$ applied to any vector lying in the subspace formed by the calculational manifold and the added dimension (x_1-x_{exp}) gives a vanishing result. Hence we can form the projection operator P_ξ from $T\mathscr{S}_0$ just as we formed $P_\perp$ from $\mathscr{S}_0$ (Appendix A). The result is

$$P_\xi = B_{exp}\,\mathscr{S}_0^{\,T}\,T^T\,G'^{-1}\,T\,\mathscr{S}_0 \tag{C19}$$

where the $(N_0-1)x(N_0-1)$ matrix G' is defined by

$$G' = T\,G\,T^T \quad . \tag{C20}$$

The operator H may now be written explicitly

$$H = B_i\,B_{bias}^{-1} \tag{C21}$$

where

$$B_i = G\,T^T\,G'^{-1}\,T\,G \tag{C22}$$

and the expression for ξ reduces to

$$\xi = (1-\lambda)\,B_{exp}\,\mathscr{S}_0^{\,T}\,G^{-1}[1-(1+H)^{-1}]\,\mathscr{S}_0(x_0-x_{exp}) \quad . \tag{C23}$$

Note G' appears only once through its inverse in the operator H.

We have yet to find the scalar λ. Setting the derivative of Expression (C7) with respect to λ equal to zero gives

$$\lambda\ \chi^2_{exp} - (1-\lambda)\ \chi^2_{ib} = 0 \tag{C24}$$

where χ^2_{ib} is found by substituting (C23) back into (C7).

$$\chi^2_{ib} = (x_1-x_{exp})^T\ \mathscr{S}_o^T\ [B_{bias} + B_i]^{-1}\ \mathscr{S}_o(x_1-x_{exp}) \quad . \tag{C25}$$

The value of λ for a minimum is

$$\lambda = \frac{\chi^2_{ib}}{\chi^2_{exp} + \chi^2_{ib}}$$

and the minimum value of the Expression (C1)

$$\chi^2 = \lambda\ \chi^2_{exp} = \frac{\chi^2_{ib}\ \chi^2_{exp}}{\chi^2_{ib} + \chi^2_{exp}} \quad . \tag{C26}$$

The final expression for the point x which minimizes (C1) summarizes many of the above results

$$x = x_{exp} + Q(x_o-x_{exp}) \tag{C27}$$

where Q is given by

$$Q = B_{exp}\ \mathscr{S}_o^T\ G^{-1}\ [1 - (1-\lambda)(1+H)^{-1}]\mathscr{S}_o \quad . \tag{C28}$$

CONTROLLED CROSS-SECTION ADJUSTMENT BY INTEGRAL DATA

U. Salmi, J.J. Wagschal, Atara Ya'ari and Y. Yeivin
Racah Institute of Physics, The Hebrew University
Jerusalem, Israel

ABSTRACT

The ENDF/B-IV cross sections of U-235, U-238, Pu-239 and Pu-240 are adjusted by the "benchmark" measured reactivities, leakage spectra, and central fission ratios and various activations of GODIVA and JEZEBEL. It is shown that by careful calculation of these integral quantities, rejection of a few inconsistent data, optimization of the relative weight of the differential data with respect to the integral data, and relaxation of the constraints on the inelastic scattering cross sections, an adjusted cross-section set, within the assumed uncertainties of the given set, is obtained, which nicely reproduces most of the experimental data. The cross-section adjustments are such that the linearity assumption, on which the adjustment procedure is based, still holds.

INTRODUCTION

Ever since the least-squares adjustment of cross sections by integral data was first proposed, in 1964, it has been unsparingly criticized. Criticism has somewhat subsided as more and more researchers involved in neutronic calculations, including former critics, have joined the ranks of the avowed practitioners.

A main argument against adjustment procedures is their specious "black box" character. An adjustment code is fed a given cross-section library (including its uncertainty-correlation data), and a set of experimental integral data (with their corresponding sensitivity profiles) by which the library is to be adjusted. The uncritical application of a typical code may indeed result in rather arbitrary or even unreasonably "wild" adjustments, spread over seemingly irrelevant cross sections. Furthermore, some of the recalculated integral quantities may still lie outside the error margins of their measured values. Whenever this happens, the fault most probably lies in poor and/or inconsistent input data. As in any other analysis, problematic input data will always result in questionable output.

The approach of "controlled" adjustment that we propose refers

to free parameters which are implicit in any adjustment procedure, and to possible rejection of dubious integral data. The validity of the linearity assumption, on which most adjustment algorithms are based, should also be verified in any particular application.

The determination of the values of the free parameters, data selection and vindication of linearity necessitate careful consideration based on feedback from repeated applications of the adjustment code.

Most problematic of all input data are commonly the uncertainties in the given cross-sections. Information on these uncertainties is vague, ambiguous and admittedly subjective. It is given in the form of relative errors β of particular cross sections over wide energy ranges. But the uncertainty in any group cross section, for instance, should be proportional to the inverse square root of the group width ΔE. Thus, apparently, $\Delta\sigma = \beta\sigma(\Delta E_0/\Delta E)^{\frac{1}{2}}$, where ΔE_0 is a dimensional constant to which there is no way to attribute a physical meaning, nor therefore to assign a numerical value. It thus remains a free parameter, the measure of the statistical importance of the set of integral data relative to that of the given cross-section library.

To determine ΔE_0, one should examine the progressive modification of the given cross-section library, and the improving reproduction of the set of integral data, as ΔE_0 increases. An optimal value is one for which all recalculated values of the integral quantities already fall within the error margins of their respective measured values, and the corresponding cross-section adjustments still remain within their assigned uncertainties.

If no such optimal value of ΔE_0 can be found, then obviously either the integral data set is inconsistent with the given library, or these data are inconsistent with each other.

Faulty data can then be detected by progressively adjusting the given library by one, two, three, etc. integral data. Whenever a bad datum is added to the partial set by which the cross sections are adjusted, the modifications will show an unusual increase, and the integral data reproduction will deteriorate.

These ideas, as well as a test for the validity of the linerarity assumption, are applied to GODIVA and JEZEBEL, assemblies for which quite a few integral measurements (reactivity, spectral indices, leakage) are available.

PROCEDURE

Experimental Input Data

The basic integral data were all taken from the CSEWG Benchmark Specifications.[1] Their values actually used in our calculations are given here in tabular form. Table 1 specifies the radii, densities and atomic compositions of the two bare homogeneous spherical critical assemblies, and Table 2 lists 18 available experimental integral data relating to GODIVA and 16 relating to JEZEBEL. The quoted errors of the leakage spectra were evaluated from Tables I and II in the article by Stewart.[2] The energy groups defining these spectra are given in Table 3. The measured leakage current of GODIVA, as given in Ref. 1, was cut off at 183.2 keV, and that of JEZEBEL at 302.0 keV.

Table 1. Specifications of GODIVA and JEZEBEL

		GODIVA		JEZEBEL
ρ (gm/cm^3)		18.74		15.61
R (cm)		8.741		6.385
Composition	U-234	1.025	Pu-239	91.951
(at. %)	U-235	93.770	Pu-240	4.346
	U-238	5.205	Pu-241	0.290
			Ga	3.413

Calculated Input Data

The calculated values of the 34 integral quantities listed in Table 2 were all obtained in a 30 group-S_8-transport corrected P_0 approximation, and then corrected so as to practically conform to an S_∞ - P_∞ approximation. These corrections, however, were really significant only for the two reactivities. Table 3 gives the 9-group structure for the measured leakage spectra, and the numbers of fine groups into which each of the 9 groups was divided to produce our 30-group structure.

All microscopic nuclear data were taken from the ENDF/B-IV library, except for gallium, the source of which was the UKNDL library. The fission spectrum was the weighing function in generating the 30-group constants, and these were weighed by the actual average flux spectrum in the appropriate assembly for collapsing each isotope's set of 30-group constants into the 9-group set.

Table 2. Experimental Integral Data

		GODIVA		JEZEBEL	
	Integral datum	value	error	value	error
k	effective multiplication	1.000	0.003	1.000	0.003
L1	relative leakage spectrum	2.00	1.00	3.10	1.50
L2		7.10	1.00	11.70	1.75
L3		13.60	1.20	17.70	1.72
L4		16.80	1.26	20.00*	
L5		18.00*		16.50	1.16
L6		18.80	0.75	13.60	0.80
L7		11.50	0.40	9.70	0.47
L8		8.00	0.32		
N_p	σ^f/σ^f_{235}			0.990	0.050
233		1.630	0.100	1.610	0.100
238		0.156	0.005	0.205	0.008
239		1.420	0.020	1.490	0.030
Th	σ^f/σ^f_{238}	0.234	0.005		
234		5.000	0.200		
238c	σ^c/σ^f_{238}	0.47	0.02		
Au	activations	0.1230	0.0030	0.1012	0.0025
Cu		0.0144	0.0006	0.0122	0.0006
Mn		0.0033	0.0002	0.0029	0.0002
Nb		0.0371	0.0030	0.0276	0.0030
V				0.0028	0.0002

* normalization value.

The calculated integral quantities, or rather their deviations from the corresponding experimental values divided by the latter's errors, are given in Table 4, under the headings "given set". In other words if $\hat{I}_i$ are our experimental integral data, $\Delta\hat{I}_i$ their errors, and $I_i(\hat{\sigma})$ the corresponding values calculated with the given cross-section set, then the "given set" columns in Table 4 list the values of

$$c_i = [I_i(\hat{\sigma}) - \hat{I}_i]/\Delta\hat{I}_i. \qquad (1)$$

In what follows we shall refer to such ratios as normalized deviations, or simply as deviations. These deviations are convenient, since they furnish a natural measure for the quality of reproduction of the measured integral data by a given cross-section set,

$$Q_I(\hat{\sigma}) = \tilde{c}c/N, \qquad (2)$$

where c is the column (and $\tilde{c}$ the row) of the c_i's, and N the dimension of the vector c (i.e., the number of integral data).

Table 3. The 9-group structure and its breakup into 30 groups.

group number	upper energy (keV)	upper lethargy	number of fine groups
1	15000.0		3
2	6065.3	0.5	2
3	3678.8	1.0	4
4	2231.3	1.5	4
5	1353.4	2.0	4
6	820.2	2.5	3
7	497.9	3.0	3
8	302.0	3.5	3
9*	183.2	4.0	4

* lower energy of group 9 is 1 keV.

Now, the "given set" columns in Table 4 obviously demonstrate that the ENDF/B-IV library is far from satisfactorily reproducing neither our GODIVA nor our JEZEBEL sets of experimental integral data. As a matter of fact, while for a reasonable reproduction of any set of experimental integral data we evidently expect that $Q_I \simeq 1$, or less, we actually find that

$$Q_I(\text{GODIVA}) = 11.5, \qquad Q_I(\text{JEZEBEL}) = 5.5.$$

Although these two numbers undoubtably indicate that the given uranium cross sections are worse than those of plutonium, even the reproduction of the JEZEBEL data is, on the whole, rather poor. The need for adjustment is obvious.

In the calculation of the integral quantities, all partial cross sections and every detail of the spectra and angular distributions of secondary neutrons were considered. On the other hand, in our adjustments we only consider sensitivities with respect to the fission, capture ((n,γ) + (n,p) + ...), inelastic ((n,n') + (n,2n) + (n,3n)), and elastic scattering cross sections, and with respect to $\bar{\nu}$, of U-235, U-238, Pu-239 and Pu-240. And the sensitivity profiles are evaluated in the 9-group structure of Table 3.

Table 4. Normalized Deviations from the Experimental Values of Calculated, Separately-Adjusted, and Final Values of the Integral Quantities.

	GODIVA			JEZEBEL		
datum	given set	adjusted	final	given set	adjusted	final
k	2.600	- 0.111	0.324	0.267	0.398	0.122
L1	0.210	0.356	-0.015	0.047	-0.008	0.320
L2	0.630	1.025	0.284	-0.914	-1.000	-0.865
L3	0.992	1.442	0.210	-0.267	-0.333	-0.157
L4	1.397	1.731	0.226			
L5				2.078	1.179	0.506
L6	-5.040	1.654	-0.218	1.287	0.491	0.207
L7	-3.525	-0.640	-0.054	-0.751	-0.866	-0.349
L8	-7.219	-1.827	-0.194			
Np				-1.000	-0.719	-0.310
233	2.550	2.872	*	-1.100	-1.107	-0.682
238	2.600	2.029	0.767	-1.250	-0.643	0.278
239	-1.750	-0.610	0.307	-3.000	-2.217	-1.319
Th	2.000	2.215	1.913			
234	-2.300	-1.888	-1.335			
238c	-1.200	-0.140	0.942			
Au	-4.200	-3.509	-2.279	0.520	-0.453	-0.130
Cu	-5.833	-5.655	*	-3.000	-3.321	*
Mn	5.335	5.565	*	6.150	5.484	*
Nb	-0.087	0.186	0.683	2.100	1.795	1.880
V				-4.100	-4.343	*

* rejected

The Adjustment Prescription

In order to formulate the adjustment prescription, we still need the so-called cross-section uncertainties. These are commonly available in the form of relative uncertainties, $\beta = \Delta\hat{\sigma}/\hat{\sigma}$, and we have employed their values as given in Table IV of the review by Pazy et al.[3] However, for β^f_{235} we had found a more recent evaluation by Bhat[4], and have therefore

revised that table as follows:

$$7\%(E \leq 700), \quad 3\%(700 < E \leq 6000), \quad 10\%(E > 6000 \text{ keV}).$$

Now, let σ_j be the (unknown) adjusted cross sections, and let ΔE_j be the energy-group width relating to σ_j. We then define the (normalized) individual adjustments,

$$x_j = (\sigma_j - \hat{\sigma}_j)\sqrt{\Delta E_j}/\beta_j\hat{\sigma}_j. \tag{3}$$

This, again, is a convenient definition, since a natural global measure for the extent of a particular adjustment is

$$\tilde{x}x \simeq \sum\int \left[\frac{\sigma(E) - \hat{\sigma}(E)}{\beta(E)\hat{\sigma}(E)} \right]^2 dE. \tag{4}$$

And similarly to the "calculated" deviations c_i, defined in Eq. (1), we also define the "adjusted" deviations,

$$y_i = [I_i(\sigma) - \hat{I}_i]/\Delta\hat{I}_i. \tag{5}$$

Then the sensitivity matrix is defined as

$$A_{ij} = \partial y_i/\partial x_j = (\beta_j\hat{\sigma}_j/\Delta\hat{I}_i\sqrt{\Delta E_j})\partial I_i/\partial\sigma_j. \tag{6}$$

In this notation the linearity assumption takes the form

$$y = Ax + c, \tag{7}$$

and the adjustment prescription reduces to minimizing the form

$$Q = \tilde{x}x + \Delta E_0\tilde{y}y, \tag{8}$$

where ΔE_0 is the dimensional parameter mentioned in the introduction, subject to the condition of Eq. (7).

The straightforward solution of this conditional minimum problem, i.e. our explicit adjustment prescription, is

$$y = (I + \Delta E_0 A\tilde{A})^{-1}c, \quad x = -\Delta E_0\tilde{A}y. \tag{9}$$

A detailed derivation of these formulas can be found in Ref. 3. ΔE_0 and its usefulness are further extensively discussed and illustrated in our Atlanta paper.[5]

ADJUSTMENT

Preliminary Data Check

Considering the given-set deviations in Table 4 again, we notice that some of the calculated activations deviate significantly more than most other calculated quantities, both in GODIVA and JEZEBEL. However, in order to determine whether the suspicious experimental activations were indeed "bad" data, we first of all adjusted the given cross sections of the two uranium isotopes by the GODIVA data, and, independently, those of the two plutonium isotopes by the JEZEBEL data. The results of these two adjustments are also listed in Table 4, under the headings "adjusted". The deviations are now indeed smaller, but we still find that

$$Q_I(\text{GODIVA}) = 6.1, \quad Q_I(\text{JEZEBEL}) = 4.6.$$

It is obvious, however, that the major contributions to these Q_I's are again those of the activations. Actually, the adjusted deviations of the Cu, Mn, and V activations are just as big as the corresponding given set deviations. We have therefore decided to eliminate these five integral data at this point. We note that without the Cu and Mn contributions $Q_I(G)$ reduces to 2.9, and without these and the V contribution $Q_I(J)$ becomes 1.1.

In these preliminary adjustments the value of ΔE_o was 200 keV. This seemingly arbitrary value we know from our experience to be quite reasonable. In any case, our data selection should not be too sensitive to the value of ΔE_o.

Overall Data Check

With the rejection of the five dubious experimental activations, we were all set to check the consistency of the remaining 29 integral data, with each other, and with the given cross sections. This was done by means of a simultaneous adjustment of the four isotopes' cross sections by all 29 data. Although the compositions of GODIVA and JEZEBEL have no common isotopes, the two assemblies are coupled through the central-fission-ratio data.

For the 29 integral data we have $Q_I(\hat{\sigma}) = 5.9$, which the adjustment reduces to $Q_I = 1.9$. This is still not quite satisfactory by our criterion, and could of course be further reduced by increasing ΔE_o (which was still 200 keV). However, before forcing Q_I further down, we should have considered the extent of the cross-section adjustment.

Let us then consider the "adjustment measure", Eq. (4). We have to determine a numerical value, up to which this measure will characterize an acceptable adjustment. Suppose that for all partial cross sections of all adjusted isotopes $(\sigma - \hat{\sigma})/\beta\hat{\sigma} \simeq 1$ everywhere. Then, since we consider five partial cross sections ($\sigma^f, \sigma^c, \sigma^{in}, \sigma^{el}$ and $\bar{\nu}$) and four isotopes,

and our energy range is 0 - 15 MeV, we would expect

$$\tilde{x}x \simeq 5 \times 4 \times 15000 = 300\ 000.$$

On the other hand we do know that our integral quantities are rather insensitive to the U-238 and Pu-240 cross sections, that they are not equally sensitive to all partial cross sections of the other two isotopes, and that the sensitivities vary widely with energy. Our estimation, based so far on limited experience, is therefore that whenever $\tilde{x}x$ reaches about 1% of the "nominal" value derived above, some of the adjusted cross sections already deviate from their given values by more than $\beta\hat{\sigma}$. Thus our criterion for a reasonable adjustment is

$$Q_\sigma = \tilde{x}x/3000 \lesssim 1. \qquad (10)$$

Returning to the adjustment under consideration, its "quality" turns out to be $Q_\sigma = 1.5$. There is therefore no point in increasing ΔE_0, which would only further increase Q_σ. Nevertheless, increasing ΔE_0 to 1000 keV results in $Q_\sigma = 4.9$ and Q_I is still over 1. Even for $\Delta E_0 = 4000$ keV, paying the heavy penalty of $Q_\sigma = 10.9$, one integral datum, 233(G) has an adjusted deviation of 3.0, in spite of $Q_I = 0.79$! In any case, the present adjustment indicates that our input cross-section and remaining integral data are still inconsistent. Even rejecting 233(G) reduces Q_I to only 1.6 (with $\Delta E_0 = 200$).

Relaxation of Cross-Section Uncertainties

Studying the individual adjustments we have found that most of the adjustments that exceed 1 relate to inelastic scattering cross sections. This is not surprising, since many of our integral quantities are quite sensitive to the neutron energy spectrum, and inelastic scattering is the principle slowing-down mechanism in the fast assemblies. And since the difficulty in measuring these cross sections is common knowledge, we felt that their estimated uncertainties might indeed be over-optimistic. We therefore now modified our "standard" inelastic cross-section uncertainties to 100%.

The adjustment of our given cross-section set with the modified uncertainty data by the 28 integral data yielded the more than reasonable result of

$$Q_I = 0.72, \qquad Q_\sigma = 0.78.$$

In this adjustment we again used $\Delta E_0 = 200$. So at this point we have studied the dependence of Q_I and Q_σ on ΔE_0. At $\Delta E_0 = 0$, $Q_I = Q_I(\hat{\sigma})$ and $Q_\sigma = 0$. As ΔE_0 is increased Q_I decreases and Q_σ increases monotonously. At $\Delta E_0 = 80$ Q_I crosses the unity downward, and at $\Delta E_0 = 320$ Q_σ crosses unity upward. Thus a reasonable adjustment obtains for all values $80 < \Delta E_0 < 320$, and $\Delta E_0 = 200$ turns out to be right at the mid-point of this interval.

We now addressed the problem of data redundancy. In other words, we wanted to see whether adjustment by a partial set of our integral data would suffice to obtain adjusted cross sections which would reasonably reproduce all the data.

This analysis consists of progressively adjusting the given cross-section set by one, two, three,..., integral data. The order in which the "active" data are added, one at a time, is such that at each step the added datum is the one for which Q_I (which always measures the reproduction of all data) is minimal. Thus starting from $Q_I(\hat{\sigma}) = 5.8$, L8(G) reduces Q_I to 4.0, L8(G) + 234(G) to 3.2, and so on. Adjustment by the nine "most important" data already yields $Q_I = 1.0$, and by 12 data $Q_I = 0.87$. The corresponding values of Q_σ are 0.10, 0.20, 0.69 and 0.73. These results seem to justify our approach.

Finally, we have checked the validity of the linearity assumption. Let $\Delta_i = I_i(\sigma) - I_i(\hat{\sigma})$, then linearity holds if each Δ_i', with $I_i(\sigma)$ evaluated by linear extrapolation, equals Δ_i'', with $I_i(\sigma)$ actually recalculated with the adjusted cross sections. It turned out that this practically was the case for 22 integral quantities. For the six σ^f/σ^f_{235}, however, Δ' was $\simeq 2\Delta''$. Still, for each ratio both adjusted values are closer to the experimental value, $\hat{I}$, than $I(\hat{\sigma})$. That linearity would not rigorously hold for these fission ratios should not come as a surprise, since the σ^f_{235} adjustments were significant, and the ratios are inversely proportional to an expression linear in the σ^f_{235}'s, and thus are strongly non-linear in these cross sections. In any case, the adjusted cross-section set does yield a much better reproduction of the experimental integral data, and thus again justifies the adjustment prescription.

CONCLUSIONS

The purpose of the excercise in adjustment presented here was to illustrate that the pitfalls of "blind" application of adjustment codes may be avoided by intelligent, continuous intervention in the procedure. The main conclusions seem to be that checking the entire input, and particularly the cross-section uncertainty information and the experimental integral data, for consistency is essential for achieving reasonable and meaningful results. Care should also be given to the adequacy of the approximation used in calculating the integral quantities and their sensitivity profiles. Finally the validity of the linearity assumption should always be examined by actually recalculating all integral quantities.

Besides rejecting integral data which refuse to fall in line, another important conclusion seems to be that uncertainties should be reconsidered liberally. Whatever their sources, they are always subjective guesses, and should never be allowed to spoil the adjustment game.

REFERENCES

1. H. Alter, R.B. Kidman, R. LaBauve, R. Protsik and B.A. Zolotar, CSEWG Benchmark Specifications, U.S. Report BNL-19302 (November, 1974).

2. Leona Stewart, "Leakage Neutron Spectrum from a Bare Pu-239 Critical Assembly," Nucl. Sci. Eng. 8, 595 (1960).

3. A. Pazy, G. Rakavy, I. Reiss, J.J. Wagschal, Atara Ya'ari and Y. Yeivin, "The Role of Integral Data in Neutron Cross-Section Evaluation", Nucl. Sci Eng. 55, 280 (1974)

4. M.R. Bhat, "Evaluation of the U-235 Fission Cross Section from 100 eV to 20 MeV", p. 307 in Proceedings of the NEANDC/NEACRP Specialists Meeting on Fast Neutron Fission Cross Sections of U-233, U-235, U-238 and Pu-239, W.P. Poenitz and A.B. Smith, Editors, US Report ANL-76-90 (June, 1976).

5. J.J. Wagschal, Atara Ya'ari and Y. Yeivin, "Cross-Section Sensitivities, Adjustments and All That", p. 536 in Advanced Reactors: Physics, Design and Economics, J.M. Kallfelz and R.A. Karam, editors, Pergamon Press, New York, N.Y., 1975.

SENSITIVITY ANALYSIS APPLIED TO THE CALCULATION OF DETECTOR-RESPONSE KERNELS

William H. Scott, Jr.
Science Applications, Inc.
La Jolla, California, USA

Patrick J. McDaniel
James H. Renken
Steven A. Wright
Sandia Laboratories
Albuquerque, New Mexico, USA

ABSTRACT

A possible method for measuring fuel motion in a melting reactor-fuel-pin test assembly is the unfolding of the signals generated by small fission-couple detectors placed in and around the test assembly. In order to perform this unfolding, the detector-response kernels for fuel movement within the test assembly must be accurately determined. This can be accomplished using the techniques of sensitivity analysis.

Forward and adjoint solutions to the neutron transport equations can be calculated with the MORSE 3D code. Then linear perturbation theory can be used to derive the response kernels as integrals of the test fuel cross sections weighted with the forward and adjoint solutions over the appropriate volumes.

Calculations have been performed to verify the accuracy of the technique. Detector responses based on the sensitivity analysis were compared with direct calculations for perturbed fuel geometries. Excellent agreement has been obtained.

INTRODUCTION

The ability to monitor fuel redistribution in fast-reactor safety experiments is important in determining the safety of fast breeder reactors. Although fuel distributions within a reactor cannot be measured directly, measurements of neutron or gamma-ray flux changes can be made to infer the fuel distribution. In this paper, sensitivity analysis will be used to determine the relationship between the flux and the fuel distribution.

The usual configuration of a safety test reactor is annular in shape with a cylindrical test assembly at the center. The test assembly may contain single pins, bundles, or even subassemblies which are irradiated by the driver reactor to simulate hypothetical core-disruptive accidents. If the driver reactor has one or more viewing slots, flux changes in the central test assembly can be measured with imaging devices such as a hodoscope,[1] a coded-aperture imaging system,[2] or a pinhole camera.[3] Until recently the hodoscope has been the only system available to monitor fuel motion, and it is used almost exclusively in the TREAT experiments.[4] The hodoscope is an array of collimators focused through a slot in the driver reactor at the test assembly. Redistribution of fuel is detected as changes in the intensity of fission neutrons observed through the collimators.

The detection of fuel motion within test sections of reactors which have no slots, such as SLSF, EBR-II, or SCARABEE, requires the use of in-core fuel motion detection systems. In this system, many small neutron or gamma-ray detectors are placed throughout the test section. Fuel motion is detected as molten fuel moves relative to the detectors. In addition to requiring no slot, this technique should be especially useful for large bundle tests since self-shielding effects are not likely to degrade the resolution as severely as in external viewing systems.

With the support of the US Nuclear Regulatory Commission, an experimental program is being conducted at Sandia Laboratories to investigate the feasibility of in-core fuel motion detection.[5] This program has two major development efforts. The first effort requires the design, construction, and testing of detectors. These detectors must be sensitive to fuel motion, withstand the extreme conditions of the test assembly environment, and be small enough to reside between individual fuel pins. The

second effort requires the development of analytical methods which can determine the fuel motion from the detector signals. This objective is accomplished in two parts. The first part develops an analytical relationship between the detector signal and fuel motion. The second part does just the reverse. It develops methods which unfold the detector responses to determine the fuel distribution. This paper addresses the first part of the problem only. A companion paper describes the unfolding problem.[6]

An experimental verification of the detector and analysis system will be provided by a series of static tests on 7-, 19-, and 37-pin bundles placed in the center of the Sandia Pulsed Reactor III (SPR III). SPR III is a fast-pulsed reactor which can deliver a neutron fluence of 6×10^{14} nvt at the center of the irradiation cavity with a pulse width of 60 μs. The core consists of 16 to 18 plates of fully enriched U-10 wt % Mo and employs external reflectors for control. The cylindrical test cavity has a diameter of 17.78 cm and a height of 31.9 cm. Figure 1 shows the 37-pin test assembly which will be placed in the SPR III. The lower 10.16 cm of the fuel pins are fixed while the upper 15.24 cm are individually attached to pullrods which can move the fuel to many static configurations. The entire fuel bundle is surrounded by a polyethylene and cadmium liner to tailor the internal spectrum to resemble a more realistic safety-test experiment. Fast-neutron-sensitive fission-couple detectors[7] and gamma-sensitive, self-powered detectors[8] will be used to monitor the fuel distribution. Approximately 30 of these detectors will be mounted on grid spacers inside the test assembly. Figure 2 shows three fission-couple detectors mounted on a grid spacer. In the SPR III tests, the reactor will be pulsed with the pins in several static positions. From analysis of the detector signals, we hope to unfold these same fuel configurations.

KERNEL DEVELOPMENT

To unfold a mass configuration from a change in response at several detectors, kernels are required that relate the change in each detector response to all possible small mass changes. Direct calculation of all of these responses would require a prohibitively large number of computer calculations. Therefore we have implemented a form of sensitivity analysis to determine the change in detector responses due to small fuel movements within the reactor test assembly. The RHOPER code has been written

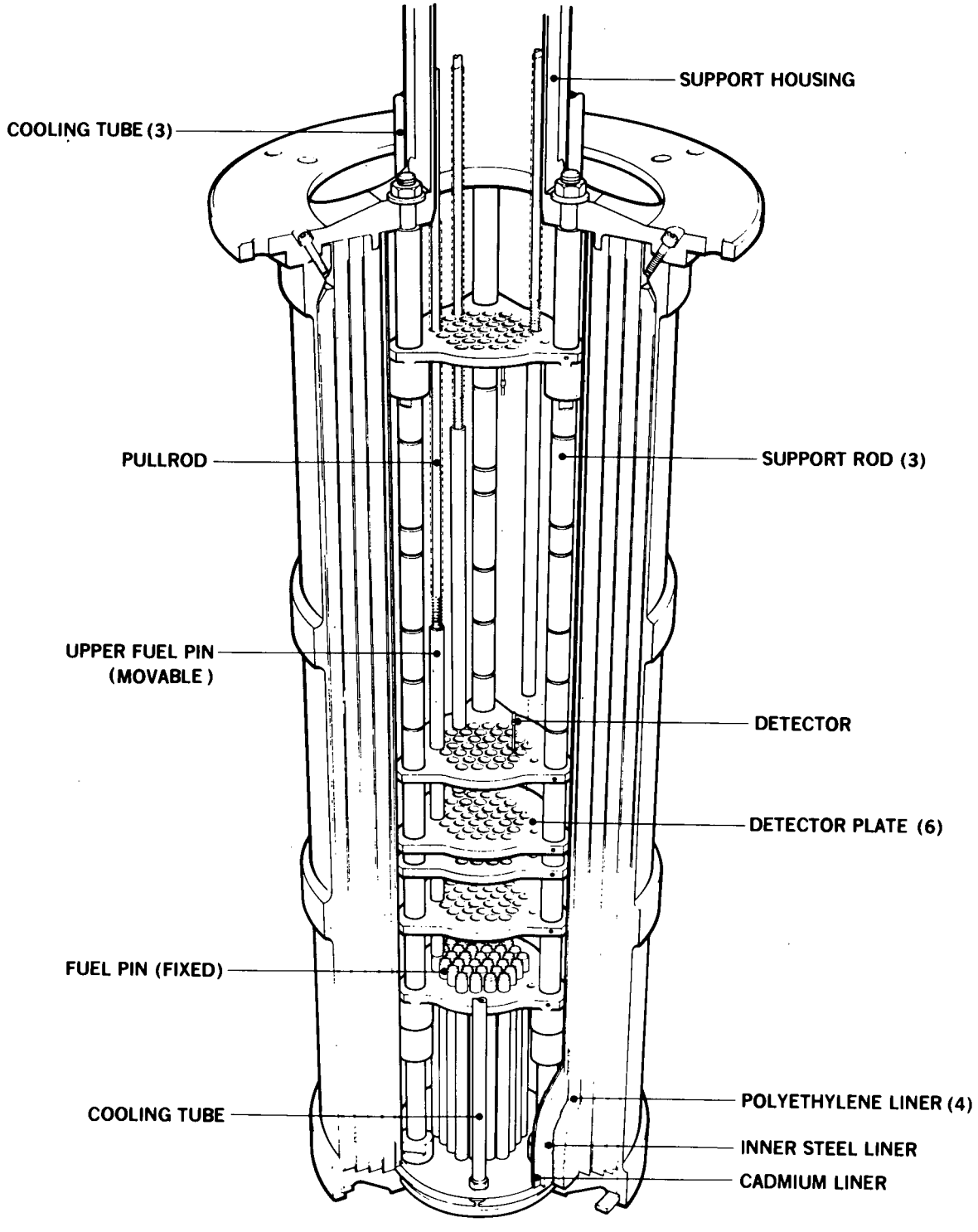

37 PIN FUEL BUNDLE

FIGURE 1

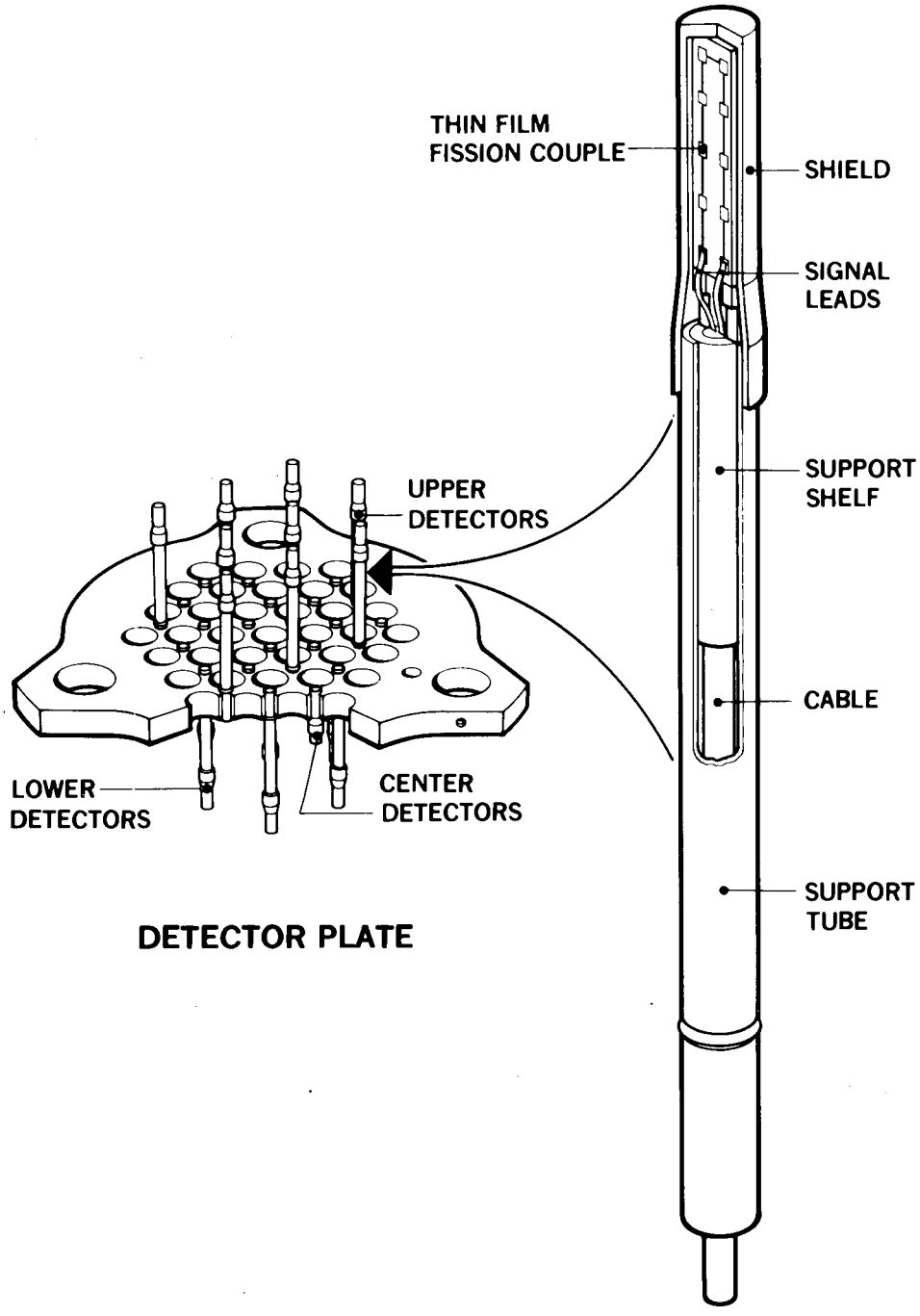

FIGURE 2 DETECTOR ASSEMBLY

to couple forward and adjoint three-dimensional angular flux densities calculated with the MORSE Monte Carlo code and to generate the response kernels required for unfolding. The actual form of the sensitivity relation used is developed below, and the actual equations used in RHOPER and MORSE follow.

The response at a detector in a perturbed geometry is given by

$$R = \int d\bar{r}\, d\bar{\Omega}\, dE\; \phi(\bar{r},\bar{\Omega},E)\, S_o^*(\bar{r},E) \tag{1}$$

where $S_o^*(r,E)$ is the detector response function. The perturbed flux $\phi(\bar{r},\bar{\Omega},E)$ could be obtained as the solution of the forward transport equation in the perturbed geometry,

$$\left[\bar{\Omega}\cdot\bar{\nabla} + \Sigma^T(r,E)\right]\phi(\bar{r},\bar{\Omega},E) = \int d\bar{\Omega}'\, dE'\, \phi(\bar{r},\bar{\Omega}',E')\, \Sigma^S(\bar{r};\bar{\Omega}',E' \rightarrow \bar{\Omega},E) \tag{2}$$

where ϕ is the angular flux density in the perturbed geometry source, and Σ^T and Σ^S are the total and differential scattering cross sections in the perturbed geometry, respectively.

Neglecting for the moment the spatial and energy dependence of the angular flux densities and the cross sections, the corresponding adjoint equation for the unperturbed geometry is

$$\left[-\bar{\Omega}\cdot\bar{\nabla} + \Sigma_o^T\right]\phi^*(\bar{\Omega}) = S_o^* + \int d\bar{\Omega}'\, \phi^*(\bar{\Omega})\, \Sigma_o^S(\bar{\Omega} \rightarrow \bar{\Omega}') \tag{3}$$

where the subscript o will indicate the unperturbed state. A relation that involves forward and adjoint angular flux densities can be derived with the following operation,

$$\int d\bar{r}\, d\bar{\Omega}\left[\phi_o^*(\bar{\Omega})\cdot(\text{eq. 2}) - \phi(\bar{\Omega})\cdot(\text{eq. 3})\right] \tag{4}$$

where V is a finite volume that contains the detector and all of the possible positions where fuel can be located. Now assuming that the forward angular flux density on the bounding surface can be measured in the perturbed geometry and performing the indicated integration over the volume under consideration, we obtain the following equation for the detector response

$$R = \int d\bar{\Omega}\, dA\, \bar{\Omega}\cdot\bar{n}\; \phi_o^*(\bar{\Omega})\, \phi_o(\bar{\Omega}) + \int d\bar{r}\, \delta\rho(\bar{r})\, d\bar{\Omega}\, \phi_o(\bar{\Omega})\left[-\Sigma_{\rho o}^T\, \phi^*(\bar{\Omega}) + \int d\bar{\Omega}'\, \Sigma_{\rho o}^S(\bar{\Omega} \rightarrow \bar{\Omega}')\, \phi^*(\bar{\Omega}')\right] \tag{5}$$

where A is the bounding surface.

The substitutions

$$\Sigma^T - \Sigma_o^T = \Sigma_{\rho o}^T \delta\rho \,, \qquad \Sigma^S - \Sigma_o^S = \Sigma_{\rho o}^S \delta\rho \,, \tag{6}$$

have been made to display the density perturbation as a separate quantity. Note also that this can be considered a fractional density change.

The first term in Eq. 5 is the unperturbed detector response, R_o, and the second term is exactly the desired response kernel times a fuel density change. This equation is the basis of the RHOPER code.

Before looking at the actual quantities calculated in MORSE and provided to RHOPER, it is worth noting that some very significant simplifications are possible. Typical experimental sections are generally placed in the center of a driving reactor. Thus over most of the test section the neutron angular flux density is relatively isotropic. If both the forward and adjoint angular flux densities are expanded in a series of spherical harmonics, the kernel integrals above can be reduced to an infinite sum of integrals of similar terms in these expansions. However, if the spherical harmonic expansion is rapidly convergent for the forward flux, then the kernel expansion will also be rapidly convergent. Thus only the first few terms need be evaluated in both the forward and adjoint expansions. Also, since the forward angular flux density is azimuthally symmetric no azimuthally dependent terms need be calculated at all.

Noting these simplifications and performing the spherical-harmonic expansions, retaining terms only up to order one (currents), Eq. 5 can be written,

$$R = R_o + \frac{1}{4\pi}\Big[-\Sigma_{\rho o}^T\left(\phi_o\phi_o^* + 3\, J_a J_a^* + 3\, J_r J_r^*\right)$$
$$+\phi_o\phi_o^*\left(\nu\Sigma_{\rho o}^F + \Sigma_{\rho o}^{S_o}\right) + 3\Sigma_{\rho o}^{S_1}\left(J_a J_a^* + J_r J_r^*\right)\Big]\delta\rho \tag{7}$$

Here the generalized scattering cross section has been broken up into $\nu\Sigma^F$ (fission) and the Legendre expansion for the actual scattering cross section. The flux density and axial and radial currents are defined by the following integrals,

$$\phi = \int_{4\pi} \phi(\bar{\Omega})\, d\bar{\Omega} \tag{8}$$

$$J_r = \int_{4\pi} \phi(\bar{\Omega})\, \bar{\Omega}\cdot\bar{e}_r\, d\bar{\Omega} \tag{9}$$

$$J_a = \int_{4\pi} \phi(\bar{\Omega})\ \bar{\Omega}\cdot\bar{e}_z d\bar{\Omega} \tag{10}$$

where $\bar{e}_r$ and $\bar{e}_z$ are the unit vectors in the radial and axial directions.

Equation 7 applies for the case of one energy group and one spatial volume bin. Including the effects of multiple energy groups and multiple fuel volume bins, Eq. 7 becomes,

$$\begin{aligned} R = R_o + \frac{1}{4\pi}\sum_K \delta\rho^K V^K \sum_i \Big[& -\Sigma^{TK}_{\rho oi} \cdot \\ & [\phi_i^K \phi_i^{K*} + 3(J_{ai}^K J_{ai}^{K*} + J_{ri}^K J_{ri}^{K*})] \\ & + \phi_i^K \sum_j [\nu \Sigma^{FK}_{\rho oi} \chi_j + \Sigma^{SoK}_{\rho oij}] \phi_j^{K*} \\ & + 3 J_{ai}^K \sum_j \Sigma^{S_1K}_{\rho oij} J_{aj}^{K*} \\ & + 3 J_{ri}^K \sum_j \Sigma^{S_1K}_{\rho oij} J_{rj}^{K*} \Big] \end{aligned} \tag{11}$$

where $_j$ is the fission neutron yield for the $_j$th group.

The unperturbed response R_o can be written as

$$R_o = \sum_i \int dA\, d\bar{\Omega}\, \bar{\Omega}\cdot\bar{n}\ \phi_i(\bar{\Omega})\ \phi_i^*(\bar{\Omega}) \tag{12}$$

where $\bar{n}$ is the inward directed unit normal to the bounding surface.

Assuming the forward angular flux density to be isotropic and neglecting the contributions from the top and bottom surfaces of the bounding volume, the unperturbed response R_o can be calculated as

$$R_o = \frac{1}{4\pi}\sum_K A^K \sum_i S_i^K (\phi_{oi}^{K*} + 2 J_{ri}^{K*}) \tag{13}$$

where

$$S_i^K = \int_{2\pi} \bar{\Omega}\cdot\bar{n}\ \phi_i^K(\bar{\Omega})\, d\bar{\Omega} \tag{14}$$

Then the response-kernel equation for the change in detector response, for the th detector, as a function changes in fuel density can be written very simply as

$$\Delta R^{\ell} = \sum_{K} K^{K\ell} \delta\rho^{K} \tag{15}$$

$$\Delta R^{\ell} = R^{\ell} - R_{o}^{\ell} \tag{16}$$

and the kernels K^K are given by $V^K/4\pi$ times the terms in braces in Eq. 11.

COMPUTATIONAL RESULTS

A calculated 16-group kernel is plotted in Fig. 3. The response function gives the effect of the change in detector signal due to density changes in volume bins along the axial dimension of a neighboring pin. Note that the shape of the kernel is roughly $1/r^2$, as would be expected from intuitive considerations.

The validity of this analysis can be verified quite easily. Two forward transport calculations can be run, one with the unperturbed fuel geometry and one with some realistic perturbation of that geometry. Then the response R_o can be calculated from the forward unperturbed calculation and from the sensitivity-theory analysis presented above. The change in the response due to the perturbation can be calculated by subtracting the detector responses calculated for the unperturbed geometry from those calculated for the perturbed geometry. This change in response can also be calculated based on the sensitivity analysis presented above. The comparison of the two R_o's and the two perturbation signals can then provide a validation of the theory.

As a test case that is representative of one of the first experiments to be run, a 7-pin bundle was studied in the 1-group approximation. A schematic of the fuel-pin geometry for both the unperturbed and perturbed cases is presented in Fig. 4. The upper two-thirds of the pins were moved approximately 8 cm upward to generate the perturbation. Note also the location of the detectors used to monitor this fuel movement.

The results of the two MORSE forward calculations and the two RHOPER calculations are presented in Fig. 5.

The agreement of the sensitivity theory results with the actual perturbation results appears to be quite good. The perturbation technique is obviously a more stable method of calculating small changes in a fairly large background

DETECTOR RESPONSE KERNAL

FIGURE 3

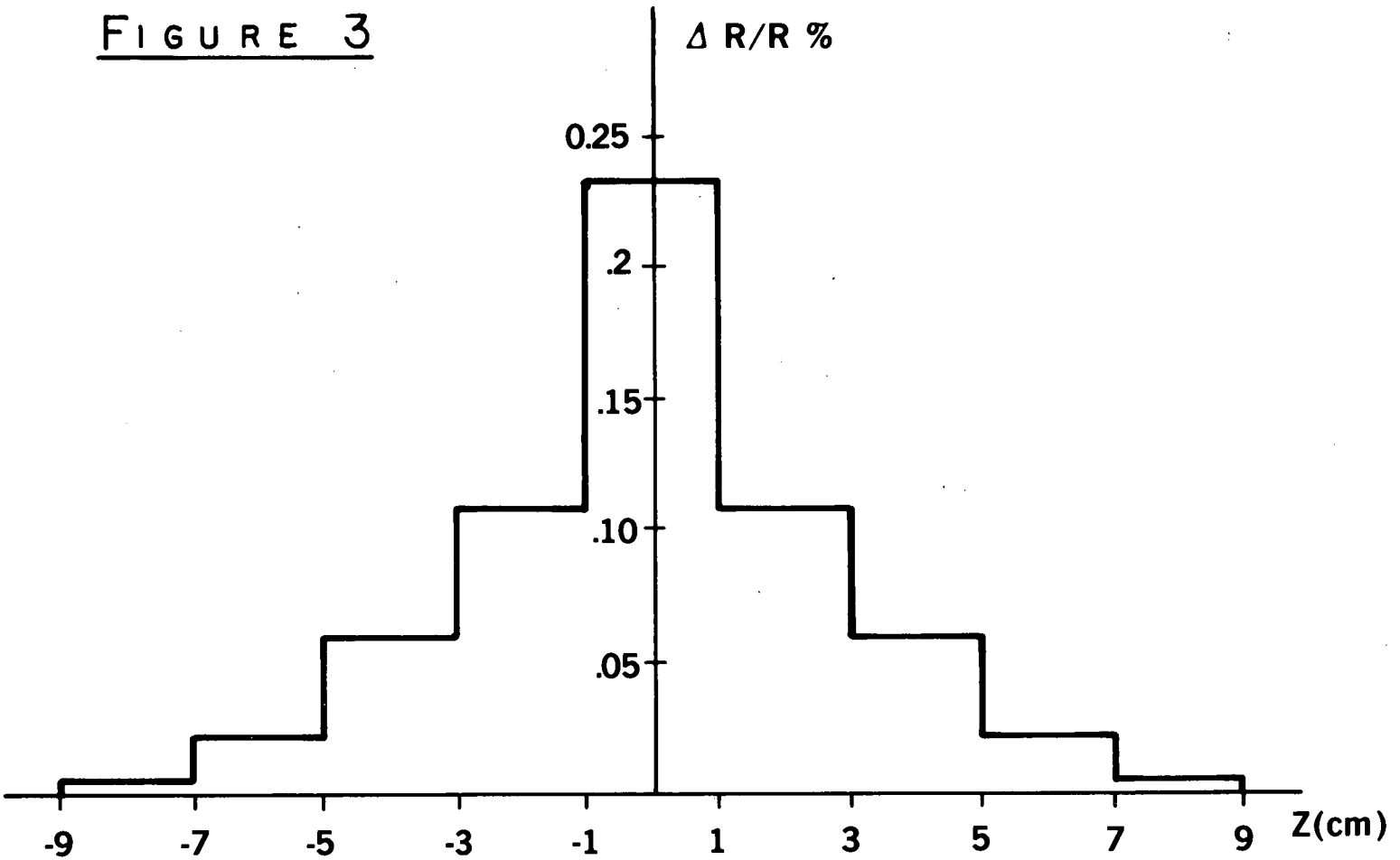

FRACTIONAL CHANGE IN DETECTOR RESPONSE AS A FUNCTION OF AXIAL DISTANCE AWAY FROM A POINT DETECTOR

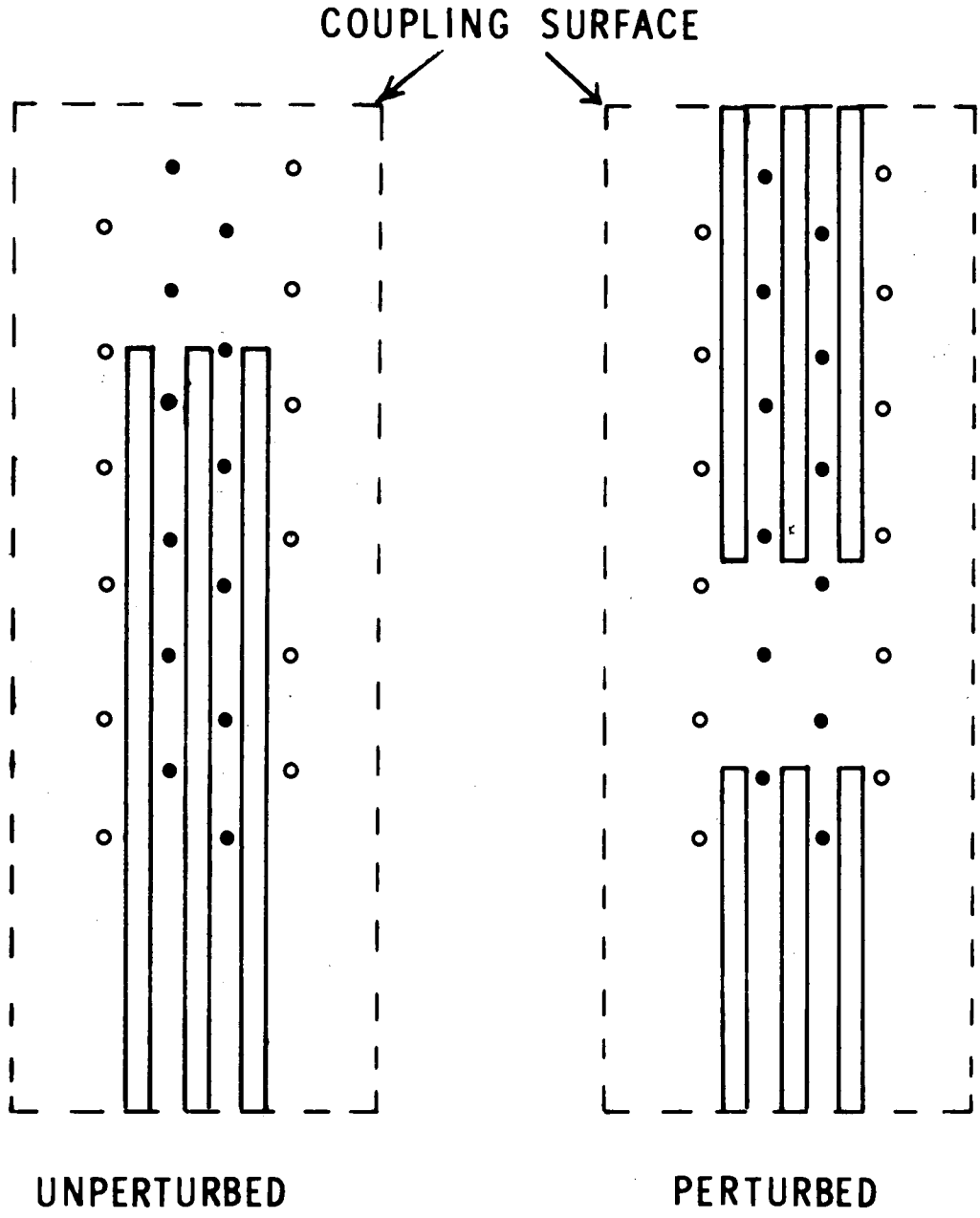

7 PIN MODEL AND DETECTOR LOCATIONS

FIGURE 4

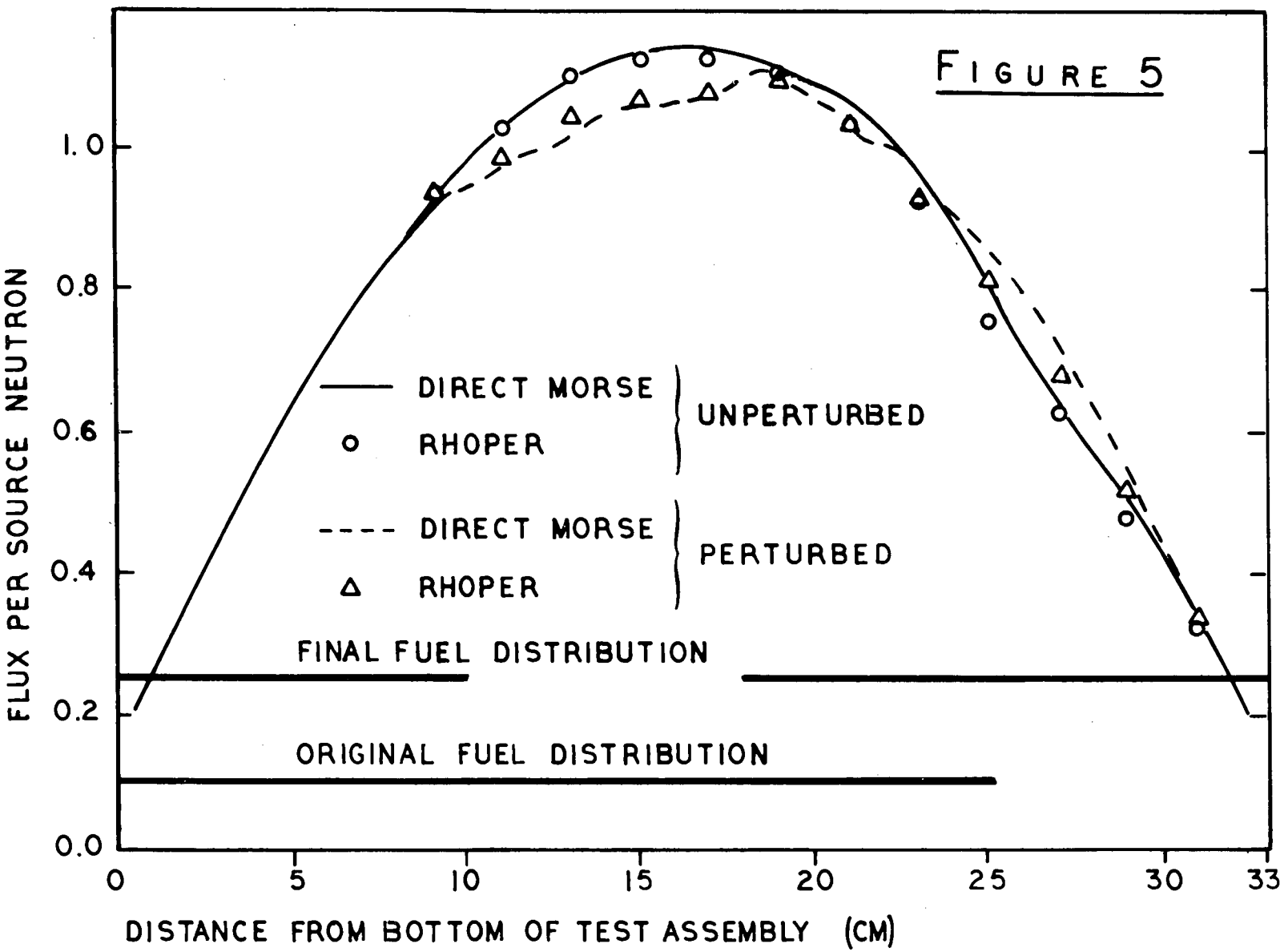
FIGURE 5
FLUX PER SOURCE NEUTRON
1.0
0.8
0.6
0.4
0.2
0.0
DIRECT MORSE
RHOPER
UNPERTURBED
DIRECT MORSE
RHOPER
PERTURBED
FINAL FUEL DISTRIBUTION
ORIGINAL FUEL DISTRIBUTION
0
5
10
15
20
25
30
33
DISTANCE FROM BOTTOM OF TEST ASSEMBLY (CM)

characteristic of this type of problem. This background will present some difficulties for the inverse problem, or unfolding, but they will be discussed in a second paper.

FUTURE WORK

Although we are relatively satisfied with the theoretical and computational development to date, the code system we are using is being expanded to include larger energy-group structures and more significant anistropies. The recent purchase of a set of gamma-ray self-powered detectors has prompted investigations into applying these techniques to coupled neutron-gamma problems. Actual experimental data will be available around the first part of FY 79. These will allow more detailed validation of the methods developed here.

REFERENCES

1. A. De Volpi, "Current Developments in TREAT Hodoscope Technology," Transactions of the Conference on Fuel and Clad Motion Diagnostics in LMFBR Safety Test Facilities, Albuquerque, NM, SAND76-5547, Nov. 1975.

2. J. G. Kelly and K. T. Stalker, "ACPR Upgrade Fuel Motion Detection System," Transactions of the Second Technical Exchange Meeting on Fuel-and Clad-motion Diagnostics for LMFBR Safety Test Facilities, Chicago, IL, Oct. 1976.

3. G. J. Berzins, K. S. Han, and W. H. Roach, "Preliminary Report on the PINEX at TREAT," Transactions of the Second Technical Exchange Meeting on Fuel-and Clad-motion Diagnostics for LMFBR Safety Test Facilities, Chicago, IL, Oct. 1976.

4. G. S. Stanford, "Performance Review--Neutron Hodoscope at TREAT," Transactions of the Second Technical Exchange Meeting on Fuel-and Clad-motion Diagnostics for LMFBR Safety Test Facilities, Chicago, IL, Oct. 1976.

5. "Fast Reactor Safety Research Program Quarterly Report," April-June 1976, SAND76-0372, Reactor Research and Development Department, Sandia Laboratories, Sept. 1976.

6. P. J. McDaniel and S. A. Wright, "Fuel Motion Unfolding Based on Point Detector Responses," these proceedings.

7. "Fast Reactor Safety Research Program Quarterly Report, October-December 1976, SAND77-0145, Reactor Research and Development Department, Sandia Laboratories, Mar. 1977.

8. G. F. Lynch, R. B. Shields and P. G. Coulter, "Characterization of Platinum Self-Powered Detectors," IEEE Transactions on Nuclear Science, Vol. NS-24, No. 1, Feb. 1977.

SENSITIVITY OF WATER REACTOR FUEL CYCLE PARAMETERS AND COSTS TO NUCLEAR DATA

M. Becker, D. R. Harris, B. Quan, and J. M. Ryskamp
Rensselaer Polytechnic Institute
Troy, New York, USA

ABSTRACT

Fuel cycle parameters including end-of-cycle reactivity, end-of-batch nuclide concentrations, and fuel cycle costs are sensitive to certain nuclear data. Sensitivity analyses for cross sections, fission yields, decay constants and other nuclear data indicate directions for worthwhile improvements in data and methods, and yield information important for selection of proper design margins. Considerable success has been achieved in understanding the relationships among various data uncertainties and water reactor fuel cycle costs. These relationships have been shown to be dependent on fuel cycle option and reactor type. Sensitivities depend in an intrinsic way on propagating and compensating effects that take place during the fuel cycle. Fuel cycle parameters and costs are found to be significantly dependent on particular thermal and resonance cross sections and flux disadvantage factors, on fission yields of neutrons and energy, and on certain other data. The results bring out the importance for power reactor sensitivity analysis of dealing with the full fuel cycle.

INTRODUCTION

Rensselaer has been engaged in the study of the relationship of uncertainties in nuclear data to implications for nuclear fuel cycle parameters, particularly fuel cycle costs.[1-10] It has been found that these relationships differ with the specific fuel cycle considered--closed cycle vs. throwaway, BWR vs. PWR, thorium cycles vs. conventional cycles. Results of the sensitivity analysis indicate directions for worthwhile improvement in data and methods. Benefits from improvements in data and methods are related to reduction of margins that are provided by designers to ensure meeting reactor and fuel objectives.

Improvements in nuclear data and methods can benefit reactor economy in several major categories of nuclear power cost: the initial capital investment cost, the operating cost, and the fuel cycle cost. For example, improvements in nuclear data may permit a reduction in the margin of U-235 enrichment that is provided in the unexposed reactor fuel to ensure that the core achieves the required cycle length

at the required power. The reduced fuel enrichment results in decreased fuel cycle cost. As another example, greater confidence in nuclear data may lead to a reduction in the number of control rods[11] and, hence, to decreased initial capital investment cost. Sensitivity analyses of core reactivities and batch nuclide concentrations through time can be used in verifying proper design margins.

Improvements in nuclear data and methods can be costly also. Accelerators and nuclear data measurement groups require long term support. Individual nuclear data measurements are funded, and the measured data are compiled, evaluated, and processed into forms required for calculation. The evaluated and processed nuclear data sets are tested against integral measurements and perhaps modified. Improvements in associated computational methods are also provided research support. If the costs of improving nuclear data and methods to the required degree cannot be borne by their contributions to the advance of basic science, then these costs must be justified by corresponding economic benefits. Improvements in nuclear data and methods thus may be contingent on demonstrations that their economic implications justify their costs.

REACTOR SENSITIVITY ANALYSIS SYSTEM

The sensitivity analysis system relates fuel cycle parameters and costs to uncertainties in nuclear data and methods by two sequences of operations broken at the few-group level. In Path A, basic cross sections are processed to multigroup cross sections and collapsed to few-group cross sections.[3,5] In Path B, few-group microscopic cross sections, radioactive decay data, and fission yields are used in depletion of a fuel batch at power levels determined by core analysis, then reactor parameters and inventories are computed, and fuel cycle costs are determined.[2,4] The sensitivity of fuel cycle parameters and costs to nuclear data uncertainties at the few-group level are determined first by Path B analysis. Path A analyses are then carried out for cases shown to be important.

The sensitivity analysis system determines changes in core reactivity and important changes in nuclide concentrations resulting directly from the original change in nuclear data and indirectly from changes in neutron flux distribution in energy and space. These changes are determined through a linked series of data processing, reactor cell, core, and cost codes either by perturbation theory methods[1,3] or by the direct method. In the direct method the code sequence is run first for a base case. Then each nuclear datum is changed, and the code sequence is run through to determine changes in physics parameters and in cost. The direct method would be prohibitively expensive if industry codes were used for the survey. It becomes feasible, however, when inexpensive special-purpose codes are used. Such fast special-purpose codes have been developed and are

applied through the RPI interactive investigator-computer-graphics system.[12] The perturbation method is much cheaper than the direct method when used in the calculation of Path A thermal region sensitivity coefficients.[10]

Path B

A sequence of batch fuel depletion, core analysis, and fuel cost codes (FASTCELL, FASTCORE, and COSTR) determines the changes in fuel cycle parameters and costs for changes in few-group microscopic cross sections, in fission yields, and in decay data by the direct method. The Path B code system exposes a fuel batch for the base case and fuel batch costs C are determined for the base case. Then a few-group microscopic cross section or fission yield or decay parameter (x) is changed by (δx), the fuel batch is reexposed, and the end-of-life cycle core reactivity and other parameters are found to differ from those of the base case. Sensitivities to core parameters and nuclide concentrations are determined at this point. To preserve the required energy production with the same cycle length, the enrichment of fresh fuel is changed until the end-of-cycle core reactivity returns to that of the base case. For mixed oxide recycle the proportion of oxides in fresh fuel may be altered as well as enrichment. Fuel cycle costs are then determined for this doubly-perturbed exposure. Sensitivity coefficients

$$S_x = \frac{x}{C} \frac{\delta C}{\delta X} \tag{1}$$

for different fuel cycle options are then computed from the changes δC from the base case.

FASTCELL is a code module designed to carry out rapid survey calculations of few-energy-group neutron fluxes, nuclide concentrations, and other quantities characterizing cell depletion in light water reactors. The code is patterned after LEOPARD[13] and LASER[14] but avoids expensive parts of these codes that are judged not to be of greatest importance. In particular, detailed space and energy calculations are avoided. Exposure-dependent few-group microscopic cross sections are determined by a base LEOPARD or LASER run and stored at major time steps during exposure. FASTCELL accurately follows 40 nuclide concentrations by forward differencing for minor time steps between the major time steps. The EPRI-CPM[15] fission product chains are used. The fission product few-group cross sections are those found in EPRI-CINDER.[16] Fission yields, decay constants and branching ratios were obtained from ENDF/B-IV[17]. Few-group fluxes scaled by demand power are recomputed at each minor time step so power demand, few-group microscopic data, few-group fluxes and nuclear concentrations are always consistent. The accuracy and cost of the calculation are controlled through the frequency of minor time steps between the major time steps. FASTCELL costs about one dollar for a full batch exposure in contrast with over a hundred dollars for LEOPARD or LASER.

FASTCORE is a code module that computes core reactivity using the batch multiplication factors generated by FASTCELL and input power fractions between nodes. The power demand imposed on a fuel batch is determined by the power demand on the core, by the distribution of power density in the core, and by cycle loading patterns for the fuel elements making up the batch. The fuel loading patterns do not change for small cross section changes. The distribution of power density in the core is determined by operator control and by thermal-hydraulic factors as well as by depletion. The Haling strategy, whereby design and control contribute to maintaining a nearly constant power shape, is often followed for BWR's and we find that PWR operation approximates this strategy. Using the cycle loading patterns and constant core power shape determined from analysis of industry experience, FASTCORE computes the core infinite multiplication factor with exposure.

COSTR is a code module that determines fuel cycle costs from fuel batch inventories before and after exposure. Fuel cycle costs are grouped into conventional cost components for which present worth values are determined referred to the mid-point of the fuel in-core residence time. Front end cost components include the costs of mining and milling ore, of conversion, of enrichment, and of fuel fabrication. Tails enrichment has either an assigned value or the optimum value in terms of feed and enrichment costs. Plutonium or U-233 values in fresh fuel are determined consistent with uranium cost, enrichment cost, and fuel handling penalties. Back end costs include storage, transportation, and disposal for the throwaway case as well as the reprocessing cost and the values of materials in spent fuel for recycle cases. Payments for materials and services, including progress payments, are on an assigned schedule relative to the fuel in-core residence time. COSTR computes the fuel cycle cost for both the throwaway and recycle options.

Path A

The sensitivities of few-group data to basic nuclear data are determined by detailed calculations (referred to as Path A). At the few-group dividing level, the uncertainties arising from data processing are indistinguishable from uncertainties in the basic nuclear data, and data processing effects are included in Path A analyses. The data processing uncertainties investigated here are not numerical in nature (these we judge should be under control) but physical, particularly in the detailed distributions of neutron flux in energy and space that are used to average cross sections. The LWR sensitivity analyses to be described in the next sections bring out the importance of thermal and resonance group cross sections. Thus most Path A analysis has been directed to these phenomena, although a fast slowing-down code combining the features of GAM[18] and MUFT[19] with adjoint capability has been prepared.

Detailed thermal region sensitivites are determined by the perturbation method. Thermal region calculations are described in detail in our other paper presented at this workshop.[10] The thermal group

code module FASTT combines features of the LEOPARD-SOFOCATE and LASER-THERMOS methods and adds an adjoint capability. A striking feature of our Path A thermal analyses has been the (usually) overwhelming importance of the Maxwellian energy region.

The resonance code module FASTR solves the slowing down equations numerically across a resonance using region-to-region collision probabilities and using resonance cross sections from the RPI multilevel code module MLEVL. Resonance group sensitivites are determined from FASTR by the direct method.[5] Resonance group sensitivities are found to result primarily from uncertainties in the resonance parameters and in Dancoff factors, with lesser contributions from multilevel effects and Doppler broadening treatments.

SENSITIVITY ANALYSES FOR CURRENT LIGHT WATER REACTORS

Sensitivity analyses have been carried out for large boiling and pressurized water reactors using slightly enriched UO_2 fuel prepared from ore.[4] The back end of the fuel cycle is considered as two alternatives, one with spent fuel reprocessing including fissile uranium and plutonium credits, and the other the throwaway case with storage and disposal costs. The representative BWR characteristics are based on data for the Montague plants.[20] The BWR fuel batch is exposed for four equilibrium cycles over four years using a scatter loading pattern. The representative PWR characteristics are based on data for the Green County plants.[21] For the first PWR cycle the batch is exposed on the core periphery and for the second and third cycles is checkerboard loaded in the core interior.

The important Path B fuel cycle cost sensitivity coefficients for 1985 are shown in Table 1 for both boiling and pressurized water reactors and for both back end alternatives. The thermal cross sections of Pu-239, U-235, and hydrogen are the most important. Epithermal cross sections of U-238 and U-235 also have large sensitivities. The U-238 fast fission cross section is the only cross section in the fast energy region that is important. Pu-240, Pu-242, structural materials, and fission products all have much smaller sensitivities to fuel cycle costs. Sensitivity coefficients for the BWR are generally less in absolute value than for the PWR. Detailed examination indicates that the lower BWR sensitivities occur because of lower initial enrichment and lower discharge exposure. Sensitivities for the closed cycle are lower than for the throwaway case. This occurs largely because changes in fissile credits after exposure tend to defray in part the changes in initial enrichment required to compensate for nuclear data changes.

The sensitivity coefficients displayed in Table 1 demonstrate the importance of considering fuel exposure in contrast to examining sensitivities at a point in time or in a mockup. For example, sensitivities to U-238 capture data are less than might have been expected because of the buildup of fissile plutonium in the throwaway case and,

Table 1. Fuel Cycle Cost Sensitivity to Few-Group Data for 1985

	BWR		PWR	
	Recycle	Throwaway	Recycle	Throwaway
^{239}Pu(Thermal,Fission)	-.522	-.688	-.560	-.753
^{239}Pu(Thermal,Capture)	.439	.578	.478	.619
^{235}U(Thermal,Fission)	-.387	-.578	-.384	-.568
^{235}U(Thermal,Capture)	.210	.232	.208	.232
H(Thermal,Capture)	.125	.169	.095	.135
^{238}U(Epithermal,Capture)	.020	.216	.043	.344
^{238}U(Fast,Fission)	-.108	-.127	-.119	-.141
^{241}Pu(Thermal,Fission)	-.094	-.123	-.099	-.130
^{235}U(Epithermal,Capture)	.089	.094	.123	.129
^{235}U(Epithermal,Fission)	-.060	-.091	-.081	-.134
^{241}Pu(Thermal,Capture)	.068	.080	.073	.089
^{238}U(Thermal,Capture)	.033	.151	.037	.147
Zr(Epithermal,Capture)	.026	.033	.020	.027
^{135}Xe(Thermal,Capture)	.017	.024	.020	.029
^{236}U(Epithermal,Capture)	.016	.020	.022	.029

additionally its credit in the recycle case. The sensitivity to Pu-240 data turns out to be small because of the high worth of the Pu-241 produced from neutron capture in Pu-240. We have shown earlier[2] that these fuel cycle sensitivities can be aggravated by applying a bias like k-reset which is determined from critical experiments.

Fuel cycle cost sensitivities to fission neutron yields ν for 1985 are shown in Table 2. These are the largest sensitivities of our entire study. The neutron yield per fission for Cf-252 is the most important because all ν values are normalized to the Cf-252 value. Although the sensitivities for Pu-241 and U-238 are smaller than those for U-235 and Pu-239, they are still large when compared with the sensitivities displayed in Table 1. The fuel cycle cost sensitivities

Table 2. Fuel Cycle Cost Sensitivity to Fission Neutron Yield (ν) for 1985

	BWR		PWR	
	Recycle	Throwaway	Recycle	Throwaway
^{252}Cf	-3.174	-3.952	-3.371	-4.326
^{235}U	-1.408	-1.764	-1.462	-1.889
^{239}Pu	-1.353	-1.696	-1.466	-1.895
^{241}Pu	-0.272	-0.342	-0.297	-0.386
^{238}U	-0.143	-0.181	-0.158	-0.205

to energy yield per fission κ are shown in Table 3. Sensitivities for U-235 and Pu-239 are quite large, while those for Pu-241 and U-238 are one order of magnitude smaller. Fuel cycle cost sensitivities to cumulative fission product yields are relatively small. When it is considered that a single fuel batch for a single reactor has a cost of some tens of millions of dollars, it can been seen that these sensitivity coefficients indicate large potential benefits from data improvement.

Table 3. Fuel Cycle Cost Sensitivity to Energy per Fission (κ) for 1985

	BWR		PWR	
	Recycle	Throwaway	Recycle	Throwaway
^{235}U	-0.504	-0.503	-0.509	-0.492
^{239}Pu	-0.226	-0.214	-0.241	-0.220
^{241}Pu	-0.031	-0.028	-0.036	-0.032
^{238}U	-0.029	-0.028	-0.035	-0.034

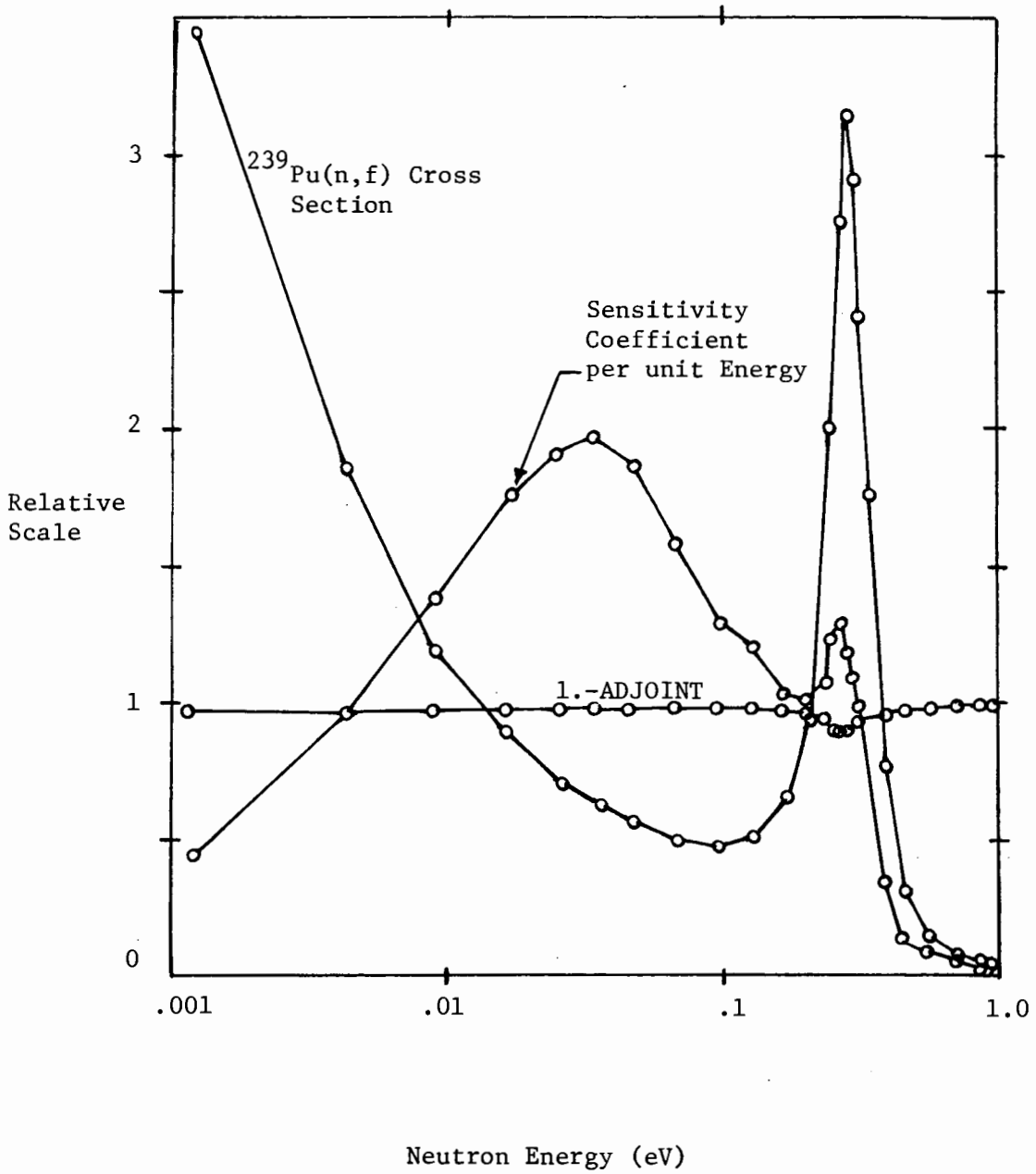

Fig. 1 Detailed Pu-239 Fission Cross Section, Sensitivity Coefficient, and Adjoint for the Maine Yankee II PWR at Middle of Batch Exposure.

Earlier it was noted that Path A analyses for these reactors bring out the importance of individual resonance parameters and Dancoff factors in the resonance range[5] and of the Maxwellian range for thermal-group cross sections.[3,10] The latter point is illustrated in Figure 1 by the case of the important Pu-239 fission cross section which is more than five times as large as its 0.3 eV resonance than at the Maxwellian peak; yet its detailed sensitivity is about 50% larger at the Maxwellian peak than at the resonance. This result is for a PWR at middle-of-exposure. At beginning-of-exposure the detailed resonance-to Maxwellian sensitivity is somewhat larger, and at end-of-exposure it is somewhat smaller.

PLUTONIUM RECYCLE SENSITIVITIES

The sensitivity code system has been modified extensively to analyze fuel cycles utilizing mixied oxide (MO_2) fuel or thorium fuel in fresh fuel loadings. Separate reference depletion calculations using LEOPARD account for different degrees of self-shielding vs. exposure. Sensitivities have been evaluated for plutonium recycle, i.e., cyles in which plutonium is loaded into the reactor as mixed oxide fuel. The cost of plutonium in the MO_2 was calculated from the consistent worth principle.[22] The core inventory for the BWR in this study consisted of 20% MO_2 fuel. The fuel enrichment of UO_2 was chosen to be 2.6% (a/o). The fissile content of the plutonium was set at 65% (a/o), about what is expected from recycle fuel of light water reactors. This MO_2 fuel thus consisted of natural uranium and plutonium in such a ratio that the overall fissile fraction is 2.8%.

The sensitivity of beginning-of-batch reactivity and end-of-cycle reactivity to thermal-group cross sections is illustrated in Table 4. In this case 20% of the core consisted of MO_2 and 80% UO_2. By comparison with conventional cycles, sensitivity to U-235 is reduced because it is no longer the only fuel present at the beginning-of-batch. Sensitivity to plutonium data is enhanced, particularly for Pu-241. The sensitivities to fuel cycle costs were also computed. Sensitivities to fuel cycle costs have a similar order of importance as the sensitivities to end-of-cycle infinite multiplication factor. This occurs because overall economics are influenced strongly by end-of-cycle conditions. Fuel cycle cost sensitivities for fertile materials are small, including both U-238 and Pu-240. Fuel cycle cost sensitivities can differ considerably depending on whether end-of-cycle criticality is maintained by enrichment of the uranium oxide fuel (the reference assumption) or by plutonium content in the mixed oxide fuel.

Table 4. Sensitivity of Beginning-of-Batch k and End-of-Cycle k to Thermal Group Cross-Sections

Thermal Cross Section	Equilibrium Thorium		Denatured Thorium		Mixed Oxide 20% Recycle	
	$\frac{\sigma\delta k_{BOE}}{k_{BOE}\delta\sigma}$	$\frac{\sigma\delta k_{EOC}}{k_{EOC}\delta\sigma}$	$\frac{\sigma\delta k_{BOE}}{k_{BOE}\delta\sigma}$	$\frac{\sigma\delta k_{EOC}}{k_{EOC}\delta\sigma}$	$\frac{\sigma\delta k_{BOE}}{k_{BOE}\delta\sigma}$	$\frac{\sigma\delta k_{EOC}}{k_{EOC}\delta\sigma}$
H (n,γ)	-.028	-.030	-.029	-.024	-.037	-.034
^{232}Th (n,γ)	-.153	-.065	-.131	-.052	—	—
^{233}Pa (n,γ)	.000	-.002	.000	-.001	—	—
^{233}U (n,γ)	-.014	-.031	-.015	-.023	—	—
^{233}U (n,f)	.087	.113	.086	.080	—	—
^{234}U (n,γ)	-.008	-.004	-.008	-.004	—	—
^{235}U (n,γ)	-.055	-.045	-.055	-.035	-.063	-.043
^{235}U (n,f)	.173	.106	.165	.088	.161	.113
^{238}U (n,γ)	∿ 0	∿ 0	-.009	-.001	-.080	-.036
^{239}Pu (n,γ)	—	∿ 0	—	-.044	-.075	-.145
^{239}Pu (n,f)	—	∿ 0	—	.053	.103	.179
^{240}Pu (n,γ)	—	∿ 0	—	-.001	-.019	-.002
^{241}Pu (n,γ)	—	∿ 0	—	-.006	-.013	-.035
^{241}Pu (n,f)	—	∿ 0	—	.009	.025	.048

THORIUM CYCLE SENSITIVITIES

Considerable interest has developed in the utilization of thorium in LWR fuel cycles, from the perspectives of utilization of thorium resources and of proliferation resistance. Fuel cycle cost sensitivities have been evaluated[8] for a basic thorium cycle[23] and for a denatured cycle related to the basic cycle. Thorium fuel cycle costs are less sensitive to U-235 data than are conventional fuel cycle costs, since U-235 constitutes only a portion of the fuel loaded in the thorium cycle. The sensitivities to fertile material data (thorium)

are smaller than sensitivities for fissile data because conversion to fissile material compensates for reactivity effects from the fertile material itself.

One interesting result in the denatured cycle is the influence of plutonium. Because of the reduced self-shielding of U-238 resonance capture, the epithermal capture cross section in U-238 in the denatured thorium cycle is substantially higher than in a conventional cycle, and fissile plutonium production still constitutes a significant factor. With one-eighth the amount of U-238, the denatured cycle leads to one-third the amount of plutonium of a conventional cycle. There is considerable sensitivity in the denatured cycle to the data for Pu-239. Indeed, Pu-239 sensitivities are comparable to those of U-233 and U-235. Thus, the presence of a modest amount of U-238 and the resulting buildup of plutonium have a significant influence on the economics of LWR fuel cycles using thorium.

The sensitivity of beginning-of-batch reactivity and end-of-cycle reactivity to thermal-group cross sections is illustrated in Table 4 for both thorium and denatured thorium cycles. Thorium and the fissile nuclides have the largest sensitivities. The sensitivities to end-of-cycle reactivity are sometimes larger than sensitivities to beginning-of-batch reactivity because some nuclides are building up. Thus, it is not a good idea to consider only sensitivities for beginning-of-batch conditions--such as for a clean critical assembly. End-of-cycle conditions are much more important from an economic standpoint.

SUMMARY

An interactive system has been developed at RPI to analyze the sensitivity of water reactor fuel cycle parameters and costs to uncertainties in nuclear data. Analyses of pressurized and boiling water reactors with recycle and throwaway options show substantial sensitivities of fuel cycle parameters and costs, particularly to thermal and resonance data for fissile nuclides. Neutron and energy yields per fission have very large sensitivities. The fact that sensitivities for fertile materials are much smaller than for fissile materials is a reflection of compensating effects. Increased absorption in fertile material (a reactivity penalty) leads to increased production of fissile material (a reactivity and economic gain). The results bring out the importance for power reactor sensitivity analysis of dealing with the full fuel cycle, as opposed to integral parameters at startup or in a critical assembly. Sensitivities to U-235 data for the thorium and mixed oxide fuel cycles are lower than in a conventional cycle, consistent with the reduction of U-235 in fuel loading. Overall economics are influenced strongly by end-of-cycle conditions. These methods and results should prove useful in setting priorities for experimental and analytical efforts aimed at the reduction of uncertainties in basic nuclear data.

ACKNOWLEDGMENT

This work was sponsored by the Electric Power Research Institute under Contract RP 975-4. The guidance of Dr. Odelli Ozer, EPRI Project Manager, is appreciated.

REFERENCES

1. D. R. Harris and M. Becker, "Nonlinear Perturbation Technique for the Nuclear Fuel Cycle," Trans. Am. Nucl. Soc. 23, 534 (1976).

2. M. Becker, D. R. Harris, J. Parillo, A. Parvez, and J. M. Ryskamp, "Fuel Cycle Sensitivity Analysis System for Light-Water Reactors," Trans. Am. Nucl. Soc. 24, 216 (1976).

3. J. M. Ryskamp, D. R. Harris and M. Becker, "Sensitivity of Light-Water Reactor Parameters to Uncertainties in Thermal Nuclear Data," Trans. Am. Nucl. Soc. 26, (1977).

4. A. Parvez, M. Becker, D. Boguslawski, D. R. Harris and J. M. Ryskamp, "Fuel Cycle Cost Sensitivity Analysis for Boiling and Pressurized Water Reactors," Trans. Am. Nucl. Soc. 27, 468 (1977).

5. A. Parvez, D. R. Harris and M. Becker, "Interactive Graphics Investigation of Relationships of Detailed Epithermal Data to Nuclear Fuel Cycle Cost," Trans. Am. Nucl. Soc. 27, 897 (1977).

6. M. Becker, D. R. Harris, A. Parvez, B. Quan, and J. M. Ryskamp, "Sensitivity of LWR Fuel Cycle Costs to Uncertainties in Nuclear Data," Proc. Topical Meeting on Advances in Reactor Physics, Gatlinburg, Tenn., April 10-12, 1978.

7. M. Becker, D. R. Harris, B. Quan and J. M. Ryskamp, "The Relationship Between Basic Nuclear Data and LWR Fuel Cycle Parameters," Proc. Topical Meeting on Nuclear Data Problems for Thermal Reactor Applications, Brookhaven National Laboratory, May 22-24, 1978.

8. A. Parvez, M. Becker, D. R. Harris, B. Quan, "Fuel Cycle Cost Sensitivity Analysis for LWR's Utilizing Thorium," Trans. Am. Nucl. Soc., 28, 385 (1978).

9. E. S. Amorim, J. M. Ryskamp, and B. K. Malaviya, "The Dependence of LWR Sensitivity Coefficients on the Macroscopic Spatial Flux Variation," Trans. Am. Nucl. Soc., 28, 766, (1978).

10. J. M. Ryskamp, M. Becker, and D. R. Harris, "Sensitivity of LWR Fuel Cycle Costs to Uncertainties in Detailed Thermal Cross-Sections," these proceedings.

11. S. Ramchandran, "Impact of the New LASL Delayed Neutron Data on FTR Design," Proc. Nat. Topical Meeting on New Developments in Reactor Physics and Shielding, Kiamesha Lake, New York, CONF-720901, p.660.

12. M. Danchak, W. R. Moyer and M. Becker, "The Rensselaer Interactive Graphics Analysis System," Trans. Am. Nucl. Soc. 18, 159 (1974).

13. R. F. Barry, "LEOPARD-A Spectrum Dependent Non-Spatial Depletion Code for the IBM-7094," Westinghouse Electric Corporation Report, WCAP-3269 (Sept. 1963).

14. C. F. Poncelet, "LASER, A Depletion Program for Lattice Calculations Based on MUFT and THERMOS," WCAP-6073 (1966).

15. A. Ahlin and M. Edenius, "The Collision Probability Module EPRI-CPM," Studsvik AB Atomenergi Sweden Report (1975).

16. T. R. England, W. B. Wilson and M. G. Stamatelatos, "Fission Product Data for Thermal Reactors, Part I, A Data Set for EPRI-CINDER Using ENDF/B-IV," EPRI NP-356 (1976).

17. P. F. Rose and T. W. Burrows, "ENDF/B Fission Product Decay Data," BNL-NCS-50545 (1976).

18. G. G. Joanou and J. S. Dudek, "GAM-II-a B_3 Code for the Calculation of Fast Neutron Spectra and Associated Multigroup Constants," Gulf General Atomics Report GA-4265 (1963).

19. W. R. Cadwell, "PDQ-7 Reference Manual," Westinghouse Electric Corporation Report WAPD-TM-678 (1967).

20. "Preliminary Safety Analysis Report, Montague Nuclear Power Station Units 1 and 2," (1974).

21. "Preliminary Safety Analysis Report, Greene County Nuclear Power Stations," (1975).

22. D. E. Deonigir, "The Value of Plutonium Recycle in Thermal Reactors," Nucl. Tech., 18, 80 (1973).

23. R. A. Matzie, J. R. Rec, "Practical Considerations in the Use of a Thorium Cycle in PWR's" Trans. Am. Nucl. Soc. 24, 220 (1976).

NONLINEAR MODEL FITTING OF THERMAL NEUTRON DATA AND ITS APPLICATION IN RESONANCE PARAMETER UNCERTAINTY ANALYSIS

J. K. Thompson
Battelle, Pacific Northwest Laboratories
Richland, Washington, U.S.A.

ABSTRACT

Nonlinear least-squares fitting techniques have been applied to experimental neutron data in the thermal region. Using theoretical forms derived from neutron-nucleus interaction theory formulated in terms of a common set of parameters, simultaneous fitting of all relevant data types may be accomplished. A formalism is established to harmonize data from divergent sources with a single stochastic model to satisfy the implicit assumptions of least-squares analysis. Following final parameter determination, rigorous statistical analysis of the residuals of the fit and the correlated parametric uncertainty fall out of nonlinear maximum-likelihood statistical theory. From the best-estimate parameters and their correlated uncertainty, one obtains not only best estimates of nuclear data but valid estimates of the uncertainty of the data. An example of the application of the formalism to ^{240}Pu data through the leV resonance is given.

INTRODUCTION

For almost two decades scientists have been attempting to develop an internally consistent set of thermal neutron data for the fissile and fertile isotopes because of their fundamental importance in the neutronic analysis of thermal fission power reactors. However, these persistent efforts have yielded only modest results, primarily due to inherent limitations of the methodological approach. Leonard, et al, have proposed(1) and demonstrated(2) an alternative approach for determining best-estimate thermal neutron data which is designed to avoid some of the previous limitations.

One of the key elements of this approach is an extremely powerful estimator of nonlinear parameters, a continually evolving computer code whose most recent generation is known as Resonance Parameter Fitting Code (RPFC). With this tool differential cross sections and ratios are simultaneously fitted to theoretical forms derived from neutron-nucleus interaction theory by iterative adjustment of the underlying physical parameters of the theoretical forms. A converged fit yields estimates of both the physical parameters of the theory and their correlated uncertainty matrix (the inverse of the covariance matrix).

With this information, the theoretical forms can be used within the energy range of the fit to predict not only the cross sections and ratios but valid measures of their uncertainty as well. Such information can be used in conjunction with the tools of sensitivity analysis to focus the attention of evaluators and experimenters on those nuclear data which most require it.

The focus of attention here will be the methodology employed in RPFC, and the underlying philosophy and motivation which have led to its current manifestation. The methodology has four distinct aspects:

- Modeling the data
- Estimating the parameters of the model
- Estimating the correlated parametric uncertainty
- Using the model for prediction of quantities of interest

A brief discussion of each of these elements demonstrates the essence of the methodology and provides the framework for critical appraisal of the philosophy and motivation of the methodology.

MODELING THE DATA

Experimental Theory

RPFC is essentially a nonlinear weighted-least-squares fitting code. As such its range of validity is restricted by the two implicit assumptions on the statistical nature of the data inherent to all least-squares analysis, viz:

- The data are not subject to significant systematic bias ($\hat{\underline{\mu}} = \mu$)
- All data are samples from a common population (σ^2 is a constant)

One further caveat concerning least-squares analysis is that a single flyer (datum "distant" from theory) can induce non-trivial local perturbations of the theory. If the data to be fitted do not meet the assumptions or exhibit flyers, the model used to describe the data must be formulated in such a way as to compensate for these deficiencies.

Unfortunately, experimental nuclear data may fail on all counts. Systematic bias may be induced by normalization errors or energy-scale errors. It is not uncommon for flyers to be present. Finally, due to differences in reporting by different experimenters, uncertainty measures, if they are reported at all, may reflect total uncertainties or only certain components of the total uncertainty. Hence, data from different experiments may exhibit widely disparate variances.

To minimize the effects of systematic bias, each data set is allowed three experimental parameters to adjust the normalization and energy-scale for those data within that data set. These parameters are not required; but if they are present, they are treated on a par with the theory parameters. An internal weight-adjustment scheme may be used to down-weight flyers and to balance the variances between data sets to satisfy the common population assumption. However, taking such liberties with reported data is not to be taken lightly, for it introduces a new set of complications. First, it forces one to work with an implicit relation between measurement and theory rather than the more common case of an explicit theory. Second, data which were in principle originally statistically independent are now correlated, and correlation introduces complexity in any statistical analysis. The first complication is merely one of mechanical detail and is readily dismissed. The second complication is actually an illusion. If the experimental parameters are statistically significant, the original data in fact were not statistically independent for they exhibited a common systematic bias. Indeed, the correlation is shifted from the measurement-space to the parameter-space, leaving the data essentially statistically independent. Furthermore, since the correlation effects are now contained in the parameter-space, a modest sophistication of the residuals analysis yields more rigorous results than could be obtained in the absence of experimental parameters.

Neutron-Nucleus Interaction Theory

The ultimate goal is to describe the thermal energy region nuclear interactions by fitting the experimental theory just described to analytic theoretical forms derived from neutron-nucleus interaction theory. By good luck, there are but a limited number of nuclear interactions of interest in the thermal range, all of which may be constructed from three fundamental theoretical forms (Table 1). A modified Adler-Adler formalism is used to describe fission and capture cross sections, while coherent, incoherent and total scattering are described by the multi-level Breit-Wigner formalism. Finally, an unnamed spin-dependent resonance formalism had to be invented to model data forms involving nu due to the evidence of energy-dependence of nu in the thermal energy range. Absorption and total cross sections and the ratios of interest may be constructed from these fundamental theoretical forms as shown in Table 2. Using the same construction logic, any theoretical form may be combined with any second theoretical form that does not involve nu in two-component sums and ratios. This feature allows simultaneous multi-isotope fitting when there exist data dependent upon two isotopes such as a limited purity sample with a single contaminant (e.g., ^{239}Pu with ^{240}Pu contaminant) or data measured relative to a standard with non-trivial shape uncertainty (e.g., $\sigma_f^{49}/\sigma_f^{25}$).

One of the primary reasons for choosing these theoretical forms is the commonality of physical theory parameters between forms. The whole purpose of performing simultaneous fitting would be lost were

TABLE 1. Fundamental Theoretical Forms

Modified Adler-Adler Formalism

$$\sigma_x(E)\sqrt{E} = \frac{\pi\hbar^2}{2M_n}\left[\sum_{r=1}^{NR}\frac{g_r\Gamma_{nr}\Gamma_{xr} + A_{xr}(E-E_r)}{(E-E_r)^2 + (\Gamma_r/2)^2} + \sum_{b=1}^{NB} Bx_b E^{b-1}\right]$$

$x = \gamma, f$

Multi-Level Breit-Wigner Formalism

$$\sigma_{coh}(E)/4\pi = [g_+b_+(E) + g_-b_-(E)]^2 + [g_+d_+(E) + g_-d_-(E)]^2$$

$$\sigma_{inc}(E)/4\pi = g_+g_-[(b_+(E) - b_-(E))^2 + (d_+(E) - d_-(E))^2]$$

$$\sigma_s(E)/4\pi = g_+[b_+^2(E) + d_+^2(E)] + g_-[b_-^2(E) + d_-^2(E)]$$

$$b_\pm(E) = R + \frac{\hbar}{\sqrt{8M_n}}\sum_{r=\pm}\frac{\Gamma^\circ_{nr}(E-E_r)}{(E-E_r)^2 + (\Gamma_r/2)^2}$$

$$d_\pm(E) = \frac{\hbar}{\sqrt{32M_n}}\sum_{r=\pm}\frac{\Gamma^\circ_{nr}\Gamma_r}{(E-E_r)^2 + (\Gamma_r/2)^2}$$

Spin-Dependent Resonance Formalism

$$\nu(E)\sigma_f(E)\sqrt{E} = \nu_+\sigma_f^+(E)\sqrt{E} + \nu_-\sigma_f^-(E)\sqrt{E} + \nu_b\sigma_f^b(E)\sqrt{E}$$

$$\sigma_f^\pm(E)\sqrt{E} = \frac{\pi\hbar^2}{2M_n}\sum_{r=\pm}\frac{g_r\Gamma^\circ_{nr}\Gamma_{fr} + A_{fr}(E-E_r)}{(E-E_r)^2 + (\Gamma_r/2)^2}$$

$$\nu_b = \lambda\nu_+ + (1-\lambda)\nu_- \qquad \nu_f^b(E)\sqrt{E} = \frac{\pi\hbar^2}{2M_n}\sum_{b=1}^{NB} B_{fb}E^{b-1}$$

NOTE: For all forms $\Gamma_r(E) = \Gamma_{fr} + \Gamma_{\gamma r} + \Gamma^\circ_{nr}\sqrt{E}$

TABLE 2. Combinations of Fundamental Theoretical Forms

Absorption

$$\sigma_a(E)\sqrt{E} = \sigma_f(E)\sqrt{E} + \sigma_\gamma(E)\sqrt{E}$$

Total

$$\sigma_t(E)\sqrt{E} = \sigma_a(E)\sqrt{E} + \sigma_s(E)\sqrt{E}$$

Alpha

$$\alpha(E) = \sigma_\gamma(E)\sqrt{E}/\sigma_f(E)\sqrt{E}$$

Eta

$$\eta(E) = (\nu(E)\sigma_f(E)\sqrt{E})/\sigma_a(E)\sqrt{E}$$

Nu

$$\nu(E) = (\nu(E)\sigma_f(E)\sqrt{E})/\sigma_f(E)\sqrt{E}$$

Sums*

$$S(E) = \lambda\sigma_x^z(E) + (1-\lambda)\sigma_{x'}^{z'}(E) \qquad \text{(possibly with } \sqrt{E} \text{ multiplier)}$$

Ratios*

$$R(E) = \sigma_x^z(E)/\sigma_{x'}^{z'}(E) \qquad \text{(possibly with } \sqrt{E} \text{ cancelling)}$$

*Sums and ratios may be formed with any theory from x for isotope z and any theory form x′ for isotope z′, except η and ν.

this commonality absent, for there would then be no competing constraints to compromise. Indeed, in some cases it is only through these competing constraints that some parameters are even marginally determinable. Furthermore, one can obtain indirect evidence of conflicting data when parameters become unphysical or exhibit large uncertainties due to these competing constraints.

The Parameters of the Model

Now that both the theory forms have been described, a complete list of the parameters can be tabulated (see Table 3). Obvisouly, in any real problem, the number of parameters could be fairly large. In general, the quality and quantity of data are inadequate to determine all of these parameters, especially due to the high degree of correlation between some of them. Furthermore, some of the parameters are generally known with fair accuracy from prior evaluations, and expediency demandsthat some use be made of this *a priori* knowledge. In RPFC there are two methods available by which this information can be used to limit the region of parameter-space to be searched. The first method is the trivial case of setting a parameter to a fixed constant, simply eliminating an entire dimension of parameter-space. In preliminary fitting in particular, where one may be interested in examining data for systematic bias, this option is very useful. Conversely, in the final stages of fitting, one would like to determine as many parameters as possible from the data alone, but subject to restricting the range of certain of the parameters to values which are physically plausible or which are demonstrably optimal from evidence of prior fitting. The second method allows one to do just that by treating a parameter estimate which has an associated uncertainty as a datum. Consequently, although the full dimensionality of the parameter-space is used, there are constraints which limit the freedom of parameter variation in some dimensions.

Summary of the Model

The description of data modeling is now complete. The data themselves are transformed via experimental theory to remove systematic bias attributable to normalization or energy-scale errors. Weight-adjustment may be used if necessary to satisfy the common variance assumption. A collection of theoretical forms derived from neutron-nucleus interaction theory based on a common set of physical parameters has been chosen to provide competing constraints in fitting the various data forms. There is arbitrary freedom in choosing which parameters are to be varied and which are to remain fixed in the fitting algorithm. Furthermore, any subset of the variable parameters may be constrained forcing each parameter in the subset to lie in the neighborhood of its *a priori* estimate. As each of these elements was introduced, the rationale involved was also discussed. That rationale is the essence of the methodology, for having prescribed a data model, all that remains of the methodology is mathematical technique. In nonlinear fitting, the exercise of parameter determination is not trivial, but it is still

TABLE 3. The Parameters of the Model

Theory Parameters for Each Isotope

Resonance Parameters		Non-Resonance Parameters	
E_r	Resonance Energy (eV)	B_{f1}, B^*_{f2}, B^*_{f3}	Coefficients of background, polynomials for fission and capture
Γ°_{nr}	Reduced Neutron width ($eV^{1/2}$)	$B_{\gamma 1}$, $B^*_{\gamma 2}$, $B^*_{\gamma 3}$	
Γ_{fr}	Fission width (eV)	R	Potential scattering radius ($b^{1/2}$)
$\Gamma_{\gamma r}$	Capture width (eV)	ν_+, ν_-, ν_b	Neutrons per fission in parallel-, anti-parallel-, and non-resonance fission respectively
A_{fr}	Fission asymmetry coefficient ($eV^{1/2}$)		
$A_{\gamma r}$	Capture asymmetry coefficient ($eV^{1/2}$)		

(g_r Input constant - statistical weight factor)

Experimental Parameters

N_s*	Normalization factor for sth data set
α_s*, β_s*	Energy-scale adjustment parameters for sth data set

$$E = E_m (\alpha_s + \beta_s \sqrt{E_m})$$

λ_s*	Composition parameter for sth data set, if applicable

* Indicates that parameter does not have to be present

simply a well-defined problem solvable by any of a broad class of techniques and hence contributes little to the methodological scheme.

ESTIMATING THE PARAMETERS OF THE MODEL

Nonlinear parameter estimation may be accomplished by any of myriad techniques outlined in its extensive literature, and, not being the central issue here, only those aspects of the particular technique used in RPFC germane to the ensuing statistical analysis will be touched upon here. For a discussion of the basic techniques see References 3, 4 and 5.

Recall that in the experimental theory of the model, to satisfy the common population assumption and to avoid local unphysical perturbations of the fit due to flyers, a scheme of weight alteration was introduced. As the weights are presumably inversely proportional to variances, and variances lie at the heart of statistical analysis, the key element of the parameter estimation algorithm from the viewpoint of statistical analysis is this weight alteration scheme. Weight alteration is optional in RPFC, and when elected may operate at two levels.

There is nothing subtle involved in the weight alteration scheme, but to demonstrate the algorithm, the foundation of the parameter estimation logic is required. The best-estimate parameters are that set of parameters which minimize the objective function, the inverse-variance weighted sum over all measurements of the squares of the residuals. Defining $Q(\underline{a})$ as the objective function, the minimization criteria are explicitly

$$\frac{\partial Q(\underline{a})}{\partial \underline{a}} = 0, \quad \frac{\partial^2 Q(\underline{a})}{\partial \underline{a} \partial \underline{a}} \text{ positive definite.} \tag{1}$$

Tables 4 and 5 define the construction of the objective function and its first two derivatives respectively, explicitly displaying the two level weighting scheme. The chain rule differentiation depicted in Table 5 cleanly divides the stochastic model from the physical theory model, a feature highly advantageous when physical theory modeling is accomplished with many theoretical forms. The stochastic model assumed is that of normally distributed residuals with zero mean and constant unknown variance. The essence of the weight alteration scheme is to force the data to satisfy the stochastic model, so that the eventual statistical analysis, which assumes the applicability of the stochastic model, is valid.

Keeping these thoughts well in mind, there is one more item to be considered in the construction of a weight alteration scheme: nonlinear parameter estimation, if it is to be successful, must proceed cautiously, always well under control. Hence, the idea to add to the thoughts above is, "THINK SMALL". Although by appeal to maximum-like-

TABLE 4. The Objective Function and its Constitutive Elements

$$Q(\underline{a}) = \sum_s W_s Q_s(\underline{a}) \qquad Q_s(\underline{a}) = \sum_{m \varepsilon s} Q_m(\underline{a})$$

$$Q_m(\underline{a}) = W_m(\underline{a}) \, [f_t^{\,m}(\underline{a}) - f_x^{\,m}(\underline{a})]^2$$

DATUM	$f_t^{\,m}$ (cf. TABLES 1 and 2)	$f_x^{\,m}$	W_m	
$\sigma_x^{\,m} \pm \delta\sigma_x^{\,m}$ @ E_m	$\sigma_x(E)\sqrt{E}$	$\sigma_x^{\,m} N_s \sqrt{E}$	$(\delta\sigma_x^{\,m} N_s \sqrt{E})^{-2}$	$x=f,\gamma,a,t$
$\sigma_x^{\,m} \pm \delta\sigma_x^{\,m}$ @ E_m	$\sigma_x(E)$	$\sigma_x^{\,m} N_s$	$(\delta\sigma_x^{\,m} N_s)^{-2}$	$x=coh,inc,s$
$R_m \pm \delta R_m$ @ E_m	$R(E)$	$R_m N_s$	$(\delta R_m N_s)^{-2}$	$R=\alpha,\eta,\nu$

NOTES: $E = E_m(\alpha_s + \beta_s\sqrt{E_m})$

m is the measurement index

s is the data set index

N_s is the normalization parameter for the sth data set (if absent, assume unity)

α_s, β_s are the energy-shift parameters for the sth data set (if absent, assume unity and zero respectively)

TABLE 5. Chain Rule Differentiation of the Objective Function

$$\frac{\partial Q(\underline{a})}{\partial \underline{a}} = \sum_s W_s \frac{\partial Q_s(\underline{a})}{\partial \underline{a}} = \sum_s W_s \sum_{m \varepsilon s} \frac{\partial Q_m(\underline{a})}{\partial \underline{a}}$$

$$\frac{\partial^2 Q(\underline{a})}{\partial \underline{a} \partial \underline{a}} = \sum_s W_s \sum_{m \varepsilon s} \frac{\partial^2 Q_m(\underline{a})}{\partial \underline{a} \partial \underline{a}}$$

$$\frac{\partial Q_m(\underline{a})}{\partial \underline{a}} = \frac{\partial Q_m(\underline{a})}{\partial \underline{M}_m(\underline{a})} \cdot \frac{\partial \underline{M}_m(\underline{a})}{\partial \underline{a}} \qquad \underline{M}_m(\underline{a}) \equiv (f_t{}^m(\underline{a}),\ f_x{}^m(\underline{a}),\ W_m(\underline{a}))$$

$$\frac{\partial^2 Q_m(\underline{a})}{\partial \underline{a} \partial \underline{a}} = \frac{\partial^2 Q_m(\underline{a})}{\partial \underline{M}_m(\underline{a})\ \partial \underline{M}_m(\underline{a})} : \frac{\partial \underline{M}_m(\underline{a})}{\partial \underline{a}} \frac{\partial \underline{M}_m(\underline{a})}{\partial \underline{a}} + \frac{\partial Q_m(\underline{a})}{\partial \underline{M}_m(\underline{a})} \cdot \frac{\partial^2 \underline{M}_m(\underline{a})}{\partial \underline{a} \partial \underline{a}}$$

lihood principles it is possible to estimate directly the variances to obtain new weights, to avoid changing the local conditions too much at once, it is better to change the weights a little at a time in such a way that in the limit the net result is the same as would be obtained via the maximum-likelihood formalism.

The weight alteration schemes outlined in Table 6 follow the "THINK SMALL" philosophy by establishing a figure of merit related to the maximum likelihood variance estimator for each weight under consideration and comparing that to an analogous figure of merit representative of all weights. In the comparison, the criteria for alteration are designed so that most weights are unchanged, and those that are changed are modified only to moderate their discrepancy from the stochastic model rather than eliminate the discrepancy entirely. It is possible to think of this process as fitting a theory of the variance (the stochastic model) while the simultaneous parameter estimation algorithm is fitting a theory of the mean. This heuristic device along with the empirical evidence that it works lend credence to the rather arbitrary methodology of weight alteration introduced here.

PARAMETRIC UNCERTAINTY AND RESIDUALS ANALYSIS

Termination of the parameter estimation logic yields a set of best-estimate parameters $\underline{\hat{a}}$ which satisfy equations (1) to some specific convergence tolerance as well as a set of effective data weights which satisfy the criteria of the stochastic model. Since the stochastic model assumptions are satisfied, it is possible to use the few derived (References 3 and 6) results from the largely uninvestigated realm of nonlinear statistics that are required here. First, the results concerning the parameters that are of interest are:

- $\underline{\hat{a}}$ is an unbiased estimator of the true parameters $\underline{A}$:

$$\langle \underline{\hat{a}} \rangle = \underline{A}$$

- The mean square correlated parametric uncertainty is given by $\langle \delta\underline{\hat{a}}\ \delta\underline{\hat{a}} \rangle = 2\hat{\sigma}^2 \left(\frac{\partial^2 Q(\underline{\hat{a}})}{\partial \underline{a} \partial \underline{a}} \right)^{-1}$, $\hat{\sigma}^2 = Q(\underline{\hat{a}})/DF$

The other result of nonlinear statistics that is used in RPFC is the determination of the probability that any particular datum would be fit with less error, i.e., the residuals analysis. Proper evaluation of this probability element requires untangling the complicated skein of data-parameter correlation. Table 7 shows the means whereby this probability is calculated. This quantitative assessment of the inherent datum quality helps to identify bad and marginal data.

TABLE 6. Weight Alteration Schemes

Data Weights

Figure of Merit

$$T_m = \sqrt{W_s Q_m}$$

Basis Figure of Merit

$$T^* = \text{Median}\ (\sqrt{W_s Q_m})$$

Algorithm:

$$\delta y_m' = \delta y_m,\ T_m < 2T^*$$

$$\delta y_m' = \delta y_m \sqrt{T_m/2T^*}\ ,\ T_m \geq 2T^*$$

$$W_m' \ \alpha\ (\delta y_m')^{-2}$$

Data Set Weights

Figure of Merit

$$T_s = W_s Q_s / DF_s$$

Basis Figure of Merit

$$T^* = \text{Average}\ (T_s)$$

Algorithm:

$$T_s' = T_s, \quad |T_s - T^*| < S^* = \text{Std. Dev.}\ (T_s)$$

$$T_s' = \sqrt{T_s T^*} \quad |T_s - T^*| \geq S^* = \text{Std. Dev.}\ (T_s)$$

$$R = \sum_s T_s / \sum_s T_s'$$

$$W_s' = R T_s' / (Q_s / DF_s)$$

TABLE 7. Probability of Less Error
(Adapted from Reference 3)

$$P(\psi_m' > \psi_m) = \int_{\psi_m}^{\pi/2} (\sin \psi_m')^{DF-1} d\psi_m' / \int_0^{\pi/2} (\sin \psi_m')^{DF-1} d\psi_m'$$

$$\cos^2\psi_m = [Q_m(\hat{\underline{a}}) - \delta^2 Q_m]/Q(\hat{\underline{a}})$$

$$\delta^2 Q_M = \underline{\underline{V}} : \underline{\underline{V}}^T$$

$$\underline{\underline{V}} = \frac{\partial^2 Q_m(\hat{\underline{a}})}{\partial \underline{M}_m \, \partial \underline{M}_m} \cdot \langle \delta \underline{M}_m \, \delta \underline{M}_m \rangle$$

$$\langle \delta \underline{M}_m \, \delta \underline{M}_m \rangle = \frac{\partial \underline{M}_m(\hat{\underline{a}})}{\partial \underline{a}} \cdot \langle \delta \hat{\underline{a}} \, \delta \hat{\underline{a}} \rangle \cdot \frac{\partial \underline{M}_m(\hat{\underline{a}})}{\partial \underline{a}}$$

PREDICTIONS OF THE MODEL

Two brief statements are now all that is necessary to conclude the methodological definition:

$$\langle f(\hat{\underline{a}}) \rangle = f(\underline{A}) + \frac{\partial^2 f(\hat{\underline{a}})}{\partial \underline{a} \partial \underline{a}} : \langle \delta \hat{\underline{a}} \delta \hat{\underline{a}} \rangle / 2 \tag{2}$$

$$\langle \delta f(\hat{\underline{a}}) \delta f(\hat{\underline{a}}) \rangle = \frac{\partial f(\hat{a})}{\partial \underline{a}} \cdot \langle \delta \hat{\underline{a}} \delta \hat{\underline{a}} \rangle \cdot \frac{\partial f(\hat{\underline{a}})}{\partial \underline{a}} \tag{3}$$

The first statement exhibits that, although the parameter estimates are unbiased, functional values estimated from those parameters are biased due to statistical resolution effects. Fortunately, for the theoretical forms of interest here, the bias is entirely negligible typically being several orders of magnitude smaller than the uncertainty, whose mean square value is given by (3).

AN EXAMPLE OF APPLICATION

Applications of SIGLEARN[5], the predecessor of RPFC, to ^{235}U[2] and ^{232}Th[7] have proven the basic formalism a useful tool to aid evaluation of thermal neutron data. Some preliminary analysis of ^{240}Pu thermal data provide a brief example of the application of RPFC in the same context. (This example is chosen to avoid an inordinately lengthy

discussion of the data base, which for ^{235}U contains more than 50 data sets.)

The thermal region in ^{240}Pu is dominated by the 1 eV resonance, but to accurately model the region a bound level and the 20 eV resonance were included in the fit with all parameters fixed, the bound level as a mirror image of the 20 eV resonance. The data base used in the studies include the capture data of Weston and Todd;[8] the total data of Leonard, et al.,[9] and Block;[10] and normalization points (see Table 9) for capture,[11] scattering[12] and fission.[13] The total data of Leonard through the resonance were corrected for Doppler broadening, and on advice from Leonard the energy scale was allowed to adjust. The capture data of Weston and Todd show evidence of ^{239}Pu contaminant and were fit as the sum of ^{240}Pu capture and ^{239}Pu cature with the impurity concentration of ^{239}Pu being an adjustable parameter. Both of these data sets, along with Block's total data, were allowed to renormalize. Furthermore, the data set weights of these three data sets were internally adjustable. This was especially important for the Weston and Todd capture data, since in the absence of measurement uncertainties, the data weights were arbitrarily set to correspond to a 5% data uncertainty with internal adjustment of the data weights allowed. The preliminary results of this data collection and data model are shown in Table 8.

TABLE 8. Preliminary Results of ^{240}Pu Data Analysis

		1 eV Resonance Parameters	
σ_t°	= 291.3 ± 1.64b	E_o	= 1.0594 ± .008 eV
σ_γ°	= 289.4 ± 1.63b	Γ_n°	= 2.451 ± .0026 meV/$\sqrt{eV}$
σ_s°	= 1.813 ± .060b	Γ_γ	= 29.72 ± .41 meV
		Γ_f	= 5.76 ± .60 μeV

1/V Capture Background at thermal is 10.4 ± 2.1b

Fitted ^{239}Pu σ_γ impurity in Weston and Todd data (.82 ± .09)%

TABLE 9. Absolute Data for ^{240}Pu Used for Normalization

	Datum	Fitted Value
σ_γ(.0253)	289.5 ± 1.4b	289.41 ± 1.63b
σ_s (.08)	1.54 ± .05b	1.537 ± .059b
σ_f PEAK	33 ± 3b	33.00 ± 3.55b

SUMMARY

The formalism of RPFC is a methodological improvement with concomitant enhancement of capabilities for simultaneous fitting of thermal neutron data from diverse sources, extending even to simultaneous fitting of several isotopes with interrelated data. This extension is made possible by incorporating into the methodology both an experimental theory which transforms all data to a common stochastic model and an analytic theory derived from neutron-nucleus interaction theory which is based on a common set of fundamental physical parameters. The common stochastic model allows rigorous statistical analysis of the estimated nonlinear parameters including the correlated parametric uncertainty, which establishes a direct link to the rapidly developing areas of sensitivity and uncertainty analysis. Via this connection, there is promise of improved understanding of the impact of data modifications which will enable the eventual development of an internally consistent best-estimate set of thermal neutron data for the fissile and fertile isotopes.

REFERENCES

1. B. R. Leonard, Jr., D. A. Kottwitz, U. P. Jenquin, K. B. Stewart and C. M. Heeb, "Cross-Section Standardization for Thermal Power Reactors," Electric Power Research Institute Report, EPRI 221 (July 1975).

2. B. R. Leonard, Jr., D. A. Kottwitz, J. K. Thompson, "Evaluation of the Neutron Cross Sections of ^{235}U in the Thermal Energy Region," Electric Power Research Institute Report, EPRI NP-167 (February 1976).

3. B. H. Duane, "Maximum Likelihood Nonlinear Correlated Fields (BNW Program LIKELY)," BNWL-390, Pacific Northwest Laboratories, September 1967), and

   G. D. Seybold, "Users Aid: Programs LEARN and LIKELY," BNWL-1057, Pacific Northwest Laboratories (May 1969), and

4. D. A. Kottwitz, "A Tandem Method for Finding Unconstrained Minima in Nonlinear Least-Squares Problems: Program LEARN-I-C," BNWL-1590, Pacific Northwest Laboratories (June 1971).

5. D. A. Kottwitz, "SIGLEARN: A Program for Simultaneous Least-Squares Fitting of Thermal Cross Sections and Related Ratios." Electric Power Research Institute Topical Report, EPRI NP-168 (February 1976).

6. Yonathan Bard, Nonlinear Parameter Estimation, Academic Press, 1974.

7. D. F. Newman, et al, "Evaluation of Temperature Coefficients of Reactivity for ^{233}U-Thorium Fueled HTGR Lattices," Electric Power Research Institute Report, EPRI NP-222 (May 1977).

8. L. W. Weston and J. H. Todd, "Neutron Capture Cross Section of Plutonium-240," NSE 63, 143 (1977)

9. B. R. Leonard, Jr., E. J. Sepp, and W. J. Friesen, "The Width of the 1 eV Resonance in Plutonium-240," NSE 5, 32 (1959).

10. R. C. Block, G. G. Slaughter, and J. A. Harvey, "Thermal Neutron Cross-Section Measurements of ^{233}U, ^{235}U, ^{240}Pu, ^{234}U, and ^{129}I with the ORNL Fast ChopperTime-of-Flight Neutron Spectrometer," NSE 8, 112 (1960).

11. M. Lounsbury, R. W. Durham, and G. C. Hanna, Proc. Conf. on Nuclear Data for Reactors, Helsinki, IAEA, 1, 287 (1970).

12. G. H. Lander and M. H. Mueller, "Coherent Scattering Amplitude of ^{240}Pu and ^{242}Pu," Acta Crystallographica/B, 27, 2284, (November 1971)

13. B. R. Leonard, Jr., E. J. Seppi, W. J. Friesen and E. M. Kinderman, "The Slow Neutron Fission Cross Section of ^{240}Pu," Bull. Am. Phys. Soc. II, 1, 248 (1956) and B. R. Leonard, Jr., and R. H. Odegaarden, USAEC Report HW-67219 (1960).

FISSION PRODUCT DECAY POWER AND UNCERTAINTIES AFTER REALISTIC REACTOR OPERATING HISTORIES

T.J. Trapp and B.I. Spinrad
Pacific Northwest Laboratory/OSU
Richland, Washington, USA

ABSTRACT

The major source of power in the first 0 to 10,000 seconds after shutdown in a LWR is the decay power of the fission products. The total decay power in LWR's results from fissions in ^{235}U, ^{238}U, ^{239}Pu, and ^{241}Pu. The fission rates of each nuclide were expanded in a series about the reactor shutdown. The contribution to the total decay power from the fission products of each fissionable nuclide was evaluated by analytically integrating the summation equations using the series expansion as the source term.

The uncertainties in the decay power must also be evaluated. The uncertainties in the decay power from each nuclide were evaluated by analytically propagating the uncertainties in the basic fission product yields and decay energies through the summation analysis into uncertainty estimates on the fission product decay power. Since the yields are constrained, a constrained variance analysis was used to reduce this component of the uncertainity. By expressing the calculated decay power from each fissioning nuclide as a ratio to the ^{235}U decay power, correlations between the energy uncertainties in the ratio were used to reduce the variance.

The decay power from a LWR and its associated uncertainty can be estimated by combining the ratios of decay power with the standard ^{235}U decay power and its uncertainty. Calculations show the actual decay power in LWR's is always less than the standard ^{235}U decay power with uncertainties of the same order of magnitude as the standard ^{235}U uncertainties.

INTRODUCTION

Energy is released in a nuclear reactor as a result of the fission process. Approximately 87% of the energy appears as kinetic energy of the fission fragments, of prompt γ-rays, and of prompt neutrons. The remaining 13% of the energy comes from the radioactive decay of the various fission products. Of this energy, approximately 4% is from β-particles, 3% from γ-rays, and 6% from neutrinos. The neutrinos escape from the reactor and deposit their energy in the far corners of

the universe. The beta and gamma energy is absorbed in the reactor.

Over one thousand fission products can result from a fission with half lives ranging from essentially 0 to thousands of years. A significant fraction of the energy released in their decay occurs at times long after the initiating fission event. After a reactor shutdown, the fission process will stop, but the fission products will continue to release energy.

In LWR, at the start of the irradiation the fission products result from fissions of ^{235}U and ^{238}U. As the irradiation progresses, the ^{238}U fission rate remains relatively constant, while the ^{235}U fission rate decreases. At the same time, neutron absorptions in ^{238}U produce ^{239}Pu and ultimately ^{241}Pu. As the ^{239}Pu and ^{241}Pu build up, their contribution to the fission rate and consequently the fission product power increases.

The decay power from ^{239}Pu is significantly less than that from ^{235}U, because the slightly lower neutron-to-proton ratio and the larger number of prompt neutrons emitted in ^{239}Pu fission, produce fission products which are, on the average, closer to beta stability. Moreover, since the average energy per fission is slightly larger for ^{239}Pu than ^{235}U, the fission product formation rate for a constant power will be slightly smaller for ^{239}Pu fissions which will tend to reduce the decay power from ^{239}Pu fissions even further.

The fission product decay power will be larger for ^{238}U then for ^{235}U, since the neutron to proton ratio is larger for ^{238}U.

A realistic assessment of the shutdown decay power must include the effects of the fission product production rates during reactor operation from all of the fissionable nuclides. In a typical LWR, these would include ^{235}U, ^{238}U, ^{239}Pu, and ^{241}Pu.

Figure 1 shows the relative decay powers of several fissionable nuclides after an infinite irradiation.

Summation Model

A fission product can result directly from fission, as a decay daughter of a fission product formed directly from fission, or both. The radioactive decay of each fission product is described mathematically by a first order differential equation which contains components accounting for both the production and depletion of the nuclide. This equation is generally called the Bateman equation, because of its initial derivation by H. Bateman[2] in 1910. Since fission products can be produced from the decay of other fission products a coupled set of equations must be solved.

After an instantaneous burst of fissions, the average concentrations per fission of the fission products in each mass chain are described by

FIGURE 1. The Ratio of the Decay Power From ^{239}Pu, ^{238}U, ^{241}Pu, and ^{233}U After an Infinite Irradiation to the ^{235}U Decay Power

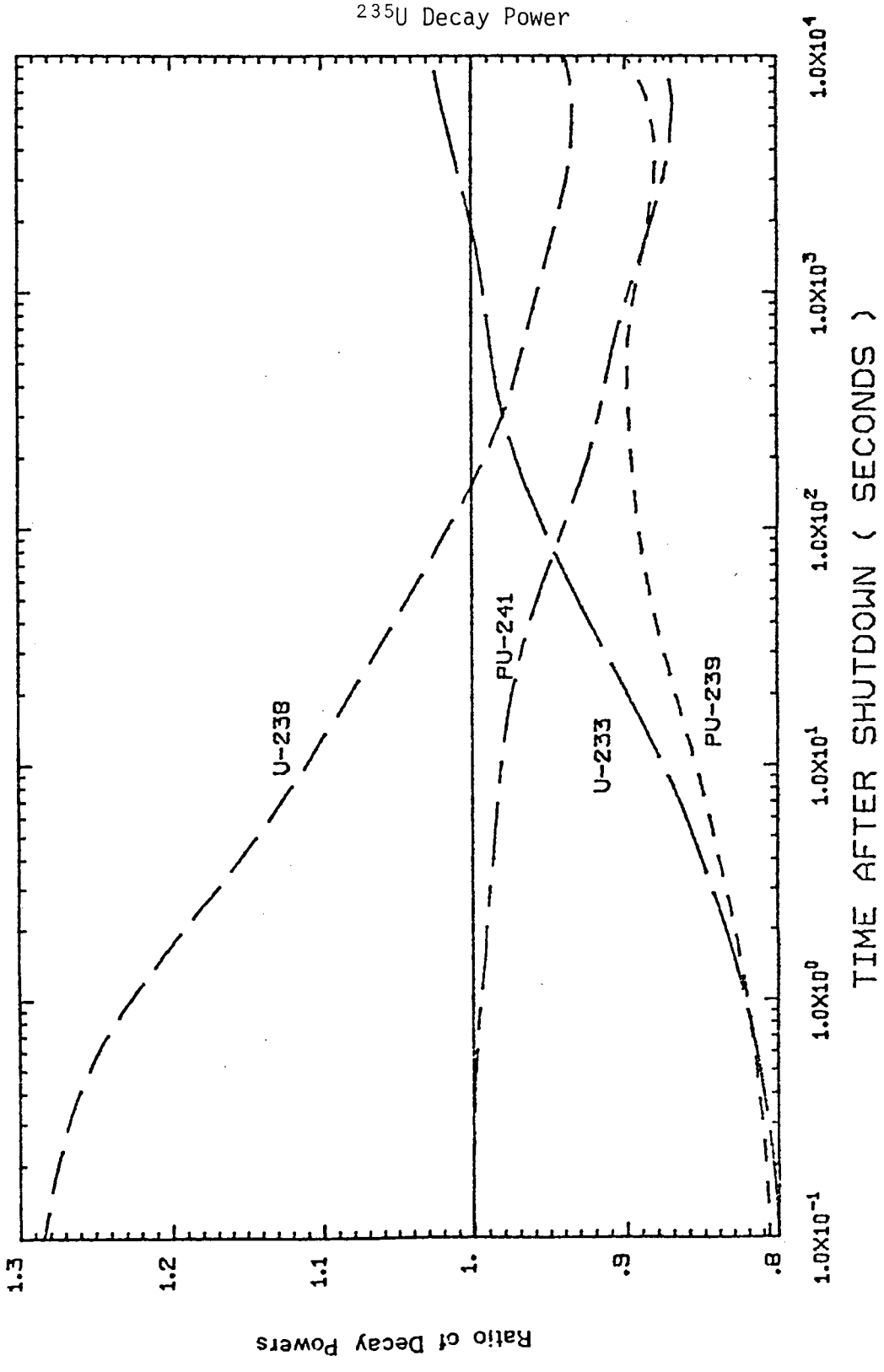

$$\frac{dN_{ij}(t)}{dt} = \sum_{k=1}^{i-1} \lambda_{kj} B_{ijk} N_{kj}(t) - \lambda_{ij} N_{ij}(t) \tag{1}$$

where

$N_{ij}(t)$ = the concentration of the ith fission product in the jth mass rope at time t.

j = the mass rope no. ordered such that the rope with smallest A number is 1.

i = the ith fission product in the jth mass rope. This is ordered such that the fission product with smallest Z number is 1.

t = time.

λ_{ij} = the decay constant for fission product i, j.

B_{ijk} = the branching ratio from fission product i, j to fission product k, j.

The initial conditions for this equation are

$$N_{ij}(t = 0) = y_j f_{ij}. \tag{2}$$

where

Y_j = the cumulative rope yield of the jth mass rope. This is normalized such that the sum of all the cumulative yields is 2.

f_{ij} = fractional independent yield of the ith fission product in the jth rope. This is normalized such that the sum of the fractional independent yields in each rope is 1.

This set of equations can be solved for each rope either by performing a direct integration of each equation or by a Laplace Transform of the system of equations. The average decay power from a single fission can be evaluated by weighting the average energy per decay with the activity and summing over all the fission products.

$$H(t) = \sum_{j=1}^{N} Y_j \sum_{k=1}^{M_j} f_{kj} \sum_{s=k}^{M_j} C_{sj} e^{-\lambda_{sj} t} \tag{3}$$

where

$$C_{sj} = \sum_{i=s}^{M_j} \lambda_{ij} E_{ij} A_{is}^{j} \tag{4}$$

and

$H(t)$ = the decay power at a time t after a fission pulse (MeV/fission-sec)

N = number of mass ropes

M_j = the number of nuclides in the jth rope

E_{ij} = the average sensible decay energy for a disintegration of the ith nuclide in the jth rope

The fission product shutdown decay power resulting from an irradiation period can be evaluated at any time after shutdown by integrating the contribution from each fission weighted by the fission rate over the reactor operating period. In general, there is no restriction on the fission rate.

In performing this analysis, a simplifying assumption has been made. This assumption is to ignore neutron capture in fission products in the equations for production and loss of radioactive nuclides. These captures greatly complicate the decay scheme which must be dealt with, and, furthermore, this effect can be easily parameterized and added in as a correction factor after the summation calculation.[3,4,5]

For a reactor which has operated from a time -T to 0 and then been shutdown for a time t, the decay power from a single fissionable nuclide, in the absence of neutron capture in the fission products is

$$H(t,T) = \sum_{j=1}^{N} Y_j \sum_{k=1}^{M_j} f_{kj} \sum_{s=k}^{M_j} C_{sj} g_{sj}(t,T) \tag{5}$$

where

$$g_{sj}(t,T) = e^{-\lambda_{sj} t} \int_{-T}^{0} R(\tau)\, e^{\lambda_{sj} \tau}\, d\tau \tag{6}$$

and

$H(t,T)$ = the decay power at time t due to the operation of a reactor for a time T.

$R(\tau)$ = the fission rate at a time τ during reactor operation for a single fissionable nuclide.

The total decay power is the sum of the decay powers from each fissionable nuclide. An evaluation of the best available experimental and calculated values for the decay power from ^{235}U after constant fission rate, no neutron capture irradiations has been made by Schenter, Schmittroth, and England.[6] This evaluation has been incorporated in a new standard[7] for fission product decay power. Formulations of the total decay power which use this standard represent a synthesis of all the available information on decay power. In addition to incorporating the standard values, it is also convenient to express the total decay power as a fraction of the operating power. A form which contains all of these features is

$$F(t,T) = \frac{H_s(t,\overline{T})}{\overline{P}} \sum_{i=1}^{N} \frac{H_i(t,T)}{H_{25}(t,\overline{T})} \tag{7}$$

where

$F(t,T)$ = the fraction of the operating power which is produced at time t after shutdown following an irradiation of length T.

$\overline{P}$ = the reference operating power.

$H_s(t,\overline{T})$ = the standard decay power from ^{235}U at a time t after a constant fission rate no neutron capture irradiation of length $\overline{T}$.

N = the number of fissionable nuclides.

If each of the decay powers in (7) is normalized to a unit fission rate and the reactor has operated at a constant power, the parameter P can be replaced by the average energy per ^{235}U fission. In other cases, a consistent definition of the reference power must be made.

Uncertainty Analysis

Evaluations of the decay power are in themselves useless, unless an estimate of the confidence in them can be made. Since the Bateman equations are known to describe radiactive decay very well, there is little question as to the adequacy of the basic model. The area in which the evaluation can be questioned is in how uncertainties in the basis nuclear data (sometimes very large) affect the final results. It is in this area, the propagation of the uncertainties in the basic nuclear data, where the summation technique has its greatest utility. If uncertainty estimates can be made for all of the basic nuclear data, these uncertainties can be propagated through the summation calculation directly into uncertainties of the decay power.

Uncertainties in the parameters arise because of the statistical uncertainties inherent in the measurements, or predictions from models of many physical parameters. The uncertainties are in the chain yields,[3] fractional independent yields, and the decay energies.[8] The uncertainties in the decay constants and branching ratios have not been considered. Schmittroth and Schenter[9] have estimated the effects of these uncertainties, and their results indicate those uncertainties tend to be small. This may not be the case at very short times after shutdown, when many of the important nuclides are not accessible to experiment.

In both the chain yields and the fractional independent yields, nature has been unusually gracious. The chain yields and independent yields are constrained such that

$$\sum_{i=1}^{N} Y_i = 2 \tag{8}$$

and

$$\sum_{k=1}^{M_i} f_{ki} = 1 \tag{9}$$

Instead of using the standard variance formulation, a constrained variance formulation can be used with a resulting decrease in the total variance of the function.[3]

The energy uncertainties are not bound to any absolute physical constraints. The decay energy uncertainties are composed of three separate components: an uncorrelated beta and an uncorrelated gamma decay energy uncertainty; and a correlated energy uncertainty. The uncorrelated uncertainties result from natural statistical variations in the experimental determination of parameters and from unbiased uncertainties in estimating decay energies from theoretical correlations and models. The correlated uncertainties result because of the possibility of a systematic bias in theoretically estimated parameters.

The variance in the decay power from a single fissionable nuclide due to the yields can be expressed as

$$\mathrm{Var}_y[\hat{A}(t,T)] = \sum_{i=1}^{N} \mathrm{Var}[Y_i] \left\{ \sum_{k=1}^{M_i} f_{ki} \sum_{s=k}^{M_i} C_{si} g_{si}(t,T) \right\}^2 - \frac{\left[\sum_{i=1}^{N} \mathrm{Var}[Y_i] \sum_{k=1}^{M_i} f_{ki} \sum_{s=k}^{M_i} C_{si} g_{si}(t,T) \right]^2}{\sum_{i=1}^{N} \mathrm{Var}[Y_i]} \tag{10}$$

$$+ \sum_{i=1}^{N} Y_i^2 \left\{ \sum_{k=1}^{M_j} \mathrm{Var}[f_{ki}] \left[\sum_{s=k}^{M_j} C_{si} g_{si}(t,T) \right]^2 - \frac{\left[\sum_{k=1}^{M_j} \mathrm{Var}[f_{ki}] \sum_{s=k}^{M_j} C_{si} g_{si}(t,T) \right]^2}{\sum_{k=1}^{M_j} \mathrm{Var}[f_{ki}]} \right\} \tag{10}$$

The variance due to decay energies can be written in the form

$$\mathrm{Var}_E[\hat{H}(t,T)] = \sum_{r=k}^{M_i} \mathrm{Var}_E[E_{ji}] \left\{ \lambda_{ri} \sum_{s=k}^{r} A_{rs}^{i} g_{si}(t,T) \right\}^2 + \sum_{r=k}^{M_i} \sum_{P=k}^{M_i} \left\{ \lambda_{ri} \sum_{s=k}^{r} A_{rs}^{i} g_{si}(t,T) \right\} \left\{ \lambda_{Pi} \sum_{s=k}^{P} A_{Ps}^{i} g_{si})t,T) \right\} \mathrm{cov}[E_{ri}, E_{Pi}] \tag{11}$$

The total variance with respect to energy is

$$\mathrm{Var}_E[E_{ri}] = \mathrm{Var}_U[E_{ri}]\, \mathrm{Var}_C[E_{Pi}] \tag{12}$$

and the covariance is

$$\mathrm{Cov}[E_{ri}, E_{Pi}] = \left(\mathrm{Var}_C[E_{ri}]\, \mathrm{Var}_C[E_{Pi}] \right)^{1/2} \tag{13}$$

where

$\mathrm{Var}_E[E_{rj}]$ = the total variance of E_{rj}

$\mathrm{Var}_C[E_{rj}]$ = the correlated component of the variance

$\mathrm{Var}_U[E_{rj}]$ = the uncorrelated component of the variance

Total Uncertainty

A confidence interval can be estimated for the decay power after an irradiation in which each nuclide fissions at a time varying rate if the variance in each of its components has been determined. The most useful form of the decay power on which to perform this analysis is the

form exhibited in (7). In this form, the uncertainties in the standard decay power form ^{235}U and the uncertainties in the operating power as well as the correlations between the calculated decay powers can all be included. The variance of this expression is

$$\mathrm{Var}[F(t,T)] = \left(\frac{H_s(t,\overline{T})}{\overline{P}}\right)^2 \left[\sum_{i=1}^{n} \mathrm{Var}[R_i] + \left(\sum_{i=1}^{n} R_i\right)^2 \left(\frac{\mathrm{Var}[H_{25}(t,T)]}{H_{25}(t,\overline{T})^2} + \frac{\mathrm{Var}[H_s(t,\overline{T})]}{H_s(t,\overline{T})^2} + \frac{\mathrm{Var}[\overline{P}]}{\overline{P}^2}\right)\right] \quad (14)$$

The variance in the standard decay power has been estimated.[7] The variance in the operating power consists of two components. The first component is due to uncertainties in the average energy per fission. The second component results from variations in the reactor power. These variations can result either from fluctuations in the actual power level or from an imprecise knowledge of the power level. Estimation of the variance which results from these fluctuations depends very strongly on external constraints which vary between different reactors.

The sources of the uncertainties in the ratio of decay powers is with one exception, completely correlated.[10,11] Any uncertainties in decay energy, half-life, or branching ratio of a fission product produce uncertainties in the decay power which are virtually the same, and in the same direction, as from a similar computation for ^{235}U. The exception is the statistical variation produced by uncertainties in fission product yields.

Differences in fission product yields would be expected to produce two types of uncertainties in the ratio of decay powers. The first uncertainity arises from the statistical variations of the yields which are uncorrelated between the two types of fission. The second uncertainty is a separate residual uncertainty in the decay power ratio due to differences in fission product yields. The decay powers have uncertainties arising from uncertainties in decay branching ratios, half-lives and decay energies Although these uncertainties for any given fission product are identical regardless of the source of fission, they are still a source of uncertainty, since the decay powers are yield-weighted.

If every uncertainty in ^{235}U decay power were matched by an equal uncertainty in the same direction, the ratios would be perfectly correlated, $\rho = 1$. Var(R) would be a small number. If the uncertainties were matched and always were in the opposite direction, the values would be perfectly anticorrelated, $\rho = -1$. Var(R) would be a maximum. If the uncertainties were completely uncorrelated then $\rho = 0$, and Var(R) would be the value conventionally assumed for the ratio of independent estimates.

The component of the uncertainty in the ratio of the decay powers due to the fission product yields will be uncorrelated. The component which results from the decay energies will be highly correlated.

The decay power functions can be represented as sums over decay energies weighted by functions of yields, half lives, and decay branching ratios. If the yields for each nuclide were the same, the partial uncertainties in the decay power functions due to decay energy uncertainties would be perfectly correlated. However, the yields for the two types of fissions are not the same, and hence the uncertainties will not be perfectly correlated. The energy uncertainties should nevertheless be highly correlated since the decay power at any time is dominated by only a few fission products.

The correlation coefficient is, by definition,[12]

$$\rho_i = \frac{\mathrm{Cov}_e[{}^{25}H,\ {}^{i}H]}{\sqrt{\mathrm{Var}[{}^{25}H]\ \mathrm{Var}[{}^{i}H]}} \tag{15}$$

where Cov_e refers to covariance due to correlations in decay energy uncertainties.

This covariance can be calculated by noting that each decay power is of the form

$${}^{i}H = \sum_j {}^{i}A_j\ E_j \tag{16}$$

where the ${}^{i}A_j$ are the activities of the fission products and the sum extends over all the fission products. Then, the covariance becomes

$$\mathrm{Cov}_e[{}^{25}H,\ {}^{i}H] = \sum_j \sum_k {}^{25}A_j\ {}^{i}A_j\ \mathrm{Cov}[E_j,\ E_k] \tag{17}$$

Each decay energy has two components to its uncertainty[8]. One component is uncorrelated, and is due to an unbiased imprecision in measuring or estimating each value. The other component is correlated due to the possibility of systematic biases in the theoretical models used to estimate some of the decay energies. The uncorrelated covariances are non-zero only when j = k, whereas the correlated component shows perfect correlation for all j, k combinations for which the correlated uncertainties in decay energies are non-zero. With this the covariance can be calculated in terms of evaluated parameters as

$$\mathrm{Cov}_e[{}^{25}H,\ {}^{i}H] = \sum_j \sum_k {}^{25}A_j\ {}^{i}A_k \sqrt{\mathrm{Var}_c[E_j]\ \mathrm{Var}_c[E_k]} + \sum_j {}^{25}A_j\ {}^{i}A_j\ \mathrm{Var}_u[E_j] \tag{18}$$

where Var_c and Var_u are the correlated and uncorrelated variances of the decay energies, respectively.

In order to determine the total variance of the decay power, a component due to flucuations in operating power must be included. These fluctuations are almost exclusively uncertainties in the absolute normalization of the reactor's power. This normalization uncertainty is an intrinsic parameter of each reactor. As an example[11] of this effect, Table 1 displays the percent uncertainty in the decay power from a BWR with standard deviations due to power fluctuations of 0%, 1%, 3%, 5%, and 10%. The magnitude of this effect can be seen by comparing the column with 0. variance due to operating power with the other columns in the table. At the larger standard deviations, the variance in the operating power dominates the uncertainty.

Even though fission product neutron capture is a small effect, it must be included in the final analysis of decay power. Neutron captures cause more decay energy to be liberated than would have been relased if the captures had not occurred. This results because a neutron capture creates a daughter nuclide which is on the average further from beta stability. The daughter nuclide requires more decays to reach beta stability, increasing the amount of energy liberated.

The effect of neutron capture has bene estimated by Spinrad and Tripathi.[5] Since it is a small change in the decay power a conservative estimate was made of the maximum addition to the decay power at irradiation times characterized by the integrated number of fissions. Table 2 shows the maximum decay power from a typical LWR with the effect of neutron captures included in the values.

For fission rates characteristic of LWR's the actual decay power is less than the standard ^{235}U decay power. The size of this reduction ranges from a minimum of about 0.8% at shutdown in a 3.5 wt% enriched LWR to a maximum of about 12% after 10,000 seconds of decay time. In the critical 10 to 100 second time span for LOCA evaluations, the reduction ranged between 3% and 5%.

REFERENCES

1. T.J. Trapp, S.M. Baker, A.W. Prichard, and B.I. Spinrad, "ROPEY, A Computer Code to Evaluate Reactor Fission Product Shutdown Decay Heat and Its Uncertainty," OSU-NE-7701, Oregon State University, Nuclear Engineering Department, August, 1977.

2. H. Bateman, "Solution of a System of Differential Equations Occuring in the Theory of Radioactive Transformations," Proc. Cambridge Phil. Soc., 15, 423 (1910).

TABLE 1. The Effect of Uncertainties in the Operating Power on Uncertainties in the Decay Power for a BWR

Decay Time (seconds)	Total Decay Power Percent Uncertainties				
	0*	1	3	5	10
0.	3.8	3.9	4.8	6.3	10.7
1.00E-01	3.8	3.9	4.8	6.3	10.7
1.50E-01	3.7	3.9	4.8	6.2	10.7
2.00E-01	3.7	3.9	4.8	6.2	10.7
3.00E-01	3.7	3.8	4.8	6.2	10.7
4.00E-01	3.7	3.8	4.8	6.2	10.7
6.00E-01	3.7	3.8	4.8	6.2	10.7
8.00E-01	3.7	3.8	4.7	6.2	10.7
1.00E+00	3.7	3.8	4.7	6.2	10.6
1.50E+00	3.1	3.3	4.3	5.9	10.5
2.00E+00	2.8	3.0	4.1	5.7	10.4
3.00E+00	2.7	2.9	4.1	5.7	10.4
4.00E+00	2.6	2.8	4.0	5.7	10.3
6.00E+00	2.5	2.7	3.9	5.6	10.3
8.00E+00	2.4	2.6	3.9	5.6	10.3
1.00E+01	2.4	2.6	3.9	5.6	10.3
1.50E+01	2.3	2.5	3.8	5.5	10.3
2.00E+01	2.3	2.5	3.8	5.5	10.3
3.00E+01	2.3	2.5	3.8	5.5	10.3
4.00E+01	2.2	2.4	3.7	5.4	10.2
6.00E+01	2.1	2.4	3.7	5.4	10.2
8.00E+01	2.1	2.3	3.7	5.4	10.2
1.00E+02	2.1	2.3	3.7	5.4	10.2
1.50E+02	2.1	2.3	3.7	5.4	10.2
2.00E+02	2.1	2.3	3.7	5.4	10.2
3.00E+02	2.1	2.3	3.7	5.4	10.2
4.00E+02	2.1	2.3	3.6	5.4	10.2
6.00E+02	2.1	2.3	3.6	5.4	10.2
8.00E+02	2.1	2.3	3.6	5.4	10.2
1.00E+03	2.1	2.3	3.6	5.4	10.2
1.50E+03	2.1	2.3	3.6	5.4	10.2
2.00E+03	2.1	2.3	3.6	5.4	10.2
3.00E+03	2.1	2.3	3.6	5.4	10.2
4.00E+03	2.1	2.3	3.6	5.4	10.2
6.00E+03	2.0	2.2	3.6	5.4	10.2
8.00E+03	2.0	2.3	3.6	5.4	10.2
1.00E+04	2.0	2.3	3.6	5.4	10.2

* Percent Uncertainty in Operating Power

TABLE 2. The Reduction in the Standard ^{235}U Decay Power for LWR's

Decay Time (seconds)	Standard ^{235}U Decay Power	% Reduction in Decay Power for LWR's without neutron capture	with neutron capture	Total Uncertainty (%)
0.	6.58	1.9	1.6	3.8
1.00E-01	6.51	2.0	1.7	3.8
1.50E-01	6.48	2.0	1.8	3.7
2.00E-01	6.45	2.1	1.8	3.7
3.00E-01	6.40	2.2	1.9	3.7
4.00E-01	6.36	2.2	1.9	3.7
6.00E-01	6.27	2.4	2.1	3.7
8.00E-01	6.20	2.4	2.1	3.7
1.00E+00	6.12	2.5	2.2	3.7
1.50E+00	5.96	2.6	2.3	3.1
2.00E+00	5.81	2.9	2.6	2.8
3.00E+00	5.58	3.1	2.8	2.7
4.00E+00	5.39	3.2	2.9	2.6
6.00E+00	5.10	3.5	3.2	2.5
8.00E+00	4.89	3.6	3.3	2.4
1.00E+01	4.73	3.8	3.4	2.4
1.50E+01	4.42	4.0	3.6	2.3
2.00E+01	4.21	4.1	3.8	2.3
3.00E+01	3.92	4.4	4.1	2.3
4.00E+01	3.72	4.6	4.2	2.2
6.00E+01	3.43	5.0	4.6	2.1
8.00E+01	3.24	5.2	4.8	2.1
1.00E+02	3.09	5.4	5.0	2.1
1.50E+02	2.84	5.7	5.3	2.1
2.00E+02	2.68	6.0	5.6	2.1
3.00E+02	2.47	6.4	6.0	2.1
4.00E+02	2.33	6.6	6.2	2.1
6.00E+02	2.14	7.1	6.6	2.1
8.00E+02	2.00	7.4	6.9	2.1
1.00E+03	1.89	7.7	7.2	2.1
1.50E+03	1.70	8.4	7.9	2.1
2.00E+03	1.57	9.0	8.4	2.1
3.00E+03	1.38	9.7	9.0	2.1
4.00E+03	1.27	10.4	9.6	2.1
6.00E+03	1.12	11.3	10.1	2.0
8.00E+03	1.02	11.6	10.2	2.0
1.00E+04	.96	12.1	10.6	2.0

3. B.I. Spinrad, "The Sensitivity of Decay Power to Uncertainties in Fission Product Yields," Nucl. Sci. Eng., 62, 35-44 (1977)

4. M. R. Shay, "Summation Evaluations of Reactor After-Heat Including the Effects of Neutron Capture in Fission Products," Master's Thesis, Oregon State University, August, 1976.

5. B.I. Spinrad and A. Tripathi, "Modeling the Effect of Fission Product Capture on Reactor Decay Power," Nucl. Sci. Eng., 68, 140-141 (1978).

6. T.R. England, M.G. Stamatelatos, R.E. Schenter, and F. Schmittroth, "Fission Product Source Terms for Reactor Applications," LA-NUREG-6917-MS (1977).

7. Proposed Revised ANS Standard, "Decay Heat Power in Light Water Reactors," November 1977.

8. S.M. Baker, "The Contribution of Fission Product Decay Energy Un-Certainties to Uncertainties in Calculated Reactor Decay Power," Master's Thesis, Oregon State University, May 1977.

9. F. Schmittroth and R.E. Schenter, "Uncertainty Analysis of Fission Product Decay Heat Summation Methods," Nucl. Sci. Eng., 59 pp. 117-139 (1976).

10. T.J. Trapp and B.I. Spinrad, "Estimation of Decay Heat From ^{239}Pu Thermal Neutron Fission by Comparison with ^{235}U Decay Heat," OSU-NE-7801, Department of Nuclear Engineering, OSU (1978) and Nucl. Sci. Eng. (to be published).

11. T.J. Trapp, "The Effect of the Depletion and Buildup of Fissile Nuclides and of ^{238}U Fast Fissions on Fission Product Decay Power," PhD. Thesis (1978).

12. A.M. Mood, F.A. Graybill, and D.C. Boes, Introduction to the Theory of Statistics, McGraw-Hill (1974).

TESTING OF ENDF/B CROSS SECTION DATA IN THE CALIFORNIUM-252 NEUTRON BENCHMARK FIELD

W. Mannhart
Physikalisch-Technische Bundesanstalt
D-3300 Braunschweig, FR Germany

ABSTRACT

The fission neutron field of Cf-252 presently represents one of the most well-known neutron benchmark fields. For 13 neutron reactions which are of importance in reactor metrology, measurements of spectrum-averaged cross sections, $\langle\sigma\rangle$, performed in this neutron field were compared with calculated average cross sections. This comparison allows to draw conclusions as to the quality of different $\sigma(E)$-data taken from ENDF/B-IV, ENDF/B-V* and from recent experiments and used in the calculation of average cross sections. The comparison includes an uncertainty analysis regarding the different uncertainty contributions of $\langle\sigma\rangle$, $\sigma(E)$ and of the spectral distribution of Cf-252 fission neutrons. Additionally, in a few examples, sensitivity studies were carried out. The sensitivity of the spectrum-averaged cross sections to individual characteristics of the $\sigma(E)$-data, such as normalization factors or shifts in the energy scale, was investigated. Similarly the sensitivity of $\langle\sigma\rangle$ to the spectral distribution of Cf-252 was determined.

INTRODUCTION

In nuclear design calculations the accuracy strongly depends on the uncertainty of both computational models and nuclear cross section data. For core and shield design of fast reactors or fusion reactors, for example, an almost direct relation between the uncertainty of calculations and financial cost is given. Therefore, in recent years much effort has been concentrated on improving the accuracy. With refined computational methods, the main source of uncertainty is now due to the neutron cross section data. A usual attempt to deduce quantitative decisions as to the quality of cross section data is to compare measurements of integral parameters, such as neutron multiplication or reactivity, with calculated results. Apart from the problem of solving the neutron transport equation for a complex system, the aforementioned procedure raises problems with regard to the attribution of uncertainties to individual cross sections.[1]

*It should be understood that the official ENDF/B-V Dosimetry File had not been released at the time this paper was prepared. The data considered are preliminary ENDF/B-V and may not be the same as those which will be in the official ENDF/B-V release.

A similar situation is given in the field of reactor dosimetry. The development of accurate and reliable reactor dosimetry techniques is of no minor importance because safety-related and economic questions such as the durability of reactor pressure vessels or the fuel cycle management are included. The topic of reactor dosimetry may be described by the measurement of reaction rates of neutron dosimetry monitors in more or less well-known neutron fields and the subsequent correlation of these data with quantities such as neutron flux density, fluence, burn up, damage rates etc. In the development of a measuring technique which can be applied for power reactors during routine operation, the verification of the measuring methods in neutron benchmark fields is a useful intermediate stage. Such benchmark fields must have a high degree of reproducibility and well-known spectral properties. In addition, they should be of a structural simplicity to facilitate the interpretation of experimental results by calculation. The credibility of the above-mentioned quantities derived from reaction rates measured in such benchmark fields mainly depends on the validity of the neutron cross sections used in the correlation procedure. Today, neutron benchmark fields are therefore mainly used for the validation and improvement of the neutron cross section data base.

The spontaneous fission neutron field of Cf-252 was recently classified as belonging to the best-known neutron benchmark fields, called "Standard Neutron Fields".[2] In these standard neutron fields, the consistency between measured spectrum-averaged cross sections and those calculated by forming the integral over the energy-dependent cross section data weighted with the well-known spectral distribution, briefly called "folding", is a valuable indication that the energy-dependent cross section data are correct. In such a consistency test of neutron cross section data, it is of course desirable to use benchmark fields with neutron spectra resembling those of power reactors. However, such benchmark fields as, for example, ΣΣ, CFRMF or Big-10[3] presently show a poorer consistency between measured and calculated reaction rates.[4] Moreover, it becomes difficult to decide which inconsistencies are due to neutron cross section data or due to uncertainties in the neutron spectrum.

AVERAGE CROSS SECTIONS IN THE NEUTRON FIELD OF CALIFORNIUM-252

The decision on the quality of energy-dependent cross section data, $\sigma(E)$, is based on the agreement between measured average cross sections, $\langle\sigma\rangle_M$, and those obtained by calculation:

$$\langle\sigma\rangle_C = \int_0^\infty \sigma(E)\ \chi_{82}(E)\ dE \qquad (1)$$

$\chi_{82}(E)$ being the normalized spectral distribution of the Cf-252 fission spectrum. In comparing both measured and calculated average cross sections, three independently measured quantities appear: the average

cross section, the spectral distribution and the energy-dependent cross section. To obtain a fair consistency, all these quantities have to be determined as well as possible.

Measurements

The measurement of <σ> requires a careful activity measurement and the determination of the neutron flux density. The problem of the neutron flux density determination, in particular, becomes simpler in the case of Cf-252 than in other benchmark fields and can be related to a neutron source strength measurement (using a manganese bath or waterbath method). For a lot of neutron reactions average cross sections in the Cf-252 neutron spectrum have been determined.[5-14] A systematic list of the results is given elsewhere.[15] The most accurate <σ>-measurements were done for fission reactions at the NBS[5,6] and for non-fission reactions at the PTB.[8,9]

Calculations

Average cross sections were calculated for all neutron reactions measured at the PTB.[8,9] In this calculation the spectral distribution of Cf-252 neutrons was folded, analogous to eq. 1, using various σ(E)-data. Details of the calculation procedure have been described elsewhere.[15] Only the input parameters of the numerical integration procedure will be discussed now.

Spectral distribution $\chi_{82}(E)$

The best description, now available, of the fission spectrum of Cf-252 is an evaluation by Grundl and Eisenhauer.[16] The evaluation is based on eight documented[17] spectrometry experiments. The spectral distribution of Cf-252 is described by a reference Maxwellian of an average energy of 2.13 MeV corresponding to a temperature parameter of kT = 1.42 MeV and five continuous segment corrections to the reference Maxwellian. In fig. 1, the result of this evaluation (indicated as $\chi_{82}^{NBS}(E)$) is plotted relative to a pure Maxwellian with kT = 1.42 MeV. The uncertainty of this evaluation (quoted at the 1σ-level) is: ± 13 % for neutron energies below 0.25 MeV, about ± 2 % between 0.25 and 8.0 MeV, and about ± 10 % between 8.0 and 20 MeV.[3]

σ(E)-data

In the calculation of average cross sections, different sets of σ(E)-data were used. The data were taken from the "Evaluated Nuclear Data File" ENDF/B-IV,[18] from Preliminary ENDF/B-V[19-21] and from recent experiments[22,23] as far as the experiment covers the total response range of a reaction in the Cf-252 fission spectrum.

It is obvious that the evaluation of neutron cross sections can-

not be better than the different σ(E)-measurements on which the evaluation is based. The crucial point in σ(E)-measurements lies in the accuracy of the neutron flux density determination. As discussed elsewhere,[2] an uncertainty of ± 5 % for σ(E)-measurements seems to be the possible lower limit which can be obtained at present. Another important point is the completeness of the nuclear cross section data base. For neutron reactions used as activation detector reactions, the energy range of importance is the range of detector response in a fission field. For threshold reactions, this energy range lies between the reaction threshold and about 6 MeV above it. Older σ(E)-measurements in particular fail to cover this energy range; they are concentrated near threshold and between 13 and 15 MeV with a typical gap between 6 and 12 MeV. Only recently it became possible to fill up this data gap, in particular, by using improved accelerator techniques.

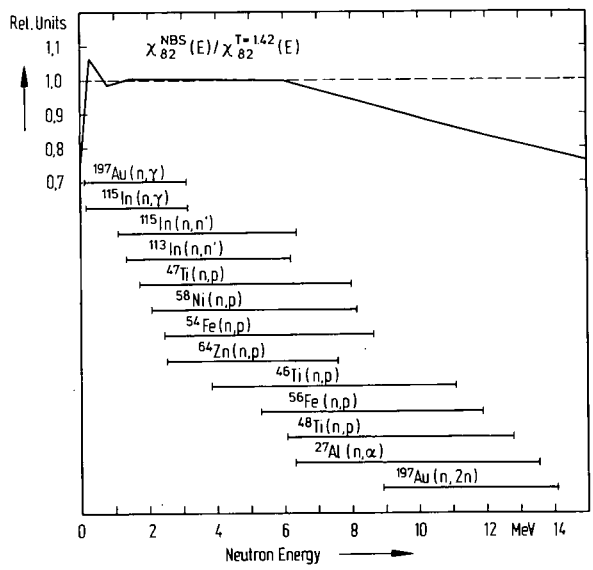

Fig. 1. Ratio of the Analytical Spectral Distribution to a Pure Maxwellian with kT = 1.42 MeV. Solid Lines indicate the Energy Range of 90 %-Response in the Fission Spectrum of Cf-252

Comparison between Measurement and Calculation

The data of this comparison are summarized in table 1. In column 1 of table 1, the neutron reactions under consideration are listed and arranged in the order of the energy ranges of 90 %-response in the Cf-252 fission spectrum as indicated by solid lines in fig. 1. Reactions classified as category I are those for which the cross section is believed to be well-known over the energy response range in standard neutron fields and for which calculated and measured reaction rates in different fields are consistent. In the unfolding of reactor spectra it is recommended to use only these category I reactions.[2]

In column 2 of table 1, the measured average cross sections and their uncertainties (1σ-level) are given. In columns 3 - 5 the calculated average cross sections are listed obtained by folding different σ(E)-data with the above-mentioned spectral distribution. The σ(E)-data of ref. 22 of the reactions In-115(n,n') and In-113(n,n') were recalculated, the reason being that in the radioactivity determination of the σ(E)-measurements[22] other values have been used for the gamma

Table 1: Comparison between measured ($\langle\sigma\rangle_M$) and calculated ($\langle\sigma\rangle_C$) average cross sections (in mb) in the ^{252}Cf fission neutron spectrum. Category I reactions are underlined and candidates of cat. I reactions are indicated by a broken line

Reaction	$\langle\sigma\rangle_M$ ref. /8,9/	$\langle\sigma\rangle_C$ This work			$\langle\sigma\rangle_M/\langle\sigma\rangle_C$		
		σ(E)-data from:					
		ENDF/B-IV+	ENDF/B-V*	other	ENDF/B-IV	ENDF/B-V*	other
^{197}Au(n,γ)	76.2 ± 1.8	79.91	76.50 a)		0.954 ± 0.047(0.069)	0.996 ± 0.047(0.069)	
^{115}In(n,γ)	124.1 ± 3.6	130.3			0.952 ± 0.043(0.109)		
^{115}In(n,n')	195 ± 5	175.5	181.9 b)	183.0 d)§	1.111 ± 0.033(0.105)	1.072 ± 0.033(0.096)	1.066 ± 0.033(0.077)
^{113}In(n,n')	160 ± 4			141.5 d)§			1.131 ± 0.033(0.077)
^{47}Ti(n,p)	18.9 ± 0.4	23.85	24.06 c)		0.793 ± 0.032(0.105)	0.786 ± 0.032(0.077)	
^{58}Ni(n,p)	118 ± 3	115.0		113.0 e)	1.026 ± 0.035(0.106)		1.044 ± 0.034(0.078)
^{54}Fe(n,p)	84.6 ± 2.0	89.09		85.58 e)	0.950 ± 0.034(0.106)		0.989 ± 0.033(0.077)
^{64}Zn(n,p)	39.4 ± 1.0			37.31 e)			1.056 ± 0.034(0.078)
^{46}Ti(n,p)	13.8 ± 0.3	12.52	13.46 c)		1.102 ± 0.040(0.108)	1.025 ± 0.040(0.080)	
^{56}Fe(n,p)	1.450 ± 0.035	1.476			0.982 ± 0.057(0.076)		
^{48}Ti(n,p)	0.42 ± 0.01	0.2653	0.4092 c)		1.584 ± 0.074(0.124)	1.026 ± 0.071(0.099)	
^{27}Al(n,α)	1.006 ± 0.022	1.059			0.950 ± 0.076(0.091)		
^{197}Au(n,2n)	5.50 ± 0.14	5.037*	5.646 a)		1.092 ± 0.103(0.144)	0.974 ± 0.103(0.144)	

\+ ENDF/B-IV Tape 412 a) ref. /19/ c) ref. /21/ e) ref. /23/

* ENDF/B-IV Tape 411 b) ref. /20/ d) ref. /22/

§ σ(E)-data renormalized; see text

* It should be understood that the official ENDF/B-V Dosimetry File had not been released at the time this paper was prepared. The data considered are preliminary ENDF/B-V and may not be the same as those which will be in the official ENDF/B-V release.

emission probability than in the <σ>-measurement.[9] The σ(E)-data were renormalized to the more reliable emission probabilities used in ref. 9. This shows that in such comparisons one has to check carefully whether the data to be compared were determined under the same conditions.

The criterion of consistency between measured and calculated average cross sections is expressed by the ratio $\langle\sigma\rangle_M/\langle\sigma\rangle_C$ given in the last columns of table 1. In order to get an impression as to which consistency is valid, the uncertainty of this ratio was also calculated. The quoted uncertainty comprises the uncertainty of the <σ>-measurement and of the spectral distribution, $\chi_{82}(E)$. As $\langle\sigma\rangle_M$ and $\chi_{82}(E)$ are uncorrelated quantities, the resulting uncertainty was calculated on quadratic error propagation. The uncertainty of $\chi_{82}(E)$ in different energy ranges (see above) was also assumed to be uncorrelated and was taken into account by weighting the various uncertainties with the corresponding portion of the total response in each neutron energy range. The uncertainty of the $\langle\sigma\rangle_M/\langle\sigma\rangle_C$-values given in brackets additionally includes the uncertainty of the σ(E)-data. As no error files are presently available for the σ(E)-data, the consideration of the uncertainty of the σ(E)-data was done only in a tentative way. Global uncertainties over the response range in the Cf-252 fission spectrum were assumed or calculated (without considering correlations) for the σ(E)-data. For all neutron reactions of ENDF/B-IV and the two gold reactions of ENDF/B-V,* the uncertainty of the σ(E)-data was assumed to be ± 5 % for category I reactions and ± 10 % for other reactions. For the remaining σ(E)-data, an average uncertainty of ± 9 % was calculated for the data of ref. 20 and of ± 7 % for the data of the ref. 21 - 23.

Generally the average cross sections calculated by means of the ENDF/B-V* data show a better agreement with the measurements than those calculated by means of the ENDF/B-IV cross section data. In the case of the reaction Ti-46(n,p) a small shift in the energy scale near the reaction threshold is mainly responsible for the better consistency of the ENDF/B-V*data. For Ti-48(n,p) experimental cross section data in the main energy response range of Cf-252 were not yet available in the calculation of the ENDF/B-IV data file. The large deviations of the $\langle\sigma\rangle_M/\langle\sigma\rangle_C$-data from unity for In-113(n,n') and Ti-47(n,p) cannot originate from an inadequate description of the neutron spectrum, as reactions with similar energy response ranges (see fig. 1) such as In-115(n,n') and Ni-58(n,p) show a satisfactory consistency.

The large uncertainty of the spectral distribution function at low and high neutron energies has only little importance for the consistency test. For the two nonthreshold reactions, Au-197(n,γ) and In-115(n,γ), only 18 % and 10 %, respectively, of the total response are below 0.25 MeV where the uncertainty of $\chi_{82}(E)$ is ± 13 %. The other range of high uncertainty in the spectral distribution (about ± 10 %) is above 8 MeV. The portion of the total energy response, which is above 8 MeV, is 58 %, 66 % and 100 % for the reactions Ti-48(n,p), Al-27(n,α) and Au-197(n,2n), respectively. The good consistency of the $\langle\sigma\rangle_M/\langle\sigma\rangle_C$-data for these reactions indicates that

*Preliminary ENDF/B-V (see footnote on title page).

the spectral distribution of. ref. 16 describes the Cf-252 spectrum in a satisfactory way at high energies.

Table 1 indicates for which energy-dependent cross section data a maximum consistency between measured and calculated average cross sections was obtained. It was found that a consistent set of σ(E)-data can be obtained by combining information from the ENDF/B-IV file, from the ENDF/B-V* file and from recent experiments. With regard to the uncertainty of the ratio $\langle\sigma\rangle_M/\langle\sigma\rangle_C$, one can state that for most reactions the consistency is given within ± 5 %. This means that presently any adjustment of the σ(E)-data within ± 5 % is rather dubious.

SENSITIVITY STUDIES

The results of table 1 allow to draw only global conclusions as to the adequacy of σ(E)-data. Any adjustment factor derived from the figures of table 1 may, of course, compensate existent disparities between measured and calculated average cross sections. However, one has to keep in mind that such an adjustment implies a doubtful simplification as it assumes the energy-dependent cross section being shifted by the same factor in the total neutron energy range. Moreover, an adjustment of σ(E)-data made to obtain convenient consistency in reactor dosimetry neglects the implication of neutron cross sections with other nuclear technologies and may yield incorrect results in other applications. Contrary to that, it is a useful procedure to investigate the dependance of average cross sections on detailed properties of the energy-dependent nuclear cross section data. It is of special importance how an uncertainty in the σ(E)-data affects the calculated average cross sections. Such statements can be derived from the sensivity studies described below. Similar studies for the fission neutron field of U-235 have already been published.[24]

Sensitivity of <σ> to Individual Properties of the σ(E)-Data

Sensitivity to an Error δσ in σ(E)

Within a small energy interval (E_1,E_2), the energy-dependent neutron cross section can be assumed to be a constant, i.e. $\sigma(E) \equiv \sigma$. If one changes the cross section by a given amount, δσ, the relative change of the average cross section of eq. 1 is described by:

$$\delta\langle\sigma\rangle/\langle\sigma\rangle(E_1,E_2) = (\delta\sigma/\sigma) \int_{E_1}^{E_2} \sigma(E)\ \chi_{82}(E)\ dE\ /\langle\sigma\rangle \qquad (2)$$

δ<σ> also meaning the uncertainty of the average cross section caused by the uncertainty, δσ, of the energy-dependent cross section. The integral term is the fractional contribution to the average cross section which results from the energy interval (E_1,E_2). The quan-

*Preliminary ENDF/B-V (see footnote on title page).

tity $(\delta\langle\sigma\rangle/\langle\sigma\rangle)/(\delta\sigma/\sigma)$ is usually called relative sensitivity or sensitivity coefficient. From eq. 2 one can see immediately that the integral of the sensitivity coefficient over all energies yields unity. Eq. 2 describes in particular the influence on the average cross section due to the normalization of $\sigma(E)$-measurements; i.e. due to the neutron flux density normalization. The influence of a further source of uncertainty on $\sigma(E)$-data will be discussed in the next chapter.

Sensitivity to an Energy Shift δE

Recently it had been discussed that inadequacies in the neutron energy determination at monoenergetic $\sigma(E)$-measurements might cause some confusion.[25] An incorrect neutron energy scale can also be caused, for example, by an insufficient treatment of the energy loss of charged particles in the neutron-producing target. By assuming a small uncertainty in the neutron energy, δE, the relation between the neutron cross sections with and without this uncertainty is:

$$\sigma(E_o+\delta E) = \sigma(E_o) + \delta E\ \sigma'(E_o) + (\delta E)^2/2\ \sigma''(E_o) + \ldots \tag{3}$$

where σ' and σ'' are the first and second derivatives of $\sigma(E)$ with respect to the energy E. Both quantities depend strongly on the slope of the excitation function of a neutron reaction. For threshold reactions the maximum slope is around threshold energy. In this energy range the cross section increases nearly exponentially, i.e.:

$$\sigma(E) \sim \exp(\ a\ E\ ) \tag{4}$$

and changes by up to a factor of 5 per MeV (in the reaction In-115(n,n'), for example) which corresponds with $a \approx 1.6\ \mathrm{MeV}^{-1}$. Inserting eq. 4 in eq. 3 yields:

$$\sigma(E + \delta E) = \sigma(E)\ \left[1 + \delta E\ a + 1/2\ (\delta E)^2 a^2 + \ldots\right] \tag{5}$$

With an uncertainty in the neutron energy of 30 keV and $a \approx 1.6\ \mathrm{MeV}^{-1}$, the quadratic term of eq. 5 is of the order of 0.1 % and can be neglected. Then the relative uncertainty of the average cross section due to a small energy shift, δE, in the energy interval (E_1,E_2) is given by:

$$\delta\langle\sigma\rangle/\langle\sigma\rangle(E_1/E_2) = \delta E \int_{E_1}^{E_2} \sigma'(E)\ \chi_{82}(E)\ dE/\langle\sigma\rangle \tag{6}$$

with δE in MeV.

Sensitivity of $\langle\sigma\rangle$ to the Spectral Distribution

The relation between the uncertainty, $\delta\chi_{82}$, of the spectral distribution and the corresponding uncertainty of $\langle\sigma\rangle$ can be obtained from eq. 2 by replacing $(\delta\sigma/\sigma)$ by $(\delta\chi_{82}/\chi_{82})$. Another feasibility

is to describe the Cf-252 neutron spectrum by a pure Maxwellian (with $T \equiv kT$)

$$\chi_{82}^{T}(E) = (2/\sqrt{\pi})\ (\sqrt{E}/T^{3/2})\ \exp(-E/T) \tag{7}$$

and to analyze the deviations from eq. 7 by a variation, δT, in the temperature parameter T. In this procedure one obtains an integral sensitivity relation of:

$$\delta\langle\sigma\rangle/\langle\sigma\rangle^{T} = (\delta T/T)\ B_1 + (\delta T/T)^2 B_2 + (\delta T/T)^3 B_3 + \ldots \tag{8}$$

with

$$B_1 = A_1 - 3/2$$

$$B_2 = 15/8 - 5/2\ A_1 + 1/2\ A_2$$

$$B_3 = 35/8\ A_1 - 7/4\ A_2 + 1/6\ A_3 - 35/16$$

and with

$$A_n = \int_0^\infty \chi_{82}^{T}(E)\ (E/T)^n\ \sigma(E)\ dE\ /\int_0^\infty \chi_{82}^{T}(E)\ \sigma(E)\ dE$$

Calculations of eq. 8 were done for T = 1.42 MeV. The results will be discussed below.

Examples

Based on eq. 2 and on eq. 6 and using the spectral distribution of ref. 16, sensitivities of cross sections averaged over the fission spectrum of Cf-252 were calculated. The results were plotted as sensitivity coefficients per lethargy width $\Delta\mu = \ln(E_2/E_1)$ with $E_2 > E_1$. Fig. 2 shows the result for the reaction In-115(n,n') and the $\sigma(E)$-data of ref. 22. Fig. 3 is valid for the reaction Au-197(n,2n) and the cross section data of ref. 19.

In the upper part of both figures, the sensitivity profile for a normalization of the $\sigma(E)$-data is given. By these graphs, the nature of the influence of a change in the $\sigma(E)$-data on the average cross section can be easily determined. Consider the following example: what is the percent change in $\langle\sigma\rangle$ due to a 10 % uniform decrease of the In-115(n,n') cross section in the energy range from 2.2 to 3.0 MeV? From the upper part of fig. 2 one obtains a value of the relative sensitivity per unit lethargy of + 0.80 for the range from 2.2 to 3.0 MeV. Then the change of $\langle\sigma\rangle$ is given by:

$$\delta\langle\sigma\rangle/\langle\sigma\rangle = 0.80\ \ln(3.0/2.2)\ (-0.10) = -0.0248$$

This means that the above-mentioned change in the cross section reduces the average cross section by 2.48 %. (The correct value is

$^{115}In(n,n')^{115}In^{m}$ ANL/NDM-14

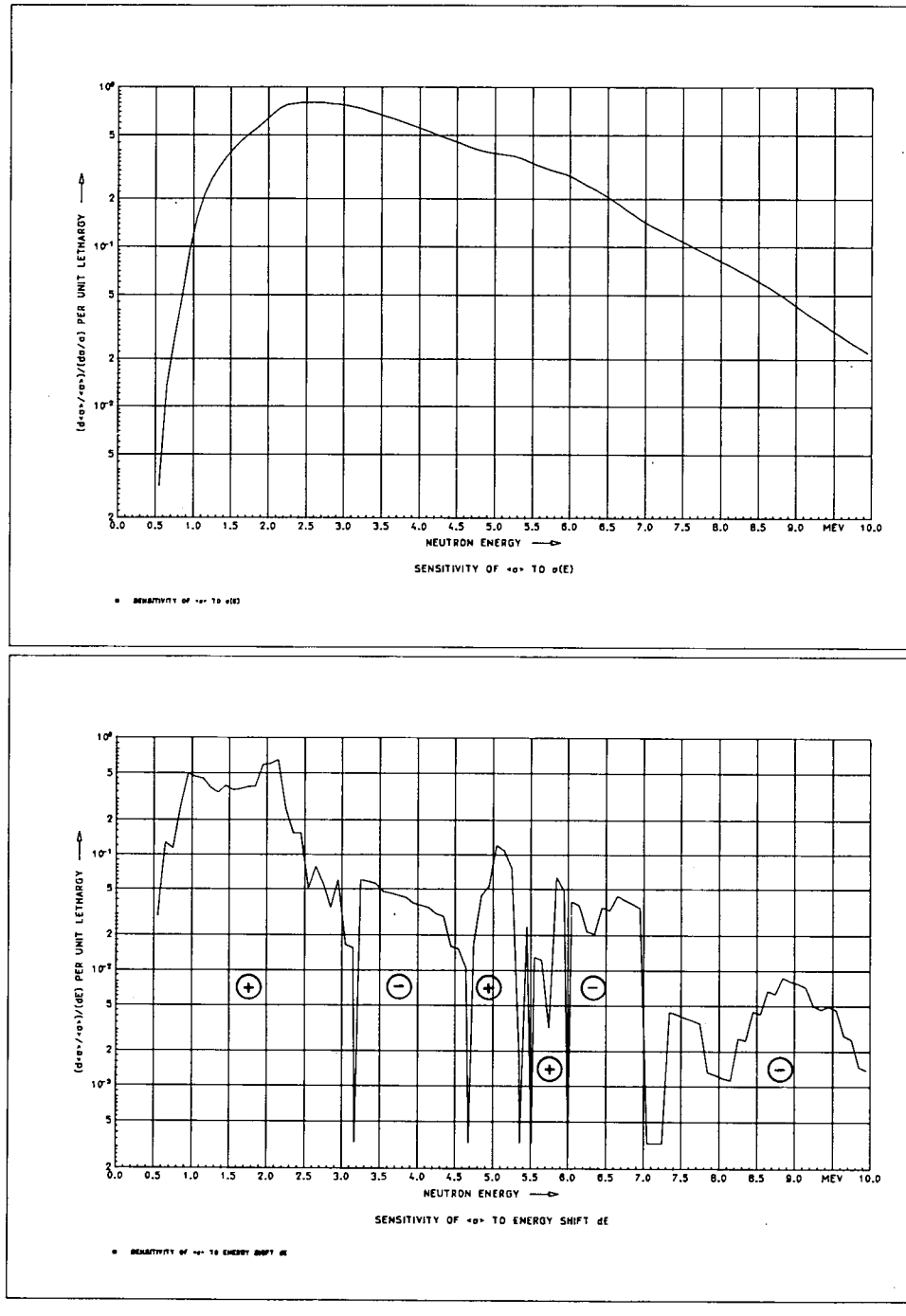

FPDIN, ERSTES FORMAT

Fig. 2. Sensitivity Profiles for $^{115}In(n,n')$

$^{197}Au(n,2n)^{196}Au$ (REF. 19)

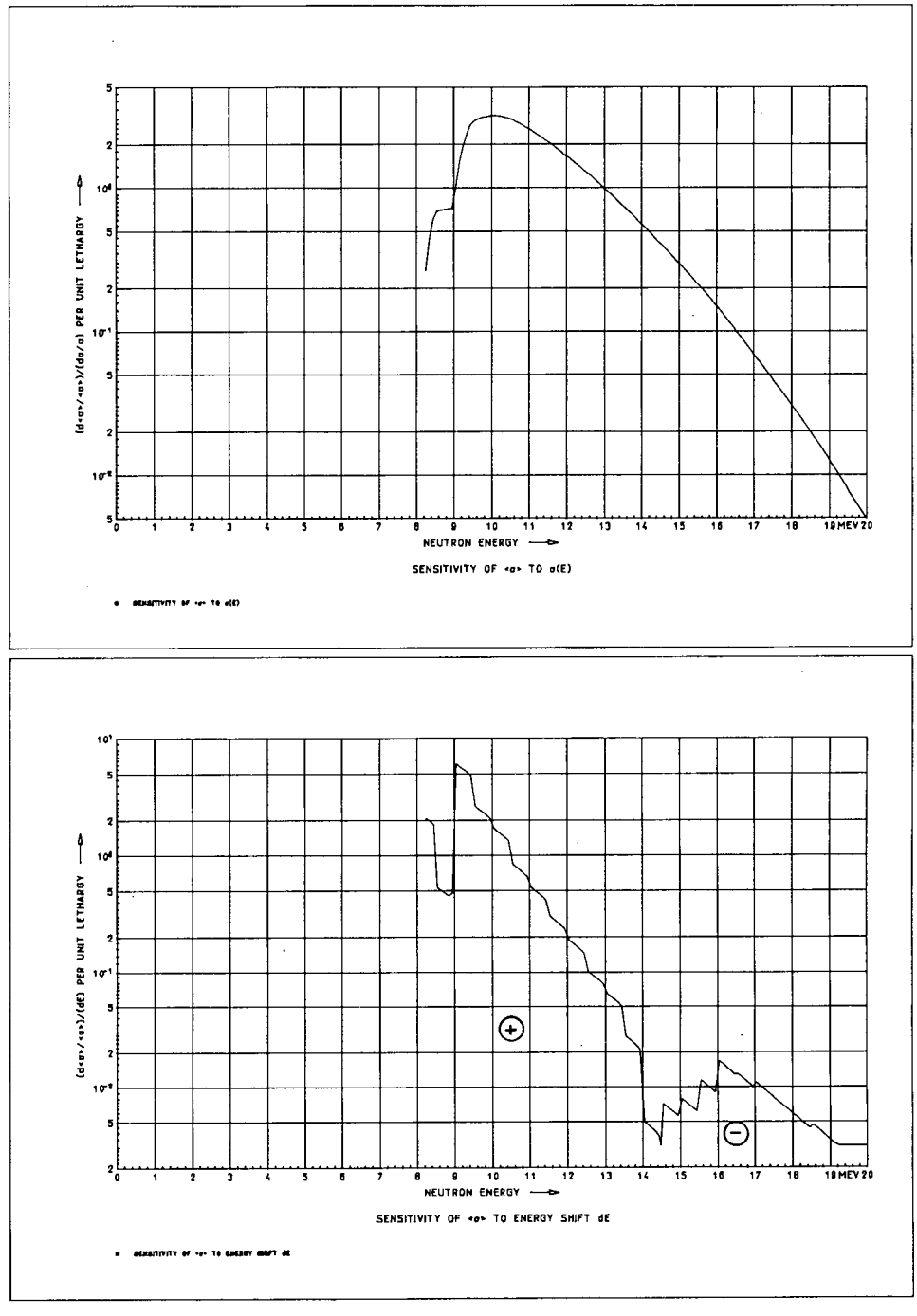

FPDIN, ERSTES FORMAT

Fig. 3. Sensitivity Profiles for $^{197}Au(n,2n)$

- 2.46 % obtained by using numerical data not given here).

In the lower part of the figs. 2 and 3 the sensitivity profile for a shift in the energy scale of the σ(E)-data is plotted. Assuming that the σ(E)-data of the reaction Au-197(n,2n) are subjected to an uncertainty of 20 keV over the total neutron energy range, this corresponds to a relative uncertainty in the energy scale of 0.25 % at the reaction threshold energy. From the data of fig. 3 follows that such a shift of 20 keV would change the average cross section by 1.33%, whereby 90% of the total effect are due to the energy range between threshold and 10.7 MeV.

The parameters which describe the sensitivity of <σ> to the form of the Cf-252 neutron spectrum, analogous to eq. 8, are listed in table 2.

Table 2. Parameters for the Calculation of the Sensitivity of <σ> to the Form of the Spectrum

Reaction	T = 1.42 <σ> (mb)	B_1	B_2	B_3
^{115}In(n,n')	183.0	+0.658	-0.58	---
^{197}Au(n,2n)	6.550	+6.263	+13.28	+7.5

For the reaction In-115(n,n') a change in the temperature parameter of ± 10 % results in a relative change of the average cross section of + 6.0 % and -7.2 %, respectively. This means that the average cross section of this reaction depends only weakly on the form of neutron spectrum. The situation is reverse for the reaction Au-197(n,2n). Here, a (δT/T) of ± 10 % corresponds to a (δ<σ>/<σ>) of +76.7 % and -50.1 %, respectively. Reactions with high threshold, such as Au-197(n,2n), are extremely sensitive to the form of neutron spectrum. From table 2 can also be gathered that a fit of the calculated average cross section value of 6.55 mb to the experimental value of 5.50 mb results in a change of (δT/T) of -2.7 %. A total overlap of both data would be given for a Maxwellian with T = 1.382 MeV instead of 1.42 MeV. This is in analogy with the trend of the analytical spectral distribution shown in fig. 1.

Finally a practical application of the sensitivity profiles is discussed. In the measurement of the σ(E)-data for the reaction In-115(n,n') of ref. 22, the energy-dependent cross section has been determined relative to the fission cross sections of U-235 and U-238. Between reaction threshold and 3.0 MeV, the reaction U-235(n,f), and above 3 MeV reaction U-238(n,f) were used as neutron flux density monitoring

reactions. For both monitor reactions, the neutron cross sections of ENDF/B-IV[18] were used. Recently it was shown that for the reaction U-235(n,f) the neutron cross section of the revised* ENDF/B-V data file deviates substantially from the data of ENDF/B-IV.[26] This effect is shown in fig. 4. In renormalizing the neutron flux density determination of ref. 22 due to the reaction U-235(n,f) one obtains, by inserting the data of fig. 4 in the senstivity profile of fig. 2, a relative change of -0.38 % in the average cross section. Although single σ(E)-data show deviations by up to 5 %, the effect on <σ> is not so dramatical as one would have expected at first glance.

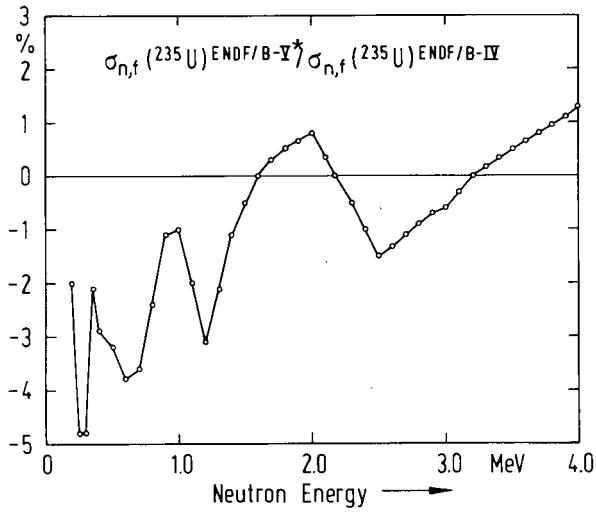

Fig. 4. Comparison of the U-235(n,f) Cross Section between ENDF/B-IV and ENDF/B-V.*

SUMMARY AND CONCLUSION

In the neutron benchmark field of Cf-252, the consistency between measured and calculated average cross sections was tested. From this comparison, conclusions as to the quality of energy-dependent neutron cross section data were drawn. An attempt was made to consider, in a tentative way, the uncertainty in this consistency test, caused by uncertainty contributions from the spectral distribution, from the σ(E)-data and from the <σ>-measurement. In addition, sensitivity profiles were set up describing the influence of σ(E)-data on the average cross section. These sensitivity profiles are at present only an intermediate step. However, combined with the uncertainty covariance files of σ(E)-data to be published in the future they will allow to estimate the uncertainty of "integral" quantities, such as average cross sections, in a mathematically more rigorous way and will then allow to draw more stringent conclusions as has been possible in the present work.

REFERENCES

1. S. A. W. Gerstl, D. J. Dudziak, and D. W. Muir, "Cross-Section Sensitivity and Uncertainty Analysis with Application to a Fusion Reactor," Nucl. Sci. Eng. 62, 137 (1977).

*Preliminary ENDF/B-V (see footnote on title page).

2. M. F. Vlasov, IAEA Consultants' Meeting on Integral Cross-Section Measurements in Standard Neutron Fields, Summary Report INDC(NDS)-81/L+M (March, 1977).

3. J. Grundl and C. Eisenhauer, "Benchmark Neutron Fields for Reactor Dosimetry," Vol. I, p. 53 in Neutron Cross Sections for Reactor Dosimetry, Technical Document IAEA-208, 1978.

4. A. Fabry, W.N. McElroy, L.S. Kellogg, E. P. Lippincott, J. A. Grundl, D. M. Gilliam, and G. E. Hansen, "Review of Microscopic Integral Cross Section Data in Fundamental Reactor Dosimetry Benchmark Neutron Fields," Vol. I, p.233 in Neutron Cross Sections for Reactor Dosimetry, Technical Document IAEA-208, 1978.

5. H. T. Heaton II, J. A. Grundl, V. Spiegel, D. M. Gilliam, and C. Eisenhauer, "Absolute U-235 Fission Cross Sections for Cf-252 Spontaneous Fission Neutrons," Vol. I, p. 266 in Nuclear Cross Sections and Technology, NBS Spec. Publ. 425, 1975.

6. D. M. Gilliam, C. Eisenhauer, H. T. Heaton II, and J. A. Grundl, "Fission Cross Section Ratios in the Cf-252 Neutron Spectrum," Vol. I, p. 270 in Nuclear Cross Sections and Technology, NBS Spec. Publ. 425, 1975.

7. V. M. Adamov, L. V. Drapchinskij, S. S. Kovalenko, G. Yu. Kudryavtsev, K. A. Petrzhak, L. A. Pleskachevskij, and A. M. Sokolov, "Absolute Measurements of Cross-Sections for Fission of U-235 und U-238 by Neutrons from the Cf-252 Fission Spectrum," p. 13 in Nuclear Physics Research in the USSR, Report INDC(CCP)-100/U (February, 1977).

8. W. G. Alberts, E. Günther, M. Matzke, and G. Rassl, "Measurements of Integral Cross Sections in the Californium-252 Fission Neutron Spectrum," Vol. II, p. 131 in Proceedings of the First ASTM-EURATOM Symposium on Reactor Dosimetry, EUR 5667 ef, 1977.

9. W. Mannhart, "Measurement of Average Cross Sections with Regard to the Low and High Energy Part of the Californium-252 Neutron Spectrum," Vol. II, p. 227 in Neutron Cross Sections for Reactor Dosimetry, Technical Document IAEA-208, 1978.

10. Z. Dezsö and J. Csikai, "Average Cross Sections for the Californium-252 Neutron Spectrum," Proceedings of the IV All Union Conference on Neutron Physics, Kiev, April 22-26, 1977 (to be published).

11. M. Buczkó, Z. T. Bödy, J. Csikai, Z. Dezsö, S. Juhász, H. M. Al-Mundheri, G. Petö, and M. Vàrnagy, "Average Cross Sections for the Cf-252 Neutron Spectrum," Proceedings of the International Symposium on Californium-252 Utilization, Paris, April 26-28, 1976 (to be published).

12. L. Green, "Absorption Cross-Section Measurements for Californium-252 Spontaneous Fission Neutrons," Nucl. Sci. Eng. 58, 361 (1975).

13. G. J. Kirouac, H. M. Eiland, and C. J. Slavic, "Fast Neutron Flux Measurements," p. 412 in Proc. Topical Meeting on Irradiation Experimentation in Fast Reactors, Jackson Lake Lodge, 1973.

14. H. Pauw and A. H. W. Aten, "Remarks on the Cf-252 Spectrum," J. Nucl. Energy 25, 457 (1971).

15. W. Mannhart, Average Cross Sections in the Neutron Benchmark Field of Californium-252: A Status Report, Report PTB-FMRB-72 (April, 1978).

16. J. Grundl and C. Eisenhauer, "Fission Rate Measurements for Materials Neutron Dosimetry in Reactor Environments," Vol. I, p. 425 in Proceedings of the First ASTM-EURATOM Symposium on Reactor Dosimetry, EUR 5667 ef, 1977.

17. J. A. Grundl and C. M. Eisenhauer, "Fission Spectrum Neutrons for Cross Section Validation and Neutron Flux Transfer," Vol. I, p. 250 in Nuclear Cross Sections and Technology, NBS Spec. Publ. 425, 1975.

18. B. A. Magurno, ENDF/B-IV Dosimetry File, Report BNL-NCS-50446 (April, 1975).

19. S. F. Mughabghab, Evaluation of the Capture Cross Section of Au-197, Informal Report BNL-NCS-21774 (1977) and priv. communication (1977).

20. D. L. Smith, Evaluation of the In-115(n,n')In-115m Reaction for the ENDF/B-V Dosimetry File, Report ANL/NDM-26 (December, 1976)

21. C. Phillis, O. Bersillon, D. Smith, and A. Smith, Evaluated (n,p) Cross Sections of Ti-46, Ti-47 and Ti-48, Report ANL/NDM-27 (January, 1977).

22. D. L. Smith and J. W. Meadows, Cross Sections for the Zn-66(n,p)Cu-66, In-113(n,n')In-113m and In-115(n,n')In-115m Reactions from Near Threshold to 10 MeV, Report ANL/NDM-14 (July, 1975).

23. D. L. Smith and J. W. Meadows, Response of Several Threshold Reactions in Reference Fission Neutron Fields, Report ANL/NDM-13 (June, 1975).

24. D. L. Smith, Analysis of the Sensitivity of Spectrum-Average Cross Sections to Individual Characteristics of Differential Excitation Functions, Report ANL/NDM-30 (March, 1977)

25. J. W. Meadows, Determination of the Energy Scale for Neutron Cross Section Measurement Employing a Monoenergetic Accelerator, Report ANL/NDM-25 (January, 1977).

26. B. A. Magurno,"ENDF/B Dosimetry File for Version V," Vol. I, p. 375 in Neutron Cross Sections for Reactor Dosimetry, Technical Document IAEA-208, 1978.

USE OF HEDL CODES IN THE SENSITIVITY AND UNCERTAINTY ANALYSIS OF THE PRESSURE VESSEL EMBRITTLEMENT DAMAGE FUNCTION PROBLEM

G. L. Guthrie, F. Schmittroth, R. L. Simons, and E. P. Lippincott
Hanford Engineering Development Laboratory (HEDL),
Richland, Washington, USA
and
C. Oster
Battelle, Pacific Northwest Laboratory (PNL)
Richland, Washington, USA

ABSTRACT

Results are given for the application of the unfolding code FERRET and two versions of SAND-II to the Light Water Reactor Pressure Vessel surveillance damage function unfolding problem. FERRET is preferred when detailed knowledge of off-diagonal covariance matrix elements is available. One of the versions of the SAND-II code allows weighting of a priori estimates of the damage function and is equivalent to a log-normal least squares procedure. For intuitive and qualitative analytical understanding, the problem of sensitivity analysis of LWR PV surveillance extrapolation is most easily understood by application of a method whereby the spectrum in which the damage is to be calculated is expressed as a linear sum of the spectra used to derive the damage function. FERRET and the two SAND-II codes have been found to give consistent results. FERRET has the advantage of providing output covariance matrices as a standard feature.

INTRODUCTION

The Nuclear Regulatory Commission (NRC) at the present time is establishing standard procedures for calculating safe operating lifetimes of nuclear reactor pressure vessels. For this purpose the USNRC has established a Light Water Reactor (LWR) Pressure Vessel (PV) Neutron Dosimetry Surveillance program. This interlaboratory program, coordinated by HEDL, involves Oak Ridge National Laboratory (ORNL), Pacific Northwest Laboratory (PNL), Hanford Engineering Development Laboratory (HEDL), CEN/SCK (Belgian Nuclear Research), KFA (West Germany Reactor Research), National Bureau of Standards (NBS), Naval Research Laboratory (NRL), and University of California at Santa Barbara (UCSB).

One of the primary goals of the program is the writing of thirteen Standard Practices, Guides and Methods dealing with various aspects of

the metallurgical and dosimetry surveillance program. One of the most important of these is a practice entitled "Extrapolating Surveillance Dosimetry Results." This deals with the problem of taking the Charpy V data and the neutron exposure data acquired from metallurgical specimens and activation foils situated at the surveillance position of an operating power reactor and using this information to predict the rate of embrittlement of the metal at the 1/4 thickness (1/4T) position in the pressure vessel wall. Since the neutron spectrum at the 1/4T position is different from that at the surveillance position, predictive calculations of this type require the use of, or at least the consideration of the use of, a damage function that describes the dependence of the embrittlement on the energy of the neutrons.[1]

Two nearly identical nuclear reactor mockups have been built at ORNL as part of the project. These consist of a low power (PCA) and a high power (PSF) mockup of an LWR reactor core and pressure vessel wall immersed in the water of a swimming pool type facility at Oak Ridge.

The high power mockup (PSF) contains provisions for exposing removable metallurgical specimens which can be irradiated at positions behind the simulated reactor thermal shield (normal surveillance position) and at the 1/4T and 1/2T positions of the PV wall and also at the front face of the PV wall.

From the metallurgical (Charpy V) data obtained at these positions, together with theoretical input on the energy dependence of the embrittlement we plan to develop a damage function and associated procedures for calculating safe lifetimes of operating reactors. For our a priori theoretical damage function we have been using the displacement cross section as given by D. G. Doran and N. J. Graves.[2]

The problem addressed to date is the following: given the values and uncertainties of the spectrum at the surveillance, 1/4T, 1/2T, and PV front face positions, and given similar information about the degree of embrittlement, and given an a priori damage function together with uncertainties, then what uncertainty can be attached to the predicted damage per unit fluence at the 1/4T position of the PV of an operating reactor? Several HEDL computer codes are being used in an attempt to learn what factors are most severely limiting our ability to make accurate predictions.

In making these assessments, we have used the Monte-Carlo version of SAND-II, a Monte Carlo version of a modified SAND-II, the code FERRET, and, on a more casual basis, a type of analysis based on the idea of expressing the 1/4T spectrum of the power reactor as a linear sum of the separate spectra used to develop the damage function. We shall briefly describe the approach used in each of these codes or methods and then give the results of the analyses.

LINEAR COMBINATION OF INPUT SPECTRA

If the true spectrum at the 1/4T position of the power reactor is given by $\Phi_{PT}(E)$ and the several true spectra at the test positions used to develop the damage function are given by $\Phi_{TT1}(E)$, $\Phi_{TT2}(E)$, etc., then we can find constants A, B, C, etc., such that

$$\Phi_{PT}(E) = A\Phi_{TT1}(E) + B\Phi_{TT2}(E) + C\Phi_{TT3}(E) + \ldots + \Psi(E) \qquad (1)$$

where the $\Psi(E)$ represents our inability to obtain a completely accurate representation from the linear combination. If the true damage function is given by $G_T(E)$, then the actual damage per unit fluence in the power reactor 1/4T position is given by

$$DR_{PT} = \int G_T(E)\,\Phi_{PT}(E)dE \quad . \qquad (2)$$

Using Eq. (1), multiplying by $G_T(E)$ on both sides and then integrating, we obtain

$$DR_{PT} = A\ DR_{TT1} + B\ DR_{TT2} + C\ DR_{TT3} + \ldots + \int G_T(E)\,\Psi(E)dE, \qquad (3)$$

where DR_{TT1} is the true damage per unit fluence at test position number one, etc. In Eq. (3) we have made the substitution

$$A\ DR_{TT1} = A \int G_T(E)\,\Phi_{TT1}(E)dE \qquad (4)$$

for the first term on the right side of the equation, and similarly for the other terms in Eq. (3). Consequently, if it is possible to express the spectrum in the power reactor as a linear sum of the so-called test spectra, then the damage per unit fluence in the power reactor can be given as a corresponding sum of the damage per unit fluence of the metallurgical samples in the test positions. Thus, if it is found possible to keep the magnitude of $\Psi(E)$ small, in Eq. (1), then there is scarcely any need to know the damage function at all, provided that the damage per unit fluence and spectra are known accurately. It may be found that it is not possible to accurately fit $\Phi_{PT}(E)$ by a choice of A, B, ... in Eq. (1) which will keep $\Psi(E)$ small for all values of E. This will not impair the usefulness of Eq. (3) as long as G(E) is small at those values of E where $\Psi(E)$ is large, so that $\int G(E)\,\Psi(E)dE$ remains small compared to DR_{PT}.

If the damage per unit fluence in the power reactor is expressed in the form of Eq. (3), then we can get the variance of DR_{PT} assuming that the variables are independent. In this case we assume that the expansion coefficients A, B, ... as well as the measured damage per unit fluence, damage function, and mismatched spectrum $\Psi(E)$ are imperfectly known. Then the variance in the calculated value of DR_{PT} calculated from Eq. (3) is given by

$$VAR(DR_{PT}) = A^2\ VAR(DR_{TT1}) + (DR_{TT1})^2\ \ VAR(A) + B^2\ VAR(DR_{TT2}) + (DR_{TT2})^2\ VAR(B) + \ldots + G^T\ VAR(\Psi)\ G + \Psi^T\ VAR(G)\ \Psi \tag{5}$$

where VAR (anything) is the variance of the item in the brackets. For the last two terms of Eq. (5) the integral of Eq. (3) has been replaced by a sum over energy space represented as the product of two vectors. In this notation, similar to that of Perey[3] and Dragt, et al.,[4] the vector is represented as a column matrix, and Ψ^T is then the transpose of the matrix Ψ. Then Var (Ψ) is the covariance matrix of Ψ, and a similar notation convention applies for G.

Some obvious facts of the calculation are that the calculated variance is lower, for a given mismatch contribution, $\int \Psi(E)\ G(E)dE$, if the power reactor spectrum can be represented as a sum of nearly equal parts of several test spectra, rather than being predominantly given by a single test spectrum contribution, assuming equal accuracies in the spectral and damage measurements in the two cases.

In this sense, the usual rule that the percentage error varies inversely as the square root of the number of measurements can be shown to apply. Also, for a given value of $\int \Psi(E)\ G(E)dE$, and equal accuracies in the spectral and damage measurements, it is generally best to avoid expansions that involve negative values of A, B, C, etc., if one wishes to have the calculated variance approximate the minimum variance limitation inherent in a more complete treatment of the data.

In actually making estimates of the variance from Eq. (5), the first step is, of course, to obtain a usable set of expansion coefficients, possibly by use of a linear least squares routine that minimizes $\int \Psi^2(E)dE$. This can also be done for an all-positive coefficients case by setting $A = a^2$, $B = b^2$, etc., and doing a nonlinear least squares fit for $\Phi_{PT}(E)$ in terms of the test spectra using the a, b, etc., as the least squares parameters. Another method is to obtain a fit which is not a least squares fit, but rather a "least sum of positive error" fit using all positive coefficients and all positive values for the mismatch $\Psi(E)$. This can be done using a linear programming code common in business optimization procedures. A further refinement consists of using, in linear programming terminology, a double set of slack variables so that $\Psi(E)$ can be either positive or negative so that the fitting procedure minimizes $\int |\ (E)|dE$. All of the above can also be done in such a way as to minimize

$$\theta = |G_{APRIORI}(E)\Psi(E)\ |\ dE \tag{6}$$

and this is done by first converting the various neutron spectra to anticipated damage as functions of energy, using the a priori damage function.

In summary, the "linear combination of input spectra," in its simpler forms, is an inexact way to calculate the variance in the damage per unit fluence incurred in the power reactor spectrum, but it is an excellent tool for estimates and is an approach that aids intuition. In this usage, it is perhaps best applied by simply plotting $G_{a\ priori}(E)\ \Phi(E)$ versus E, for the various $\Phi(E)$. Then a casual visual observation tells whether it is possible to expand DR_{PT} in the form given by Eq. (3) with a small contribution from the integral $\int G(E)\ \Psi(E)dE$. If so, the percentage uncertainty in RD_{PT} can be directly estimated from the errors in the measured damage values, even if G(E) is not accurately known. In our current work it is found that the power reactor 1/4T spectrum is very close to the 1/4T and 1/2T position spectra of the PSF mock-up. Therefore, our final error in the predicted damage rate depends heavily on the measurement error of damage per unit fluence at the 1/4T position of the PSF mockup.

SAND-II CODE

SAND-II type codes have been used in a sensitivity and error analysis of the damage function determination and damage per unit fluence prediction problem referred to above. For this type of analysis it was assumed that dosimetry and damage per unit fluence data were available from the four PSF test position at the 1/4T, 1/2T, PV front face, and surveillance positions. The true neutron spectra in the test reactor was assumed to be that calculated at ORNL using a 1D transport code.[5] The true damage function was assumed to be the DPA function given by D. G. Doran, et al.[2] and the true 1/4T power reactor spectrum was that given for a typical pressurized water reactor by M. L. Gritzner, et al.[6] The true damage per unit fluence at each of the four test positions (ORR-PSF) was assumed to be given by

$$DR_t = \int G_{D.D.}(E)\ \Phi_t\ (E)\ dE \qquad (7)$$

where G_{DD} (E) is the displacement cross section, the Φ_t are the test reactor spectra, or the power reactor spectra.

The Monte Carlo method used with the standard (RSIC) version of SAND-II was the following. A basic group structure of 75 energy groups was chosen. The difference between group boundaries closely approximated a constant difference in lethargy. These 75 groups were divided into 15 super groups of 1 to 6 (usually 4 to 6) adjacent small groups. Twenty one Monte Carlo passes were run with the standard SAND-II code. The initial pass was not a Monte Carlo pass in the usual sense. In the first, or zero level pass, the Doran DPA function was used as the a priori input guess for the true damage function. All spectra and damage measurements were assumed to be correct so that the measured integral damage data equaled the calculated damage and no adjustment in the a priori guess was needed. For the next ten Monte Carlo trials. the a priori damage function

was perturbed** by being multiplied by $E^{+.3}$ and for the following ten trials the a priori damage function was multiplied by $E^{-.3}$.

Concurrently, standard deviation (percentage) limits were put on the normal distributions assumed for the test reactor spectra measurement errors, and a value was chosen for the standard deviation (%) in the mechanical measurements. Normally distributed independent random errors were generated for both the spectral input and the measured damage per unit fluence values for the twenty trials which followed the zero level pass of the program algorithm.

Twenty damage functions were unfolded and twenty predictions made for the damage per unit fluence in the power reactor spectrum at the 1/4T position. Deviations from the "true" value were noted, and a standard deviation was calculated. The "random" variation in the spectrum in the test reactor is achieved by using a bulk variation of each of the 15 supergroups and then renormalizing to maintain the value of the integral flux. This renormalization does not imply that the integral flux is assumed to be well known, but rather that the integral flux uncertainty is entered as an uncertainty in the damage per unit fluence.

Calculations of this type can be used in several ways. In the present application we wanted to know the necessity or lack thereof for obtaining improved dosimetry data, better input a priori damage functions, additional damage data in other spectra, etc. We now estimate that the most critical item is the measurement of damage per unit integral fluence although of course improvements in the other areas are also helpful.

In the matter of supplying a designer with a damage function for a given standard material, two approaches are possible. A nominal damage function can be generated from the data plus several Monte Carlo trials to determine the uncertainty in the damage function. An engineer can then apply the nominal function to get a prediction of reactor lifetime, and he can use the Monte Carlo retrial functions to estimate the uncertainty. Alternatively, Monte Carlo trials can be used to generate a covariance matrix for the damage function, using the basic definition of a covariance matrix.

MODIFIED SAND-II CODE

Recent analysis of the SAND-II algorithm[8] has shown that the code uses a method of steepest descent to achieve a log-normal least squares solution when the code is presented with an overdetermined problem. It

**This corresponds to a highly correlated tilt in the mean slope of the Doran displacement cross section, which can be approximated by

$$G_{D.D}(E) = C \cdot E^{0.7}$$

where C is a constant.

is possible to include the a priori damage function information as a type of weighted data, thus making every problem overdetermined. The increase in running time for the code is similar to that incurred in adding one integral measurement to the data set. Thus in unfolding a damage function using five damage measurements in five separate spectra with any number of energy groups, the increase in running time is less than 20% with the modified code compared to the current RSIC code.

The modified code has been used on the PCA-PSF sensitivity analysis problem with results similar to those found for the standard code. An analysis of the SAND-II algorithm, and a comparison with the algorithm used by Perey in STAY'SL[3] shows that, for a problem with diagonal input covariance matrices, the SAND-II algorithm first pass is equivalent to the Perey algorithm, except for the difference created by the assumption of a log-normal distribution in place of a normal distribution in the former.

FERRET CODE

The FERRET code uses assumptions of log-normal distributions of errors in the damage function, combined with a normal distribution of errors in the integral damage. The code searches for those "best values" which indicate a maximum likelihood, and uses all the information inherent in a complete set of covariance matrices. It is more completely described in a paper by F. Schmittroth in this same conference proceedings.

RESULTS AND CONCLUSIONS

The FERRET code and the two versions of the SAND-II code were used to calculate damage per unit fluence and damage per unit fluence uncertainties at the 1/4T position of a power reactor, using assumed input data accumulated at the surveillance, 1/4T, 1/2T, and pressure vessel front face positions of the PSF (high power version of the dual Oak Ridge Light Water Pressure Vessel Mockup). The spectra used were as given in references (5) and (6). Uncertainties in the integral flux were combined with those in the mechanical measurements to give an uncertainty in the damage-per-unit-integral-fluence. Spectral shape uncertainties were introduced as described previously. The SAND-II codes were used with the smoothing option inoperative, for both the RSIC version and the modified version. The results of the analysis are shown in Table 1.

For the introduction of the uncertainty in the a priori damage function in FERRET, the uncertainty in $G_{D.D}(E)$ was introduced as a covariance matrix having diagonal elements with values chosen to give uncertainties similar to those introduced by the tilt functions described earlier for use with SAND-II. As can be seen from the table, the results of the three codes are similar for the cases tried. The running times were about equal, being usually one to two minutes per case. It would seem that the

Table 1. Calculated Damage per unit fluence Uncertainty (%) in a Power Reactor for Three Combinations of Uncertainties in Input Data Required in a Test Reactor

CODE	$\frac{P}{S}$*	$\frac{5}{15}$	$\frac{15}{25}$	$\frac{25}{35}$
FERRET		6.5	11.2	15.1
MODIFIED SAND-II		7.8	10.9	12.7
REGULAR SAND-II		6.7	9.1	15.1

*The quantity (P) is the uncertainty (%) in the damage per unit fluence while the quantity S is the uncertainty (%) in the spectral shape, as defined in the text.

choice of codes depends somewhat on the familiarity of the user with the codes and the availability of input information. For cases where detailed covariance information on the input parameters is lacking but where semi-quantitative information is known about short range correlations, FERRET has a utility subroutine for generating covariance matrices which are then available for additional analysis.

REFERENCES

1. C. Z. Serpan Jr. and W. N. McElroy, " Elevated-Temperature Damage Functions for Neutron Embrittlement in Fluence Vessel Steels," Nuclear Technology, Vol 13, February 1972.

2. D. G. Doran and N. J. Graves "Neutron Displacement Damage Cross Sections for Structural Metals," in Irradiation Effects on the Microstructure and Properties of Metals, ASTM STP 611, American Society for Testing and Materials, 1976, pp. 463-482.

3. F. G. Perey, "Least Squares Dosimetry, Unfolding: The Program STAY'SL," ORNL/TM-6062, ENDF-254 Oak Ridge National Laboratory.

4. J. B. Dragt, J. W. M. Dekker, H. Greeppelaar, and A. J. Janssen, Nuclear Science and Engineering, Vol 62, p. 117, 1977.

5. F. B. K. Kam and J. H. Swanks, "Pool Critical Facility," (in LWR Pressure Vessel Irradiation Surveillance Dosimetry Quarterly Progress Report), HEDL-TME 77-4, Westinghouse-Hanford, Richland, Washington, 1977.

6. M. L. Gritzner, G. L. Simmons, T. E. Albert, and E. A. Straker, PWR and BWR Radiation Environments for Radiation Damage Studies, EPRI-NP-152, Electric Power Research Institute, Palo Alto, California, 1977.

7. F. Schmittroth, "Generalized Least Squares for Data Analysis," HEDL-TME 77-51, Westinghouse Hanford, Richland, Washington, 1977.

8. G. L. Guthrie and R. L. Simons, "Analysis and Extension of the SAND-II Code, in LWR Pressure Vessel Irradiation Dosimetry Quarterly Progress Report HEDL-TME-78-4," Westinghouse Hanford, Richland, Washington, 1977.

VARIED APPLICATIONS OF A NEW MAXIMUM-LIKELIHOOD CODE WITH COMPLETE COVARIANCE CAPABILITY

F. Schmittroth
Hanford Engineering Development Laboratory
Richland, Washington, USA

ABSTRACT

Applications of a new data-adjustment code are given. The method is based on a maximum-likelihood extension of generalized least-squares methods that allow complete covariance descriptions for the input data and the final adjusted data evaluations. The maximum-likelihood approach is used with a generalized log-normal distribution that provides a way to treat problems with large uncertainties and that circumvents the problem of negative values that can occur for physically positive quantities.

The computer code, FERRET, is written to enable the user to apply it to a large variety of problems by modifying only the input subroutine. The following applications are discussed: A 75-group a priori damage function is adjusted by as much as a factor of two using 14 integral measurements in different reactor spectra. Reactor spectra and dosimeter cross sections are simultaneously adjusted based on both integral measurements and experimental proton-recoil spectra. The simultaneous use of measured reaction rates, measured worths, microscopic measurements, and theoretical models are used to evaluate dosimeter and fission-product cross sections. Applications in the data reduction of neutron cross section measurements and in the evaluation of reactor after heat are also considered.

INTRODUCTION

In recent years, the methods of generalized least-squares[1-6] have been successfully applied to a variety of data-adjustment and unfolding problems; not only in the fields of reactor physics and nuclear data, but in fields as diverse as aerospace and communications. In this study, we discuss a useful extension of these ideas and present several examples that illustrate the method. Brief consideration is also given to the computer-code implementation of the method.

The term, generalized least-squares, connotes two important extensions of the usual least-squares in the present context: the use of

complete covariance matrices rather than diagonal matrices to describe both input and output information, and the use of a priori information to obtain solutions for what are otherwise underdetermined problems.

METHOD

Review of Least-Squares

A detailed description of the method will be given elsewhere. Here we present important features that distinguish it from earlier work and enough detail to discuss subsequent examples.

The usual least-squares equations may be obtained by minimizing[1]

$$S_g = [g_m - g(w)]^t \, M_g^{-1} \, [g_m - g(w)] \tag{1}$$

where g_m is a vector of measured values, and where w is a vector of least-squares parameters that are to be determined. The vector function g(w) may be linearized as $g(w) \cong g(w^*) + \nabla_w g \cdot (w - w^*)$ if g is not already linear. The covariance matrix M_g describes the known uncertainties and correlations in the measured data g_m:

$$(M_g)_{ij} = \mathrm{Cov}\,(g_{mi}, g_{mj}) \; . \tag{2}$$

A priori knowledge of the parameters w can be included by minimizing[2-6]

$$S = S_g + S_o \tag{3}$$

rather than S_g alone where

$$S_o = (w_o - w)^t \, M_{wo}^{-1} \, (w_o - w) \; . \tag{4}$$

The a priori values are denoted by the vector w_o. The uncertainties and correlations in the values w_o are also considered as a priori knowledge and are described by the covariance matrix M_{wo}. With the definitions,

$$f = g_m - g^* \qquad M_f = M_g \tag{5a}$$

$$x = w - w^* \tag{5b}$$

$$x_o = w_o - w^* \qquad M_{xo} = M_{wo} \tag{5c}$$

the solution to the minimization problem is given by[6]

$$\hat{x} - x_o = M_{xo} \, A^t \, D^{-1} \, (f - A x_o) \tag{6}$$

where

$$D = A\, M_{xo}\, A^t + M_f \tag{7}$$

and where $\hat{x}$ denotes the "best" estimate of the parameters $x = w-w^*$. The uncertainties and correlations in this estimate are described by the covariance matrix M_x which can be calculated from

$$M_x - M_{xo} = M_{xo}\, A^t\, D^{-1}\, A\, M_{xo}\ . \tag{8}$$

As is well known, the least-squares method is equivalent to a maximum-likelihood approach that makes the assumption of normal distributions.[1] It is also well known that the least-squares equations can be derived without the assumption of normality from the principle of a "minimum-variance unbiased estimator".[1]

Description of A Priori Information and its Inclusion in a Maximum-Likelihood Approach

The description and use of a priori information plays an important role in the present method. As mentioned earlier, a priori knowledge includes covariance information, M_{wo}, as well as a priori values, w_o. A common reason for using a priori data is to provide a unique solution to the least-squares equations in a situation that would be mathematically underdetermined otherwise. However, mathematically overdetermined problems do not negate the practical use of a priori knowledge.

A particular type of a priori information led us to consider a maximum-likelihood approach in contrast to a least-squares approach. Many physical values, especially in reactor physics and nuclear data, are a priori positive. In fact, their physical character frequently dictates that they be described (e.g. plotted) logarithmically. For instance, one might be able to estimate a particular nuclear cross section to within a factor of 2. The a priori value might be 10, for example, with upper and lower bounds of 2x10=20 and 10/2=5, respectively. The factor of 2 uncertainty might itself be quite uncertain; and yet, one might be very certain that the value sought was not a factor of 100 smaller. The least-squares equations do not allow the accurate description of this type of a priori knowledge. The problem is evident in Eq. (4) if one considers a diagonal covariance matrix M_{wo}. The value S_o is a sum of squared residuals and gives a measure of the deviation of w from the a priori values w_o. Clearly, S_o is a symmetric function of w about the values w_o and does not adequately represent the asymmetric limits discussed above. In fact, for large uncertainties as described by M_{wo}, the value of S_o may not even strongly dictate against negative values for w, even though it may be a priori known with complete assurance that w cannot be negative.

An obvious solution is to replace S_o by a term that explicitly accounts for a logarithmic description of the a priori information. Very simple treatments have been considered previously.[2] Specifically, we replace S_o by

$$S_o' = (z_o - z)^t \, M_{zo}^{-1} \, (z_o - z) \ , \tag{9}$$

where

$$z = \ln(w) \tag{10a}$$

$$z_o = \ln(w_o) \ , \tag{10b}$$

so that the minimization of S in Eq. (4) requires that ln(w) be close to $\ln(w_o)$ in lieu of the requirement that w be close to w_o. Negative values for w are completely ruled out. The covariance matrix M_{zo} in Eq. (9) is related to M_{wo} by

$$\frac{(M_{wo})_{ij}}{\langle w_i \rangle \langle w_j \rangle} = e^{(M_{zo})_{ij}} - 1 \ . \tag{11}$$

Analytic solutions that correspond to Eqs. (6), (7), and (8) are no longer possible. However, Eq. (6) can be used in an iterative fashion to find the desired minimum of

$$S' = S_g + S_o' \ .$$

In line with a logarithmic picture, it is desirable to express uncertainties (covariances) in fractional form as alluded to in Eq. (11). At the same time, we take a step toward a more practical description of the needed covariance matrices. One can show that M_{wo} can be rewritten as

$$\frac{(M_{wo})_{ij}}{\langle w_i \rangle \langle w_j \rangle} = (1+c^2)(1+r_i r_j \rho_{ij}) - 1 \tag{12}$$

where c is a fractional normalization uncertainty (c=1 implies a 100% uncertainty completely correlated for all values $\{w_i\}$). The values $\{r_i\}$ denote any additional point by point fractional uncertainty, and ρ_{ij} is a matrix that describes any further correlations. From Eqs. (11) and (12) we now find

$$M_{zo} = \ln(1+c^2) + \ln(1+r\rho r) \ . \tag{13}$$

Even for relatively large uncertainties, one can usually use

$$M_{zo} \approx c^2 + r\rho r \ . \tag{14}$$

In any event, M_{zo} can be completely specified in terms of fractional as opposed to absolute uncertainties.

A completely rigorous replacement for Eq. (8) is not available. A solution that one can show works well in many cases is given by Eq. (8) with M_{xo} replaced by M_{zo} and with A appropriately redefined to reflect the change from absolute to relative values. For small uncertainties, the method is equivalent to the usual least-squares treatment.

APPLICATIONS

The FERRET Code

The formalism sketched above was implemented in the FERRET computer code.[7] Additional features include maximum use of partitioning to eliminate unneeded subspaces in covariance matrices and to allow sequential use of independent data subsets. Also, indexing techniques were used that make maximum use of available core memory. A secondary advantage of the indexing method is a computational module that can handle vastly different types of problems by simply modifying the input subroutine. Practical experience has demonstrated the algorithms to be reasonably fast and efficient. The examples discussed below were all easily treated with less than 38K with running times on the order of a minute or less on a CDC 6600 computer.

Before proceeding to specific examples, we want to discuss a further parameterization used in the description of the a priori covariance matrix. The computational module of the code does not impose any restrictions on the allowable covariance matrices. However, in practice we have relied on an intuitive parameterization of the covariance matrices for the measured and a priori data. Equations (12-14) already display one step toward this parameterization. As discussed above, the covariance matrices are separated into two components: an overall fractional normalization uncertainty, c, and a second term, $r_i r_j \rho_{ij}$, that describes any additional uncertainties and correlations. In practice, the correlation matrix ρ_{ij} has been used primarily to describe short-range correlations, and we have further parameterized it by the form[6]

$$\rho_{ij} = (1-\theta)\delta_{ij} + \theta e^{-\frac{(i-j)^2}{2\gamma^2}} \tag{15}$$

where θ denotes the strength of short-range correlations and γ denotes their range. For example, completely uncorrelated data or a priori values are described by $\theta=0$ so that $\rho_{ij}=\delta_{ij}$. The values $\{r_i\}$ are the point-by-point fractional uncertainties.

It is important to emphasize the role of the correlation matrix ρ_{ij} for the a priori covariance matrices. A priori knowledge consists of more than preliminary estimates w_0 of least-squares parameters. For highly underdetermined problems, stiffness or smoothness constraints can be crucial in obtaining final solutions with uncertainties small enough to be of practical value. Any unfolding code must apply some constraint of this nature to obtain useful solutions for this type of problem (e.g., minimization of second derivative terms). Note that ρ_{ij} does not necessarily dictate smoothness, only a particular degree of correlation among neighboring points. An advantage of using covariance matrices to obtain unique solutions is that final uncertainties are obtained that describe the uniqueness of these solutions. If sufficient data or a priori information are supplied, the problem will be apparent from large final

uncertainties. The user must then seek additional physical information such as new data values or stronger a priori correlations.

75-Group Damage Function Analysis

The first example is a 75-group damage function unfolding problem chosen for its large uncertainties and adjustments. The damage D_i in a neutron flux ϕ_i is assumed to be given by

$$D_i = \sum_{g=1}^{75} \phi_{ig} \, \sigma_{Dg} \tag{16}$$

where $\{\sigma_{Dg}\}$ are the multigroup values of the damage function $\sigma_D(E)$ being sought. This equation is linearized by the expansion

$$D_i \approx D_i^{(o)} + \sum_g \phi_{ig}^{(o)} \, (\sigma_{Dg} - \sigma_{Dg}^{(o)}) + \sum_g \sigma_{Dg}^{(o)} \, (\phi_{ig} - \phi_{ig}^{(o)}) \; . \tag{17}$$

The flux spectra ϕ_i are assumed to have small uncertainties and are adjusted simultaneously with the damage function $\sigma_D(E)$.

This example included 14 "measured" damage values corresponding to 14 separate spectra and which were computed from a so-called "exact" damage function. These 14 values were then used to adjust an a priori damage function which can then be compared with the "exact" solution. Figure 1(a) shows the results for the damage function $\sigma_D(E)$.

The adjusted damage function is in good agreement with the exact function for neutron energies between about 30 keV and 4 MeV where the fast spectra have a strong response. Thermal spectra were also included among the 14 fluxes, but Figure 1(a) centers on the higher energies for clarity. The agreement is particularly good in light of adjustments of nearly a decade. In regions of low response, as near the edges of Figure 1(a), there is still a strong downward adjustment which is a consequence of the large a priori normalization uncertainty. In the absence of a priori correlations, such as normalization uncertainties, a priori values in regions of low response will tend not to be adjusted.

Briefly, a few of the covariance parameters used are as follows. The 14 damage values were assumed to have an uncertainty of 15% independent of each other. The uncertainties on the multigroup fluxes were typically 10-15% for the better known energy groups. No normalization uncertainty was assumed, and neighboring groups were taken to be partially correlated over about ±2 groups ($c=0$, $r_g \approx 0.10$-0.15, $\theta=0.5$, $\gamma=2$). A priori uncertainties for the damage function were taken to be much larger, 1000% normalization uncertainty and 300% group-by-group uncertainties ($c=10$, $r_g=3$), although somewhat stronger short-range correlations were assumed ($\theta=0.9$, $\gamma=5$).

(a)

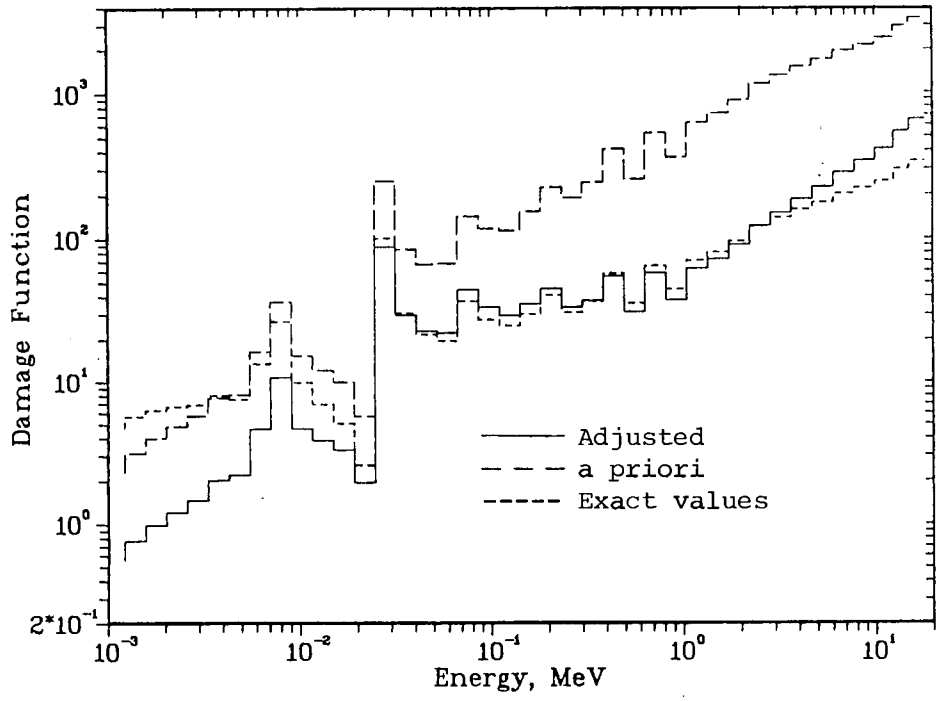

(b)

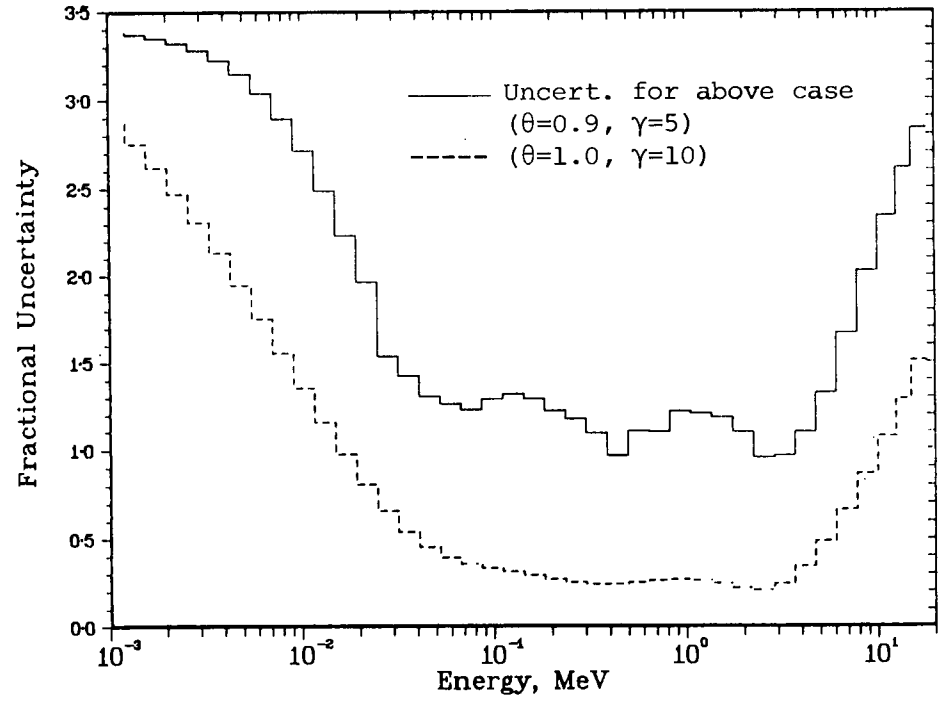

Figure 1. 75-group damage-function analysis. Although the analysis extended to thermal energies, only the top 39 groups are shown for clarity: (a) damage function; (b) uncertainties for adjusted results. θ and γ are short-range correlation parameters (see text).

The final uncertainties are shown by the solid line in Figure 1(b). Typical uncertainties in regions of low response near the edges of the plot are on the order of 300%. This value reflects the original 300% group-by-group uncertainties. Most of the 1000% overall normalization error is removed by the integral measurements. The energy ranges of high sensitivity to integral values are sharply delineated by about an additional factor-of-3 reduction in the final group damage-function uncertainties to about 100%, a value still large in the face of the striking agreement shown in Figure 1(a). In part, the good agreement in Figure 1(a) is an artifact of an artificial problem (in reality, exact damage values cannot be known) and illustrates the potential danger in using such comparisons as a means for testing the accuracy of the final solution. There are some indications that the present algorithm overestimates final uncertainties in loosely constrained systems such as the present example; although it gives reliable uncertainties for more constrained problems or where the uncertainties are smaller. Even so, one can explicitly demonstrate that all the correlations in the final damage function induced by the integral values are present to the following extent. If one computes the uncertainty in a particular damage value from the adjusted covariance matrix, uncertainties as small as the original "measured" values are obtained.

For comparison, a second example was run with a more constrained a priori damage function. The strength θ of the short-range correlation was increased from 0.9 to 1.0 and the range γ was increased from ±5 groups to ±10. The final uncertainties are compared to the previous case in Figure 1(b). As clearly shown, the increased a priori knowledge as specified by the stronger short-range correlations greatly reduces the uncertainties in the adjusted damage function, especially in the high-response energy groups where the final uncertainties drop from about 100% to near 25%. The values, themselves, for the adjusted damage function did not change significantly.

Fast-Neutron Spectrum Analysis

A second example we consider is the unfolding or adjustment of fast-neutron spectra based on dosimeter and proton recoil measurements. This example is similar in form to the previous example. It does show, however, how many-channel data (in this case proton-recoil data) can be easily included in the few-channel problem. Dosimeter reaction rates are related to multigroup fluxes and cross sections by

$$R_i = \sum_g \phi_g \sigma_{ig} \tag{18}$$

where i specifies the various dosimeter foils. As an aside, we note that the present code can include multiple spectra (e.g. from different locations within a reactor) at the same time as multiple foils.

This example is based on 12 actual dosimeter measurements in the Engineering Mockup Critical (EMC) as well as proton recoil measurements.[8]

It was reported on earlier[9] but without the proton-recoil measurements which are included directly in the analysis here. The 12 dosimeters include resonance detectors, threshold detectors, and broad range detectors. Dosimeter cross sections are based on ENDF/B-IV. The reported reaction rate measurements were typically 3-6% uncertain. The calculation used to generate an a priori flux was assumed to have a normalization uncertainty of 100c=50% and additional group-by-group uncertainties of $100r_g$=30% with short-range correlations specified by θ=0.5 and γ=5. Cross section uncertainties were evaluated and typically were much smaller. The analysis was carried out in 42 energy groups and proton-recoil measurements were included for the high-energy groups 4-22. Proton-recoil uncertainties were taken to be 5% with an additional 10% overall normalization uncertainty.

Results for the neutron flux are shown in Figure 2. Rather than pursue a detailed discussion, we draw attention to one particular feature of this example. Prior to inclusion of the proton recoil results, the neutron flux along with the multigroup representations of the 12 cross section sets were adjusted based solely on the dosimeter reaction rates. As shown by the dotted line in Figure 2, there was a rather noticeable upward adjustment of the neutron flux near 20 keV. Moreover, this adjustment was not confirmed by comparisons with proton-recoil measurements. Therefore, the proton-recoil measurements were included in the same analysis to provide a more direct constraint on the adjusted flux. As seen from the dashed line in Figure 2, the comparatively small uncertainties for the proton-recoil measurements effectively eliminate the previously noted upward flux adjustment. Instead the nuclear cross sections are adjusted, in particular $^{45}Sc(n,\gamma)$ which has a response in this energy region. Figure 3 shows that the scandium cross section had been adjusted upward a little prior to the inclusion of the proton-recoil data. But with the proton-recoil data, the adjustment is greater, more than 9% in spite of assigned uncertainties of only 6% for the a priori cross section in this energy range. There is a strong implication that the scandium cross section should be reexamined.

Multichannel Unfolding

The FERRET code was used to reduce data on recent D-Li neutron yield studies. The data reduction required the subtraction of a background measurement from a foreground measurement and accounted for detector response broadening. Also, although the problem was not underdetermined as in the previous examples, important a priori information was included: a presumed smoothness was specified by the use of a priori short-range correlations, and conservation of energy dictated that the neutron yield was rigorously zero above a known energy. The problem is summarized by Figure 4 which shows both the experimental neutron-yield measurements and the reduced data as a function of the neutron energy. The fluctuations seen in the measurements are due to counting statistics. Relative channel 30 corresponds to 50 MeV neutrons, and represents the highest energy for which neutrons are emitted.

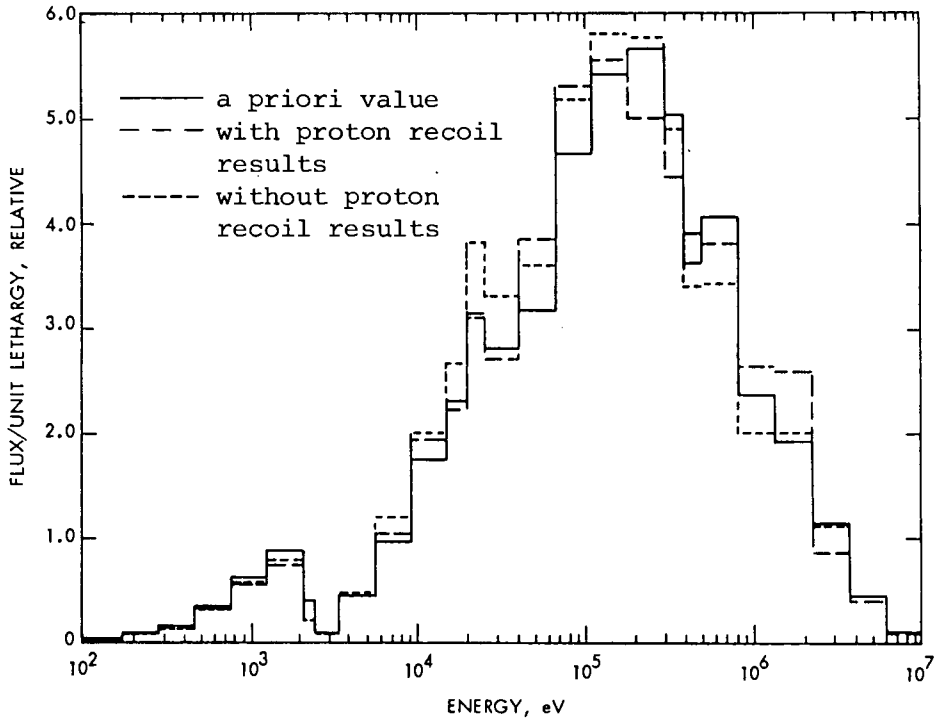

Figure 2. 42-group analysis for the Engineering Mockup Critical (EMC), neutron flux.

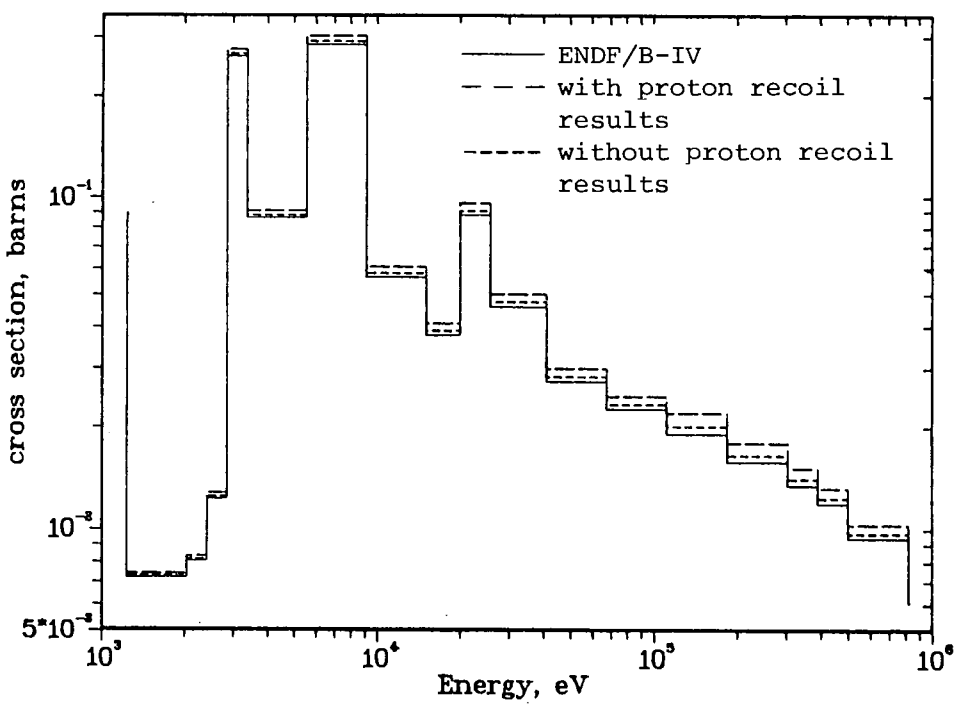

Figure 3. 42-group analysis for the Engineering Mockup Critical (EMC), $^{45}Sc(n,\gamma)$ cross section.

(a)

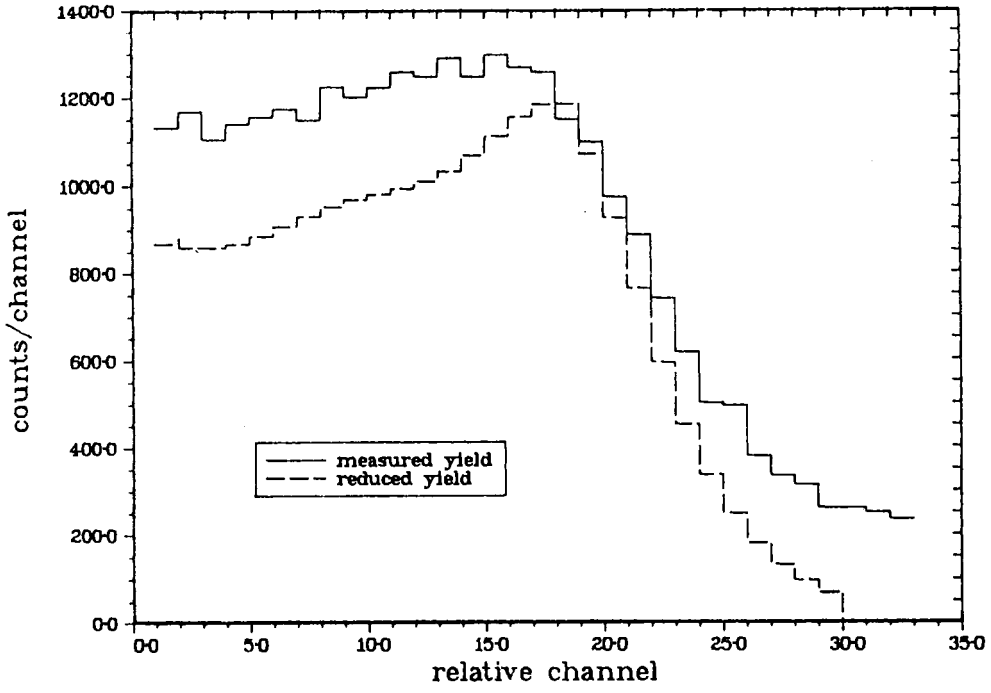

(b)

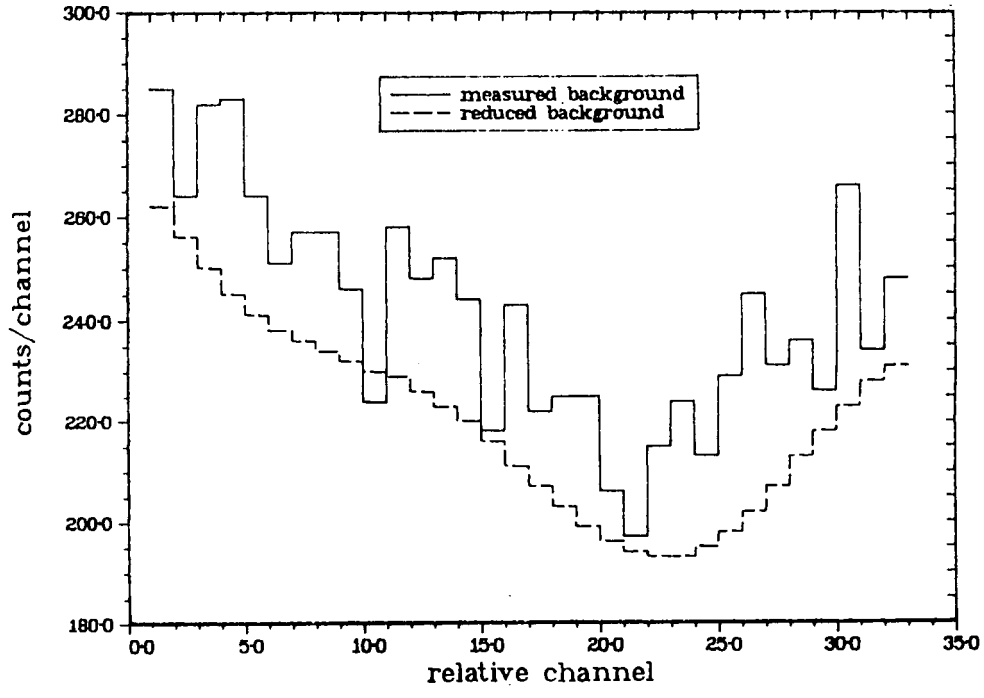

Figure 4. Measured and evaluated neutron yield data at 12°: (a) foreground results; (b) background results.

A particular advantage of the present method is apparent in Figure 5 which shows a sharp rise in the reduced-yield uncertainties above channel 25. As the foreground values become smaller at the higher energies (channels), one obtains the increased error associated with the background subtraction as the background becomes increasingly important.

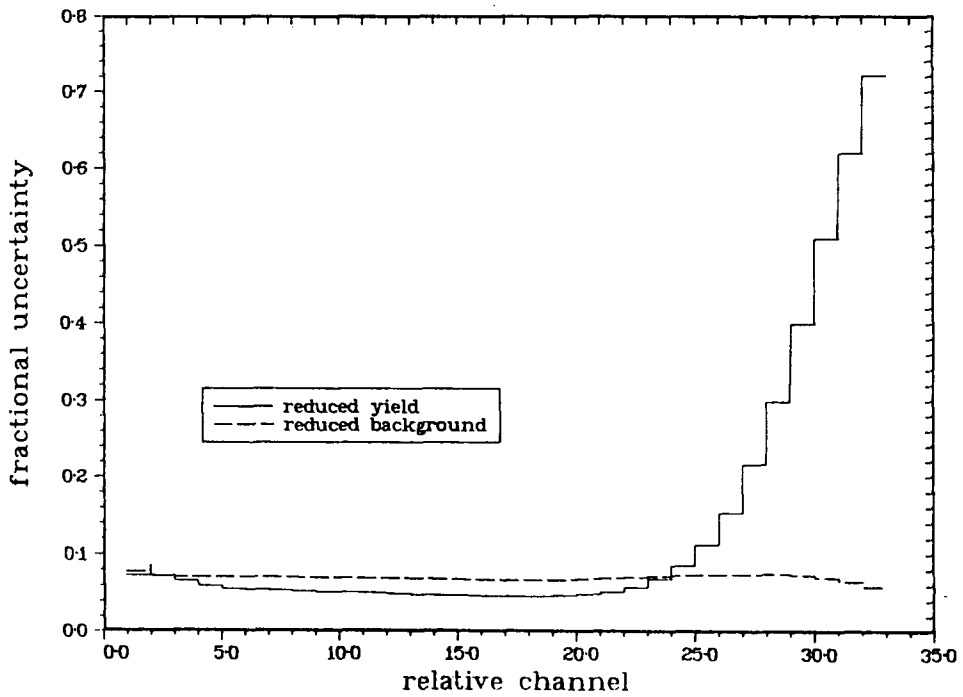

Figure 5. Final uncertainties for reduced neutron-yield data.

Cross Section Evaluation

Figure 6 summarizes the results of an evaluation for the neutron-capture cross section for the fission-product ^{109}Ag. Space precludes a detailed discussion. An important feature of this example is the simultaneous use of different types of integral measurements along with direct microscopic data to obtain a final evaluation. In addition to the microscopic data shown, integral worth measurements from several STEK cores[2,10] and a reaction rate measurement from the Coupled Fast Reactor Measurement Facility[11] (CFRMF) were included. Another feature is the use of a pointwise representation for the cross section in contrast to the multigroup-like representations used in the earlier examples. It is interesting to note that the integral measurements, in a sense, rule in favor of the Weston microscopic measurements.[12] The different microscopic measurements had comparable uncertainties. A final point concerns the character of the uncertainties. By their nature, neutron-capture measurements are often subject to overall normalization errors. This important correlation must be included if a measurement with a relatively large number of data points is not to be unduly weighted. The statistical weighting of the single degree-of-freedom associated with normalization generates less weight than a set of statistically-independent values.

The uncertainties are shown in Figure 6(b). For low energies, the reductions in the uncertainties for the adjusted values are due to integral measurements. At the higher energies, the uncertainty reduction to 12% arises from the elimination of a 40% a priori normalization error assumed above 1 keV.

(a)

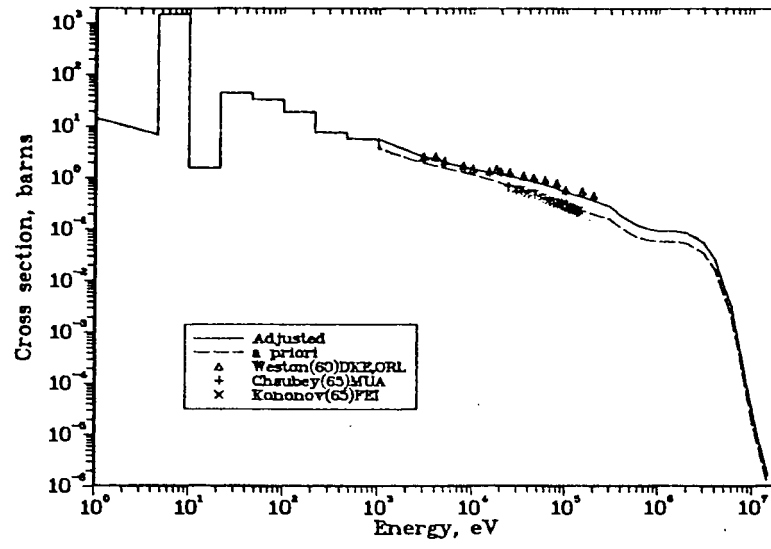

(b)

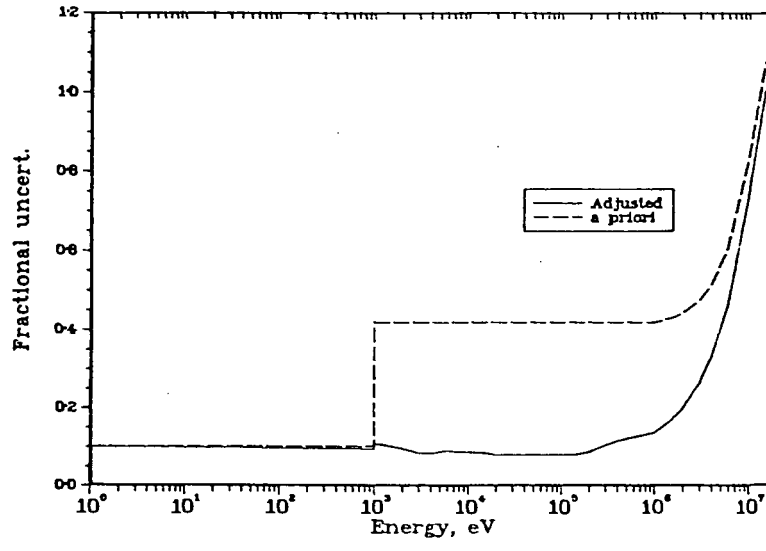

Figure 6. Neutron-capture cross section evaluation for ^{109}Ag: (a) cross section, (b) uncertainties.

SUMMARY

The examples discussed illustrate the diversity of problems that can be treated by the present method. Their common link is the need to simultaneously consider integral and differential data in a common evaluation. In common with a generalized least-squares approach, final uncertainties and covariances are generated that describe the accuracy of the final results. Particular attention was devoted to the problem of large a priori uncertainties for physical quantities known to be positive.

ACKNOWLEDGMENT

The use of preliminary data on recent D-Li neutron yield measurements by D. L. Johnson and F. M. Mann is gratefully acknowledged. The data for the damage function were provided by R. L. Simons. And finally, much of the work on the fission-product example was in conjunction with R. E. Schenter's group. All the above people are with the Hanford Engineering Development Laboratory (HEDL).

REFERENCES

1. Walter Clark Hamilton, Statistics in Physical Science, The Ronald Press Company, New York (1964).

2. J. B. Dragt, et al., Nucl. Sci. and Eng., 62, 117 (1977).

3. A. Gandini, Nuclear Data and Integral Measurements Correlation of Fast Reactors, Part 2: "Review of Methods", RT/Fi (73) 22, Comitato Nazionale Energia Nucleare (1973).

4. "A Review of Radiation Energy Spectra Unfolding, Proc. of a Seminar-Workshop, April 12-13, 1976", compiled by D. K. Trubey, ORNL/RSIC-40, Oak Ridge National Laboratory, Oak Ridge, TN, October 1976.

5. F. G. Perey, Least-Squares Dosimetry Unfolding: The Program STAY'SL, ORNL/TM-6062 (ENDF-254), October 1977 and Contributions to Few-Channel Spectrum Unfolding, ORNL/TM-6267 (ENDF-259), February 1978, Oak Ridge National Laboratory, Oak Ridge, TN.

6. F. Schmittroth, Generalized Least-Squares for Data Analysis, HEDL-TME 77-51, Hanford Engineering Development Laboratory, Richland, WA, March 1978.

7. F. Schmittroth, "Methods Development", Core Engineering Technical Progress Report, October, November, December 1977, HEDL-TME 77-49, pp. 51-60, Hanford Engineering Development Laboratory, Richland, WA, April 1978.

8. J. V. Nelson, et al., Measurement and Calculation of Neutron Spectra in the FTR Engineering Mockup Critical, HEDL-TME 76-88, Hanford Engineering Development Laboratory, Richland, WA, February 1977.

9. F. Schmittroth and J. A. Rawlins, "Dosimeter Based Adjustments of Fast-Neutron Spectra", HEDL-SA-1480, Hanford Engineering Development Laboratory, Richland, WA (June 1978); and in ANS Trans., Vol. 28, pg. 621 (June 18-22, 1978).

10. J. W. M. Dekker and H. Ch. Rieff, Adjusted Capture Cross Sections of Fission-Product Nuclides from STEK Reactivity Worths and CFRMF Data, ECN-28, Netherlands Energy Research Foundation (ECN), Petten, The Netherlands (August 1977).

11. Y. D. Harker, et al., Fission Product and Reactor Dosimetry Studies at Coupled Fast Reactivity Measurements Facility, TREE-1259, EG&G Idaho, Inc. (March 1978).

12. Microscopic neutron-capture data was obtained from the CSISRS data file available from the National Nuclear Data Center (NNDC), Brookhaven National Laboratory, Upton, New York.

SENSITIVITY AND UNCERTAINTY ANALYSIS APPLIED TO THE NBS-ISNF*

B. L. Broadhead
University of Tennessee
Knoxville, Tennessee

and

J. H. Marable
Oak Ridge National Laboratory
Oak Ridge, Tennessee

ABSTRACT

Sensitivities and uncertainties have been obtained for input into a least squares consistency analysis of the NBS-ISNF flux spectrum. One-dimensional ANISN transport calculations were used in the calculation of sensitivity coefficients. These sensitivity coefficients were then folded with covariance files to obtain the uncertainty in the NBS-ISNF central region flux spectrum due to cross section and fission spectrum uncertainties. This flux covariance file along with reaction rate ratio sensitivities and reaction cross sections with their covariances were used to adjust the NBS-ISNF flux spectrum, reaction cross sections and activations based on integral reaction rate ratio measurements and their uncertainties.

An initial calculated vs. experimental discrepancy for 28f/25f of 12.6% was removed by the adjustment. However, the cross sections and fluxes were adjusted by more than their standard deviations and the resulting chi-square per degree of freedom was 7, which indicated extreme inconsistency.

A finer energy mesh and replacement of a Maxwellian fission source by a preliminary-ENDF/B-V fission source gave a calculated vs. experimental discrepancy of only 4.3%. The resulting revised adjustment yielded a chi-square per degree of freedom of 1.2 which indicates good consistency among the various data. This revised adjustment included off-diagonal elements of the flux covariance matrix. If these off-diagonal elements are omitted, the chi-square per degree of freedom becomes 1.6 indicating only fair consistency.

*Research sponsored under U.S. NRC Interagency Agreement 40-552-75 with the Dept. of Energy under contract W-7405-eng-26 with Union Carbide Corp.

INTRODUCTION

The FORSS system[1] has been suggested as a tool for analysis of dosimetry unfolding problems.[2] Previously the FORSS system has been applied to Fast Reactor Benchmarks,[3,4] Radiation Transport[5] problems, LMFBR design uncertainties,[6] ENDF/B-V projections,[7] and others. This study applies the FORSS system to the analysis of a benchmark standard neutron field, the National Bureau of Standards-Intermediate Energy Standard Neutron Field (NBS-ISNF),[8] to obtain the "most likely" estimates for both the NBS-ISNF flux spectrum and several dosimetry cross sections as well as their covariances based on several experiment measurements. The maximum likelihood estimator is a linear least squares adjustment scheme such as reported in several other studies.[9,10,11]

Presently, much of the adjustment work is in the area of cross sections for the improvement of performance parameter predictions. However, very little work has been done in the area of dosimetry unfolding, where the aim is to adjust both dosimetry cross sections and the flux spectrum. One difficulty arises from the continuous nature of the flux; hence each group flux must be treated as an individual response (whereas with performance parameter predictions, there is only one response, the performance parameter itself). Also, the *a priori* flux covariance matrix is needed before an adjustment of the flux spectrum can be made. The sensitivities obtained using FORSS can be folded with constituent cross section covariance data to obtain this flux covariance matrix.

The motivation for this work arises from the economic incentive of the reduction in uncertainties of operating LWR fluences. Fluence uncertainties mandate conservatism in reactor pressure vessel lifetime estimates and therefore premature shutdown. Several reactors face shutdown within the next couple of years if these fluence uncertainties are not reduced. However, with the use of the techniques demonstrated in this study along with experimental measurements in both standard and reference fields, it is felt that predictions of operating fluences can be made with significantly more confidence; thus reducing unnecessary design conservatism.

APPROACH TO THE PROBLEM

This study has been broken into essentially two separate problems. Part I consists of the calculation of an *a priori* flux spectrum covariance matrix for the NBS-ISNF. Here we define the response of interest as the NBS-ISNF flux spectrum, since we are interested in the effect of cross section uncertainties on the flux spectrum. Part II uses integral data and its covariance matrix, dosimetry cross sections and their covariance matrices, and the NBS-ISNF flux spectrum and its covariance matrix to obtain "most likely" estimates of all of the above. Here the response of interest is the measured activity or activity ratio, since we are interested in the effect of cross section and flux spectrum changes on the activity or activity ratio.

SENSITIVITY ANALYSIS

Relative sensitivity coefficients form the basis for a study of this nature. In Part I relative sensitivity values allow an importance ranking of major system constituents according to the response which in our case is the NBS-ISNF central region flux. The energy-dependent relative sensitivity coefficients along with cross section covariance data are used to obtain the *a priori* flux covariance matrix. In Part II the relative sensitivity coefficients show the effect of cross section and flux adjustments on the calculated activity or activity ratio.

The total (summed over space and cross section energy) relative sensitivity coefficients for each group flux response are shown in Table 1. These quantities represent the indirect effect only since the NBS-ISNF constituent cross sections do not appear explicitly in the response. The energy-dependence (both flux spectrum and cross section) of these sensitivities is necessary for the *a priori* flux spectrum covariance matrix calculation. A plot of the energy dependence of the sensitivity of the total flux to the boron-10 absorption cross section is shown in Figure 1. Plots such as these are obtained for every response and cross section. The total relative sensitivity coefficients indicate the NBS-ISNF central region flux spectrum is very sensitive to the fission spectrum and carbon cross sections. Boron and aluminum are relatively unimportant in the intermediate and fast energy range (i.e., the range of interest in the NBS-ISNF). For a more detailed discussion of the procedures and results, see Reference 12.

For the relative sensitivities used in the adjustment (Part II), there were two responses, $^{28}f/^{25}f$ and $^{49}f/^{25}f$.[13] For these responses, it was necessary only to calculate the direct effect, since it was assumed that a perturbation in these cross sections would not change the flux.

UNCERTAINTY ANALYSIS

Folding of energy dependent relative sensitivity coefficients with ENDF/B-IV, and ORNL-generated covariance data yields the *a priori* estimate of the flux spectrum covariance matrix shown in Table 2. This flux spectrum covariance matrix is presented as a correlation matrix with its elements multiplied by 1000 for clarity. It contains contributions from carbon and the fission source. Boron and aluminum were not included; however, their contribution to the flux uncertainty is felt to be small since boron is a standard material, coupled with its low sensitivities at energies of interest and since aluminum has a very low sensitivity. The sensitivity matrix is formed from the previously calculated relative sensitivity coefficients with the columns representing various cross section energy intervals and the rows representing various flux spectrum intervals. The carbon covariance matrix was processed[14] using PUFF[5], while the fission spectrum covariance matrix was generated[12] assuming

a Maxwellian spectrum with a mean energy of 2 MeV ±2%. Once the sensitivity and covariance matrices for all materials is obtained the flux spectrum covariance matrix is obtained by: $\underline{M}_{\phi} = \sum_{mat.} \underline{S}^{T} \cdot \underline{M}_{\Sigma} \cdot \underline{S}$ where $\underline{S}$ is the sensitivity matrix, $\underline{M}_{\Sigma}$ the cross section covariance matrix, and $\underline{M}_{\phi}$ the flux spectrum covariance matrix.

The resulting flux covariance matrix is strongly correlated with relatively small standard deviations. It should be pointed out that these uncertainties are due to nuclear data only. The relatively low estimates for the uncertainties in the flux spectrum confirms the potential usefulness of this field as a standard.

ADJUSTMENT

The adjustment utilized the method of Gandini and Salvatores[11] to reduce the uncertainty in both the flux and dosimetry cross sections based on integral measurements made in the NBS-ISNF facility. The data used for the adjustment is shown in Table 3. A newly developed code UNCOVER,[15] which allows partitioned matrices to be brought into the core as needed, was used for the adjustment. A schematic of the partitioned covariance matrix used in this analysis is shown in Figure 2. The Pu-239f, U-238f, and U-235f covariance data were processed into a 15-group structure using PUFF. The AMPX system[16] processed dosimetry cross sections from the 171- group VITAMIN-C library.[17] A Pu-239 fission spectrum weight function was used to collapse from 171 to 126 groups, then an approximate NBS-ISNF flux spectrum in 126-groups was used to collapse from 126 to 15 groups. The $\frac{\text{exp. - calc.}}{\text{calc.}}$ values shown in Table 4 show a 12% discrepancy in the measured vs. calculated value for $^{28}f/^{25}f$. The adjustment removed this discrepancy as also shown, but the cross sections were adjusted beyond their standard deviations and the resulting chi-square test for goodness of fit was ∿7 per degree of freedom. This indicates extreme inconsistency in the measured (± uncertainty) vs. the calculated (± uncertainty) values.

REVISED ADJUSTMENT

The first attempt to resolve this discrepancy utilized an ENDF/B-V U-235 fission spectrum as the fixed source in a 15-group *a priori* flux spectrum calculation, as opposed to the previous calculation which used an NBS supplied source.[18] The result was a decrease in the magnitude of the 28/25 discrepancy of 3.5%. The second attempt utilized an ENDF/B-IV U-235 (since a 171-group NBS source was not available) fission spectrum in a 171-group *a priori* flux spectrum calculation. The 28/25 discrepancy was reduced 4.5% from the reference case.

A final revised adjustment utilized a preliminary ENDF/B-V U-235 fission source in 171-groups to reduce the *a priori* calculated vs. experimental discrepancy of the $^{28}f/^{25}f$ response from 12.6% to 4.3% as shown in Table 5. Also the $^{49}f/^{25}f$ discrepancy was reduced from 4.7% to 2.7%. As can be seen in Table 5, these *a priori* discrepancies are now within combined experimental and calculational uncertainties such that chi-square per degree is now 1.2. The resulting adjustment further decreased these discrepancies to 1.5% and 0.5% for $^{49}f/^{25}f$ and $^{28}f/^{25}f$, respectively, as shown in Table 5. Also, inspection of Tables 6, 7, 8, and 9 show that the cross section and flux adjustments are well within their standard deviations.

For comparison, the revised adjustment was repeated assuming the off-diagonal elements of the flux spectrum covariance were 0. Flux spectrum changes for these two cases are shown in Table 9. The resulting chi-square per degree of freedom was 1.6 as compared to 1.2 for the case which did consider the off-diagonal elements. These chi-square values have corresponding probabilities where 1.2 has a probability of 0.3 (the standard deviation has 30% chance of being higher, 70% lower) and 1.6 has a probability of 0.2. Thus it appears the inclusion of off-diagonal elements of the flux covariance matrix does affect the adjustment and a more consistent adjustment is obtained if you consider the off-diagonal elements.

SUMMARY AND CONCLUSIONS

An *a priori* flux spectrum covariance matrix for the NBS-ISNF was generated for the calculation of "most likely" estimates for the NBS-ISNF flux spectrum and dosimetry cross sections based on two integral experiment values. Additional covariance data included dosimetry cross section covariances, processed from ORNL internal point-covariance files, and covariance data for the integral experiments, obtained from NBS. The resulting adjustment decreased large $^{28}f/^{25}f$ and $^{49}f/^{25}f$ calculated vs. experimental discrepancies (12.6% and 4.6% respectively) to acceptable values. However, many group cross sections and fluxes were adjusted beyond the limits of their standard deviations and the resulting chi-square test showed the adjustments to be extremely inconsistent (chi-square/degree=7.2).

Upon recalculation of the two experiments using a 171-group cross section set with a preliminary ENDF/B-V U-235 fission spectrum, the calculated vs. experimental discrepancies were reduced from 12.6% to 4.2% and 4.6% to 1.6% for $^{28}f/^{25}f$ and $^{49}f/^{25}f$, respectively. The resulting revised adjustment further decreased these discrepancies, to 0.5% and 1.5%, respectively, and the chi-squared test indicated the adjustments were now consistent with the standard deviations of the cross sections and fluxes.

It is interesting to note that the primary difference between the first and second adjustment is due to a correction in the calculation

based on a finer group structure and an improved fission spectrum. The 171-group calculation allows, in essence, a correction to the 15-group cross sections and fluxes for methods and data deficiencies.

As a final note, it can be seen in Table 9 that inclusion of the off-diagonal elements of the flux spectrum covariance matrix gives a more consistent adjustment. This is an important conclusion since many adjustment codes neglect these off-diagonal elements.

ACKNOWLEDGMENTS

The authors wish to thank the following persons for their contributions to this paper: C. R. Weisbin for his suggestion of this study and his valuable comments, F. G. Perey for his many valuable comments and suggestions, J. L. Lucius for his guidance in the sensitivity coefficient generation, J. D. Drischler for suggestions regarding processing of cross section covariance data, J. E. White and R. Q. Wright for their guidance in cross section processing, H. L. Dodds, Jr. for his guidance and encouragement, C. Eisenhauer and J. Grundl for supplying model and integral data, and Nancy Allen, Brenda Neely, Barbara Beem and Kathy Oldham for typing and editing this manuscript.

REFERENCES

1. C. R. Weisbin, E. M. Oblow, F. R. Mynatt, and G. F. Flanagan, "The FORSS Sensitivity Analysis Code System," *Trans. Am. Nucl. Soc.*, *22*, 792 (1975) and these proceedings.

2. W. N. McElroy, R. Gold, E. P. Lippincott, A. Fabry, and J. H. Roberts, "Spectral Characterization by Combining Neutron Spectroscopy, Analytical Calculations, and Integral Measurements," *Neutron Cross Sections for Reactor Dosimetry*, (Proceedings of a Consultants' meeting on Integral Cross-Section Measurements in Standard Neutron Fields for Reactor Dosimetry), IAEA-208, Vienna, 147, (1978).

3. C. R Weisbin, E. M. Oblow, J. G. Marable, R. W.Peelle, J. L. Lucius, "Application of Sensitivity and Uncertainty Methodology to Fast Reactor Integral Experiment Analysis," *Nucl. Sci. and Eng.*, *66*, 307 (1978).

4. J. H. Marable, J. L. Lucius, and C. R. Weisbin, *Compilation of Sensitivity Profiles for Several CSEWG Fast Reactor Benchmarks*, ORNL-5262 (1977).

5. C. R. Weisbin, E. M. Oblow, J. Ching, J. E. White, R. Q. Wright, and J. D. Drischler, *Cross Section and Method Uncertainties: The Application of Sensitivity Analysis to Study Their Relationship in Radiation Transport Benchmark Problems*, ORNL-TM-4847 (ENDF-218) (August 1975) see also, RSIC Code Collection PSR-93.

6. J. H. Marable and C. R. Weisbin, "Uncertainties in the Breeding Ratio of a Large LMFBR," Proceedings of an American Nuclear Society Topical Meeting, Gatlinburg, Tennessee, 231 (June 1978).

7. C. R. Weisbin, J. H. Marable, J. Hardy, Jr., and R. D. McKnight, "Projections of ENDF/B Version V Performance for Fast and Thermal Reactors Using Sensitivity Coefficients," Proceedings of an American Nuclear Society Topical Meeting, Gatlinburg, Tennessee, 79 (June 1978).

8. C. M. Eisenhauer, J. A. Grundl, A. Fabry, C. D. Bowman, A. D. Carlson, H. O. Lisken, "Neutron Standards and Applications," *Proceedings of International Symposium on Neutron Standards and Applications, NBS* -- special publication 493 (1977).

9. J. B. Dragt, *Statistical Considerations on Techniques for Adjustment of Differential Cross Sections with Measured Integral Parameters*, RCN-122 (August 1970).

10. F. G. Perey, *Least-Squares Dosimetry Unfolding: The Program STAY'SL*, ORNL/TM-6062, ENDF-254 (October 1977).

11. A. Gandini, et al., *Nuclear Data and Integral Measurements Correlation for Fast Reactors*, Parts I, II, and III, RT/FI(73)5, RT/FI(73)22, and RT/(74)3 (1973 and 1974).

12. B. L. Broadhead, J. L. Lucius, F. G. Perey, C. R. Weisbin, and H. L. Dodds, Jr., "Calculation of the Flux Covariance Matrix for the National Bureau of Standards-Intermediate Energy Standard Neutron Field (NBS-ISNF)," Trans. Am. Nucl. Soc., 30 (November 1978).

13. C. M. Eisenhauer, private communication (1978).

14. J. D. Drischler and C. R. Weisbin, *Compilation of Multigroup Cross Section Covariance Matrices for Several Important Reactor Materials*, ORNL-5318, ENDF-235 (October 1977).

15. UNCOVER is a revision of the AMARA program permitting the solution of problems with a large number of groups. See also A. Gandini and M. Petilli, "AMARA: Code Using the Lagrange Multiplier Method for Nuclear Data Adjustment, private communication, M. Salvatores (1975).

16. N. M. Greene, J. L. Lucius, L. M. Petrie, W. E. Ford, III, J. E. White, R. Q. Wright, *AMPX: A Modular Code System for Generating Coupled Multigroup Neutron-Gamma Libraries from ENDF/B*, ORNL/TM-3706 (March 1976).

17. R. W. Roussin, C. R. Weisbin, J. E. White, N. M. Greene, R. Q. Wright, and J. B. Wright, *The CTR Processed Multigroup Cross Section Library for Neutronic Studies*, ORNL/RSIC-37 (1978).

18. J. Grundl and C. Eisenhauer, "Benchmark Neutron Fields for Reactor Dosimetry," *Neutron Cross Sections for Reactor Dosimetry*, Vol I, IAEA, Vienna (1978).

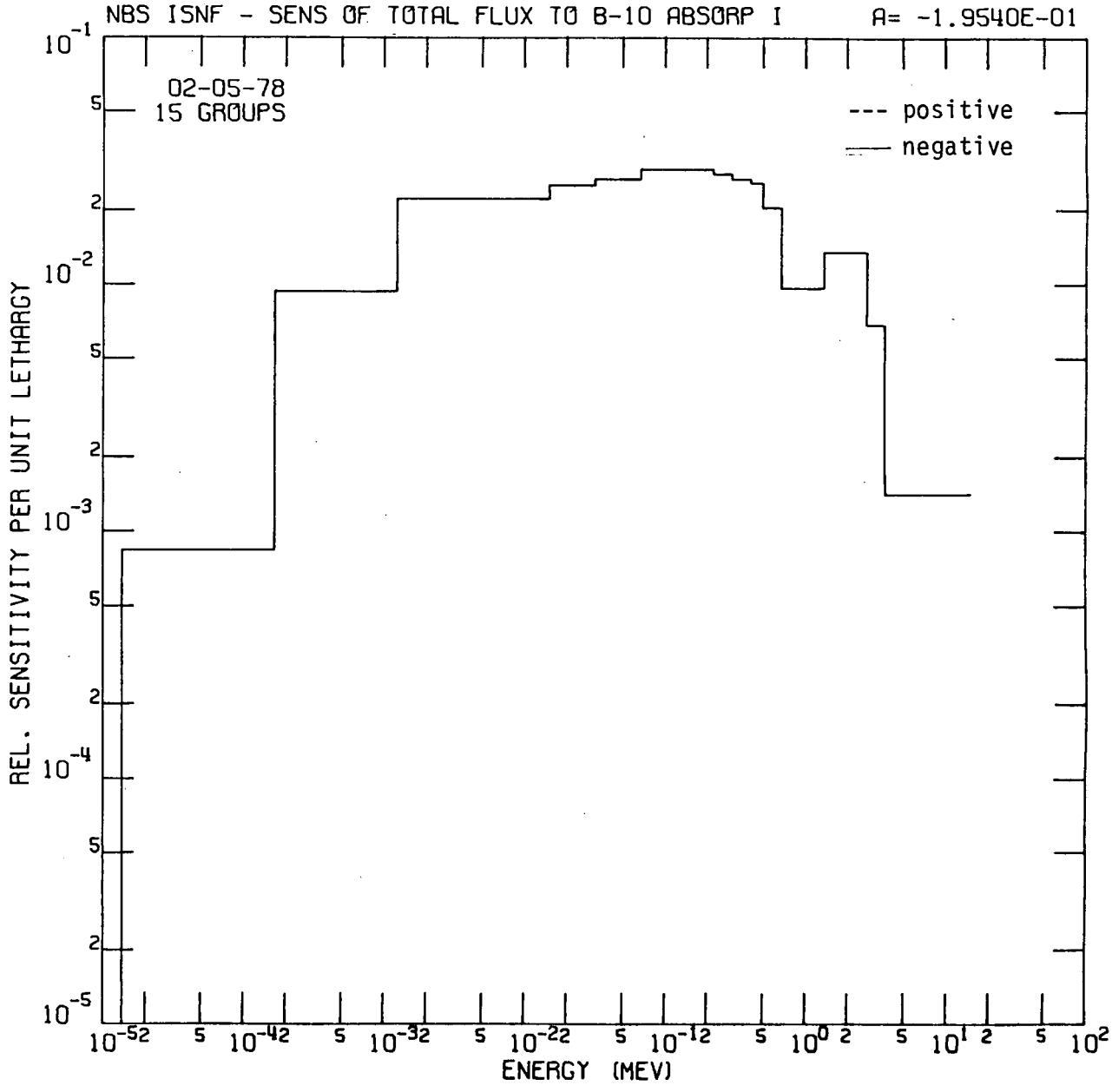

Fig. 1. Sensitivity of the flux integrated over all energies in the NBS-ISNF central region to B-10 absorption cross section in various energy intervals.

	I.E.	28f	49f	25f	ϕ
I.E.	X				
28f		X	X	X	
49f		X	X	X	
25f		X	X	X	
ϕ					X

Note: Blank boxes were assumed to be zero, crosses represent quanities that were used in the analysis.

Figure 2. Extended covariance matrix partitions used in UNCOVER code.

TABLE 1. RELATIVE SENSITIVITY COEFFICIENTS FOR EACH GROUP FLUX TO CROSS SECTIONS SUMMED OVER ENERGY AND SPACE.

CENTRAL REGION FLUX RESPONSE	ALUMINUM-27 TOTAL	BORON-10 ABSORPTION	CARBON-12 TOTAL	FISSION[a] SPECTRUM
GROUP 1	-.0301	-.0316	.0834	1.0
GROUP 2	-.0290	-.0304	.0637	1.0
GROUP 3	-.0163	-.0404	.2302	1.0
GROUP 4	.0011	-.0326	.3130	1.0
GROUP 5	-.0020	-.0636	.3653	1.0
GROUP 6	-.0089	-.0917	.3950	1.0
GROUP 7	.0031	-.1127	.4285	1.0
GROUP 8	.0074	-.1444	.4584	1.0
GROUP 9	-.0090	-.2426	.5735	1.0
GROUP 10	-.0910	-.3442	.6415	1.0
GROUP 11	.0386	-.4564	.7210	1.0
GROUP 12	-.0132	-.8085	.8038	1.0
GROUP 13	-.0203	-2.0197	.8524	1.0
GROUP 14	-.0239	-4.3922	.8938	1.0
TOTAL	-.0112	-.1954	.4154	1.0

[a]These are derived quantities.

TABLE 2. NBS ISNF FLUX CORRELATION MATRIX (10**3)

NOTE: GROUP 15 HAS BEEN OMITTED

GROUP BOUNDARY	% REL. ST. DEV.																
0.1733D 08	5.0	1	1000														
0.3679D 07	2.8	2	998	1000													
0.2725D 07	0.9	3	963	959	1000												
0.1353D 07	0.4	4	-802	-803	-631	1000											
0.6721E 06	0.8	5	-920	-920	-815	965	1000										
0.4979D 06	0.9	6	-937	-936	-849	923	995	1000									
0.4076D 06	1.1	7	-937	-936	-855	892	978	997	1000								
0.3020D 06	1.2	8	-947	-946	-872	889	978	991	994	1000							
0.2237D 06	1.2	9	-933	-932	-860	893	968	981	983	994	1000						
0.6738D 05	1.2	10	-854	-854	-780	844	899	904	901	928	955	1000					
0.3183D 05	1.1	11	-821	-820	-740	841	892	894	890	912	951	965	1000				
0.1503D 05	1.0	12	-673	-672	-593	749	785	780	774	797	836	852	884	1000			
0.1234D 04	0.9	13	-586	-585	-504	698	730	720	722	729	774	753	798	815	1000		
0.1670D 03	0.8	14	-475	-474	-399	627	644	641	641	639	700	680	734	791	991	1000	
0.1371D 02		15															
0.1000D-03																	

TABLE 3. EXPERIMENTAL DATA[13]

Response	Exp.	S-D(%)
$\frac{49f}{25f}$	1.155	1.8
$\frac{28f}{25f}$	0.0923	1.1

Correlation Matrix for Integral Data

1.000	.266
.266	1.000

TABLE 4. RESULTS OF FIRST ADJUSTMENT

Response	Exp.	Calc.	[a]E-C Old / C (%)	[b]E-A New / A (%)	St. Dev. Exp. (%)	St. Dev. Old Calc.(%)	St. Dev. New Adj. (%)
$\frac{49f}{25f}$	1.1550	1.1006	4.9	2.3	1.8	2.3	1.1
$\frac{28f}{25f}$	.0923	0.0820	12.6	1.3	1.1	3.4	1.0

chi-square/degree = 7.2

[a]a priori

[b]a posteriori

TABLE 5. RESULTS OF REVISED ADJUSTMENT

Response	Exp.	Calc.	[a]E-C Old / C (%)	[b]E-A New / A (%)	St. Dev. Exp. (%)	St. Dev. Old Calc.(%)	St. Dev. New Adj. (%)
$\frac{49f}{25f}$	1.1550	1.1243	2.7	1.5	1.8	2.2	1.1
$\frac{28f}{25f}$	.0923	.0885	4.3	0.5	1.1	3.3	1.0

chi-square/degree = 1.2

[a]a prior

[b]a posteriori

TABLE 6. U-235$_f$ CROSS SECTION ADJUSTMENTS

Group Number	Group Boundaries (eV)	Change (%)	St. Dev. Old (%)	St. Dev. New (%)
1	1.733E+07	1.19	2.99	2.81
2	3.679E+06	1.38	3.00	2.79
3	2.725E+06	1.09	2.26	2.10
4	1.353E+06	0.39	2.48	2.47
5	6.721E+05	-0.08	3.50	3.46
6	4.979E+05	-0.08	3.50	3.46
7	4.076E+05	-0.55	2.95	2.87
8	3.020E+05	-0.58	3.00	2.92
9	2.237E+05	-1.02	2.61	2.46
10	6.738E+04	-1.82	2.97	2.68
11	3.183E+04	-2.43	3.54	3.12
12	1.503E+04	-3.16	4.91	4.42
13	1.234E+03	-1.74	3.17	2.95
14	1.670E+02	-1.37	3.10	2.96
15	1.371E+01	-0.92	2.56	2.49
	1.000E-04			

TABLE 7. U-238$_f$ CROSS SECTION ADJUSTMENTS

Group Number	Group Boundaries (eV)	Change (%)	St. Dev. Old (%)	St. Dev. New (%)
1	1.733E+07	1.24	3.01	2.83
2	3.679E+06	1.49	3.01	2.76
3	2.725E+06	1.18	2.31	2.12
4	1.353E+06	0.57	2.60	2.57
5	6.721E+05	-0.07	3.79	3.75
6	4.979E+05	-0.07	3.95	3.91
7	4.076E+05	-0.62	4.20	4.13
8	3.020E+05	-0.67	4.55	4.48
9	2.237E+05	-1.01	7.01	6.96
10	6.738E+04	-1.73	36.69	36.67
11	3.183E+04	-2.18	109.59	109.58
12	1.503E+04	-2.91	109.59	109.57
13	1.234E+03	-1.48	109.59	109.59
14	1.670E+02	-1.12	109.59	109.59
15	1.371E+01	-0.66	109.59	109.59
	1.000E-04			

TABLE 8. Pu-239$_f$ CROSS SECTION ADJUSTMENTS

Group Number	Group Boundaries (eV)	Change (%)	St. Dev. Old (%)	St. Dev. New (%)
1	1.733E+07	1.21	3.01	2.84
2	3.679E+06	1.41	3.03	2.82
3	2.725E+06	1.12	2.30	2.14
4	1.353E+06	0.44	2.57	2.54
5	6.721E+05	-0.05	3.52	3.48
6	4.979E+05	-0.05	3.52	3.47
7	4.076E+05	-0.52	3.01	2.93
8	3.020E+05	-0.56	3.07	2.99
9	2.237E+05	-0.99	2.66	2.52
10	6.738E+04	-1.78	3.16	2.89
11	3.183E+04	-2.43	3.60	3.18
12	1.503E+04	0.69	9.42	8.40
13	1.234E+03	3.05	10.49	9.13
14	1.670E+02	3.43	10.47	9.09
15	1.371E+01	3.88	10.34	8.92
	1.000E+04			

TABLE 9. COMPARISON OF REVISED FLUX ADJUSTMENTS WITH AND WITHOUT OFF-DIAGONAL ELEMENTS OF THE FLUX SPECTRUM COVARIANCE MATRIX.

Group Number	Group Boundaries (eV)	Change With (%)	Change w/o (%)	St. Dev. Old (%)	St. Dev. New w/ (%)	St. Dev. New w/o (%)
1	1.733E+07	3.77	2.06	4.97	3.75	4.75
2	3.697E+06	2.11	0.60	2.79	2.10	2.76
3	2.725E+06	0.64	0.19	0.88	0.69	0.87
4	1.353E+06	-0.28	-0.01	0.44	0.37	0.44
5	6.721E+05	-0.55	-0.01	0.76	0.57	0.76
6	4.979E+05	-0.70	-0.01	0.96	0.72	0.94
7	4.076E+05	-0.80	-0.02	1.09	0.84	1.09
8	3.020E+05	-0.88	-0.03	1.18	0.90	1.18
9	2.237E+05	-0.91	-0.10	1.22	0.93	1.22
10	6.738E+04	-0.83	-0.05	1.18	0.95	1.18
11	3.183E+04	-0.75	-0.04	1.09	0.89	1.09
12	1.503E+04	-0.60	-0.18	1.00	0.87	1.00
13	1.234E+03	-0.48	-0.03	0.92	0.82	0.92
14	1.670E+02	-0.38	-0.002	0.84	0.78	0.84
15	1.371E+01					
	1.000E-04					

SENSITIVITY ANALYSIS APPLIED TO AN INTEGRAL TEST OF NIOBIUM CROSS SECTIONS

D. T. Ingersoll
Oak Ridge National Laboratory
Oak Ridge, Tennessee, U.S.A.
and
B. W. Wehring
University of Illinois at Urbana-Champaign
Urbana, Illinois, U.S.A.

ABSTRACT

Simultaneous neutron and gamma-ray measurements were made of the leakage spectra from a Cf-252 spontaneous fission source located at the center of a solid, 9.6-cm thick, spherical shell of niobium. The NE-213 data were unfolded above 1 MeV and compared on an absolute basis to one-dimensional transport calculations, thus providing an integral test of Nb cross section data and multi-group processing. Several neutron, gamma-ray coupled cross section sets were investigated including the fine group VITAMIN-C library.

Calculations based on ENDF/B-III and IV data were in good agreement with the measured neutron spectrum below 10 MeV but diverged from the measurement above 10 MeV. ENDF/B-III data were in generally good agreement with the gamma-ray measurement while ENDF/B-IV gave an overestimation of the leakage. Sensitivity analysis showed that inelastic reactions were the dominant gamma-ray production mechanism for Nb, and that the gamma-ray leakage had much larger cross section sensitivities than the neutron leakage. Based on this integral test, it is suggested that a reevaluation of ENDF/B-IV Nb data for inelastic processes above 1 MeV and all processes above 10 MeV be made.

INTRODUCTION

An integral test of nuclear data uses a comparison of measurements and calculations to provide information on the accuracy of the data and/or the data processing. For a valid test, both the experiment and the calculations must use proven methods, and the geometry of the problem must be sufficiently simple to insure interpretable measurements and reliable computations. An integral test of niobium cross sections has

*Research sponsored by the Division of Nuclear Research and Applications, U.S. Department of Energy under contract W-7405-eng-26 with the Union Carbide Corporation.

been made within the energy range of 1 to 14 MeV. A measurement of the neutron and gamma-ray leakage spectra from a ^{252}Cf spontaneous fission source located at the center of a spherical shell of niobium was compared to several one-dimensional transport calculations which utilized ENDF/B cross sections and accepted multigroup processing methods. The extreme simplicity of the geometry and the use of standard experimental and analytic techniques satisfied the necessary requirements for an accurate test of the relevant niobium cross sections. Sensitivity analysis proved useful in understanding the complex relationship between the neutron and gamma-ray leakage spectra and in locating the source of the disagreement between the measurement and the calculations.

EXPERIMENTAL PROCEDURE

The procedure used at the University of Illinois (UIUC) to measure the neutron and gamma-ray spectra will be described briefly. A 4 μg ^{252}Cf spontaneous fission source was placed at the center of a spherical shell of niobium which was positioned 2m above a concrete floor. The sphere had an outside radius of 12.7 cm and an inside radius of 3.1 cm. An NE-213 spectrometer system[1] was used to simultaneously collect the neutron and gamma-ray pulse height data. The 5-cm NE-213 scintillation detector was also positioned 2m above the floor at a distance of 200 ± 1 cm from the Nb sphere. A lead and paraffin shadow shield was placed between the sphere and detector to obtain background data. The pulse height spectra were unfolded with the FORIST code[2] which used NE-213 neutron and gamma-ray response matrices prepared at UIUC.[1,3] The unfolded spectra are shown in Fig. 1 together with the Gaussian "window" function used to smooth the unfolded solution. Although the high energy data was collected for nearly 75h, statistical error in the data was unacceptably large above 14 MeV neutron energy and 6 MeV gamma-ray energy. The lower limit of approximately 1 MeV was determined by pulse shape discrimination considerations. The spectra were normalized on an absolute basis using the known source strength, the measured source-detector separation, and the absolute detector efficiency.

CALCULATION OF LEAKAGE SPECTRA

The neutron and gamma-ray leakage spectra were calculated at both UIUC and ORNL using the one-dimensional discrete ordinates code ANISN.[4] Thirty-five mesh intervals were used, with an S_{32} annular quadrature and P_3 cross sections. The ^{252}Cf source was distributed uniformly in the first interval and was assumed for neutrons to be a Maxwellian distribution with a temperature of 1.43 MeV. For gamma rays, the source was assumed to be an exponential with a "decay constant" of 1.13 $MeV.^{-1}$ The shape of both the neutron and the gamma-ray source distributions were determined from bare source measurements.

Several multigroup coupled neutron and gamma-ray cross section sets based on ENDF/B data were used in the transport calculations. All sets were obtained from the Radiation Shielding Information Center (RSIC) and

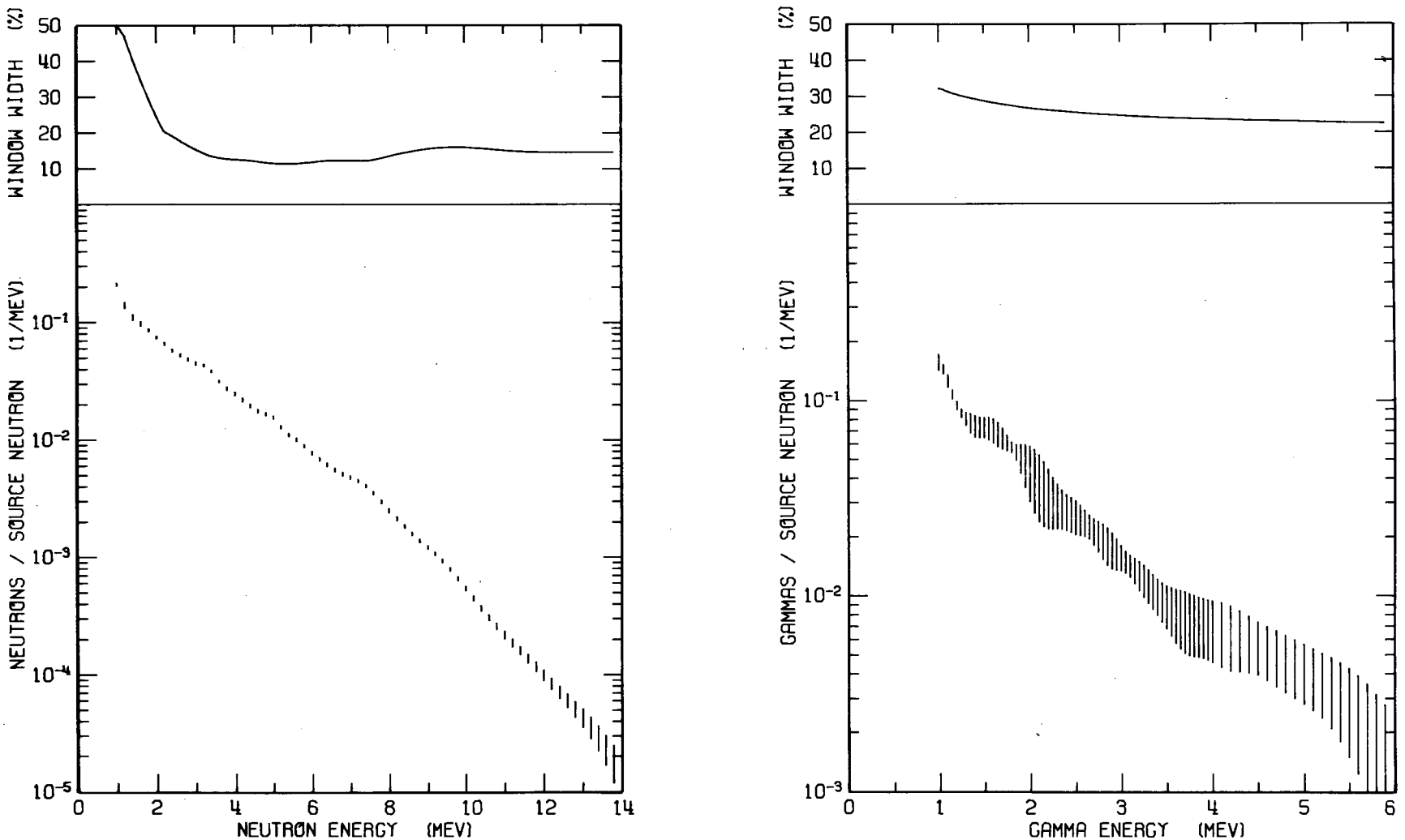

Fig. 1. Measured neutron (left) and gamma-ray (right) leakage spectra from a ^{252}Cf source in a niobium sphere. The upper curves represent the full-width-at-half-maximum of a Gaussion window function used to smooth the unfolded data.

included: DLC-28,[5] DLC-37C,[6] DLC-41,[7] and DLC-47.[8] Only DLC-28 was based on ENDF/B-III, MAT-1164 data, while the other sets used ENDF/B-IV, MAT-1189 data. The DLC-47 set containing 45 neutron and 16 gamma-ray groups was derived from the 171/36-group DLC-41 set and will not be discussed further. The DLC-28 and 37C sets were prepared using a 1/E flux weighting, while DLC-41 used a Maxwellian-1/E-fission-fusion peak weighting function. All sets assumed infinitely dilute media for niobium.

Calculated leakage spectra from the Nb sphere are given in Fig. 2 which compares the DLC-28, 37C, and 41 results. All spectra have been smoothed by the Gaussian window function which was used to smooth the unfolded measurements (see Fig. 1). The two ENDF/B-IV data sets gave nearly identical results despite the differences in group structure and multigroup processing. However, the version-III data gave significantly different results, especially for the gamma-ray leakage.

COMPARISON OF MEASUREMENT AND CALCULATIONS

The comparison of measured and calculated leakage spectra are shown in Fig. 3. To facilitate the comparison, the calculations have been approximated by a line passing through the center of each energy group. The neutron spectra compared well, except above 10 MeV where the calculations diverged from the measurements. At 14 MeV, the calculations overpredicted the measurement by a factor of 3. The DLC-28 data also gave too high a result between 2 and 3 MeV. The gamma-ray spectra showed considerable differences, with DLC-28 appearing to give the better results. While the DLC-41 calculation was generally 30 to 50% too high over the entire energy range, the DLC-28 results were only 10 to 20% high between 2 and 4 MeV.

In trying to understand the differences between the DLC-28 and 41 results and the measurement, an obvious starting point was to compare the ENDF/B-III and IV evaluations for niobium. This comparison is shown in Fig. 4 which was taken from the ENDF/B-IV evaluation report for MAT 1189.[9] In the relevant energy range (above 1 MeV) the most significant differences in the two evaluations are in the elastic and inelastic cross sections. Above 4 MeV, the elastic cross section was raised for version-IV by approximately 10%. The continuum inelastic, which was treated as a floating parameter to establish consistency with the total cross section, was thereby reduced 10 to 60%. Since the average energy loss per interaction near 10 MeV is only 0.2 MeV for elastic scattering compared to several MeV for inelastic reactions, the inelastic process is more important in terms of removal from higher to lower energies. Therefore, the increase in the elastic cross section and the compensating decrease in the inelastic might have been responsible for the larger neutron leakage calcualted above 10 MeV using DLC-41. However, it does not explain why the DLC-41 gamma-ray leakage was also higher than DLC-28. Also, the difference between the version-III and IV calculations was small compared to the calculation-measurement discrepancy. Thus the cause of the observed disagreements is not obvious. Sensitivity analysis was used to further investigate the problem.

ORNL-DWG-78-16453

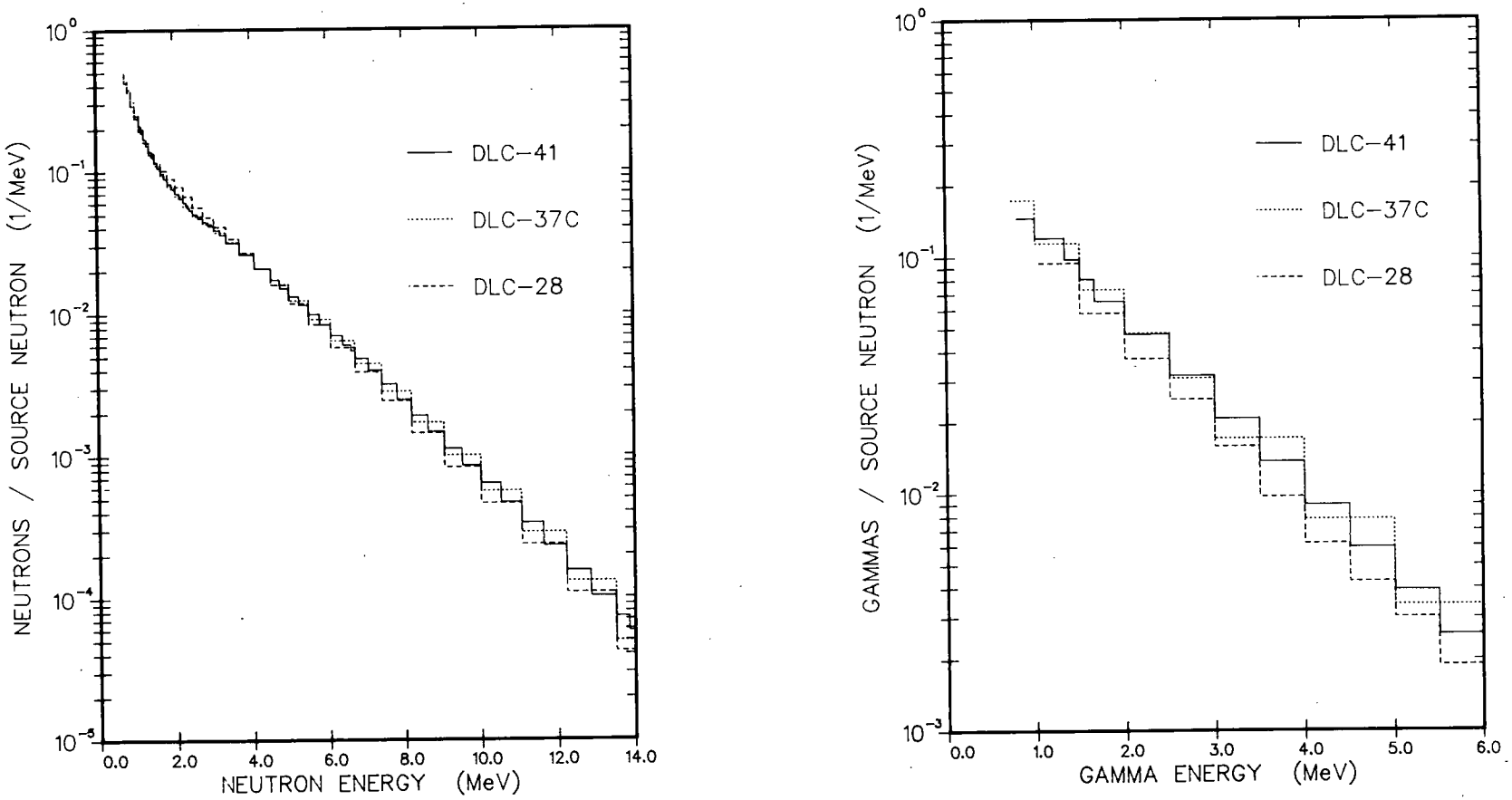

Fig. 2. Calculated neutron (left) and gamma-ray (right) leakage spectra. The DLC-41 and 37C cross section sets were based on ENDF/B-IV while DLC-28 was from version-III.

ORNL-DWG-78-16454

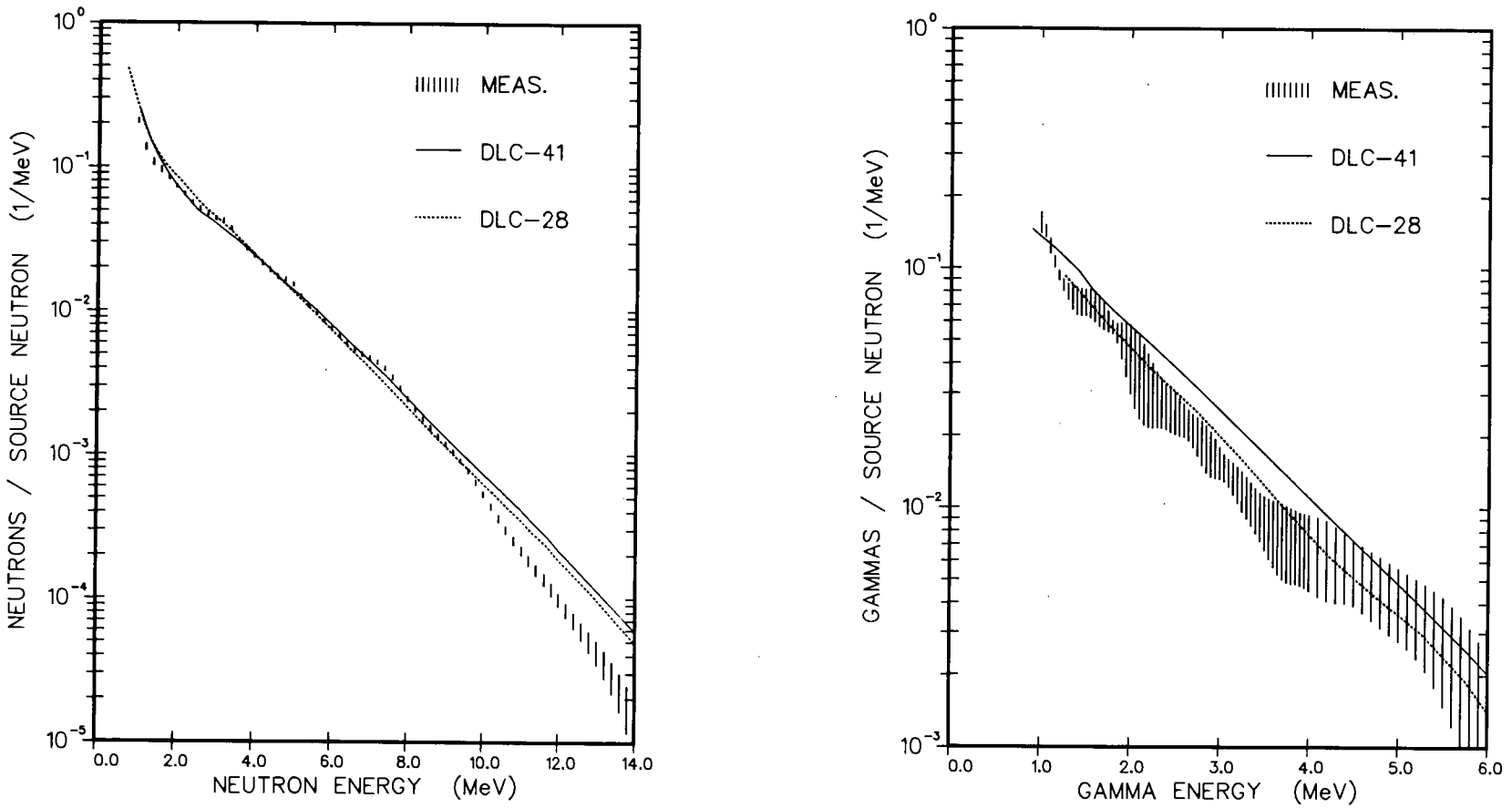

Fig. 3. Comparison of measured and calculated leakage spectra for neutrons (left) and gamma-rays (right).

ORNL-DWG-78-16455

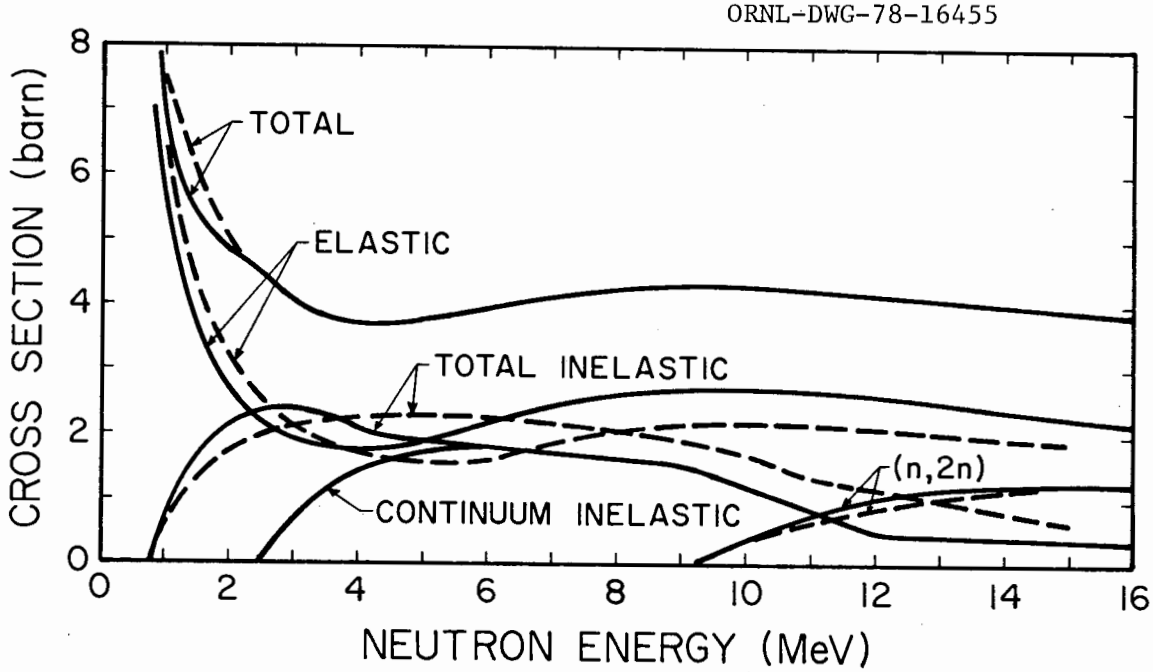

Fig. 4. Comparison of niobium cross sections for the ENDF/B-IV (solid line) and ENDF/B-III (broken line) evaluations (taken from ref. 9).

SENSITIVITY ANALYSIS

Sensitivity analysis was employed in this integral test in order to understand and define the complex relationship between the neutron and gamma-ray spectra and to establish the source of the disagreement between the calculations and the measurements. The information could have been obtained by performing several forward transport calculations; however, sensitivity analysis simplified the procedure. For all of the analysis reported here, the DLC-41 cross section set was used. The sensitivity calculation was performed using SWANLAKE[10] with an adjoint flux calculated by ANISN. The source for the adjoint calculation was properly taken to be the "response" in the forward calculation, i.e., leakage from the outside surface of the niobium sphere. Sensitivities due to neutron transport and gamma-ray production were isolated by performing two adjoint calculations where the neutron and gamma-ray leakages were considered separately. In all cases, the agreement between the forward response (forward flux folded with adjoint source) and the adjoint response (adjoint flux folded with forward source) was excellent, which indicated a proper selection of angular and spatial mesh.

The total sensitivity of the neutron leakage to neutron cross sections is given in Fig. 5. As expected, the sensitivities were negative except above 10 MeV where the (n, 2n) reaction contributes. With an integrated value of only -0.12%, the neutron leakage appeared to be relatively insensitive to the neutron cross sections. The structure in the sensitivity distribution was likely due to the discrete inelastic

ORNL-DWG-78-16456

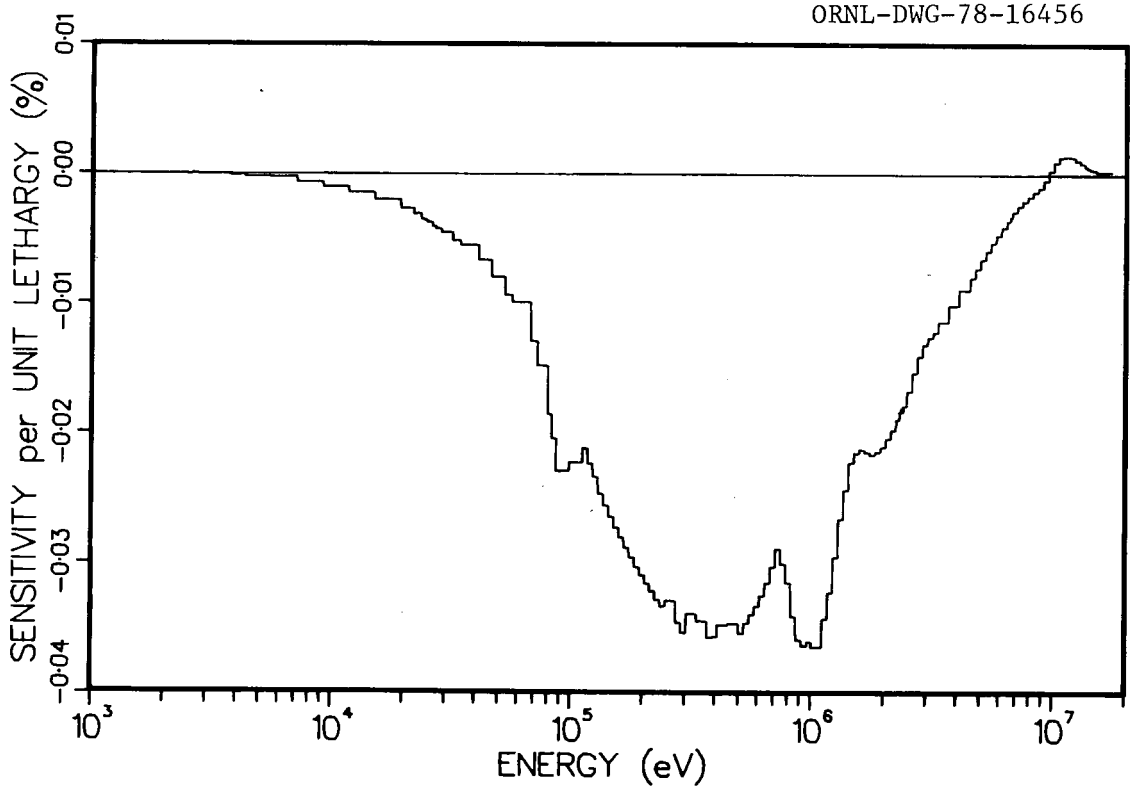

Fig. 5. Total sensitivity (by group) of the neutron leakage to neutron cross sections. The integrated sensitivity is -0.12%.

partial cross sections which constitute a significant portion of the total in the energy range of 0.1 to 4 MeV. This appears even more evident in Fig. 6 which gives the total sensitivity of the gamma-ray leakage to neutron cross sections. In this case, the integrated sensitivity was 0.73%. The three obvious peaks relate to corresponding clusters of excited levels in niobium. Unlike the neutron leakage, the gamma-ray leakage was strongly influenced by Nb cross sections with 62% of the calculated leakage resulting from neutron-induced secondary gamma rays. Also unlike neutrons, the gamma-ray leakage was more dependent on the order of cross section expansion. The difference between using P_0 versus P_3 cross section expansion would cause an estimated 0.4% change in the neutron response compared to 31.3% for gamma rays. The P_1 sensitivities were 0.01% and 2.1% for neutrons and gamma rays, respectively.

Finally, Fig. 7 gives the total sensitivity of the gamma-ray leakage to the gamma-ray cross sections. The sensitivities are relatively large, with an integrated value of -1.2%. The spike at 511 keV which actually extends to -2.3% was partially due to the relatively large number of anihilation photons present but was also a consequence of plotting a very narrow energy group (510 to 512 keV) on a per unit lethargy basis.

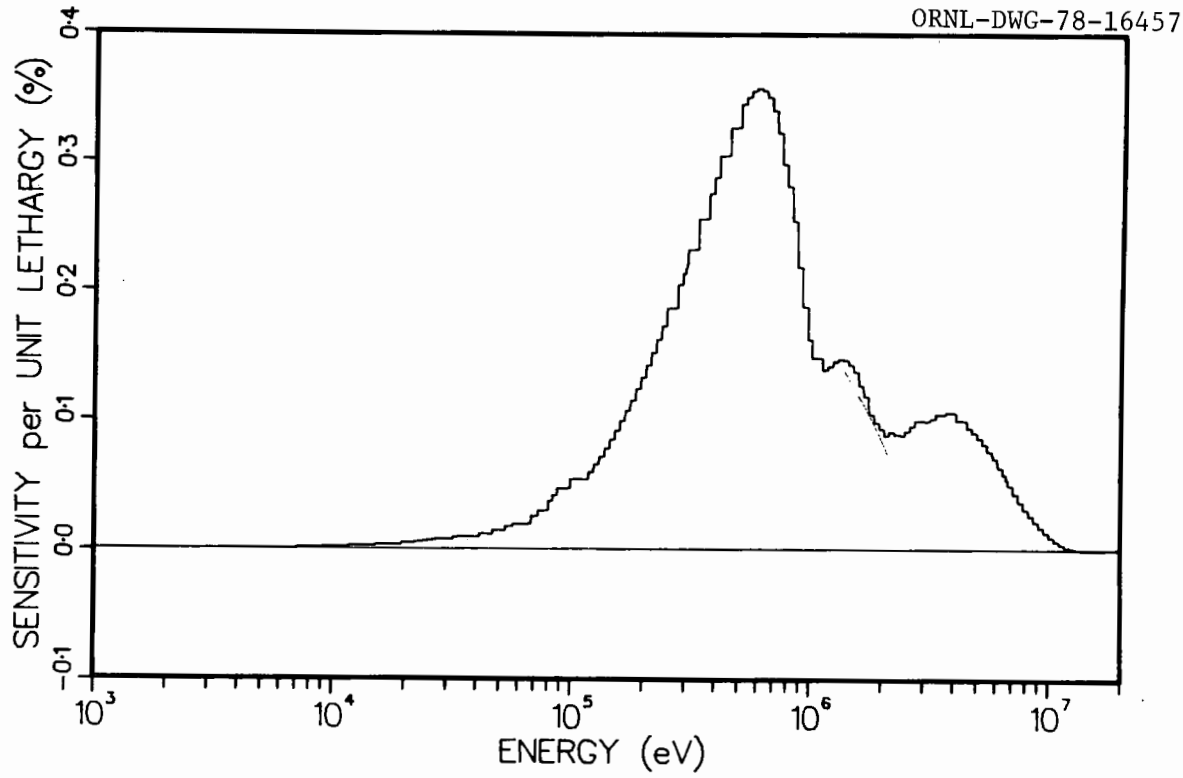

Fig. 6. Total sensitivity (by group) of the gamma-ray leakage to neutron cross sections. The integrated sensitivity is 0.73%.

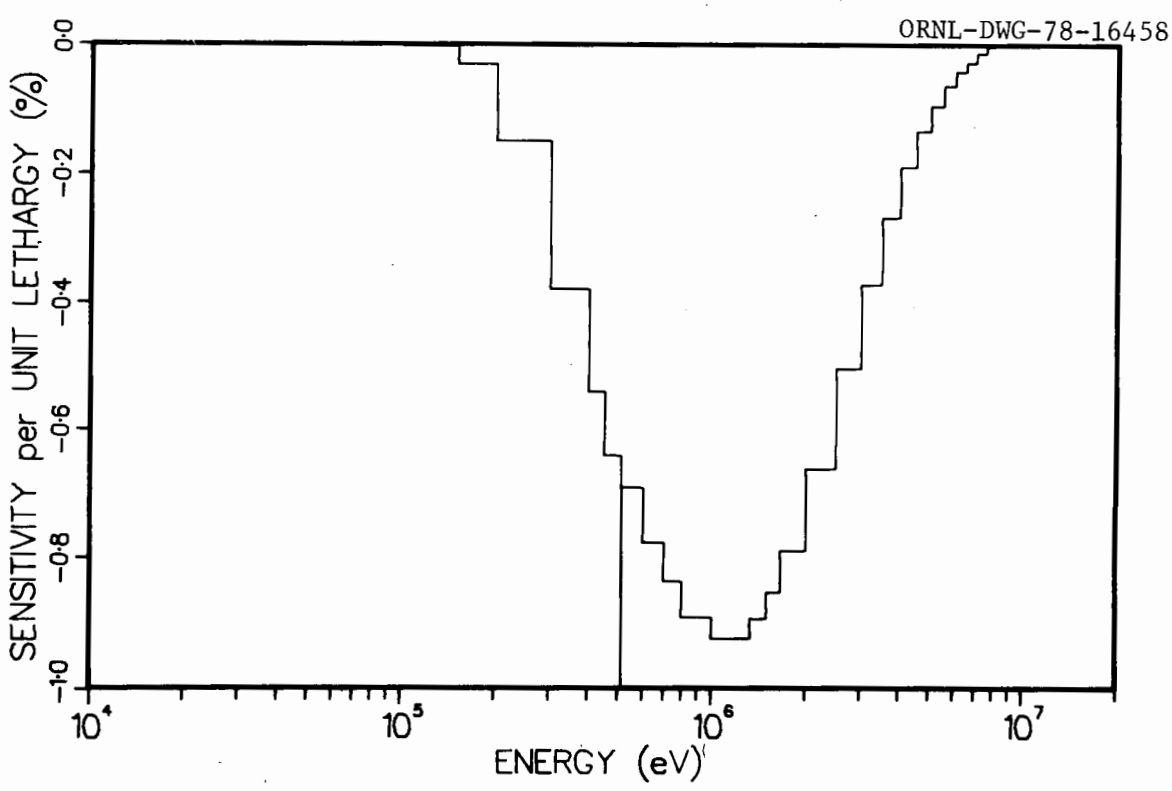

Fig. 7. Total sensitivity (by group) of the gamma-ray leakage to gamma-ray cross sections. The integrated sensitivity is -1.2%.

CONCLUSIONS AND RECOMMENDATIONS

With respect to this integral test, ENDF/B-III and IV neutron cross sections appear adequate for medium penetration (2-3 mean-free-paths) through niobium for energies between 1 and 10 MeV. Above 10 MeV, both evaluations appear to overpredict the neutron leakage. The gamma-ray production and transport data appear marginally adequate for version-III and inadequate for version-IV, which leads to an overprediction of the gamma-ray leakage.

In light of the calculated sensitivities, and considering the magnitude of the disagreements between the measurement and calculations, it appears that cross section adjustments outside the assigned error limits would be required to bring the calculations into agreement with the measured neutron leakage above 10 MeV. However, the gamma-ray results could probably be brought into good agreement with only modest adjustments to the production data. The adjustments should be guided by the ENDF/B-III evaluation since that data was more consistent with the measured gamma-ray spectrum.

Analysis of this integral test will be continued with emphasis on the sensitivity to various partial cross sections followed by trial adjustments to the cross section data. For the long term, integral tests on niobium using a 14-MeV fusion source are planned to help resolve the high energy discrepancies.

REFERENCES

1. R. H. Johnson, D. T. Ingersoll, B. W. Wehring, and J. J. Dorning, "NE-213 Neutron Spectrometry System for Measurements From 1.0 to 20 MeV," Nucl. Instr. and Meth. 145, p. 337 (1977).

2. "FORIST Spectra Unfolding Code," Radiation Shielding Information Center, Oak Ridge, Tenn., PSR-92.

3. D. T. Ingersoll and B. W. Wehring, "Gamma-Ray Pulse-Height Response of an NE-213 Scintillation Detector," Nucl. Instr. and Meth. 147, p. 551 (1977).

4. W. W. Engle, Jr., "A Users Manual for ANISN, A One-Dimensional Discrete Ordinates Transport Code with Anisotropic Scattering," K-1693, CTC, UCC-ND (1967).

5. J. T Kriese, "Coupled Neutron and Gamma-Ray Cross Section Sets for Fusion Reactor Calculations," ORNL-TM-4277 (1973).

6. W. E. Ford, R. T. Santoro, R. W. Roussin, D. M. Plaster, "Modification Number One to the Coupled 100n-21γ Cross Section Library for EPR Calculations," ORNL-TM-5249 (1976).

7. R. W. Roussin, C. R. Weisbin, J. E. White, N. M. Greene, R. Q. Wright, and J. B. Wright," The CTR Processed Multigroup Cross Section Library for Neutronics Studies," ORNL-RSIC-37 (draft).

8. "BUGLE, Coupled 45 Neutron, 16 Gamma-Ray, P_3, Cross Sections for Studies by the ANS 6.1.2 Shielding Standards Working Group on Multigroup Cross Sections," RSIC-DLC-47.

9. R. Howerton, A. Smith, P. Guenther, and J. Whalen, "Evaluated Neutronic Cross Section File for Niobium," ANL/NDM-6 (1974).

10. D. E. Bartine, F. R. Mynatt, and E. M. Oblow, "SWANLAKE, A Computer Code Utilizing ANISN Radiation Transport Calculations for Cross Section Sensitivity Analysis," ORNL-TM-3809 (1973).

THE APPLICATION OF UNCERTAINTY ANALYSIS IN CONCEPTUAL FUSION REACTOR DESIGN

T. Wu and C. W. Maynard
Nuclear Engineering Department
University of Wisconsin-Madison
Madison, Wisconsin, USA

ABSTRACT

We briefly describe the theories of sensitivity and uncertainty analysis and then apply them to a new conceptual tokamak fusion reactor design - NUWMAK. NUWMAK is a moderately sized tokamak fusion reactor of medium toroidal field, high power density and high neutron wall loading and is designed to minimize thermal cycling and provide internal thermal energy storage by use of the eutectic $Li_{62}Pb_{38}$ compound both as the breeding and energy storage material. Neutronics calculations are performed in P_3S_4 by DOT and ANISN.

The responses investigated in this study include the tritium breeding ratio, first wall Ti dpa and gas productions, nuclear heating in the blanket, energy leakage to the magnet, and the dpa rate in the superconducting magnet aluminum stabilizer. The sensitivities and uncertainties of these responses are calculated. The cost/benefit feature of proposed integral measurements is also studied through the uncertainty reductions of these responses.

I. INTRODUCTION

The theories of sensitivity and uncertainty analysis have been developed[1-12] in the past decade to deal with the problem of estimation of nuclear response uncertainties, nuclear data adjustments, etc., which then provide vital information for nuclear reactor design. Most of the applications have been in the field of fast breeder reactors. In this study, the methodology of sensitivity and uncertainty analysis will be applied to the field of fusion reactor design.

Basically, sensitivity analysis is developed to answer questions of the relationship between the changes of a design quantity and of the basic data field. The sensitivity coefficient, mathematically the first derivative of the response with respect to the basic cross sections, can be calculated and used quantitatively for indicating the rate of change of a reactor performance parameter with respect to changes in the cross sections. It also points out what cross section data, as a function of nuclide, reaction type, and energy, are important in analyzing a given reactor system. Moreover, it connects the uncertainty of a given design

quantity and the uncertainties of the basic data field through a simple mathematical expression.

Nuclear reactor design calculations have always been limited in their accuracies by both computational methods and uncertainties in nuclear data. After a period of extensive refinements in calculational methods and computer codes, the main uncertainty has been believed to be in the basic nuclear data. The calculation of the uncertainty of a design quantity is made possible by implementing the statistical error propagation model in connection with sensitivity analysis. For the case where the calculated accuracy of certain design quantities are unsatisfactory for meeting the design criteria, one must improve the basic data considerably. The cross section adjustment methodology, by which one utilizes information from integral measurements by fitting the calculated integral quantity to the experimental results, is used as a tool to improve our current knowledge of the basic data. Here, we also consider the differential measurement as a special integral experiment without confusion.

Sometimes our best knowledge about the basic data field, which may include the information from available integral experiments, still leads to an unsatisfactory result for the design performance parameters of concern. Therefore a new measurement should be proposed. In this study the benefit of the proposed measurement is evaluated through the error reduction of the responses. The cost to benefit ratios of the proposed measurements are then obtainable if we know the cost of the experiment as a function of experiment errors. The cost to benefit ratio should serve as the indicator of how well the measurement has to be done for an optimal design. It also gives a reference for the funding agency if several measurements are proposed.

In the following section, the theories of sensitivity and uncertainty analysis are reviewed and a procedure for analyzing the economical aspects of integral experiments is given. Section III gives the calculational results and analyses for a tokamak fusion reactor design as an application of the theories. The conclusions are given in Section IV.

II. THEORY

II-1. Sensitivity Methodology for a Fixed Sources System

In the neutronic and photonic calculations of fusion reactor blanket and shield desgin, we have always encountered transport problems with fixed sources. The main objective in such problems is to calculate a certain result which is a flux-integrated quantity or more simply a response. By using the conventional and convenient operator notation, the forward and adjoint fluxes, $\phi(\xi)$ and $\phi^*(\xi)$, can be calculated from the forward and adjoint Boltzmann equations:

$$L\phi = S \tag{1}$$

and

$$L^{\dagger}\phi^* = S^*, \tag{2}$$

where L and $L^{\dagger}$ are the forward and adjoint transport operators, S is the physical source distribution, and S* is the functional derivative of the result of interest.

In this study we will concentrate on the responses which are linear functionals of the flux $\phi(\xi)$. By using the notation (,) to indicate integration over the phase space, we can define a response, R, by the following expression:

$$R = (\Sigma_R, \phi), \tag{3}$$

where Σ_R is the response function associated with the result of interest.

The variation of the response, δR, due to the variations of the transport operator and of the response function itself, can be easily derived from the well-developed generalized perturbation theory[1,2] or variational principles[6,7] in connection with the forward and adjoint fluxes. That is,

$$\delta R = (\delta\Sigma_R, \phi) - (\phi^*, \delta L\phi). \tag{4}$$

The first term on the right-hand side of Eq. (4) could be called the direct effect (or detector term) which measures the effect of the response function itself to the response and is relatively easy to calculate. In contrast, the second term, called the indirect effect (or flux perturbation term) which affects the response through the transport operator, is relatively difficult to calculate due to the complexity of the transport operator and requires some computer programming efforts.

Let us concentrate on a set of multigroup nuclear data $\{\Sigma_i\}$ which is contained in L_i, where L_i is a subset of the transport operator L. The linearity of the transport operator enables us to evaluate the contribution of L_i to the response R and therefore the variation of the response due to the variation of L_i can be expressed as

$$\delta R_i = (\delta\Sigma_R, \phi) - (\phi^*, \delta L_i\phi). \tag{5}$$

From Eq. (5) we can obtain the sensitivity coefficient of R with respect to Σ_i which is defined as

$$S_i = \partial R/\partial\Sigma_i \tag{6}$$

and the relative sensitivity,

$$P_i = (\partial R/R)/(\partial\Sigma_i/\Sigma_i). \tag{7}$$

If the group cross sections are concerned, then, for group i, we have

$$P_i(E) = \{ - \iint d^3\underline{r}d\underline{\Omega}\Sigma_i(\underline{r},E)\phi(\underline{r},E,\underline{\Omega})\phi^*(\underline{r},E,\underline{\Omega})$$

$$+ \iiiint d^3\underline{r}d\underline{\Omega}d\underline{\Omega}'dE'\phi^*(\underline{r},E,\underline{\Omega})\Sigma_i^s(\underline{r},E'\to E,\underline{\Omega}'\to\underline{\Omega})\phi(\underline{r},E',\underline{\Omega}')\}/R \qquad (8)$$

The first term on the right hand side of Eq. (8) represents the collision term which removes the particle from that point in phase space and the second term is the collective gain term for the particles emerging from such collision at other energies and angles.

The sensitivity profile, a graphical display of $P_i(E)$, can be presented for a series of spatial zones as a function of energy. By looking at these graphs one can immediately determine how sensitive the response is to a particular cross section set in a particular energy range. Therefore, the sensitivities are useful in determining which cross section uncertainties are important in a given system and should serve as a quantitative guide to nuclear data measurements and evaluations.

II-2. Uncertainty Analysis

Assuming that the response R can be related to a set of cross section data $\{\Sigma_i\}$ by a symbolic expression $R = R(\Sigma_i)$ which, in general, is a non-linear function of Σ_i, we linearize the function R and use the definition of the sensitivity coefficients S_i to get the following expression:

$$R - E(R) = \sum_i S_i(\Sigma_i - E(\Sigma_i)), \qquad (9)$$

where E denotes the expectation value. Furthermore, we let $D = \{d_{ij}\}$ be the covariance or dispersion matrix for the cross section set $\{\Sigma_i\}$. That is,

$$d_{ij} = E((\Sigma_i - E(\Sigma_i))(\Sigma_j - E(\Sigma_j))). \qquad (10)$$

Following the general derivation of statistical error propagation, the variance of R, V(R), can be obtained as

$$V(R) = \sum_{i,j} S_i S_j d_{ij}. \qquad (11)$$

The uncertainty or standard deviation of R defined as $\Delta R = \sqrt{V(R)}$, has the following matrix expression:

$$(\Delta R)^2 = SDS^t, \qquad (12)$$

where, $S = (S_1, S_2, \ldots, S_k)$ is a row matrix representing the sensitivities of R with respect to a set of cross sections. S^t is the transpose of S, and k is the total number of cross sections of interest. A common

practice in the uncertainty calculations is that the relative sensitivity coefficients are provided from the sensitivity analysis. Therefore a modified mathematical form is implemented, that is,

$$(\Delta R/R)^2 = P\hat{D}P^t, \tag{13}$$

where P is the relative sensitivity matrix, and $\hat{D} = \{\hat{d}_{ij}\}$ the relative covariance matrix of the cross section defined as

$$\hat{d}_{ij} = d_{ij}/\Sigma_i\Sigma_j. \tag{14}$$

Eq. (12) mathematically connects the uncertainty of the response and the uncertainties of the cross sections through the associated sensitivity coefficients. It also clearly demonstrates that both the highly sensitive and uncertain cross sections are most responsible for the uncertainty of the response and therefore gives the designer a direction to focus on if the accuracy criteria for some design parameters are not satisfied.

II-3. Statistical Inference in Cross Section Adjustment

Cross section adjustment techniques (utilizing the available information from integral experiments to improve our knowledge about the basic data set) have been developed extensively[3-5,9-12] over the past decade. Sometimes no statistical justification or physical basis is given for the adjustment procedure or the usefulness of the method is limited by some strict assumptions. A general method based on the Bayesian inference in statistical analysis proposed by Dragt[12] will be outlined here.

Basically the concept of probability distribution could be used to describe our degree of belief that a certain parameter (e.g., cross section) has a certain value or distribution, the so-called prior distribution. After an experiment is carried out, the posterior knowledge about the parameter contained in the posterior distribution should be improved by drawing inferences from the experimental data. As a result, the uncertainty of the basic nuclear data decreases and so does the uncertainty of the design parameter of interest.

The consistent method, proposed by Gandini[3], is basically a maximum likelihood estimation (least square method) of the integral quantities and basic differential data constrained by their functional relationship. The approach of this method - sampling theory in statistical analysis - ends up with the same result as the Bayesian approach when the probability distributions are assumed normal. However, the Bayesian method is easier to use when dealing with non-normal distributions. It provides a satisfactory way of explicitly introducing and keeping track of assumptions about prior knowledge or ignorance. For instance, after a study of residuals had suggested model (or assumption) inadequacy, it might be desirable to reanalyze the data in relation to a less restrictive model into which the initial model was embedded. If

non-normality was suspected, for example, it might be sensible to postulate that the sample came from a wider class of parent distributions of which the normal was a member. The consequential analysis could be difficult via sampling theory but is readily accomplished in a Bayesian framework[14].

Let us consider a nuclear data field (mostly group cross sections) combined into a column vector Σ of order m. Let us also assume that the prior distribution of Σ is an m-dimensional multi-variate normal distribution with prior mean $\overline{\Sigma}$ and prior covariance matrix D, i.e., $p_o(\Sigma) \sim N_m(\overline{\Sigma},D)$. The assumption of normality, a common practice to simplify the analysis procedure in scientific investigation, is not absolutely necessary which will be discussed later. Suppose we are interested in n integral quantities, denoted as a column matrix $\underline{Y}$, which can be expressed as a function of Σ, i.e., $Y = Y(\Sigma)$. Let $\overline{Y}$ be the calculated values of Y. From sensitivity theory, we have

$$\overline{Y}(\Sigma) = \overline{Y}(\overline{\Sigma}) + S(\Sigma - \overline{\Sigma}), \tag{15}$$

where, $S = \{s_{ij}\}$ is the sensitivity matrix and s_{ij} represents the sensitivity coefficient of the ith integral quantity with respect to the jth cross section.

An important function which plays a very significant role in Bayesian inferences is the likelihood function $L(\Sigma|Y^{ex})$, where Y^{ex} represents the experimental result for Y. It is "the" function through which the experimental data Y^{ex} modifies prior knowledge of Σ; it can therefore be regarded as representing the information about Σ coming from the data. The likelihood function is formally identical with the conditional probability function of Y^{ex}, given Σ, i.e., $p(Y^{ex}|\Sigma)$. The only difference between these two functions is that in $p(Y^{ex}|\Sigma)$ Y^{ex} represents a vector of variables and Σ a vector of constant parameters, while in $L(\Sigma|Y^{ex})$ Y^{ex} represents a vector of fixed values and Σ a vector of parameters of which optimal estimators are to be determined.

The Bayes' theorem states that

$$p_n(\Sigma|Y^{ex}) = \frac{p_o(\Sigma)L(\Sigma|Y^{ex})}{\int p_o(\Sigma)L(\Sigma|Y^{ex})d\Sigma} \tag{16}$$

where $p_n(\Sigma|Y^{ex})$, or simply $p_n(\Sigma)$ without confusion, is the posterior distribution of the vector Σ after n observations Y^{ex} have been obtained. Again, we assume that the likelihood function is normally distributed with covariance E of order n and mean $Y(\Sigma)$, that is, $L(\Sigma|Y^{ex}) \sim N_m(\overline{Y}(\Sigma),E)$. Then we have two mathematical expressions:

$$L(\Sigma|Y^{ex}) = \text{const} \cdot \exp\{-1/2[Y^{ex} - \overline{Y}(\Sigma)]^t E^{-1}[Y^{ex} - \overline{Y}(\Sigma)]\} \tag{17}$$

and

$$p_o(\Sigma) = \text{const} \cdot \exp\{-1/2(\Sigma - \overline{\Sigma})^t D^{-1}(\Sigma - \overline{\Sigma}). \tag{18}$$

By using Eq. (15), we get

$$Y^{ex} - \overline{Y}(\Sigma) = Y^{ex} - \overline{Y}(\overline{\Sigma}) - S(\Sigma - \overline{\Sigma})$$

$$= V - S(\Sigma - \overline{\Sigma}) \tag{19}$$

where

$$V = Y^{ex} - \overline{Y}(\overline{\Sigma}). \tag{20}$$

It is clear that V represents the differences between the experimental values of Y and the calculated values associated with the prior mean $\overline{\Sigma}$.

The posterior distribution of Σ can be derived by combining Eq. (16), (17), (18) and (19).

$$p_n(\Sigma) = \text{const} \cdot \exp\{-1/2(\Sigma - \overline{\Sigma}')^t D'^{-1}(\Sigma - \overline{\Sigma}')\} \tag{21}$$

where

$$\overline{\Sigma}' = \overline{\Sigma} + (S^t E^{-1} S + D^{-1})^{-1} S^t E^{-1} V \tag{22}$$

$$D'^{-1} = D^{-1} + S^t E^{-1} S \tag{23}$$

Therefore, the posterior distribution of Σ is also normally distributed with posterior mean $\overline{\Sigma}'$ and covariance matrix D' defined by Eq. (22) and (23).

Usually the number of differential data m is much larger than the number of integral quantities n. The matrix D with order m x m has to be inverted in both Eq. (22) and (23). That would pose a potential problem if m gets too large. A reduction of matrix order is therefore required for practical applications. The final result without showing the tedious matrix manipulations is given as follows:

$$\overline{\Sigma}' - \overline{\Sigma} = DS^t(E + SDS^t)^{-1} V \tag{24}$$

$$D' = D - DS^t(E + SDS^t)^{-1} SD \tag{25}$$

Equations (24) and (25) are the basic formulae employed as the computer algorithm in the cross section adjustment procedure. Notice that the matrix to be inverted, i.e., $E + SDS^t$, is a square matrix of order n which is much smaller than the order m of matrix D.

The characteristic of sequential inferences in Baye's theory provides the possibility of a further matrix reduction in the procedure for cross section adjustments. If Y consists of k statistically independent subsets, Y_1, Y_2,...,Y_k, the adjustment can be performed in k steps. First, a new nuclear data set with covariance matrix is obtained by an adjustment by Y_1. Then this new set is used as the prior data set for an adjustment on the basis of Y_2. This procedure continues until the final set $\overline{\Sigma}'$ and covariance matrix D' are obtained with the final adjustment on the basis of Y_k. In the extreme case, if

all experiments are uncorrelated, the calculation can be done without any matrix inversion at all.

The assumptions of normality for the prior distribution and likelihood function eventually lead to the result that the posterior distribution is also normally distributed with the posterior mean and covariance matrix defined in Eq. (24) and (25) respectively. If one has a strong feeling that either the prior distribution or the likelihood function should not be normally distributed, the adjustment procedure could be carried out by using the real probability density function for Eq. (16). In that case, the posterior mean and covariance could still be calculated by implementing a computer program and using the relatively complicated posterior probability density function.

II-4. Economical Aspect of Integral Experiments

In practical nuclear reactor design we always want to know the mean values and the accuracies of certain design quantities. It is not the accuracy of the differential data that really concerns us. If the accuracy of a certain response is not able to satisfy our design criteria after using our best knowledge about the differential data, some experimental measurements may have to be carried out in order to reach the design goal. Here we discuss a procedure to preanalyze the economic values of these proposed integral experiments and to provide a quantitative basis for the choice of the proposed experiments.

Following the derivation from the previous section, let us assume that the current estimation (which may include information from the available integral experiments) of a set of differential nuclear data Σ is $\bar{\Sigma}$ with covariance matrix D, and the integral parameter y of the proposed integral experiment has an experimental uncertainty e and the sensitivity vector S with respect to Σ. The adjusted data $\bar{\Sigma}'$ and covariance matrix D' can be obtained from Eq. (24) and (25) or

$$\bar{\Sigma}' - \bar{\Sigma} = DS^t(e^2 + SDS^t)^{-1}V \tag{26}$$

$$D' = D - DS^t(e^2 + SDS^t)^{-1}SD \tag{27}$$

Suppose that R is the design quantity we are interested in and S_R is a row matrix representing the sensitivity of R with respect to Σ. From Eq. (12) we can get the prior and posterior variance of R, i.e.,

$$(\Delta R)^2 = S_R D S_R^t$$

$$(\Delta R')^2 = S_R D' S_R^t$$

$$= S_R D S_R^t - S_R D S^t (e^2 + SDS^t)^{-1} SDS_R^t \tag{28}$$

Since $e^2 + SDS^t$ is just a number, Eq. (28) can be rearranged:

$$(\Delta R)^2 - (\Delta R')^2 = \frac{(S_R D S^t)^2}{e^2 + S D S^t} \tag{29}$$

Eq. (29) gives a simple analytical dependence of the error reduction on the accuracy of the new integral experiment in the most general case. It is clear that the more accurate the new integral experiment, the larger the error reduction. In the extreme cases, when e approaches infinity, Eq. (29) is zero, i.e., we can not get any information from the experiment, which is expected. On the other hand, we expect to get the maximum information which can be extracted from the new experiment when we have the limit of an infinitely small measuring error. The maximum extractable information, or the maximum variance reduction in R, is called the information content[10] (IC) for the given experiment and the response R and can be defined as

$$IC = \frac{(S_R D S^t)^2}{S D S^t} \tag{30}$$

Half of the IC can be gained when $e^2 = SDS^t \equiv e_H^2$. In general, e_H gives a quantitative value of how accurate the experiment should be to obtain some value from it.

Eq. (30) allows one to compare the quantitative error reduction in R (or a set of R) in a nuclear reactor design when several integral measurements are proposed. However, it does not include some very important information, namely, what the experiment will cost and how much the error reduction is worth. A more objective comparison of different experiments therefore requires a full economic analysis of the benefits resulting from the error reduction.

To simplify the problem, we assume that the cost of electricity from a power plant is a function of a set of nuclear responses R_r and therefore a function of errors in R_r, ΔR_r. That is,

$$C = C(\Delta R_r) \tag{31}$$

For a set of changes $\delta(\Delta R_i)$, the cost changes by

$$\delta C = \sum_r \frac{\partial C}{\partial(\Delta R_r)} \delta(\Delta R_r), \tag{32}$$

where $\partial C/\partial(\Delta R_r)$ can be called the cost sensitivity coefficient with respect to the error in the response R_r. The benefit for the integral experiment through error reduction is then

$$C_B = \delta C = \sum \frac{\partial C}{\partial(\Delta R_r)} \delta(\Delta R_r)$$

$$= \sum_r \frac{\partial C}{\partial(\Delta R_r)} \sqrt{\Delta R_r^2 - \Delta R_r'^2}$$

$$= \sum_r \frac{\partial C}{\partial(\Delta R_r)} \frac{S_{R_r} DS^t}{(e^2 + SDS^t)^{1/2}} \tag{33}$$

The benefit sensitivity vector with respect to the basic nuclear data, B, can be defined to further simplify the problem:

$$B = \sum \frac{\partial C}{\partial(\Delta R_r)} S_{R_r} \tag{34}$$

By assuming C_I to be the cost of the integral experiment we can get a mathematical expression for the cost-to-benefit ratio (CTBR).

$$CTBR = \frac{C_I}{C_B} = \frac{C_I(e^2 + SDS^t)^{1/2}}{BDS^t} \tag{35}$$

The calculated value of CTBR should provide a quantitative basis for comparing different experiments. Usually one should choose the one with the smallest value of CTBR. Since C_I is also a function of e (C_I decreases when e increases) and the sensitivity S is influenced by the materials, geometry, compositions, etc., of the experiment, an optimal value of CTBR could be obtained by properly choosing the experimental error and experimental setups. An optimal integral experiment is therefore attainable through the pre-analysis of the cost-to-benefit ratio even before the experimental facility is built.

III. APPLICATION OF UNCERTAINTY ANALYSIS TO NUWMAK DESIGN

III-1. Neutronics Analysis of NUWMAK

A new conceptual design of a tokamak reactor, called NUWMAK[15], has the characteristics of medium field, high power density, high degree of modularity, and moderate size. This design is especially attractive from the viewpoints of system accessibility, low levels of long term radioactivity and minimum penetrations. The power density (10 MW/m^2) and electrical power output (660 MW) are chosen as typical of a full scale reactor operating in a base-loaded mode. The TF coil set is unique in that just eight superconducting coils are used. A set of 16 small water cooled copper trim coils that do not encircle the vacuum chamber correct the field ripple to below 2%. The blanket is designed to minimize thermal cycling, to provide internal energy storage, and to eliminate the need for an intermediate heat exchanger. A lithium-

lead eutectic, $Li_{62}Pb_{38}$, with a melting point of 464°C is used as the tritium breeding and thermal energy storage material. The titanium alloy, Ti-6Al-4V, is used as structural material to maintain a low level of long term radioactivity. Table 1 gives the major features of the NUWMAK design.

Table 1
Major Features of NUWMAK Design

Power	
Total Thermal Power	2097 MW_t
Net Electric Power	660 MW_e
Plasma	
Major Radius	5.13 m
Minor Radius	1.13 m
Plasma Height to Width Ratio (b/a)	1.64
Plasma Current	7.2 MA
Toroidal Beta	6%
$n_e \tau_E$	2×10^{14} cm^{-3}-sec
q(a)	2.64
Magnet	
On-Axis Toroidal Field	6.05 Tesla
Toroidal Field at NbTi Conductor	11.5 Tesla
Stabilizer	Aluminum
Number of Toroidal Field Coils	8
Number of Cu Trim Coils	16
Blanket	
Structural Material	Titanium Alloy
Coolant	Boiling Water
Breeding Material	$Li_{62}Pb_{38}$
Average Neutron Wall Loading	4.34 MW/m^2

A schematic of the blanket and shield design is shown in Fig. 1. The neutronics analysis makes use of the two-dimensional discrete ordinate transport code DOT[16]. The calculation was performed with the P_3S_4 approximation in r-z geometry. The nuclear cross section library is a 25 neutron and 21 gamma coupled ANISN-formatted library processed from DLC-41B/VITAMIN-c by AMPX[17] modules MALOCS and NITAWL.

The neutronics results[18] are summarized in Table 2. In NUWMAK, the breeding ratio associated with the outer blanket alone is 1.24. However, the Li-Pb zone on the inside has been retained so as to maintain minimum thermal cycling of the structure. The total tritium breeding ratio is 1.54, of which 90% is contributed by $^6Li(n,\alpha)T$ reactions. This is due to the large Pb(n,2n) and W(n,2n) reaction rates, ~0.57 per source neutron and the sufficient amount of ^6Li in natural

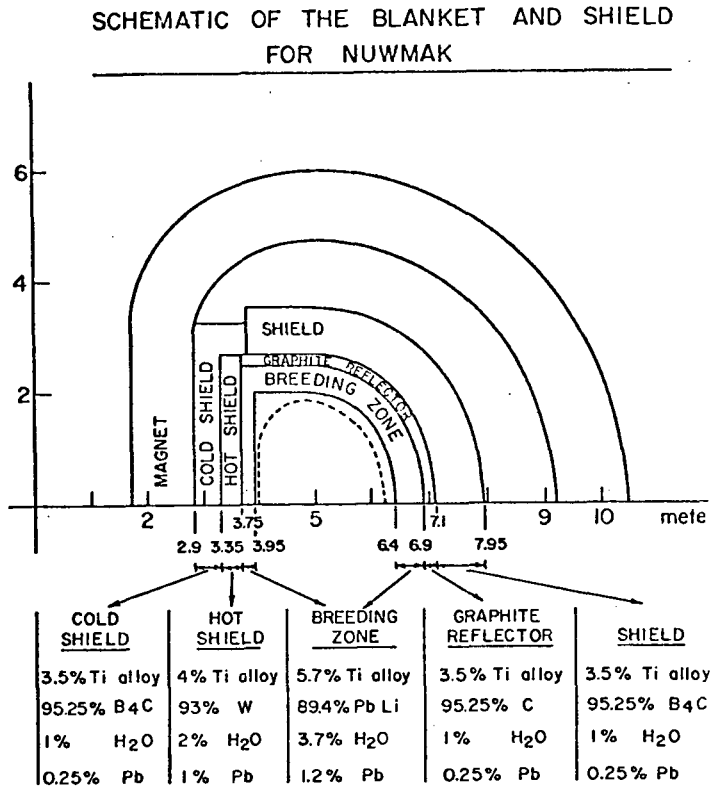

Figure 1

lithium within the lithium lead eutectic. However, the tritium breeding ratio is not very sensitive to the enrichment of ^{6}Li in the total lithium inventory. It shows a maximum value of 1.64 at ~30% ^{6}Li and a value of 1.51 at 90% ^{6}Li enrichment. In the inner shield design, the most restrictive criterion is found to be the resistivity change of the Al stabilizer. The resistivity of the Al at 1.8°K is estimated to increase by 15%/year due to the Al atomic displacement rate (2×10^{-6} dpa/year) and will necessitate periodic annealing approximately every two years. As for the superinsulation, it is found that the dose to mylar would exceed dose limits before plant life. An epoxy based superinsulation whose dose limit is $1 - 5 \times 10^9$ rads is therefore selected. At a dose rate of 3×10^7 rad/yr, the epoxy should last the plant life.

III-2. Sensitivity Analysis

The one-dimensional sensitivity code SWANLAKE has been used to calculate the sensitivity coefficients for the NUWMAK blanket and shield. Forward and adjoint fluxes are calculated by using the one-dimensional discrete ordinate transport code ANISN[20] with the P_3S_4 approximation. Cylindrical geometries based on the minor radius are assumed for both inner and outer blanket/shield to simulate the compact-

Table 2
Summary of NUWMAK Neutronics Calculations

Tritium Production	Inner	Outer	Total
$^6Li(n,\alpha)T$	0.2604	1.1249	1.3853
$^7Li(n,n'\alpha)T$	0.0375	0.1192	0.1567
TOTAL	0.2979	1.2441	1.5420

Neutron Multiplication	Inner	Outer	Total
Pb(n,2n)	0.1339	0.4181	0.5520
W(n,2n)	0.0137	----	0.0137
TOTAL	0.1476	0.4181	0.5657

Nuclear Heating (MeV/D-T Neutron)	Inner	Outer	Total
Neutron	2.2665	8.9298	11.1963
Gamma-Ray	2.4143	3.5422	5.9565
TOTAL	4.6808	12.4720	17.1528

Maximum Atomic Displacement Rate in the Aluminum Stabilizer (dpa/year)	2×10^{-6}
Maximum Dose Rate in the Epoxy Based Superinsulators (rad/year)	3×10^{7}
Maximum Neturon Flux in the NbTi Superconductors ($n/cm^2/year$)	7×10^{15}
Total Nuclear Heating in TF Coils (Watts)	~500

ness of the system. The one-dimensional fluxes are then normalized to the result from DOT and used for the sensitivity analysis. No gamma-ray transport calculations are performed in order to reduce the computing cost. Partial transfer matrices are processed from DLC-41B/VITAMIN-C by AMPX module NITAWL.

In this study we have chosen six key quantities for our sensitivity analysis, namely, the tritium breeding ratio, nuclear heating, first wall dpa and gas production rates, energy leakage to the inner magnet, and dpa rate in the Al stabilizer. A tritium breeding ratio of greater than 1.1 is required as a common practice, otherwise its only impact on the reactor design is through the tritium recovery system. The nuclear heating in the blanket will directly influence the electric power output and the heat transfer design, therefore one needs a more accurate value for this quantity. The first wall lifetime will be strongly affected by the dpa and gas production rates in the first wall

material which could be the determining factor for the choices of the first wall material and wall loading. Since NUWMAK is designed to be compact there is only a 1.05 m thick region for the entire inner blanket and shield, which leads to the use of tungsten as the hot shield material. The responses of dpa rate in Al stabilizer and energy leakage to the inner magnet therefore serve as an indication of the effectiveness of the inner shield design.

Table 3 shows the energy-integrated sensitivities of the above-mentioned six responses to various cross sections of the constituents of the MUWMAK blanket and shield. Caution must be exercised on interpreting these results. The values of Table 3 come directly from SWAN-

Table 3
Energy-Integrated Relative Sensitivities for NUWMAK

R_1 --- Outer Blanket Breeding Ratio
R_2 --- Outer Blanket Neutron Heating
R_3 --- First Wall Ti dpa Rate
R_4 --- First Wall Ti Gas Production Rate
R_5 --- Neutron Energy Leakage to Inner Magnet
R_6 --- dpa Rate in Al Stabilizer

Cross Section	R_1	R_2	R_3	R_4	R_5	R_6
Ti total	-0.050	-0.079	-0.016	-0.039	-0.349	-0.334
Pb total	0.137	-0.051	0.120	-0.003	-1.598	-1.238
^{12}C total	0.048	-0.024	---	---	-0.633	-0.595
^{10}B total	---	-1.795	---	---	-2.106	-2.094
^{6}Li total	-0.865	-0.652	-0.011	---	-0.025	-0.024
^{7}Li total	-0.011	-0.105	---	0.013	-0.319	-0.303
W total					-5.214	-5.282
Pb(n,2n)	0.115	0.006	0.064	---	-1.078	-0.712
inel. level	0.002	-0.025	-0.024	---	-0.146	-0.154
inel. cont.	-0.022	-0.031	-0.002	---	-0.181	-0.127
elastic	0.040	0.001	0.085	---	-0.181	-0.231
^{6}Li(n,α)T	-0.864	-0.644	-0.011	---	-0.001	-0.001
^{7}Li(n,n'α)T	-0.036	-0.047	---	-0.007	-0.132	-0.129
elastic	0.023	-0.042	---	0.018	-0.131	-0.119
Ti(n,2n)	0.011	---	0.004	-0.025	-0.097	-0.084
inel. cont.	-0.028	-0.037	-0.017	-0.028	-0.157	-0.152
elastic	0.007	---	0.014	0.018	-0.052	-0.054
W(n,2n)					-4.123	-4.030
inel. cont.					-0.474	-0.622
inel. level					-0.126	-0.143
elastic					-0.451	-0.449

LAKE calculations which only represents the indirect effect (or flux perturbation term) and does not include the variation of the response function itself (direct effect or detector term). As an example, the

breeding ratio for the outer blanket has a largest negative sensitivity with respect to ^{6}Li total cross section, i.e, -0.865. From the sensitivity theory we would expect a 0.865% decrease in the breeding ratio if the ^{6}Li density increases 1%. This is misleading. Since ^{6}Li(n,α)T reaction contributes 90% to the total tritium production, the relative sensitivity from direct effect is 0.9 and the net effect is 0.9 - 0.865 = 0.035. That is, as the tritium breeding decreases 0.865% from the flux perturbation, it also gains 0.9% from the increases of ^{6}Li(n,α)T macroscopic cross sections. The same trend also happens to the sensitivity of neutron heating with respect to the ^{6}Li total cross section. It has a value of -0.652 from indirect effect and 0.685 from the direct effect and therefore only 0.685 - 0.652 or 0.033 for the net result.

The characteristic of the breeding ratio being insensitive to most of the materials in the blanket can be explained by the fact that a 50 cm thick breeding zone is more than enough and the tritium production saturates. A result from a variational interpolation[21] study also shows[18] that the total breeding ratio is about 1.51 at 90% ^{6}Li, 1.64 at ~30% ^{6}Li which is a maximum, and 1.54 for natural lithium. Incidentally, the sensitivity of neutron heating, with the fact that the ^{6}Li(n,α)T reaction contributes most of the neutron heating, has roughly the same behavior as the sensitivity of the breeding ratio, excepting the contribution of boron-10.

Neither the gas production nor dpa rates in the Ti first wall have sensitivities high enough to warrant further investigation. In contrast, the responses in the inner magnet far from the plasma are relatively sensitive to the neutron transport media. The integral sensitivities of the dpa rate in the Al stabilizer are -5.282, -2.094, -1.238, -0.595 and 0.334 to the total cross sections of tungsten, ^{10}B, lead, graphite and titanium, respectively. Further investigation of the partial cross section sensitivity analysis shows that the (n,2n) cross sections of the tungsten and lead are the dominant reactions. The neutron energy leakage to the inner magnet also shows the same tendency. As the energy dependencies of the sensitivities are concerned, the highest energy group has absolute dominance for these two responses.

From Fig. 2 to Fig. 7, we present some typical graphs, the sensitivity profiles, for a combination of various responses and cross section types. The solid lines represent negative sensitivities, i.e., the response increases as the cross section decreases, and the dashed lines represent positive sensitivities, i.e., the response increases as the cross section increases. Notice that only the flux perturbation terms are presented here. By visualizing these profiles one can have a clear idea for a particular response, in what energy range a particular cross section type would have the greatest impact. Information from the sensitivity profiles would further simplify the procedure in uncertainty analysis by allowing the neglect of the cross section types and energy ranges which have negligible sensitivities.

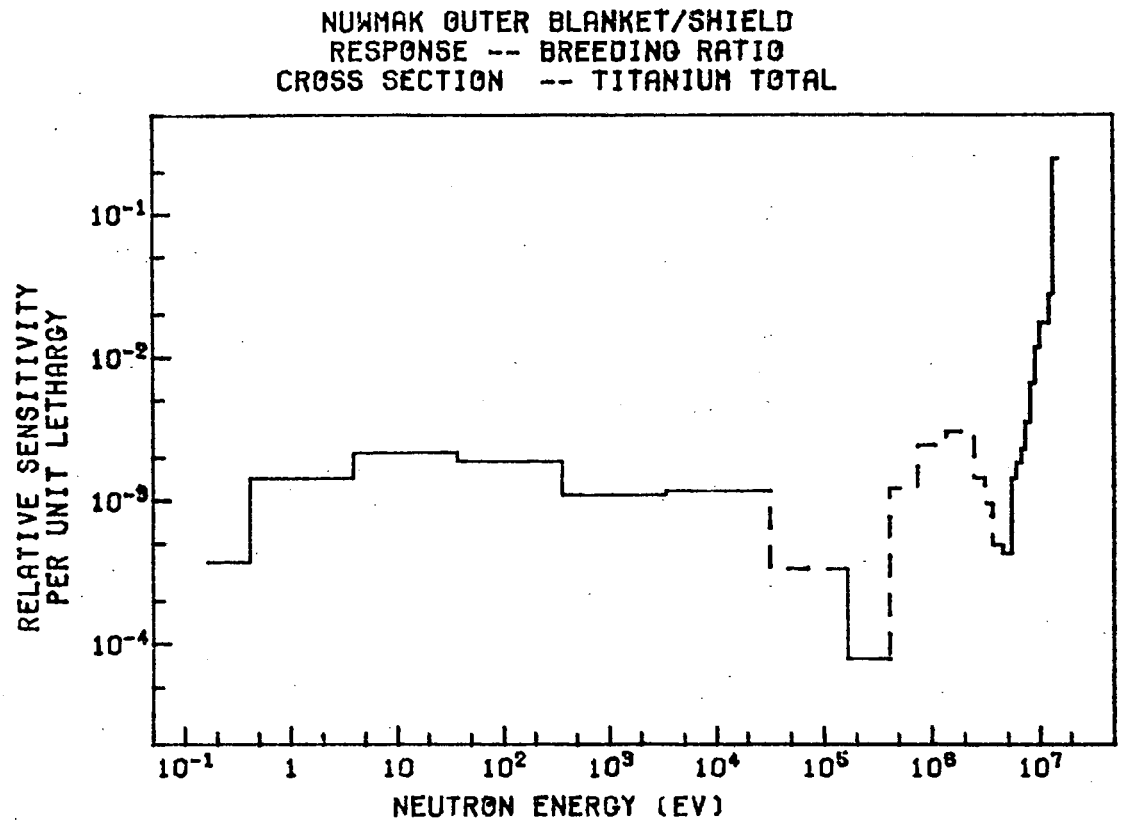

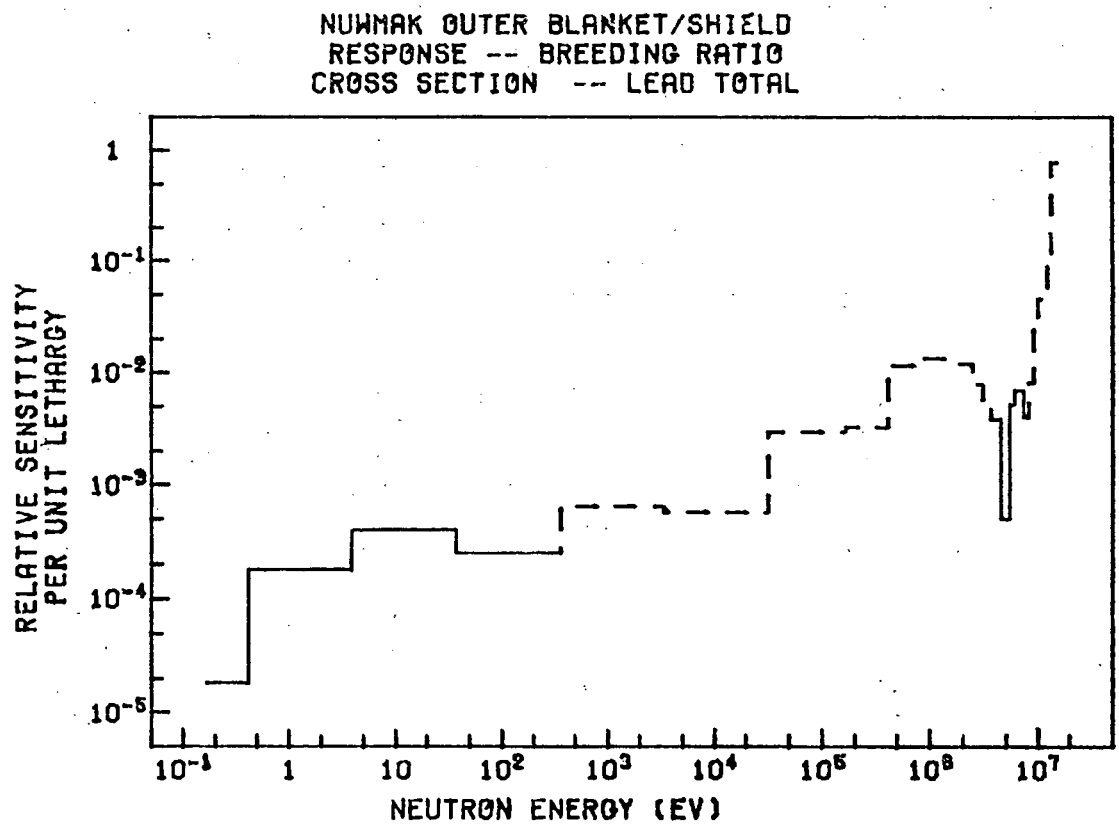

Fig. 2. Sensitivity Profiles of NUWMAK Outer Breeding Ratio to Ti and Pb Total Cross Sections.

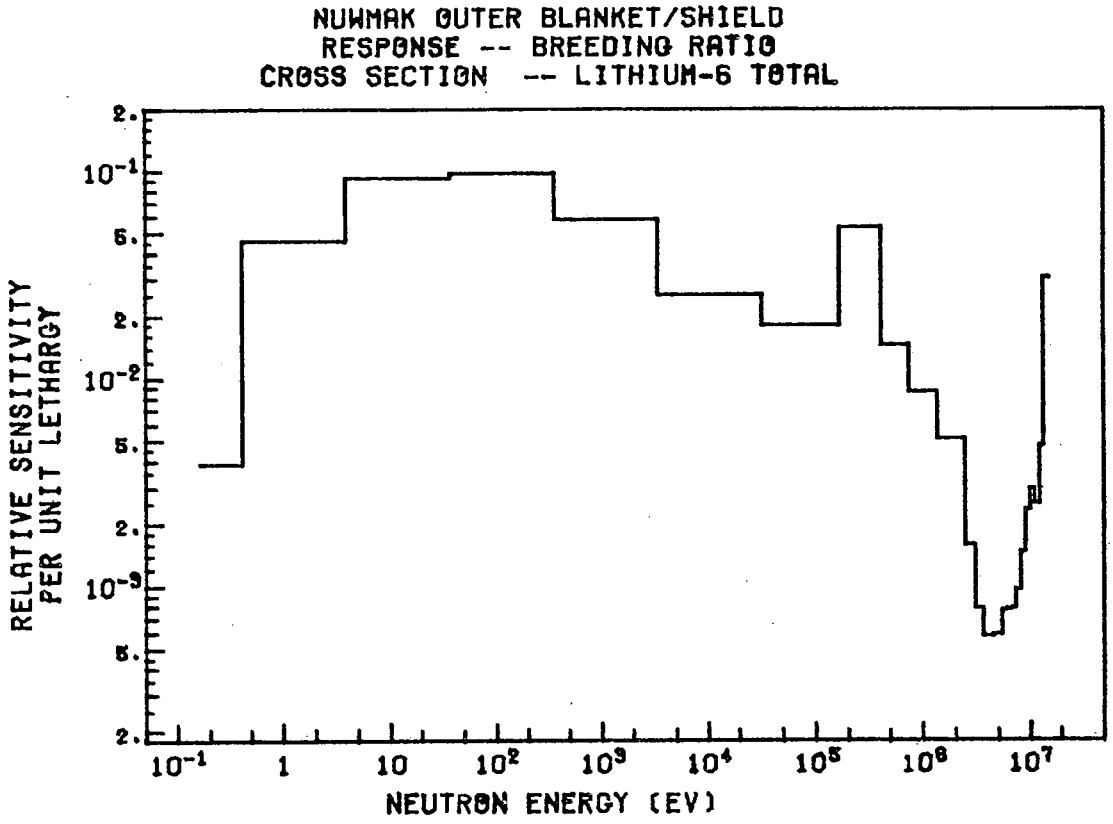

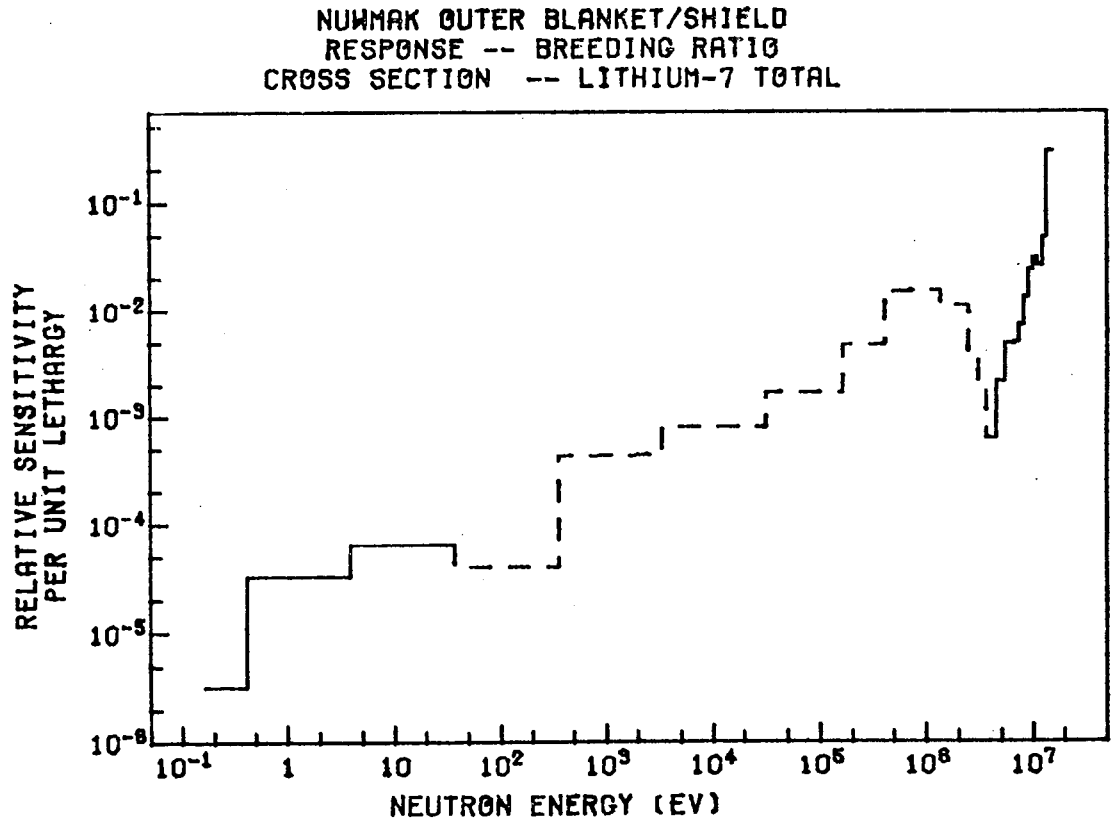

Fig. 3. Sensitivity Profiles of NUWMAK Outer Breeding Ratio to ^{6}Li and ^{7}Li Total Cross Sections.

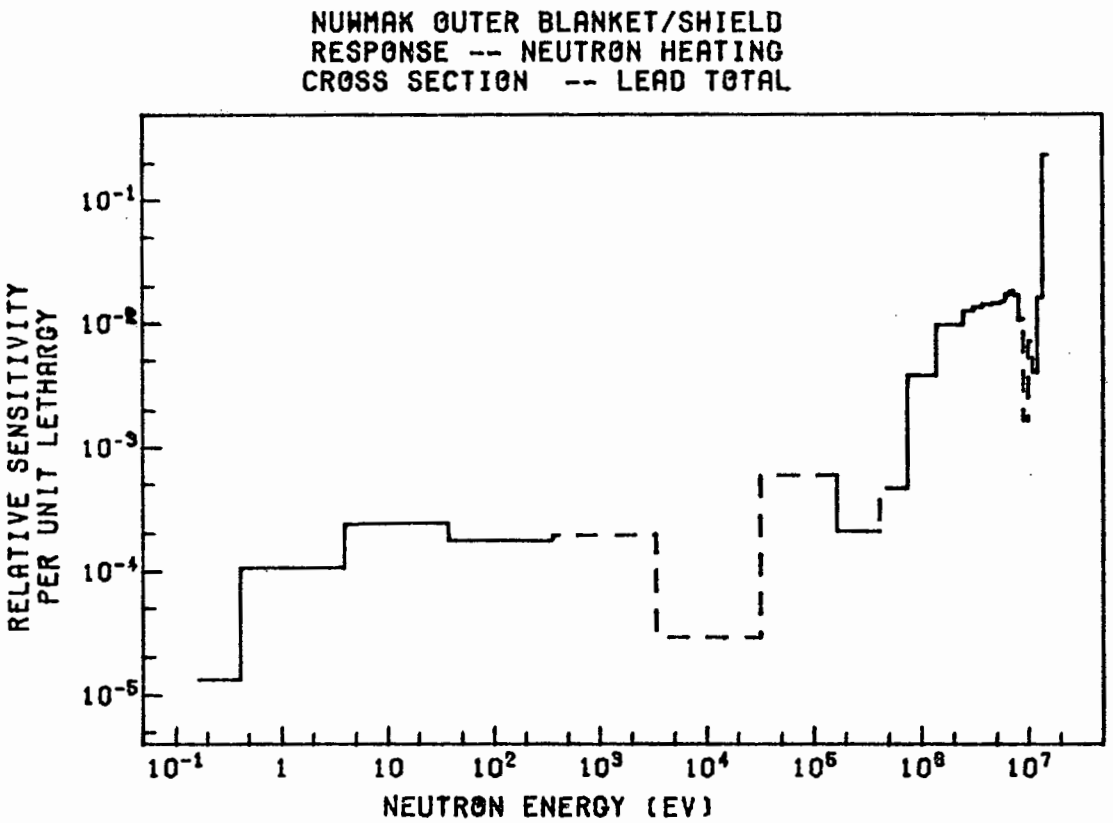

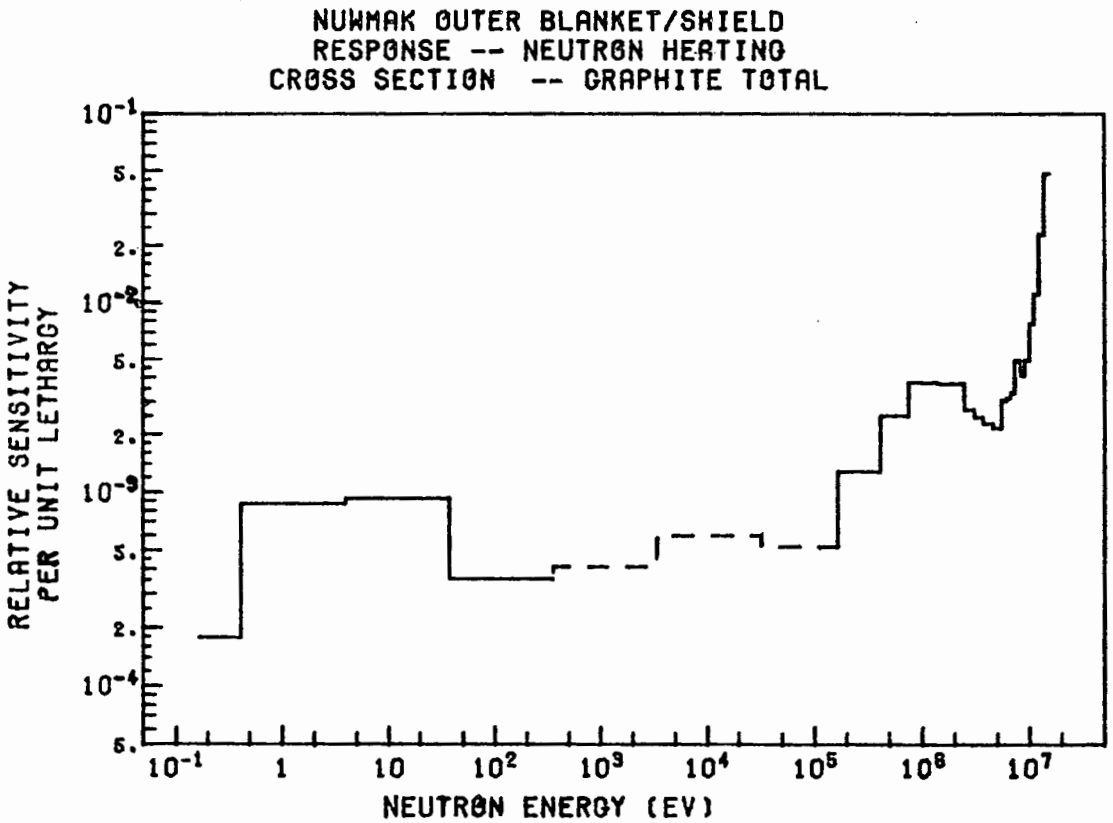

Fig. 4. Sensitivity Profiles of NUWMAK Outer Neutron Heating to Pb and ^{12}C Total Cross Sections.

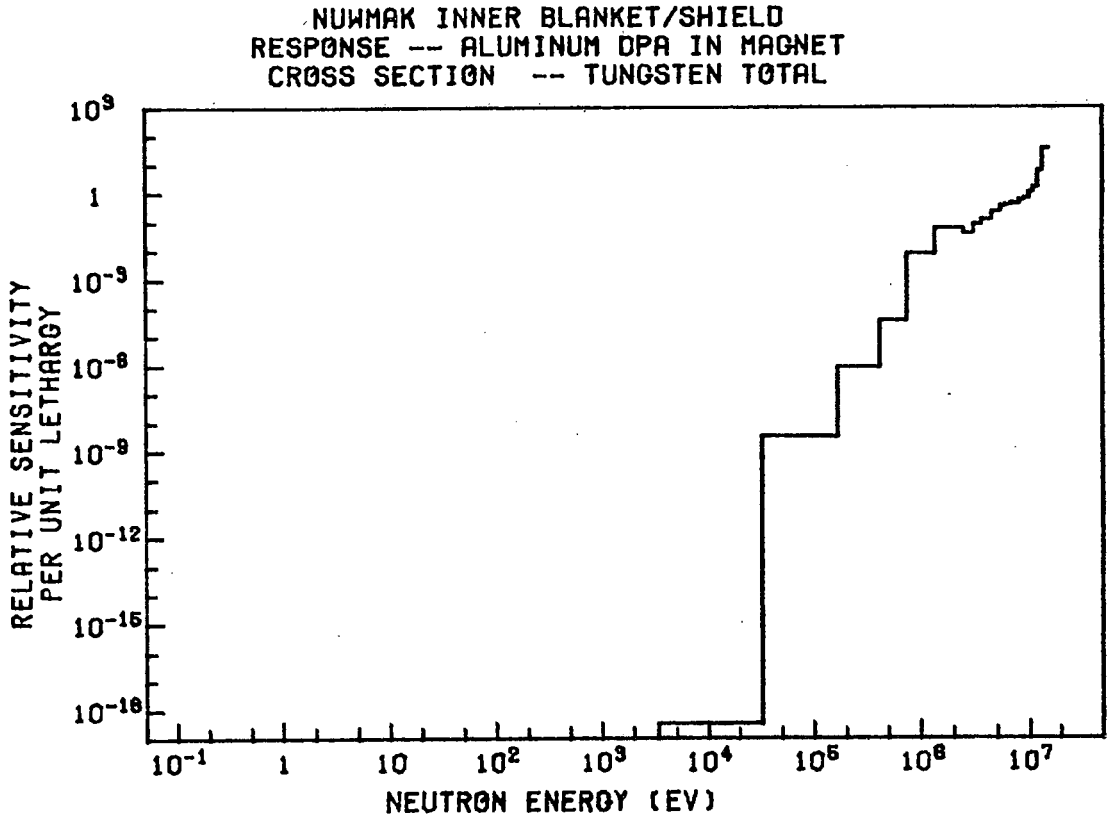

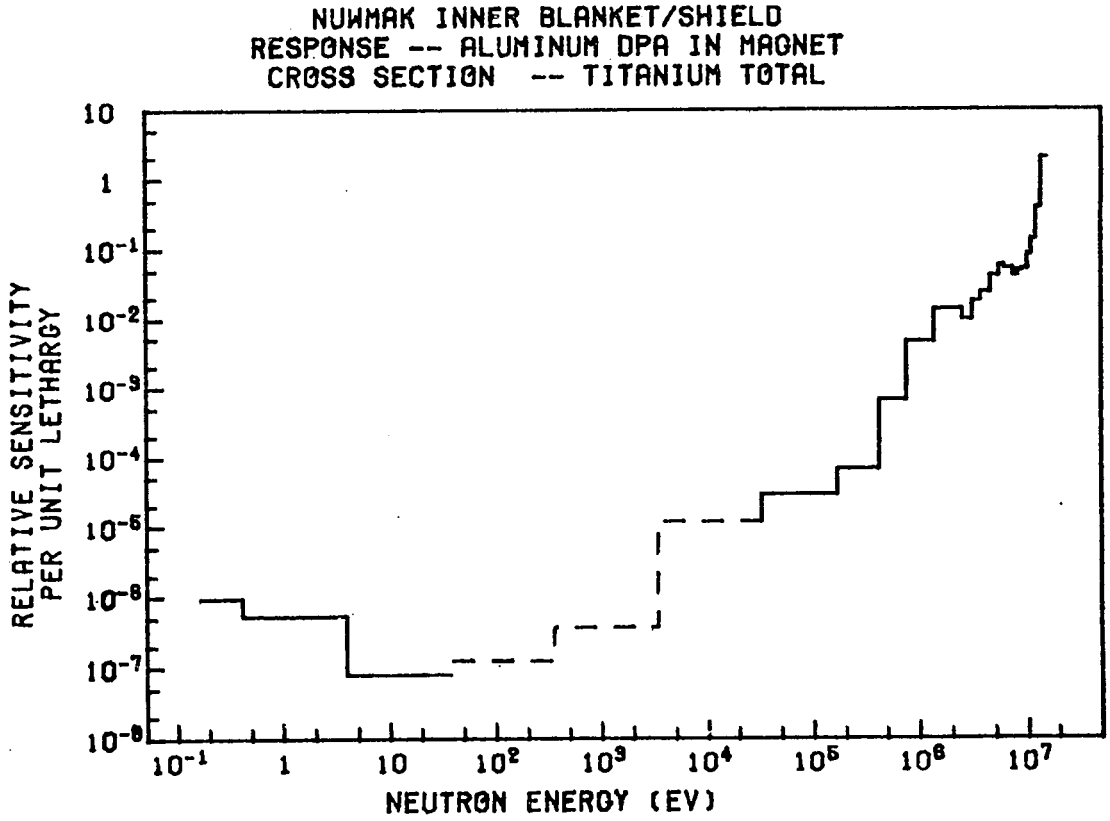

Fig. 5. Sensitivity Profiles of NUWMAK dpa Rate in Al Stabilizer to W and Ti Total Cross Sections.

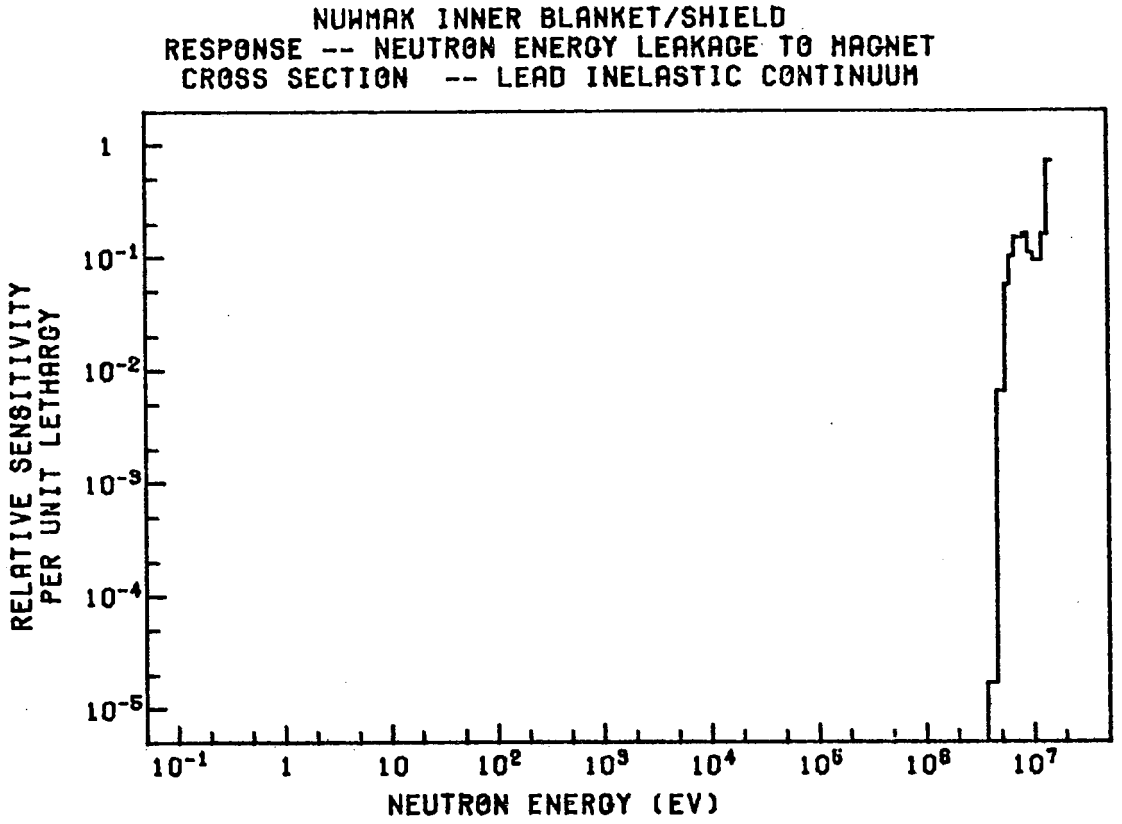

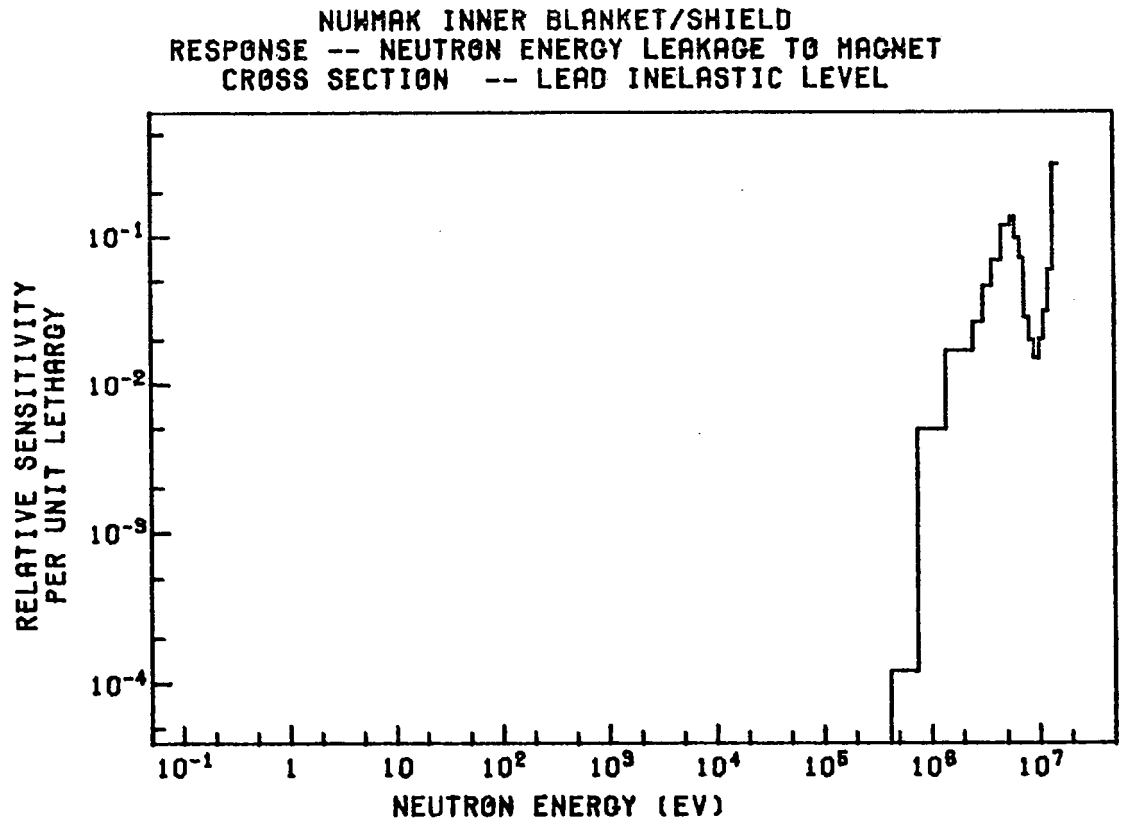

Fig. 6. Sensitivity Profiles of NUWMAK Neutron Energy Leakage to Inner Magnet to Pb Inelastic Continuum and Inelastic Level Cross Sections.

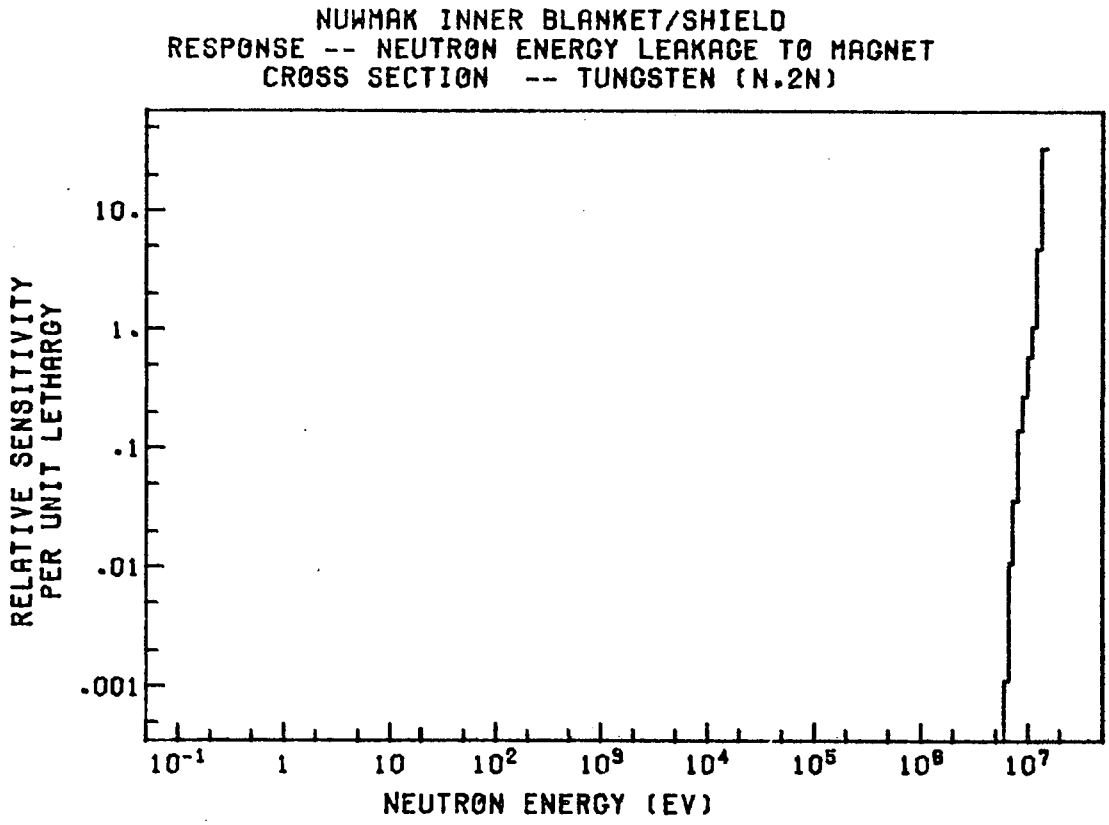

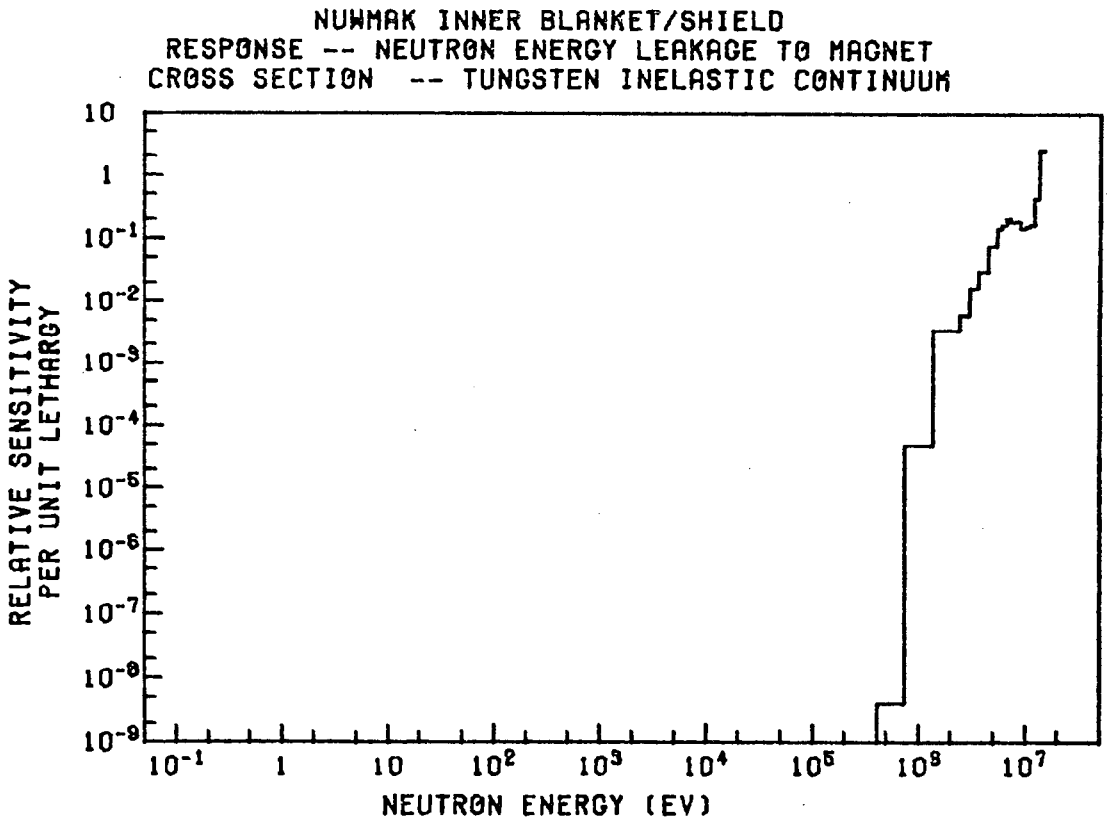

Fig. 7. Sensitivity Profiles of NUWMAK Neutron Energy Leakage to Inner Magnet to W(n,2n) and Inelastic Continuum Cross Sections.

III-3. Uncertainty Analysis

As derived in Section II, Eq. (13) is the basic formula for calculating the uncertainty of a design quantity through its sensitivity coefficients and the covariance matrices of the basic nuclear cross sections. The sensitivity coefficients are obtainable by implementing transport and sensitivity codes. However, the incompleteness of the covariance data seems to cause the most difficulties in the process of uncertainty analysis.

A computer code, called PUFF, is available to process the covariance matrices from error files in the ENDF/B-IV library. In this study, we have modified PUFF to take care of the format changes[22] in the pre-preliminary ENDF/B-V file. The following are some major modifications:

(1) A new subroutine written to read the entire error file to pick up every energy boundary contained in the error file and then to form an error energy grid.

(2) Subroutine DANNY revised such that it will process the error file in order, i.e., first the sub-subsection of the NI-type for the same reactions, then sub-subsection of the NI-type for different reactions, and finally the sub-subsection of the NC-type.

(3) Modifications of subroutine PUFF for processing the NI type, LB = 4 and 5.

(4) The restriction on total number of standard deviations being lifted by storing the standard deviations in a temporary file.

(5) Adding a new subroutine for plotting the correlation matrices, group cross sections and relative standard deviations in user group structure.

The data covariance matrices of four materials, ^{6}Li, Pb, ^{10}B, and ^{12}C, have resulted from the preliminary ENDF/B-V files by PUFF processing. Notice that these data have not yet been tested and may contain some errors. Both ^{6}Li and ^{10}B only contain error files for the energy regime below 1 MeV. However, it seems to be good enough for NUWMAK application since the responses under investigation in NUWMAK are only sensitive to the low energy absorption cross sections for ^{6}Li and ^{10}B. As far as the other materials are concerned, there are no error files for Ti, W, ^{7}Li, ^{10}B in the pre-preliminary version of ENDF/B-V and no Al data are available at the present time.

Table 4 gives a summary of the relative uncertainties for six design quantities in NUWMAK contributed from the uncertainties of total cross sections. Those six quantities are defined in Table 3. The first four responses, which are the breeding ratio, neutron heating, Ti dpa in first wall, and Ti gas production in first wall, all have

Table 4
Relative Uncertainty (%) of the Responses Contributed From the Uncertainties of Total Cross Sections in NUWMAK

Material	ΔR/R (%)					
	R_i	R_2	R_3	R_4	R_5	R_6
^6Li	0.72	0.55	----	0.03	----	----
Pb	0.34	0.10	0.02	0.39	5.02	3.89
^{12}C	0.02	0.02	----	----	1.89	1.78
^{10}B	----	0.39	----	----	----	----
^7Li					2.89	2.65
W					42.35	39.86
Ti					2.46	2.14
^{11}B					1.50	1.07
TOTAL ($\sqrt{\Sigma(\Delta R/R)^2}$)	0.80	0.68	0.02	0.39	42.88	40.24

uncertainties below 1% which should satisfy the design criteria. The remainders are the neutron energy leakage to the inner magnet and dpa rate in the Al stabilizer which have uncertainties of 42.88% and 40.24% respectively. The results are based on the assumption of 10% uncorrelated uncertainties throughout the entire energy range for the ^7Li, W, Ti, and ^{11}B total cross sections. From Table 4 it is clear that the uncertainties of these two responses are dominated by the tungsten cross sections and could be cut down significantly if considerable efforts were made to improve the accuracy of the 14 MeV tungsten total cross sections.

III-4. Error Reduction

As noted earlier, the uncertainty of the dpa rate in the Al stabilizer for NUWMAK is 40.24% from all the materials and 39.86% from tungsten alone. A major error reduction is possible by simply refining the tungsten 14 MeV cross section. Here we propose pulsed-sphere type[23] experiment with a 5 cm thick tungsten sphere surrounding the 14 MeV neutron source. The 14 MeV neutron flux is to be measured outside the sphere such that the 14 MeV total cross section can be derived easily from the flux attenuation.

The response chosen in this analysis is the dpa rate in the Al stabilizer which has a 39.26% uncertainty contributed from the tungsten 14 MeV total cross section alone. Therefore, the calculations will be done just for the first energy group. The sensitivity for the experiment is calculated by SWANLAKE and has a value of -1.1. The design

quantity we are interested in has a sensitivity of -3.93 and the standard deviation of the tungsten cross section is assumed to be 10%. Therefore we have $S_R = -3.93$, $S = -1.1$, $D = (0.1)^2 = 0.01$, and $\Delta R = 0.3926$ (all in relative units). From Eq. (30)

$$IC = \frac{(S_R D S^t)^2}{S D S^t} = S_R^2 D = (\Delta R)^2 = 0.1541,$$

i.e., the information content of the experiment is exactly equal to the variance of the response. This is just a characteristic of one group analysis and is not generally true. By substituting S_R, D, S, and ΔR into Eq. (29), we have

$$(\Delta R')^2 = 1541 - \frac{186461}{e^2 + 121}$$

where e is the experimental error, $\Delta R'$ is the posterior uncertainty of the response, and both e and $\Delta R'$ are in percentage units.

By our definition, $e_H \equiv \sqrt{SDS^t}$ is the experimental error which would reduce the variance of the response by half. In this case, e_H = 11%, which indicates that if our proposed experiment were to be performed with 11% error the uncertainty of the Al dpa would be cut from 39% to 28%. The following gives a one-to-one correspondence between the experimental error and the reduced response uncertainty.

e (%)	0	2	4	6	8	10	11	∞
$\Delta R'$(%)	0	7.0	13.4	18.8	23.1	26.4	27.8	39.3

Since a full-scale economic analysis for the NUWMAK design is not available, the economic analysis of the error reduction from the proposed experiment will not be presented here.

IV. CONCLUSIONS

The theories of sensitivity and uncertainty analysis for fixed source problems have been outlined and their application to a new conceptual tokamak fusion reactor, NUWMAK, is studied. Several conclusions can be drawn from this study.

(1) Sensitivity calculations show that the breeding ratio and neutron heating in the outer blanket of the NUWMAK design are most sensitive to the ^{6}Li and Pb cross sections with integral sensitivities of -0.865 and -0.652 for ^{6}Li and 0.137 and -0.051 for Pb respectively. However, due to the

relatively thick breeding zone design, these sensitivities are comparatively small. A detailed partial cross section analysis also shows that Pb(n,2n) and $^{6}Li(n,\alpha)T$ cross sections are the most dominant in this respect.

(2) First wall dpa and the gas production rate in the Ti alloy have small sensitivities with respect to all materials, while the neutron energy leakage to the inner magnet and the dap rate in the Al stabilizer are noteable with their high sensitivities to most of the materials in the blanket and shield, especially tungsten. Sensitivity profiles indicate the importance of the 14 MeV tungsten cross section as far as these two responses are concerned.

(3) Detailed calculations from uncertainty analysis conclude that the uncertainties of the breeding ratio, neutrons heating, Ti dpa, and first wall gas production are all below 1% which should satisfy the design criteria. However, the relatively high uncertainties of neutron energy to the magnets and dpa rate in the Al stabilizer, 43% and 40% respectively, suggest that a refinement in the tungsten 14 MeV cross section may be worthwhile.

(4) For a pulsed sphere type tungsten cross section measurement, we have found that with an experimental error of 11% and 6%, the uncertainty of the Al dpa rate could be cut from 39% to 28% or 19% respectively. However, the economic value of the error reduction requires a full scale economic analysis and is not presented here. Nevertheless, a study of the NUWMAK design indicates the reactor costs are quite sensitive to the thickness of the tungsten zone which will in turn place a relatively high value on an accurate knowledge of the tungsten cross section. Since the pulsed sphere experiments are of reasonable cost, it is almost a certainty that the complete analysis would show a favorable cost benefit ratio for such an experiment if the NUWMAK design is the basis.

ACKNOWLEDGEMENTS

The authors would like to thank Dr. E.T. Cheng for his contribution in the two-dimensional neutronics analysis. This work is supported in part by the Department of Energy and the Wisconsin Electric Utilities Research Foundation.

REFERENCES

1. L.N. Usachev, J. Nucl. Energy, Parts A/B, 18, 571 (1964).

2. A. Gandini, J. Nucl. Energy, 21, 755 (1967).

3. A. Gandini, "Nuclear Data and Integral Measurements Correlation for Fast Reactors," Parts I, II, and III, RT/FI (73) 5, RT/FI (73) 22, and RT/FI (74) 3, Comitato Nazionale Energia Nucleare, Casaccia, Italy (1973 and 1974).

4. J.B. Dragt et al., Nucl. Sci. Eng., 62, 117 (1977).

5. C. Campbell and J. Rowlands, "The Relationship of Microscopic and Integral Data," IAEA-CN-26/116, Int. Conf. Nuclear Data for Reactors, Helsinki, International Atomic Energy Agency, Vienna (June 1970).

6. G.C. Pomraning, J. Math. Phys., 8, 149 (1967).

7. W.M. Stacey, Jr., J. Math. Phys., 13, 1119 (1972).

8. E.M. Oblow, Nucl. Sci. Eng., 59, 187 (1976).

9. A. Pazy et al., Nucl. Sci. Eng., 55, 280 (1974).

10. L.N. Usachev and Y.G. Bobkov, "Determination of Required Accuracy of Nuclear Data," INDC(CCP)-33/L, IAEA, Vienna (1973).

11. H. Mitani and H. Kurui, J. Nucl. Sci. Technol., 9, 383, and 642 (1972).

12. J.B. Dragt, "Statistical Considerations on Techniques for Adjustment of Differential Cross Sections with Measured Integral Parameters," Reactor Center of Netherlands Report RCN-122 (1970).

13. R.V. Hogg and A.T. Craig, Introduction to Mathematical Statistics, 3rd edition, MacMillan Publishing Co., Inc., New York (1970).

14. G.E.P. Box and G.C. Tiao, Bayesian Interference in Statistical Analysis, Addison-Wesley Publishing Company, Inc., Reading, Mass., 1973.

15. R.W. Conn et al., "NUWMAK: An Attractive Medium Field, Medium Size, Conceptual Tokamak Reactor," Proc. of Third Topical Meeting on the Technology of Controlled Thermonuclear Fusion, American Nuclear Society, Santa Fe, New Mexico, (May 1978).

16. F.R. Mynatt et al., "The DOT-III Two-Dimensional Discrete Ordinates Transport Code," ORNL/TM-4280, Oak Ridge National Laboratory (1973).

17. N.M. Greene et al., "AMPX: A Modular Code System for Generating Coupled Multigroup Neutron Gamma Libraries from ENDF/B," ORNL/TM-3706, Oak Ridge National Laboratory (1976).

18. E.T. Cheng, private communication, (July 1978).

19. D.E. Bartine, E.M. Oblow, and F.R. Mynatt, "SWANLAKE--A Computer Code Utilizing ANISN Radiation Transport Calculations for Cross Section Sensitivity Analysis," ORNL/TM-3809, Oak Ridge National Laboratory (1973).

20. W.W. Engle, Jr., "A User's Manual for ANISN," K-1693, Oak Ridge Gaseous Diffusion Plant (1967).

21. E.T. Cheng and R.W. Conn, Nucl. Sci. Eng., 62, 601 (1977).

22. F.G. Perey, "The Data Covariance Files for ENDF/B-V," ORNL/TM-5938, Oak Ridge National Laboratory (1977).

23. C. Wong et al., "Livermore Pulse Sphere Program: Program Summary Through July, 1971," UCRL-51144, Rev. I., Lawrence Livermore Laboratory (1972).

UNCERTAINTY ANALYSIS FOR SECONDARY ENERGY DISTRIBUTIONS

S. A. W. Gerstl
University of California, Los Alamos Scientific Laboratory
Theoretical Division
Los Alamos, New Mexico, USA

ABSTRACT

In many transport calculations the integral design parameter of interest (response) is determined mainly by secondary particles such as gamma rays from (n,γ) reactions or secondary neutrons from inelastic scattering events or (n,2n) reactions. Standard sensitivity analysis usually allows to calculate the sensitivities to the production cross sections of such secondaries, but an extended formalism is needed to also obtain the sensitivities to the energy distribution of the generated secondary particles. For a 30-group standard cross-section set 84% of all non-zero table positions pertain to the description of secondary energy distributions (SED's) and only 16% to the actual reaction cross sections. Therefore, any sensitivity/uncertainty analysis which does not consider the effects of SED's is incomplete and neglects most of the input data. This paper describes the methods of how sensitivity profiles for SED's are obtained and used to estimate the uncertainty of an integral response due to uncertainties in these SED's. The detailed theory is documented elsewhere and implemented in the LASL sensitivity code SENSIT. SED sensitivity profiles have proven particularly valuable in cross-section uncertainty analyses for fusion reactors. Even when the production cross sections for secondary neutrons were assumed to be without error, the uncertainties in the energy distribution of these secondaries produced appreciable uncertainties in the calculated tritium breeding rate. However, complete error files for SED's are presently nonexistent. Therefore, methods will be described that allow rough error estimates due to estimated SED uncertainties based on integral SED sensitivities.

As the number of cross-section sensitivity and uncertainty analyses (that are being performed for many specific design or research applications) increases, it is more and more realized that most of them are incomplete. In fact very often only the effects of uncertainties in total cross sections or some other conveniently defined composit cross sections (such as inelastic scattering or absorption cross sections) on integral design parameters (responses) are considered. However, even if the uncertainties of all partial cross sections for all materials used in the calculation were included in such studies - which is at present not possible because of the nonexistence of complete covariance data - the analysis would still be incomplete because the energy and angular distributions of secondaries from neutron reactions which produce secondary particles [e.g., (n,2n), (n,γ), inelastic scattering, etc.] are assumed to be without error. It is the goal of this paper to present a formalism which will allow the incorporation of uncertainties in secondary energy distributions into cross-section uncertainty analyses by using basically the same computational algorithms that are already available in existing analysis codes.

Figure 1 summarizes the classical formalism[1-3] which allows the calculation of an uncertainty in any computed integral response R due to uncertainties in any input parameters X_i which, in this context, are taken to be

RESPONSE $R = R(X_i)$

SENSITIVITY COEFFICIENT	SENSITIVITY PROFILE
$S_{X_i} = \frac{\partial R}{\partial X_i}$	$P_{X_i} = \frac{\partial R/R}{\partial X_i/X_i}$ (% per %)

ASSUMING LINEAR PERTURBATION THEORY
(small changes):

$\Delta R \approx S_{X_i} \cdot \Delta X_i$	$\frac{\Delta R}{R} \approx P_{X_i} \cdot \frac{\Delta X_i}{X_i}$

FOR DATA UNCERTAINTIES $\{\delta X_i\}$ or $Cov(X_i, X_j)$:

$Var(R) = \sum_{i,j} S_{X_i} S_{X_j} Cov(X_i, X_j)$	$\left(\frac{\Delta R}{R}\right)^2 = \sum_{i,j} P_{X_i} P_{X_j} \frac{Cov(X_i, X_j)}{X_i X_j}$

Fig. 1. Summary of conventional sensitivity and uncertainty analysis methods.

input cross-section data, e.g., a multigroup cross-section set $\{\Sigma_i^g\}$. In order to use this formalism to incorporate uncertainties in secondary energy distributions (SED's), we must define appropriate sensitivity profiles and covariance matrices for SED's. Figure 2 shows the structure of a typical multigroup neutron cross-section set (gamma rays are excluded for simplicity), where those data which describe the SED's are encircled. Obviously, since for each incident neutron energy (index g') a whole

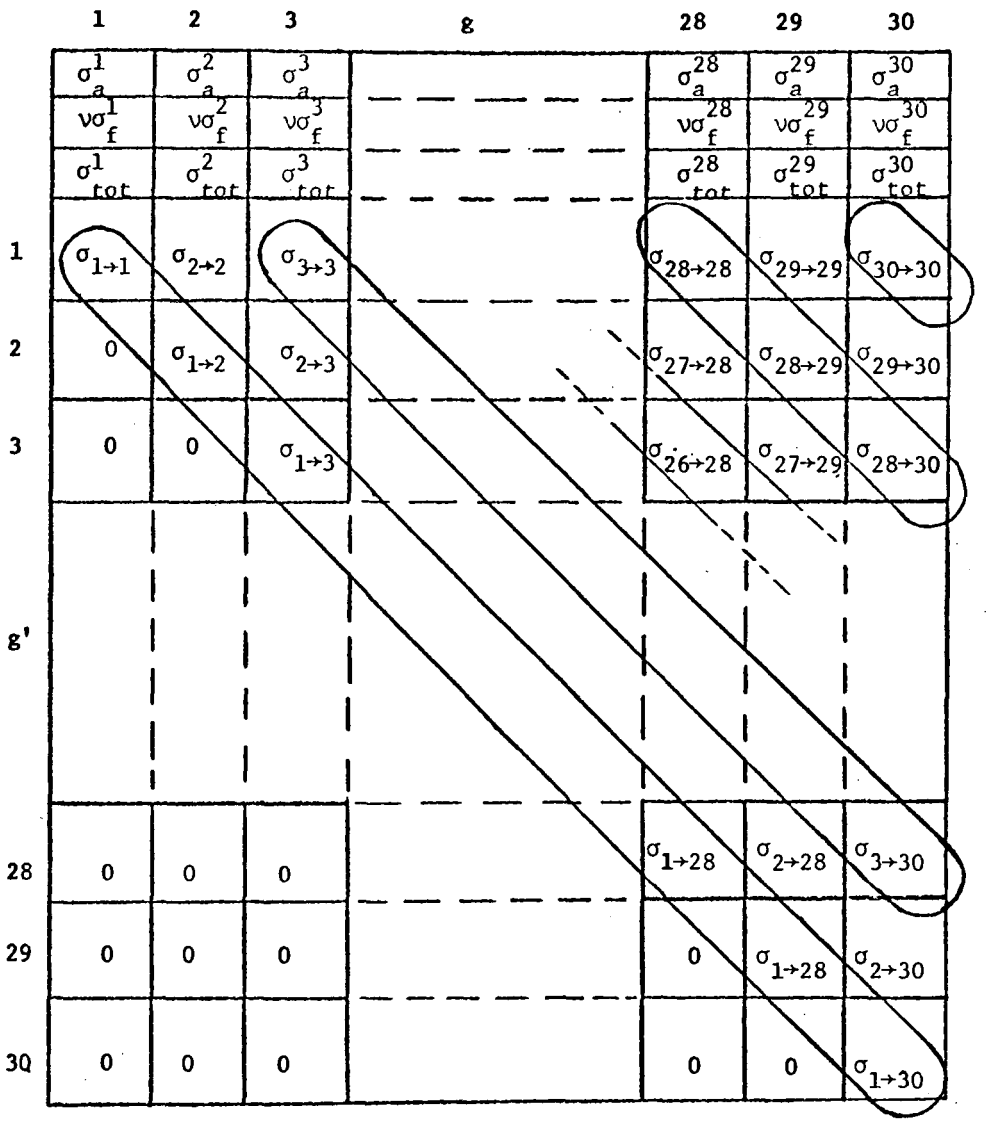

Total nonzero positions describing XS-set = 555

Total nonzero positions describing SED's = 465 (= 84% of total)

Fig. 2. Multigroup cross-section set for a 30 neutron-group structure, including only downscattering: σ_a, $\nu\sigma_f$, σ_{tot}, $\sigma_{g'\to g}$.

spectrum of secondaries may be produced (index g), the two-dimensional array of the scattering matrix is needed to describe SED's. As a consequence, in the 30-group structure shown in Fig. 2, 84% of all cross-section data describe exclusively SED's. To convey some feeling for possible uncertainties in such SED data we reproduce in Fig. 3 a comparison of a recently measured secondary neutron energy spectrum[4] for $^{9}Be(n,2n)$ with data contained in ENDF/B-IV. Although these large discrepancies may be smoothed out after the data are converted into multigroup form, it appears nevertheless that the data uncertainties in SED's are considerable and should not be neglected. We shall return later to the question on how to quantify these uncertainties conveniently.

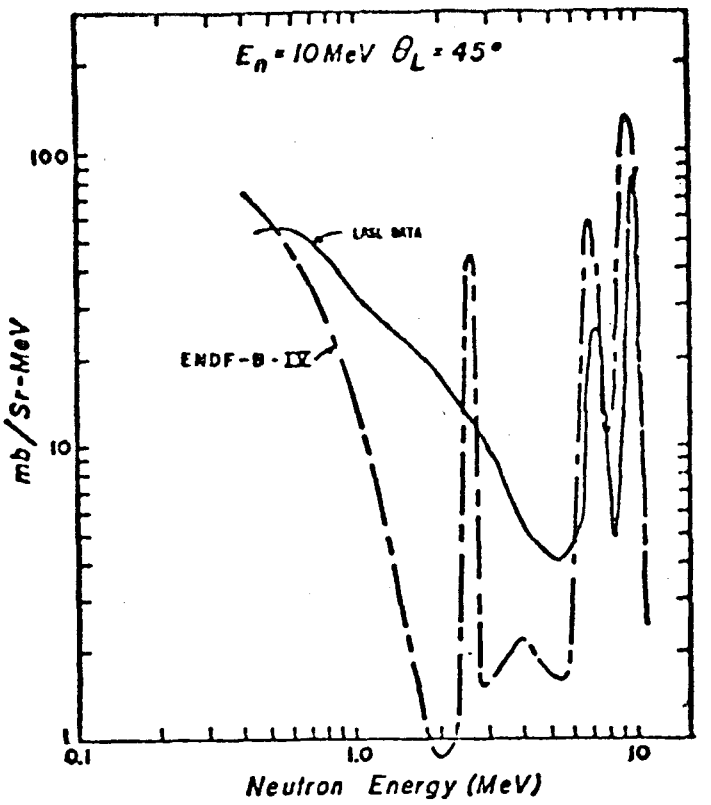

Fig. 3. Comparison of newly measured secondary energy distribution (smooth curve) with ENDF/B-IV data.

Fig. 4 gives a summary on how an analytical expression for the cross-section sensitivity profile P_{XS} can be derived[5] and shows at the same time that sensitivity profiles for SED's may be calculated from the adjoint expression of that for P_{XS}. The detailed analytical expression for an SED sensitivity profile[6] is shown in Fig. 5. Taking the incident neutron energy E' as a parameter and the emerging neutron energy E (energy of the secondary particle) as the continuous variable, we note that $P^{SED}_{\Sigma^{E'}_{x}}(E)$ spans again a two-dimensional array which means that in a multigroup representation one may expect one full SED sensitivity profile for each energy group specifying the incident neutron energy. From the expression in Fig. 5 it is obvious that P^{SED} can be physically interpreted in complete analogy to P_{XS} as the percentage change of the response R due to a one percent change in the value of $\sigma_{g'\to g}$:

$$P^{SED}_{\sigma_{x,g'}}(E_g) = \frac{\partial R/R}{\partial\sigma_{g'\to g}/\sigma_{g'\to g}} \quad . \tag{1}$$

SENSITIVITY ANALYSIS METHODS

FORWARD	ADJOINT
$L\phi = Q$	$L^*\phi^* = \Sigma_R$
$R = \langle\phi,\Sigma_R\rangle$	$R = \langle\phi^*,Q\rangle$
$= \langle\phi,L^*\phi^*\rangle$	$= \langle\phi^*,L\phi\rangle$
$P_{\text{CROSS-SECT.}} \sim (\phi,L^*_\Sigma\phi^*)/R$	$P_{\text{SECONDARIES}} \sim (\phi^*,L_\Sigma\phi)/R$

Fig. 4. Derivation of equations for cross-section and SED sensitivity profiles.

SENSITIVITY PROFILES FOR SECONDARY ENERGY (SED) AND ANGULAR (SAD) DISTRIBUTIONS

$$P^{SED}_{\Sigma^{E'}_x}(E) = \frac{1}{R}\int d^3r\int d^2\Omega\int d^2\Omega'\phi^*(r,E,\Omega)\Sigma_x(r;E'\to E,\Omega'\to\Omega)\phi(r,E',\Omega')$$

$$P^{SAD}_{\Sigma^{E'}_x}(\Omega) = \frac{1}{R}\int d^3r\int dE\int d^2\Omega'\phi^*(r,E,\Omega)\Sigma_x(r;E'\to E,\Omega'\to\Omega)\phi(r,E',\Omega')$$

Fig. 5. Detailed analytic expressions for SED and SAD sensitivity profiles.

One may also note that SED sensitivity profiles are always positive, i.e., they express "gain-terms" only. A specific example of two SED sensitivity profiles[6] is reproduced in Fig. 6, where also the associated secondary energy distributions $\sigma_{2\to g}$ and $\sigma_{3\to g}$ for incident energy groups 2 and 3 are shown with broken lines. The numbers above the top histogram indicate group numbers of our 30 energy group structure employed for this specific analysis.

The two-dimensionality of SED sensitivity profiles and of the secondary energy distribution itself often presents an obstacle when uncertainties of SED's are to be quantified in practice, especially when correlations are also considered. As a first step to quantify SED uncertainties, we introduce the concept of an integral SED uncertainty which can then be conveniently used for a comprehensive cross-section uncertainty analysis in connection with the definition of an integral SED sensitivity.[6] Figure 7 summarizes the definition of an integral SED sensitivity as introduced in Ref. 6. The basis for this definition is the fact that each secondary energy distribution itself may be subdivided into a "hot", i.e., high-energy part, and a "cold", i.e., low-energy part by identifying the median energy group g_m which is defined as that group into which the median energy of all secondaries (for a given initial neutron energy) falls. Then the associated SED sensitivity profile can be integrated separately over its cold part and its hot part. Subtracting these two integrals from each other, as indicated on Fig. 7, defines an integral SED sensitivity, S^{SED}, which may be labeled "HOT" if the difference is positive and "COLD" if it is negative. S^{SED} is then a quantitative measure of how much more sensitive the response R is to high-energy secondaries (if S^{SED} is "HOT") than to low-energy secondaries.

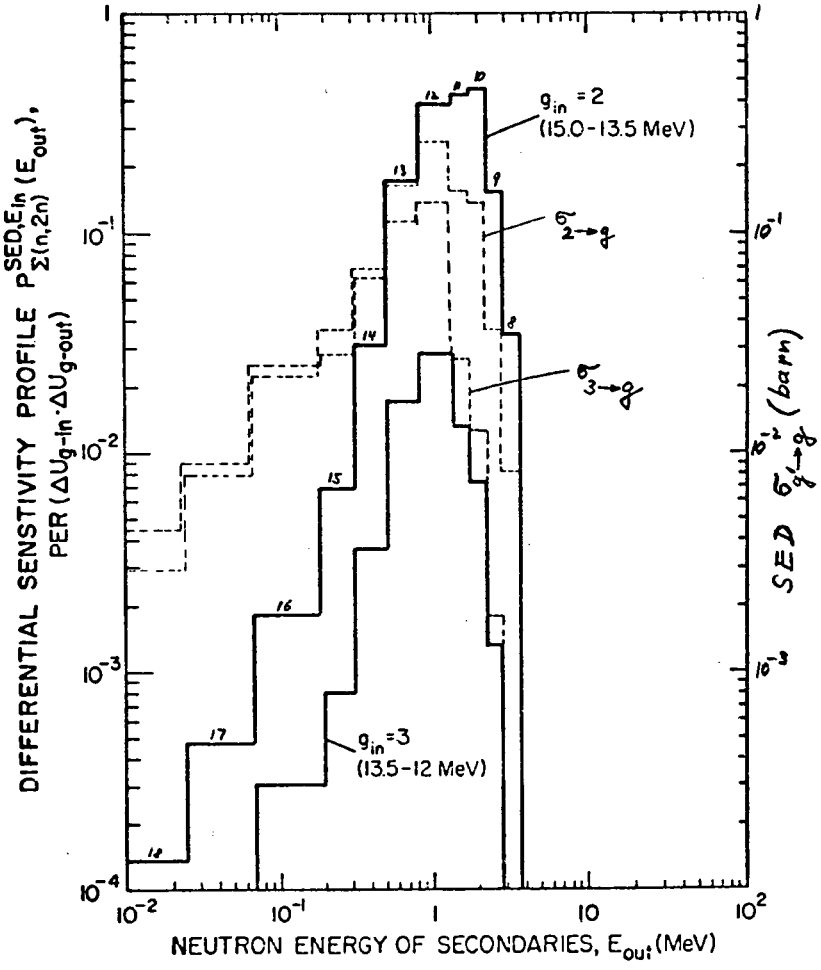

Fig. 6. Double-differential sensitivity profiles for the secondary energy distributions of Fe(n,2n) reactions for each energy group of initial neutrons, per lethargy widths of initial and final energy groups.

Since in general we have an SED for each incident energy group g', this definition of S^{SED} holds for all g'. If we abbreviate $P^{SED}_{\sigma_{x,g'}}(E_g)$ with $P^{SED}_{g'g}$ we have

$$S^{SED}_{g'} = \sum_{g=1}^{g_m} P^{SED}_{g'g} - \sum_{g=g_m+1}^{G} P^{SED}_{g'g} \quad . \tag{2}$$

Within this concept it follows quite naturally then to also define an integral SED uncertainty as shown in Fig. 8. The spectral shape uncertainty parameter f may be considered as the width of an uncertainty band that can be drawn around an average secondary energy distribution which encompasses all credible data available for this particular SED. Consequently, if the number of hot secondaries is increased by a fraction

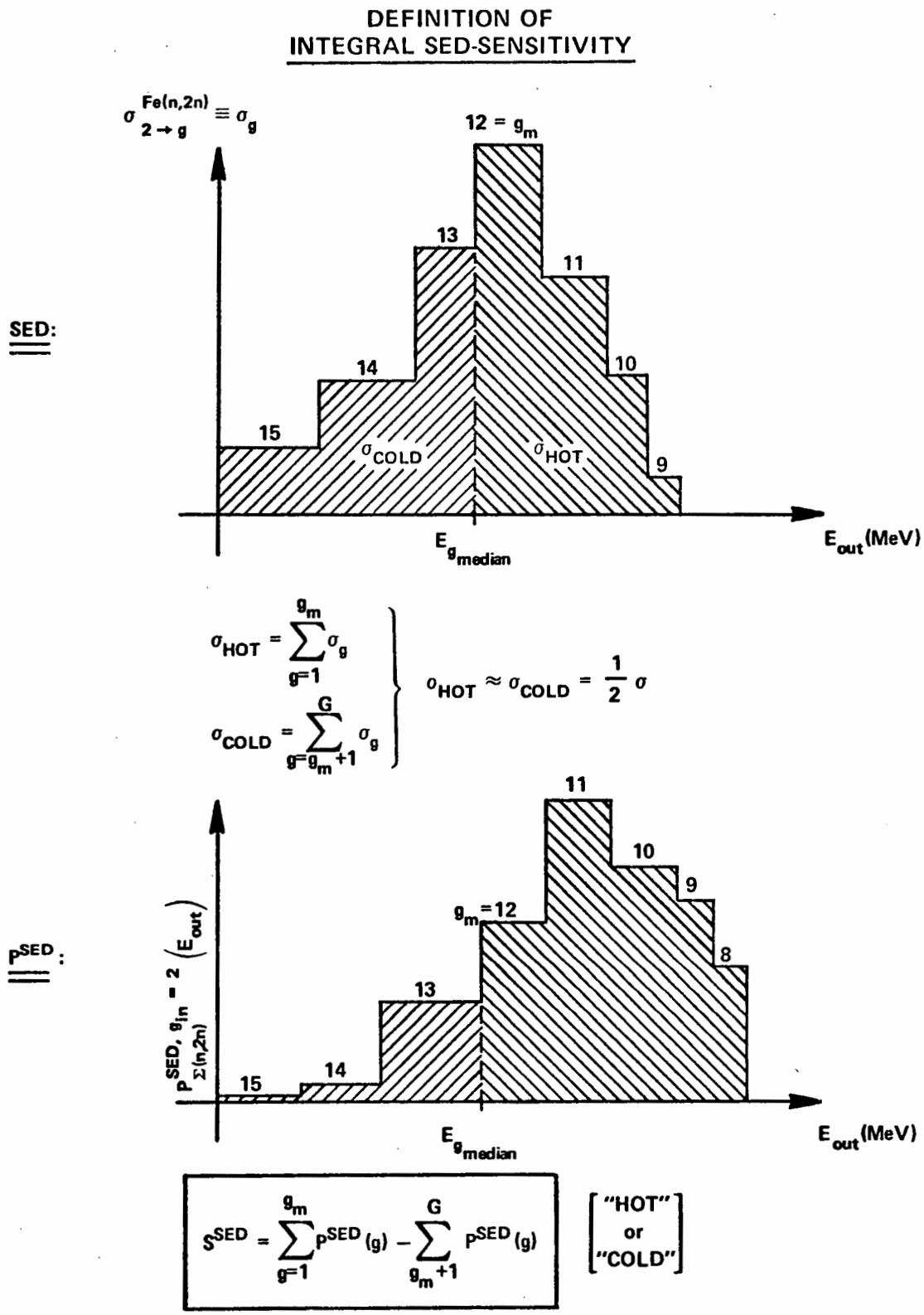

Fig. 7. Definition of median energy and integral SED sensitivity.

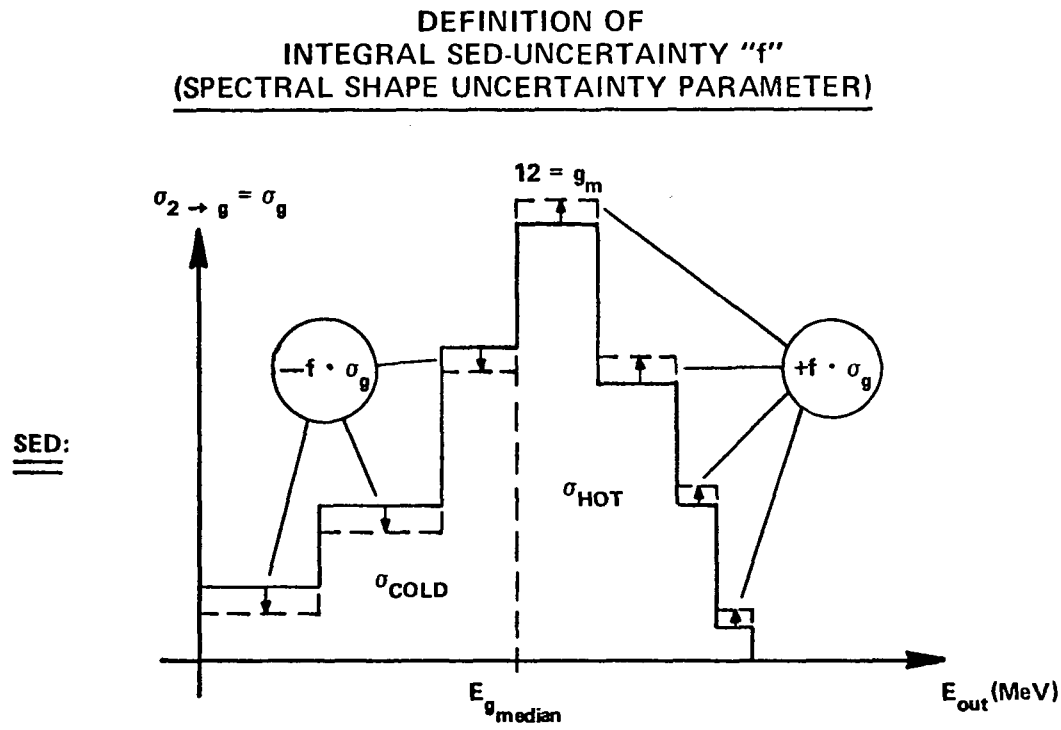

$$\frac{\delta\sigma_g}{\sigma_g} = \begin{cases} +f \text{ if } g \leqslant g_m \\ -f \text{ if } g > g_m \end{cases}$$

Fig. 8. Interpretation of integral SED uncertainty as spectrum shape perturbation.

f of all secondaries, while the number of cold secondaries is decreased by this same number, then f quantifies only the uncertainty in the shape of the SED while the total number of secondaries, i.e., the normalization of the SED remains unchanged. Thus f may also be interpreted as a measure for a spectrum shape perturbation which can be written as

$$\frac{\delta\sigma_{g'\to g}}{\sigma_{g'\to g}} = \begin{cases} +f_{g'} \text{ if } g \leq g_m \\ -f_{g'} \text{ if } g > g_m \end{cases} . \tag{3}$$

Returning for a moment to our original goal, namely to treat SED uncertainties within the same formalism than ordinary cross-section uncertainties (compare Fig. 1), we are attempting to propagate SED changes into a response change via an equation of the form

$$\left(\frac{\delta R}{R}\right)_{SED} = \sum_{g'g} P^{SED}_{g'g} \frac{\delta\sigma_{g'\to g}}{\sigma_{g'\to g}} , \tag{4}$$

if a spectrum perturbation $\delta\sigma_{g'\to g}$ is considered. Inserting Eq. (3) into Eq. (4) and using Eq. (2) we obtain

$$\left(\frac{\delta R}{R}\right)_{SED} = \sum_{g'} S_{g'}^{SED} f_{g'} \quad , \tag{5}$$

which is exactly analog to the classic equation used to estimate the effects of a reaction cross-section perturbation on a response R. Continuing the exact analogy we can infer from Eq. (5) immediately the formalism required to treat correlated uncertainties. Let us denote with f_i the value of f for a specific nuclear reaction, e.g., (n,2n), at a specific incident neutron energy, e.g., $g_{in} = 2$, and let f_j correspond to some different reaction/energy combination, then the uncertainty in R due to correlated uncertainties of all SED's considered for one specific isotope is given by

$$\left(\frac{\Delta R}{R}\right)^2_{SED} \equiv \frac{Var(R)}{R^2} = \sum_{i,j} S_i^{SED} S_j^{SED} Cov(f_i, f_j) \quad . \tag{6}$$

An illustration of how the values of f may be obtained by an evaluator who has N independent measurements of the same SED available is shown in Fig. 9. Muir[7] has written a short FORTRAN program SPEC which performs these numerical operations on a set of input energy spectra.

FOR n=1,..,N INDEPENDENT MEASUREMENTS OF σ_g:

XS-EVALUATOR ASSIGNS WEIGHTS w_n, THEN

$$f^n = \frac{\sigma^n_{HOT} - \sigma^n_{COLD}}{\bar{\sigma}} \text{, WHERE } \bar{f} = \sum_{n=1}^{N} w_n f_n = 0$$

$$Var(f) = \overline{(f-\bar{f})^2} = \overline{f^2}$$

$$= \sum_{n=1}^{N} w_n \frac{\left(\sigma^n_{HOT} - \sigma^n_{COLD}\right)^2}{\bar{\sigma}^2}$$

Fig. 9. A sample evaluation of the spectral shape uncertainty parameter f.

Figure 10 summarizes the five steps necessary to perform a quantitative uncertainty analysis for SED's. The most difficult and time consuming part is listed as Step 3 which requires a cross-section evaluation to establish the numerical values for f_i. Our preliminary calculations and evaluations indicate that for a fusion reactor design problem (14 MeV neutron source) where the responses are taken to be total tritium production and nuclear heating, the integral SED sensitivities S_i range from 0.05 to 0.5 while the integral SED uncertainties f_i are of the order of 0.5 to 1.0.

In conclusion it should be noted that the methodology to include SED uncertainties into routine cross-section uncertainty analyses as

SED-UNCERTAINTY ANALYSIS (SUMMARY)

1) COMPUTE E_{median} OR g_m FOR ALL SED's

2) COMPUTE INTEGRAL SENSITIVITIES S^{SED}

→ REQUIRES SENSITIVITY ANAL.

3) OBTAIN SPECTRAL SHAPE PARAMETERS f_i FOR SED's

→ REQUIRES XS-EVALUATION

4) COMPUTE $Cov(f_i, f_j)$ FOR SPECIFIC REACTIONS AND SED's OF INTEREST

5) COMPUTE $$\left(\frac{\Delta R}{R}\right)^2_{SED} = \sum_{i,j} S_i^{SED} S_j^{SED} Cov(f_i, f_j)$$

Fig. 10. A five-step summary to perform SED uncertainty analysis.

presented here, requires a minimum of additional computations and allows rough estimates of spectral shape uncertainties to be considered quantitatively. If the correlations of the f_i's are unknown, certain conservative assumptions may be made to obtain at least an upper limit estimate for Var(R) as outlined in Ref. 3. If higher precision might be desired than the present model is able to give, an extension of the hot/cold subdivision of SED's appears straightforward to the point where individual energy groups may be considered. Also, it is clear that this formalism is not restricted in its application to secondary energy distributions but can be applied to quantify any spectral shape uncertainties, e.g., that of the fission spectrum.

REFERENCES

1. S. A. W. Gerstl, "The Application of Perturbation Methods to Shield and Blanket Design Sensitivity Analyses," AP/CTR/TM-28 or FRA/TM-67, Applied Physics Division, Argonne National Laboratory (1974).

2. D. E. Bartine, E. M. Oblow, and F. R. Mynatt, Nucl. Sci. Eng. 55, 147 (1974).

3. S. A. W. Gerstl, D. J. Dudziak, and D. W. Muir, "Cross-Section Sensitivity and Uncertainty Analysis with Application to a Fusion Reactor," Nucl. Sci. Eng. 26, 137-156 (1977).

4. D. M. Drake, G. F. Auchampaugh, E. D. Arthur, C. E. Ragan, and P. G. Young, "Double-Differential Beryllium Neutron Cross Sections at Incident Neutron Energies of 5.9, 10.1, and 14.2 MeV," Los Alamos Scientific Laboratory report LA-6257, August 1976.

5. S. A. W. Gerstl and W. M. Stacey, Jr., Nucl. Sci. Eng. 51, 339 (1973).

6. S. A. W. Gerstl, "Sensitivity Profiles for Secondary Energy and Angular Distributions," Proc. of the Fifth Int'l. Conf. on Reactor Shielding, Knoxville, Tenn., April 1977; R. W. Roussin, L. S. Abbott,

and D. E. Bartine (editors), Science Press, Princeton, USA, 1977 (pg. 101-111).

7. C. I. Baxman and P. G. Young (Eds.), "Applied Nuclear Data Research and Development, April 1-June 30, 1977," Los Alamos Scientific Laboratory report LA-6971-PR (1977).

HIGH ORDER EFFECTS IN CROSS SECTION SENSITIVITY ANALYSIS*

E. Greenspan, Y. Karni and D. Gilai
Nuclear Research Center - Negev
Beer-Sheva, ISRAEL
and
Ben-Gurion University of the Negev
Department of Nuclear Engineering
Beer-Sheva, ISRAEL

ABSTRACT

Two types of high order effects associated with perturbations in the flux shape are considered: Spectral Fine Structure Effects (SFSE) and non-linearity between changes in performance parameters and data uncertainties. SFSE are investigated in Part I using a simple single resonance model. Results obtained for each of the resolved and for representative unresolved resonances of ^{238}U in a ZPR-6/7 like environment indicate that SFSE can have a significant contribution to the sensitivity of group constants to resonance parameters. Methods to account for SFSE both for the propagation of uncertainties and for the adjustment of nuclear data are discussed.

A Second Order Sensitivity Theory (SOST) is presented, and its accuracy relative to that of the first order sensitivity theory and of the direct substitution method is investigated in Part II. The investigation is done for the non-linear problem of the effect of changes in the 297 keV sodium minimum cross section on the transport of neutrons in a deep-penetration problem. It is found that the SOST provides a satisfactory accuracy for cross section uncertainty analysis. For the same degree of accuracy, the SOST can be significantly more efficient than the direct substitution method.

PREFACE

Two subjects related to cross section sensitivity theory are addressed in this work: Spectral Fine Structure Effects (SFSE) on sensitivity coefficients and Second Order Sensitivity Theory (SOST) for problems in which the change in performance parameters is not linear with the change in cross sections. Even though completely distinct, the two subjects have a common denominator--they are concerned with indirect effects on sensitivity coefficients caused by changes in the cross sections via perturbations in the flux shape. These "high order" effects are not taken into account by the perturbation theory based sensitivity methodologies developed

*This research was partially sponsored by the Electric Power Research Institute and was performed in part at ORNL, operated by Union Carbide Corporation under Contract W-7405-eng-26 with the Department of Energy.

so far. As the two subjects to be considered are independent, they are presented as two separate parts.

SPECTRAL FINE-STRUCTURE EFFECTS IN CROSS SECTION SENSITIVITY ANALYSIS

Introduction

The ultimate goal of cross section uncertainty analysis based on sensitivity methodology is to relate uncertainties in performance parameters to uncertainties in basic nuclear data. The common practice in uncertainty analysis is to use multi-group formulations and to apply the sensitivity methodology starting from the group constants. Group sensitivity coefficients are generated to provide linear relations between the perturbation (or, a change, in general) in the performance parameter and the uncertainty in any of the group constants.

In the framework of the group formulation, the sensitivity methodology is fairly well established. The situation is not as clear with regard to the relation between the uncertainty in the basic nuclear data and that of the group constants.

Approaches for relating uncertainties in nuclear data with uncertainties in group constants were proposed, for example, by Gandini and Salvatores[1] and by Perey[2]. Perey outlined a general approach for propagating the uncertainties from the resonance parameters to the group constants and Gandini and Salvatores provided[1] detailed prescriptions. In the resonance energy range, where the question is most problematic, they propose to associate all the uncertainties in the nuclear data with the uncertainty in the corresponding infinite dilution cross section. This proposal reflects their assessment[1] that "the inaccuracies of the self-shielding coefficients are second-order with respect to those of the infinite dilution cross sections." The above procedure was adopted as the common practice in cross section uncertainty methodology.

The self-shielding coefficients (or f-factors) account for the effect of the fluctuations in the neutron spectrum, caused by the resonance structure of the cross section in an energy scale which is much finer than the group width, on the group constants. A change in the resonance parameters (as well as in the background cross section) affects, in principle, the fine structure details of the flux spectrum and, through it, also the group constants. We shall refer to these effects on the group constants as spectral fine structure effects (SFSE).

In a recent study[3,4] it was found that SFSE can have a significant contribution to the reactivity worth associated with changes in the amplitude or temperature of resonances. Perturbation theory expressions for reactivity worth use, in fact, sensitivity coefficients of a certain type. This observation appears to be in contradiction with the assertion[1] that

the effects of uncertainties due to SFSE are negligible.

The purpose of this work is to investigate the magnitude of SFSE on cross section sensitivity coefficients. A specific question we address is whether or not it is justified to neglect the propagation of uncertainties from the basic resonance parameters to the group constants via the f-factor channels.

The investigation is system independent and differential in nature; we investigate the contribution of uncertainties in the parameters of a given resonance to the uncertainty in the group constants. This is done for each of the resolved resonances and of selected unresolved resonances of ^{238}U using a simple single-resonance model.

The results presented pertain to a ZPR-6/7 like assembly. The type of the assembly enters into the model through the atomic density of ^{238}U and the background cross section.

General Considerations

Consider the self-shielding approach for the expression of group constants. Using the notation of Ref. 1, the group constant of type x of isotope i, $\langle\sigma_x^i\rangle$ is expressed as

$$\langle\sigma_x^i\rangle = \sigma_{x\infty}^i \, f_x^i \tag{1}$$

where

$$\sigma_{x\infty}^i = \frac{1}{\Delta u}\int_{u_1}^{u_2} \sigma_x^i(u)\,du \tag{2}$$

is the infinite dilution group constant and

$$f_x^i = \frac{1}{\sigma_{x\infty}^i}\,\frac{\displaystyle\int_{u_1}^{u_2} \frac{\sigma_x^i(u)}{\Sigma_t(u)}\,du}{\Delta u\,\langle 1/\Sigma_t\rangle} \tag{3}$$

is the resonance self-shielding, or f-factor. In the above

$$\left\langle\frac{1}{\Sigma_t}\right\rangle \equiv \frac{1}{\Delta u}\int_{u_1}^{u_2} \frac{1}{\Sigma_t(u)}\,du \tag{4}$$

Σ_t is the total cross section (of all the constituents of the assembly), and $\Delta u = u_2 - u_1$ is the group width, in lethargy units.

The change in the group constant $\langle\sigma_x^i\rangle$ due to a change in a given input parameter q_k is

$$\frac{\partial\langle\sigma_x^i\rangle}{\partial q_k} = f_x^i \frac{\partial\sigma_{x\infty}^i}{\partial q_k} + \sigma_{x\infty}^i \frac{\partial f_x^i}{\partial q_k} . \tag{5}$$

If $\sigma_{x\infty}^i \partial f_x^i/\partial q_k \ll f_x^i \partial\sigma_{x\infty}^i/\partial q_k$, as suggested for example in Ref. 1, then there is a simple linear relation between a change in the infinite dilution cross section (and therefore, in the basic nuclear data) and the change in the group constant. If, however, the $\partial f_x^i/\partial q_k$ term of Eq. (5) is not negligible (that is, if the SFSE are not negligible) the relation between a change in the nuclear data and a change in the group constant becomes much more complicated.

The self-shielding factor, f_x^i, depends in principle on all the partial cross sections of the ith constituent [that contributes to $\sigma_t^i(u)$] and on all the other constituents of the assembly. This dependence comes via the weighting function $1/\Sigma_t(u)$ [see Eq. (3)]

$$\Sigma_t(u) = \sum_{j=1}^{J} N_j \sigma_t^j(u) \tag{6}$$

where N_j is the atomic density of the jth constituent and J is the total number of constituents present. Consequently,

$$\frac{\partial f_y^n}{\partial q_k} = \frac{\partial f_y^n}{\partial\sigma_y^n}\frac{\partial\sigma_y^n}{\partial q_k} + \sum_{j=1}^{J}\frac{\partial f_y^n}{\partial\sigma_t^j}\frac{\partial\sigma_t^j}{\partial q_k} . \tag{7}$$

The scripts y and n are to emphasize that a change in a given input parameter q_k can effect many different f-factors and therefore, group constants!

Consider now the uncertainty in a performance parameter, R, due to uncertainty in an input parameter q_k. The uncertainty in q_k can propagate to the uncertainty in R via many channels--including all group constants their corresponding $\partial f_y^n/\partial q_k$ are not negligible. Thus in general, the sensitivity coefficient of performance parameter R to the nuclear parameter q_k is:

$$S_{Rq} \equiv \frac{\partial R}{R}\Big/\frac{\partial q_k}{q_k} = \sum_i\sum_x \left[\frac{\partial R}{R}\Big/\frac{\partial\langle\sigma_x^i\rangle}{\langle\sigma_x^i\rangle}\right]\left[\frac{\partial\langle\sigma_x^i\rangle}{\langle\sigma_x^i\rangle}\Big/\frac{\partial q_k}{q_k}\right] \equiv \sum_i\sum_x G_{Rx}^i\, P_{xq}^i \tag{8}$$

We shall refer to G_{Rx}^{i} as the sensitivity coefficient of the performance parameter to the group constant and to P_{xq}^{i} as the group constant sensitivity coefficient (to the input parameter).

Most sensitivity analysis performed to date dealt with sensitivity coefficients to group constants (the G_{Rx}^{i}s). The subject matter of the present work are the group constant sensitivities, the P_{xq}^{i}s. From Eq. (5) we get, dropping the superscript i for the type of isotope,

$$P_{xq} \equiv \frac{\partial\langle\sigma_x\rangle}{\langle\sigma_x\rangle}\Big/\frac{\partial q_k}{q_k} = \frac{\partial\sigma_{x\infty}}{\sigma_{x\infty}}\Big/\frac{\partial q_k}{q_k} + \frac{\partial f_x}{f_x}\Big/\frac{\partial q_k}{q_k} \tag{9}$$

which we shall express as follows:

$$P_{xq} \equiv D_{xq} + I_{xq} \equiv D_{xq}(1+R_{xq}) \ . \tag{10}$$

In the above, D_{xq} is the direct effect of the change in the input parameter on the group constant, i.e., the effect via the infinite dilution cross section; I_{xq} is the indirect effect, which is the effect via the self-shielding factor (i.e., SFSE). The parameter $R_{xq} \equiv I_{xq}/D_{xq}$ will be referred to as the relative sensitivity of the group constant, or the "relative sensitivity." The quantities D_{xq} and I_{xq} will also be referred to as the infinite dilution cross section sensitivity and the f-factor sensitivity, respectively. Our main concern in the following sections is R_{xq}, that is, the relative contribution of the SFSE to the group constant sensitivities.

Model for Analysis

The investigation of SFSE is performed using a simple single resonance space-independent model similar in its general approach to that used in Ref. 3. Following is a brief description of this model, starting with a list of assumptions:

1) Each resonance is taken to be centered in a group having a prescribed width. There is only one resonance per group.

2) The resonance cross sections are expressed by the single-level Brei-Wigner formula.

3) The resonance satisfies either the narrow resonance or the narrow resonance infinite mass approximation.

4) The scattering cross section of the mixture, excluding the resonance cross section, is constant. Perturbations in the resonance parameters do not vary this background cross section.

5) The absorption cross section, excluding that of the resonance, is zero.

6) The asymptotic flux distribution is taken to be constant across the group. That is, we neglect the 1/E dependence of the flux weighting spectrum within the group. This should be a fairly valid assumption for our model, in view of the fact that the flux weighting within the group has a meaning only in the vicinity of the resonance. Thus we use

$$\phi(E) \propto 1/\Sigma_t(E) \tag{11}$$

for the flux weighting spectrum, where

$$\Sigma_t(E) = \Sigma_b + {}^{28}N^{28}\sigma_t(E) \tag{12}$$

and Σ_b is the total macroscopic background cross section.

In the resolved resonance energy region we consider each of the ^{238}U resonances. In the unresolved region we examine selected fictitious resonances taken to have the average resonance parameters specified by ENDF/B-IV.

For each group (i.e., resonance, in our model) we calculate the group constant sensitivities P_{xq} for capture ($x=\gamma$) and for scattering ($x=n$) pertaining to each one of the three input variables Γ_γ, Γ_n and Σ_b. We shall use for q the subscripts γ, n and b to denote these three variables. In the following, the superscript 28 (for i) will be omitted.

The direct and indirect effects of the change in the input variables were calculated as the difference between a perturbed and the reference values of $\sigma_{x\infty}$ and f_x, respectively. The perturbed values were calculated from the basic definitions, Eqs. (1) and (3), with the value of the input parameter slightly varied (usually by 1%) from the reference value.

Results

In this work we shall restrict our consideration to the sensitivities of capture group constants--the group constants of most relevance to the contribution of ^{238}U to performance parameters of interest. All the results pertain to groups having a width of 0.25 lethargy units--a typical width for many multi-group cross section sets.

Figures 1 through 4 summarize the results obtained for the ^{238}U resolved resonances. Each point in the figures represents the group sensitivity (or relative sensitivity) corresponding to the ^{238}U resonance the energy of which is marked by the location of the point.

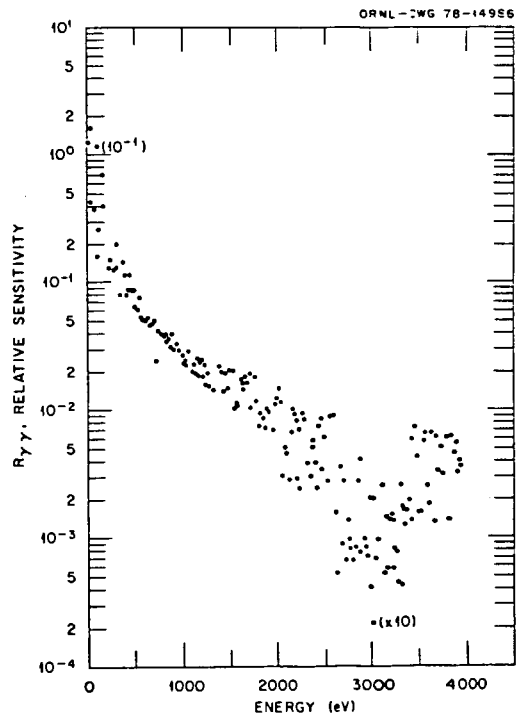

Fig. 1. Relative Sensitivities $R_{\gamma\gamma}$ of ^{238}U in ZPR-6/7 Like Assembly.

$\gamma\gamma$ Sensitivities

There is a tendency for the indirect contribution to $P_{\gamma\gamma}$ (that due to SFSE) to become smaller with energy, relative to the direct contribution. That is, the $R_{\gamma\gamma}$ data (Fig. 1) exhibit a general decline as the energy of the resonances increases. It appears that in the energy range of interest for fast reactors the SFSE are negligible; above 2 keV $R_{\gamma\gamma}$ is smaller than 1%. $R_{\gamma\gamma}$ is of the order of 2-3% in the vicinity of 1 keV and keeps increasing significantly at lower energies; in the energy range below about 400 eV $R_{\gamma\gamma}$ exceeds 10%. Hence in the energy range $E \lesssim 400$ eV, the neglect of the SFSE is expected to lead to non-negligible errors. This energy range is of importance for thermal and epithermal systems.

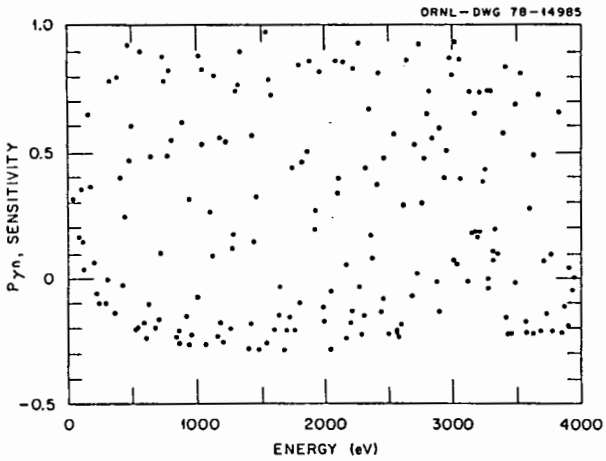

Fig. 2. Group Constant Sensitivities $P_{\gamma n}$ of the Resolved Resonances of ^{238}U in ZPR-6/7 Like Assembly.

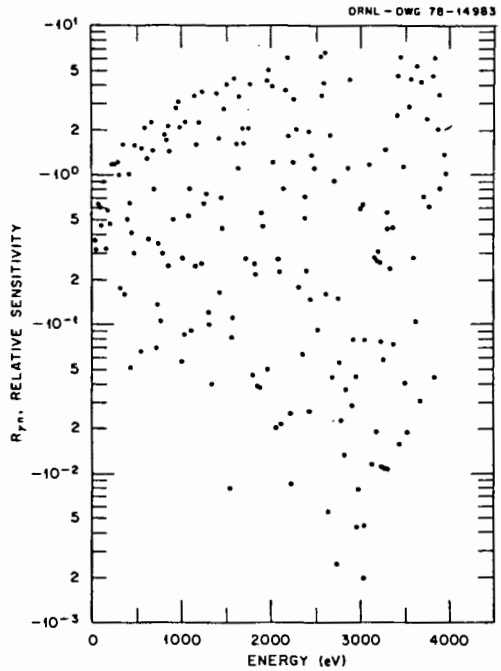

Fig. 3. Relative Sensitivities $R_{\gamma n}$ of the Resolved Resonances of ^{238}U in ZPR-6/7 Like Assembly.

γn Sensitivities

Most interesting are the $P_{\gamma n}$ sensitivities (Fig. 2); they can be either positive or negative, depending on the particular resonance parameters. This behavior reflects the fact that $D_{\gamma n}$ and $I_{\gamma n}$ are of opposite signs and of widely varying magnitude (see Fig. 3). Notice that for many resonances $|R_{\gamma n}|>>1$!

Table 1 summarizes the $D_{\gamma n}$, $P_{\gamma n}$ and $R_{\gamma n}$ sensitivities of samples of predominantly scattering and of predominantly capture resonances. A strong correlation is observed between the γ_n sensitivities and the type of the resonance:

a) The highest $P_{\gamma n}$ sensitivities are associated with predominantly capture resonances. The corresponding SFSE are relatively small (with the exception of the low energy resonances).

b) Very large SFSE are associated with the predominantly scattering resonances. For these resonances $I_{\gamma n}$ provides the dominant contribution to $P_{\gamma n}$.

In the case of the γ_n sensitivities the SFSE have a negative contribution. This phenomenon can be explained, qualitatively, as follows: An increase in Γ_n tends to increase the amplitude of the total cross section (the resonance part of which being roughly proportional to Γ_n) more than that of the capture cross section [which is proportional to $\Gamma_n/(\Gamma_\gamma+\Gamma_n)$].

Consequently $\Sigma_t(E)$ becomes more pronounced relative to $\sigma_\gamma(E)$ causing an increase in the self-shielding factor and thus a negative $I_{\gamma n}$ component.

Table 1. - Sensitivities $D_{\gamma n}$, $P_{\gamma n}$, and $R_{\gamma n}$ and the Effective Capture Group Constant $\langle\sigma_\gamma\rangle$ for a Sample of Predominantly Scattering Resonances and a Sample of Predominantly Capture Resonances.

Resonance Energy (eV)	$\frac{\Gamma_\gamma}{\Gamma}$	$\langle\sigma_\gamma\rangle$	$D_{\gamma n}$	$P_{\gamma n}$	$R_{\gamma n}$
116.8	.454	1.477	.453	.0411	- .909
237.2	.447	.631	.446	-.0929	-1.208
518.3	.321	.242	.321	-.1987	-1.619
936.6	.147	.091	.147	-.2641	-2.797
1522.3	.089	.043	.089	-.2623	-3.953
2547.2	.041	.025	.040	-.2089	-6.164
3856.4	.045	.013	.045	-.2219	-5.928
6.67	.945	38.05	.944	.598	- .35
311.2	.955	.1475	.955	.786	- .18
454.1	.981	.0342	.981	.930	- .05
1533.0	.983	.0027	.983	.976	- .008
2241.0	.940	.0046	.940	.932	- .008
3015.1	.934	.0028	.934	.933	- .002

As the $P_{\gamma n}$ sensitivities are of significant magnitude it is apparent that for an accurate uncertainty analysis the contribution of uncertainties in Γ_ns to uncertainties in the capture group constants should be accounted for and vice versa: In adjusting cross sections the adjustment of the Γ_ns capture group constant should be correlated with the adjustment of the Γ_γ (in addition to the Γ_γs). Realizing that the SFSE have a very large contribution to the $P_{\gamma n}$s (for many of the more important resonances $|I_{\gamma n}| > D_{\gamma n}$), it is concluded that the neglect of SFSE in cross section uncertainty analysis may not be justified for many problems.

γb Sensitivities

The $P_{\gamma b}$ sensitivities (Fig. 4) stem entirely from SFSE so that $R_{\gamma b} = 0$. Increasing Σ_b leads to a relative flattening of the $\Sigma_t(E)$ distribution thus causing a reduction in the resonance self-shielding, and hence, an increase in the group capture cross section. It is observed (Fig. 4) that for many resonances $P_{\gamma b} > 0.3$ but the $P_{\gamma b}$ values spread over about two decades.

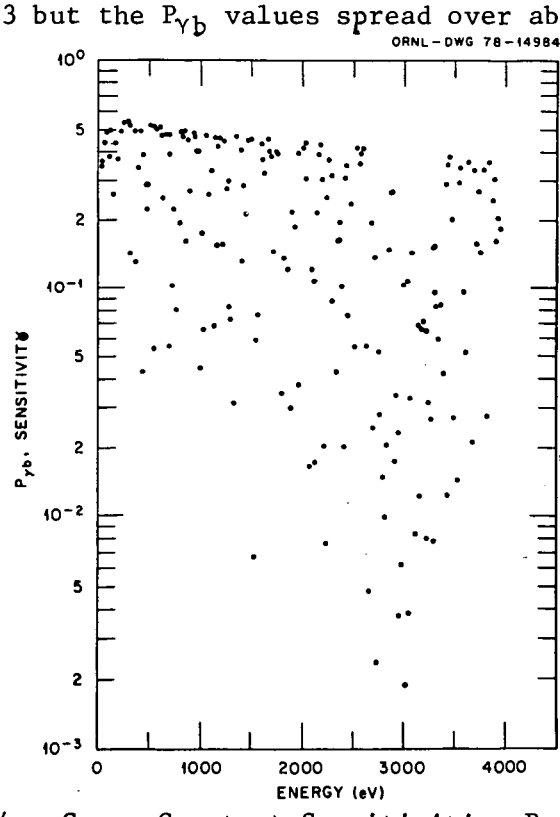

Fig. 4. Group Constant Sensitivities $P_{\gamma b}$ of the Resolved Resonances of ^{238}U in ZPR-6/7 Like Assembly

The systematics of the $P_{\gamma b}$ behavior can be deduced from Table 2 which presents the sensitivities of samples of predominantly scattering and predominantly capture resonances. It is observed that the high $P_{\gamma b}$ values are associated with the predominantly scattering resonances. Realizing that these resonances are the relatively large ones it is concluded that uncertainties in Σ_b can have non-negligible contributions to uncertainties in the group capture cross section and vice versa--the adjustment of the group capture cross section should be propagated back also to the adjustment in the background cross section.

Table 2. - Capture Group Constant Sensitivities to the Background Cross Section ($P_{\gamma b}$) for a Sample of Predominantly Scattering Resonances and a Sample of Predominantly Capture Resonances.

Resonance Energy (eV)	$\frac{\Gamma_\gamma}{\Gamma}$	$\langle\sigma_\gamma\rangle$	$P_{\gamma b}$
116.8	.454	1.477	.496
237.2	.447	.631	.541
518.3	.321	.242	.516
936.6	.147	.091	.481
1522.3	.089	.043	.451
2547.2	.041	.025	.410
3856.4	.045	.013	.357
311.2	.945	.1475	1.435-1
454.1	.955	.0342	4.267-2
1533.0	.983	.0027	6.55-3
2241.0	.940	.0046	7.51-3
3015.1	.934	.0028	1.85-3

Unresolved Resonances

In the unresolved resonance energy range we found that the $P_{\gamma\gamma}$ sensitivities approach unity and they result, essentially, from the direct effects ($R_{\gamma\gamma}\to 0$). The $P_{\gamma n}$ sensitivities are pretty small with the SFSE playing the major role. The $P_{\gamma b}$ sensitivities are of the order of 20% at the lower energies of the unresolved range, but drop to below 10% for energies exceeding 15 keV. These sensitivities come entirely from SFSE.

In summary, even though SFSE are generally significantly lower, for the unresolved resonances than for the resolved ones, errors of the order of 10% might be expected in certain problems due to the neglect of SFSE in the unresolved resonance energy range.

Methods to Account for SFSE

The single resonance model results do not give the overall inaccuracy that might be introduced in sensitivity analysis of specific reactors due to the neglect of SFSE.* These results indicate, nevertheless, that SFSE are expected to be significant enough for certain real problems so that it is desirable to have an uncertainty analysis methodology that could take these SFSE into account.

The most straightforward way to account for SFSE is to use an energy mesh which is fine compared with the fluctuations in the cross sections. Such an approach might be justified for certain applications such as for thermal reactor lattices[7] but does not appear to be practical for general use.

*Such weighted effects are being investigated for the ZPR-6/7 using the FORSS sensitivity machinery[5,6].

A procedure compatible with the computational capability of fast systems is to propagate uncertainties in the basic nuclear data through self-shielding factors (and vice versa) in addition to their propagation through the infinite dilution cross sections. This propagation of uncertainties can use analytic expressions of the form

$$\frac{\partial f_x^i}{\partial q_k} = \frac{1}{\Delta u \langle \frac{1}{\Sigma_t} \rangle} \int_{u_1}^{u_2} \frac{1}{\Sigma_t(u)} \frac{\partial \Sigma_t(u)}{\partial q_k} \left[f_x^i - \frac{\sigma_x^i(u)}{\sigma_{x\infty}^i} \right] du$$

$$+ \frac{1}{\Delta u \; \sigma_{x\infty}^i} \int_{u_1}^{u_2} \frac{\partial \sigma_x^i(u)}{\partial q_k} \left[\frac{1}{\langle \frac{1}{\Sigma_t} \rangle} \; \frac{1}{\Sigma_t(u)} - f_x^i \right] du \qquad (13)$$

derived[1] from Eq. (3). These f-factor sensitivities could be generated by the cross section processing codes.

Discussion

Regardless of whether SFSE are to be taken into account or not, uncertainties in the nuclear data can be propagated to an uncertainty in a performance parameter via uncertainties in group constants. The calculation of uncertainties in performance parameters can be performed using a two-phase procedure: First the nuclear data uncertainties are propagated to the group constants uncertainties. Then the group constants uncertainties are propagated to the uncertainty in the performance parameters with the aid of the sensitivity coefficient to the group constants. The second phase is the standard procedure in sensitivity analysis to date. The inclusion of SFSE in the analysis increases the number of channels through which uncertainties can propagate to the group constants. Moreover, SFSE open channels for the propagation of uncertainties to group constants pertaining to isotopes other than the isotope the uncertainty in the nuclear data of which is being considered.

More complex is the question of cross section adjustment. When SFSE can be neglected, the two-phase procedure can be reversed. First, the infinite dilution cross sections can be adjusted using results of integral experiments from many assemblies. This is, in fact, the conventional procedure for cross section adjustments. In the second phase, the resonance parameters can be adjusted, with the adjusted infinite dilution cross sections playing the role of the integral experiment results in the first phase.

When SFSE cannot be neglected, however, current procedures for the adjustment of group constants can be applied only to a single assembly. This is rather a severe limitation for cross section uncertainty analysis. This difficulty may be overcome either by adjusting the self-shielding factors

along with the infinite dilution cross sections or by adopting a more general procedure: The direct adjustment of the basic nuclear parameter (i.e., skipping the group constant adjustment stage). The basis for this one-phase adjustment procedure are the sensitivity coefficients S_{Rq} defined by Eq. (8). The resulting one-phase adjustment procedure is, in fact, the consistent method for data adjustment proposed by Gandini and Salvatores[1] modified to include SFSE. It conforms with the data adjustment philosophy proposed by Perey[2].

Concluding Remarks

Spectral fine structure changes in the neutron spectra caused by changes in the nuclear data in the resonance energy range can have significant effects on the value of the group constant sensitivity coefficients and thus, on the sensitivity of a performance parameter to the nuclear data. The overall magnitude of SFSE is strongly problem dependent. It is recommended that the sensitivity and uncertainty analyses methodologies be extended to include the capability of taking these SFSE into account. It appears that the approach for taking SFSE into account most compatible with the existing computational machinery is through f-factor sensitivities for fast reactors and through the point-energy mesh for thermal lattices.

When SFSE are not negligible, the adjustment of group constants becomes more complicated. It is possible, however, to adjust the nuclear data directly using the consistent method with SFSE accounted for. It is therefore recommended that the feasibility of developing the methodology and machinery required for a full-scale application of the direct adjustment of nuclear data will be studied.

If developed for practical applications, the cross section uncertainty analysis methodology that includes the capability for direct adjustment of nuclear data could be a very useful aid for the evaluators of nuclear data. For this computational capability to be useful, one should also have the data bases of uncertainties of nuclear data, of integral experiments as well as of methods. Should not the development of such a computational capability and data bases be set as a goal associated with the preparation of one of the forthcoming versions of ENDF/B, perhaps even of ENDF/B-VI?

SECOND ORDER SENSITIVITY THEORY

Introduction

The perturbation theory based cross section sensitivity methodologies developed in recent years are based on linear perturbation theory formulations; linear in the sense that the fractional change in the performance parameter is linear with the fractional change in the cross section (or input parameter, in general). We shall refer to the above as First Order Sensitivity Theory (FOST). Herb Goldstein has recently pointed out[8] to

situations in which performance parameters vary significantly non-linearly with cross section changes. A most convincing illustration for such non-linear situations is the effect of changes in the cross section of the 297 keV sodium minimum in deep penetration problems; Goldstein found[8] that even for quite modest changes of 5-10% in the cross section at the minimum, the correct value of the sensitivity coefficient differs by 20-50% from the predictions of the FOST! In such "pathological" or non-linear situations (which are expected to occur mainly in certain deep penetration problems), Goldstein suggests[8] to calculate the correct sensitivity coefficients using the direct substitution approach, i.e., from the difference of two direct calculations.

Another possible approach for the analysis of non-linear problems is to apply high order sensitivity theory formulations. The work summarized in this part is a preliminary investigation of the adequacy and feasibility of applying a Second Order Sensitivity Theory (SOST) formulation for the analysis of the non-linear problems. The investigation is done by comparing the prediction ability of the SOST and of FOST against the exact result (as calculated with the direct substitution approach) for a problem of deep penetration in sodium, similar to Goldstein's problem[8].

The theoretical basis for the SOST is the Second Order generalized Perturbation Theory (SOPT) recently derived and summarized in a general formulation in Ref. 9. A special case of the SOPT in which the variables are the material densities has been tried[9,10] for shield optimization studies and found very useful for this type of application.

In the following section we derive expressions for a special case of the SOST pertaining to a certain type of cross sections. The resulting SOST formulation is then applied for the analysis of the effect of changes in the cross section of the sodium 297 keV minimum.

The SOST Formulation

Consider a performance parameter of the form of reaction rate

$$R = \int d\underline{r} \int dE \; \phi(\underline{r},E) \; S^*(\underline{r},E) \tag{14}$$

where $S^*(\underline{r},E)$ is the response function of the detector measuring R. Suppose the perturbation (causing the non-linear effects) is in a specific cross section to be denoted here simply as $\sigma(E)$ (i.e., we ignore, for notational simplicity, possible angular dependence). We shall also assume that neither S^* nor the neutron source S depend on σ.

Let us express the performance parameter in the system in which σ is perturbed as a functional Taylor series around its value in the reference system:

$$\bar{R} = R + \int d\underline{r} \int dE \int dE' \, \frac{\partial\phi(\underline{r},E)}{\partial\sigma(E')} \, S^*(\underline{r},E)\delta\sigma(E')$$

$$+ \frac{1}{2!} \int d\underline{r} \int dE \int dE' \int dE'' \, \frac{\partial^2\phi(\underline{r},E)}{\partial\sigma(E')\partial\sigma(E'')} \, S^*(\underline{r},E)\delta\sigma(E')\delta\sigma(E'') + \ldots \tag{15}$$

where the flux is the solution of the Boltzmann equation

$$\underset{\sim}{H} \, \phi(\underline{r},E,\underline{\Omega}) = S(\underline{r},E,\underline{\Omega}), \tag{16}$$

and the flux perturbation can be obtained, to first order, from

$$\underset{\sim}{H} \, \frac{\partial\phi(\underline{r},E,\underline{\Omega})}{\partial\sigma(E')} = - \frac{\partial\underset{\sim}{H}}{\partial\sigma(E')} \, \phi(\underline{r},E,\underline{\Omega}). \tag{17}$$

Using the adjoint function, ϕ^*, defined by

$$\underset{\sim}{H}^* \, \phi^*(\underline{r},E,\underline{\Omega}) = S^*(\underline{r},E) \tag{18}$$

the first integral at the right side of Eq. (15) can be expressed as follows:

$$\left\langle \frac{\partial\phi(\underline{r},E,\underline{\Omega})}{\partial\sigma^*E')}, S^*(\underline{r},E) \right\rangle = - \left\langle \phi^*(r,E,\underline{\Omega}), \frac{\partial\underset{\sim}{H}}{\partial\sigma(E')} \, \phi(r,E,\underline{\Omega}) \right\rangle \equiv S_1(E') \tag{19}$$

where <, > stands for integration over the phase space $(\underline{r},E,\underline{\Omega})$ and $S_1(E')$ is directly related to the conventional (i.e., first order) sensitivity profile.

Let us turn now to the second order term of Eq. (15). The second order derivative of the flux can be obtained from the solution of the Boltzmann equation

$$\underset{\sim}{H} \, \frac{\partial^2\phi(\underline{r},E,\underline{\Omega})}{\partial\sigma(E')\partial\sigma(E'')} = - \frac{\partial\underset{\sim}{H}}{\partial\sigma(E')} \, \frac{\partial\phi(\underline{r},E,\underline{\Omega})}{\partial\sigma(E'')} - \frac{\partial\underset{\sim}{H}}{\partial\sigma(E'')} \, \frac{\partial\phi(\underline{r},E,\underline{\Omega})}{\partial\sigma(E')} . \tag{20}$$

Using this equation and Eq. (18), the second integral at the right side of Eq. (15) can be expressed as follows:

$$\left\langle \frac{\partial^2\phi(\underline{r},E,\underline{\Omega})}{\partial\sigma(E')\partial\sigma(E'')}, S^*(\underline{r},E) \right\rangle = - \left\langle \phi^*(\underline{r},E,\underline{\Omega}), \left[\frac{\partial\underset{\sim}{H}}{\partial\sigma(E')} \, \Psi(\underline{r},E,\underline{\Omega};E'') + \right.\right.$$

$$\left.\left. + \frac{\partial\underset{\sim}{H}}{\partial\sigma(E'')} \, \Psi(\underline{r},E,\underline{\Omega};E') \right] \right\rangle \equiv S_2(E';E'') \tag{21}$$

where $\Psi(\underline{r},E,\underline{\Omega};E') \equiv \partial\phi(\underline{r},E,\underline{\Omega})/\partial\sigma(E')$ is the solution of Eq. (17) and $S_2(E';E'')$ is directly proportional to the sensitivity of the sensitivity coefficient:

$$S_2(E';E'') = \frac{\partial S_1(E')}{\partial \sigma(E'')} . \tag{22}$$

With these definitions, Eq. (15) can be converted to

$$\delta R \equiv \overline{R} - R = \int dE' \; S_1(E')\delta\sigma(E') + \frac{1}{2}\int dE' \int dE'' \; S_2(E';E'')\delta\sigma(E')\delta\sigma(E''). \tag{23}$$

Consider now the special case in which the cross section perturbation can be expressed in the form

$$\delta\sigma(E) = \alpha f(E) \tag{24}$$

in which the shape f(E) of the perturbation is known (or postulated) but its amplitude, α, is a variable. For this case Eq. (23) can be reworked to the form

$$\delta R = S_1 \; \alpha + \frac{1}{2} S_2\alpha^2 \tag{25}$$

where

$$S_1 \equiv \int dE' \; S_1(E')f(E') \tag{26}$$

and

$$S_2 \equiv \int dE' \int dE'' \; S_2(E';E'')f(E')f(E'') . \tag{27}$$

The sensitivity coefficient

$$\frac{\partial R}{R}\Big/\frac{\partial \alpha}{\alpha} = \frac{1}{R}\left[S_1\alpha + S_2\alpha^2\right] = \frac{\alpha}{R}S_1 \left[1 + \alpha\frac{S_2}{S_1}\right] \tag{28}$$

is quadratic with the amplitude of the cross section perturbation. The FOST formulation is obtained by ignoring the S_2 terms.

An Example

The problem chosen for checking the accuracy of the SOST formulation is a sodium deep penetration problem in which the non-linearity in the performance parameters due to changes in the cross section at the sodium 297 keV minimum is aniticipated to be representative of the class of the most extreme non-linear situations to be encountered in cross section uncertainty analysis.

To reduce computer memory requirements we have used a smaller sodium assembly than that of Ref. 8 and applied a coarser spatial, angular and energy mesh for its solution. The problem uses one-dimensional slab geometry. A sodium slab, 260 cm in thickness, is subjected to an isotropic

source of 360 keV (monoenergetic) neutrons located at one of its faces. A (fictitious) detector set to monitor the flux of neutrons pertaining to the next to the lowest energy group (around 160 keV) is located at the other face of the assembly. Vacuum boundary conditions are imposed on both sides.

The cross section perturbation considered is of the form of Eq. (24) but restricted to the energy range of the window (around the 297 keV minimum). The shape of the perturbation is defined so that $\sigma(E) + f(E) = 2.8$ where $\sigma(E)$ is the sodium total cross section and 2.8 is representative of the sodium background cross section. In other words, when $\alpha=1$, the sodium window is completely filled up. Twenty-five energy groups, spanning the energy range from 150 keV to 360 keV are used with six of them covering the range of the window. The cross section set was generated from ENDF/B-IV. Scattering anisotropy was accounted for using the P_1 approximation. The calculations were performed with SWAN[12]. For this purpose the cross section perturbations were introduced in the form of changes in the atomic density of a fictitious material the cross sections of which are f(E) and the density of which determines α.

The sensitivity coefficients obtained for the problem under considerations are $S_1 = 13.17$ and $S_2 = -81.09$. In other words, the second order term becomes the dominant one for αs exceeding about 0.16. Fig. 5 compares the results obtained using the SOST, FOST and direct substitution method (considered as the "exact" results). The relative detector response is plotted as a function of the cross section at the 297 keV minimum (denoted in the figure by σ) relative to its reference value (σ_0). The corresponding actual change in the cross section is described by Eq. (24). A σ/σ_0 value of 0.75 or 1.25, for example, corresponds approximately to α of -0.2 or 0.2 respectively. Following are several observations:

1) In the σ/σ_0 range considered, the SOST results are more accurate than the FOST ones.

2) As the window becomes more shallow, the SOST overestimates the detector reading while the FOST underestimates it. For σ/σ_0 values exceeding 1.23, the FOST predicts negative detector readings! At this point the SOST overpredicts the reading by about 30%.

3) In the $\delta\sigma/\sigma_0 = \pm 10\%$ range, the SOST formulation is accurate to within 4% (actually, from about o to 4%). In this range FOST can deviate by as much as 17% (from -17% to +1%).

4) In the $\delta\sigma/\sigma_0 = \pm 20\%$ range, the SOST formulation is accurate to within 11% (from -4% to +11%). In this range FOST can deviate by as much as 70% (from +27% to -70%)!

Uncertainties in cross sections of importance for the design of nuclear systems are usually confined within the 10% range and seldom exceeding the 20% range. It thus appears that SOST does provide an adequate accuracy for cross section uncertainty analysis.

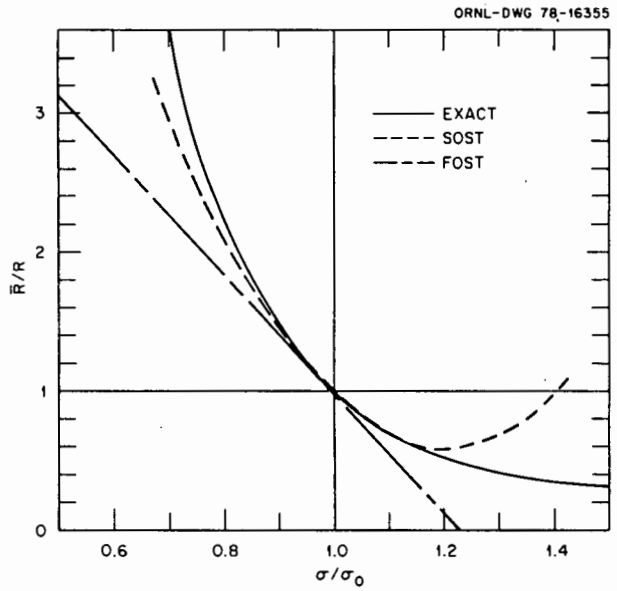

Fig. 5. Relative Detector Response $\bar{R}/R$ as a Function of the Relative 297 keV Na Minimum Cross Section Change σ/σ_0 Calculated Using Three Methods: Direct Substitution ("Exact"), SOST and FOST.

Discussion

Three transport calculations are required for applying the SOST formulation to the example dealt with in the preceeding section: One for the flux, one for the adjoint function and one [Eq. (17)] for the perturbation in the flux $\Psi(\underline{r},E,\underline{\Omega})$ with $-\int dE'[\partial \underset{\sim}{H}/\partial\sigma(E')]\phi(\underline{r},E,\underline{\Omega})f(E')$ for the source term. To get comparable information using the direct substitution approach, one also needs three transport (flux) calculations; the resulting three points in the δR - α space could provide a quadratic expression for the relation between δR and α. Thus, for the single variable problem the SOST does not save computational effort relative to the direct substitution method.

Let us consider now a multi-variable problem having n independent input variables. For example n can stand for the total number of different group constants the uncertainties of which is to be propagated independently (and/or which are to be adjusted independently). To apply the SOST to such a problem one needs to solve n transport equations for the flux perturbation due to a change in each of the n variables [similar to Eq. (17)] in addition to the two regular flux and adjoint equations. To construct an n-dimensional paraboloid (which is the equivalent of the SOST formulation for the problem) one needs to have n(n+3)/2 points in the n-dimensional space necessitating n(n+3)/2 solutions of the transport equation in addition to the calculation of the reference point. It is concluded that for a comparable degree of accuracy, the SOST has the potential of saving a

large computational effort relative to the direct substitution method. The number of extra runs required by the direct substitution method relative to the number of runs required by the SOST method for an n-variable problem is:

$$\frac{[n(n+3)/2+1]-(n+2)}{(n+2)} = \frac{n-1}{2} \xrightarrow[n>>1]{} \frac{n}{2} .$$

As the number of the performance parameters to be considered increases, the relative advantage of the SOST decreases, but not significantly. The reason being that the SOST requires an adjoint function for each performance parameter. The flux and flux perturbations, however, are applicable to all of the performance parameters. Thus for a problem involving m performance parameters and n independent variables the relative number of extra transport calculations required by the direct substitution method is $[n(n+1)-2m]/2(n+m+1)$.

Concluding Remarks

SOST appears to provide satisfactory accuracies for most non-linear problems associated with cross section changes encountered in practice. The use of higher (than second) order sensitivity theories like the one recently proposed by Gandini[11] is not likely to be desirable--the added accuracy provided, say, by a third order formulation is not likely to justify the additional computational effort required for its application.

The SOST formulation addressed to in this work is more efficient than the direct substitution method. The larger the number of independent variables, the larger becomes the advantage of the SOST. The direct substitution method can, however, provide a better accuracy over a wider range of perturbations and can be applied with existing tools.

The SOST can be useful for a variety of applications, including the study of the effect of specified changes in the system for problems which are non-linear, and the estimation of the effect of design changes on cross section sensitivity coefficients. It is doubtful, however, that the general application of the SOST for cross section uncertainty analysis (including the incorporating of the SOST formulation within the uncertainty analysis machinery) could be done without significant effort, and whether such an effort is justified at present.

Acknowledgment

The help of P. Levin in obtaining the SOST results for Fig. 5, and useful discussions with J. H. Marable, F. G. Perey and C. R. Weisbin are appreciated.

REFERENCES

1. A. Gandini and M. Salvatores, "Nuclear Data and Integral Measurements Correlation for Fast Reactors. Part 3: The Consistent Method," CNEN-RT/FI (74)3 (1974).

2. F. G. Perey, "Estimated Uncertainties in Nuclear Data--An Approach," Proc. Conf. Nucl. Cross Sections and Tech., R. A. Schreck and C. D. Bowman, Edts., p. 842, NBS SP 425 (1978).

3. E. Greenspan and Y. Karni, "Spectral Fine-Structure Effects on Material and Doppler Reactivity Worths," Nucl. Sci. and Eng. (to be published).

4. E. Greenspan, "Developments in Perturbation Theory," Advances in Nucl. Sci. and Tech., vol. 9, p. 181, Academic Press (1976).

5. See "Workshop on FORSS," Proc. of the RSIC Seminar-Workshop on the Theory and Application of Sensitivity and Uncertainty Analysis (August 1978).

6. C. R. Weisbin, J. H. Marable, J. L. Lucius, E. M. Oblow, F. R. Mynatt, R. W. Peelle, and F. G. Perey, "Application of FORSS Sensitivity and Uncertainty Methodology to Fast Reactor Benchmark Analysis," ORNL/TM-5563, ORNL (1976).

7. E. T. Tomlinson, G. de Saussure, and C. R. Weisbin, "Sensitivity Analysis of TRX-2 Lattice Parameters with Emphasis on Epithermal ^{238}U Capture," EPRI Research Project 612 Final Report (EPRI NP-346) (1977).

8. Herbert Goldstein, "A Survey of Cross Section Sensitivity Analysis as Applied to Radiation Shielding," pp. 73-90, Proc. Fifth Int. Conf. on Reactor Shielding, R. W. Roussin, L. S. Abbott and D. E. Bartine, Edts., Science Press, Princeton (1977).

9. E. Greenspan, D. Gilai and E. Oblow, "Second Order Generalized Perturbation Theory for Source-Driven Systems," Nucl. Sci. and Eng. (to be published).

10. D. Gilai, E. Greenspan, P. Levin and W. G. Price, Jr., "Optimal Iron-Water Shields for Fusion Reactors," pp. 731-738, Proc. Fifth Int. Conf. on Reactor Shielding, R. W. Roussin, L. S. Abbott and D. E. Bartine, Edts., Science Press, Princeton.

11. A. Gandini, "Higher Order Time-Dependent Generalized Perturbation Theory," Nucl. Sci. and Eng., 67, 91 (1978).

12. E. Greenspan, W. G. Price, Jr. and H. Fishman, "SWAN: A Code for the Analysis and Optimization of Fusion Reactor Nucleonic Characteristics," MATT-1008 (1973). Also RSIC Computer Code Collection CCC-248.

SENSITIVITY THEORY FOR REACTOR THERMAL-HYDRAULICS PROBLEMS

E. M. Oblow
Oak Ridge National Laboratory
Oak Ridge, Tennessee 37830

ABSTRACT

A sensitivity theory based on reactor physics experience was successfully developed for a reactor thermal-hydraulics problem. The new theory is derived for the case of non-linear, transient heat and mass transfer in a typical reactor subassembly. Suitable adjoint equations for heat and fluid flow are presented along with methods for deriving the sources and boundary and final conditions for these equations. Expressions for the sensitivity of any integral temperature response to problem input data are also presented. The theory is applied to a sample problem describing the steady-state thermal-hydraulic conditions in a CRBR fuel channel. For this case, sensitivity coefficients are derived for several thermal response functions (i.e. peak clad and peak fuel temperature) for all physical input data (i.e. the heat transfer coefficient, thermal conductivities, etc.). A typical uncertainty analysis for peak clad and peak fuel temperature was also performed using uncertainty information about the physical data. Conclusions are drawn about the applicability of this approach to more general problems and the procedures for its implementation in conjunction with large safety or thermal-hydraulics codes are outlined. The method is also compared with currently used response surface techniques.

I. Introduction

Thermal-hydraulics calculations play an essential role in the design and safety analysis of nuclear reactor systems. The importance of these calculations has led to the development of a variety of large computer code systems which model heat, momentum, and mass transfer problems in great detail (e.g. the RELAP4[1] code for LWR design work and the SAS3A[2] and MELT-III[3] codes for fast reactor safety studies). Although these codes readily provide solutions to difficult design problems, the large number of physical effects they treat and their high running costs make them ill-suited to applications of a parametric or survey nature. It is precisely this latter capability, however, that is needed to answer the typical sensitivity questions which arise frequently in all design and

safety studies. Such difficult tasks as assessing confidence levels and uncertainties in calculated design parameters and determining the effect of changes in engineering data on the results of lengthy calculations are typical of the results required from any sensitivity analysis. To address these problems for a complex reactor system, it is essential to have available a sensitivity methodology that works within the existing design framework which relies so heavily on large computer code systems.

Currently, most successful deterministic solutions to the sensitivity problem are based in one form or another on response surface methods.[4] In this approach, a small subset of the data field needed as input for a large computer run is first chosen for study. Specific changes to be made in these data to address sensitivity questions are then derived from a variety of experimental design theories.[5-7] A number of additional calculations are then made using these altered data sets to estimate the changes which occur in the calculated response of interest. These calculated results are then used to construct the response surface (i.e. the behavior of the response as a function of input data) which is fit with a simple functional form for later use.

With any of the experimental design theories, a large number of additional calculations are in general required to map the response surface for even a small data field (typically, 50 runs are needed to study the effects of changes in seven input data variables). To limit computer costs for these studies so that they are not excessive, fast-running versions of the large design codes are usually used (e.g. SACO[8] was developed for SAS3A studies and a 12-volume version of RELAP4[9] is available for LWR sensitivity studies). Despite the sophisticated theories used and the extensive code development effort which has been undertaken, current sensitivity methods: (a) are still limited in scope by the choices which must be made beforehand, (b) require a great many time consuming calculations and (c) still rely on approximate methods for calculating sensitivities whose accuracy may be questionable if the changes in the data produce changes in the response which are either too large or too small.

To remedy the situation just outlined, this report explores the possibility of applying the differential sensitivity theory developed for radiation transport problems[10] to the larger set of equations governing the thermal-hydraulics behavior of a reactor. This theory has the advantage of (a) being global in nature, in that the sensitivity to all data used in a calculation can be studied without a priori choices being made and (b) being fast and efficient, since only one additional set of equations needs to be solved for each response studied. The only major shortcoming of this theory is that to be really efficient it must be restricted to finding the linear behavior of the response surface in the vicinity of a specific calculated design point. This drawback can be overcome in many cases by using high order interpolation schemes which combine the results of several design point calculations. In practice this is not a serious problem and the theory has been successfully applied in many fields of engineering and physics.[11-22] With all the experience that has been acquired using this theory the advantages of the approach seem to far

outweigh the disadvantages even for problems which are inherently non-linear in nature.

The purpose of this paper is to outline the development of a sensitivity theory for a general, yet tractable, problem in reactor core thermal-hydraulics and indicate how the theory can be used with existing codes for more applications-oriented research. In Section II this general theory is developed for a transient reactor thermal-hydraulics problem. The connection with the theory for steady-state problems is made in Section III. A general discussion of the results of a sample steady-state problem are discussed in Section IV and conclusions about the general applicability of the method are drawn in Section V.

II. Theory for a General Transient Problem

Consider the problem of heat transfer and fluid flow in a representative fuel-coolant channel of a nuclear reactor core. Figure 1 represents the cylindrically symmetric configuration of a typical reactor fuel rod (which includes the fuel pin, gap, and cladding) surrounded by a coolant which removes the fission heat generated in the fuel pin. If we consider a problem with negligible axial heat flow in the fuel and radially averaged fluid properties in the coolant channel (i.e. the use of bulk fluid properties), the following set of coupled non-linear differential equations can be used to represent the transient heat and mass balance in the system.

In the fuel rod, the radial heat conduction equation is:

$$\rho\frac{\partial H}{\partial t} + \frac{1}{r}\frac{\partial}{\partial r}[rq] = Q \tag{1}$$

where

$$q \equiv -k\frac{\partial T}{\partial r} \tag{2}$$

and ρ is the density in gm/cm^3; $H = \int_0^T c_p dT$ is the enthalpy in joules/gm; k is the thermal conductivity in watts/cm^2(°C/cm); $T(r,z,t)$ is the fuel temperature as a function of space and time in °C; $Q(r,z,t)$ is the nuclear heat source in watts/cm^3; $q(r,z,t)$ is the heat flux in watts/cm^2; $0 \le r \le R$; $0 \le z \le L$; and $0 \le t \le t_f$.

The boundary and initial conditions for the fuel region are:

$$T(r,z,0) = \tilde{T}(r,z) \tag{3}$$

$$q(0,z,t) = -k\frac{\partial T}{\partial r}\bigg|_{r=0} = 0 \tag{4}$$

$$q(R,z,t) = -k\frac{\partial T}{\partial r}\bigg|_{r=R} = h[T(R,z,t)-T_c(z,t)] \tag{5}$$

where $\tilde{T}(r,z)$ is the steady-state temperature profile in the fuel in °C; $T_c(z,t)$ is the bulk coolant temperature at axial position z and time t; h is the heat transfer coefficient in the coolant in watts/cm^2 °C; $0 \leq z \leq L$; and $0 \leq t \leq t_f$.

In the coolant channel, the axial heat convection equation is:

$$\frac{\partial}{\partial t}[A\rho_c c_{pc} T_c] + \frac{\partial}{\partial z}[w c_{pc} T_c] = 2\pi R q(R,z,t) \tag{6}$$

where, $A = \pi(R_{max}^2 - R^2)$ is the area of the coolant channel in cm^2; ρ_c is the coolant density in gm/cm^3; $w \equiv A\rho_c V_z$ is the coolant mass flow rate in gm/sec; c_{pc} is the coolant heat capacity in joules/gm °C; $T_c(z,t)$ is the coolant temperature in °C as a function of axial position z and time t; $q(R,z,t) = h[T(R,z,t)-T_c(z,t)]$ is the heat flux into the coolant from the fuel rod wall in watts/cm^2; and h is the heat transfer coefficient of the coolant in watts/cm^2 °C. The boundary and initial conditions in the coolant channel are:

$$T_c(z,0) = \tilde{T}_c(z) \tag{7}$$

$$T_c(0,t) = T_i(t) \tag{8}$$

where $\tilde{T}_c(z)$ is the steady-state axial temperature profile in the coolant and $T_i(t)$ is the inlet coolant temperature.

For sensitivity purposes, the quantity of interest resulting from the solution of the above equations is called a system response. For this case it is convenient to define this response as an integral averaged temperature.

$$P \equiv \iiint_{rzt} 2\pi r\, f(r,z,t)T(r,z,t)drdzdt + \iint_{zt} g(z,t)T_c(z,t)dzdt \tag{9}$$

where f and g are arbitrary weighting functions. They can be Heaviside or Dirac delta functions if needed to define useful results such as peak clad or peak fuel temperature and outlet coolant temperature.

The general problem in sensitivity analysis is to evaluate the rate of change of P with respect to changes in any element, α, of the data

field used in Eqs. (1) and (6) to calculate P. That is, we want to know $dP/d\alpha$, the derivative of P with respect to α. For the sake of generality it is assumed that all the data are functionally dependent on α and either the coolant or fuel temperatures. That is, we assume the following forms for the input data: $c_p(T,\alpha)$, $c_{pc}(T_c,\alpha)$, $k(T,\alpha)$, $h(T_c,\alpha)$, $\rho(T,\alpha)$, $A\rho_c(T_c,\alpha)$, $w(T_c,\alpha)$, and $T_i(\alpha)$. Differentiating Eq. (9) with respect to α we find that the sensitivity derivative $dP/d\alpha$ is:

$$\frac{dP}{d\alpha} = \frac{\partial P}{\partial \alpha} + \iiint_{rzt} 2\pi r f \frac{dT}{d\alpha}\, drdzdt + \iint_{zt} g\, \frac{dT_c}{d\alpha}\, dzdt \tag{10}$$

where, $\partial P/\partial\alpha$, the "direct effect" term representing the explicit dependence of P on α is:

$$\frac{\partial P}{\partial \alpha} \equiv \iiint_{rzt} 2\pi r\, \frac{\partial f}{\partial \alpha}\, T\, drdzdt + \iint_{zt} \frac{\partial g}{\partial \alpha}\, T_c dzdt \tag{11}$$

and the remaining two integral terms in Eq. (10) are the "indirect effect" terms representing the implicit dependence of P on α through the temperatures which solves Eqs. (1) and (6).

In order to evaluate Eq. (10), the behavior of $dT/d\alpha$ as a function of r,z, and t and the behavior of $dT_c/d\alpha$ as a function of z and t must be known. Both of these functions obey partial differential equations similar to Eqs. (1) and (6) and they are functions of the quantity, $d\alpha$ whose sensitivity is being studied. These equations will be developed in the next few paragraphs but only as a preliminary step in the development of the terms in Eq. (10). This adjoint approach is the basic strength of sensitivity theory since it avoids the necessity of having to solve equations for $dT/d\alpha$ and $dT_c/d\alpha$ which depend explicitly on $d\alpha$ (as will be seen later, the adjoint equations are independent of $d\alpha$). Such an approach is essential if a large number of input parameters are to be studied (i.e. if α can take on many different definitions). It would become prohibitively expensive to keep resolving the basic partial differential equations for $dT/d\alpha$ and $dT_c/d\alpha$ over and over again to answer all the sensitivity questions which could arise.

As a step toward the development of the appropriate adjoint equations, the equations which $dT/d\alpha$ and $dT_c/d\alpha$ obey must first be derived. This is done easily by differentiating Eqs. (1) and (6) with respect to α about $\alpha=\alpha_o$ which represents a specific solution point in the response space. In performing this operation care must be taken to note those terms in the equation which are non-linear in nature. For such terms, functional derivatives[10] must be used and it should be understood that this procedure is implied in the notational shorthand which follows.

Letting $\phi \equiv dT/d\alpha$ and $\chi \equiv dT_c/d\alpha$, Eq. (1) can then be differentiated with respect to α, to get:

$$\rho c_p \frac{\partial \phi}{\partial t} + \left[\frac{\partial(\rho c_p)}{\partial \alpha} + \frac{\partial(\rho c_p)}{\partial T}\phi\right]\frac{\partial T}{\partial t} - \frac{1}{r}\frac{\partial}{\partial r}\left[rk\frac{\partial \phi}{\partial r} + r\frac{\partial k}{\partial \alpha}\frac{\partial T}{\partial r} + r\frac{\partial k}{\partial T}\phi\frac{\partial T}{\partial r}\right] = \frac{\partial Q}{\partial \alpha} \tag{12}$$

with initial and boundary conditions:

$$\phi(r,z,0) \equiv \frac{\partial \tilde{T}(r,z)}{\partial \alpha} \tag{13}$$

$$\left(\frac{\partial k}{\partial \alpha} + \frac{\partial k}{\partial T}\phi\right)\frac{\partial T}{\partial r} + k\frac{\partial \phi}{\partial r}\bigg|_{r=0} = 0 \tag{14}$$

$$\left[\left(\frac{\partial k}{\partial \alpha} + \frac{\partial k}{\partial T}\phi\right)\frac{\partial T}{\partial r} + k\frac{\partial \phi}{\partial r}\right]_{r=R} = -\left(\frac{\partial h}{\partial \alpha} + \frac{\partial h}{\partial T_c}\chi\right)(T-T_c) - h(\phi-\chi)\bigg|_{r=R} \tag{15}$$

Similarly, differentiating Eq. (6) with respect to α gives:

$$\frac{\partial}{\partial t}[A\rho_c c_{pc}\chi] + \frac{\partial}{\partial t}\left[\left(\frac{\partial(A\rho_c c_{pc})}{\partial \alpha} + \frac{\partial(A\rho_c c_{pc})}{\partial T_c}\chi\right)T_c\right] + \frac{\partial}{\partial z}[wc_{pc}\chi] + \frac{\partial}{\partial z}\left[\left(\frac{\partial(wc_{pc})}{\partial \alpha} + \frac{\partial(wc_{pc})}{\partial T_c}\chi\right)T_c\right] = 2\pi R\left[\left(\frac{\partial h}{\partial \alpha} + \frac{\partial h}{\partial T_c}\chi\right)(T-T_c) + h(\phi-\chi)\right]\bigg|_{r=R} \tag{16}$$

with initial and boundary conditions:

$$\chi(z,0) = \frac{\partial \tilde{T}_c(z)}{\partial \alpha} \tag{17}$$

$$\chi(0,t) = \frac{\partial T_i(t)}{\partial \alpha} \tag{18}$$

In order to simplify the notation, the following new functions are defined:

$$S_\phi\ (r,z,t) \equiv \frac{\partial Q}{\partial \alpha} - \frac{\partial(\rho c_p)}{\partial \alpha}\frac{\partial T}{\partial t} + \frac{1}{r}\frac{\partial}{\partial r}\left[r\ \frac{\partial k}{\partial \alpha}\frac{\partial T}{\partial r}\right] \tag{19}$$

$$S_\chi\ (z,t) \equiv 2\pi R\ \frac{\partial h}{\partial \alpha}\ (T-T_c) - \frac{\partial}{\partial t}\left[\frac{\partial(A\rho_c c_{pc})}{\partial \alpha}\ T_c\right] - \frac{\partial}{\partial z}\left[\frac{\partial(wc_{pc})}{\partial \alpha}\ T_c\right] \tag{20}$$

$$h' \equiv h - (T-T_c)\ \frac{\partial h}{\partial T_c}\Bigg|_{r=R} \tag{21}$$

$$(\rho_c c_{pc})' \equiv \rho_c c_{pc} + T_c \frac{\partial(\rho_c c_{pc})}{\partial T_c} \tag{22}$$

$$(wc_{pc})' \equiv wc_{pc} + T_c\ \frac{\partial(wc_{pc})}{\partial T_c} \tag{23}$$

$$a \equiv -\frac{\partial k}{\partial \alpha}\frac{\partial T}{\partial r} - \frac{\partial h}{\partial \alpha}\ (T-T_c)\Bigg|_{r=R} \tag{24}$$

Using these new functions, the Eq. (12) for the fuel region can be rewritten simply as:

$$\frac{\partial}{\partial t}\left[\rho c_p \phi\right] - \frac{1}{r}\frac{\partial}{\partial r}\left[r\ \frac{\partial(k\phi)}{\partial r}\right] = S_\phi \tag{25}$$

with boundary and initial conditions,

$$\phi(r,z,0) = \frac{\partial \tilde{T}(r,z)}{\partial \alpha} \tag{26}$$

$$\frac{\partial(k\phi)}{\partial r}\Bigg|_{r=0} = 0 \tag{27}$$

$$\frac{\partial(k\phi)}{\partial r} + h\phi\Bigg|_{r=R} = h'\chi + a \tag{28}$$

Here the central boundary condition on T (i.e., Eq. (4)) was used to get Eq. (27) and because of the local temperature dependence of k(T) and $\rho c_p(T)$ it was possible to write:

$$\frac{\partial k}{\partial T}\,\phi\,\frac{\partial T}{\partial r} + k\,\frac{\partial \phi}{\partial r} = \frac{\partial (k\phi)}{\partial r} \tag{29}$$

$$\rho c_p\,\frac{\partial \phi}{\partial t} + \frac{\partial (\rho c_p)}{\partial T}\,\frac{\partial T}{\partial t}\,\phi = \frac{\partial}{\partial t}\left[\rho c_p \phi\right] \tag{30}$$

Similar simplifications can be made in Eq. (16) to get:

$$\frac{\partial}{\partial t}\,[A(\rho_c c_{pc})'\chi] + \frac{\partial}{\partial z}\,[(wc_{pc})'\chi] = 2\pi R\,(h\phi - h'\chi) + S_\chi \tag{31}$$

with boundary and initial conditions,

$$\chi(z,0) = \frac{\partial \tilde{T}_c(z)}{\partial \alpha} \tag{32}$$

$$\chi(0,t) = \frac{\partial T_i(t)}{\partial \alpha} \tag{33}$$

Eqs. (25) and (31) now represent linearized versions of the original heat conduction and convection equations (i.e., Eqs. (1) and (6)), henceforth referred to as the "forward" equations). It should be noted that they are no longer nonlinear equations since all the physical constants are functions of the temperatures T and T_c and are not functions of ϕ and χ. In order to solve such equations (which will not be necessary for this theory but might be for other applications), the forward equations must be solved for a specific problem to determine the functional dependence on T and T_c of the constants in the linearized equations. These latter equations are therefore coupled to the forward equations in that the former must be solved first to set up the constants for the latter case.

Since the linearized equations only have source terms that depend on $d\alpha$ and their solution is really needed only to evaluate the integral terms in Eq. (10), it is far simpler to define a set of adjoint equations independent of $d\alpha$ to solve this same problem. The adjoint operators for Eqs. (25) and (31) are easily derived and what remains to be done in the derivation is to identify appropriate source terms and boundary and initial conditions for these new equations.

Using the definition of an adjoint operator,

$$\int_V pHq\,dV = \int_V qH^* p\,dV \tag{34}$$

where p and q are arbitrary functions and H^* is the adjoint operator of H, we can write down equations which are adjoint to Eqs. (25) and (31) after some manipulations as:

$$-\rho c_p \frac{\partial T^*}{\partial t} - k \frac{1}{r}\frac{\partial}{\partial r}\left[r \frac{\partial T^*}{\partial r}\right] = S_T^* \tag{35}$$

and

$$-A(\rho_c c_{pc})' \frac{\partial T_c^*}{\partial t} - (wc_{pc})' \frac{\partial T_c^*}{\partial z} + 2\pi R h' T_c^* = S_{Tc}^* \tag{36}$$

The equation needed to define the source terms and boundary and initial conditions for these equations is derived as follows: (a) multiply Eq. (25) by T^* and Eq. (35) by ϕ, subtract the two and integrate over r,z, and t; (b) multiply Eq. (31) by T_c^* and Eq. (36) by χ, subtract the two and integrate over z and t; (c) add the two equations derived in (a) and (b) together. The following equation results from these operations:

$$\begin{aligned}
&\iiint_{r\,z\,t} \phi S_T^* \, 2\pi r dr dz dt + \iint_{z\,t} \chi S_{Tc}^* \, dz dt = \iiint_{r\,z\,t} T^* S_\phi \, 2\pi r dr dz dt + \iint_{z\,t} T_c^* \, S_\chi \, dz dt \\
&+ \iint_{z\,t} 2\pi R \left[T^* \frac{\partial(k\phi)}{\partial r} - k\phi \frac{\partial T^*}{\partial r}\right]_0^R dz dt + \iint_{z\,t} 2\pi R T_c^* h\phi \, dz dt \\
&- \iint_{r\,z} \left[\rho c_p \, \phi T^*\right]_0^{t_f} 2\pi r dr dz - \int_t \left[(wc_{pc})' \chi T_c^*\right]_0^L dt - \int_z \left[A(\rho_c c_{pc})' \chi T_c^*\right]_0^{t_f} dz
\end{aligned} \tag{37}$$

where all the integrals were evaluated where possible (using integration by parts when necessary).

Since an adjoint equation which is independent of $d\alpha$ is desired, boundary and <u>final</u> conditions as well as sources must be chosen to eliminate any terms which contain unknown values of ϕ or χ. Using the known boundary

and initial conditions for ϕ and χ, the following conditions can be shown to satisfy the desired criteria:

$$T_c^*(z,t_f) = 0 \tag{38}$$

$$T_c^*(L,t) = 0 \tag{39}$$

$$T^*(r,z,t_f) = 0 \tag{40}$$

$$- k \left.\frac{\partial T^*}{\partial r}\right|_{r=0} = 0 \tag{41}$$

$$- k \left.\frac{\partial T^*}{\partial r}\right|_{r=R} = h(T^*-T_c^*) \tag{42}$$

Collecting terms and rewriting Eq. (39) with these new conditions gives:

$$\begin{aligned}
&\int_r\int_z\int_t \phi S_T^* \, 2\pi r dr dz dt + \int_z\int_t \chi(S_{Tc}^* - 2\pi R h' T^*) dz dt = \int_r\int_z\int_t T^* S_\phi 2\pi r dr dz dt + \int_z\int_t T_c^* S_\chi dz dt \\
&+ \int_z\int_t [2\pi r T^* a]_{r=R} \, dz dt + \int_r\int_z \left[\rho c_p \; T^* \frac{\partial \tilde{T}(r,z)}{\partial \alpha} \right]_{t=0} 2\pi r dr dz \\
&+ \int_t \left[(wc_{pc})' T_c^* \frac{\partial T_i(t)}{\partial \alpha} \right]_{z=0} dt + \int_z \left[A(\rho_c c_{pc})' \; T_c^* \frac{\partial \tilde{T}_c(z)}{\partial \alpha} \right]_{t=0} dz
\end{aligned} \tag{43}$$

Since everything on the right-hand side of Eq. (43) is known from solutions of the forward or adjoint equation, all that remains is to properly choose the source terms S_T^* and S_{Tc}^*. Looking back at Eq. (10), it is clear that the left-hand side of Eq. (43) can be made equivalent

to the two integrals in Eq. (10) (remembering that $\phi \equiv dT/d\alpha$ and $\chi \equiv dT_c/d\alpha$) if the sources for the adjoint equation are chosen as follows:

$$S_T^* = f \tag{44}$$

$$S_{Tc}^* = g + 2\pi R h' T^* \tag{45}$$

With these final definitions, Eq. (10) can be recast in terms of adjoint functions with each term an explicit function of α as:

$$\begin{aligned}
\frac{dP}{d\alpha} = & \iiint_{r\,z\,t} \frac{\partial f}{\partial \alpha} T\, 2\pi r dr dz dt + \iint_{z\,t} \frac{\partial g}{\partial \alpha} T_c\, dz dt \\
& + \iiint_{r\,z\,t} T^* \left[\frac{\partial Q}{\partial \alpha} - \frac{\partial(\rho c_p)}{\partial \alpha} \frac{\partial T}{\partial t} + \frac{1}{r}\frac{\partial}{\partial r}\left[r \frac{\partial k}{\partial \alpha}\frac{\partial T}{\partial r}\right]\right] 2\pi r dr dz dt \\
& - \iint_{z\,t} T_c^* \left[\frac{\partial}{\partial t}\left[\frac{\partial(A\rho_c c_{pc})}{\partial \alpha} T_c\right] + \frac{\partial}{\partial z}\left[\frac{\partial(wc_{pc})}{\partial \alpha} T_c\right]\right] dz dt \\
& - \iint_{z\,t} 2\pi R \left[\frac{\partial h}{\partial \alpha}(T-T_c)(T^*-T_c^*) + T^* \frac{\partial k}{\partial \alpha}\frac{\partial T}{\partial r}\right]_{r=R} dz dt \\
& + \int_t \left[(wc_{pc})' T_c^* \frac{\partial T_i(t)}{\partial \alpha}\right]_{z=0} dt \\
& + \iint_{r\,z} \left[\rho c_p\, T^* \frac{\partial \tilde{T}(r,z)}{\partial \alpha}\right]_{t=0} 2\pi r dr dz + \int_z \left[A(\rho_c c_{pc})' T_c^* \frac{\partial \tilde{T}_c(z)}{\partial \alpha}\right]_{t=0} dz
\end{aligned} \tag{46}$$

The terms involving T and T_c can be evaluated once the forward equations (i.e., Eqs. (1) and (6)) have been solved and the adjoint functions T^* and T_c^* solve the following set of equations:

(a) in the fuel region,

$$-\rho c_p \frac{\partial T^*}{\partial t} - k \frac{1}{r}\frac{\partial}{\partial r}\left[r \frac{\partial T^*}{\partial r}\right] = f \tag{47}$$

with boundary and <u>final</u> conditions,

$$T^*(r,z,t_f) = 0 \tag{48}$$

$$- k \left.\frac{\partial T^*}{\partial r}\right|_{r=0} = 0 \tag{49}$$

$$- k \left.\frac{\partial T^*}{\partial r}\right|_{r=R} = h(T^*-T_c^*) \tag{50}$$

(b) in the coolant channel,

$$-A(\rho_c c_{pc})' \frac{\partial T_c^*}{\partial t} - (wc_{pc})' \frac{\partial T_c^*}{\partial z} = 2\pi Rh' (T^*-T_c^*) + g \tag{51}$$

with boundary and <u>final</u> conditions,

$$T_c^*(z,t_f) = 0 \tag{52}$$

$$T_c^*(L,t) = 0 \tag{53}$$

With this derivation of the adjoint equations completed, the general features of a sensitivity theory for thermal-hydraulics problems begin to become more evident. A single forward and a single adjoint problem solution is all that is needed to evaluate all the derivatives of the response with respect to input data. The adjoint equations required are independent of $d\alpha$ and $d\alpha$ appears explicitly only in the defining expression for $dP/d\alpha$ (i.e., Eq. (46)). The adjoint equations, however, do depend explicitly on the particular response being studied through the source terms in Eqs. (47) and (51).

It is important to also note that the adjoint equations are linear in T^* and T_c^* making them easier to solve than the nonlinear forward equations. They are not, however, independent of the forward equations. In order to

solve the adjoint problem a particular forward problem solution (called a design point solution) must be available to evaluate the physical constants that go into the adjoint equations. This dependence of the constants on T and T_c is a double-edged sword--it linearizes the adjoint equations but also ties the solution of the adjoint equations to a specific design point solution.

Another important point to observe is that the forward and adjoint equations are very similar in form. Both have differential operators which are very much alike and the canonical form of the equations (i.e., hyperbolic, parabolic, etc.) remains unchanged. The adjoint equations are simply linearized forward equations reversed in time and space with slightly different input data. The same numerical methods (and possibly the same codes) that solve the forward problem can be used to solve its adjoint. This observation strongly suggests that the method will be applicable for more practical problems.

Looking more closely at the nature of the adjoint equations it is also interesting to note that they are final value problems. That is, the adjoint functions are solved by starting at a final time at the spatial position of the response function and moving backwards toward the initial conditions. This fact leads directly to an interpretation of the adjoint solutions as "importance" functions. The adjoint equation solutions starts at the response and traces this value back into the problem phase space along paths which include only those physical phenomena which contribute to the response. The adjoints therefore determine the importance of the physical phenomena for the particular response under investigation. The units of these functions are °C per joule for a temperature response defined in terms of weighting functions f and g which are density functions per unit volume and time. In numerical terms they represent the change in °C of the temperature response for one joule of heat put into any differential element in phase space. They are very physical quantities and can clearly be studied in their own right to understand the complex phenomena occurring in any particular thermal-hydraulics problem.

III. Theory for a Steady-State Problem

One further development is needed before this illustrative example of a sensitivity theory for thermal-hydraulics problems can be said to be complete. The item remaining deals with the sensitivity terms in Eq. (46) containing the initial conditions for this problem. Typically, the initial conditions are derived from the solution of a suitable steady-state problem. The steady-state solution describes the stable conditions which existed in the reactor system prior to the initiation of any transient event. Insofar as this steady-state problem is the solution to Eqs. (1) and (6) without time derivatives, it also depends on the same input data as the transient problem (i.e., k, c_{pc}, w, etc.). To derive expressions for these additional sensitivity terms, one further general aspect of sensitivity theory must first be dealt with--the extension of the theory to cover sensitivity coefficients which require solutions of other sets of equations.

To see clearly how the theory is extended, the last two terms in Eq. (46) (i.e., those dealing with the derivatives of the initial conditions) can be viewed as the derivative of a new integral response functions P', defined as follows:

$$\frac{dP'}{d\alpha} \equiv \iint_{r\,z} \left[\rho c_p \quad T^* \frac{\partial \tilde{T}(r,z)}{\partial \alpha} \right]_{t=0} 2\pi r dr dz + \int_z \left[A(\rho_c c_{pc})' T_c^* \frac{\partial \tilde{T}_c(z)}{\partial \alpha} \right]_{t=0} dz \tag{54}$$

Here $\tilde{T}(r,z)$ and $\tilde{T}_c(z)$ are the solutions of steady-state forward problems which can be derived from Eqs. (1) and (6) by ignoring the time derivatives.

In the fuel region, the steady-state equation to be solved is:

$$\frac{1}{r} \frac{\partial (r\tilde{q})}{\partial r} = \tilde{Q} \tag{55}$$

where

$$\tilde{q}(r,z) \equiv - \tilde{k} \frac{\partial \tilde{T}(r,z)}{\partial r} \tag{56}$$

and

$$\tilde{q}(0,z) = - \tilde{k} \frac{\partial \tilde{T}(r,z)}{\partial r} \bigg|_{r=0} = 0 \tag{57}$$

$$\tilde{q}(R,z) = - \tilde{k} \frac{\partial \tilde{T}(r,z)}{\partial r} \bigg|_{r=R} = \tilde{h}(\tilde{T}(R,z) - \tilde{T}_c(z)) \tag{58}$$

In the coolant channel, the corresponding equation is:

$$\frac{\partial (\tilde{w}\tilde{H})}{\partial z} = 2\pi R \tilde{q}(R,z) \tag{59}$$

where

$$\tilde{H}(z) = \tilde{c}_{pc} \, \tilde{T}_c(z) \tag{60}$$

and

$$\tilde{T}_c(0) \equiv \tilde{T}_i \tag{61}$$

As before, the derivative of Eqs. (55)-(61) with respect to α is taken to derive the linearized equations which $\partial\tilde{T}/\partial\alpha$ and $\partial\tilde{T}_c/\partial\alpha$ solve. Defining $\tilde{\phi} \equiv \partial\tilde{T}/\partial\alpha$ and $\tilde{\chi} \equiv \partial\tilde{T}_c/\partial\alpha$, these new equations can be written down by inspection if we refer back to the transient problem equations (i.e., Eqs. (25) and (31)) and ignore all time derivative terms.

In the fuel region we therefore get:

$$-\frac{1}{r}\frac{\partial}{\partial r}\left[r\frac{\partial}{\partial r}(\tilde{k}\tilde{\phi})\right] = \tilde{S}_\phi \tag{62}$$

where

$$\left.\frac{\partial(\tilde{k}\tilde{\phi})}{\partial r}\right|_{r=0} = 0 \tag{63}$$

$$\left[\frac{\partial(\tilde{k}\tilde{\phi})}{\partial r} + \tilde{h}\tilde{\phi}\right]_{r=R} = \tilde{h}'\tilde{\chi} + \tilde{a} \tag{64}$$

and

$$\tilde{S}_\phi = \frac{\partial\tilde{Q}}{\partial\alpha} + \frac{1}{r}\frac{\partial}{\partial r}\left[r\frac{\partial\tilde{k}}{\partial\alpha}\frac{\partial\tilde{T}}{\partial r}\right] \tag{65}$$

$$\tilde{h}' = \tilde{h} - (\tilde{T}-\tilde{T}_c)\frac{\partial\tilde{h}}{\partial\tilde{T}_c} \tag{66}$$

$$\tilde{a} = -\frac{\partial\tilde{k}}{\partial\alpha}\frac{\partial\tilde{T}}{\partial r} - \frac{\partial\tilde{h}}{\partial\alpha}(\tilde{T}-\tilde{T}_c) \tag{67}$$

In the coolant we get:

$$\frac{\partial}{\partial z}\left[(\tilde{w}c_{pc})'\tilde{\chi}\right] = 2\pi R(\tilde{h}\tilde{\phi} - \tilde{h}'\tilde{\chi}) + \tilde{S}_\chi \tag{68}$$

where

$$\tilde{X}(0) = \frac{\partial \tilde{T}_i}{\partial \alpha} \tag{69}$$

and

$$(\widetilde{wc}_{pc})' \equiv \tilde{w}\tilde{c}_{pc} + \tilde{T}_c \frac{\partial(\tilde{w}\tilde{c}_{pc})}{\partial \tilde{T}_c} \tag{70}$$

Again, by analogy with the transient problem, the integral response function derivative $dP'/d\alpha$ given by Eq. (54) is best evaluated using adjoint functions for the steady-state problem. Looking at the transient adjoint results given in Eqs. (46)-(53), a steady-state expression can be derived by ignoring time derivatives and integrals as:

$$\begin{aligned}
\frac{dP'}{d\alpha} = & \iint_{r\,z} \tilde{T}^* \left[\frac{\partial \tilde{Q}}{\partial \alpha} + \frac{1}{r}\frac{\partial}{\partial r}\left[r \frac{\partial \tilde{k}}{\partial \alpha}\frac{\partial \tilde{T}}{\partial r}\right]\right] 2\pi r dr dz \\
& - \int_z \tilde{T}_c^* \frac{\partial}{\partial z}\left[\frac{\partial(\tilde{w}\tilde{c}_{pc})}{\partial \alpha}\tilde{T}_c\right] dz \\
& - \int_z 2\pi R \left[\frac{\partial \tilde{h}}{\partial \alpha}(\tilde{T}-\tilde{T}_c)(\tilde{T}^*-\tilde{T}_c^*) + \tilde{T}^* \frac{\partial \tilde{k}}{\partial \alpha}\frac{\partial \tilde{T}}{\partial r}\right]_{r=R} dz \\
& + \left[(\widetilde{wc}_{pc})' \tilde{T}_c^* \frac{\partial \tilde{T}_i}{\partial \alpha}\right]_{z=0}
\end{aligned} \tag{71}$$

The source terms for the steady-state case can be obtained by comparing Eqs. (10) and (54) thereby properly defining f and g for this case. The steady-state adjoint equation in the fuel region is then:

$$-\tilde{k}\frac{1}{r}\frac{\partial}{\partial r}\left[r\frac{\partial \tilde{T}^*}{\partial r}\right] = [\rho c_p \quad T^*(r,z,t)]_{t=0} \tag{72}$$

where

$$- \tilde{k} \left. \frac{\partial \tilde{T}^*}{\partial r} \right|_{r=0} = 0 \tag{73}$$

$$- \tilde{k} \left. \frac{\partial \tilde{T}^*}{\partial r} \right|_{r=R} = \tilde{h} \, (\tilde{T}^* - \tilde{T}_c^*) \tag{74}$$

In the coolant channel we likewise have:

$$- (\tilde{w} c_{pc})' \frac{\partial \tilde{T}_c^*}{\partial z} = 2\pi R \tilde{h}' \, (\tilde{T}^* - \tilde{T}_c^*) + [A(\rho_c c_{pc})' T_c^*(z,t)]_{t=0} \tag{75}$$

where

$$\tilde{T}_c^*(L) = 0 \tag{76}$$

The final expression for $dP'/d\alpha$ (i.e., Eq. (71)) can now be used to replace the last two terms in Eq. (46). Because the procedure for solving the transient problem in this case also involves the solution of a steady-state problem, the sensitivity coefficients for most of the input parameters have two terms: one describing the effects of changes in α on the steady-state solution (i.e., the initial conditions for the transient) and a second describing the effect of these changes on the transient solution.

It is interesting to note that the procedures for solving the adjoint equations are now completely the opposite of those which would be used in a forward problem. The adjoint problem solution is started at a final time, with the response function as the source and the transient equations are solved first moving backwards in time. When the initial time is reached the transient solution is used in Eqs. (72) and (75) as the source for a steady-state problem which is solved next. This reversal of procedures is typical of all adjoint problems and is consistent with the physical interpretation of the adjoint solutions as "importance" functions for a particular final response.

The method just used to develop adjoint equations for the terms in $dP/d\alpha$ derived from the solution of a steady-state problem is also the general approach needed to expand any of the derivative terms in Eqs. (46) and (71). For instance, the heat transfer coefficient is generally a complicated function of temperature and flow conditions in the coolant stream and is described by empirical correlations. In many cases, these correlations require the solutions to momentum balance equations (or simplified approximations of them) to understand the velocity profiles in the coolant channel.

These auxiliary equations can also be cast in adjoint form and coupled with the main heat balance adjoint equations if sensitivity questions concerning the heat transfer coefficient correlation functions are to be answered.

IV. Solution of a Sample Sensitivity Problem

To make the results of the derivations in the preceding sections more understandable in a practical sense, a sample steady-state, thermal-hydraulics problem for the Clinch River Breeder Reactor (CRBR) was devised. Although a full transient treatment could have been pursued, it is more instructive to look in depth at the results of the simpler steady-state problem. The sensitivity derivatives for this case (see Eq. (71)) are very similar in form to those for the transient problem (see Eq. (46)) if the time functions are ignored. It is also easier to show the behavior of the complete solution to the adjoint problem and derive a physical feeling for these functions in this more restrictive case.

A description of a typical CRBR fuel pin and coolant channel is given in Table I, along with some initialization data for the steady-state problem. The physical input data for $\tilde{k}$, $\tilde{c}_{pc}$, and $\tilde{h}$ were all taken to be functions of temperature[2] and are given in Fig. 2 and Table II. A small nonlinear, ordinary differential equation solution code was written to solve both the forward and adjoint heat balance equations (Eqs. (55) and (59) and Eqs. (72) and (75), respectively). The source term in the fuel for the forward problem was taken to be a cosine distribution axially and flat radially. For the adjoint equations, however, the sources were not derived from the initial conditions of a transient adjoint equation. The response for the steady-state problem was taken to be of the same form as the general response function given in Eq. (9) with time behavior ignored. Several typical responses such as: coolant outlet temperature, peak clad temperature, and peak and center-line average fuel temperature, were then defined by suitable choices of f(r,z) and g(z) thus providing appropriate adjoint sources.

The results of a run with the typical CRBR data presented are given in Fig. 3. Here the steady-state temperature profile at the center of each radial and axial node is plotted as a function of space in both the fuel and coolant regions. The fuel temperature has the same general cosine shape axially as the nuclear heat source and peaks near the center (both axially and radially) of the pin. The coolant temperature on the other hand increases monotonically in the axial direction as more heat enters from the fuel rod. The clad temperature, therefore, peaks somewhere near the end of the coolant channel.

To investigate the sensitivity of the steady-state CRBR temperature profile to the physical input data used, several figures of merit for the temperature distribution were chosen as responses for study. The two most interesting were: 1) peak fuel temperature, and 2) peak clad temperature. Adjoint equations for each of these responses were solved and the results were used for a complete sensitivity and uncertainty analysis of all the

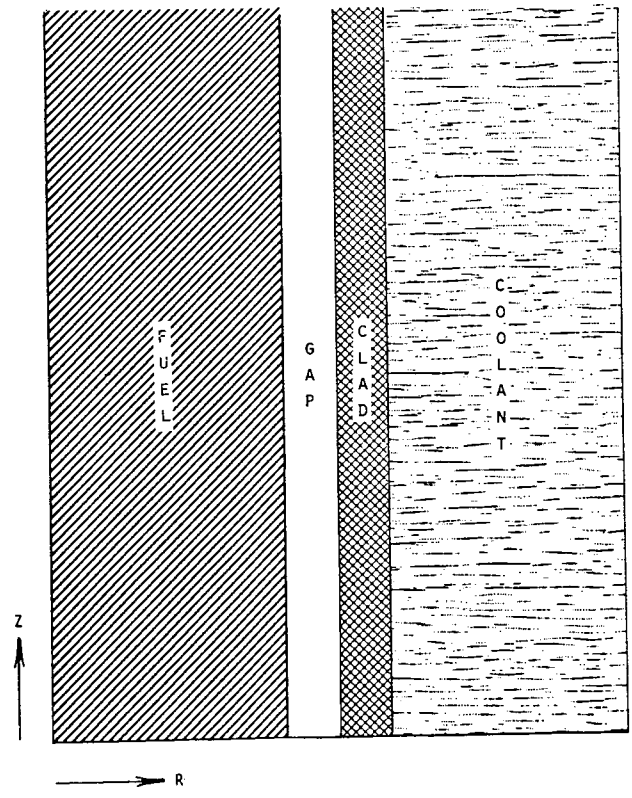

Fig. 1. Typical Geometric Configuration of a Fuel-Coolant Channel.

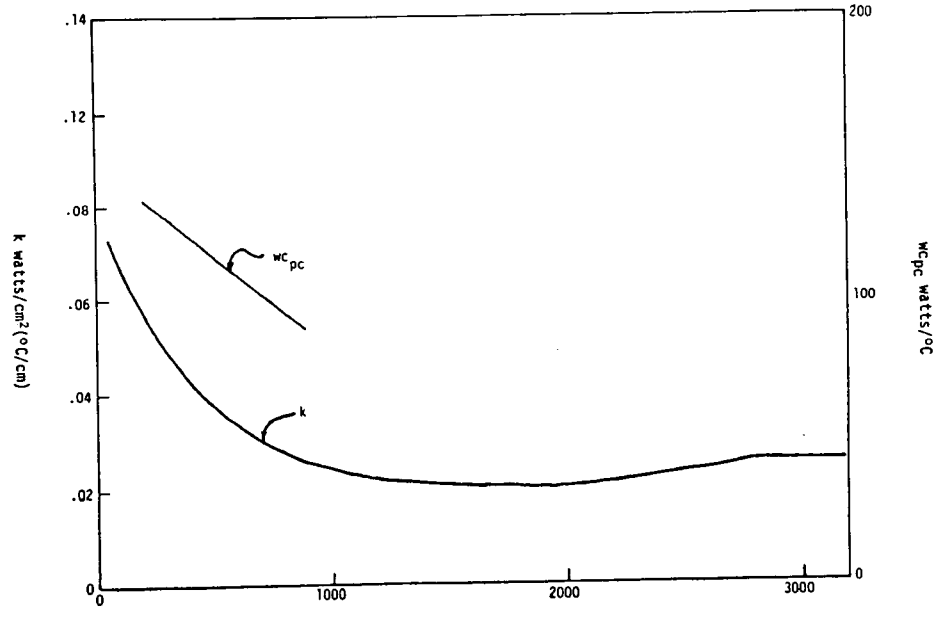

Fig. 2. Physical Data for CRBR Problem as a Function of Temperature.

Table I. CRBR Sample Problem Input Specifications

Fuel Pin (mixed Pu-U oxide) Outer Radius	0.2457 cm
Gap (helium and fission products) Outer Radius	0.254 cm
Clad (stainless steel) Outer Radius (R)	0.2921 cm
Coolant Channel (sodium) Cross Sectional Area (A)	0.359 cm^2
Coolant Channel Length	162.6 cm
Fuel Pin Power ($\tilde{Q}$)	2.427×10^4 watts
Power Distribution	Flat Radially and Cosine Axially
Coolant Flow Rate ($\tilde{w}$)	112 gm/sec
Inlet Coolant Temperature ($\tilde{T}_i$)	388°C

Table II. Physical Data for CRBR Sample Problem

Clad Thermal Conductivity	0.21 watt/cm^2(°C/cm)
Gap Equivalent Thermal Conductivity	0.002 watt/cm^2(°C/cm)

Heat Transfer Coefficient Correlation:

$$\tilde{h} = (7.0 + 0.025\ Pe^{.8})\ \frac{\tilde{k}_c}{D}\ \text{watt/cm}^2\ °\text{C}$$

where

$$Pe = \frac{\tilde{w}\tilde{c}_{pc} D}{\tilde{k}_c A}$$

$$\tilde{k}_c = 0.66\ \text{watt/cm}^2(°\text{C/cm})$$

$$D = 4A/2\pi R$$

physical input data. The behavior of the adjoint functions for these two cases is shown in Figs. 4 and 5. Here the adjoints with units of °C per watt represent the differential change in the temperature response in °C for a differential change in the power source in watts made at the center of each axial or radial node plotted.

Close inspection of these adjoint functions reveals a wealth of physical information about the heat conduction and convection processes in this sample problem. For instance, in the plot of the adjoint for a peak fuel temperature response (see Fig. 4), the "importance" of a differential unit of power put into the system at any axial level is negligible unless it is put at the level where the peak temperature occurs. This effect is primarily the result of the absence of any axial heat conduciton in the fuel. The only way power at axial positions other than the one where the fuel temperature peaks can influence the peak temperature is by radial conduction followed by axial convection in the coolant. This mode of heat transfer produces very small temperature increases in the coolant due to the high mass flow rate and therefore only these very small temperature increases are passed from the coolant to the center of the fuel.

ORNL-DWG 78-3632

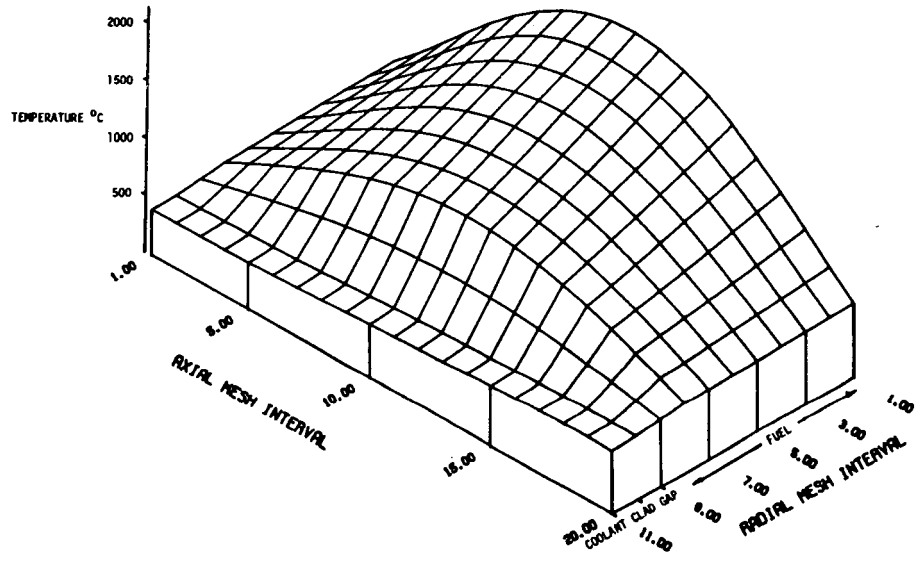

Fig. 3. Steady-State Temperature Profile in CRBR Channel.

ORNL-DWG 78-3633R

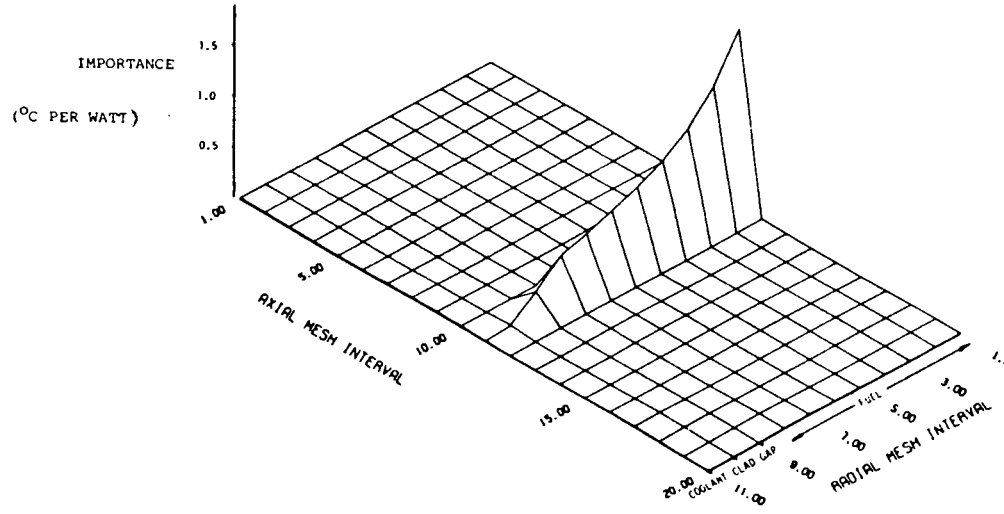

Fig. 4. Adjoint Temperature Profile for Peak Fuel Temperature Response in CRBR Channel.

ORNL-DWG 78-3635R

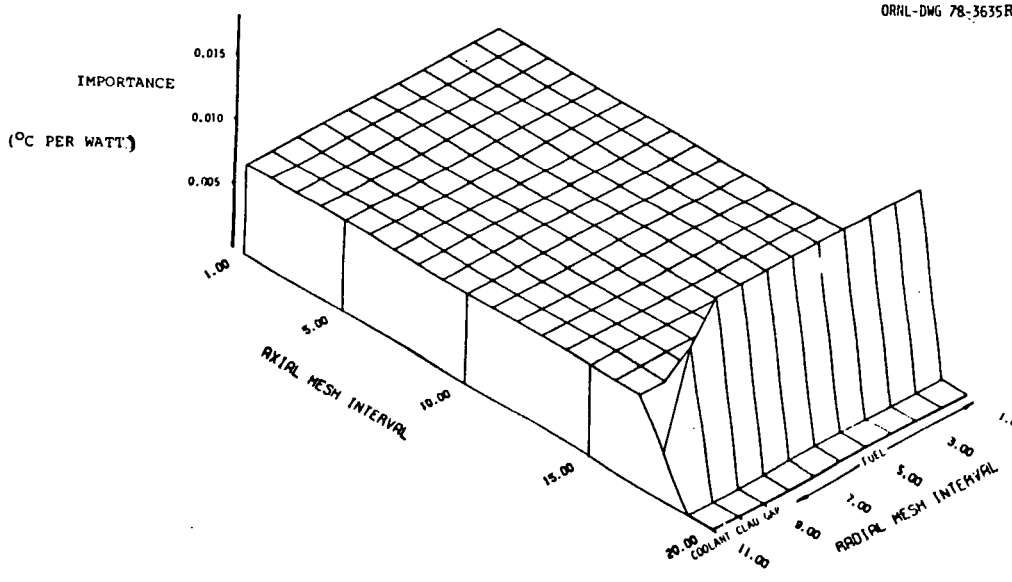

Fig. 5. Adjoint Temperature Profile for Peak Clad Temperature Response in CRBR Channel.

Another example of the usefulness of the adjoint functions is obtained from analysis of Fig. 5. Here the "importance" of a differential unit of power is zero for all axial positions downstream from the peak position (the peak occurs at axial interval 18). Again, because there is no axial conduction in the fuel, any power source downstream from the peak cald temperature can only influence the clad temperature through coolant convection. Since the coolant flows in only one direction, a downstream power source has no influence on the clad or any other region's temperature. These comments also apply to the results given in Fig. 4 although the scale in this figure makes it more difficult to see.

The fact that all upstream differential power sources have equal importance is a result of the fact that at steady-state power put into the fuel will eventually be transferred to the coolant. This power will produce about the same temperature rise in the coolant across an axial mesh interval if wc_{pc} is fairly constant, as it was for this case. The higher importance of a power source at the axial position of the peak clad temperature (i.e., axial interval 18) is due to the fact that both conduction and convection processes in this axial interval can effect the clad temperature as opposed to convection alone at all upstream positions.

It is also interesting to observe that the absolute magnitude of the importance at the peak axial position (about 0.015 °C per watt) for this response is about two orders of magnitude lower than the highest importance value in Fig. 4. This is the result of two effects. First, the peak cald temeprature (561°C) is about a factor of four lower than the peak fuel temperature (1940°C) and second, the number of axial levels that can influence the peak clad temperature is about 20 compared to effectively only one for the peak fuel temperature. This latter condition has the effect of spreading out the total importance and therefore lowering its absolute value at any one axial or radial position.

Continuing on to the next phase of the study, the forward and adjoint solutions were used to evaluate the expression for $dP/d\alpha$ (Eq. (71)) and a full sensitivity analysis was performed for the CRBR problem. A small code was written to perform the integrals needed and several responses of interest were studied. Some of the results obtained are summarized in Table III. It should be noted that the column labeled sensitivity contains the evaluated derivatives $dP/d\alpha$ multiplied by α/P to form a logarithmic derivative $(dP/P)/(d\alpha/\alpha)$ which is commonly referred to as the sensitivity of P to α. In addition, it should be clear that α was used only symbolically in the derivations to represent any of the data that were being studied. The sensitivity results reported for each input parameter were obtained by defining α to be a scale factor for that particular parameter, thereby reducing the expression for $dP/d\alpha$ to only the one or two terms involving that parameter. For instance, the sensitivity of peak fuel temperature to the nuclear heat source, $\tilde{Q}$, would involve defining $\alpha \equiv \tilde{Q}_0$ (a scale factor for the power) in Eq. (71) and setting all terms except the one for $\partial\tilde{Q}/\partial\alpha$ equal to zero. The sensitivities thus obtained are known as "integral sensitivities" and can be thought of as the percent change (positive or negative) in the response for a 1% increase in the scale (i.e. magnitude) of the input parameter. In other

applications, α can be allowed to be a function (i.e. the spatial behavior of $\hat{Q}(r,z)$) and a "sensitivity profile" can be defined as a spatial density function using functional derivative notation.

Looking at the results presented in Table III, it is easy to see how the particular behavior of each of the adjoint functions shown in Figs. 4 and 5 gives rise to the reported sensitivities of each of the individual input parameters. The parameters with the largest sensitivities in absolute magnitude are those which by and large affect the temperature profile in regions of high importance for this problem and those that have small sensitivities only affect unimportant regions. Since the nuclear heat source directly affects the heat balance in the fuel region, both the peak clad and peak fuel temperatures are very sensitive to it. On the other hand, the heat transfer coefficient and clad thermal conductivity have very little effect on these two responses because they have a relatively minor effect on the steady-state temperatures in the fuel rod. In general, a dramatic difference in sensitivity from one case to another (i.e. for fuel and gap conductivity) is a reflection of large differences in the value of the adjoint function.

Table III. Typical Sensitivity Results for CRBR Test Problem

Response	Parameter	Sensitivity*	Parameter** Uncertainty (%)	Response*** Uncertainty (%)
Peak Clad Temperature (561°C)	Coolant Inlet Temperature	.69	10	7.7
	Heat Source	.31	5	
	Coolant wc_{pc}	-.29	10	
	Clad Thermal Conductivity	-.009	20	
	Coolant Heat Transfer Coefficient	-.006	30	
	Fuel and Gap Conductivity	—		
Peak Fuel Temperature (1940°C)	Heat Source	.89	5	14
	Fuel Thermal Conductivity	-.45	15	
	Gap Thermal Conductivity	-.37	30	
	Coolant Inlet Temperature	.23	10	
	Coolant wc_{pc}	-.06	10	
	Coolant Heat Transfer Coefficient	-.005	30	

*Can be interpreted as the per cent change in the response function for a 1% increase in the system parameter.

**Estimated standard deviation for parameter.

***Calculated standard deviation for response assuming no correlations between parameter uncertainties.

For this case, the most dramatic effect present appears to be the sensitivity of both the peak fuel and peak clad temperature responses to the thermal conductivity in the fuel-clad gap region (treated in this case with an equivalent gap conductance). Since there is such a large temperature change across the gap (about 500°C; see Fig. 3), it is not surprising that the peak fuel temperature is very sensitive to the gap

conductivity. Even though the gap is very small, the large temperature drop that occurs crossing it is almost 30% of the change over the whole fuel rod. This results in a gap sensitivity which is close to 30% of the heat source sensitivity for this response. On the other hand, the gap conductivity has little effect at steady-state on the amount of heat getting out of the fuel into the coolant (the total amount generated will always be conducted into the coolant) and therefore has little effect on the peak clad temperature. This response is affected mostly by clad coolant properties or direct changes in the heat source itself.

In addition to their usefulness in the foregoing discussion of relative importance of data and heat transfer mechanisms, sensitivity derivatives can also be used to formulate a first order perturbation theory. This theory is based on establishing an anlaytic relationship between the response and the input data. The simplest form for this relationship is derived from a first order Taylor series expansion of the response about a particular calculated design point, symbolized by the vector of all input data at a particular point $\bar{\alpha}_0$. This relationship, written out to second order accuracy, is:

$$P(\bar{\alpha}_0 + \overline{\delta\alpha}) \cong P(\bar{\alpha}_0) + \int_V \left[\frac{dP}{d\bar{\alpha}(v)}\right]_{\alpha=\alpha_0} \cdot \overline{\delta\alpha}(v)\, dv \qquad (77)$$

where $[dP/d\bar{\alpha}(v)]_{\bar{\alpha}=\bar{\alpha}_0}$ is the vector of derivatives for each separate α of input data field evaluated at $\bar{\alpha} = \bar{\alpha}_0$; $\overline{\delta\alpha}(v)$ is the vector of finite changes in the input data as a function of the problem phase space (i.e. space and time); $P(\bar{\alpha}_0)$ is the response evaluated at $\bar{\alpha}_0$; and $P(\bar{\alpha}_0 + \overline{\delta\alpha})$ is the response evaluated with the altered input data set.

Rearranging, this expression can be cast into a linear perturbation theory form as follows:

$$\frac{\delta P}{P} \equiv \frac{P(\bar{\alpha}_0+\overline{\delta\alpha})-P(\bar{\alpha}_0)}{P(\bar{\alpha}_0)} = \int_V \bar{s}_\alpha \cdot \frac{\overline{\delta\alpha}}{\alpha}\, dv \qquad (78)$$

where $\bar{s}_\alpha$ is the vector of sensitivity coefficients each element of which has the form $(dP/P)/(d\alpha_i/\alpha_i)$ and $(\overline{\delta\alpha/\alpha})$ is the fractional perturbation vector with elements $(\delta\alpha_i/\alpha_i)$ as a function of the problem phase space.

The usefulness of Eq. (78) as a perturbation theory expression has already been pointed out in Table III where the sensitivities were interpreted as a percent change in P for a percent increase in α. In this case the fractional change vector has only one element which is constant (i.e. 0.01) for the particular α being looked at and the sensitivity coefficient vector is the total sensitivity for that particular α (i.e. $\int s_\alpha\, dv$). For other applications it is possible to estimate the change in the response caused by any arbitrary change in the input data field using Eq. (78). The limitation of this formula is the range within which P is a linear

function of the input data (i.e. close to the calculated design point at which P ($\bar{\alpha}_0$) and the sensitivities are evaluated).

With these comments in mind, it is possible to consider the statistical nature of the input data base as forming an ensemble of finite (and hopefully small) perturbations of the data about $\bar{\alpha}_0$. Since most of the input data are experimentally derived, information about the standard deviation of the distribution function of $\bar{\alpha}$ about its nominal value, $\bar{\alpha}_0$, and correlations between the different input data can be put into Eq. (78) to formulate a first order uncertainty theory. This is done by squaring Eq. (78) and taking its expectation value over the correlated ensemble of statistical input data variations, to get:

$$\sigma_p^2 = \bar{s}^{tr} C \bar{s} \tag{79}$$

where, σ_p is the standard deviation in the response; C is the correlation matrix with elements along the diagonal representing the standard deviations in the input data and off-diagonal elements representing the correlations between the input data; and $\bar{s}$ and $\bar{s}^{tr}$ are the total sensitivity vector and its transpose. For the simple case of uncorrelated input data, C will be a diagonal matrix of standard deviations.

To illustrate the use of Eq. (79), a very crude estimate was made of the uncertainties in the input data for the CRBR problem, under the assumption of no data correlations. The estimated standard deviations of some of the input parameters are given in Table III along with the standard deviation in the responses resulting from these uncertainties.

Form these results it is clear that the major data uncertainty contributing to the 7.7% uncertainty in the peak clad temperature response is the 10% uncertainty in the coolant inlet temperature. The fact that 20-30% uncertainties exist in the conduction and convection properties of the fuel and coolant are of little concern because of their low sensitivities. On the other hand, for the 14% uncertainty in the central fuel temperature almost nothing but the 30% uncertainty in the gap conductivity and the 15% uncertainty in the fuel conductivity is of much concern. It should be noted that these results are expected to be strongly influenced by the nature of the correlations which exist between the data. A more refined uncertainty analysis would require careful evlauations of the uncertainties of all data of significant importance in this problem. Despite the crudeness of the current analysis, these results underscore the need to take both the uncertainty and sensitivity results into account in analyzing the uncertainty in any particular response. Since sensitivities are in general problem and response dependent care must be taken in using this information properly.

V. Summary and Conclusions

The extension of reactor sensitivity theory to non-linear thermal-hydraulics problems was successfully outlined in this paper. These

developments provide the framework for a powerful new approach to analyzing both the physics and safety aspects of LWR and FBR designs. The theory has several strong points which were highlighted in reactor sensitivity applications. First, for a large input data base, the use of adjoint functions to develop a sensitivity theory allows all the data to be anlayzed using only a single forward and adjoint run for each system response function being studied. This tremendous savings in computer time compared with currently used response surface methods is a strong incentive to apply the adjoint approach whenever possible. Second, the adjoint functions offer strong physical insight into the processes which occur in any particular problem, making a potentially black-box code somewhat more understandable. Last, the same usefulness of sensitivity coefficients in formulating a linear perturbation theory and a theory for uncertainty analysis is also present.

For more general applications several other benefits of the method are also apparent. For instance, the adjoint equations for non-linear forward problems are linear, making them easier to solve. In addition, the form of these adjoint equations and their boundary and final conditions strongly resemble the forward equations. This makes it conceptually possible to use the same computer codes and numerical methods to solve both the forward and adjoint equations. A test of this theory should now be possible within the framework of an existing thermal-hydraulics or safety code.

While the benefits of reactor sensitivity theory appear for the most part to apply to thermal-hydraulics problems, some additional complications must be overcome in this new application. The least worrisome of these, although it still must be dealt with, is the tendency of the solution of non-linear equations to behave in a more non-linear fashion as a function of input parameter variation. This factor makes it more difficult to apply a linear theory in perturbation applications. Here, however, some experience with non-linear reactor physics problems offers the possibility of using multiple forward and adjoint runs and high order interpolation schemes to map out non-linear response surfaces. The derivatives around a single design point available from a single adjoint run actually make it possible to more efficiently choose the data for the new calculations (i.e. a steepest descent approach using the derivatives to from a multi-phase space gradient).

More of a problem is the fact that the adjoint problem requires the solution of the forward problem to determine its input data base. This means that in addition to saving the forward problem solution at all points in phase space, the behavior of all physical data which depend on this solution (i.e. all non-linear data) must also be saved as a function of phase space. This means that essentially the whole forward solution path including all model changes for the data must be saved for an adjoint calculation. At best this will be a large bookkeeping problem and for applications with some large computer codes it might well nullify the inherent advantages of the adjoint approach.

A further problem is the inherent diversity of physical constants needed in a thermal-hydraulics or safety calculation. This results in a large number of terms of differing form in the expression for the sensitivity coefficient. Compared to the expressions which arise in reactor physics applications, the thermal-hydraulics problem is an order of magnitude larger. The sensitivity code that utilizes the results of forward and adjoint equations will therefore have to be larger. On the relative scale of these larger thermal-hydraulics and safety codes, the adjoint approach is still cost effective and this sensitivity code scale-up only poses problems of a theoretical nature. In practice there should be little difficulty with this coding problem.

On balance, it appears that there will be significant practical thermal-hydraulics and safety problems for which adjoint sensitivity theory can be used profitably. In a future paper an easier approach to deriving the adjoint equations for these more practical cases will be explored. An effort will be made to use more symbolic notations and illustrate the approach for the case of adding point kinetics and momentum balance equations to the heat balance equations. The solution to this expanded problem will more clearly delineate those areas in which the adjoint theory will or will not be successful. In the meantime practical applications with specific computer codes will be undertaken to test the theory on a case-by-case basis.

REFERENCES

1. K. V. Moore and W. H. Rettig, "RELAP4--A Computer Program for Transient Thermal-Hydraulic Analysis," ANCR-1127, Aerojet-Nuclear Corp. (December 1973).

2. F. E. Dunn, et al, "The SAS3A LMFBR Accident Analysis Computer Code," ANL/RAS 75-17, Argonne National Laboratory (1975).

3. A. E. Waltar, et al, "MELT-III: A Neutronics, Thermal-Hydraulics, Computer Program for Fast Reactor Safety Analysis," HEDL-TME 74-47, Hanford Engineering Development Laboratory (1974).

4. R. H. Myers, Response Surface Methodology, Allyn and Bacon, Inc., Boston (1971).

5. N. D. Cox, "Comparison of Two Uncertainty Analysis Methods," Nucl. Sci. Eng. 64, 258 (1977).

6. J. K. Vaurio and C. Mueller, "A Probabalistic/Deterministic Procedure for Analyzing LMFBR Core Disruptive Accidents," Proc. Int. Mtg. Fast Reactor Safety and Related Physics, Chicago (1976).

7. M. D. McKay, W. J. Conover and D. E. Whiteman, "Report on the Application of Statistical Techniques to the Analysis of Computer Codes," LA-NUREG-6526-MS, Los Alamos Scientific Laboratory (1976).

8. C. Mueller, et al, "SACO-1: A Fast-Running LMFBR Accident Analysis Code," ANL/RAS 77-50, Argonne National Laboratory (1977).

9. M. E. Wells and C. B. Davis, "Quarterly Technical Report on Water Reactor Safety Programs," July-September 1975, ANCR-1296, Aerojet Nuclear Corp. (1976).

10. E. M. Oblow, "Sensitivity Theory from a Differential Viewpoint," Nucl. Sci. Eng. 59, 187 (1976); see also, E. M. Oblow, "Reactor Cross Section Sensitivity Studies Using Transport Theory," ORNL/TM-4437 (April 1974).

11. G. C. Pomraning, J. Math, Phys., 8, 149 (1967).

12. L. N. Usachev, "Perturbation Theory for the Breeding Ratio and for Other Number Ratios Pertaining to Various Reactor Processes," J. Nucl. Energy, Pts. A/B 18, 571 (1964).

13. A. Gandini, "A Generalized Perturbation Method for Bilinear Functionals of the Real and Adjoint Neutron Fluxes," J. Nucl. Energy 21, 755 (1967).

14. W. M. Stacey, Jr., Variational Methods in Nuclear Reactor Physics, Academic Press, N.Y. (1974).

15. D. E. Bartine, E. M. Oblow, and F. R. Mynatt, "Radiation Transport Cross Section Sensitivity Analysis - A General Approach Illustrated for a Thermonuclear Source in Air," Nucl. Sci. Eng. 55, 147 (1974).

16. E. Greenspan, "Developments in Perturbation Theory," Advances in Nuclear Science and Technology, 9 (1977).

17. S. A. W. Gerstl, D. J. Dudziak, and D. W. Muir, "Cross Section Sensitivity and Uncertainty Analysis with Application to a Fusion Reactor," Nucl. Sci. Eng. 62, 137 (1977).

18. D. R. Harris, "Sensitivity of Nuclear Fuel Cycle Costs to Uncertainties in Nuclear Data and Methods," Doctoral Thesis, Rennselaer Polytechnic Institute, Troy, N.Y. (October 1976).

19. M. L. Williams and C. R. Weisbin, "Sensitivity and Uncertainty Analysis for Linear Functionals of the Time-Dependent Nuclide Density Field," ORNL/TM-5799 (1977).

20. A. Gandini, "A Method of Correlation of Burnup Measurements for Physics Prediction of Fast Reactor Life," Nucl. Sci. Eng. 38, 1-7 (1969).

21. M. Becker, "Perturbation Theory for Ratios in Linear and Non-linear Problems", Nucl. Sci. Eng. 62, 296 (1977).

22. C. R. Weisbin et al, "Application of Sensitivity and Uncertainty Methodology to Fast Reactor Integral Experiment Analysis", Nucl. Sci. Eng. 66 (1978).

A NEW APPROACH TO THE ADJUSTMENT OF GROUP CROSS-SECTIONS FITTING INTEGRAL MEASUREMENTS

Yung-An Chao
Nuclear Science and Engineering Division, Carnegie-Mellon University
Pittsburgh, Pennsylvania 15213

ABSTRACT

The adjustment of group cross-sections fitting integral measurements is viewed as a process of uncovering theoretical and/or experimental negligence errors to bring statistical consistency to the integral and differential data so that they can be combined to form an enlarged ensemble, based on which an improved estimation of the physical constants can be made. An approach with three steps is suggested and its formalism of general validity is developed. In step one, the data of negligence error is extracted from the given integral and differential data. The method of extraction is based on the concepts of prior probability and information entropy. It automatically leads to vanishing negligence error as the two sets of data are statistically consistent. The second step is to identify the sources of negligence error and adjust the data by an amount compensating the extracted negligence discrepancy. And in the last step the two data sets, already adjusted to mutual consistency, are combined as a single unified ensemble. Standard methods of statistics can then be applied to reestimate the physical constants. A simple example is shown as a demonstration of the method.

I. INTRODUCTION

The adjustment of group constants fitting integral measurements consists of two parts. One is the calculation of the sensitivity matrix relating the integral quantities to the differential ones. The other is the treatment of uncertainties and errors. The former is a problem of reactor physics and has been formulated on relatively sound grounds through the development of the theory of generalized pertubation. The latter is largely a problem of application of statistics and is still relatively loose in structure. Considerable disagreement exists among specialists in how to assess properly the errors of the group constants and adjust them accordingly.

In a recent paper[1] by the author, the inadequacy of current approaches to the problem is pointed out and ideas of a new approach based on Bayesian principle and information entropy are discussed. Considerable refinements and developments on these ideas have been carried out since then. A rather complete scheme of this new approach is now established and the general formalism of the methodology worked out. These results will be reported in this paper, as an updated revision of the quoted earlier work.

My basic view of the problem and ideas of the approach are first reviewed in Section II. Following that a method is devised to implement these ideas. For clarity of presentation, the method itself is described for a simple case. Necessary generalizations of that to realistic problems are subsequently worked out in Section III. A very simple example is shown in Section IV to demonstrate the method.

II. FUNDAMENTALS

A set of group constants calculated via a theoretical model from basic cross-section data, when used to calculate certain integral parameters may not agree with the experimentally measured values. The question is how to adjust the group constants to new values compatible with the integral measurements. It is important to notice here that any adjustment to be made is a consequence of the observed discrepancy. If there is no discrepancy, why should any adjustment be made? Thus, whatever adjustments eventually made must be deduced or inferred from the observed discrepancy. Therefore, the result of data adjustment necessarily depends on the assessment of discrepancy by the person who is making the adjustment. However, since the discrepancy is never absolute but always probable in nature, the assessment of it is highly susceptible to one's subjective bias. This in my opinion is one of the major reasons for the diversity in current approaches to the problem. I will therefore first address to this issue.

The discrepancy may originate in two different ways: (1) statistical uncertainties, arising from finiteness of the data ensemble; and (2) negligence errors* arising from some negligence in experiments (e.g., calibration) or in theory (e.g., approximations). If a discrepancy is due to the first cause (called henceforth a statistical discrepancy), it will decrease and eventually disappear as the statistics improve with more data collection. But for given data sets, this discrepancy <u>cannot</u> be <u>corrected</u>, although unification of the data sets can be made for a reestimation within statistical uncertainties. On the other hand, if it is due to the second cause (called henceforth a negligence discrepancy), the discrepancy will always be there regardless of any improvement of

* To avoid possible confusion, the term systematic error used in ref. 1 is replaced by negligence error.

the statistics. However, if the negligence error is uncovered and corrected accordingly, the discrepancy will be removed. A statistical discrepancy may appear among the affected parameters in an uncorrelated or correlated way, while a negligence discrepancy due to a single source of error necessarily appears among the affected parameters in a completely correlated (systematic) manner. A simple example is that when the disagreement between a total cross-section (an integral measurement) and the sum of differential cross-sections (differential measurements) is due to a negligence error, this is an error in normalization affecting all the data by a systematic shift. Whether the discrepancy is a statistical one or not is usually checked by the statistical consistency of the two sets of data: for example, agreement within standard deviations. A statistical discrepancy can be handled in a well-defined and straightforward way via the standard methods of statistics for combination and propagation of uncertainties. It is the treatment of negligence error that bears ambiguity and is often disputable. It should be pointed out that the commonly adopted term adjustment makes sense only when two sets of data are not statistically consistent so that they need to be "adjusted" to become consistent. Otherwise one merely puts two consistent distributions on top of each other to make a reestimation based on the enlarged ensemble and nothing needs to be adjusted at all.

Currently there are, generally speaking, two approaches to the problem of resolving the discrepancy. One[2,3] is to regard the integral and differential data as experimental measurements of the same physical constants, since the former can be related to the latter through the sensitivity matrix. The adjustment is then simply done by fitting the two sets of data simultaneously with the "adjusted" group constants. This approach implies that the discrepancy is statistical in nature. However, unless the discrepancy lies within statistical uncertainties, it does not seem proper to exclude the possibility of a negligence error. Namely the two sets of data may not be interpreted as measurements of the same physical constants because of the possible negligence error indicated by the statistical inconsistency. With the discrepancy assumed statistical, this method should always reduce the uncertainties of the adjusted group constants from those of the original group constants because of the increase in data ensemble. This would not be reasonable if the two data sets are not statistically consistent. To remedy this drawback, a user of the method has to alter (enlarge) the covariance (or dispersion, or error) matrices of the data sets. The amount of alteration, of course, depends again on his own assessment of the discrepancy.

Another adopted approach[4], somewhat counter to the preceding one, is to use only the integral measurements in determining the adjusted group cross-sections. The differences between the adjusted and the original group constants are regarded as due to some negligence error which is just being corrected through this adjustment procedure. However, contrary to the first one, this method would not be appropriate if the discrepancy does lie within the statistical uncertainties,

because it then does not use in this case all of the consistent data. Furthermore, since this method cannot apply to the case of having more group constants to be adjusted than integral parameters being fitted to, one has to decide on which subset of the group constants is responsible for the discrepancy. The other deficiency of the method is that if the integral measurements carry large uncertainties the deduced adjustments may be unrealistically large.

The approach that I shall suggest is based on the view that because of the probable rather than absolute nature of the discrepancy, the assessment of it, which directly affects the subsequent adjustment, should make use of as much as possible statistics principles so that subjective bias may be reduced. (It goes without saying that additional information established prior to the undertaking of data adjustment is certainly not regarded as a bias and should by all means be included into the data to start.) It will be seen that my method turns out comprising both of the two preceding methods as limiting cases in the proper respective limits. In my approach of data adjustment there are three steps. The first is to extract from the given data an estimated "data" of negligence discrepancy. The second is to try to understand where this extracted negligence error may come from, namely to identify the sources of the error (theoretical or experimental). After the negligence error has been explained away (corrected for), the integral and differential data are necessarily in statistical agreement. They can now be interpreted as measurements of the same constants. Step three is therefore to unify the two consistent sets of integral and differential data by the standard method of data combination. The outcome of step two must bear uncertainties larger or equal to those of the income, while the outcome of step three must be less uncertain than those of the income. Steps one and three involve only statistics, while step two is mostly a problem of physics rather than mathematics. Since negligence errors and statistical uncertainties are due to different causes, a separation of the two helps in sorting out entanglement and in defining the right problem. Since it is the negligence error that can be <u>corrected</u>, not the statistical uncertainties which <u>cannot</u> be improved until more data are collected, one may run into the trap of introducing a fictitious correction to compensate for poor statistics if the two are not handled separately as suggested here.

To work out the basic formulation of the problem, we first consider for convenience and clarity a very simple case. Let there be two independent experiments attempting to measure the same physical parameter. If the two reported data, $y \pm \delta_y$ and $x \pm \delta_x$ are not consistent within their standard deviations despite the claimed sufficiency of statistics, one would think that there is some negligence error, which may be caused by some negligence in either one or both of the experiments. We shall consider the question of how to estimate this negligence error, $\bar{g} \pm \delta_g$, with no other information than the given data.

First of all, we have <u>no</u> direct <u>measurement</u> (<u>data</u>) of the negligence error $\bar{g}$. From the reported data, we can deduce the difference between

them as $g = y - x$ with an uncertainty of $\delta_g = (\delta_x^2 + \delta_y^2)^{1/2}$. However, $g \pm \delta_g$ cannot be identified with full confidence as a measurement of the negligence error. The reason is that if $|g| \leq \delta_g$ the two data are statistically consistent and we have no evidence at all, based on the data available, that there exists an error. The question of negligence error would not arise in such a case at all and we should therefore conclude with full confidence that there is no negligence error, namely $\bar{g} \pm \bar{\delta}_g = 0 \pm 0$ instead of $g \pm \delta_g$. However, if $|g| >> \delta_g$, it would seem reasonable to regard $g \pm \delta_g$ as a measurement of $\bar{g} \pm \bar{\delta}_g$. In this sense we call $g \pm \delta_g$ the "conjectured data" of the negligence error.* How reliable the conjecture is depends on how significant the difference is between the reported data. Since the conjectured data is all what we have for estimating $\bar{g} \pm \bar{\delta}_g$, we have to have a method of incorporating into the estimation procedure the reliability of the conjecture. If the data g were a genuine measurement of $\bar{g}$ we would have the data distribution function as

$$p(g|\bar{g}) = \frac{1}{\delta_g} \exp(- \frac{1}{2\delta_g^2} (g - \bar{g})^2) \tag{1}$$

and could simply apply the maximum likelihood principle to $p(g|\bar{g})$ to estimate $\bar{g}$. To take into consideration the reliability of the conjecture we assume a probability distribution function of $\bar{g}$ as the following

$$p(\bar{g}|\lambda) = \frac{\lambda^{1/2}}{\delta_g} \exp(- \frac{\lambda}{2} (\bar{g}/\delta_g)^2) \tag{2}$$

which peaks at $\bar{g} = 0$, namely zero negligence error, with λ as a confidence parameter measuring the subjective confidence on non-negligence. The actual distribution function of the data g is then given by the joint distribution function of g and $\bar{g}$ as

$$p(g,\bar{g}|\lambda) = g(g|\bar{g})p(\bar{g}|\lambda) = [\frac{1}{\delta_g} \exp(- \frac{1}{2\delta_g^2} (g - \bar{g})][\frac{\lambda^{1/2}}{\delta_g} \exp(- \frac{\lambda}{2} (\bar{g}/\delta_g)^2)] \tag{3}$$

The value of the confidence parameter λ is a priorily unknown and should be determined in such a way that it reflects on the reliability of the conjectured data, namely the relative value of $|g|$ and δ_g. If $|g| >> \delta_g$, λ should turn out small so that the estimation of $\bar{g}$ is dominated by the highly significant (therefore reliable) conjectured data $g \pm \delta_g$. On the other hand for $|g| \leq \delta_g$, λ should approach infinity so that zero negligence error is guaranteed through the complete dominance of the assumed distribution $p(\bar{g}|\lambda)$. There is an obvious resemblance of $p(\bar{g}|\lambda)$ to the prior distribution in Bayesian statistics[5], except that λ is to be determined posteriorly. The choice of a normal distribution for $p(\bar{g}|\lambda)$

* It will become clear with eq. (10) that $g \pm \delta_g$ itself cannot be used as an independent data for any consistent calculation.

was argued in ref. 1 with the idea of information entropy, where λ can be regarded as a Lagrange multiplier. This argument is reproduced in the Appendix for completeness. This choice for $p(\bar{g}|\lambda)$ will also be posteriorly justified by its convenience in use and the surprisingly simple yet very reasonable results it leads to. It is important to recognize that this choice of $p(\bar{g}|\lambda)$ satisfies the requirement of the formulation, eq. (3), being invariant under any linear transformation of the variable, which, although looks trivial in this very simple example of only one variable, becomes an important condition in the case of multi-variables in Section III.

In the joint distribution $p(g,\bar{g}|\lambda)$ of eq. (3), g and $\bar{g}$ are random variables and λ is a parameter. If both g and $\bar{g}$ were given, λ could be determined by applying the maximum likelihood principle to $p(g,\bar{g}|\lambda)$. However, only g is known and $\bar{g}$ is to be estimated, the outcome of which depends on the choice of λ. We therefore consider all possible values of $\bar{g}$ by integrating $p(g,\bar{g}|\lambda)$ over $\bar{g}$ to find $p(g|\lambda)$, which can be maximized to determine the most probable value, $\bar{\lambda}$, of the confidence parameter, λ. A more formal way of presenting this is to use Bayes theorem[5] and rearrange eq. (3) to the following form:

$$p(g,\bar{g}|\lambda) = p(g|\bar{g})p(\bar{g}|\lambda) = p(\bar{g}|g,\lambda)p(g|\lambda) \tag{4}$$

where

$$p(\bar{g}|g,\lambda) = \frac{(1+\lambda)^{1/2}}{\delta_g} \exp[-\frac{(1+\lambda)}{2\delta_g^2}(\bar{g} - g/(1+\lambda))^2] \tag{5}$$

is the distribution function of $\bar{g}$ for a given g and λ, and

$$p(g|\lambda) = (\frac{\lambda/\delta_g^2}{1+\lambda})^{1/2} \exp[-\frac{1}{2}(\frac{\lambda/\delta_g^2}{1+\lambda})\, g^2] \tag{6}$$

is the distribution function of g for a given confidence parameter λ. The most probable value $\bar{\lambda}$ of the confidence parameter is determined in terms of g and δ_g by applying the maximum likelihood principle to $p(g|\lambda)$. The distribution function $p(g|\lambda)$ regarded as a function of λ for a given g has two maxima as shown in Fig. (1). One is at $\lambda = \bar{\lambda}$ where $\bar{\lambda}$ is given by the condition

$$1 = (\frac{\bar{\lambda}}{1+\bar{\lambda}})(g^2/\delta_g^2), \tag{7a}$$

or

$$\bar{\lambda} = 1/((g/\delta_g)^2 - 1), \tag{7b}$$

and the other being asymptotic at $\lambda = \infty$. If $|g| > \delta_g$, $\lambda = \bar{\lambda}$ is the absolute maximum. As $|g|$ approaches δ_g the maximum at $\bar{\lambda}$ approaches the asymptotic maximum at $\lambda = \infty$, and for $|g| \leq \delta_g$ it disappears from

the positive λ region and moves into the unphysical negative λ region. Thus, for $|g| < \delta_g$, the absolute maximum switches to $\lambda = \infty$.

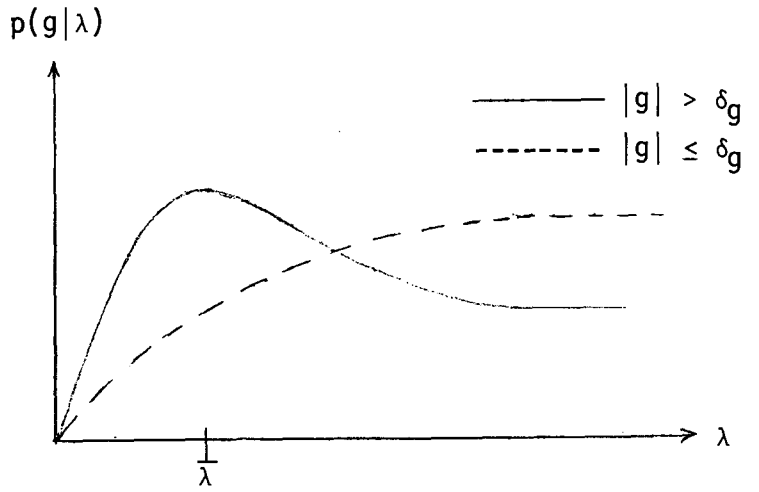

Figure (1)

The most probable value of the confidence parameter is therefore given by

$$\bar{\lambda} = \begin{cases} 1/((g/\delta_g)^2 - 1) & \text{for } |g| \geq \delta_g \\ \infty & \text{for } |g| \leq \delta_g \end{cases} \tag{8}$$

$$\bar{g} = \begin{cases} g(1 - \delta_g^2/g^2) & \text{for } |g| \geq \delta_g \\ 0 & \text{for } |g| \leq \delta_g \end{cases} \tag{9a}$$

$$\bar{\delta}_g = \begin{cases} \delta_g(1 - \delta_g^2/g^2)^{1/2} & \text{for } |g| \geq \delta_g \\ 0 & \text{for } |g| \leq \delta_g \end{cases} \tag{9b}$$

This result is remarkably simple and in the limits of $|g| \leq \delta_g$ and $|g| >> \delta_g$ gives exactly what we hope for.

It is worth pointing out that the condition on $\bar{\lambda}$, eq. (7a), makes both the χ^2-value of $p(g|\lambda)$ of eq. (6) and the minimum χ^2-value of $p(g,\bar{g}|\lambda)$ of eq. (4) equal to exactly one. We will see in Section III that for the multi-variable case these χ^2-values will always turn out equal to the number of degree of freedom. Thus the method of determining

$\bar{\lambda}$ by maximizing the likelihood function of $p(g|\lambda)$ is consistent with a χ^2-test* on the proposed distribution function $p(g,\bar{g}|\lambda)$.

A very important advantage of this approach is that the negligence error extracted can be treated consistently as an independent quantity in data adjustment. More specifically, let us consider as an example the case when $y \pm \delta_y$ is believed to be a more reliable data and any possible negligence error is attributed to the measurement of $x \pm \delta_x$. We then try to adjust the data $x \pm \delta_x$ to $\hat{x} \pm \hat{\delta}_x$ by adding $\bar{g} \pm \bar{\delta}_g$ to it,

$$\hat{x} = x + \bar{g} = \begin{cases} y - \dfrac{\delta_x^2 + \delta_y^2}{y - x} & \text{for } |y-x| \geq (\delta_x^2+\delta_y^2)^{1/2} \\ x & \text{otherwise} \end{cases} \tag{10a}$$

$$\hat{\delta}_x = (\delta_x^2+\bar{\delta}_g^2)^{1/2} = \begin{cases} [(\delta_x^2+\delta_y^2)(2 - \dfrac{\delta_x^2+\delta_y^2}{(y-x)^2}) - \delta_y^2]^{1/2} & \text{for } |y-x| \geq (\delta_x^2+\delta_y^2)^{1/2} \\ \delta_x & \text{otherwise} \end{cases} \tag{10b}$$

It is a consistency check that when $|y - x| \leq (\delta_x^2 + \delta_y^2)^{1/2}$, namely no statistical inconsistency, $\hat{x} = x$ and $\hat{\delta}_x = \delta_x$. This would not have been the case had we used $g \pm \delta_g$ instead of $\bar{g} \pm \bar{\delta}_g$ as the negligence error. To check for consistency that the adjusted data $\hat{x} \pm \hat{\delta}_x$ is always in agreement with the other data $y \pm \delta_y$, we calculate the difference between the two,

$$t = y - \hat{x} = \frac{\delta_x^2 + \delta_y^2}{y - x} \tag{11a}$$

$$\delta_t = (\delta_y^2 + \hat{\delta}_x^2)^{1/2} = [(\delta_x^2 + \delta_y^2)(2 - \frac{\delta_x^2 + \delta_y^2}{(y - x)^2})]^{1/2} \tag{11b}$$

It is easy to see that $|t| \leq \delta_t$. Now that the adjusted data $\hat{x} \pm \hat{\delta}_x$ is statistically consistent with $y \pm \delta_y$, we can regard them as two measurements of the same physical parameter. They can thus be combined for an estimation of the value of the physical parameter as

$$p = (\hat{\delta}_x^2 y + \delta_y^2 x)/(\delta_y^2 + \hat{\delta}_x^2) \tag{12a}$$

---

* In response to the work of ref. 1, Gandini[6] suggested for the determination of $\bar{\lambda}$, a χ^2-test, however apparently not to this proposed distribution function $p(g,\bar{g}|\lambda)$.

$$\delta_p = \hat{\delta}_x \delta_y / (\delta_y^2 + \hat{\delta}_x^2)^{1/2} \tag{12b}$$

The most severe adjustment occurs as $|y - x| >> (\delta_x^2 + \delta_y^2)^{1/2}$ in which case we have

$$\hat{x} \pm \hat{\delta}_x \cong y \pm (2\delta_x^2 + \delta_y^2)^{1/2} \tag{13a}$$

$$p \pm \delta_p \cong y \pm \delta_y \left(1 - \frac{\delta_y^2}{2(\delta_x^2 + \delta_y^2)}\right)^{1/2} \tag{13b}$$

Now that we have completed step one of extracting the "data" of the negligence discrepancy, we consider next step two of what to do with it. Obviously one should try to analyze all sorts of possibilities in an attempt to explain away the negligence discrepancy. This, as remarked before, is mainly a problem of physics rather than mathematics, and is basically common to all different approaches to data adjustment. It will involve complicated and painstaking analyses, as much as possible, of all experimental data and theoretical models used. (In this sense my approach is not really of any fundamental conflict to other suggested or adopted approaches. The main difference is that I single out step one and three specifically and suggest a different route on the treatment of statistics involved.) The laborious exploration of the sources of negligence error may end up with one of the following results. The first one is that a source is discovered and the correction can be explicitly calculated. In this case one simply adds in the corrections to remove the negligence discrepancy. The other possibility is that a source of error is identified but one cannot compute the correction explicitly or estimate it accurately. Then we can parameterize the correction due to the identified or highly suspected source of error, fit it to the extracted data of negligence discrepancy and subsequently remove it from the data. The last possibility is that after all these efforts, none of the sources can be identified. This is unlikely to happen and we really should not stop until something is found. However one situation may actually occur in practice. Namely after all the efforts, still some negligence discrepancy is left unexplained; and one knows that whatever negligence left must be associated with a certain subset of the data because they are particularly difficult to check and all the other data have been carefully examined. In such a case one would assign the negligence discrepancy to the "unclean" subset and adjust the subset in the way described in eq. (10). A particularly likely case is that when all the integral experiments have been examined very carefully without any error uncovered and no obvious mistake in any differential experiment has been noticed. Then the error must be in theory, either in the group constant calculation or the sensitivity matrix calculation. But one may not have any better theoretical model or computational approximation available than what is used. In this case we can adjust the group constants as described in

eq. (10) and define the adjusted group constants as the fudged group constants associated with the theoretical model or approximation. These fudged group constants should of course be updated when better models or more data become available.

After all the adjustments* (corrections) of the data are done so that the induced adjustments fit the extracted data of negligence discrepancy to a statistically accepted level, namely of a χ^2 smaller than the number of degree of freedom, all integral and differential data are now statistically consistent. One can then make a further adjustment* by simply unifying all the data and reestimate the best values of the parameters as described in eq. (12). This last step is undisputable and straightforward, and will not be discussed here.

III. GENERAL METHODOLOGY

Now we consider necessary generalizations of the above adjustment procedure to a realistic situation, where we have

- G' or G: a m component vector of group constants, G' being the variable and G the data,
- Q: a m by m precision matrix** associated with G,
- I: a k component vector of integral measurements,
- R: a k by k precision matrix associated with I,
- S: a k by m sensitivity matrix theoretically relating the group constants to the integral measurements.

Let g be the m-component vector of "conjectured data" of the negligence discrepancy. The joint probability density $p(g,G'|G,I)$ for given G and I can be written as

$$p(g,G'|G,I) \alpha \exp - \frac{1}{2}[(S(g+G')-I)^T R(S(g+G')-I) + (G'-G)^T Q(G'-G)] \tag{14}$$

From which one can derive, by using Bayes Theorem $p(g,G') = p(G'|g)p(g)$, the probability density $p(g|G,I)$ as

$$p(g|G,I) \alpha \exp - \frac{1}{2}[(S(g+G)-I)^T (R - R^T S(S^T RS + Q)^{-1} S^T R)(S(g+G)-I)] \tag{15}$$

* The adjustment in step one is really correction, while in step three it is really unification of consistent data and should not be called adjustment.

**A precision matrix is the inverse of the covariance or error or dispersion matrix.

From this probability function one can deduce the conjectured data and its precision matrix as

$$g = \tilde{R}^{-1} S^T R I - G \tag{16}$$

$$V = \tilde{R} - \tilde{R}(\tilde{R} + Q)^{-1}\tilde{R} \tag{17}$$

where

$$\tilde{R} = S^T R S \tag{18}$$

is a m by m matrix, which is not reversible if $k < m$ because of the S being a non-square matrix. For the moment we will ignore the non-inversability of $\tilde{R}$ for $k < m$ and later justify the general applicability of the method. The two probability density functions $p(g|\bar{g})$ and $p(\bar{g}|\lambda)$ in eqs. (1) and (2) are now generalized to

$$p(g|\bar{g}) = (\det V)^{1/2} \exp[-\frac{1}{2}(g - \bar{g})^T V (g - \bar{g})] \tag{19}$$

$$p(\bar{g}|\lambda) = \lambda^{1/2} (\det V)^{1/2} \exp(-\frac{\lambda}{2} \bar{g}^T V \bar{g}) \tag{20}$$

The route of generalizing $p(\bar{p}|\lambda)$ is chosen to preserve the invariance of the (posterior) joint distribution $p(g|\bar{g})p(\bar{g}|\lambda)$ under any linear transformation of the variables*. The most probable value of λ and the best estimate $\bar{g}$ with its precision matrix $\bar{V}$ are found in complete analogy to eqs. (7) and (9) of the previous case of a single variable as

$$n = (\frac{\bar{\lambda}}{1 + \bar{\lambda}})(g^T V g) \tag{21a}$$

or

$$\bar{\lambda} = n/(g^T V g - n) \tag{21b}$$

$$\bar{g} = g/(1 + \bar{\lambda}) = (1 - n(g^T V g)^{-1})g \tag{22}$$

$$\bar{V} = (1 + \bar{\lambda})V = V/(1 - n(g^T V g)^{-1}) \tag{23}$$

where n is the rank of the matrix V and $g^T V g \geq n$ is assumed. If $g^T V g \leq n$, $\bar{\lambda}$ is infinite. The negligence discrepancy, $\bar{g}$, may be associated with either the group constants G or the integral measurements I. In the latter case one simply redefines the m-component vector g by multiplying it with the sensitivity matrix S to transform it to a k-component vector,

$$g = I - SG \tag{24}$$

---

* The function $p(\bar{g}|\lambda)$ suggested in ref. 1 does not include V. That formulation is therefore not invariant and should be revised to this one.

Similarly, the m by m precision matrix V is also transformed to a k by k one,

$$V = R - RS(\tilde{R} + Q)^{-1}S^{T}R \tag{25}$$

And the rest of the formulae remain the same.

If the negligence error is in I, we see from eqs. (24) and (25) that no inversion of any singular matrix is involved. In this case whether m < k or m > k is irrelevant. However, if the negligence error is in G, we see in eq. (16) $\tilde{R}^{-1}$ is singular and thus undefined for m > k. In such a case we are facing the problem of having m group cross-sections subject to consistency correction, while there are only k less than m constraints. How do we select the G's? Obviously there is only a subspace of G, spaced by the k linear combinations of G's specified by the sensitivity matrix S, that can be affected by the consistency check. The question is then how to define the other m - k linear combinations. This leads to the question of defining orthogonality conditions, which is equivalent to matrix diagonalization. We see in eq. (17) that both real symmetric matrices $\tilde{R}$ and Q can be diagonalized, $\tilde{R}$ having m - k zero eigenvalues while Q having all positive eigenvalues. The diagonalization of each of the two is unique only if we restrict the diagonalizing matrix to be orthonormal. However with an orthonormal diagonalizing matrix, $\tilde{R}$ and Q cannot be diagonalized simultaneously because the two in general do not commute. But if we do not use an orthonormal diagonalizing matrix, the two can be diagonalized simultaneously and uniquely. This unique transformation is then the one to define the other m - k linear combinations of the m G's. First of all, $Q^{1/2}$ and $Q^{-1/2}$ can be uniquely defined because Q is a real symmetric and positive definite matrix. This can be easily seen by diagonalizing Q. Thus we can transform Q to the unit matrix by using $Q^{1/2}$ as the transformation matrix. Under this transformation $\tilde{R}$ goes to $Q^{-1/2}\tilde{R}Q^{-1/2}$ which is again a real symmetric matrix. Now we can diagonalize $Q^{-1/2}\tilde{R}Q^{-1/2}$ and the unit matrix simultaneously. This diagonalization is unique and the transformation matrix is orthonormal, namely the orthonormal matrix diagonalizing $Q^{-1/2}\tilde{R}Q^{-1/2}$. Therefore both $\tilde{R}$ and Q can be diagonalized by the unique matrix D such that

$$(D^{-1})^{T}QD^{-1} = \text{unit matrix} \tag{26a}$$

$$(D^{-1})^{T}\tilde{R}D^{-1} = r, \text{ a diagonal matrix with } m - k \text{ zero eigenvalues} \tag{26b}$$

where

$$D = uQ^{1/2} \tag{27}$$

and u is the unique orthonormal matrix diagonalizing the symmetric matrix $Q^{-1/2}\tilde{R}Q^{-1/2}$.

Applying the transformation D to G renders the precision matrix V in eq. (17) to the diagonal from r/(1 + r) which vanishes in the subspace spanned by the last m-k vectors of D. The transformation will also

remove the singularity of $\tilde{R}^{-1}$ in eq. (16) and leave the last k - m components of Dg finite but undetermined. Therefore in terms of the new bases Dg, the probability densities $p(Dg|D\bar{g})$ and $p(D\bar{g}|\lambda)$ transformed from eqs. (19) and (20) will cover only the subspace spanned by the first k components of Dg and Dg. The last m - k components disappear from $p(Dg|\hat{D}g)$ and $p(Dg|\lambda)$ entirely. Thus we reach the conclusion that if we use G = DG as the bases, then only $(G_1, G_2, \ldots G_k)$ will be related to the k integral measurements. All the other $\hat{G}$'s are completely decoupled from I's and thus carry no information at all on the negligence discrepancy*.

In step two, if we need to parametrize a correction on G for a certain identified source of negligence error to fit the data of negligence discrepancy, the parametrization may unavoidably affect the last m - k of $\hat{G}$'s. In that case in addition to fitting the parametrized correction to the negligence discrepancy $D\bar{g}$, we must at the same time fit to the last m - k of $\hat{G}$'s. After the negligence discrepancy is removed, all of the G's will be unified with the integral measurements for a final reestimation of the group constants. If the parametrized correction is made on I, there is no complication because no inversion of any singular matrix is encountered.

IV. EXAMPLE

To get more insight of the method of Section III, we demonstrate it by explicitly working out a very simple example. Measurements of partial cross-sections, $\sigma_m{}^\circ \pm \varepsilon_m$, are checked by a measurement of the total cross-section $\Omega^\circ \pm \bar{\varepsilon}$. For simplicity we assume only two σ° and that the theoretical relation between the integral and differential data is simply $\Omega = \sigma_1 + \sigma_2$. If we find that

$$|\Delta| = |\Omega^\circ - \sigma_1{}^\circ - \sigma_2{}^\circ| > \delta = (\varepsilon^2 + \varepsilon_1{}^2 + \varepsilon_2{}^2)^{1/2} \tag{28}$$

there is an indication of some negligence error. The experimentalists believe that the total cross-section experiment is very clean and the partial cross-section experiment is subject to possible errors in identifying different nuclei, missing counts of multi-body events, too high an energy threshold in a detector for certain reactions and so on. The negligence error is thus most likely in the partial cross-sections. We then have the problem of having two data to adjust, while there is only one constraint. We shall try to extract the negligence discrepancy and cast it into the diagonal representation.

Using the notions of Section III, we have

---

* This separation of the total space into two "orthogonal" subspaces also facilitates the handling of negligence errors in both G and I simultaneously.

$$G = \begin{pmatrix} \sigma_1^\circ \\ \sigma_2^\circ \end{pmatrix} \quad ; \qquad Q = \begin{pmatrix} 1/\varepsilon_1^2 & 0 \\ 0 & 1/\varepsilon_2^2 \end{pmatrix}$$
$$I = \Omega^\circ \quad ; \qquad R = 1/\varepsilon^2 \tag{29}$$
$$S = (1, 1)$$

To work out the diagonalizing matrix $D = uQ^{1/2}$, we first calculate u by diagonalizing $Q^{-1/2}\tilde{R}Q^{-1/2}$, which from eq. (18) equals

$$Q^{-1/2}\tilde{R}Q^{-1/2} = \frac{1}{\varepsilon^2}\begin{pmatrix} \varepsilon_1^2 & \varepsilon_1\varepsilon_2 \\ \varepsilon_1\varepsilon_2 & \varepsilon_2^2 \end{pmatrix} \tag{30}$$

The orthonormal matrix u is easily found as

$$u = \frac{1}{(\varepsilon_1^2 + \varepsilon_2^2)^{1/2}}\begin{pmatrix} \varepsilon_1 & \varepsilon_2 \\ -\varepsilon_2 & \varepsilon_1 \end{pmatrix} \tag{31}$$

and D as

$$D = (\varepsilon_1^2 + \varepsilon_2^2)^{-1/2}\begin{pmatrix} 1 & 1 \\ -\varepsilon_2/\varepsilon_1 & \varepsilon_1/\varepsilon_2 \end{pmatrix}; \quad D^{-1} = (\varepsilon_1^2 + \varepsilon_2^2)^{-1/2}\begin{pmatrix} \varepsilon_1^2 & -\varepsilon_1\varepsilon_2 \\ \varepsilon_2^2 & \varepsilon_1\varepsilon_2 \end{pmatrix} \tag{32}$$

Applying this transformation of bases to the quantities in eq. (29), we readily find their <u>redefined</u> transformed forms as

$$G = (\varepsilon_1^2 + \varepsilon_2^2)^{-1/2}\begin{pmatrix} \sigma_1^\circ + \sigma_2^\circ \\ -\sigma_1^\circ\ \varepsilon_2/\varepsilon_1 + \sigma_2^\circ\ \varepsilon_1/\varepsilon_2 \end{pmatrix}; \qquad Q = \begin{pmatrix} 1 & 0 \\ 0 & 1 \end{pmatrix}$$
$$I = \Omega^\circ \quad ; \qquad R = 1/\varepsilon^2 \tag{33}$$
$$S = ((\varepsilon_1^2 + \varepsilon_2^2)^{1/2}, 0)$$

Plugging the above redefined quantities into eq. (18) the <u>redefined</u> matrix $\tilde{R}$ is equal to

$$\tilde{R} = \begin{pmatrix} (\varepsilon_1^2 + \varepsilon_2^2)/\varepsilon^2 & 0 \\ 0 & 0 \end{pmatrix} \tag{34}$$

The conjectured data of negligence discrepancy and its precision matrix in this new representation are, from eqs. (16) and (17),

$$g = \begin{pmatrix} (\varepsilon_1^2 + \varepsilon_2^2)^{-1/2}\,\Delta \\ \text{undetermined} \\ \underline{\text{finite}}\ \text{constant} \end{pmatrix} \tag{35}$$

$$V = \begin{pmatrix} (\varepsilon_1^2 + \varepsilon_2^2)/\delta^2 & 0 \\ 0 & 0 \end{pmatrix} \tag{36}$$

where Δ and δ are defined in eq. (28). Since the second component of g in eq. (35) is undetermined yet <u>finite</u> with a <u>zero</u> precision as shown in eq. (36), only the linear combination $\sigma_1^\circ + \sigma_2^\circ$ can sense any negligence discrepancy. This is a trivial result. What is not trivial is that the other linear combination in G of eq. (33) is <u>uniquely</u> specified by the diagonalization. Now we can substitute eqs. (35) and (36) into eqs. (21) to calculate the confidence parameter $\bar{\lambda}$

$$\bar{\lambda} = \begin{cases} n/(g^T V g - n) = \delta^2/(\Delta^2 - \delta^2) & \text{if } |\Delta| > \delta \\ \infty & \text{if } |\Delta| < \delta \end{cases} \tag{37}$$

where n equals one because the rank of V is one. It should be pointed out that because of the invariance of the formulation of the method under linear transformations, built in via the prior probability $p(g|\lambda)$. The value of $\bar{\lambda}$ is independent of the bases chosen. Had we used the original definition of G, we would have still obtained the same result. Finally, we obtain the data of negligence discrepancy as

$$\bar{g} = \begin{cases} \dfrac{\Delta}{(\varepsilon_1^2 + \varepsilon_2^2)^{1/2}} \cdot \left(1 - \dfrac{\delta^2}{\Delta^2}\right) \\ \text{unknown} \end{cases} \tag{38}$$

$$\bar{V} = \begin{pmatrix} \dfrac{\varepsilon_1^2 + \varepsilon_2^2}{\delta^2}\Big/\left(1 - \dfrac{\delta^2}{\Delta^2}\right) & 0 \\ 0 & 0 \end{pmatrix} \tag{39}$$

where $|\Delta| \geq \delta$ is assumed otherwise both of them vanish.

APPENDIX

Here we shall present the argument for the proposed prior probability of eq. (2) based on the concept of information entropy. A basic theorem in information theory (Shanon's theorem[7]) states that under rather general requirements* of an appropriate definition of a measure of information, such as additivity and continuity, the existence and uniqueness of the measure can be proven. This unique measure, called information entropy, is shown to be

$$S_I = -\sum_i P_i \ln P_i \tag{A1}$$

where i stands for the ith outcome. (A nice discussion of the theorem is given in the book by Khinchin[8].) The most unbiased and therefore most reasonable probability distribution function is obtained by maximizing this information entropy S_I. If no information is available at all, maximizing S_I gives a uniform distribution independent of i. However, if there is information available (either theoretical or experimental), the information is imposed mathematically as auxiliary constraints. And S_I is maximized conditionally to give the most unbiased probability distribution function compatible with the constraints. An especially interesting case is when the expectation value F of a quantity f is measured

$$\langle f(x)\rangle = \sum_i P_i\, f(x_i) = F \tag{A2}$$

The conditional maximum leads to

$$P_i = P(x_i) = \text{normalization} \cdot \exp[-\lambda f(x_i)] \tag{A3}$$

where λ is the Lagrange multiplier that can be determined through eq. (A2) in terms of the expectation value F. A familiar example of this case is classical statistical mechanics where f is the energy of a system, λ turns out to be $1/kT$ and $P(x_i)$ the partition function of the familiar Maxwellian form. For further discussions and illustrations, readers are suggested to consult references 9,10 and 6.There is a well-known ambiguity as one goes from a discrete distribution to a continuous one; namely, the prior distribution may not be invariant with respect to transformation of its distribution variables[11]. This is resolved in our case by requiring the (posterior) joint probability distribution $p(g,\bar{g}|\lambda)$ be invariant under linear transformations. This is actually an unavoidable consistency condition on the formulation of the method.

In the auxiliary condition, eq. (A2), if we keep specifying higher order moments, the result will be like expanding the logarithm of the

---

* It is crucial for the proof that the least informative distribution is defined to be the uniform one.

probability function in a Tayler series. Thus, we could regard it as a way of constructing a probability function in terms of its moments. Usually the importance (in informativeness) of the moments is to decrease with the order of the moments. The moments can only be determined posteriorly when measurements are taken. Now we apply this idea to the prior probability distribution for the negligence discrepancy. Let us assume that only the first two moments will be sensitive to the data. Since the prior probability $p(\bar{g}|\lambda)$ represents our confidence on non-negligence, the mean value of $\bar{g}$ must be set at zero to mean non-negligence. The second moment indicates our confidence, which depends on how consistent statistically the two sets of data are and therefore is a priorily unknown. Thus in the auxiliary condition, $\langle(\bar{g} - 0)^2\rangle = D$, the moment D is an unknown parameter. The most unbiased distribution is therefore according to eq. (A3)

$$p(\bar{g}|\lambda) = \sqrt{\lambda}\, \exp(-\frac{1}{2}\lambda\bar{g}^2)$$

which is eq. (2).

REFERENCES

1. Y. A. Chao, "On the Treatment of Uncertainties in Adjusted Group Cross-sections Fitting Integral Measurements," Proceedings of the ANS Topical Conference on Advances in Reactor Physics, Gatlinburg, April, 1978, pp 245-257.
2. J. B. Dragt, J.W.M. Dekker, H. Gruppelaar and A. Janssen, Nucl. Sci. Eng., 62, 117 (1977) and references 10-16 therein.
3. J. Kuroi and H. Mitani, J. Nucl. Sci. Tech., 12, 663 (1975).
4. J. P. Chaudat, J. Y. Barre and A. Khairallah, Proceedings of the International Symposium on Physics of Fast Reactors, Tokyo, Japan, October 1973, pp 1207-1238.
5. For example, G.E.P. Box and G. C. Tiao, "Bayesian Inference in Statistical Analysis," Addison-Wesley Pub. Co., 1973.
6. A. Gandini, "Nuclear Data and Integral Measurements Correlation for Fast Reactors, Part 4: Second Order Adjustments and Systematic Errors," preprint RT/F1 (78) 10 of Comitato Nazionale Energia Nucleare-C.S.N. Casaccia, Rome, Italy,1978
7. C. E. Shanon, Bell System Tech. J. 27, 379, 623 (1948).
8. A. I. Khinchin, Mathematical Foundations of Information Theory, Dover Publications, Inc. (1957).
9. E. T. Jaynes, 1962 Brandies Lectures, Vol. 3 (Statistical Physics), p 181, W. A. Benjamin, Inc., (1963).
10. Y. A. Chao, "Application of Information Theory to High-Energy Inclusive Phenomenology," Nucl.Phys. B40, 475 (1972), Section 2.
11. E. T. Jaynes, IEEE Transactions on Systems Science and Cybernetics, Vol. SSC-4, No. 3, September 1968.

SENSITIVITY THEORY FOR DEPLETION ANALYSIS*

M. L. Williams, J. R. White, J. H. Marable, E. M. Oblow
Oak Ridge National Laboratory
Oak Ridge, Tennessee, USA

ABSTRACT

This study discusses a general perturbation theory for two of the common approximations used in burnup analysis. In this text these types are called the uncoupled and the coupled formalisms. The distinction lies in how the interaction between the nuclide and neutron fields is treated. It is shown that based on the coupled approximation three adjoint equations (for the flux shape, the flux normalization, and the nuclide density) are required to fully develop a perturbation theory which accounts for the coupled variations in the neutron and nuclide fields, arising from variations in initial conditions and nuclear data. The adjoint equations are derived in detail using a variational principle.

A sensitivity methodology is established which seeks to estimate the change in various computed quantities when the input parameters to the burnup calculation are varied. The perturbation expressions are used to define sensitivity coefficients for responses that depend on the coupled interaction between the neutron and nuclide fields. The relation between coupled and non-coupled sensitivity theory is illustrated.

I. INTRODUCTION

The area of nuclear engineering known as burnup analysis is concerned with predicting the long-term isotopic changes in the material composition of a reactor. Analysis of this type is essential in order to determine optimum fissile loading, efficient refueling schedules, and a variety of operational characteristics that must be known to ensure safe and economic reactor performance. Burnup physics is unique in that it is concerned not only with computing values for the neutron flux field within a reactor region, but also with computing the time-dependent behavior of the nuclide-density field. In general the flux and nuclide fields are coupled nonlinearly, and solving the so-called burnup equations is quite a formidable task which must be approached with approximate techniques.

*Research sponsored by the U.S. DOE Division of Reactor Research and Technology under contract W-7405-eng-26 with the Union Carbide Corporation.

It is the purpose of this paper to summarize the development of various methodologies that allow extension of sensitivity theory to include depletion analysis. Details of different derivations and applications can be found in the list of references.

The specific approaches discussed in the present study are the time-continuous, coupled case; the uncoupled case; and the time-discontinuous coupled case.

II. THE NONLINER SYSTEM OF BURNUP EQUATIONS

The purpose of this section is to review the burnup equations, expressing them in the operator form which will be followed throughout this study. We are interested in the interaction between the neutron flux field and the nuclide density field, both of which change with time and both of which influence the other.

A material reactor region is completely described by its nuclide density vector, which is defined by

$$\underline{N}(\hat{r},t) = \left(N_1(\hat{r},t),\ N_2(\hat{r},t),\ \ldots,\ N_n(\hat{r},t)\right) \tag{1}$$

where $N_i(\hat{r},t)$ = atom density of nuclide i at position $\hat{r}$ and time t.

While in operation, the reactor volume will also contain a population of neutrons whose distribution is described by the neutron flux field $\phi(\hat{\rho})$, where

$\hat{\rho}$ = vector in the 7-dimensional phase space of $(\hat{r},\ t,\ \hat{\Omega},\ E)$.

Note that the phase space over which $\underline{N}$ is defined is a subdomain of ρ-space.

Given an initial reactor configuration that is described by $\underline{N}_o(\hat{r})$ at t = 0, and that is exposed to the neutron flux field for $t \geq 0$, all future reactor configurations, described by the nuclide field $\underline{N}(\hat{r},t)$, will obey the nuclide transmutation equation (Bateman equation)*

$$\frac{\partial}{\partial t}\underline{N}(\hat{r},t) = [\phi(\hat{\rho})\underline{\underline{R}}(\sigma)]_{E,\Omega}\,\underline{N}(\hat{r},t) + \underline{\underline{D}}(\Lambda)\underline{N}(\hat{r},t) + \underline{C}(\hat{r},t) \tag{2}$$

where

$\underline{\underline{R}}$ is a cross section matrix whose elements are

$\sigma_{ij}(\hat{r},E)$ = microscopic cross section and yield data for production of nuclide i by nuclide j, and

$\sigma_{ii} = -\sigma_{ai}$ = absorption cross section for nuclide i

*$[\ \ ]_{x,y,\ldots}$ indicates integration over x,y,... .

$\underline{\underline{D}}$ is a decay matrix whose elements are

Λ_{ij} = decay constant for decay of nuclide j to nuclide i, and

$\Lambda_{ii} = -\Lambda_i$ = total decay constant for nuclide i

$\underline{C}(\hat{r},t)$ is an external source of nuclides, accounting for refueling, control rod motion, etc.

We will find it convenient to define a transmutation operator by

$$\underline{\underline{M}} = \underline{\underline{M}}(\phi(\hat{\rho}),\ \sigma(\hat{r},E),\ \Lambda) = [\phi(\hat{\rho})\underline{\underline{R}}(\sigma)]_{E,\Omega} + \underline{\underline{D}}(\Lambda) \quad . \tag{3}$$

Then the equation for the nuclide field vector becomes

$$\frac{\partial}{\partial t}\underline{N}(\hat{r},t) = \underline{\underline{M}}(\phi,\sigma,\Lambda)\underline{N}(\hat{r},t) + \underline{C}(\hat{r},t) \quad . \tag{4}$$

The neutron flux field is assumed to obey the homogeneous time-dependent transport equation expressed by (as usual for depletion analysis, the delayed neutrons and time derivative of the flux are ignored),

$$\hat{\Omega}\cdot\nabla\phi(\hat{\rho}) + \underline{N}(\hat{r},t)\cdot\underline{\sigma}_t(\hat{r},E)\phi(\hat{\rho}) = \tag{5}$$
$$\underline{N}(\hat{r},t)\cdot\left[\underline{\sigma}_s(\hat{r},E',\Omega'\to E,\Omega)\ \phi(\hat{\rho}) + \frac{\chi(E)}{4\pi}\ \underline{\nu\sigma}_f(E')\phi(\hat{\rho})\right]_{E',\Omega'}$$

where

$\underline{\sigma}_t$ is the total cross-section vector, whose components are the total microscopic cross sections corresponding to the components of $\underline{N}$,

$\underline{\sigma}_s$ is the differential scatter cross-section vector,

$\underline{\nu\sigma}_f$ is the fission-production cross-section vector,

and

$\chi(E)$ = neutron fission spectrum.

Defining the Boltzmann operator in the indicated manner, $B = B[\underline{N}(r,t),\underline{\sigma}(r,E)]$, Eq. (5) becomes

$$B(\underline{N})\phi(\hat{\rho}) = 0 \quad . \tag{6}$$

Equation (6) is homogeneous and thus at any given time will have nontrivial solutions only for particular values (an infinite number) of $\underline{N}$. To simulate the effect of control-rod motion, we will single out one of the components of $\underline{N}$ which will be designated the control nuclide N_c. Also, we will express the B operator as the sum of a fission operator and a loss plus inscatter operator:

$$B = L - \lambda F \quad , \tag{7}$$

so that Eq. (6) becomes

$$\left[L(\underline{N},N_c) - \lambda F(\underline{N},N_c)\right]\phi(\rho) = 0 \quad , \tag{8}$$

where

$$\lambda = \frac{1}{k_{eff}} = \text{instantaneous lambda mode eigenvalue.}$$

The value for N_c is usually found indirectly by adjusting its magnitude until $\lambda = 1$. The concentration of the control nuclide is thus fixed by the eigenvalue equation and does not need to be considered as an unknown in the transmutation equation.

An alternate method of solving Eq. (6) is to directly solve the lambda mode eigenvalue equation (given $\underline{N}$, λ is sought from Eq. 8). In this case λ may or may not equal one. For both of these techniques, only the flux shape can be found from Eq. (8), i.e., Eq. (8) alone is not sufficient to fix the normalization of the flux. We will find it convenient to write $\phi(\rho)$ as the product of a time-dependent normalization factor and a shape function which is the solution to Eq. (8), normalized to unity:

$$\phi(\rho) = \Phi(t)\ \psi(\rho) \quad . \tag{9}$$

The magnitude of $\Phi(t)$ is determined by fixing the power output of the reactor to be constant:

$$\left[\underline{N}(r,t)\cdot\underline{\sigma}_f(\hat{r},E)\phi(\rho)\right]_{E,\Omega,V} \equiv F(\underline{N},\underline{\sigma}_f,\psi)\cdot\Phi = P \quad . \tag{10}$$

In this study, the system of coupled, non-linear equations given by Eqs. (4), (8), and (10) is referred to as the time-continuous burn-up equations, because the flux is a continuous function of time. The equations expressed in matrix notation are:

$$\begin{bmatrix} B(\underline{N},\alpha) & 0 & 0 \\ 0 & F(\underline{N},\psi,\alpha) & 0 \\ 0 & 0 & \underline{\underline{M}}(\Phi,\psi,\alpha) \end{bmatrix} \begin{bmatrix} \psi \\ \Phi \\ \underline{N} \end{bmatrix} = \begin{bmatrix} 0 \\ P \\ \frac{\partial}{\partial t}\underline{N} \end{bmatrix} \tag{11}$$

where α stands for any arbitrary nuclear data used in the calculation.

III. SENSITIVITY THEORY FOR COUPLED NEUTRON/NUCLIDE FIELDS

The desired end result of virtually all design calculations is an estimated value for some set of reactor performance parameters. Each such parameter will be called a "response" in this study. For the case of burnup analysis, the generic response will be an integral of the flux and nuclide fields; i.e., it is mathematically a functional of both fields, which in turn are coupled through the respective field equations. As an example, the desired response may be the final ^{239}Pu mass at shutdown (a pure nuclide response); it may be the time-integrated damage to some non-depleting structural component (a flux response); or it may be some macroscopic reaction rate (a nuclide and flux functional). These functionals all take the general form of

$$R = R\left[\phi(\hat{\rho}),\ \underline{N}(\hat{r},t),\ \underline{h}\right] \quad . \tag{12}$$

In these expressions $\underline{h}$ is a "realization vector" which can have the form of a cross section or of some unit vector which determines the response of interest. A discussion of some explicit forms for response functionals and their associated realization vectors appears in ref. 1.

It is the goal of sensitivity analysis to find the effect that varying some nuclear data parameter (e.g., a cross section, a decay constant, a branching ratio, etc.) will have on the response R. This will be accomplished by defining a "sensitivity coefficient" for the data in question, which will relate the percent change in R to the percent change in the data.

For example, let α be a nuclear data parameter contained in either or both the B and the $\underline{\underline{M}}$ operators. Then the sensitivity of R to α is given by

$$\delta R/R = \left[S_\alpha(\hat{\rho})\ \frac{\delta\alpha}{\alpha}\ (\hat{\rho})\right]_\rho + \text{second-order terms} \quad . \tag{13}$$

For small $\delta\alpha$, we obtain the familiar linear relation between $\delta R/R$ and $\delta\alpha/\alpha$, with $S_\alpha(\hat{\rho})$ serving as the sensitivity coefficient at position $\hat{\rho}$ in phase space. A change in the value of α in general will perturb both the nuclide and flux fields in some complex manner, depending on the specific $\delta\alpha(\hat{\rho})$.

Treating the response as an implicit function of α, $\underline{N}$, ψ, and Φ, the differential of R to first order is

$$\Delta R = \left[\frac{\partial R}{\partial\alpha}\,\Delta\alpha + \frac{\partial R}{\partial\psi}\,\Delta\psi + \frac{\partial R}{\partial\Phi}\,\Delta\Phi + \frac{\partial R}{\partial\underline{N}}\cdot\Delta\underline{N}\right]_\rho \quad . \tag{14}$$

It is important to realize that the variations in α, ψ, Φ, and N are in general not independent. This can be seen by considering perturbations about some reference state described by Eq. (11). After linearizing the perturbed expressions, Eq. (11) reduces to

$$\begin{bmatrix} B & 0 & \frac{\partial B}{\partial \underline{N}}\psi \\ \frac{\partial F}{\partial \psi}\Phi & F & \frac{\partial F}{\partial \underline{N}}\Phi \\ \frac{\partial \underline{\underline{M}}}{\partial \psi}\underline{N} & \frac{\partial \underline{\underline{M}}}{\partial \Phi}\underline{N} & \underline{\underline{M}} \end{bmatrix} \begin{bmatrix} \Delta\psi \\ \Delta\Phi \\ \Delta\underline{N} \end{bmatrix} = \frac{\partial}{\partial t}\begin{bmatrix} 0 \\ 0 \\ \Delta\underline{N} \end{bmatrix} - \begin{bmatrix} \frac{\partial B}{\partial \alpha}\psi \\ \frac{\partial F}{\partial \alpha}\Phi \\ \frac{\partial \underline{\underline{M}}}{\partial \alpha}\underline{N} \end{bmatrix}\Delta\alpha \quad . \tag{15}$$

In theory the above system of equations could be solved and ΔR estimated using Eq. (14). In reality this is not practical since the "source" on the right-hand side of the equation depends on α. Instead, it is much more efficient to use the adjoint system to define sensitivity coefficients independent of the particular data being perturbed.

IV. TIME-CONTINUOUS ADJOINT EQUATIONS

Consider the following inhomogeneous system of equations, adjoint[a] to Eq. (15):

$$\begin{bmatrix} B^* & \left(\frac{\partial F}{\partial \psi}\Phi\right)^* & \left(\frac{\partial \underline{\underline{M}}\,\underline{N}}{\partial \psi}\right)^* \\ 0 & F^* & \left(\frac{\partial \underline{\underline{M}}\,\underline{N}}{\partial \Phi}\right)^* \\ \left(\frac{\partial B}{\partial \underline{N}}\psi\right)^* & \left(\frac{\partial F}{\partial \underline{N}}\Phi\right)^* & \underline{\underline{M}}^* \end{bmatrix} \begin{bmatrix} \Gamma^* \\ P^* \\ \underline{N}^* \end{bmatrix} = -\frac{\partial}{\partial t}\begin{bmatrix} 0 \\ 0 \\ \underline{N}^* \end{bmatrix} - \begin{bmatrix} \frac{\partial R}{\partial \psi} \\ \frac{\partial R}{\partial \Phi} \\ \frac{\partial R}{\partial \underline{N}} \end{bmatrix} \quad . \tag{16}$$

Note that the "adjoint source" (i.e., the second term on RHS) depends only on the response of interest. This specific form for the source was chosen for the following reason: multiply Eq. (15) by (Γ^*, P^*, $\underline{N}^*$) and Eq. (16) by ($\Delta\psi$, $\Delta\Phi$, $\Delta\underline{N}$); integrate over Ω, E, and V; and subtract,

$$\frac{\partial}{\partial t}\,[\Delta\underline{N}\cdot\underline{N}^*]_V - \left[\left(\Gamma^*\frac{\partial B\psi}{\partial \alpha} + P^*\frac{\partial F}{\partial \alpha}\Phi + \underline{N}^*\frac{\partial \underline{\underline{M}}\,\underline{N}}{\partial \alpha}\right)\Delta\alpha\right]_{\Omega,E,V}$$

$$+ \left[\frac{\partial R}{\partial \psi}\Delta\psi + \frac{\partial R}{\partial \Phi}\Delta\Phi + \frac{\partial R}{\partial \underline{N}}\Delta\underline{N}\right]_{\Omega,E,V} = 0 \quad . \tag{17}$$

Defining $\underline{N}^*(t=T_f) = 0$, Eq. (17) can be integrated over time and simplified using Eq. (14) to

$$\Delta R/R = \left[\Delta\underline{N}_o\cdot\underline{N}^*\right]_V + \int\left[\frac{\alpha}{R}\left(\frac{\partial R}{\partial \alpha} + \frac{\Gamma^*\partial B\psi}{\partial \alpha} + \frac{P^*\partial F}{\partial \alpha}\Phi + \underline{N}^*\frac{\partial \underline{\underline{M}}\,\underline{N}}{\partial \alpha}\right)\frac{\Delta\alpha}{\alpha}\right]_{\Omega,E,V} dt \tag{18}$$

and thus

$$S_\alpha(\rho) = \frac{\alpha}{R}\left(\frac{\partial R}{\partial \alpha} + \frac{\Gamma^*\partial B\psi}{\partial \alpha} + \frac{P^*\partial F}{\partial \alpha}\Phi + \underline{N}^*\frac{\partial}{\partial \alpha}\underline{\underline{M}}\,\underline{N}\right) \quad .$$

---

[a] "*" indicates an adjoint operator, defined by $[fLg]_\rho = [gL^*f]_\rho$.

Having defined the appropriate sensitivity coefficient, the depletion sensitivity and uncertainty analyses proceed as in the well known static case.

We have shown that for the time-continuous case, the appropriate adjoint equations are quite easy to derive — they are simply the equations arising from transposing the linearized forward system, and then taking the adjoint operator for each matrix element. Similar equations have been derived earlier by Lewins;[2] and more recently Harris[3] has applied related equations to analysis of fuel cycle cost. However, for complex reactor depletion studies these equations are not practical, since the flux shape equation (space-energy dependent) must be solved at every instant in time. In reality this is not done; instead, suitable approximations are made. Two methods which appear most attractive for depletion sensitivity analysis will be discussed next.

V. UNCOUPLED PERTURBATION THEORY FOR THE NUCLIDE FIELD

The uncoupled perturbation formalism assumes that the flux and nuclide fields can vary independently about the reference state (this does not exclude a coupled, non-linear calculation to determine the reference state). Mathematically, this amounts to neglecting the off-diagonal terms in Eq. (15). The adjoint system is then described by a diagonal matrix, and hence there is no coupling between the various adjoint functions. If we further assume that the response of interest depends explicitly only on the nuclide field, then the sensitivity coefficient becomes[1]

$$S(\rho) = \underline{N}^* \frac{\partial}{\partial \alpha} \underline{\underline{M}}\, \underline{N} \quad , \tag{19}$$

where $\underline{N}^*$ obeys the final value problem

$$\underline{\underline{M}}^* \underline{N}^* = - \frac{d}{dt} \underline{N}^* - \frac{\partial R}{\partial \underline{N}} , \quad \underline{N}^*(T_f) = 0 \quad .$$

This equation has been derived by Gandini[4] for the case when R is a delta function in time. For application of the methodology to sensitivity and uncertainty analysis, see references 5 and 6.

VI. SENSITIVITY THEORY FOR COUPLED NEUTRON/NUCLIDE FIELDS: "QUASI STATIC" FORMULATION

As previously stated, the adjoint equations in (16) cannot be solved economically because the time scale for the flux calculation has the same hierarchy as the calculation for the nuclide field. In realistic burn-up calculations, solving the transport (or diffusion) equation accounts for the majority of computing cost; and therefore the usual procedure is to solve a "quasi-static depletion" (not to be confused with quasi-static kinetics) problem, rather than the time-continuous problem.

The quasi-static problem is formulated by breaking the time domain into a number of "broad-time intervals":

$$\left\{ (0,t_1),\ (t_1,t_2),\ \ldots\ (t_i,\ t_{i+1}),\ \ldots\ (t_{F-1},\ T_F) \right\} . \tag{20}$$

Over each broad interval, it is assumed that the flux does not change with time:

$$\phi(\rho) \ = \ \Phi_i\ \psi_i(r,E,\Omega) \quad , \qquad t_i^+ < t < t_{i+1}^- \quad . \tag{21}$$

Note the discontinuity in the flux at each time boundary. The ith shape function is found by solving Eq. (8) at $t = t_i$, and the normalization is determined by Eq. (10) at $t = t_i$.

Over each broad time interval, the nuclide field is computed from the transmutation equation with the initial condition for the interval set equal to the final value for the previous interval:

$$\underline{\underline{M}}(\Phi_i,\psi_i)\ \underline{N} \ = \ \frac{d}{dt}\underline{N} \qquad\qquad t_i^+ < t < t_{i+1}^- \tag{22}$$

$$\underline{N}(t_i^+) \ = \ \underline{N}(t_i^-) \quad . \tag{23}$$

The nuclide field is continuous across the time boundaries.

This procedure is employed by virtually all space-energy dependent depletion codes; and therefore to be consistent, the adjoint burnup equations should also be derived from the quasi-static formulation.

For the derivation, we will use a variational technique described by Pomraning[7] and Stacey.[8] With this method, the quasi-static burnup equations are treated as constraints on the response and as such are appended to the response functional using Lagrange multipliers. We will specifically examine the case in which the shape function is obtained by solving the lambda mode eigenvalue equation, rather than the case in which ψ is obtained from a control variable ("N_c") search. The two cases are quite similar, the only difference being that the latter has a "k-reset." (See reference 9 for details.)

Let us consider the following functional

$$\begin{aligned} K[\underline{N},\ \psi_i,\ \Phi_i,\ \alpha,\ \lambda,\ h] \ &= \ R[\underline{N},\ \psi_i,\ \Phi_i,\ h] \\ &+ \sum_{i=1}^{T} \int_{t_i^+}^{t_{i+1}^-} \left[dt\ \underline{N}^*(\hat{r},t)\ \left([\psi_i \underline{\underline{R}}]_{E,\Omega}\ \Phi_i + \underline{\underline{D}} - \frac{\partial}{\partial t} \right) \underline{N}(\hat{r},t) + \underline{C} \right]_V dt \\ &- \sum_{i=1}^{T} \left[\Gamma_i^*(\hat{\rho})\ \left(L(\underline{N}_i) - \lambda_i F(\underline{N}_i) \right)\ \psi_i(\hat{\rho}) \right]_{\Omega,E,V} \\ &- \sum_{i=1}^{T} P_i^* \left([\psi_i\ \underline{\sigma}_f\ \underline{N}_i]_{\Omega,E,V}\ \Phi_i - P_i \right) - \sum_{i=1}^{T} a_i \left([\psi_i]_{\Omega,E,V} - 1 \right) \end{aligned} \tag{24}$$

where

T = number of broad intervals in the quasi-static calculation,

$\underline{N}_i = \underline{N}(\hat{r},t_i)$, and

$\underline{N}^*(\hat{r},t)$, $\Gamma_i^*(\rho)$, P_i^* are the Lagrange multipliers.

Expanding the perturbed functional K' about the unperturbed state, and neglecting second-order terms, we obtain

$$K' = K + \left[\frac{\partial K}{\partial \alpha}\ \delta\alpha + \frac{\partial K}{\partial \underline{N}}\ \delta\underline{N} + \frac{\partial K}{\partial \underline{h}}\ \delta\underline{h} + \sum\left(\frac{\partial K}{\partial \psi_i}\ \delta\psi_i + \frac{K}{\partial \Phi_i}\ \delta\Phi_i + \frac{\partial K}{\partial \lambda_i}\ \delta\lambda_i\right)\right] \tag{25}$$

If we can force the quantities $\partial K/\partial \underline{N}$, $\partial K/\partial \psi_i$, $\partial K/\partial \Phi_i$, $\partial K/\partial \lambda_i$ to vanish, then (see ref. 9)

$$\delta R/R = \left[\frac{\alpha}{R}\left(\frac{\partial K}{\partial \alpha} + \frac{\partial R}{\partial \underline{h}}\frac{\partial \underline{h}}{\partial \alpha}\right)\frac{\delta\alpha}{\alpha}\right]_\rho \quad . \tag{26}$$

The conditions which make K stationary to variations in the indicated variables are given below:

$$1.\quad \frac{\partial K}{\partial \Phi_i} = 0 \rightarrow P_i^* = \frac{\displaystyle\int_{t_i^+}^{t_{i+1}^-} \left[\underline{N}^*[\psi_i \underline{\underline{R}}]_{\Omega,E}\ \underline{N}\right]_V dt + \frac{\partial R}{\partial \Phi_i}}{[\psi_i\ \underline{\sigma}_f\ \underline{N}_i]_{\Omega,E,V}} \quad \text{at } t = t_i \tag{27}$$

$$2.\quad \frac{\partial K}{\partial \psi_i} = 0 \rightarrow \left\{L^*(\underline{N}_i) - \lambda_i F^*(\underline{N}_i)\right\}\ \Gamma_i^*(\hat{\rho}) = Q_i^* \ , \quad \text{at } t = t_i \tag{28}$$

where

$$Q_i^*(\hat{\rho}) = \frac{\partial R}{\partial \psi_i} + \Phi_i \int_{t_i^+}^{t_{i+1}^-} \underline{N}^*(\hat{r},t)\ \underline{\underline{R}}(\sigma)\ \underline{N}(\hat{r},t)dt - \Phi_i P_i^*\ \underline{\sigma}_f\ \underline{N}_i - a_i \tag{29}$$

At this point is should be noted that Eqs. (29) and (8) require that the flux shape function be orthogonal to the adjoint source, i.e.,

$$[\psi_i\ Q_i^*]_{\Omega,E,V} = 0 \ , \text{ at all } t_i \ .$$

It is easily shown that this condition implies

$$\left[\psi_i \frac{\partial R}{\partial \psi_i}\right]_{E,\Omega,V} - \Phi_i \left[\frac{\partial R}{\partial \Phi_i}\right]_{E,\Omega,V} = a_i \tag{30}$$

which fixes the value of "a". For most cases of practical interest, this term is zero. For example if R is bilinear in ψ_i and Φ_i, or is a bilinear ratio, then "a" will vanish.

$$3. \quad \frac{\partial K}{\partial \lambda_i} = 0 \rightarrow [\Gamma_i^*(\hat{\rho})\ F(\underline{N}_i)\ \psi_i]_{\Omega,E,V} = 0 \ , \tag{31}$$

which forces $\Gamma_i^*(\hat{\rho})$ to be orthogonal to the fission source at $t = t_i$.

$$4. \quad \frac{\partial K}{\partial \underline{N}} = 0 \rightarrow \underline{\underline{M}}^* \ \underline{N}^* + \frac{\partial R}{\partial \underline{N}} = -\frac{\partial}{\partial t} \underline{N}^* \ , \ t_i < t < t_{i+1}^- \tag{32}$$

together with the time boundary conditions

$$\underline{N}^*(T_f) = 0, \text{ at } t = T_f \quad , \tag{33}$$

and

$$\underline{N}^*(\hat{r},t_i^-) = \underline{N}^*(\hat{r},t_i^+) - \left[\Gamma_i^* \frac{\partial}{\partial \underline{N}_i} (L - \lambda F)\psi_i + \Phi_i\ P_i^*\ \underline{\sigma}_f\ \psi_i\right]_{\Omega,E} \quad \text{at } t_i,\ i \neq f \tag{34}$$

The above expression specifies a "jump condition" on the nuclide adjoint.

In summary, we have shown that there exist adjoint equations corresponding to the nuclide transmutation equation, to the flux-shape equation (transport equation), and to the power-constraint equation. In addition, we have found that it is convenient to ascribe additional restrictions on the adjoint fields--namely, that Γ_i^* be orthogonal to the fission source and that $\underline{N}^*$ be discontinuous at each time boundary. The adjoint field equations are coupled, linear equations which contain the unperturbed forward values for $\underline{N}$, ψ_i, and Φ_i. An appropriate algorithm for solving these equations is given in reference 9.

As an example of a data sensitivity coefficient, consider the hypothetical data $\alpha(r,E)$. The sensitivity coefficient for α is

$$S_\alpha(\hat{r},E) = \frac{\partial R}{\partial \alpha(r,E)} +$$

$$+ \sum_i \int_{t_i^+}^{t_{i+1}^-} \underline{N}^*(\hat{r},t) \frac{\partial}{\partial \alpha(r,E)} \underline{\underline{M}}_i \ \underline{N}(\hat{r},t)dt$$

$$-\sum_i \left[\Gamma_i^* (\hat{\rho}) \frac{\partial}{\partial\alpha(r,E)} B_i \psi_i (\hat{\rho})\right]_\Omega$$

$$-\sum_i P_i^* \left[\psi_i (\hat{\rho}) \frac{\partial}{\partial\alpha(r,E)} \underline{\sigma}_f \underline{N}_i (\hat{r})\right]_\Omega . \tag{35}$$

VII. SUMMARY

Sensitivity coefficients have been obtained for responses which are functionals of both the neutron and nuclide fields, as encountered in depletion analysis. The sensitivity coefficients are defined using first-order perturbation expressions containing various "adjoint functions," which are computed independently of any specific data perturbation. Equations for the adjoint functions were derived for several formulations of the burnup equations.

The technique for depletion sensitivity analysis appears to have potential in assessing uncertainties in depletion related responses, and in relating changes in beginning of life composition to changes in performance parameters at end of life. The latter case could be useful in fuel cycle optimization and in design scoping studies.

REFERENCES

1. M. Williams, C. Weisbin, "Sensitivity and Uncertainty Analysis for Functionals of the Time-Dependent Nuclide Density Field," ORNL-5393 (1978).

2. J. Lewins, "A Variational Principle for Non-Linear Systems," Nuclear Science and Engineering 12, 10-14, (1962).

3. D. R. Harris, "Sensitivity of Nuclear Fuel Cycle Costs to Uncertainties in Data and Methods," Ph.D. thesis, Rensselaer Polytechnic Institute, 1976.

4. A. Gandini, "Time-Dependent Generalized Perturbation Theory for Burn-up Analysis," CNEN RT/FI(75) 4, CNEN, Rome (1975).

5. L. Tondinelli, "Sensitivity of Actinide Concentration during Burn-up with Respect to Nuclear Data," CNEN RT/FI(76) 1, CNEN Rome (1976).

6. M. Williams, S. Raman, "Calculational and Experimental Analysis of ^{239}Pu Sample Irradiated in EBR II," Vol. 28, Transactions Winter ANS meeting, Washington, D. C., Nov., 1978.

7. G. Pomraning, "Variation Principle for Eigenvalue Equations," J. Math. Phys. 8, 149 (1967).

8. W. Stacey, Variational Methods in Nuclear Reactor Physics, Academic Press, N.Y., 1974.

9. M. Williams, "Development of Depletion Perturbation Theory for Coupled Neutron-Nuclide Fields," Submitted to Nuclear Science and Engineering, August 1978.

EXPECTATIONS FOR ENDF/B-V COVARIANCE FILES: COVERAGE, STRENGTH AND LIMITATIONS*

F. G. Perey
Oak Ridge National Laboratory
Oak Ridge, Tennessee 37830 U.S.A.

ABSTRACT

The concept of the estimated data covariance files of ENDF/B is explored in detail. The relationship between uncertainties and "possible mistakes" is discussed in order to avoid likely misunderstanding concerning the use of the data covariance files. Some perceived strengths and weaknesses of the ENDF/B-V data covariance files are mentioned.

INTRODUCTION

It has long been perceived that an important contribution to the uncertainties we should associate with the results of most neutronic calculations arises from the uncertainties in the nuclear data used as input. The Cross Section Evaluation Working Group, CSEWG, several years ago decided to investigate the possibility of improving its method of communication with users in the area of the estimated uncertainties in the evaluated data files it produces. Until ENDF/B-IV the only method the evaluators had available to them for communicating such information was through the documentation of the evaluations. During the preparation of ENDF/B-IV a subcommittee was appointed to make recommendations in this area. The initial effort was directed toward a standardization of the reporting method in the documentation. It was only after considerable debate that the concept of incorporating the information with the "data files" on the tape was approved. There were two major factors which influenced this decision. The first one was that the dominant features of the uncertainties are the correlations in the data and these are not easily handled in the documentation. The second one was that the uncertainty information needs to be processed together with the differential data to obtain the uncertainties in the quantities of interest to the users. It has been a major goal of the Data Covariance Subcommittee of the CSEWG, of which I am the current chairman, to develop a formalism whereby the evaluators could communicate the uncertainties in their evaluations in such a way that they could be readily processed. For

---

*Research sponsored by the Division of Reactor Research and Technology, U. S. Department of Energy, under contract W-7405-eng-26 with the Union Carbide Corporation.

ENDF/B-IV only three general purpose evaluations were released with some covariance files, C, N, and O. These were prepared at Oak Ridge and Los Alamos and very little pressure was exerted on evaluators to avail themselves of this new facility to report estimated uncertainties. Much additional work went on at both Los Alamos and Oak Ridge to generate more of these files for ENDF/B-IV, but much of it was in-house effort to investigate the potential usefulness of this kind of data. The general conclusion reached at both Los Alamos and Oak Ridge was that the concept of these files was quite sound and worth the effort put into them. Consequently, much pressure is being put to bear upon the evaluators of ENDF/B-V to contribute covariance files with their evaluations. I am pleased to report that the response has been very good and it is the purpose of this paper to share some of our expectations concerning the ENDF/B-V covariance files.

THE CONCEPT OF DATA COVARIANCES

It has been tacitly assumed for the many years that the subject has been under consideration within the CSEWG that a major problem was the representation of the uncertainty data in the files. Certainly this problem of representation had to be overcome and it has taken a lot of effort within the Data Covariance Subcommittee to develop a solution to it since there was no procedent to guide us. A report is available describing the formats and procedures adopted for ENDF/B-V[1] in order to represent the estimated uncertainties in the evaluated data. We shall not go here into the details of these formats. They were based upon a thorough analysis of the methods used to obtain estimated uncertainties in the results of experiments (including their correlations), the evaluation process, and by giving full consideration to the fact that the data need to be processed.

It has been our experience with the CSEWG community of measurers, evaluators and users that even though the concept of "errors" in experimental and evaluated data seems to be very familiar to all, many difficulties tend to arise when their meaning and uses are discussed. The only motivation for providing in ENDF/B a quantitative and precise measure of the uncertainties in the evaluated data was the perceived need for such data in order to use evaluations to achieve meaningfully and credibly some specific and useful goals. During the early discussions within the CSEWG some strong reservations were expressed by many members about this new endeavor because of fears that the data may be misused. Of course the CSEWG cannot prevent the data from being misused, but we find some justification for concern in this area in view of the apparent sharp differences of opinion as to what the uncertainty data mean and can be justifiably used for. A survey of the literature indicates that these diverging opinions are not specific to the CSEWG members, but are quite general throughout the nuclear community. With the impending release of ENDF/B-V and the fairly large amount of covariance files it will contain, the Data Covariance Subcommittee of the CSEWG has

the responsibility to attempt to clarify the situation. In this communication we cannot provide the comprehensive treatment that this subject requires and we will do so elsewhere.[2] We will only share here some thoughts and make a few suggestions which we believe will help greatly.

Very early in the discussions within the CSEWG about data uncertainties we discovered that many misunderstandings could be alleviated if we were very careful about the terminology we use. Since uncertainties are such a frequent occurrence in daily life (they underly practically all of our activities) we have acquired a common vocabulary to deal with them which is familiar to everyone. Therefore, when discussing uncertainties, very few people feel any compulsion to define exactly what they mean when they use words which may have several different meanings, the exact meaning being often clear only from the context in which the words are used. Many misunderstandings with respect to data uncertainties occur because we have not yet learned to identify which meaning must be applied to each word. For this reason we have found it more convenient to use very technical terms not used in the common language and to avoid words which have several different meanings substituting for them synonyms which are less ambiguous. This is the reason we decided to use the term "estimated data covariances" instead of "estimated errors." You will find the covariance files occasionally still referred to as "error files" as they were originally called. We think that the use of the word "error," by itself or with qualifiers, is very frequently the cause of misunderstandings and should be banned from any technical discussion where it is possible to interpret it in two totally different ways: as uncertainty or mistake. These synonyms should be used instead as the case may be. We have unfortunately many occasions to use the word mistake in our work. The word mistake should also very often be used with qualifiers. Mistakes fall into two categories: they are either "known mistakes" or "suspected mistakes." There is only one known remedy for mistakes — they must be eliminated (i.e., corrected). This is clearly possible for "known mistakes" in many cases. It is clearly not possible to correct "suspected mistakes" which still remain unidentified, and unfortunately often many known mistakes also cannot be corrected because of lack of appropriate data to do so. The subject of "suspected mistakes" is a very important one which unfortunately we cannot fully explore here and in any event is totally irrelevant to our discussion of the concept of "estimated data covariances" since these deal with uncertainties and not mistakes. In fact, we will show that the covariance information is only valid if no mistakes, known or suspected, have been made in obtaining them.

We shall now indicate what the covariance files are purported to be. In the covariance files the evaluator provides a measure of the uncertainty in the data. What is exactly the meaning of uncertainty? The uncertainty assigned to the value of a quantity is related to how confident we are, on the basis of the information available, that this value corresponds to the unknown true value. In the process of "deriving" the value of the quantity from whatever specific information we have we must often make some assumptions because the information is in some sense incomplete since

it does not allow us to deduce the true value. It does not make any sense to think that these assumptions are right or wrong on the basis of the information we have, and all we can do is assign to them a degree of plausibility. The degree of plausibility associated to these assumptions is, in a direct way, a measure of the "completeness" of the information we have. It is perfectly natural to use the language of probability theory to designate these levels of confidence or degree of plausibility. The estimated values of the data and its uncertainty can be used to define an estimated probability density function for the "true value" of the quantity which we do not have. The job of the evaluator is to assemble all of the information available about the quantities of interest and use it to estimate the joint probability density function for their values. We say joint probability density function because many of the uncertainties impact upon several of the quantities and therefore lead to important correlations. The evaluated files contain the estimated expectation values and estimated covariances corresponding to this joint probability density function.

We have just described the evaluations without introducing the idea of mistakes or the concept of probabilities based upon frequency distributions as is done in statistics and will discuss briefly these points. It is clear that we can make mistakes in our evaluation work; if we do, then the evaluations are wrong and we must correct these mistakes. The important point to remember is that the uncertainties in the file are a quantitative statement based upon the completeness of the information available to the evaluator and in no way whatsoever correspond to a statement he makes about his or anybody else's actual or suspected mistakes. Therefore to interpret or use the files as a statement concerning mistakes is totally wrong. It is evident to anyone familiar with the experimental techniques and evaluation work that for practically all of the important data in most applications the dominant uncertainties do not arise from the "counting statistics." The uncertainties related to the finite number of "events" recorded in most of the experiments are usually very small compared to the uncertainties in the various assumptions which must be made to extract from the experiment an estimate of the value of the quantities of interest. Most of the books available today to experimentalists and evaluators on probability theory deal with statistics and define probabilities as a frequency distribution. It is therefore not surprising that most experimentalists feel quite comfortable about the handling of uncertainties related to the frequency of observed events in the experiments and almost always state quite explicitly the uncertainties coming from counting statistics, the so-called "statistical error." It is usually perceived that there are few misunderstandings possible about these uncertainties, they do not deal with mistakes and their numerical values can be very precisely calculated. Concerning uncertainties arising from other sources, the assumptions which must be made in order to reduce the data, and for which almost universally they use the term "estimated systematic errors," much confusion occurs. It seems quite readily accepted that in some sense probability theory is capable of dealing with them since they are expressed quantitatively as

standard deviations of some probability density functions. The situation here is usually viewed as totally different from the one of "statistical errors" and is thought to represent merely some opinion as to the possible correctness of the assumptions and in a direct sense deals with possible mistakes. There is also the perception that one should assign a large uncertainty to these estimated uncertainties. Of course, no one denies that personal opinions are entitled to consideration and respect if they are based on factual evidence. We believe, however, that the notion of personalistic probability belongs to the field of psychology and has no place in our evaluations. Objectivity and credibility in our evaluations require that we should make use, not of anybody's personal opinions, but rather the specific factual data on which those opinions are based. It appears that very few people seem to be aware that there is a fully consistent way to treat these problems within probability theory. This theory[3] deals with logical inferences which can be made on the basis of limited or incomplete information, is closely related to decision theory, and is fully rigorous. Although most workers in the field of nuclear data and its applications do not appear to know the formal aspects of this theory, much of what they do, in particular in experimental and evaluation work, is an attempt to apply it in specific circumstances. In many areas such as experimental measurements, because of long experience with this activity, we feel quite confident about how to proceed and assign uncertainties on the basis of the specific information available in the experiment. We feel that the uncertainties we quote are reasonable, i.e. logical; any knowledgeable experimentalist we think would come essentially to the same conclusion. It is therefore not appropriate to call these uncertainties a statement of personal opinions since they are the conclusions which any experienced worker would reach. In the area of evaluation, since this activity is much more recent, we have not developed yet such a confidence about how to proceed and in general have not paid much attention to methodology. The consequence is that uncertainties tend to be more perceived as a statement of personal opinion and are formally on much less secure grounds. It is, we think, for this reason that much confusion occurs concerning the possible meaning and uses of uncertainties in evaluations. We believe that the situation could be very much improved, and probably will in the future as we pay more attention to methodology. We have been caught in a vicious circle to the extent that since uncertainties in experimental data, as provided by experimentalists, were not used in a formal way we have not demanded that experimental uncertainties be reported in an unambiguous manner, and as a consequence they usually are not. We hope that as we pay more attention to methodology and indicate more clearly to experimentalists what is needed to do credible evaluation with generally believable uncertainties the situation will improve.

COVARIANCE FILES OF ENDF/B-V

A number of covariance files have already been turned in for ENDF/B-V. In the table below is shown the list of files which had been received by the last CSEWG meeting in June 1978 for the general purpose evaluations. In addition to these we expect for the fissile and fertile nuclides 232-Th, 233-U, 235-U, 238-U, and 239-Pu covariance information on $\bar{\nu}$, the fission spectrum, the fission, capture and inelastic cross sections. All of the dosimetry cross sections of ENDF/B-V will also have some covariance files.

General Purpose Evaluation Covariance Files for ENDF/B-V

Element	Content
^{1}H	33;2
^{6}Li	33;1,2,105,<1 MeV
^{10}B	33;1,2,107,780,781
C	33;1,2,3,51-68,91,102-4,107
^{14}N	33;1,2,4,102,103,107
^{16}O	33;1,2,4,103,107
^{19}F	33;1-4,16,51,52,102,103,107
^{23}Na	32;151.33;1-4,16,51-68,91,102,103,107
^{27}Al	33;1,2,4,16,102,103,107
Si	33;1-4,52,61,103,107
Cr	33;1-4,16,17,22,28,51-89,91,102-107
Fe	32;151.33;1-4,16,22,28,51-76,91,102-107
Ni	33;1,2,4,16,22,28,51-76,91,102-104,107,111
Pb	33;1-4,16,17,51,52,64,102
^{232}Th	33;18,102.31;452
^{233}U	
^{235}U	31;452.33;18,102
^{238}U	31;452.33;18,102,inelastic
^{239}Pu	31;452.33;18,102
^{240}Pu	31;452.32;151.33;18,102
^{241}Pu	31;452.33;18,102
^{242}Pu	33;1,2,4,16,18,102.32
^{241}Am	33;1,2,4,16,18,102.32
^{237}Np	33;18.32

The covariance files of ENDF/B-V are currently undergoing review within the Data Covariance Subcommittee of the CSEWG, and it is hoped that they will be released at the same time as the "data files" or shortly afterward. We shall now discuss briefly our own perception of the strengths and weaknesses of the covariance files at this time. These comments are very general and should be valid for most covariance files of ENDF/B-V. More specific comments will be released by the subcommittee after review of the files is completed.

The major strength of the covariance files of ENDF/B-V will be their very existence, establishing a precedent. They represent an unambiguous statement of the uncertainties, including the important correlations in the data which arise from these uncertainties, as "perceived" by the evaluators who did the evaluations. Until now the best that could be done in this area was to collect various opinions as to how good the data were likely to be from people who usually had not done the evaluations or when they had the statements were likely ambiguous in particular concerning the correlations which were consequently often ignored or very poorly treated. Although most cross sections of ENDF/B-V will not have uncertainty estimates in the files, it is hoped that there will be some for many of the most important cross sections of interest in fast reactor applications. Unfortunately, we perceive many more weaknesses in these files than strengths. In a sense this is a strength of these files since they focus on various areas where specific improvements should be sought and will likely be made in future versions. In our mind, as we have gathered from comments made to us by most evaluators who have attempted to generate these covariance files, the most important contribution which these files are likely to make has already been made!! We refer to the fact that they point out a number of general weaknesses in our overall evaluation effort. They have caused evaluators to ask in a more directed way a number of questions which in the past, in our opinion, remained too aften unworded, such as: What are really the uncertainties in the data and theories used in evaluation? Upon what hard evidence do we base these uncertainties? How do we establish credible evaluations in the face of these uncertainties? By what methodology? Are we getting from experimentalists and "data compilers" the necessary information to perform rational evaluations? We believe that many of these questions, which are only now being more precisely formulated as a result of attempting to generate the covariance files for the evaluations, if we find satisfactory answers for them, will transform both experimental and evaluation work from an art into a science and reduce considerably the subjectivity currently used in obtaining recommendations for applied purposes. This effort, if we pursue it, will make for much more credible evaluations.

There are obvious weaknesses to these files of ENDF/B-V which can be stated prior to their complete review. There will not be any uncertainty estimates for two important classes of data: angular and energy distributions. This deficiency of the files will limit in many cases their usefulness since in only few applications can sensitivity to angular and energy distributions be properly neglected. As far as we have been able to ascertain from communications from most evaluators, they do not feel

confident about the uncertainty assignments. They are often felt to be little more than "guesses" indicating that at this stage we are dealing mostly with "subjective" or "personal probabilities." As we have already pointed out, the opinion of experts is quite valuable, but we are really only interested in "opinions" which can be objectively substantiated on the basis of the information available. When evaluators state that their covariance files are at this stage "mostly guesses," they are in fact telling us that they are not sure they correspond to the facts. We should therefore suspect that many mistakes may have been made. If such is the case, then they can be used with very little confidence. However, as we have very strongly made the point before, they should be corrected for these mistakes before they are used and not interpreted as being themselves statements about possible mistakes. During the review process of the files, the Data Covariance Subcommittee will endeavor to eliminate as much as possible this element of "personal probability" from the files by attempting to secure some sort of "consensus" of experts. We realize this is a very unsatisfactory situation which is almost unavoidable until we gain more experience with the concept of data covariances. We caution the users of the data to beware of the quality of the data in the covariance files and refrain from treating them as hard facts upon which strong conclusions can be based. At this stage they should be used very cautiously and taken more as an indication of things to come.

CONCLUSIONS

After several years of discussion within the CSEWG, a somewhat extensive set of estimated data covariance files describing some of the uncertainties in the recommended cross sections will be released with ENDF/B-V. Even though much work has gone into them, they are not expected to be free from mistakes. The concept of quantified uncertainties in evaluated differential data is rather new and it is likely to present some problems to users just as it has to evaluators. We do not expect at this stage that the quality of the files will be such that strong conclusions can be based upon them. However, we hope that their appearance will assist in a reappraisal of the concept of uncertainties in many aspects of applied neutronics, in particular in connection with "methods" and "integral data." This reappraisal should allow us to gain a better perception of the role which our different types of information play in achieving a goal such as the design or performance analysis of reactors.

REFERENCES

1. F. G. Perey, "The Data Covariance Files for ENDF/B-V," ORNL/TM-5938 (ENDF-249) July 1977.

2. F. G. Perey, to be published.

3. E. T. Jaynes, IEEE Transactions on Systems Science and Cybernetics 4, 277 (1968), and private communication.

FUEL-MOTION UNFOLDING BASED ON POINT DETECTOR RESPONSES

Patrick J. McDaniel
Steven A. Wright
Sandia Laboratories
Albuquerque, New Mexico, USA

ABSTRACT

The detection of fuel-motion in a fast-reactor fuel test assembly using in-core point detectors requires an extensive data-analysis system to infer fuel movements from detector responses. The detector-response kernels must be inverted using noisy data. This procedure is inherently unstable, but it can be stabilized by applying singular-value analysis and appropriate physical constraints.

An unfolding code, MOVUN, has been written specifically for this problem. It treats the instabilities in a consistent manner and applies the known constraints to provide reasonable resolution on fuel mass movements within a test assembly inside the Sandia SPR-III reactor.

INTRODUCTION

As part of the Nuclear Regulatory Commission's program of fast reactor research, Sandia Laboratories is developing an in-core fuel-motion detection system. In order to provide an accurate assessment of the capabilities of this system, a series of experiments will be conducted in Sandia's SPR-III reactor. A test assembly containing positions for up to 37 fuel pins has been designed and will be placed in the central cavity of this reactor. The fuel pins have been manufactured so that the upper two-thirds are movable and may be held fixed with gaps of up to 15 cm between the upper and lower portions. This will allow a large number of arbitrarily shaped fuel voids to be introduced into the test assembly. In this manner the actual fuel positions can be mechanically measured for direct comparison with the positions determined by the in-core fuel-motion detection system.

A previous paper[1] has dealt with the computational procedures used to develop detector response kernels for this system. Based on the results of this analysis, the data available from an in-core system can

be characterized as a small signal riding on a large background. Though the absolute noise in the fission-couple detectors developed for this system is very small, the signal-to-noise ratio available for fuel-motion detection is not very good due to the large background. Therefore, the inversion procedure used to calculate fuel-motion must explicitly consider the noisy data and filter this noise in some manner. An algorithm has been developed to treat this problem based on a singular-value analysis of the response matrix.

In addition to being able to filter the noisy data, information from a number of physical constraints is available to assist in unfolding realistic fuel movements. The most obvious constraint is conservation of fuel mass. During the course of the experiment the total fuel mass should remain constant. A second constraint is that negative fuel densities are not possible. A third constraint, related to the second one, is that fuel densities must be less than some maximum. Incorporation of these constraints into the analysis procedure precludes physically unrealistic fuel movements.

Based on these techniques, it has been possible to unfold computer-simulated data with reasonable accuracy. Obviously, actual experimental data are the real test of the analysis procedure, but the simulations conducted so far will provide a powerful tool for analyzing the actual experiments. The code developed for this analysis has been called MOVUN for MOVement UNfolding.

ANALYSIS PROCEDURE

The differential response of an in-core detector to signals generated by fuel movements can be represented by[1]

$$\Delta R = \sum_{k=1}^{N} K_k \, \delta\rho_k \quad , \tag{1}$$

where

ΔR is the differential detector response,

$\delta\rho_k$ is the fuel movement within the kth subvolume of the test assembly,

K_k is the kernel for the detector response due to fuel movement within the kth subvolume.

Note it has been assumed that the test assembly volume may be divided into N subvolumes which cover all possible locations that can contain fuel.

If M such equations, one for each detector, are combined, this can be written in matrix form as

$$[\Delta R]^{Mx1} = [K]^{MxN} [\delta\rho]^{Nx1} \tag{2}$$

In this equation the $[\Delta R]$ vector is known and the $[\delta\rho]$ vector is to be determined. To do this, the matrix [K] must be inverted. However, since [K] is derived from a real physical response that is not singular, an inversion process of this type is known to be very unstable.[2,3,4] That is, small errors in the data will generally produce large errors in the solution.

In order to avoid this problem we have used the following techniques. First, each equation is weighted with the inverse error expected in the measured detector response. This scales the data vector so that each measurement has the same absolute uncertainty. The resulting matrix is factored with a singular value decomposition algorithm[5] to give

$$[\Delta R'] = [K'][\delta\rho] = [U][S][V^T][\delta\rho] \quad , \tag{3}$$

where

[U] is unit-orthogonal of order M,

[S] is diagonal with its elements order from largest in the first row to smallest in the Nth row and zero in the N + 1st to Mth row,

$[V^T]$ is unit-orthogonal of order N,

and the primes on $[\Delta R']$ and $[K']$ indicate the original quantities scaled by the error estimates.

Now the [U] matrix can be inverted by multiplying by its transpose. This is a stable process due to the characteristics of a unit-orthogonal matrix. In doing this we have reduced the dimensionality of the $[S][V^T]$ matrix from M (the number of detectors) to N (the number of fuel subvolumes). It can be shown that this procedure is equivalent to finding the least squares solution to Equation 3.[5] Also, since $[S][V^T][\delta\rho]$ is an N vector and it is equal to the M vector $[U^T][\Delta R']$, the last (M-N) elements of $[U]^T [\Delta R']$ must represent the residuals obtained when Equation 3 is solved in a least-square sense. Thus if the vector [G] is defined as $[U]^T [\Delta R']$ then,

$$\sum_{i=N+1}^{M} G_i^2 = \sum_{j=1}^{M} \left(\Delta R'_j - \sum_{k=1}^{N} K'_{jk} \delta\rho_k \right)^2$$

Recognizing this fact, it is now possible to treat the instability problems generated by the inversion process. The elements of the $[\Delta R']$ vector are statistical quantities, each with an error estimate of 1.0, due to the scaling by inverse errors. Thus the sum-of-residuals-squared, given by

$$R^2 = \sum_{i=N+1}^{M} G_i^2 \quad ,$$

will also be a statistical quantity. It can be shown[6] that the expected value for R^2 is (M-N) for this problem. Now if the detector response kernels represent a real physical system, as they do, the actual value obtained for R^2 will be very much smaller than its expected value. This is the condition that causes the instabilities in the inversion process. We are in fact trying to fit the measured data much more accurately than it warrants, based on its known errors. Relaxing the accuracy we are trying to obtain in fitting the measured data should overcome these instabilities, and provide a realistic filter for the inversion process.

The procedure is rather straightforward. We neglect the last row of the $[V^T]$ matrix and add the square of the corresponding element of the [G] vector to R^2. The new value of R^2 can be compared with its expected value. If R^2 is less than its expected value the process is repeated on the next row of $[V^T]$. If R^2 is now greater than its expected value, the last row of $[V^T]$ that was deleted, must be retained. Note that as each row of $[V^T]$ is deleted, the value of R^2 must be increased by 1.0 to allow for the increase in the expected error due to using fewer basis functions for the solution space.

When $[V^T]$ has been reduced to the minimum number of rows that will keep R^2 less than its expected value, the matrix inversion can proceed. The matrix [S] is inverted by taking the reciprocals of each of its elements. Then the vector [G] is multiplied by $[S]^{-1}$ and $[V_R R]$. This gives the filtered solution for $[\delta\rho]$,

$$[\delta\rho] = [V_R]\,[S]^{-1}\,[G] \quad ,$$

where $[V_R]$ is the matrix $[V]$ with the appropriate zero columns generated during the stabilization process.

This procedure produces the best estimate of fuel movement based strictly on the noisy data measured by the detectors. However, additional physical constraints are available to improve this estimate. For the SPR-III experiments, at least, fuel mass must be conserved and there exists upper and lower bounds on the amount of fuel in each volume bin.

The conservation of mass constraint is easiest to apply. This constraint can be written as an equation that says the sum of the fuel density changes must be zero. In the algorithm used by MOVUN, it is applied prior to performing the singular value decomposition of the response matrix. An orthogonal transformation is applied to the response matrix that reduces the number of independent parameters (fuel-density changes) by one. The singular value analysis is performed on this reduced solution space. The maximum density change constraints are then applied to this reduced solution space also. Then the inverse of the orthogonal transformation is applied to the solution in this reduced space to obtain a best estimate for the fuel-density changes. This procedure conserves fuel mass to machine accuracy and somewhat reduces the work involved in the matrix factorization process.

The bounding constraints are treated by noting that they are actually inequalities. That is, for example, the fuel in each volume bin must be greater than or equal to zero. If the filtered solution obtained from singular value analysis indicates some negative fuel densities, then some of these should be, in actuality, zero fuel densities. The densities in these subvolumes may be set to zero, and the effect of this change on the solution, in the value obtained for R^2, calculated. The optimum solution would appear to be the one that minimizes the increase in R^2 due to increasing some fuel densities to a zero or positive value. Lawson and Hanson[5] have developed an algorithm that finds this minimum increase in R^2 very efficiently. This algorithm has been incorporated into the MOVUN code to perform this operation.

The resulting solution satisfies some of the inequality constraints exactly and produces the minimum increase in R^2 (the sum of the squared residuals for the detector equations) possible.

Thus the basic algorithm proceeds in four steps. First, the solution space is reduced by applying the conservation of mass constraint; second, a best estimate for the fuel movement in the reduced space is obtained from singular value analysis; third, this solution is perturbed to meet the bounding constraints and increase least squares error by the minimum amount possible; and finally the estimated fuel movement is transformed back into the full solution space.

COMPUTATIONAL RESULTS

In order to test the MOVUN code and estimate the effects of measurement errors on the resolution obtainable by an in-core system, a number of computer simulations have been run. A specified fuel movement can be described for the RHOPER code[1] and simulated detector responses can be generated. Errors can be introduced into these responses that are typical of expected measurement errors. This data can then be unfolded by MOVUN to obtain an estimated fuel movement. Finally, this fuel movement can be compared with the actual fuel movement, to determine the accuracy of the technique.

This type of computer experiment was run for the fuel movement described in a previous paper.[1] Basically, the upper two-thirds of seven pins were moved upward 8 cm to produce a voided region in the middle of the pins. The anticipated detector responses for this movement were calculated with RHOPER. These responses were perturbed with normally distributed errors having a standard deviation of 2% of the total signal. The unfolded results for this problem are presented in Figure 1. Note that twelve fuel volumes were chosen to represent the fuel movement. For this problem each volume bin measured 6.4 cm^3 with a nominal density of 8.5 gm/cm^3, and the maximum density obtainable was set at 17.0 gm/cm^3. The estimated errors in the unfolded fuel densities were approximately 18 grams per volume bin, or one-third of the starting density for volumes initially containing fuel.

As the magnitudes of the errors in the actual detector signals can only be estimated at this time, this particular fuel movement was rerun with a number of different error estimates. In an attempt to obtain a more general measure of system capability an average signal-to-noise ratio was defined

$$SNR_{AVE} = \sqrt{\frac{\sum_{i=1}^{M} \left(\frac{\Delta R_i}{\varepsilon_i}\right)^2}{M}} ,$$

where ε_i is the estimated error in ΔR_i.

The results of these computer experiments are presented in Figure 2. Error estimates were chosen to be 1%, 2%, and 3% of total measured detector signals. These estimates correspond to average signal-to-noise ratios of 4.2, 2.2, and 1.7, respectively. Based on the data presented in Figure 2, mass resolutions of the order of 10 to 20 grams should be obtainable in a 6.4 cm^3 volume.

CONCLUSIONS

The application of linear perturbation theory to generate detector response kernels and the unfolding of the measured responses for in-core detectors appears very feasible. Singular value analysis and the application of simple physical constraints can produce adequate fuel movement information, if the detector signals are reasonably accurate. Best estimates for detector signal accuracy indicate fuel mass resolutions of 10-20 grams.

REFERENCES

1. Scott, W. H., Jr., P. J. McDaniel, J. H. Renken, and S. A. Wright, "Sensitivity Analysis Applied to the Calculation of Detector Response Kernels," RSIC Seminar-Workshop on the Theory and Application of Sensitivity and Uncertainty Analysis, Oak Ridge, Tennessee, August 22-24, 1978.

2. Tikhonov, A. N. and V. Y. Cersenin, Solutions of Ill-Posed Problems, V. H. Winston and Sons, Washington, D. C., 1977.

3. Hanson, Richard J., "A Numerical Method for Solving Fredholm Integral Equations of the First Kind using Singular Values," SIAM Journal of Numerical Analysis, Vol. 8, No. 3, September 1971, pp. 616-622.

4. Miller, G. F., "Fredholm Integral Equations of the First Kind," Chapter 13 in Numerical Solution of Integral Equations, L. M. Delves and J. Walsh, ed. Clarendon Press, Oxford, 1974.

5. Lawson, Charles L. and Richard J. Hanson, Solving Least Squares Problems, Prentice-Hall, Inc., Englewood Cliffs, New Jersey, 1974.

6. Meyer, Stuart L., Data Analysis for Scientists and Engineers, John Wiley and Sons, Inc., New York, 1975.

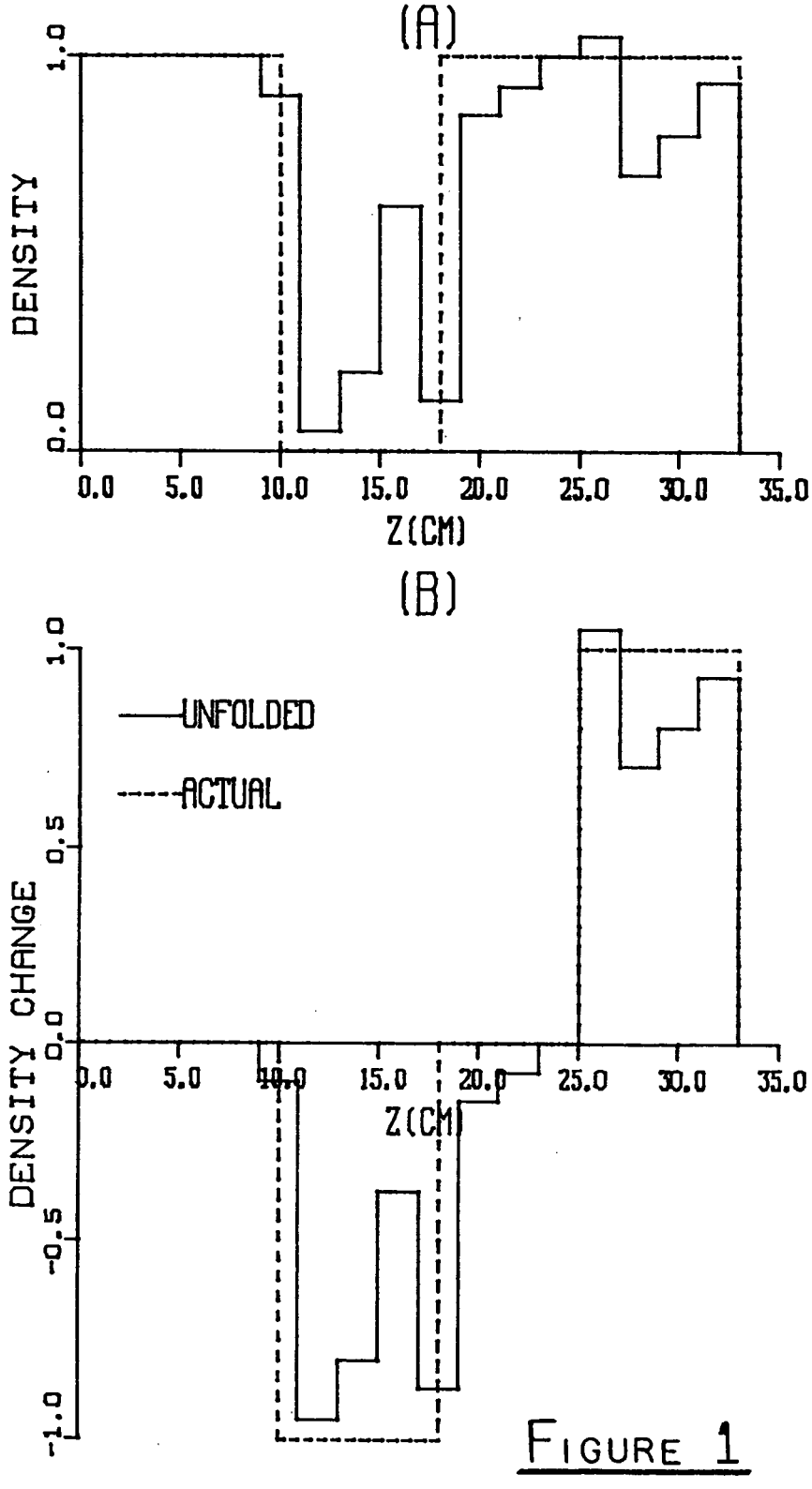
(A)
DENSITY
1.0
0.0
0.0
5.0
10.0
15.0
20.0
25.0
30.0
35.0
Z(CM)
(B)
UNFOLDED
ACTUAL
DENSITY CHANGE
1.0
0.5
0.0
-0.5
-1.0
0.0
5.0
10.0
15.0
20.0
25.0
30.0
35.0
Z(CM)

FIGURE 1

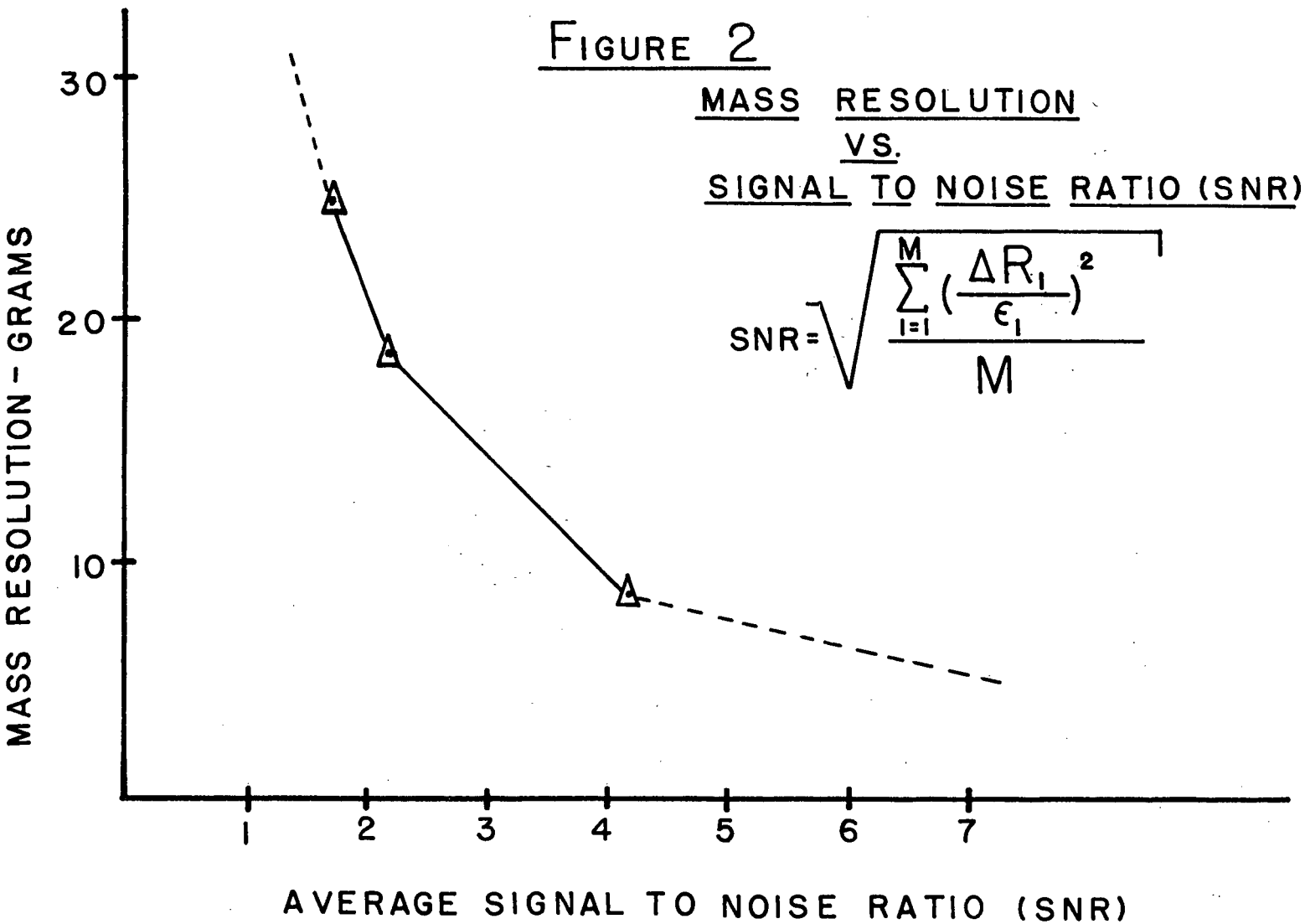

FIGURE 2

MASS RESOLUTION VS. SIGNAL TO NOISE RATIO (SNR)

$$SNR = \sqrt{\frac{\sum_{i=1}^{M} \left(\frac{\Delta R_i}{\epsilon_i}\right)^2}{M}}$$

SENSITIVITY OF LWR FUEL CYCLE COSTS TO UNCERTAINTIES IN DETAILED THERMAL CROSS SECTIONS

J. M. Ryskamp, M. Becker, and D. R. Harris
Rensselaer Polytechnic Institute
Troy, New York U.S.A.

ABSTRACT

Cross sections averaged over the thermal energy (<1 or 2 eV) group have been shown to have an important economic role for light-water reactors. Cost implications of thermal cross section uncertainties at the few-group level were reported earlier. When it has been determined that costs are sensitive to a specific thermal-group cross section, it becomes desirable to determine how specific energy-dependent cross sections influence fuel cycle costs. Multigroup cross-section sensitivity coefficients vary with fuel exposure. By changing the shape of a cross section displayed on a view-tube through an interactive graphics system, one can compute the change in few-group cross section using the exposure dependent sensitivity coefficients. With the changed exposure dependent few-group cross section, a new fuel cycle cost is computed by a sequence of batch depletion, core analysis, and fuel batch cost code modules. Fuel cycle costs are generally most sensitive to cross section uncertainties near the peak of the hardened Maxwellian flux.

INTRODUCTION

An interactive system has been developed at RPI to analyze the sensitivity of water reactor fuel cycle parameters and costs to uncertainties in nuclear data. The sensitivities of few-group cross sections to uncertainties in detailed thermal nuclear data (referred to as Path A) are determined by methods presented in this paper. A sequence of batch depletion, core analysis, and fuel cycle cost codes (referred to as Path B) determines the changes in fuel cycle parameters and costs for changes in few-group microscopic cross sections, in fission yields, and decay data. These Path B methods and results are discussed in detail in our other paper presented at this workshop.[1]

Cross sections averaged over the thermal energy (<1 or 2 eV) group have been shown to have an important economic role for light-water reactors.[2,3] When it has been determined that fuel cycle parameters and costs are sensitive to a specific thermal-group cross section, it becomes desirable to determine how specific energy-dependent cross sections influence fuel cycle parameters and costs. A cross section can be

modified and viewed easily, along with the base cross section, flux, adjoint, and sensitivity coefficient, with the aid of Rensselaer's Interactive Graphics Analysis System (RIGAS)[4]. After computing the changed exposure-dependent thermal-group cross section, a new fuel cycle cost is computed by the sequence of Path B code modules. We can therefore obtain the change in fuel cycle cost for different fuel cycle options induced by a change in the shape of a detailed thermal cross section. This type of analysis on thermal cross section uncertainties can be used to indicate directions for worthwhile improvements in thermal nuclear data and methods.

METHODS FOR COMPUTING THERMAL REGION SENSITIVITY COEFFICIENTS

Path A analyses examine the sensitivities of few-group microscopic cross sections to changes in basic nuclear data. These sensitivities have two components, one associated directly with the nuclear data change and one associated with the change in flux resulting from the change in nuclear data. This change in flux affects few-group microscopic cross sections for other reactions as well as for that originally changed. Sensitivities of thermal group cross sections to uncertainties in multigroup cross sections can be calculated by direct and by perturbation methods. Each method has advantages and disadvantages.

In the direct method the change in thermal-group cross section σ^{i}_{rG} of nuclide i and reaction type r contingent on a change $\delta\sigma^{i'}_{r'g}$ in the multigroup cross section $\sigma^{i'}_{r'g}$ is computed directly by subtracting the changed case calculation from the base case calculation. The flux calculation is performed once with base multigroup cross sections. This flux is used to collapse the multigroup cross-sections σ^{i}_{rg} to the few-group cross-section σ^{i}_{rG}. The flux is computed again with a changed multigroup cross section $\sigma^{i'}_{r'g} + \delta\sigma^{i'}_{r'g}$, where $\delta\sigma^{i'}_{r'g}$ is the uncertainty. The few-group cross section σ^{i}_{rG} is then computed again with this changed flux. By subtracting the changed value from the base value, one determines the microscopic cross section sensitivity coefficients

$$S^{i,i'}_{gr,r'} = \frac{\sigma^{i'}_{r'g} \quad \delta\sigma^{i}_{rG}}{\sigma^{i}_{rG} \quad \delta\sigma^{i'}_{r'g}} \quad . \tag{1}$$

Direct methods are conceptually simple but require a new flux calculation for each data change, which can be prohibitively expensive when several sensitivities must be computed. Direct methods, however, are not limited to small cross section uncertainties.

Perturbation methods permit calculation of many sensitivity coefficients from a practicable number of forward and adjoint calculations.

Industry codes could be used for this purpose if they were capable of computing adjoint solutions; however, they do not have this capability. The FASTT code, to be described later, was written to perform the flux and adjoint calculations in the thermal energy region and combine these to yield the required sensitivity coefficients. Perturbation methods are limited to small changes, however, yielding partial derivatives $\partial\sigma^i_{rG}/\partial\sigma^{i'}_{r'g}$ instead of $\delta\sigma^i_{rG}/\delta\sigma^{i'}_{r'g}$.

Few-group cross-sections are usually determined in LWR design by solving inhomogeneous equations,

$$L\phi = S \quad , \tag{2}$$

for the position, direction, and energy dependent neutron flux $\phi(\underline{r},E,\underline{\Omega})$ in a unit cell or other region of a reactor. The source S in the thermal energy region has the shape of neutrons slowing down from higher energies. If thermal nuclear data are changed, the transport operator L will change, and the flux will change as required by the transport equation. To first order, the change in flux is given by the equation

$$\delta L\phi + L\delta\phi = 0 \quad . \tag{3}$$

It is customary to compute few-group microscopic cross sections, σ^i_{rG}, by reaction rate averaging,

$$\sigma^i_{rG} = \frac{\langle\sigma^i_r C^i \phi\rangle_G}{\bar{C}^i\langle\phi\rangle_G} \quad . \tag{4}$$

Here the symbol $\langle f\rangle_G$ represents the integral of $f(\underline{r},E,\underline{\Omega})$ over position in the region, over the energy band G, and over all directions. $\bar{C}^i$ is the cell averaged concentration for nuclide i.

The change in few-group cross section σ^i_{rG} can be computed directly by calculations using Eqs. 2 and 4 both with and without the change in multigroup cross section $\sigma^{i'}_{r'g}$,

$$\delta\sigma^i_{rG} = \frac{\langle(\sigma^i_r + \delta_{ii'}\delta_{rr'}\delta\sigma^{i'}_{r'})C^i(\phi+\delta\phi)\rangle_G}{\bar{C}^i\langle\phi + \delta\phi\rangle_G} - \frac{\langle\sigma^i_r C^i\phi\rangle_G}{\bar{C}^i\langle\phi\rangle_G} \quad . \tag{5}$$

The Kronecker delta $\delta_{ii'}$ is equal to 1 when i = i', and $\delta_{rr'}$ is equal to 1 when r = r'; both are equal to zero otherwise. This is referred to as the direct technique. Using Eq. 4, after the terms in Eq. 5 have been placed on the common denominator and expanded, gives to first order,

$$\delta\sigma^i_{rG} = \frac{\langle\delta_{ii'}\delta_{rr'}\delta\sigma^{i'}_{r'}C^{i'}\phi\rangle_G}{\bar{C}^i\langle\phi\rangle_G} + \frac{\langle(\sigma^i_r C^i - \sigma^i_G\bar{C}^i)\delta\phi\rangle_G}{\bar{C}^i\langle\phi\rangle_G} \quad . \tag{6}$$

From this expression we can see that if $i \neq i'$ or $r \neq r'$, the first term is zero and the change in few-group cross-section results from the change in flux alone.

Perturbation theory is applied as follows; the equation adjoint to Eq. 2 is

$$L^{+}\phi^{+} = S^{+} \quad , \tag{7}$$

where the operator L^{+} has the usual linear adjoint property

$$\langle \chi^{+}, L\psi \rangle_G = \langle L^{+}\chi^{+}, \psi \rangle_G \quad . \tag{8}$$

Commas are introduced at times in these equations to delimit operations, e.g., the operator L^{+} operates on χ^{+} but not on ψ. Using the last two equations we find

$$\langle S^{+}, \delta\phi \rangle_G = \langle L^{+}\phi^{+}, \delta\phi \rangle_G = \langle \phi^{+}, L\delta\phi \rangle_G \quad . \tag{9}$$

By comparing the first term of this expression with the last term in Eq. 6, we choose the adjoint source,

$$S^{+}_{ir} = \sigma^{i}_{r}(E)C^{i}(\underline{r}) - \sigma^{i}_{rG}\bar{C}^{i} \quad . \tag{10}$$

From Eqs. 3, 9 and 10 we obtain,

$$\langle (\sigma^{i}_{r}C^{i} - \sigma^{i}_{rG}\bar{C}^{i}), \delta\phi \rangle_G = -\langle \phi^{+}_{ir}, \delta L\phi \rangle_G \quad . \tag{11}$$

Using the adjoint we have elminated the need to compute the change in flux. Using Eq. 11, Eq. 6 becomes

$$\delta\sigma^{i}_{rG} = \frac{\langle \delta_{ii'}\delta_{rr'}\delta\sigma^{i'}_{r'}C^{i'}\phi \rangle_G}{\bar{C}^{i}\langle \phi \rangle_G} - \frac{\langle \phi^{+}_{ir}, \delta L\phi \rangle_G}{\bar{C}^{i}\langle \phi \rangle_G} \quad . \tag{12}$$

The change δL is just $C^{i'}\delta\sigma^{i'}_{r'}(E)$ for a reaction cross-section change.

One forward flux calculation and one adjoint flux calculation suffice to yield the dependence of the group cross-section σ^{i}_{rG} on all small changes $\delta\sigma^{i'}_{r'}(E)$ as arbitrary functions of energy. For a reaction cross section change, we are actually interested in the sensitivity coefficient defined by the partial derivative,

$$S^{i,i'}_{gr,r'} = \frac{\sigma^{i'}_{r'g}}{\sigma^{i}_{rG}} \frac{\partial\sigma^{i}_{rG}}{\partial\sigma^{i'}_{r'g}} = \frac{\langle (\delta_{ii'}\delta_{rr'} - \phi^{+}_{ir})\sigma^{i'}_{r'}C^{i'}\phi \rangle_g}{\langle \sigma^{i}_{r}C^{i}\phi \rangle_G} \quad . \tag{13}$$

In arriving at this equation it was assumed that the cross-section was perturbed slightly only in group g.

The sensitivities of thermal-group average cross sections to changes in detailed energy-dependent cross sections in the thermal range are calculated by the code FASTT. This code combines selected features of the thermal neutron treatments in LASER[5] and LEOPARD[6] to compute both the multigroup neutron flux and adjoint, then combines these to yield the required sensitivities. Sensitivity coefficients computed by both the direct and perturbation methods are shown in Table 1. The results agree with reasonable accuracy, thus confirming both methods.

THERMAL REGION CALCULATIONS: THE FASTT CODE

Cross sections averaged over the thermal energy (<1 or 2 eV) group play an important role in computational methods for light-water reactors. The thermal-group cross sections are computed in reactor cell programs by code modules that can be classified as being like SOFOCATE[7] or like THERMOS[8]. In the former case the emphasis is on the neutron energy spectrum with simplified spatial treatments when these are included at all. In the latter case there is a more balanced treatment of spatial and spectral effects, but there is a corresponding penalty in running time. Because a large part of the power reactor industry utilizes SOFOCATE in the form included as a module in cell codes like LEOPARD[6] and CHEETAH[9], and because this approach is simpler, less costly, and hence, suited for sensitivity analysis, the FASTT code to be described utilizes this approach.

Neutrons slowing down in the moderator from energies above 1 or 2 eV provide the transport into the thermal range. This equation is solved in LWR design for the order of 10 or 10^2 energy points or groups using spatial calculations of greater or lesser accuracy. Codes solving this problem are reasonably complex, and their adjoint versions could be complex also. Fortunately, we have developed a technique for computation of adjoints using forward codes. The adjoint source, $\sigma(E)C(\underline{r}) - \sigma_G\bar{C}$, appropriate to the present application requires a particular transformation for solution with conventional methods.

The reactor parameters calculated by FASTT and the procedures used to determine them are similar to those in other industry type codes. The microscopic cross sections read by FASTT must be Doppler broadened to the proper temperature. D. E. Cullen et al.[10] have presented a comparison of Doppler broadening methods in the thermal energy range. We have chosen to use the LASER[5] 35 group structure with an upper cutoff of 1.855 eV in order to include the effects of the Pu-240 resonance. The FASTT code is quite general and can run with any group structure.

Table 1. Comparison Between Direct and Perturbation Methods for the Green County PWR at Middle of Exposure (1% changes for Direct Method)

	SENSITIVITY COEFFICIENTS					
Energy Midpoint of Group(eV)	U-235(n,f)		Boron(n,γ)		Pu-240(n,γ)	
	Direct	Pert.	Direct	Pert.	Direct	Pert.
.001139	.003081	.003091	.005888	.005885	.000487	.000491
.036685	.086202	.086267	.088536	.088541	.015800	.015799
.165080	.058685	.058711	.063540	.063545	.015564	.015566
.295940	.003922	.003934	.003631	.003635	.001028	.001031
.564090	.011168	.011176	.015874	.015877	.013222	.013224
1.047700	.000140	.000147	.000309	.000310	.042377	.042540
1.237200	.004546	.004546	.005722	.005723	.034977	.034980
1.790500	.000916	.000923	.003094	.003089	.001170	.001171

The simplest model of neutron thermalization yielding results of sufficient accuracy is that which treats the reactor core as a free proton gas, neglecting chemical binding. In this Wigner-Wilkins[11] model the protons are assumed to be in thermal equilibrium with a Maxwell-Boltzman energy distribution. FASTT can compute scattering cross-sections using the free proton model or the Nelkin[12] model, in which the chemical binding is accounted for by a set of discreet molecular frequencies. In FASTT only the downscattering part of the kernel is calculated and stored. The upscattering is calculated as needed from the condition of detailed balance,

$$M(E)\sigma_s(E\rightarrow E') = M(E')\sigma_s(E'\rightarrow E) \quad . \tag{14}$$

where M is the Maxwellian flux

$$M(E) = \frac{E}{(kT)^2} e^{-E/kT} \quad . \tag{15}$$

The FASTT code has the option to read in any scattering kernel in the proper group structure.

The unit cell consists of the cylindrical fuel pellet, a cylindrical annular clad region, and a coolant region between fuel rods. A modified Amouyal-Benoist-Horowitz method defined by Strawbridge is used to calculate the spatial variation of flux within the pin cell. The fuel-to-moderator flux ratio and the clad-to-moderator flux ratio are computed by FASTT at each energy group. The macroscopic cross sections are then computed with respect to the moderator.

In FASTT we have included the spatial flux dependence with the use of flux ratios and are therefore able to simplify the linear transport equation (Eq. 2) to

$$\Sigma_t(E)\phi(E) - \int\Sigma_s(E'\rightarrow E)\phi(E')dE' = S(E) \quad , \tag{16}$$

where the slowing down source S(E) from energies above the thermal range is uniform into the effective pin cell. This forward balance equation can be solved by iteration,

$$(\Sigma_{ag} + \Sigma_{sg})\phi_g^{(m+1)} = \sum_{g'} \Sigma_{g'\rightarrow g}\phi_{g'}^{(m)} + S_g \quad . \tag{17}$$

The initial flux $\phi_g^{(o)}$ is assumed to be a Maxwellian distribution,

$$\phi_g^{(o)} = M_g \sum_{g'} S_{g'} / \sum_{g'} M_{g'}\Sigma_{ag'} \quad , \tag{18}$$

which is normalized so that the spectrum averaged absorption equals the total source. FASTT renormalizes each iterate flux so that $\sum_g \Sigma_{ag}\phi_g^{(m)}$ equals the source $\sum_g S_g$ into the thermal group. Convergence is very

rapid; in fact, even the first iterate may be adequate for some sensitivity studies.

Earlier it was shown that few-group sensitivities are readily computed in terms of solutions to the forward and adjoint transport problems. The difficulty is that industry codes for the thermal energy range do not have adjoint capability. Fortunately, a method has been developed for computation of the thermal adjoint using forward codes[14]. The adjoint equation corresponding to the forward equation for the effective uniform cell, Eq. 16, is

$$\Sigma_t(E)\phi^+(E) - \int \Sigma_s(E\to E')\phi^+(E')dE' = S^+(E) \quad . \tag{19}$$

Multiply this by M(E), and replace $M(E)\Sigma_s(E\to E')$ by its detailed balance equivalent from Eq. 14. Then

$$\Sigma_t(E)\psi(E) - \int \Sigma_s(E'\to E)\psi(E')dE' = M(E)S^+(E) \quad , \tag{20}$$

where the auxiliary function $\psi(E)$ is defined by

$$\psi(E) = \phi^+(E)M(E) \quad . \tag{21}$$

Eq. 20 has the structure of a forward equation, so the adjoint ϕ^+ can be computed from any code that solves this forward equation. Here a source $M(E)S^+(E)$ is used, and the auxiliary function $\psi(E)$ is divided by M(E) to yield the adjoint $\phi^+(E)$.

It is required that the scattering function $\Sigma_s(E'\to E)$ actually obeys detailed balance. In LWR codes this is so for hydrogen scattering. Scattering of thermal neutrons from other nuclides usually is taken to be monoenergetic, in which case the detailed balance equation is satisfied automatically.

As was noted earlier, the adjoint source appropriate for the group averaged cross-section σ_G^i for isotope i in region j is $\sigma_g^i C_j^i - \sigma_G^i \bar{C}^i$. This source is positive for some groups and negative for others. It is convenient to further transform the adjoint equation as follows:

$$(\Sigma_{ag} + \Sigma_{sg})\phi_g^+ = \sum_{g'} \Sigma_{g\to g'}\phi_{g'}^+ + \sigma_g^i C_j^i - \sigma_G^i \bar{C}^i \quad . \tag{22}$$

Subtract $\Sigma_{ag} + \Sigma_{sg}$ from both sides, then multiply by -1.

$$(\Sigma_{ag}+\Sigma_{sg})(1-\phi_g^+) = \sum_{g'} \Sigma_{g\to g'}(1-\phi_{g'}^+)+\sigma_G^i\bar{C}^i+(\Sigma_{ag}-\sigma_g^i C_j^i) \quad . \tag{23}$$

The source to this balance equation is non-negative. Now convert this to a forward equation as developed previously,

$$(\Sigma_{ag}+\Sigma_{sg})\psi_g = \sum \Sigma_{g'\to g}\psi_{g'} + M_g\left[\sigma_G^i\bar{C}^i+\Sigma_{ag}-\sigma_g^i C_j^i\right] \quad , \tag{24}$$

where the auxiliary function ψ_g is

$$\psi_g = M_g(1-\phi_g^+) \quad . \tag{25}$$

FASTT calculates the auxiliary function ψ_g by the iteration technique described earlier, and since the source approximates the Maxwellian, convergence is even faster for the auxiliary function than for the forward flux.

The sensitivities of thermal group average cross sections to changes in detailed energy-dependent cross sections in the thermal range can be calculated from the flux and proper adjoint. The macroscopic sensitivity coefficient is computed from

$$D_g = \frac{\Sigma_{ag}}{\Sigma_{aG}} \frac{\partial \Sigma_{aG}}{\partial \Sigma_{ag}} = \frac{(1-\phi_g^+)\Sigma_{ag}\phi_g}{\sum_{g'} \Sigma_{ag'}\phi_{g'}} \quad . \tag{26}$$

The microscopic sensitivity coefficients for a change in a few group cross section for nuclide i and reaction type r, induced by a change in multigroup cross section for nuclide i' and reaction type r', are calculated by

$$S^{i,i'}_{gr,r'} = \frac{\sigma^{i'}_{r'g}}{\sigma^{i}_{rG}} \frac{\partial \sigma^{i}_{rG}}{\partial \sigma^{i'}_{r'g}} = \frac{\sum_j (\delta_{ii'}\delta_{rr'} - \phi^{+i}_{rjg}) C^{i'}_j V_j \sigma^{i'}_{r'g} (\frac{\phi_j}{\phi_M})_g \phi_{Mg}}{\sum_g \phi_{Mg} \sum_j C^{i}_j V_j \sigma^{i}_{r} (\frac{\phi_j}{\phi_M})_g} \quad . \tag{27}$$

Here V_j refers to the volume of region j, and M refers to the moderator.

We are also interested in determining the change in a few-group cross section for a change in the shape in the detailed cross section. Using the definition of microscopic sensitivity coefficient, we find,

$$\frac{\delta \sigma^{i}_{rG}}{\sigma^{i}_{rG}} = \sum_g S^{i,i'}_{gr,r'} \frac{\delta \sigma^{i'}_{r'g}}{\sigma^{i'}_{r'g}} \quad , \tag{28}$$

where the fractional changes in $\sigma^{i'}_{r'g}$ are input quantities. For example, we may wish to investigate the effects of an uncertainty in the 1/v component of a cross section or in a resonance parameter. The cross section can be modified and viewed easily, along with the base cross section, flux, adjoint, and sensitivity coefficient, with the aid of Rensselaer's Interactive Graphics Analysis System (RIGAS)[15].

Some sensitivity coefficients have large variations with exposure due to self-shielding and the hardening of the flux spectrum as

plutonium builds up. Even 1/v cross section sensitivity coefficients have large variations with exposure in certain energy regions, primarily due to flux dipping at plutonium resonances. Therefore, the fractional changes in σ^i_{rG} from Eq. 28 will vary with exposure. Once these changes are computed at each exposure time step, they can be used in the Path B code sequence as input to the fuel depletion module FASTCELL[16]. We can therefore obtain the change in fuel cycle cost for different fuel cycle options induced by a change in the shape of a detailed thermal cross section. Thus we have the necessary tools to investigate fuel cycle cost implications to improvements in ENDF data sets.

COMPUTED SENSITIVITY COEFFICIENTS

The sensitivity of fuel cycle costs to uniform thermal-group cross section changes with exposure were determined for the 40 nuclides included in the FASTCELL fuel depletion module. Path B sensitivity coefficients for 1985 are shown in Table 2 for both pressurized and boiling water reactors and for two back end fuel cycle alternatives. Nuclides with sensitivities less than .006 are not listed. Pu-239 and U-235 have the largest sensitivities, followed by H, Pu-241, and U-238. Fission products and structural materials have much smaller sensitivities. Sensitivity to the Pu-240 thermal capture cross section turns out to be small because of the high worth of the Pu-241 produced from neutron capture in Pu-240.

The sensitivities of thermal-group average cross sections to changes in detailed energy-dependent cross sections in the thermal range are calculated by the FASTT code. Figure 1 shows the energy dependent Pu-240 capture sensitivity coefficient per unit energy at three different exposures. This figure illustrates the importance of self-shielding effects with exposure. (Analogous effects are observed with Pu-239). The region of the 1.058 eV resonance is much more important at beginning of exposure. The Maxwellian region, however, becomes more important towards the end of exposure. This shifting of importance occurs because as the Pu-240 builds up in the pin cell, the flux dips at the resonance. Since there is less flux, a change in a resonance parameter will perturb the few-group cross-section less than it would have at beginning of exposure. This strong exposure dependence of sensitivity coefficients illustrates the importance of considering the fuel cycle as a whole, rather than considering any single time.

Figure 1 of our other paper in this proceedings illustrates the Pu-239 fission cross-section, adjoint, and sensitivity coefficient as a function of energy. The cross-section is more than five times as large at its 0.3 eV resonance than at the Maxwellian peak; yet its detailed sensitivity is about 50% larger at the Maxwellian peak than at the resonance. This illustrates the importance of the hardened

Table 2. Fuel Cycle Cost Sensitivity to Thermal Group Cross-Sections for 1985

	BWR		PWR	
	Recycle	Throwaway	Recycle	Throwaway
Pu-239 (n,f)	-.522	-.688	-.560	-.753
Pu-239 (n,γ)	.439	.578	.478	.619
U-235 (n,f)	-.387	-.578	-.384	-.568
U-235 (n,γ)	.210	.232	.208	.232
H (n,γ)	.125	.169	.095	.135
Pu-241 (n,f)	-.094	-.123	-.099	-.130
Pu-241 (n,γ)	.068	.080	.073	.089
U-238 (n,γ)	.033	.151	.037	.147
Fission Product Lump (n,γ)	.037	.052	.035	.049
B (n,γ)	—	—	.024	.045
Xe-135 (n,γ)	.017	.024	.020	.029
Zr (n,γ)	.019	.025	.011	.015
Nd-143 (n,γ)	.018	.024	.019	.027
Rh-103 (n,γ)	.008	.011	.008	.011
Pu-240 (n,γ)	.005	.012	.009	.020
Eu-153 (n,γ)	.004	.005	.004	.006

Maxwellian energy range for thermal-group cross sections.

SUMMARY

Cross sections averaged over the thermal energy group have been shown to have an important economic role for light-water reactors. Pu-239 and U-235 have the largest sensitivities (Path B), followed by H, Pu-241, and U-238. Fission products and structural materials have much smaller sensitivities.

The methods used to compute the sensitivity of few-group cross sections to uncertainties in basic nuclear data have been presented

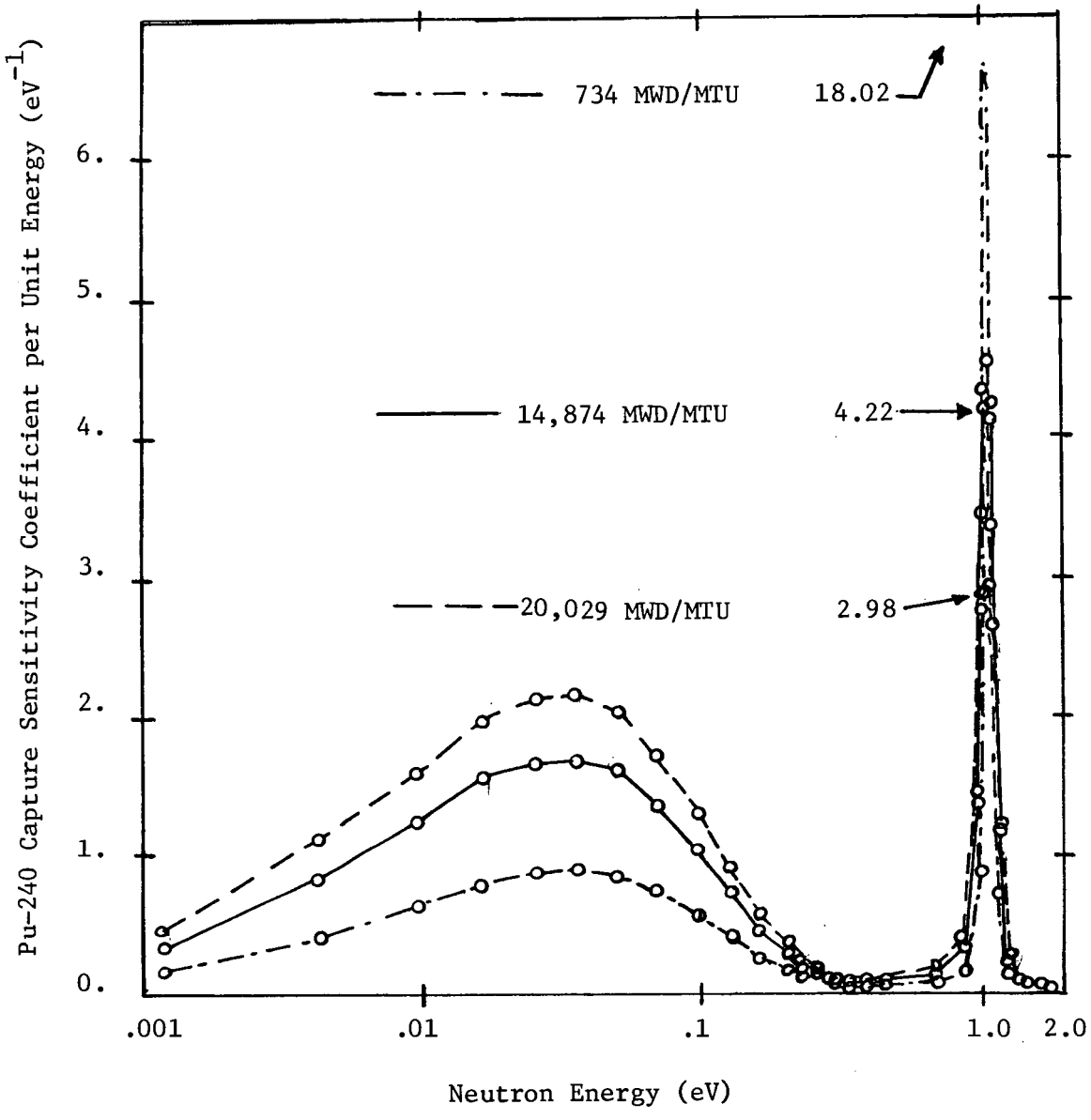

Fig. 1. Detailed Pu-240 Sensitivity Coefficient for the Montague BWR at Different Exposures.

and have been implemented in the FASTT code. Multigroup cross section sensitivity coefficients (Path A) vary with fuel exposure. A striking feature of our thermal analyses has been the (usually) overwhelming importance of the hardened Maxwellian energy region. Both Path A and Path B analyses indicate that it is very important to analyze the fuel cycle as a whole, rather than to consider one time only.

ACKNOWLEDGEMENT

This work was sponsored by the Electric Power Research Institute under Contract RP-975-4. The guidance of Dr. Odelli Ozer, EPRI Project Manager, is appreciated.

REFERENCES

1. M. Becker, D. R. Harris, B. Quan, and J. M. Ryskamp, "Sensitivity of Water Reactor Fuel Cycle Parameters and Costs to Nuclear Data," these proceedings.

2. M. Becker, D. R. Harris, J. Parillo, A. Parvez, and J.M. Ryskamp, "Fuel Cycle Sensitivity Analysis System for Light-Water Reactors," Trans. Am. Nucl. Soc., 24, 216 (1976).

3. A. Parvez, M. Becker, D. Boguslawski, D. R. Harris and J. M. Ryskamp, "Fuel Cycle Cost Sensitivity Analysis for Boiling and Pressurized Water Reactors," Trans. Am. Nucl. Soc., 27, 468 (1977).

4. M. Danchak, W. R. Moyer and M. Becker, "The Rensselaer Interactive Graphics Analysis System," Trans. Am. Nucl. Soc., 18, 159 (1974).

5. C. F. Poncelet, "LASER, A Depletion Program for Lattice Calculations Based on MUFT and THERMOS," WCAP-6073 (1966).

6. R. F. Barry, "LEOPARD-A Spectrum Dependent Non-Spatial Depletion Code for the IBM-7094," Westinghouse Electric Corporation report, WCAP-3269 (Sept. 1963).

7. H. Amster and R. Suarey, "The Calculation of Thermal Constants Averaged Over a Wigner-Wilkins Flux Spectrum: Description of the SOFOCATE Code," Westinghouse Electric Corporation report, WAPD-TM-39 (1957).

8. H. C. Honeck, "THERMOS, A Thermalization Transport Theory Code for Reactor Lattice Calculations," Brookhaven National Laboratory report, BNL-5826 (1961).

9. "CHEETAH-P," Nuclear Associates International Corporation report, (1974).

10. D. E. Cullen, C. R. Weisbin, R. Q. Wright, and J. E. White, "Comparison of Doppler Broadening Methods," NBS Special Publication 425, Vol. 1, 392 (1975)

11. E. P. Wigner and J. E. Wilkins, Jr., "Effect of the Temperature of the Moderator on the Velocity Distribution of Neutrons with Numerical Calculation for Hydrogen as Moderator," U. S. AEC report, AECD-2275 (1944).

12. M. Nelkin, "The Scattering of Slow Neutrons by Water," Phys. Rev., 119, 741 (1960).

13. L. E. Strawbridge, "Calculation of Lattice Parameters and Criticality for Uniform Water Moderated Lattices," Westinghouse Electric Corporation report, WCAP-3269-25 (1963).

14. J. M. Ryskamp, D. R. Harris and M. Becker, "Sensitivity of Light-Water Reactor Parameters to Uncertainties in Thermal Nuclear Data," Trans. Am. Nucl. Soc., 26, 581 (1977).

15. M. Danchak, W. R. Moyer, and M. Becker, "The Rensselaer Interactive Graphics Analysis System," Trans. Am. Nucl. Soc., 18, 159 (1974).

16. J. M. Ryskamp, "FASTCELL, A Code for Fast Computation of Reactor Cell Characteristics Over a Fuel Cycle," Master's Thesis, Rensselaer Polytechnic Institute (1976).

THE LINEARITY ASSUMPTION IN ADJUSTMENT PROCEDURES

Yehuda Yeivin
Racah Institute of Physics, The Hebrew University
Jerusalem, Israel

ABSTRACT

A numerical experiment was devised to illustrate the application of the cross-section adjustment code ISPRAD. The experiment relates to the Pavia shielding experiment, which consists of an iron block irradiated by a fission plate at the end of the thermal column of the Pavia reactor. A set of five ideal activation detectors was postulated, and their response functions and sensitivity profiles were evaluated for three positions in the iron block. The "experimental" values of the response functions were generated with a modified cross-section set. In the first test the experimental activations were obtained by increasing Σ_6 , the iron total cross section in group 6, by 0.6%. The assumed cross-section uncertainties were 10%, and the errors of the integral data 1%. The given cross-section set was successively adjusted by one, two,..., fifteen integral data. The adjustment of Σ_6 was progressively enhanced, but while most other adjustments practically disappeared, a significant secondary peak persisted throughout. This failure was attributed to the non-linear dependence of the activations on the cross sections. A second test, in which the change in Σ_6 was only 0.17%, resulted in a perfect reproduction of the modified set. The full text elaborates on the analyses of the two tests, on a procedure to check the validity of the linearity assumption, and on a proposed procedure to handle cases in which the linearity criterion fails.

INTRODUCTION

The code ISPRAD (ISpra PRocedure for cross-section ADjustment) incorporates a standard adjustment prescription, which is briefly described in the Appendix. The present version does not include correlations. A numerical experiment was devised to illustrate the application of the code. The present contribution describes this experiment and discusses the results. The main point in the discussion concerns the linearity assumption, upon which most adjustment procedures are based.

The numerical experiment relates to the Pavia shielding experiment, which consists of an iron block irradiated by a fission plate at the end of the thermal column of the Pavia reactor. This assembly was approximated

by a one-dimensional plane-geometry model, which, together with 15-group cross sections, was used as input in the necessary calculations.

A set of five ideal activation detectors was "invented," and their response functions and sensitivity profiles (for the 15 group total cross sections) were evaluated at three positions in the iron block. The assumed detectors were all of a constant (10 barn) capture cross section. Detector 1 was flat. The threshold of detector 2 coincided with the lower energy boundary of group number 12. And detectors 3, 4 and 5 had their thresholds at the lower energy boundaries of groups 9, 6 and 3, respectively.

A direct-flux ANISN calculation yields the angular flux distribution in the assembly, of course, and the activations of the five detectors at each and every space division. Thus, from such a run with the given cross-section set we obtain the calculated values of the response functions of each detector at each of the three positions.

To evaluate the sensitivity profile of a detector, we need the direct flux (obtained from the above-mentioned ANISN run), and also the adjoint flux in the assembly with the detector as source.

Let $S = S(\vec{x},\vec{v})$ be the actual neutron source distribution in the assembly (the fission-plate source in our case), and let $D = D(\vec{x},\vec{v})$ be the detector "distribution". Then the direct and adjoint fluxes that we need are, respectively, the solutions of the two equations

$$H\psi = S, \quad H^{\dagger}\psi^{\dagger} = D. \tag{1}$$

Now, the detector's response is obviously

$$R = \langle\psi D\rangle = \ldots = \langle\psi^{\dagger}S\rangle, \tag{2}$$

where $\langle\ldots\rangle$ denotes integration over all six variables ($\vec{x}$ and $\vec{v}$). Considering any perturbation in the assembly, and denoting

$$\delta H = H - H_0 , \quad \delta\psi = \psi - \psi_0 , \tag{3}$$

it is a straightforward matter to show that the corresponding variation of the response function is given by

$$\delta R = -\langle\psi_0^{\dagger}\delta H\psi\rangle \simeq -\langle\psi_0^{\dagger}\delta H\psi_0\rangle . \tag{4}$$

In our particular study we are interested in the detector's sensitivities to the iron total cross sections, and therefore

$$\delta H\psi = \delta\Sigma\psi . \tag{5}$$

Thus the sensitivities in which we are interested are given by

$$\delta R/\delta\Sigma_g = -\int d^3x\int d^2\Omega\psi_g^{\dagger}(\vec{x},\vec{\Omega})\psi_g(\vec{x},\vec{\Omega}) \quad . \; . \; . \; . \quad g = 1,2,\ldots,15 \tag{6}$$

where the space integration obviously refers to the iron block only.

The code SWANLAKE, the input for which consists of the direct and adjoint fluxes and the given cross-section set, evaluates these integrals (as well as the other integrals which enter into the expressions of the detector's sensitivities to all the cross sections in the given set), and thus generates the complete sensitivity profile of the detector which was used as source in the calculation of the adjoint flux.

To apply ISPRAD we also needed experimental values of the response functions. These were generated by direct-flux runs of ANISN with modified cross-section sets. The clear advantage of such "games", from the viewpoint of testing the code, is that in each case we know beforehand what adjustments to expect.

As already mentioned, in the first tests of the adjustment code the total cross sections only were modified, and they alone were allowed to be adjusted. Thus in each run of ISPRAD there were 15 parameters to be adjusted in order to improve the fit between the calculated and "experimental" values of the response functions.

RESULTS AND DISCUSSION

In the first test Σ_6, the macroscopic total cross section in group 6 ($32<E\leq 110$ keV), was modified from its "given" value of 0.3258 to 0.32776 cm^{-1}, i.e. by 0.6%. This may seem a rather small modification, but modifying the total cross section alone amounts to just modifying the capture cross section, and the corresponding modification of the latter is from 0.00054 to 0.0025 cm^{-1}, which is quite substantial.

Unless otherwise stated, the cross-section errors in all ISPRAD runs were always $\Delta\hat{\Sigma}=10\%$, and those of the "experimental" response functions were $\Delta\hat{r}=1\%$.

In the first run the given total cross sections were adjusted by just one integral datum, the experimental activation of detector 1 at position 1 (100 cm from the iron-block face touching the fission plate). The resulting adjustments (in %) are shown as the dotted curve in Fig. 1.

Compared with the 0.6% modification of Σ_6, let alone with the 10% error allowed to each total cross section, it is seen that the adjustments are indeed very small. The fit between the recalculated response function and its experimental value is excellent. Regarding the "shape" of the dotted curve, however, not much can be said. It is, as it should be, proportional to the sensitivity profile of response function (11), i.e. "position 1, detector 1".

In further runs of ISPRAD the given cross sections were successively adjusted by two, three, four and five integral data, all relating to the detectors at position 1, namely by the experimental values of activations (11) and (12), then by those of activations (11), (12) and (13), etc. The dashed curve in Fig. 1 shows the adjustments resulting from data on

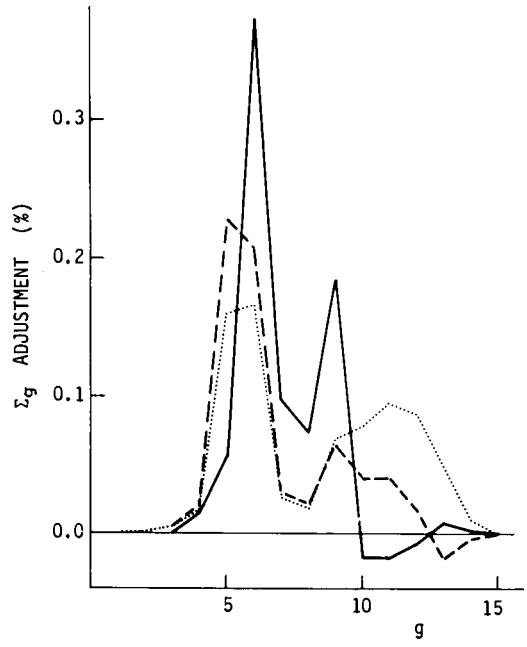

Fig. 1. The relative total-cross-section adjustments by data generated by increasing the given Σ_6 by 0.6%. The dotted curve refers to the adjustment by just one datum, the "experimental" response (11); the dashed curve to the adjustment by (11),(12) and (13); and the full curve refers to the adjustment by all five responses at position 1.

(11),(12) and (13); and the full curve gives the adjustments by all five detectors at position 1.

We notice that the adjustment of Σ_6 is progressively enhanced, as was to be expected, and that in the case of adjustment by all the data at position 1, already reached more than half the actual modification of this parameter. At the same time, most other adjustments decrease to a mere "noise" level, except for a spurious secondary peak at Σ_9.

The next step was to adjust the given set by all data of positions 1 and 2 (150 cm from the fission plate), namely by 10 integral data. The results are shown in Fig. 2 (the dashed curve). Now the adjustment of Σ_6 is over 0.5%, almost its full "nominal" value. The secondary peak at Σ_9 has disappeared, and except for a Σ_7 adjustment of 0.13%, it seems that we now have a rather satisfactory reconstruction of the modified cross-section set with which the experimental activations were generated.

Finally the cross sections were adjusted by all 15 integral data, i.e. by the experimental activations of all detectors at positions 1, 2 and 3 (125 cm from the fission plate). However, expecting to further improve the reconstruction of the modified set, we actually obtain the adjustments shown by the full curve in Fig. 2. The adjustment of Σ_6 has somewhat decreased to 0.46%, that of Σ_7 has doubled, and a high peak of 0.33% appears at Σ_4.

Now, the adjustment of the 15 total cross sections by 15 integral data, whatever the adjustment algorithm, is unique, and should just reproduce the modified set. Furthermore, this result should be independent of the assumed errors $\Delta\hat{r}$. But on repeating the last run with $\Delta\hat{r}$=0.25% (instead of 1%) we find the absurd adjustments shown by the dash-point curve in Fig. 2.

This seemingly striking failure of our adjustment procedure indicates that something rather fundamental must have been overlooked, and an obvious suspicion is a failure of the linearity assumption over the range of modification of Σ_6.

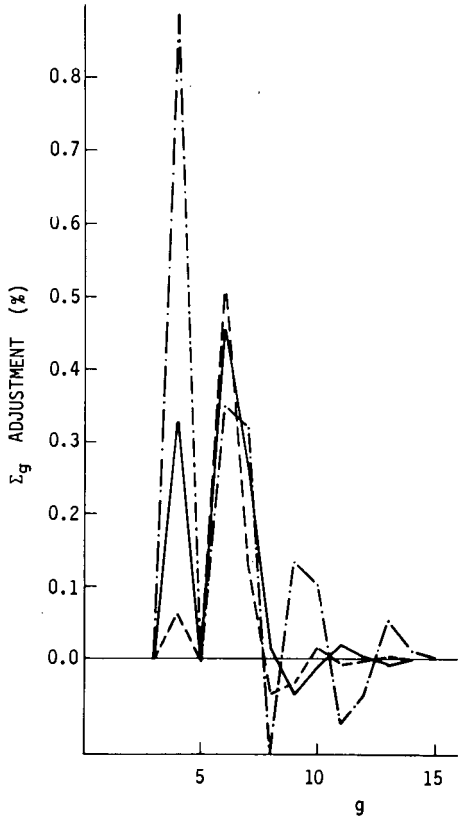

Fig. 2. The relative total-cross-section adjustments by data generated by increasing the given Σ_6 by 0.6%. The dashed curve refers to the adjustment by all data at positions 1 and 2; the full curve to the adjustment by all 15 data, at positions 1, 2 and 3; and the dash-point curve refers to the adjustment by all 15 data, but with all $\Delta\hat{r}$ reduced to 0.25% (instead of the standard 1%).

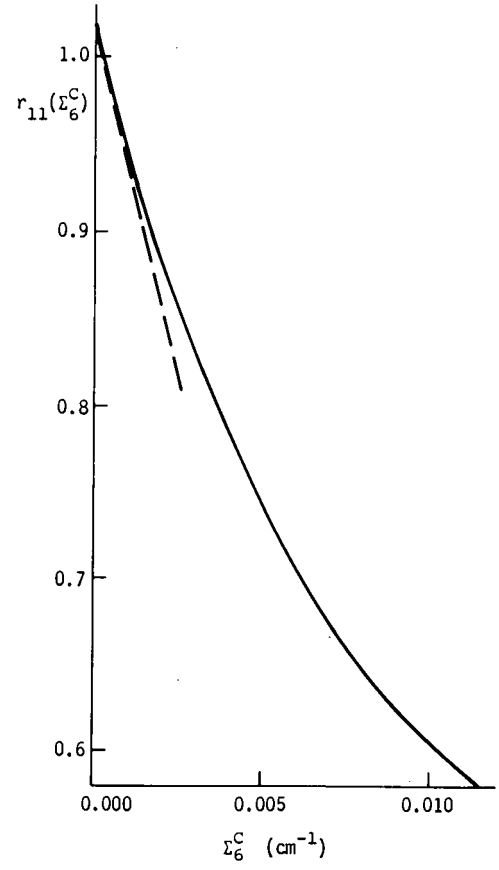

Fig. 3. The dependence of activation (11) on Σ_6^c. The dashed line is the tangent to the curve at the given-library value of Σ_6^c.

Let us then consider Fig. 3, which shows the dependence of activation (11) on Σ_6. The curve is also typical of the behaviour of the other activations as functions of Σ_6. The tangent to the (11) curve at the point corresponding to the given value of Σ_6, i.e. the point at which the sensitivities are calculated, is also shown. It is evident that linear adjustment over the range up to the modified value of Σ_6 is inconsistent with our "experimental" activations, generated with this value by ANISN. It is thus not suprising that we have failed to reconstruct the nominal cross-section modification.

In order to verify this argument, the complete set of calculations has been repeated with "experimental" activations generated by a Σ_6 modification of -0.17%, which just corresponds to setting $\Sigma_6^c=0$. Notice that this modification is 3.5 times smaller than the previous one. The results are summarized in Fig. 4. The dotted curve shows the total-cross-section adjustments by the 5 data at position 1, the dashed curve the adjustments by the 10 data at positions 1 and 2, and the full curve represents the adjustment of the given set by all 15 data, at positions 1, 2 and 3.

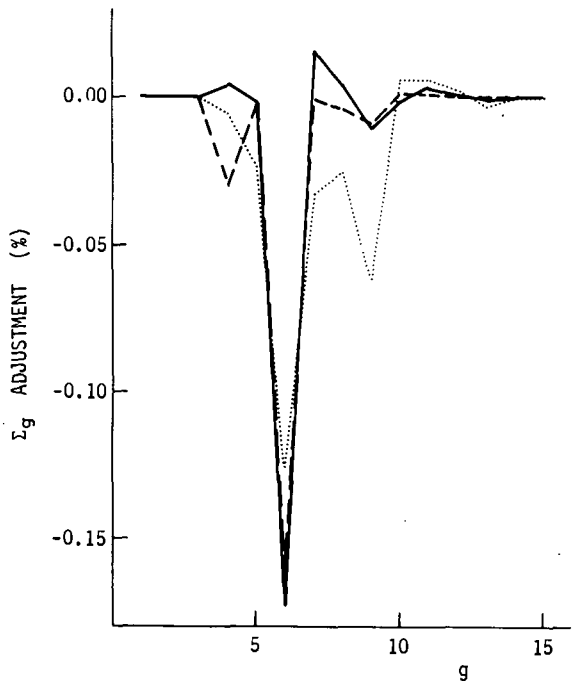

Fig. 4. The relative total-cross-section adjustments by data generated by decreasing the given Σ_6 by 0.17%. The dotted curve refers to adjustment by all data at position 1; the dashed curve to the adjustment by data at positions 1 and 2; and the full curve refers to the adjustment by the data at positions 1, 2 and 3.

The adjustment by the activation data at one position already indicates the actual modification, but still generates a "ghost" adjustment at Σ_9. When data at two positions are used to adjust the cross sections we already obtain a reasonable reconstruction of the modified set, and the adjustment by all 15 integral data yields yet a marginally better reconstruction.

CONCLUDING REMARKS

Reported above were just preliminary results. Nevertheless, we may comment on several important problems that arise with respect to cross-section adjustment in general, and to the discussion of which even our preliminary results already make certain contributions.

First of all, since in practical situations we do not know, of course, what to expect, we should always be aware that the linearity assumption might not be valid over the range of the resulting adjustments. In principle, the assumption may be checked by comparing the values of the integral quantities re-evaluated by linear extrapolation, using the sensitivities, with their values recalculated by the transport code using the adjusted cross sections. However, our results indicate a possible alternative, which is much simpler. We could progressively reduce Δr, and judge the validity of the linearity assumption by studying the behaviour of the ensuing adjustments.

Another problem, which is at least just as important, arises if and when it turns out that the linearity assumption is definitely in-

valid. A most reasonable procedure, lengthy and tedious as it might be, would be to reduce, by a constant factor, all deviations of the experimental values of the integral quantities from their corresponding values calculated with the given set of cross sections. In other words, to replace the vector c by αc, with $\alpha<1$, in the adjustment prescription. The resulting adjusted cross-section set should then be considered as a given set, and be re-adjusted, again substituting $\alpha' c'$ for c' if necessary. These steps would be repeated until the nth-adjusted cross-section set satisfactorily reproduces the $\hat{r}$'s. With the α's small enough, the validity of the linearity assumption in each step will obviously be guaranteed.

A last comment refers to a problem of great practical significance, namely that of the optimal number of integral data necessary to adjust a cross-section set in a given typical adjustment problem. As we have just noticed, if this number is too small, then the adjustments only reflect the nature of the sensitivities (and whenever cross sections are adjusted by just one datum, the adjustments are exactly proportional to the sensitivity profile of the single integral quantity). On the other hand, we have seen that integral data above a certain number may be redundant. In designing integral experiments, such as the shielding experiment that we have considered, this is certainly an important problem. However, it seems that more numerical experiments are necessary in order to intelligently discuss the problem of the optical number and the nature of the desirable integral data.

Acknowledgement

The author wishes to express his gratitude to the EURATOM centre at Ispra, and to the ESIS group in particular, for their hospitality and for the opportunity to spend three months with them, during which time ISPRAD was written and the results reported here obtained.

Special thanks are due to Mr. K. Burn for his help with the ANISN and SWANLAKE calculations.

APPENDIX: THE ADJUSTMENT PRESCRIPTION

Consider a given cross-section set $\hat{\sigma}_i$, i=1,...,N, where N = (number of energy groups)×(number of partial cross sections considered)× (number of isotpes), and a set of measured responses of various detectors (in a typical shielding experiment) $\hat{r}_j$, j=1,...,n. Let $\Delta\hat{\sigma}_i$ be the cross-section uncertainties, and $\Delta\hat{r}_j$ the experimental errors of the measured responses. Further, denote the calculated values of the response function by $r_j(\hat{\sigma})$.

Now, if σ_i are the (unknown) adjusted cross sections, we denote

the dimensionless cross-section adjustments by

$$x_i=(\sigma_i-\hat{\sigma}_i)/\Delta\hat{\sigma}_i, \tag{A.1}$$

and since $r_j(\sigma)$ should be the "true" values of the response functions, we denote their dimensionless deviations from the corresponding experimental values by

$$y_j=(r_j(\sigma)-\hat{r}_j)/\Delta\hat{r}_j. \tag{A.2}$$

We further denote the (negatives of the) deviations of the calculated responses from the experimental values by

$$c_j= -(r_j(\hat{\sigma})-\hat{r}_j)/\Delta\hat{r}_j. \tag{A.3}$$

The sensitivity matrix is defined as

$$A_{ji}=\frac{\partial y_j}{\partial x_i} = \frac{\Delta\hat{\sigma}_i}{\Delta\hat{r}_j}\frac{\partial r_j}{\partial\sigma_i}, \tag{A.4}$$

where the derivatives are evaluated at $x=0$ $(\sigma=\hat{\sigma})$. Then the linearity assumption, i.e. the assumption of a linear dependence of the response functions on the cross sections,

$$r_j(\sigma)\simeq r_j(\hat{\sigma})+\sum\frac{\partial r_j}{\partial\sigma_i}(\sigma_i-\hat{\sigma}_i), \tag{A.5}$$

reduces, in matrix notation, to

$$y=Ax-c. \tag{A.6}$$

The adjustment procedure then boils down to the following conditional minimum: to find the vectors x and y which minimize the form

$$Q=\tilde{x}x+\tilde{y}y, \tag{A.7}$$

subject to the constraint of equation (A.6).

The straightforward solution of this problem is

$$x=\tilde{A}(I+A\tilde{A})^{-1}c, \quad y= -(I+A\tilde{A})^{-1}c. \tag{A.8}$$

FIRST AND HIGHER ORDER PERTURBATION TECHNIQUES AND THEIR APPLICATION IN SYSTEM ANALYSIS AND DATA ADJUSTMENTS.

A. Gandini
CNEN-CSN Casaccia, Rome (Italy)

ABSTRACT

Owing to their ability to allow with relatively limited effort to account for and analyze the more or less complex processes which are involved when an alteration is induced into a given system, perturbation methods in general and generalized perturbation methods in particular have been encountering an increasing interest among reactor physicists. Most applications of these methods have been so far characterized by linear approaches. In the present paper, the scope and limits of these linear approaches are discussed and second or higher order ones are proposed in some significant cases.

For what concerns the multiplying systems at critical conditions for which ratios of functionals linear with the flux are generally considered, explicit methods adopting higher mode eigenfunctions are illustrated, whereas higher order generalized perturbation techniques are proposed for time-dependent and source problems.

INTRODUCTION

Perturbation methods in general, and generalized perturbation theory (GPT) methods in particular, have been playing a major role in several fields of multiplying and non-multiplying systems. An effort of this kind seems highly justified under many respects, in particular:

1 - by the need for a full analytical comprehension of the physical phenomena occuring in a reactor system also in connection with interrelated effects;
2 - by the need of a more accurate correlation between integral and differential data so that a more adequate procedure may be adopted in cases where the adjustments result too high for a linear approach, especially in cases in which the second order sensitivities result significantly high, as may occur in propagation experiments when the optical distances between the real sources and the detectors are large;
3 - by the need in certain circumstances to adopt existing non-linear programming techniques in reactor (core, blanket and shield) optimization problems for which quadratic (or higher order) sensitivity coefficients should also be known.

Most applications of these methods have been so far characterized by linear approaches. In the present paper the scope and limits of these linear approaches are discussed and second or higher order ones are proposed in some significant cases.

PERTURBATION METHODS FOR CRITICAL SYSTEM

The quantities which are of major interest in reactor physics analysis at critical conditions fall generally within three main categories:

1 - Those given by ratios of quantities linear with the real neutron fluxes, as reaction rate ratios, breeding ratios, etc.
2 - Those given by ratio of quantities linear with the real and adjoint neutron fluxes, as reactivity coefficients and prompt neutron lifetimes.
3 - Those given by functionals of the neutron flux density different from those described above, as, for example, the doubling time of the critical mass of a reactor system.

Integral quantities of the first category may be assumed to have the general form (in multigroup notation):

$$R = \frac{\langle \underline{h}_A^+ \underline{\varphi} \rangle}{\langle \underline{h}_B^+ \underline{\varphi} \rangle} \tag{1}$$

$\underline{h}^+(\underline{\vartheta})$ representing assumed vector functions, $\underline{\varphi}(\underline{\vartheta})$ the neutron flux density satisfying the equation

$$(A + \lambda_1 \mathcal{F})\underline{\varphi} = 0 \quad , \tag{2}$$

and $\langle\ \rangle$ indicating integration over the space variables $\underline{\vartheta}$.

Integral quantities of the second category may be assumed of the form:

$$\rho = \frac{\langle \underline{\varphi}^* \mathcal{H}_A \tilde{\underline{\varphi}} \rangle}{\langle \underline{\varphi}^* \mathcal{H}_B \tilde{\underline{\varphi}} \rangle} \tag{3}$$

where $\underline{\varphi}^*$ represents the adjoint flux, $\mathcal{H}$ assigned matrix operators and $\tilde{\underline{\varphi}}$ a zero, first, etc. order approximation of the flux altered by system parameter variations (in reactivity expressions inherent in matrices $\mathcal{H}$).

Quantities of the third category may be assumed to have the form

$$F = F(\underline{\varphi}) \tag{4}$$

$F(\underline{\varphi})$ denoting a most general dependence on the flux $\underline{\varphi}$.

A perturbation introduced into a given system* generally gives rise to changes $\delta\underline{\varphi}$, $\delta\underline{h}^{+}$, $\delta\underline{\varphi}^{*}$, $\delta\tilde{\underline{\varphi}}$, $\delta\mathcal{H}$ of $\underline{\varphi}$, $\underline{h}^{+}$, $\underline{\varphi}^{*}$, $\tilde{\underline{\varphi}}$, $\mathcal{H}$ leading to changes δR, $\delta\rho$ and δF of R, ρ and F, respecively. In view of such parameter alterations, it is the object of perturbation methods to allow the evaluation of the consequent changes in these integral quantities, to first or higher order of approximation, avoiding the direct calculation of the perturbed fluxes and, if possible, explicitly in terms of unperturbed functions.

First order evaluations of the variations $\delta R/R$ and $\delta\rho/\rho$ can be obtained by means of the generalized perturbation theory (GPT) methods**, which may also be used to account, to first order, for the altered density $\tilde{\underline{\varphi}}$. Since these GPT methods imply, in their derivation, the neglecting of a second order term***, there is generally no possibility to further improve their accuracy when this is requested. The only practical ways to obtain significant second and higher order terms appear then to consist in methods expressing perturbatively the altered real and adjoint fluxes to be adopted directly in Eqs. (1), (3), or (4), which after all is a standard procedure in classical perturbation theory.

The Standard Method

In order to obtain the expressions giving the flux $\delta\underline{\varphi}$ in terms of the perturbed parameters, the "standard method" is derived [2], so called since it leads to perturbative expressions analogous to those relevant to the classical quantum mechanics. If we assume that the perturbation does

---

* In case of quantities of the second category, this perturbation is assumed independent, in general, of the parameter changes which may be inherent (as in reactivity expression) in operator $\mathcal{H}$ and on which $\tilde{\underline{\varphi}}$ depends.

** For comments and ample bibliography on these methods, see Ref. /1/

*** For instance, considering the second order expression

$$\delta R = R\left(\frac{\delta\langle\underline{h}_A^{+}\underline{\varphi}\rangle}{\langle\underline{h}_A^{+}\underline{\varphi}\rangle} - \frac{\delta\langle\underline{h}_B^{+}\underline{\varphi}\rangle}{\langle\underline{h}_B^{+}\underline{\varphi}\rangle}\right)\left(1 - \frac{\delta\langle\underline{h}_B^{+}\underline{\varphi}\rangle}{\langle\underline{h}_B^{+}\underline{\varphi}\rangle}\right),$$

obtained from Eq. (1), the GPT methods resul neglecting the coefficient $(1 - \delta\langle\underline{h}_B^{+}\underline{\varphi}\rangle/\langle\underline{h}_B^{+}\underline{\varphi}\rangle)$.

not alter the criticality, and limiting here our attention to second order terms, we may obtain the expression:

$$\delta\underline{\varphi} = -\langle\delta\underline{\varphi}\,\underline{h}\rangle + \langle\delta\underline{h}\,\underline{\varphi}\rangle^2 - \sum_{n=2}^{\infty}\langle\underline{f}_n^*\delta\mathcal{B}_1\underline{\varphi}\rangle\left\{[1-\langle\delta\underline{h}\,\underline{\varphi}\rangle]\underline{\Psi}_n - \right.$$
$$\left. -\langle\delta\underline{h}\,\underline{\Psi}_n\rangle\underline{\varphi}\right\} + \sum_{n,j=2}^{\infty}\langle\underline{f}_j^*\delta\mathcal{B}_1\underline{\varphi}\rangle\langle\underline{f}_n^*\delta\mathcal{B}_1\underline{\Psi}_j\rangle\underline{\Psi}_n \tag{5}$$

where

$$\delta\mathcal{B}_1 = \delta\mathcal{A} + \lambda_1\delta\mathcal{F} \tag{6}$$

$$\underline{f}_n^* = \underline{\Phi}_n^*/(\lambda_1-\lambda_n) \tag{7}$$

$$\underline{\Psi}_n = \underline{\Phi}_n - \langle\underline{h}\,\underline{\Phi}_n\rangle\underline{\varphi} \quad , \tag{8}$$

$\underline{h}$ is an assigned vector characterizing the flux normalization criterion (to be satisfied before and after the perturbation and implying, for instance, the conservation of the total reactor power)

$$\langle\underline{h}\,\underline{\varphi}\rangle = \langle\underline{h}'\underline{\varphi}'\rangle = 1 \quad , \tag{9}$$

$\underline{\Phi}_n$ and $\underline{\Phi}_m^*$ represent the real and adjoint n-th eigenfucntions, respectively, and satisfy the equations

$$(\mathcal{A}+\lambda_m\mathcal{F})\underline{\Phi}_m = 0 \tag{10}$$

$$(\mathcal{A}^*+\lambda_m\mathcal{F}^*)\underline{\Phi}_n^* = 0 \tag{11}$$

(λ_m being the n-th eigenvalue) and the normo-orthogonality relation

$$\langle\underline{\Phi}_m^*\mathcal{F}\underline{\Phi}_n\rangle = \begin{cases} 1 & \text{for } n=m \\ 0 & \text{for } n\neq m \end{cases} . \tag{12}$$

If no particular flux normalization is imposed as in the course of reactivity or reaction rate studies, Eq. (5) reduces to

$$\delta \underline{\varphi} = -\sum_{n=2}^{\infty} \langle \underline{f}_n^* \delta \mathcal{B} \underline{\varphi} \rangle \underline{\phi}_n + \sum_{n,j=2}^{\infty} \langle \underline{f}_j^* \delta \mathcal{B} \underline{\varphi} \rangle \langle \underline{f}_n^* \delta \mathcal{B} \underline{\phi}_j \rangle \underline{\phi}_n \, . \tag{13}$$

If, for instance, a flux expansion up to three harmonics is considered, there would be only six terms $\langle\,\rangle$ to be calculated in either expression (5) or (13). Simplified formulations of this kind may be of interest in optimization problems in which large material changes may occur, or in problems of (second-order) adjustments of nuclear data to force statistical consistency with measured integral parameters given by ratios of functionals linear with the neutron flux. In all then cases, in fact, all the material density changes, or the nuclear data adjustments, should amount to a change $\delta\mathcal{B}$ of the Boltzman operator, which does not alter the criticality.

The above method is based on the knowledge of the higher mode eigenfunctions $\underline{\phi}_n$ and $\underline{\phi}_n^*$ and of the eigenvalues λ_n . These quantities can be evaluated by the method proposed by Saito and Katsuragi[3] which can be extended to any order of eigenfunctions desired[2]. In the most general case, given the real source

$$\underline{\mathcal{S}}_n = (\mathcal{A} + \lambda_1 \mathcal{F}) \mathcal{F}^{-1} (\mathcal{A} + \lambda_2 \mathcal{F}) \mathcal{F}^{-1} (\mathcal{A} + \lambda_3 \mathcal{F}) \ldots$$
$$\ldots \mathcal{F}^{-1} (\mathcal{A} + \lambda_{n-1} \mathcal{F}) \underline{\phi}^{guess} \tag{14}$$

and the system

$$\begin{cases} \mathcal{A} \underline{f}_n^{(1)} = \underline{\mathcal{S}}_n \\ \cdot \quad \cdot \quad \cdot \quad \cdot \quad \cdot \quad \cdot \quad \cdot \\ \mathcal{A} \underline{f}_n^{(i)} = -\bar{\lambda}_n^{(i-1)} \mathcal{F} \underline{f}_n^{(i-1)} \, , \qquad (i = 2, 3, \ldots) \end{cases} \tag{15}$$

where

$$\bar{\lambda}_n^{(i-1)} = 1 / \langle \underline{u} \, \mathcal{F} \underline{f}_n^{(i-1)} \rangle \tag{16}$$

($\underline{u}$ being a unit vector), function $\underline{f}_n^{(i)}$ is shown to converge, for $i \to \infty$, to the n-th real eigenvalue $\underline{\phi}_n$. An analogous procedure may be obtained with respect to the n-th adjoint eigenfunction. It is interesting to notice that the recurrent system (15), apart from the ri-normalization coefficient $\bar{\lambda}_n^{(i)}$, resembles those adopted for the calculation of the integral importance function in the GPT methods. Therefore, existing methods for the calculation of this latter function can be adapted, with little

effort, to this new purpose.

PERTURBATION METHODS FOR TIME DEPENDENT AND SOURCE PROBLEMS

Let us generally consider an integral quantity (or detection) of the type

$$Q = \int_{t_I}^{t_F} dt \, \langle \underline{s}^+(\underline{\vartheta}, t) \underline{c}(\underline{\vartheta}, t) \rangle \quad , \tag{17}$$

(t_I ,t_F) being the time of detection, $\underline{s}^+$ and assigned vector, and $\underline{c}$ representing the particle density satisfying the equation

$$\frac{\partial \underline{c}}{\partial t} = \mathcal{H} \underline{c} + \underline{s} \quad , \tag{18}$$

$\mathcal{H}$ and $\underline{s}$ being an assigned linear matrix operator and the real source, respecively. By repeated use of the time-dependent GPT methods[4], the following expression may be obtained[5] relevant to a perturbation $\delta\mathcal{H}$ in the time interval (t_1 , t_F):

$$\delta Q = \int_{t_1}^{t_F} dt \, \langle \underline{c}^* \delta\mathcal{H} \underline{c} \rangle + \frac{1}{2!} \sum_{i=1}^{I} \int_{t_1}^{t_F} dt \left[\langle \underline{c}^*_{/i} \delta\mathcal{H} \underline{c} \rangle + \langle \underline{c}^* \delta\mathcal{H} \underline{c}_{/i} \rangle \right] \delta p_i +$$

$$+ \frac{1}{3!} \sum_{i,j=1}^{I} \int_{t_1}^{t_F} dt \left[\langle \tilde{\underline{c}}^*_{/i,j} \delta\mathcal{H} \underline{c} \rangle + \langle \underline{c}^*_{/j} \delta\mathcal{H} \underline{c}_{/i} \rangle + \langle \underline{c}^*_{/i} \delta\mathcal{H} \underline{c}_{/j} \rangle + \right.$$

$$\left. + \langle \underline{c}^* \delta\mathcal{H} \tilde{\underline{c}}_{/i,j} \rangle \right] \delta p_i \delta p_j \quad , \tag{19}$$

where

$$\delta\mathcal{H} = \sum_{k=1}^{I} \frac{\partial \mathcal{H}}{\partial p_k} \delta p_k \quad , \tag{20}$$

p_i is the generic i-th (j = 1, ..., I) parameter characterizing matrix $\mathcal{H}$, and functions $\underline{c}^*$, $\tilde{\underline{c}}^*_{/i,j}$, $\underline{c}_{/i}$, $\tilde{\underline{c}}_{/i,j}$ satisfy the equations:

$$-\frac{\partial \underline{c}^*}{\partial t} = \mathcal{H}^* \underline{c}^* + \underline{s}^+ \tag{21}$$

(with $\underline{c}^* = 0$ for $t > t_F$)

$$-\frac{\partial \underline{c}^*_{/i}}{\partial t} = \mathcal{H}^* \underline{c}^*_{/i} + \frac{\partial \mathcal{H}^*}{\partial p_i} \underline{c}^* \tag{22}$$

$$-\frac{\partial \tilde{\underline{c}}^*_{/i,j}}{\partial t} = \mathcal{H}^* \tilde{\underline{c}}^*_{/i,j} + \frac{\partial \mathcal{H}^*}{\partial p_i} \underline{c}^*_{/j} + \frac{\partial \mathcal{H}^*}{\partial p_j} \underline{c}^*_{/i} \tag{23}$$

$$\frac{\partial \underline{c}_{/i}}{\partial t} = \mathcal{H} \underline{c}_{/i} + \frac{\partial \mathcal{H}}{\partial p_i} \underline{c} \tag{24}$$

$$\frac{\partial \tilde{\underline{c}}_{/i,j}}{\partial t} = \mathcal{H} \tilde{\underline{c}}_{/i,j} + \frac{\partial \mathcal{H}}{\partial p_i} \underline{c}_{/j} + \frac{\partial \mathcal{H}}{\partial p_j} \underline{c}_{/i} \quad . \tag{25}$$

If, as is the case with most shielding problems, the source $\underline{s}$ is the time-independent, so result also the density $\underline{c}$. If also the perturbation $\delta\mathcal{H}$ is assumed time-independent, Eq. (19) may be transformed into the following:

$$\begin{aligned} \delta Q = {} & \langle \underline{\Psi}^* \delta\mathcal{H} \underline{c} \rangle + \frac{1}{2!} \sum_{i=1}^{I} [\langle \underline{\Psi}^*_{/i} \delta\mathcal{H} \underline{c} \rangle + \langle \underline{\Psi}^* \delta\mathcal{H} \underline{c}_{/i} \rangle] \delta p_i + \\ & + \frac{1}{3!} \sum_{i,j=1}^{I} [\langle \tilde{\underline{\Psi}}^*_{/i,j} \delta\mathcal{H} \underline{c} \rangle + \langle \underline{\Psi}^*_{/j} \delta\mathcal{H} \underline{c}_{/i} \rangle + \langle \underline{\Psi}^*_{/i} \delta\mathcal{H} \underline{c}_{/j} \rangle + \\ & + \langle \underline{\Psi}^* \delta\mathcal{H} \tilde{\underline{c}}_{/i,j} \rangle] \delta p_i \delta p_j \end{aligned} \tag{26}$$

where $\underline{\Psi}^*, \underline{\Psi}^*_{/i}, \underline{\Psi}^*_{/i,j}$ are given by the expression:

$$\underline{\Psi}^*(\underline{\vartheta}) = \int_{-\infty}^{t_F} \underline{c}^*(\underline{\vartheta}, t)\, dt \tag{27}$$

$$\underline{\Psi}^*_{/i}(\underline{\vartheta}) = \int_{-\infty}^{t_F} \underline{c}^*_{/i}(\underline{\vartheta}, t)\, dt \tag{28}$$

$$\underline{\tilde{\Psi}}^{*}_{/i,j}(\underline{\vartheta}) = \int_{-\infty}^{t_F} \underline{\tilde{c}}^{*}_{/i,j}(\underline{\vartheta}, t)\,dt \tag{29}$$

and satisfy the equations:

$$\mathcal{M}^{*}\underline{\Psi}^{*} + \underline{w}^{+} = 0 \tag{30}$$

$$\mathcal{M}^{*}\underline{\Psi}^{*}_{/i} + \frac{\partial \mathcal{M}^{*}}{\partial p_i}\underline{\Psi}^{*} = 0 \tag{31}$$

$$\mathcal{M}^{*}\underline{\tilde{\Psi}}^{*}_{/i,j} + \frac{\partial \mathcal{M}^{*}}{\partial p_i}\underline{\Psi}^{*}_{/j} + \frac{\partial \mathcal{M}^{*}}{\partial p_j}\underline{\Psi}^{*}_{/i} = 0 \tag{32}$$

with

$$\underline{w}^{+}(\underline{\vartheta}) = \int_{t_1}^{t_F} \underline{s}^{+}(\underline{\vartheta}, t)\,dt \quad . \tag{33}$$

Alternatively, if a perturbation expression of $\delta\underline{c}$ is preferred, which is desirable when a large number of functionals Q have to be studied on the some system (and/or the number of parameters p_i is reduced, for instance by adopting the so called consistent method[6]), the following expression may be used (always limiting our attention to the third order):

$$\delta\underline{c} = \sum_{i=1}^{I} \underline{\tilde{c}}^{(1)}_{/i}\,\delta p_i + \sum_{i\leq j=1}^{I} \underline{\tilde{c}}^{(2)}_{/i,j}\,\delta p_i\,\delta p_j + \sum_{i\leq j\leq k=1}^{I} \underline{\tilde{c}}^{(3)}_{/i,j,k}\,\delta p_i\,\delta p_j\,\delta p_k \ , \tag{34}$$

$\underline{\tilde{c}}^{(1)}_{/i}$, $\underline{\tilde{c}}^{(2)}_{/i,j}$ and $\underline{\tilde{c}}^{(3)}_{/i,j,k}$ satisfying the equations

$$\frac{\partial \underline{\tilde{c}}^{(1)}_{/i}}{\partial t} = \mathcal{M}\underline{\tilde{c}}^{(1)}_{/i} + \frac{\partial \mathcal{M}}{\partial p_i}\underline{c} \tag{35}$$

$$\frac{\partial \underline{\tilde{c}}^{(2)}_{/i,j}}{\partial t} = \mathcal{M}\underline{\tilde{c}}^{(2)}_{/i,j} + \frac{1}{\alpha_i}\frac{\partial \mathcal{M}}{\partial p_i}\underline{\tilde{c}}^{(1)}_{/j} + \frac{1}{\alpha_j}\frac{\partial \mathcal{M}}{\partial p_j}\underline{\tilde{c}}^{(1)}_{/i} \tag{36}$$

$$\left(\begin{array}{c} i\leq j = 1, 2, \ldots, I \\ \alpha_s = \delta_{si} + \delta_{sj} \end{array}\right)$$

$$\frac{\partial \underline{\tilde{c}}^{(3)}_{/i,j,k}}{\partial t} = \mathcal{M}\,\underline{\tilde{c}}^{(3)}_{/i,j,k} + \frac{1}{\alpha_i}\frac{\partial \mathcal{M}}{\partial \mu_i}\underline{\tilde{c}}^{(2)}_{/j,k} + \frac{1}{\alpha_j}\frac{\partial \mathcal{M}}{\partial \mu_j}\underline{\tilde{c}}^{(2)}_{/i,k} +$$

$$+ \frac{1}{\alpha_k}\frac{\partial \mathcal{M}}{\partial \mu_k}\underline{\tilde{c}}^{(2)}_{/i,j} \quad , \quad \left(\begin{array}{l} i \leq j \leq k = 1,2,\ldots,I \\ \alpha_s = \delta_{si} + \delta_{sj} + \delta_{sk} \end{array} \right) \tag{37}$$

δ_{ij} being the Kronecker's symbol. The coefficients $1/\alpha$ are introduced to account for possible repetitions of equal indexed terms. At steady state conditions, which is the case of interest in shielding studies, the time--derivatives in the above equations may be set equal to zero.

The above method giving the density variation $\delta \underline{c}$ in terms of the perturbed parameters is mandatory if higher order terms are requested and direct changes of vector $\underline{s}^+$ are also considered. In fact, in this case it is not possible to apply the higher order formulations for δQ as given by Eq. (19) [or (26)], since the source $\underline{s}^+$ represents the final condition of function $\underline{c}^*$; therefore, its change would influence directly all the other higher order auxiliary functions. In other words, accounting for the variation $\delta \underline{s}^+$ would make the method implicit, whereas we are looking for explicit forms. In these cases the only way out of this difficulty consists adopting the above method. For instance, to second ordern we would obtain:

$$\delta Q = \int_{t_I}^{t_F} dt \Big[\sum_{i=1}^{I} \langle (\underline{s}^+ + \delta \underline{s}^+)\underline{\tilde{c}}^{(1)}_{/i} \rangle \delta \mu_i + \sum_{i \leq j=1}^{I} \langle \underline{s}^+ \underline{\tilde{c}}^{(2)}_{/i,j} \rangle \delta \mu_i \delta \mu_j + \langle \delta \underline{s}^+ \underline{c} \rangle \Big] . \tag{38}$$

If $\underline{s}$ of Eq. (18) results time-independent, so that the system is at steady state conditions, the above expression may also be written:

$$\delta Q = \sum_{j=1}^{I} \langle (\underline{w}^+ + \delta \underline{w}^+)\underline{\tilde{c}}^{(1)}_{/j} \rangle \delta \mu_j + \sum_{i \leq j=1}^{I} \langle \underline{w}^+ \underline{\tilde{c}}^{(2)}_{/i,j} \rangle \delta \mu_i \delta \mu_j + \langle \delta \underline{w}^+ \underline{c} \rangle , \tag{39}$$

with $\underline{w}^+$ given by Eq. (33).

FIRST AND SECOND ORDER ADJUSTMENTS

Once an expresssion for δQ, for instance of the type given by expression (39) or (26) (limited here to second order) is available, the problem arises of adopting adequate adjustment methods which may account also for second order terms at least in relation to a few parameters, i.e. those affected by larger variations. If we consider the fractional changes y_{Q_j} $(j = 1,\ldots,J)$ and y_{σ_i} $(i = 1, \ldots,I)$ of the integral and differential parameters, respectively (with respect to initial values), these result satisfying the (second order) constraints

$$y_{Q_j} = \sum_{i=1}^{I} s_{j,i}\, y_{\sigma_i} + \sum_{i,k=1}^{I} s_{j,i,k}\, y_{\sigma_i}\, y_{\sigma_k} \quad , (j=1,\ldots,J) \tag{40}$$

$s_{j,i}$ and $s_{j,i,k}$ representing first and second order sensitivities, respectively, obtainable by the methods described previously. Assuming estimates $\tilde{y}_{\sigma_i}^{(m-1)}$ are available, the following recurrent scheme may be considered for linearizing the constraints:

$$\begin{aligned} y_{Q_j}^{(m)} &= \sum_{i=1}^{I} \left(s_{j,i} + \sum_{k=1}^{I} s_{j,i,k}\, \tilde{y}_{\sigma_k}^{(m-1)} \right) y_{\sigma_i}^{(m)} \\ &= \sum_{i=1}^{I} s_{j,i}^{(m-1)}\, y_{\sigma_i}^{(m)} \end{aligned} \tag{41}$$

Starting with a linear approach for obtaining $\tilde{y}_{\sigma_i}^{(o)}$, and adopting iteratively the same standard linear techniques already available, the value $\tilde{y}_{\sigma_i}^{(m)}$ should converge rapidly to the best estimators $\tilde{y}_{\sigma_i}$.

REFERENCES

1. A. Gandini, Nucl. Sci. Eng., 57, 248 (1975)
2. A. Gandini, Nucl. Sci. Eng. (in print)
3. R. Saito and S. Katsuraghi, J. Nucl. Sci. Technol. 6, 303 (1969)
4. A. Gandini, Nucl. Sci. Eng., 35, 141 (1964)
5. A. Gandini, Nucl. Sci. Eng. (in print)
6. A. Gandini and M. Salvatores, "Nuclear Data and Integral Measurement Correlation for Fast Reactors. Part 3: the Consistent Method", A CNEN Report, RT/FI(74)3
7. A. Gandini, "Nuclear Data and Integral Measurement Correlation for Fast Reactors. Part 4: Second Order Adjustments and Systematic Errors", A CNEN Report, RT/FI(78)10.

THE USE OF ERROR FILES IN UNCERTAINTY ANALYSIS AND DATA ADJUSTMENT

M. M. Chestnutt ** and A. K. McCracken *
** Imperial College, London
*AEE Winfrith, Dorset

ABSTRACT

Some results are given from uncertainty analyses on Pressurised Water Reactor (PWR) and Fast Reactor Theoretical Benchmarks. Upper limit estimates of calculated quantities are shown to be significantly reduced by the use of ENDF/B data covariance files and recently published few-group covariance matrices.

Some problems in the analysis of single-material benchmark experiments are discussed with reference to the Winfrith iron benchmark experiment. Particular attention is given to the difficulty of making use of very extensive measurements which are likely to be a feature of this type of experiment. Preliminary results of an adjustment in iron are shown.

1. INTRODUCTION

The use of sensitivity analysis to predict uncertainties in calculated quantities - so-called uncertainty analysis - has until recently been inhibited by the lack of adequate information on the accuracy of cross-section data used in calculations. Despite this, estimates had perforce to be made of the accuracy of calculation of some quantities; in this situation there has been a natural tendency to make pessimistic assumptions in order to arrive at a safe upper limit for the estimated standard deviation on calculated quantities. In many cases these overestimates proved acceptable to designers but there is clearly an economic incentive to limit as far as possible the element of overdesign implicit in such "upper limit" methods. In section 2 we consider the improvement achieved by the use of up-to-date information on the probability distributions of errors on basic data.

The other principal use of sensitivity analysis, which might reasonably be called consistency analysis, is the comparison of calculation with measurement in benchmark experiments in order to assess the adequacy of calculational methods and data. The experiments may be carried out in a single material or in an assembly of materials intended to simulate, at least approximately, a typical reactor

environment of interest. The extreme generality of the former type of experiment suggests that extensive measurement at all energies is required in order to be certain that one can pass comment on the whole range of cross-sections which may be of interest in a wide variety of practical environments. In section 3 some problems of the analysis of such an experiment are considered.

2. UNCERTAINTY ANALYSIS IN THEORETICAL BENCHMARKS

Given the Oak Ridge programmes ANISN and SWANLAKE or their equivalents, uncertainty analysis on specific design parameters can be carried out provided information can be found on the error distributions of data used in the calculations. Such information has not always been easy to find in convenient form although much expertise was possessed by individual data experts and cross-section measurers. The 1966 evaluation of Schmidt [1] has been a useful source of error estimates for fast reactor materials. It made quite clear which are independently measured and which are derived cross-sections, but no attempt was made to consider subleties like energy-dependent correlations and their effective energy range. Thus - (and this is much better than no information) - one has to make use of the following typical statement for the total cross-section of iron:- "This gives an overall accuracy of about 5% above 1.5 MeV. Below 1.5 MeV it should be slightly more accurate."

An upper bound is easily established for the uncertainty induced by such error estimates in a calculated quantity R.

Let A_i, X_i, T_i be group cross-sections of independently measured absorption, non-elastic and total cross-sections.

Let U_{Ai}, $U_{N'i}$, U_{Ni}, be sensitivities of R to absorption, inelastic and elastic cross-section derived from SWANLAKE.

Then: $$\frac{\delta R}{R} = \sum_i \left\{ Z_{Ai}\,\delta A_i + Z_{Xi}\,\delta X_i + Z_{Ti}\,\delta T_i \right\} \qquad (1)$$

Where: $$Z_{Ai} = \left(\frac{U_{Ai}}{A_i} - \frac{U_{N'i}}{N'_i}\right); \quad Z_{Xi} = \left(\frac{U_{N'i}}{N'_i} - \frac{U_{Ni}}{N_i}\right); \quad Z_{T_i} = \frac{U_{Ni}}{N_i} \qquad (2)$$

Squaring and taking the expectation of equation (1) gives for an upper limit:

$$\left(\frac{\sigma^2(R)}{R^2}\right)_{Max} = \sum_j \sum_i \left\{ Z_{Ai}Z_{Aj}\sigma_{Ai}\sigma_{Aj} + Z_{Xi}Z_{Xj}\sigma_{Ai}\sigma_{Aj} + Z_{Ti}Z_{Tj}\sigma_{Ti}\sigma_{Tj} \right\} \qquad (3)$$

if the correlation coefficients between groups i and j for the group cross-sections are taken as unity.

Similar attempts can be made to find a lower limit by setting $r_{ij} = 0$ but these are much more subjective depending on the group structure chosen and are of little practical importance to a designer.

Equation (3) has been applied to the calculation of uncertainties in the iron displacement rate in the pressure vessel of a typical PWR caused by oxygen cross-section errors, and the activation rate of sodium in the heat exchanger of a fast breeder reactor caused by sodium cross-section errors using data uncertainties from Schmidt's compilation. These two calculational benchmark problems were posed respectively by Hehn [2] and Barre [3]. The latter is not generally available and tables 1 and 2 summarise the essential configuration.

Table 1. Spherical Shield Geometry for Fast Reactor Benchmark

Zone	Number	Inner Radius (cm)	Outer Radius (cm)	Thickness (cm)	Mixture Number
Source	1	236.5	236.51	0.01	1
Lateral Shield	2	236.51	416.5	179.99	1
Sodium Tank	3	416.5	916.5	500	2
Heat Exchanger	4	916.5	966.5	50	3
Sodium	5	966.5	1016.5	50	2

Table 2. Composition of Shield for Fast Reactor Benchmark

Medium	Source and Lateral Shield	Sodium	Heat Exchanger
Mixture Number	1	2	3
Volume Fractions			
Steel	0.53	0	0.15
Sodium	0.47	1.0	0.85
Atoms/cm^3 x 10^{24}			
Sodium	0.01045	0.02223	0.01890
Iron	0.03200	0	0.00906
Nickel	0.00423	0	0.00120
Chrome	0.00860	0	0.00243

These calculations were carried out in 42 groups by ANISN and a direct comparison of the above simple method with more sophisticated methods was achieved by generating the 42-group correlated error matrix from the ENDF/B data covariance file for oxygen [4] which is generally available. The full error file for sodium is not yet available but condensed 15 group information for both sodium and iron is given in a compilation of covariance matrices (Drischler and Weisbin [5]) which has recently appeared. Use was made of these matrices by approximate collapsing of the 42 group sensitivities into 15 groups according to the recipe:-

$$Z_p = U \sum_i P_i \, z_{pi} \Big/ \sum P_i U_i \qquad (4)$$

where Z_p, z_{pi} are respectively the collapsed broad group sensitivity and the sensitivity of a fine group contained within the broad group to cross-section type p, and U, Ui are broad and fine group lethargy widths. This type of collapsing is, of course, approximate, but it is seen below that for oxygen it gives results which are not disturbingly different from those given by the more accurate 42-group treatment, and short of a complete new 15 group sensitivity analysis makes the best use of the available information for sodium. These results are summarised in table 3.

Table 3. Uncertainties on Calculated Reaction Rates caused by Data Uncertainties

Relative standard deviation %				Quantity
	15 group matrices [a]	ENDF error file	Schmidt data	
Diagonals [b] Total Max [c]	2.7 2.9 -	2.1 3.0 -	3.7(2.7) [d] - 8.5(6.2)	Uncertainty in displacement-rate of Fe in PWR pressure vessel caused by uncertainties in Oxygen data. Benchmark of Hehn.
Diagonals Total Max	30 40 -	- - -	17(30) - 57(100)	Uncertainties in activation-rate of Na in Fast Reactor heat-exchanger caused by uncertainties in Na data. Benchmark of Barre

a 42 group sensitivities collapsed into 15 groups
b Contains only contributions from the diagonal elements of covariance matrices
c Calculated according to equation (3)
d Figures in brackets are with diagonals normalised to the first column

The differences between columns 1 and 3 in table 3 are largely caused by the different error assignments which are not detailed here. For ease of comparison the figures in brackets in column 3 have been scaled to agree with the diagonal components of column 1. The reasonable agreement between the approximate 15-group collapsed treatment and the more exact 42-group treatment for oxygen in the first case gives confidence that the 15-group treatment for sodium is not seriously incorrect. The above figures do no more than quantify approximately the magnitude of the safety factor (or overdesign factor) involved in the use of upper-limit estimates. Quite clearly the use of correlated error files in uncertainty analysis can reduce the uncertainty quoted to a designer by up to a factor 2 or more - in some cases (though by no means all) this could represent a considerable economic gain.

3. ANALYSIS OF SINGLE MATERIAL BENCHMARK EXPERIMENTS

The simplest form adjustment of calculational data to give consistency between calculation and experiment requires an adjoint calculation and a perturbation for each measurement included in the process. The use of many channel spectrometers in such an experiment can therefore require prohibitive amounts of computation unless some simplifying treatment can be found. In the Winfrith iron benchmark experiments, for example, threshold detectors, hydrogen-filled proportional counters and an NE213 organic liquid scintillator have been used in each of four measuring positions. This raw data amounts to thousands of channels of information - this is collapsed into ~500 channels for the analysis. Further collapsing is of course possible until a manageable number of channels is reached; this is tantamount to admitting that one can not use very detailed information and that it should not have been measured in the first place.

There appear to be three alternative methods of dealing with this problem. If we ignore, for simplicity of notation, uncertainties due to absolute sensitivity of detector counting, source calibration, and energy calibration of spectrometers we can write:-

$$\chi^2 = \sum_i \omega_i (C_i - M_i + \delta C_i)^2 + \sum_j \left\{ \omega_{xj} (\delta X_j)^2 + \omega_{Tj} (\delta T_j)^2 + \omega_{Aj} (\delta A_j)^2 \right\} \quad (5)$$

for the function to be minimized where:

C_i, M_i are respectively the calculation of the ith quantity and its measurement; X_j, T_j, A_j are respectively the independently-derived j^{th} group non-elastic total and absorption cross-section; ω_i, ω_{xj}, ω_{Tj}, ω_{nj} are respectively the weights (inverse variances) of the ith measurement and the cross-sections indicate in group j. (Equation (5) corresponds to the further simplification that the group cross-sections for a given variable are independent - this in no way affects the arguement).

If a_{ij} is the reaction cross-section of detector i in energy group j we require simply to carry out an adjoint calculation with source $H_j^+ = a_{ij}$ for each value of i (ie each detector). As the number of detectors becomes very large interpolation could be tried: thus one might carry out an adjoint ANISN and a SWANLAKE calculation for every tenth or twentieth detector and attempt to interpolate the cross-section sensitivities given by SWANLAKE to give an approximate sensitivity for every channel.

A similar approach would be to carry out a limited number of adjoint calculations for $H_j^+ = 1$ with corresponding SWANLAKE calculations. In this case one would be interpolating the sensitivity of group flux to the calculational data.

The success of the above approaches would depend on something that the authors have not investigated, i.e. the smoothness or otherwise of the sensitivities given by SWANLAKE with the variation of spectrometer channel chosen as adjoint source. The successful implementation of such a method, if it is possible, leads to an essentially simple method of data adjustment and derivation of the dispersion relations of the adjusted data. There is, however, a clear risk of introducing unacceptable approximations for the sensitivities if accurate interpolation can not be guaranteed.

An alternative approach which has been adapted for the Winfrith iron benchmark experiment uses an approximate adjoint source in an iterative procedure - in this case the approximation causes little apprehension, for convergence to the most probable solution can be guaranteed. In equation (5), noting that $C_i - M_i$ is constant, and that $\delta C_i = \sum_j a_{ij}\, \delta \phi_j$ where ϕ_j is the flux in group j, we can make the approximation:

$$\chi^2 = 2\sum_j \sum_i \omega_i (C_i - M_i)\, a_{ij}\, \delta\phi_j + \sum_j \left\{ \omega_{Xj} (\delta X_j)^2 + \omega_{Tj} (\delta T_j)^2 + \omega_{Aj} (\delta A_j)^2 \right\} \quad (6)$$

This suggests immediately for choice of adjoint source:

$$H_j^+ = 2 \sum_i \omega_i (C_i - M_i) a_{ij} \quad (7)$$

Now putting:

$$2h = \sum_j H_j^+ \phi_j \quad (8)$$

we find:

$$\sum_j H_j^+ \delta\phi_j = 2h \sum_k \left\{ \frac{U_{AK}}{A_k} \delta Ak + \frac{U_{N'k}}{N'k} \delta N'k + \frac{U_{Nk}}{Nk} \delta N_k \right\} \quad (9)$$

If $\delta N'_k$, δN_k are expressed in terms of δA_k, δX_k, δT_k and the notation of equation (2) is used the object function for minimization becomes:

$$\chi^2 = 2h \sum_k \left\{ Z_{Ak}\,\delta A_k + Z_{Xk}\,\delta X_k + Z_{Tk}(\delta T_k) + \omega_{Ak}(\delta A_k)^2 + \omega_{Xk}(\delta X_k)^2 + \omega_{Tk}(\delta T_k)^2 \right\} \quad (10)$$

and the first interation adjustments δA_k, δX_k, δT_k are immediately found for example:

$$\delta A_k = -hZ_{Ak}/\omega_{Ak} \quad (11)$$

The derivation of the dispersion relations for the adjusted cross-sections requires a further SWANLAKE calculation and adjoint ANISN calculation in which a strategem similar to the above is adopted in the choice of an adjoint source. At this stage the variables and their dispersion parameters are updated and new ANISN and SWANLAKE calculations are carried out for the next iteration.

The above exposition represents a considerable simplification of the procedure adopted in practice - but it contains all the essentials of the method needed to optimise a large number of data variables using information from a very large number of detectors.

The number of iterations required is now being investigated but worthwhile adjustments and improvements in the agreement of calculation and measurement have already been achieved after two cycles of iteration in an analysis which takes account of all known sources of uncertainty in the measurements and the calculations.

Figure 1 shows the adjustments achieved in the iron inelastic cross-section after one iteration in an early, slightly simplified, analysis. The iron group cross-sections were derived from the UK data library DFN 908 which is essentially the same as that of ENDF/B-3 above 860 KeV. The rather large fractional changes at energies near the threshold are not reproduced at higher energies. This does not necessarily indicate that the cross-sections at these energies are satisfactory; it reflects the lack of sensitivity of the experiment to these cross-sections. This can be seen in figure 2 which shows the inelastic cross-section sensitivities given by SWANLAKE for the "total experiment detector" with cross-section defined by equation (7). (Since this time special, rather lengthy, measurements have been made with an organic liquid scintillator spectrometer to increase the amount of experimental information at energies up to 10 MeV).

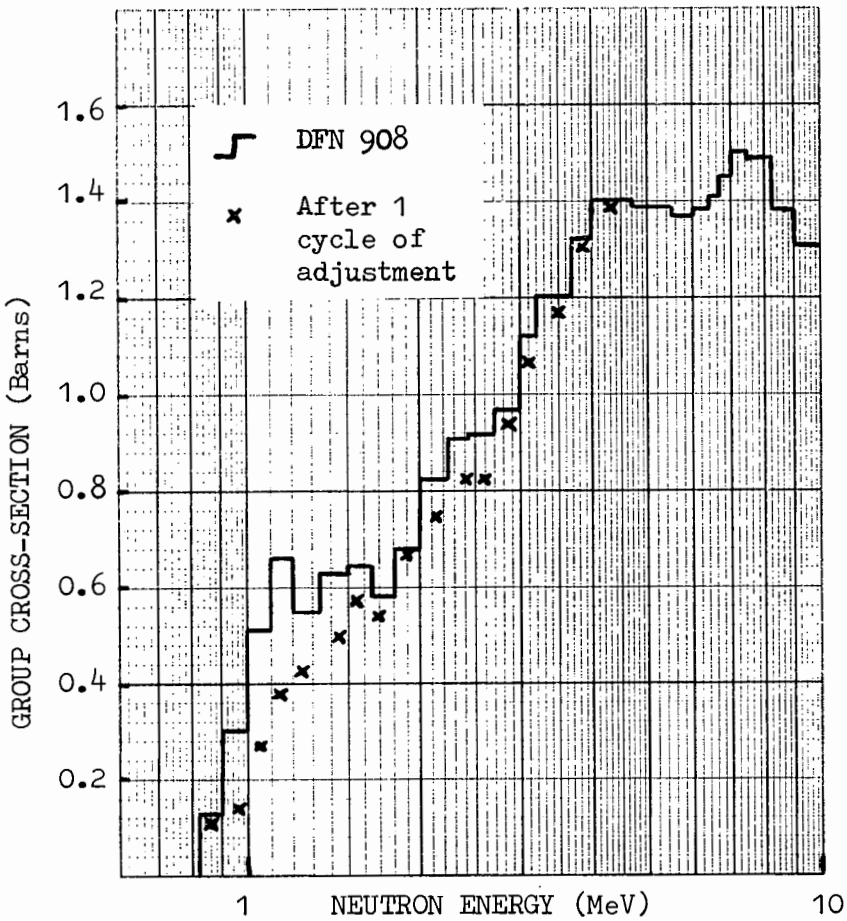

Fig. 1. Group Inelastic Cross-sections before and after Adjustment

Figure 3 shows the composite unfolded spectrum at a penetration of 76 cm of iron and the spectrum predicted by ANISN before and after the 1 - cycle adjustment - a worthwhile improvement in fit is obtained. Figure 3 shows one other feature of this type of experiment which merits attention; the accuracy of the energy calibration of the spectrometers may be important. Little can be done when the spectrum is rapidly fluctuating near 27 KeV and some deresolution is perhaps indicated here. Above 860 KeV, however, there is a rapid monotonic decrease in flux with energy and we find $\frac{\delta\phi(E)}{\phi(E)} \Big/ \frac{\delta E}{E} \sim 5$ for the amplification of flux uncertainties caused by calibration errors. We are not yet sure what influence this has on the adjustment procedure but allowance has been made for it in the latest series of iterations.

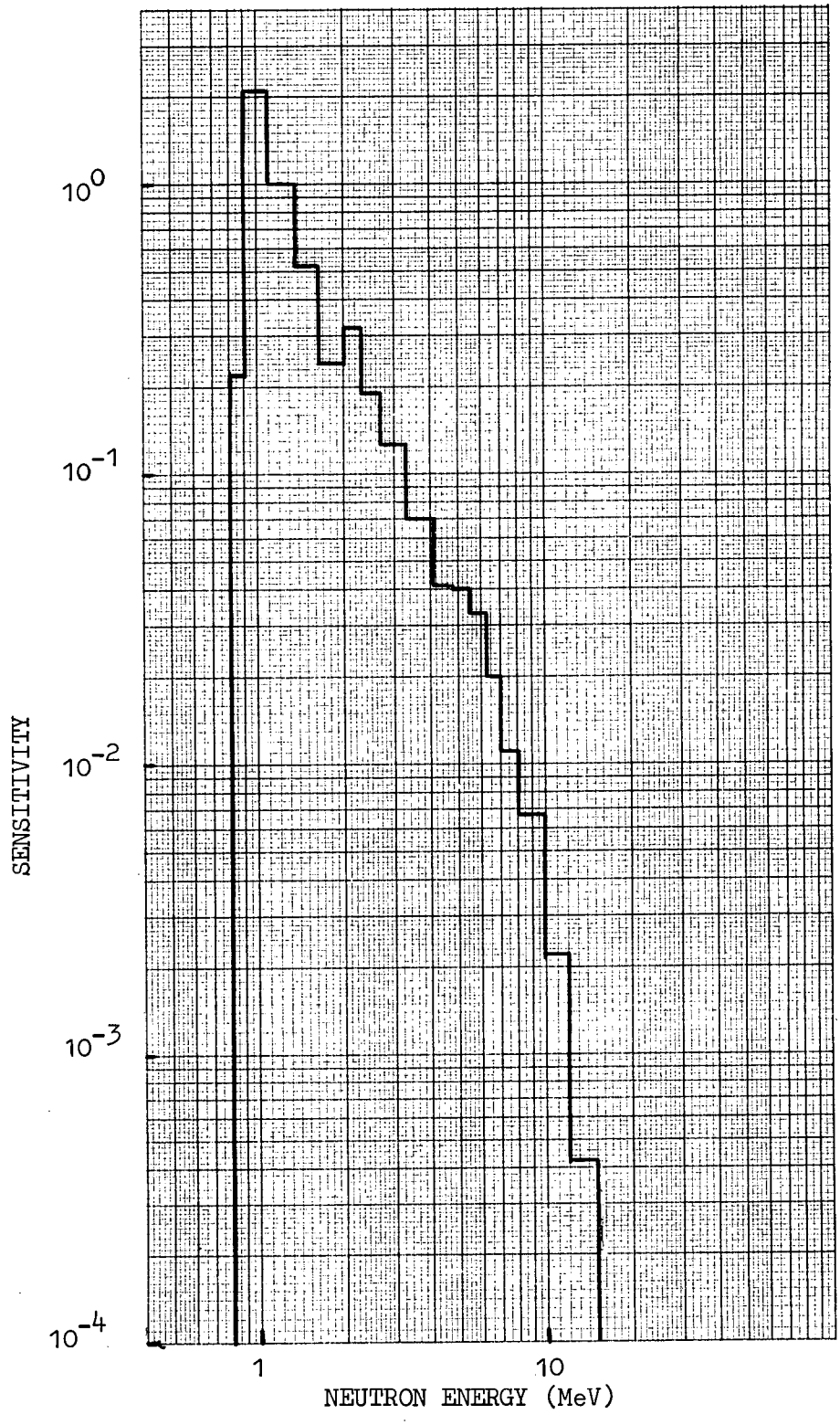

Fig. 2. Initial Experiment Sensitivity to Inelastic Cross-sections in the Winfrith Iron Benchmark Experiment

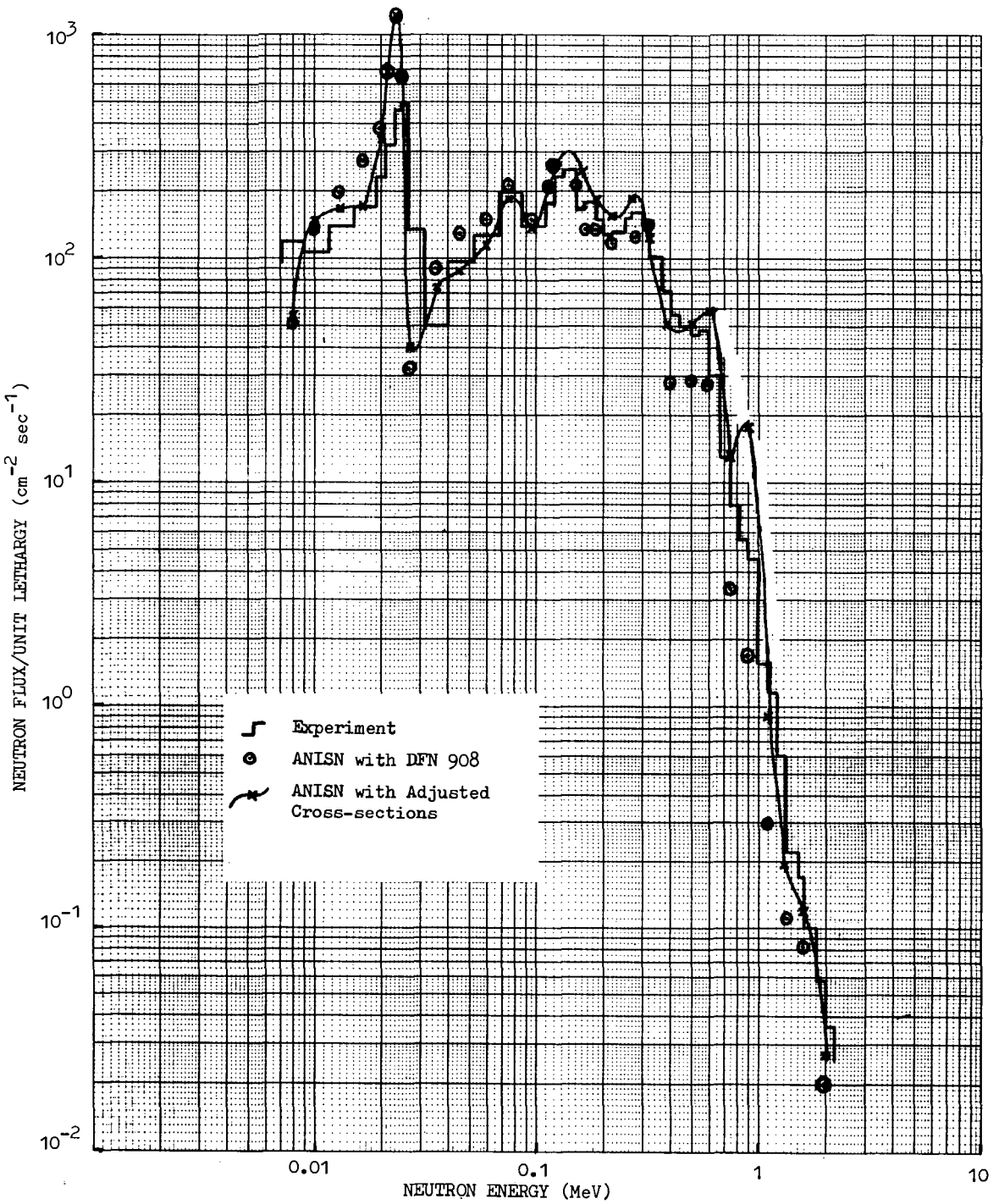

Fig. 3. Comparison of Calculated and Measured Flux Spectra at 76 cm in the Winfrith Iron Benchmark Experiment.

ACKNOWLEDGEMENTS

We are obliged to Mr A F Avery, Mr M J Grimstone and Mr A Packwood for contributing at various times to this work, and to Mr M D Carter and Mr J Samways on whose measurements this work is based.

REFERENCES

1. J. J. Schmidt, Neutron Cross-sections for Fast Reactor Materials Part I; Evaluation, Report KFK 120 (EANDC-E-35U) (February 1966).

2. G. Hehn, J. Koban, Reactor Shield Benchmark No 2, Special Issue No 4 ESIS Newsletter.

3. J. Y. Barre, Fast Reactors: Definition of a Standard Configuration for the Comparison of Shielding Calculations, Unpublished.

4. F. G. Perey, The Data Covariance Files for ENDF/B-V, ORNL/TM - 5938 (ENDF-249) (1977)

5. J. D. Drischler, C. R. Weisbin, Compilation of Multigroup Covariance Matrices for Several Important Reactor Materials, ORNL-5318 (ENDF-235) (December 1977)

INFLUENCE OF CROSS-SECTION STRUCTURE ON UNFOLDED NEUTRON SPECTRA

C. Ertek, M.F. Vlasov, B. Cross, P.M. Smith
International Atomic Energy Agency
Vienna, Austria

ABSTRACT

The influence of cross-section structure on neutron spectra unfolded by multiple foil activation technique, SAND-II case, has been studied. For three reactions with evident structure in neutron cross-section above threshold: 27Al(n,α)24Na, 31P(n,p)31Si and 32S(n,p)32P, two remarkably different sets of evaluated data were selected from the available evaluations; one set of data was "smooth", the structure having been averaged over by a smooth curve; the other set was "sharp" with structure given in detail. These data were used in unfolding procedure together with other reactions, the same in both cases (as well as input spectra and measured reaction rates). It was found that during unfolding calculations less iteration steps were needed to unfold the neutron flux spectrum with the set of "sharp" data. In case of "smooth" data it was difficult to obtain an agreement between measured and calculated activity values even by increasing the number of iteration steps. Contrary to expectations, considerable deformation of unfolded neutron flux spectrum has been observed in the case of the "smooth" data set.

This work has been performed within the IAEA programme on standardization of reactor radiation measurements, one of the important objectives of which is assistance to laboratories in member states to implement the multiple foil activation technique for neutron spectra unfolding, an especially useful technique for in-pile neutron measurements. The importance of this method, e.g. for radiation damage studies is well recognized [1,2].

In order to unfold a neutron spectrum, the following information is required:

a) measured saturation activities of the irradiated detector foils;

b) a set of energy-dependent neutron cross-sections for each foil;

c) a computer programme for unfolding spectra using an input spectrum and data noted in (a) and (b).

The ENDF/B Dosimetry File is finding increasing use as a reference cross-section data set; however, it does not include some important dosimetry reactions. Therefore, the IAEA Nuclear Data Section has initiated an

activity to evaluate these additional reactions. It is hoped that this expanded file will form a basis for an internationally recommended data set for neutron dosimetry applications.

The IAEA Seibersdorf Laboratory, with the support of the IAEA Computer Section, is currently involved in the intercomparison of available computer programmes for spectrum unfolding to recommend the best one (or a few) for general use. For the time being, the SAND-II [3] and CRYSTAL BALL [4] programmes have been implemented [5-7]. The RFSP-Jül [8] programme is under consideration and preparation have been started to implement the STAY'SL[9] unfolding code. The SAND-II programme has been compared with a new generalized least squares method by J.T. Routti [10].

As a part of these activities, we plan to investigate related problems such as the influence of input spectra on the solution spectrum, consistency of measured reaction rates, effects of structure in the energy-dependent neutron cross sections on the shape of the unfolded spectrum, etc. As the first step, we have studied the influence of cross-section structure on spectra unfolded with the SAND-II programme. The pressurized water reactor (PWR) type spectrum was chosen.

Three reactions ($^{27}Al(n,\alpha)^{24}Na$, $^{31}P(n,p)^{31}Si$ and $^{32}S(n,p)^{32}P$) with evident energy dependent cross-section structure were selected. For each reaction two sets of the evaluated data, "smooth" (structure averaged by smooth curve) and "sharp" (structure given in detail), were taken from the available evaluations and converted, where necessary, into SAND-II format. The cross sections together with the response functions in a Watt neutron spectrum are given in Fig. 1-6. In addition to these three reactions, seven other reactions, with identical evaluations in both "smooth" and "sharp" cases, were used to unfold the PWR type neutron spectrum. The saturation activities calculated with this spectrum were compared with the measured ones. This comparison is given in Table 1, from which it can be seen, that for the $^{31}P(n,p)^{31}Si$ reaction, the deviation of the measured from the calculated activity is ~7% in the "smooth" case, while it is only 0.5% in the "sharp" case.

For the $^{32}S(n,p)^{32}P$ reaction this deviation is ~-6% and -3% respectively. Less than 0.1% deviation is observed in both cases for $^{27}Al(n,\alpha)^{24}Na$ reaction. The overall standard deviation of the measured activities is ~3% in the "smooth" case as compared to 1.5% in the case of "sharp" data. Increasing the number of the iteration steps in the case of "smooth" data does not decrease the final deviation of the measured from calculated activity.

At first, one might expect that sharp structure in the cross-section would perturb the smooth shape of the unfolded spectrum; however, contrary to expectations, considerable deformation of the unfolded neutron flux spectrum has been observed in the case of the "smooth" data set in the energy range from 2.2 MeV up to ~6 MeV as shown in Fig. 8. It is difficult to explain in detail the observed results. However, it is clear that the "sharp" data, which more accurately represent the measured neutron cross sections, are preferable. At the same time these results suggest, that

smoothing of the input cross-section data should be done very carefully in order to avoid introducing distortions of the type seen in this work.

ACKNOWLEDGEMENTS

The authors would like to thank Dr. D.W. Muir for useful discussions and Mr. K. McLaughlin for assistance with computer plotting programmes.

REFERENCES

[1] 1st ASTM-EURATOM Symposium on Reactor Dosimetry, Petten, Netherlands, EUR 5667 e/f parts I and II (September 1975).

[2] 2nd ASTM-EURATOM Symposium on Reactor Dosimetry, Palo Alto, Calif., USA (October 1977) to be published.

[3] W.N. McElroy et al., "SAND-II, Neutron Flux Spectra Determinations by Multiple Foil Activation Iterative Method", RSIC Computer Code Collection CCC112, ORNL, (May 1969).

[4] F.B.K. Kam, F.W. Stallman, CRYSTAL BALL, Report ORNL-TM-4601 (June 1974).

[5] C. Ertek, "On the Penetration of Mono-energetic Neutrons Inside the Detector Foils and Related Problems", IAEA/RL/44 (February 1977).

[6] C. Ertek, et al. "Progress Report on the IAEA Activity on Neutron Spectra Unfolding by Activation Technique", paper presented at the Second ASTM-EURATOM symposium on Reactor Dosimetry, Palo Alto, Calif., USA (October 1977).

[7] C. Ertek, "Report on Some Interlaboratory IAEA Activities on Neutron Spectra Unfolding by Activation Technique", IAEA/RL/47 (May 1978).

[8] A. Fischer, "RESP-JÜL: A Programme for Unfolding Neutron Spectra from Activation Data", Jül-1475 (December 1977).

[9]. F.G. Perey, "Least-Squares Dosimetry Unfolding: The Programme STAY'SL", ORNL/TM-6062 (October 1977).

[10] J.T. Routti et al. "Threshold Detector Measurements of Fast Neutron Spectra in TRIGA Reactor with Application of a New Unfolding Method", Atomkernenergie (ATKE) Bd. 26(1975), Lfg. 2.

Table 1

RESULTS OBTAINED AFTER 12 ITERATIONS ("SMOOTH")

Foil Reaction	Saturated Measured Activity (DPS/Nucleus)	Saturated Calculated Activity (DPS/Nucleus)	Ratio Measured to Calculated Activities	Deviation of Measured from Calculated Activity (Percent)
Sc45(n,γ)Sc46	1.713E-24	1.734E-24	0.9880	-1.20
Na23(n,γ)Na24	3.997E-26	3.974E-26	1.0057	0.57
Au197(n,γ)Au198	6.836E-23	6.839E-23	0.9996	-0.04
Co59(n,γ)Co60	4.936E-24	4.936E-24	1.0001	0.01
Th232(n,f)FP	1.727E-26	1.749E-26	0.9877	-1.23
Fe54(n,p)Mn54	1.825E-26	1.822E-26	1.0019	0.19
U235(n,f)FP	4.084E-23	4.065E-23	1.0047	0.47
Al27(n,α)Na24	1.281E-28	1.281E-28	1.0000	0.00
P31(n,p)Si31	7.836E-27	7.324E-27	1.0699	6.99
S32(n,p)P32	1.474E-26	1.564E-26	0.9425	-5.75
		Standard Deviation of Measured Activities (Percent)		3.08

RESULTS OBTAINED AFTER 12 ITERATIONS ("SHARP")

Sc45(n,γ)Sc46	1.713E-24	1.733E-24	0.9883	-1.17
Na23(n,γ)Na24	3.997E-26	3.973E-26	1.0061	0.61
Au197(n,γ)Au198	6.836E-23	6.837E-23	0.9999	-0.01
Co59(n,γ)Co60	4.936E-24	4.934E-24	1.0004	0.04
Th232(n,p)FP	1.727E-26	1.738E-26	0.9938	-0.62
Fe54(n,p)Mn54	1.825E-26	1.771E-26	1.0305	3.05
U235(n,f)FP	4.084E-23	4.064E-23	1.0049	0.49
S32(n,p)P32	1.474E-26	1.515E-26	0.9727	-2.73
P31(n,p)Si31	7.836E-27	7.796E-27	1.0052	0.52
Al27(n,α)Na24	1.281E-28	1.283E-28	0.9981	-0.19
		Standard Deviation of Measured Activities (Percent)		1.47

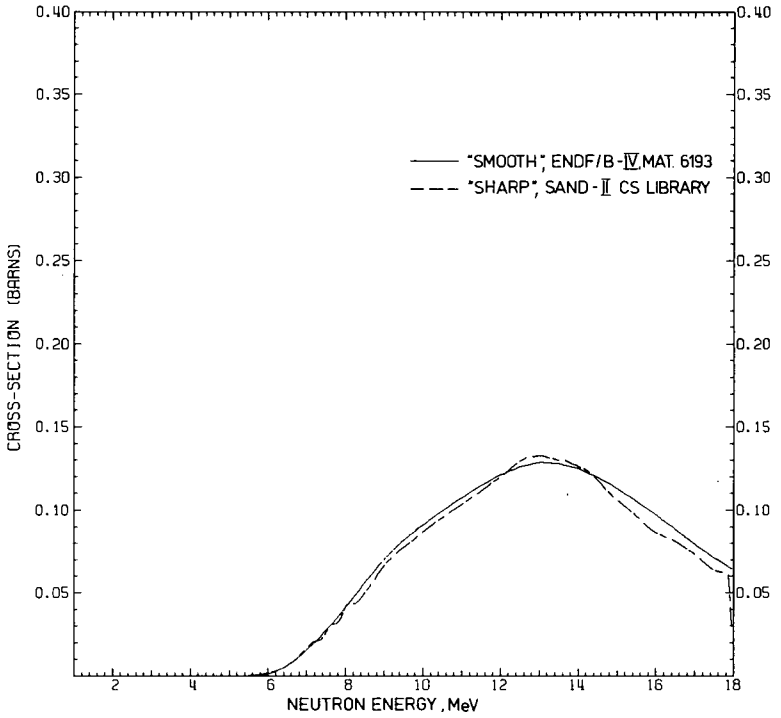

Fig. 1. 27Al(n,α)24Na neutron cross section.

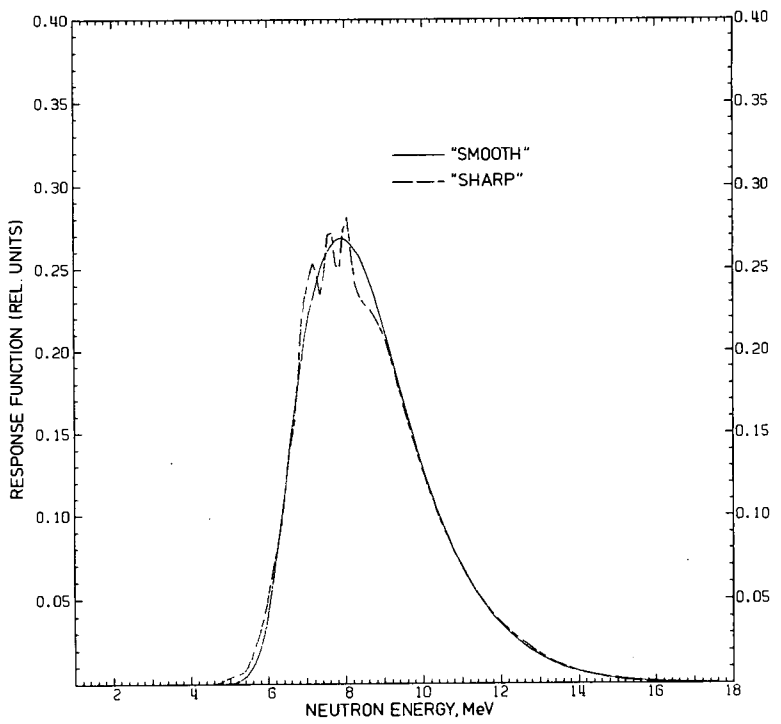

Fig. 2. 27Al(n,α)24Na response in Watt spectrum.

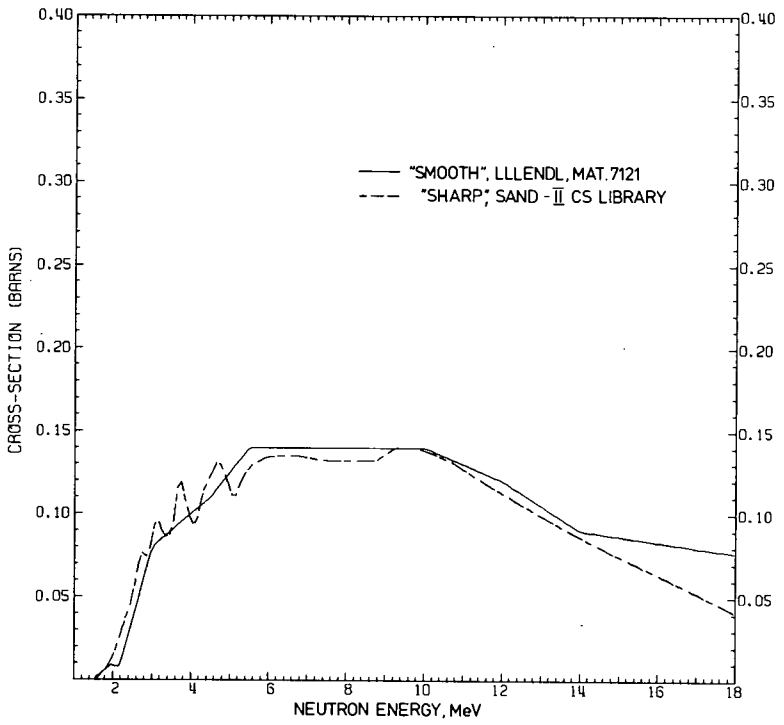

Fig. 3. 31P(n,p)31Si neutron cross section.

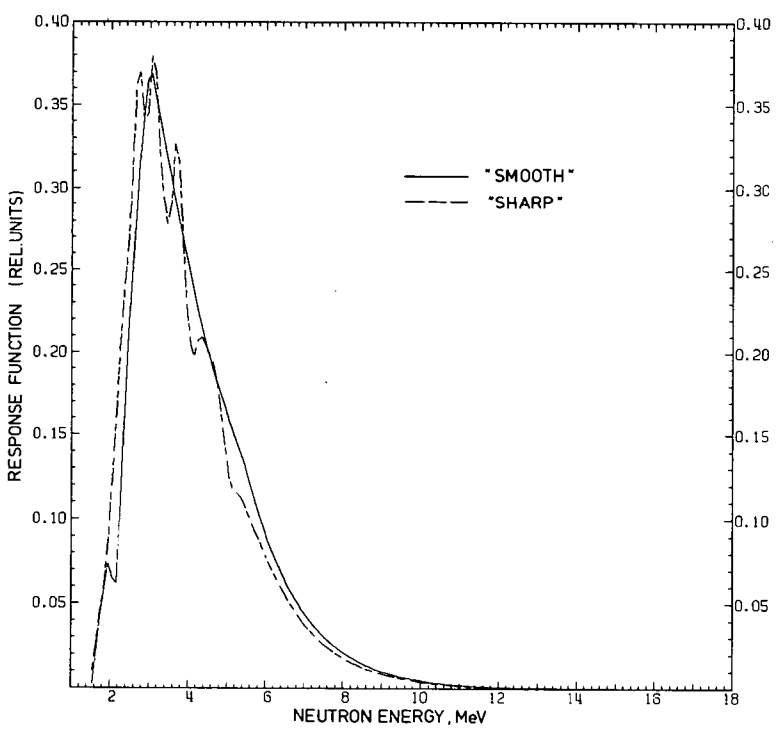

Fig. 4. 31P(n,p)31Si response in Watt spectrum.

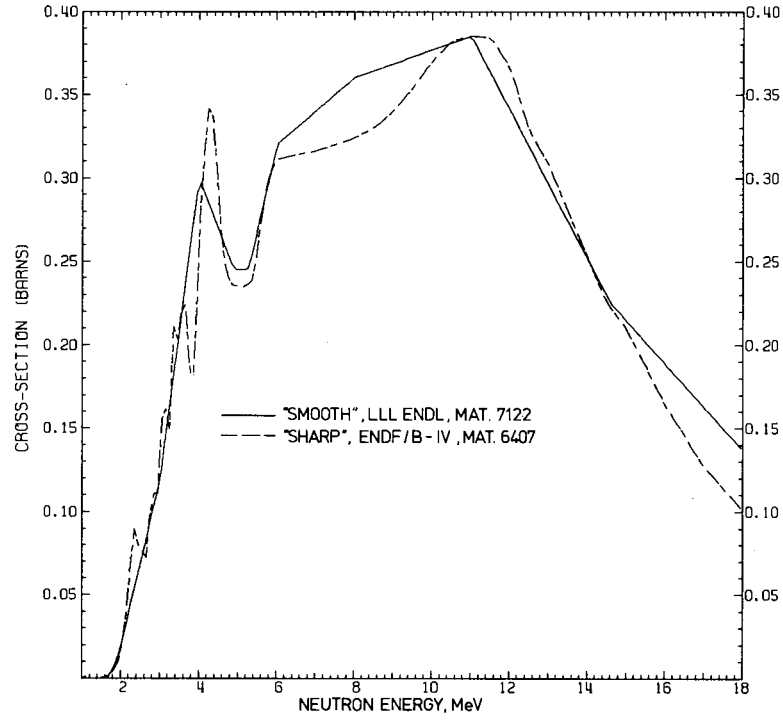

Fig. 5. 32S(n,p)32P neutron cross section.

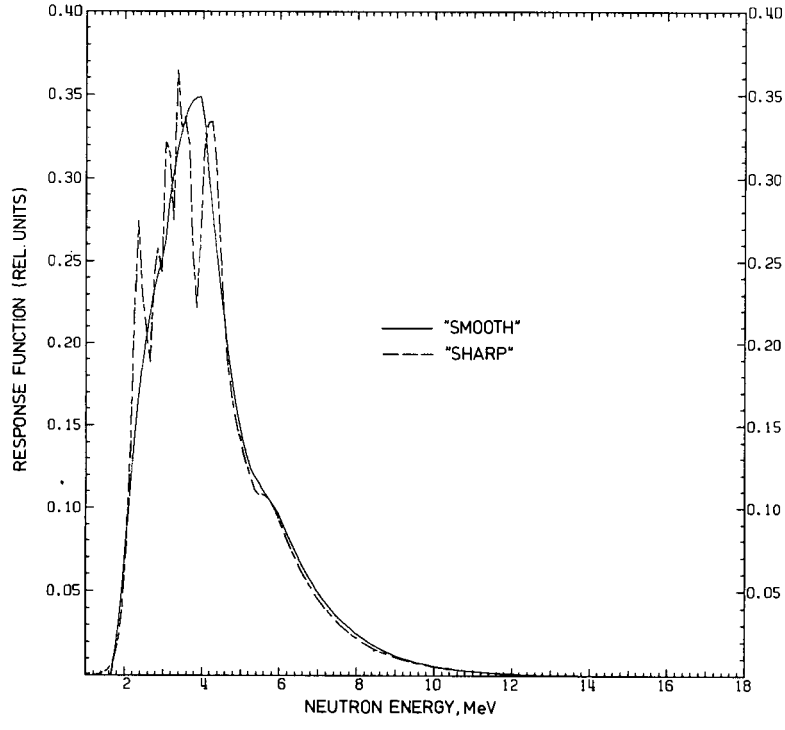

Fig. 6. 32S(n,p)32P response in Watt spectrum.

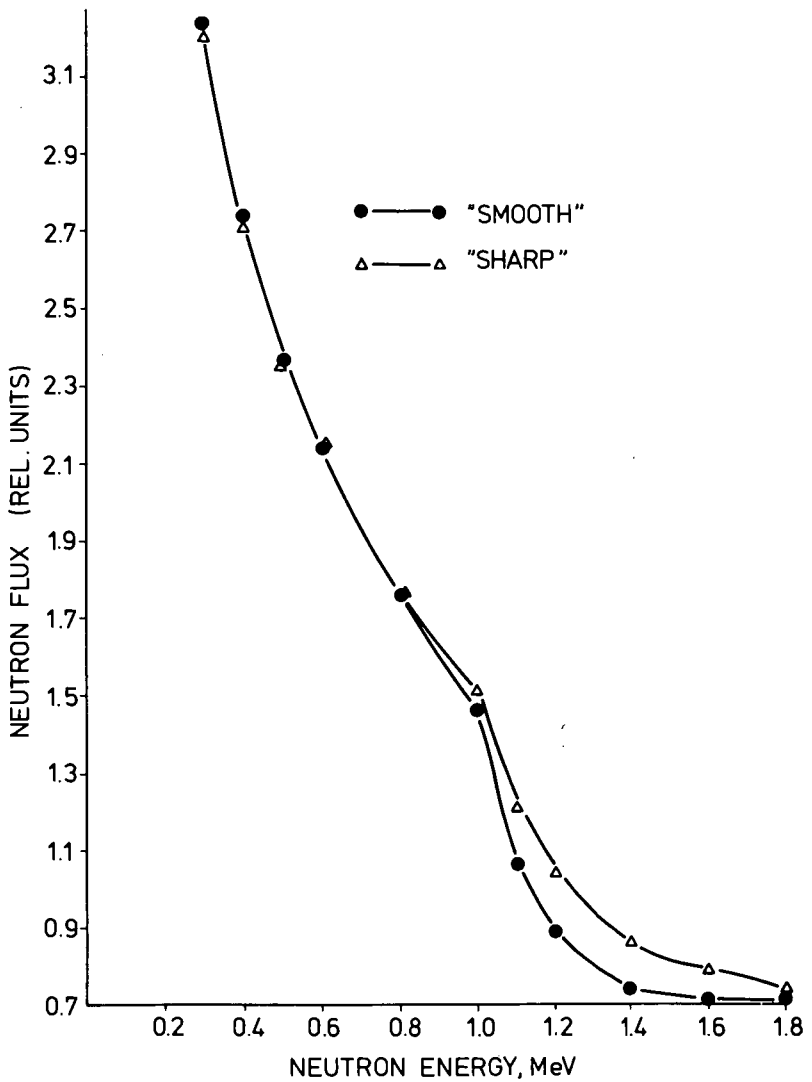

Fig. 7. PWR unfolded flux spectrum.

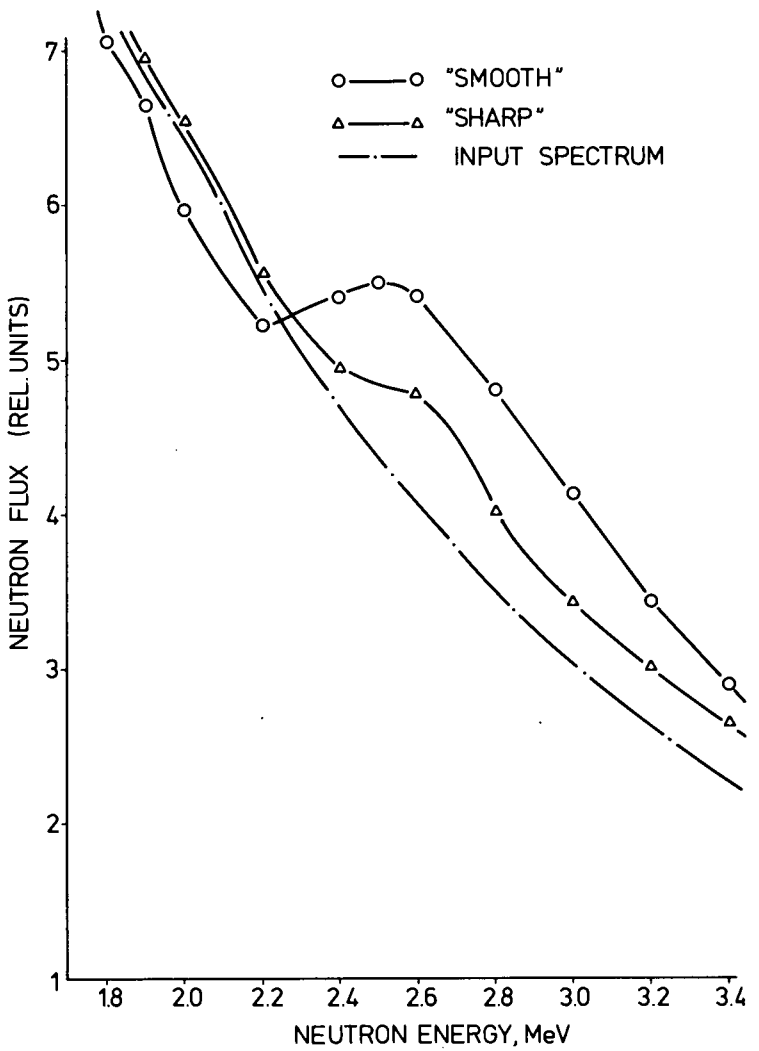

Fig. 8. PWR unfolded flux spectrum.

INTERNAL DISTRIBUTION

1. L. S. Abbott
2. R. G. Alsmiller, Jr.
3. D. E. Bartine
4. L. Berry
5. G. F. Flanagan
6. F. C. Maienschein
7. F. R. Mynatt
8. R. W. Peelle
9. H. Postma
10. M. W. Rosenthal
11. D. B. Trauger
12. C. R. Weisbin
13. A. Zucker
14. H. Goldstein (consultant)
15. Paul Greebler (consultant)
16. W. B. Loewenstein (consultant)
17. R. Wilson (consultant)
18. R. E. Uhrig (consultant)

19-193. RSIC Distribution

194-195. Central Research Library

196. ORNL-Y-12 Technical Library Document Reference Section

197-198. Laboratory Records Department

199. Laboratory Records, ORNL R.C.

200. ORNL Patent Office

EXTERNAL DISTRIBUTION

201. P. B. Hemmig, Division of Reactor Research and Technology, U. S. Department of Energy, Washington, D.C. 20545
202. David Auton, Defense Nuclear Agency, Washington, D.C. 20305
203. Frank Coffman, Office of Fusion Energy, U.S. Department of Energy, Washington, D.C. 20545
204. R. H. Odegaarden, Transportation Branch, U.S. Nuclear Regulatory Commission, Washington, D.C. 20545
205. Myrna Steele, U.S. Nuclear Regulatory Commission, M/S LA-212, Washington, D.C. 20545
206. Henry Till, Electric Power Research Institute, 3412 Hillview Ave., Palo Alto, CA 94304
207. Charles Head, Office of Fusion Energy, U.S. DOE, Washington, D.C. 20545
208. Harry Alter, Reactor Research & Technology Division, U.S. DOE, Washington, D.C. 20545
209. Burt Zolotar, EPRI, 3412 Hillview Ave., Palo Alto, CA 94304
210. Odelli Ozer, EPRI, 3412 Hillview Ave., Palo Alto, CA 94304
211. J. Lewellen, Division of Reactor Research & Technology, U.S. DOE, Washington, D.C. 20545
212. George L. Rogosa, Division of Physical Research, U. S. DOE, Washington, D.C. 20545
213. Office of Nuclear Reactor Regulation, U.S. Nuclear Regulatory Commission, Washington, D.C. 20545, Attn: Director
214. Office of Nuclear Regulatory Research, U.S. Nuclear Regulatory Commission, Washington, D.C. Attn: Director
215. Office of Standards Development, U.S. Nuclear Regulatory Commission, Washington, D.C., Attn: Director

216-217. Technical Information Center, U.S. DOE, Oak Ridge, Tennessee 37830

218. Office of Assistant Manager, Energy Research and Development, DOE-ORO, Oak Ridge, Tennessee 37830
219. Patent Office, U.S. DOE, Oak Ridge, Tennessee 37830

220-294. RSIC Distribution

☆U.S. GOVERNMENT PRINTING OFFICE: 1979-748-189/396